U.S. Department
of Transportation

**United States
Coast Guard**

Bulletin of the United States Coast Guard

Report of the International Ice Patrol in the North Atlantic

**1984 Season
Bulletin No. 70**
CG-188-39

INTERNATIONAL
ICE PATROL

DEPARTMENT OF TRANSPORTATION
UNITED STATES COAST GUARD

MAILING ADDRESS G-OIO
U. S. COAST GUARD
WASHINGTON, D. C. 20593
(202) 426-1881

2 JUL 1985

Bulletin No. 70

REPORT OF THE INTERNATIONAL ICE PATROL SERVICES IN THE NORTH ATLANTIC OCEAN

Season of 1984

CG-188-39

FOREWORD

Forwarded herewith is Bulletin No. 70 of the International Ice Patrol describing the Patrol's services, ice observations and conditions during the 1984 season.

M. J. O'BRIEN
Acting Chief, Office of Operations

DISTRIBUTION - SDL No. 121

	a	b	c	d	e	f	g	h	i	j	k	l	m	n	o	p	q	r	s	t	u	v	w	x	y	z
A	1*	1*		1	1	1*																				
B		1	1		10					2				2	5		1									
C	1*															1*										
D																							60			
E																										
F																										
G																										
H																										

NON-STANDARD DISTRIBUTION:

*A;abf LANTAREA only
*B;b LANTAREA (5); B:b PACAREA (5)
*C: aq LANTAREA only
SML CG-4

Summary

From 23 March to 7 September 1984, the International Ice Patrol (IIP), a unit of the U.S. Coast Guard, conducted the International Ice Patrol Service, which has been provided annually since the sinking of the RMS TITANIC on April 15, 1912. During past years, Coast Guard ships and/or aircraft have patrolled the shipping lanes off Newfoundland within the area delineated by 40°N - 52°N, 39°W - 57°W, detecting icebergs and warning mariners of these hazards. During the 1984 Ice Patrol season, Coast Guard HC-130 aircraft deployed out of Gander, Newfoundland to search for icebergs in the Grand Banks region of the North Atlantic. These aircraft flew 78 ice reconnaissance sorties, logging over 476 flight hours. New detection equipment, the AN/APS-135 Side-Looking Airborne Radar (SLAR), was introduced into Ice Patrol duty during the 1983 season. It proved to be an excellent tool for the detection of both icebergs and sea ice, and alone provided 78 percent of the 1984 sightings on IIP reconnaisance flights. A total of 2202 icebergs were estimated south of 48°N latitude, a new record. The record number of icebergs south of 48°N this year was the result of colder than normal conditions (see Environmental Conditions section) and increased iceberg detection due to the use of SLAR (see Appendix C). To evaluate the iceberg drift and deterioration models used by International Ice Patrol, an oceanographic cruise was conducted by USCGC HORNBEAM. This cruise conducted the first hydrographic survey since 1978, and included drift and deterioration studies on a medium iceberg (see Appendix B).

Introduction

This is the 70th annual report of the International Ice Patrol Service in the North Atlantic. It contains information on ice conditions and Ice Patrol operations for 1984. The U.S. Coast Guard conducts the International Ice Patrol Service in the North Atlantic under the provisions of Title 46, U.S. Code, Sections 738, 738a through 738d; and the International Convention for the Safety of Life at Sea (SOLAS), 1960, regulations 5-8. This service has been provided annually since the sinking of the RMS TITANIC on April 15, 1912. Commander, International Ice Patrol under Commander, Coast Guard Atlantic Area, directed the International Ice Patrol from offices located at Groton, Connecticut. The unit analyzes ice and environmental data, prepares the daily ice bulletins and facsimile charts, and replies to any requests for special ice information. It also controls the aerial Ice Reconnaisance Detachment and any surface patrol cutters when assigned, both of which patrol the southeastern, southern, and southwestern limits of the Grand Banks region (40°N to 52°N) and 39°W to 57°W for icebergs. The International Ice Patrol makes twice-daily radio broadcasts to warn mariners of the limits of iceberg distribution.

Vice Admiral Wayne E. Caldwell, U.S. Coast Guard, was Commander, Atlantic Area until he was relieved on 1 July 1984. Vice Admiral P.A. Yost was Commander, Atlantic Area from then until the season's end on 7 September 1984. Commander Norman C. Edwards, Jr., U.S. Coast Guard, was Commander, International Ice Patrol during the 1984 Ice Patrol season.

Two pre-season deployments were made from 31 January - 3 February and 7-14 March 1983 to determine the early season iceberg distribution. Based on these trips, regular deployments started on 21 March with the 1984 season officially opening on 22 March.

From that date until 3 September 1984, an aerial Ice Reconnaisance Detachment (ICERECDET) operated from Gander, Newfoundland one week out of every two. The season officially closed on 7 September 1984.

No U.S. Coast Guard cutters were deployed to act as surface patrol vessels this year. The USCGC HORNBEAM was deployed to provide oceanographic support to Ice Patrol from 26 June - 31 July.

During the 1984 season, an estimated 2202 icebergs drifted south of 48°N latitude. Table 1 shows monthly estimates of icebergs that crossed 48°N.

Table 1. Icebergs South of 48° North

	1984	Total 1946-84	Average 1946-84	Total 1900-84	Average 1900-84
OCT	0	2	0	109	1
NOV	0	4	0	110	1
DEC	0	13	0	93	1
JAN	0	74	2	194	3
FEB	0	437	11	888	16
MAR	101	1397	36	3499	56
APR	953	4423	113	9268	150
MAY	484	3842	99	11025	169
JUN	227	2260	58	5778	92
JUL	335	900	23	2096	31
AUG	93	197	5	586	8
SEP	9	19	0	265	3
Annual total	2202	13568	347	33911	399

Data Collection and Dissemination

Ice Reconnaisance Detachment Deployments	No. of Flights	Number of Hours Flown
Pre-season	13	75.2
In-season	93	543.1
Post-season	2	10.7
Total	108	629.0

Note: In-season ICERECDET flights include transit and logistics flights to and from Gander during the Ice patrol season.

There were 78 sorties dedicated solely to ice reconnaisance with a total of 476.1 flight hours. They are summarized as follows:

Month	Number of Sorties	Flight Hours
FEB	3	15.5
MAR	10	60.7
APR	16	101.0
MAY	15	93.6
JUN	10	59.5
JUL	10	60.1
AUG	12	74.8
SEP	2	10.9
TOTAL	78	476.1

Table 2. Aircraft Deployments from 1 October 1983 to 30 September 1984

During the 1984 Ice Patrol year (from 1 October through 30 September 1984), 108 aircraft sorties were flown in support of the International Ice Patrol. These included pre-season flights, ice observation and logistics flights during the season, and post-season flights. Pre-season flights determined iceberg concentrations north of 48°N, necessary to estimate the time when icebergs would threaten the North Atlantic shipping lanes in the vicinity of the Grand Banks of Newfoundland. During the active season, ice observation flights located the southwestern, southern, and southeastern limits of icebergs. Logistics flights were necessary for unusual aircraft maintenance. Post-season flights were made to retrieve parts and equipment from Gander and to close out all business transactions from the season.

U.S. Coast Guard aircraft, deployed from Coast Guard Air Station Elizabeth City, North Carolina, conducted all the aircraft missions. SLAR-equipped HC-130 aircraft were utilized exclusively for aerial ice reconnaisance, HU-25A aircraft were used on two logistics flights, and the VC-4A aircraft was utilized for post season deployment. Table 2 shows aircraft utilization during the 1984 season.

U.S. Coast Guard Communications Station Boston, Massachusetts, NMF/NIK, was the primary radio station used for the dissemination of the daily ice bulletins and facsimile charts after preparation by the Ice Patrol office in Groton. Other transmitting stations for the 0000Z and 1200Z ice bulletins included Canadian Coast Guard Radio Station St. John's/VON, Canadian Forces Radio Station Mill Cove/CFH, and U.S. Navy LCMP Broadcast Stations Norfolk/NAM; Thurso, Scotland; and Keflavik, Iceland.

Canadian Forces Station Mill Cove/CFH as well as AM Radio Station Bracknell/GFE, United Kingdom are radio facsimile broadcasting stations which used Ice Patrol limits in their broadcasts. Canadian Coast Guard Radio Station St. John's/VON provided special broadcasts.

The International Ice Patrol requested that all ships transitting

Table 3
Iceberg and SST Reports

Number of ships furnishing Sea Surface Temperature (SST) reports	86
Number of SST reports received	353
Number of ships furnishing ice reports	220
Number of ice reports received	586
First Ice Bulletin	230000Z MAR 84
Last Ice Bulletin	071200Z SEP 84
Number of facsimile charts transmitted	169

the area of the Grand Banks report ice sightings, weather, and sea surface temperatures via U.S. Coast Guard Communications Station Boston, NMF/NIK. Response to this request is shown in Table 3, and Appendix A lists all contributors. Commander, International Ice Patrol extends a sincere thank you to all stations and ships which contributed.

Table 4
Sources of International Ice Patrol Iceberg Reports

Sighting Source	No. of Sightings	% of Total
Coast Guard SLAR	2487	49.3
Coast Guard Visual	722	14.3
CanadianRadar	10	0.2
Canadian Visual	48	1.0
CommercialRadar	367	7.3
CommercialVisual	1157	22.9
Mobil Oil Canada, LTD	171	3.4
Other	31	0.6

Environmental Conditions, 1984 Season

Weather in Labrador and east Newfoundland during the 1984 International Ice Patrol season tended to be cooler and wetter than normal (Table 5). The weather stations listed were selected to give a cross section of weather patterns throughout the province. Months that ran contrary to the cool, wet trend were February and May, which were warmer than normal, and July, which was warmer and drier than normal. The overall wet, cool trend had the effect of allowing sea ice to persist longer than normal in the Davis Strait and Labrador Sea, thereby offering some protection to icebergs in that region.

January: The Iceland Low was deeper than normal during January and the distribution of pressure funnelled in cold continental air (Figure 1), causing the air temperatures to be well below normal (Table 5).

February: The Iceland Low was again deeper than normal, but pressure patterns allowed warm, moist marine air to flow over the Maritimes (Figure 2) and temperatures and precipitation were above normal.

March: Average surface flow during the month was almost the opposite of the normal pattern (Figure 3) with easterly and northeasterly winds, which brought cool, moist marine air over the Grand Banks and the Maritimes, resulting in slightly lower than normal temperatures and greater than normal precipitation.

April: The unusual high pressure system over Labrador in April (Figure 4), coupled with lows south of the Avalon Peninsula and over Iceland, caused northeasterly flow across the Labrador coast and easterly flow across Newfoundland and the Grand Banks, with above average precipitation on the Avalon Peninsula (St. John's) and below average temperatures throughout the region (Table 5).

May: Southwesterly flow over Newfoundland and Labrador (Figure 5) brought in marine air and raised temperatures and precipitation above normal.

June: Under the influence of low pressure over the Labrador Sea (Figure 6), southerly flow over the region brought in marine air which was cooler and moister than the continental air normal for June.

July: With near normal pressures (Figure 7), precipitation was slightly below normal and temperatures slightly above normal during July, suggesting more of a continental influence than normal.

August: With the cooling of the northern continental air mass that normally takes place in August, a stronger than normal marine influence (Figure 8) brought warmer temperatures and more precipitation over the region.

September: The Bermuda High was farther south than normal in September (Figure 9), bringing marine air into the area and causing above normal precipitation with near normal temperatures.

Table 5
Environmental Conditions for 1984 International Ice Patrol Season

	Station	Temp °C Monthly Mean	Temp °C Diff. from Norm.	Total Precipitation (mm)	% of Normal Precipitation	% of Normal Snowfall
OCT 1983	Hopedale	1.8	-0.6	47.0	75	73
	Goose	2.6	-0.1	91.3	119	87
	Gander	6.9	0.9	42.2	40	25
	St. John's	7.7	0.8	214.6	147	27
NOV	Hopedale	-3.8	-0.6	99.1	173	159
	Goose	-4.9	-1.1	155.1	206	264
	Gander	1.3	0.5	126.4	118	168
	St. John's	2.4	-1.0	118.9	73	84
DEC	Hopedale	-13.6	-2.9	109.9	194	181
	Goose	-15.3	-2.3	126.7	74	215
	Gander	-4.4	-0.6	84.4	78	92
	St. John's	-1.5	0.0	111.7	69	53
JAN 1984	Hopedale	-22.4	-6.6	34.4	55	48
	Goose	-23.0	-6.6	51.8	70	82
	Gander	-9.4	-3.2	157.7	145	158
	St. John's	-5.5	-1.6	188.8	121	65
FEB	Hopedale	-17.7	-2.6	111.6	223	174
	Goose	-14.4	0.1	90.7	150	219
	Gander	-4.7	2.1	142.7	143	67
	St. John's	-1.9	2.6	151.1	108	10
MAR	Hopedale	-12.1	-1.6	100.1	181	149
	Goose	-10.3	-1.7	82.9	115	116
	Gander	-3.9	-0.4	174.4	158	160
	St. John's	-1.6	0.7	142.7	108	173
APR	Hopedale	-6.9	-2.0	25.0	54	54
	Goose	-3.6	-1.9	50.8	83	108
	Gander	-0.6	-1.5	97.8	105	79
	St. John's	-0.2	-1.4	235.2	203	51
MAY	Hopedale	1.8	0.4	68.0	134	119
	Goose	5.8	0.8	89.6	140	143
	Gander	8.9	2.7	92.2	132	31
	St. John's	8.3	2.9	156.0	153	*
JUN	Hopedale	4.7	-1.7	71.8	112	126
	Goose	9.3	-2.0	120.6	130	432
	Gander	9.4	-2.4	115.9	144	36
	St. John's	9.9	-1.0	144.0	168	*
JUL	Hopedale	9.6	-0.9	178.3	211	*
	Goose	16.8	1.0	91.8	87	*
	Gander	18.0	1.5	63.2	92	*
	St. John's	17.9	2.4	41.4	50	*
AUG	Goose	23.0	3.7	23.6	23	*
	Gander	16.6	1.0	181.8	187	*
	St. John's	17.3	2.0	204.3	168	*
SEP	Nain	5.1	----	134.3	----	----
	Goose	13.0	-0.7	121.3	137	*
	Gander	14.9	-0.7	113.4	140	*
	St. John's	16.9	1.0	157.8	141	*

* No snowfall recorded during this month.

NOTE: In August 1984, the Canadian weather reporting at Hopedale was discontinued. The new station is at Nain on the Labrador coast, approximately 150km northwest of Hopedale.

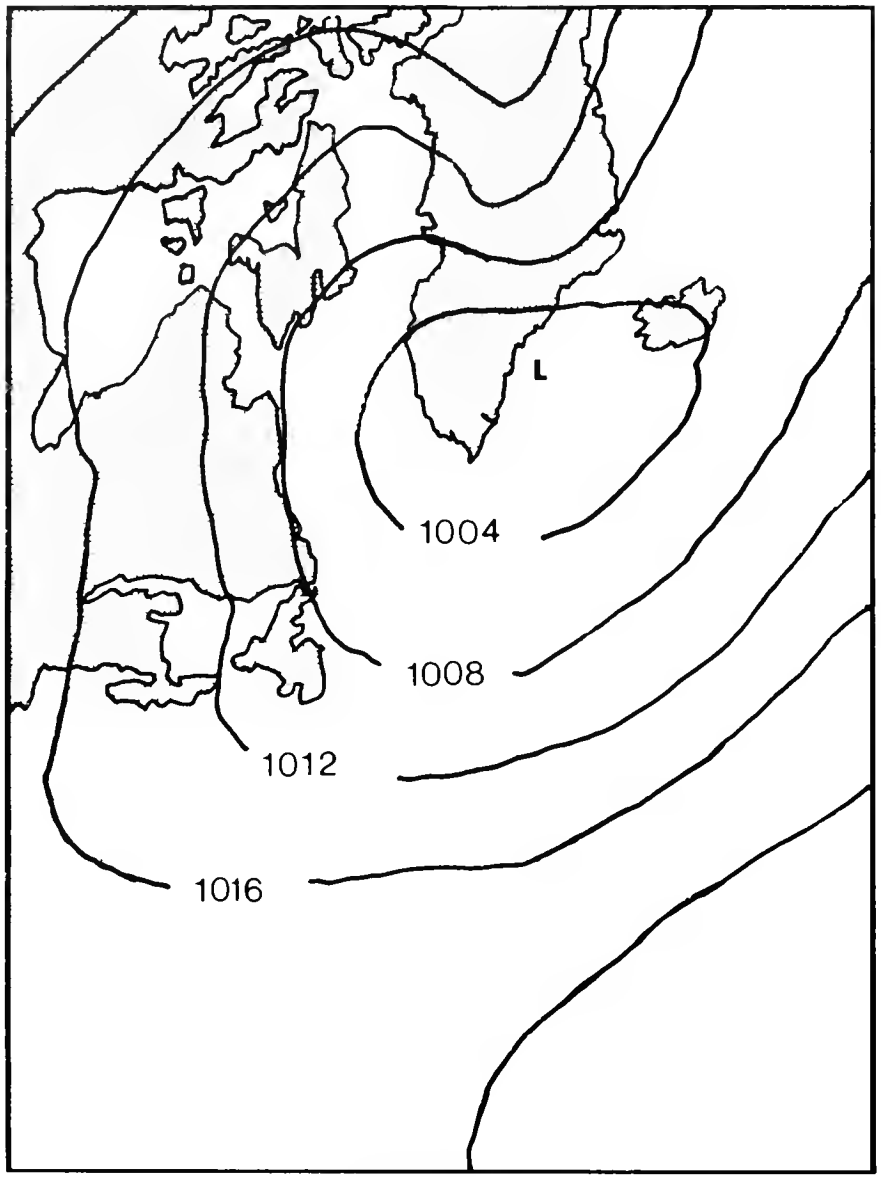

Normal

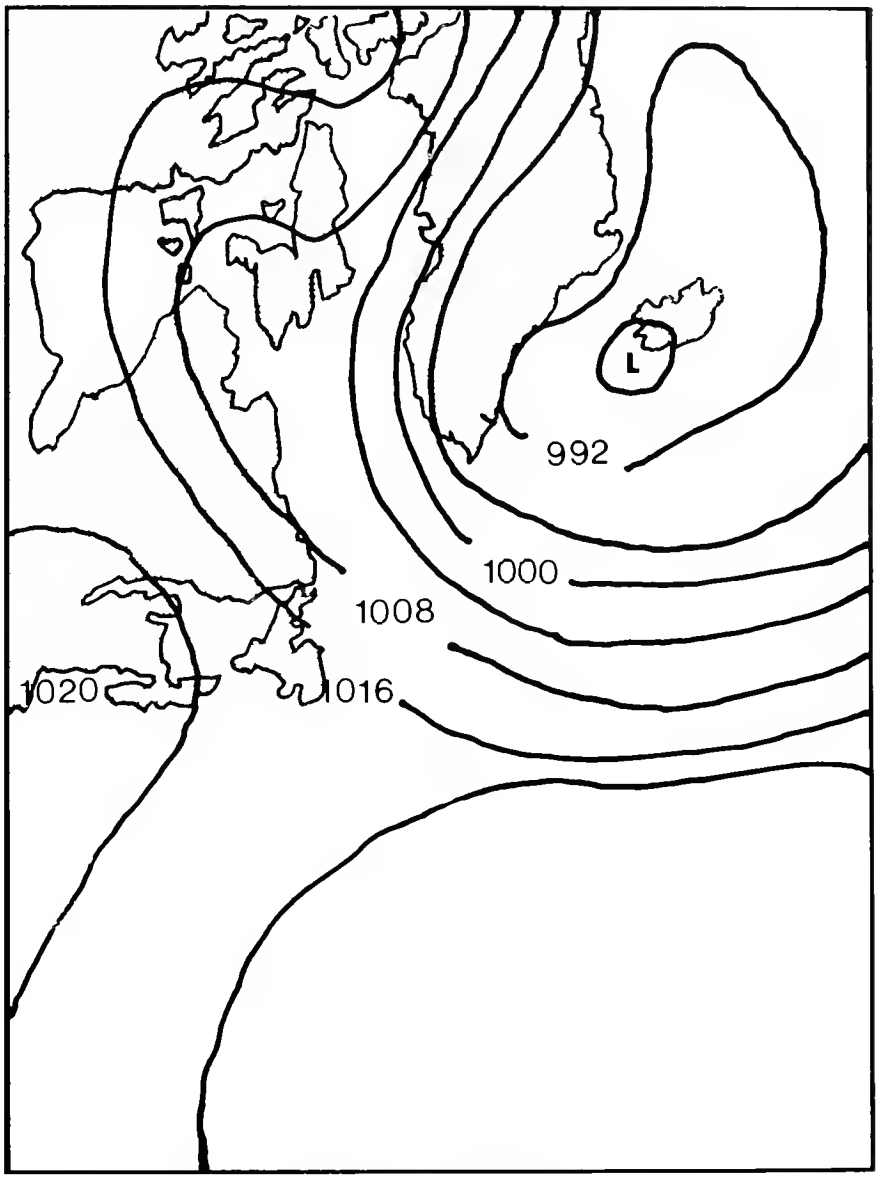

January 1984

Figure 1

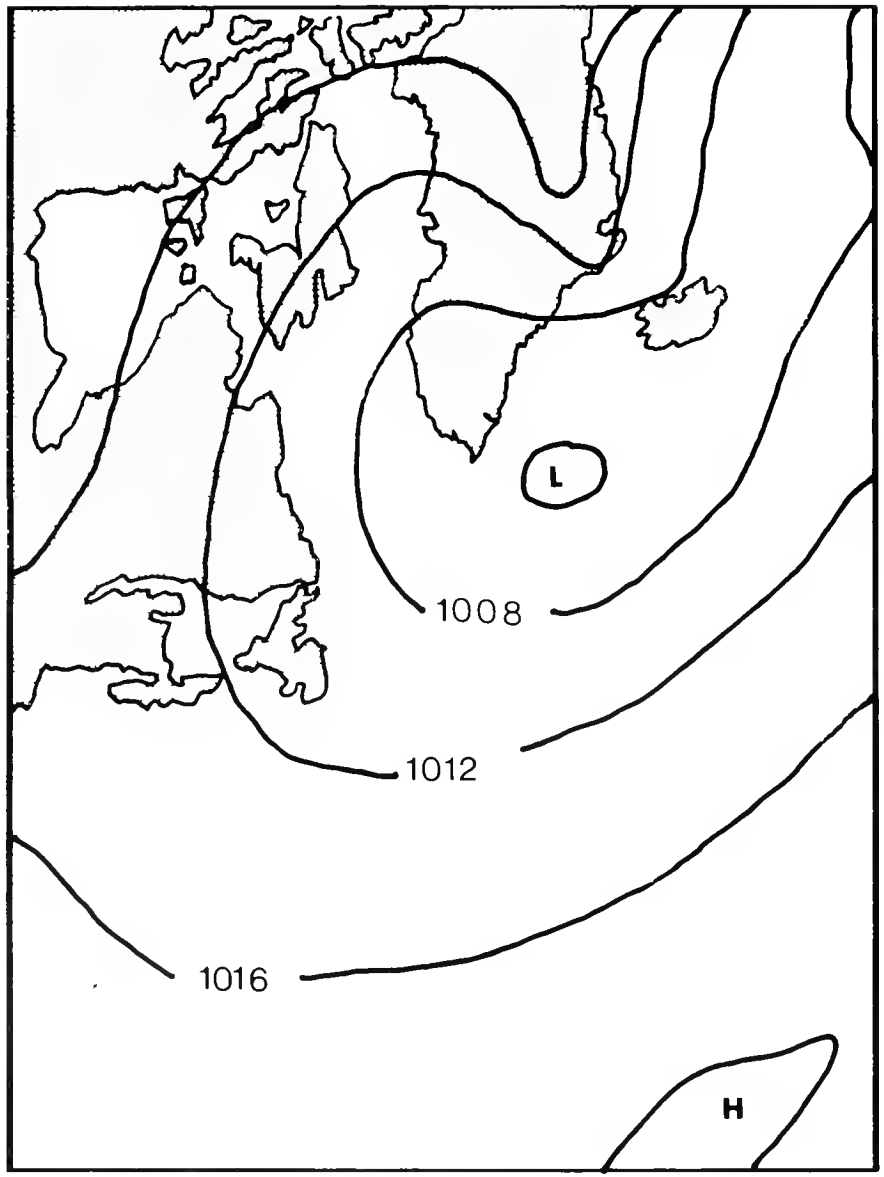

Normal

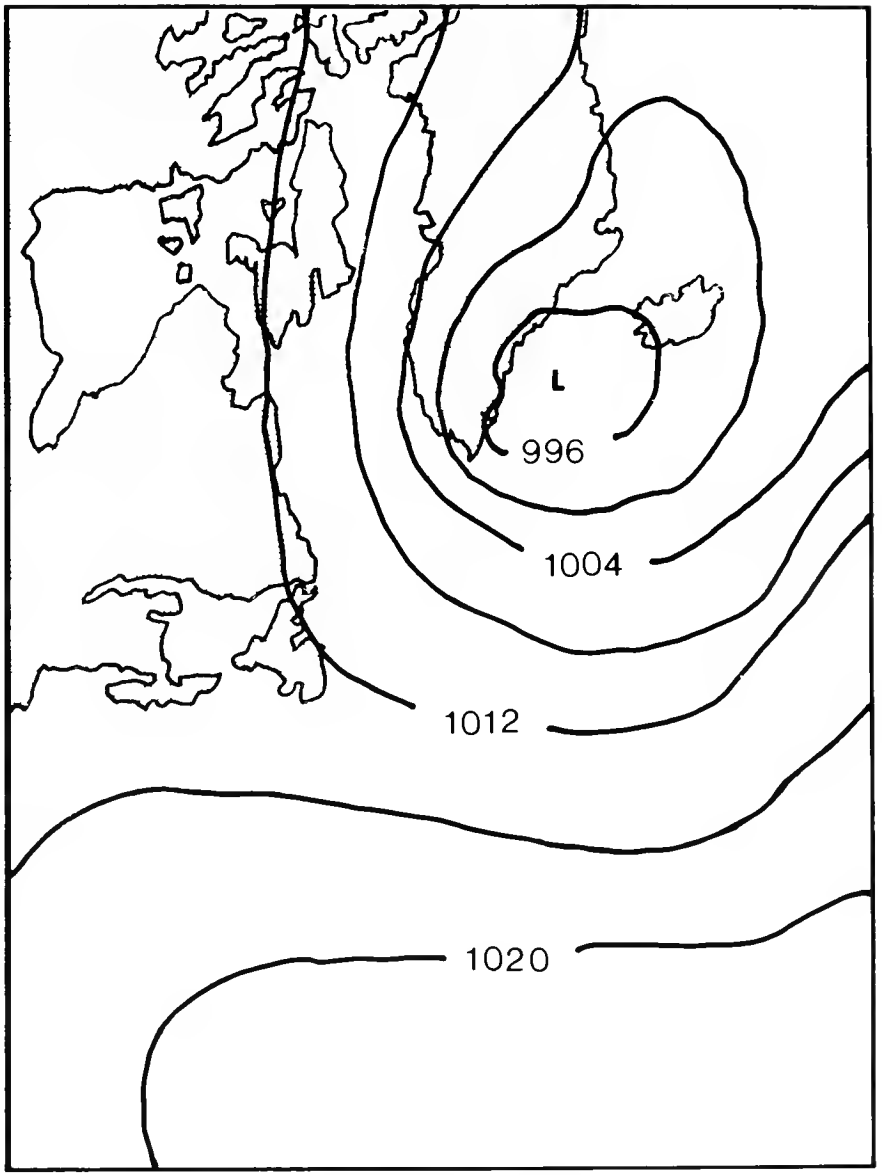

February 1984

Figure 2

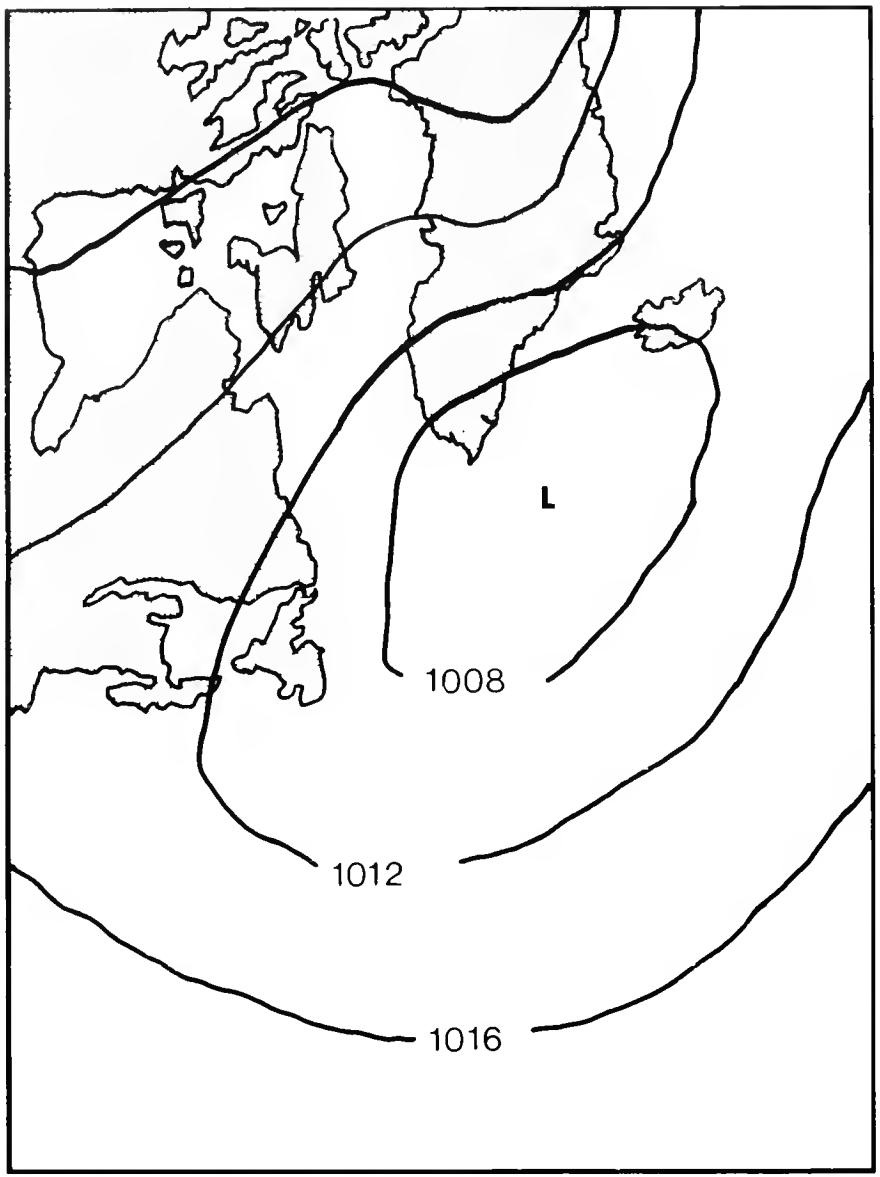

Normal

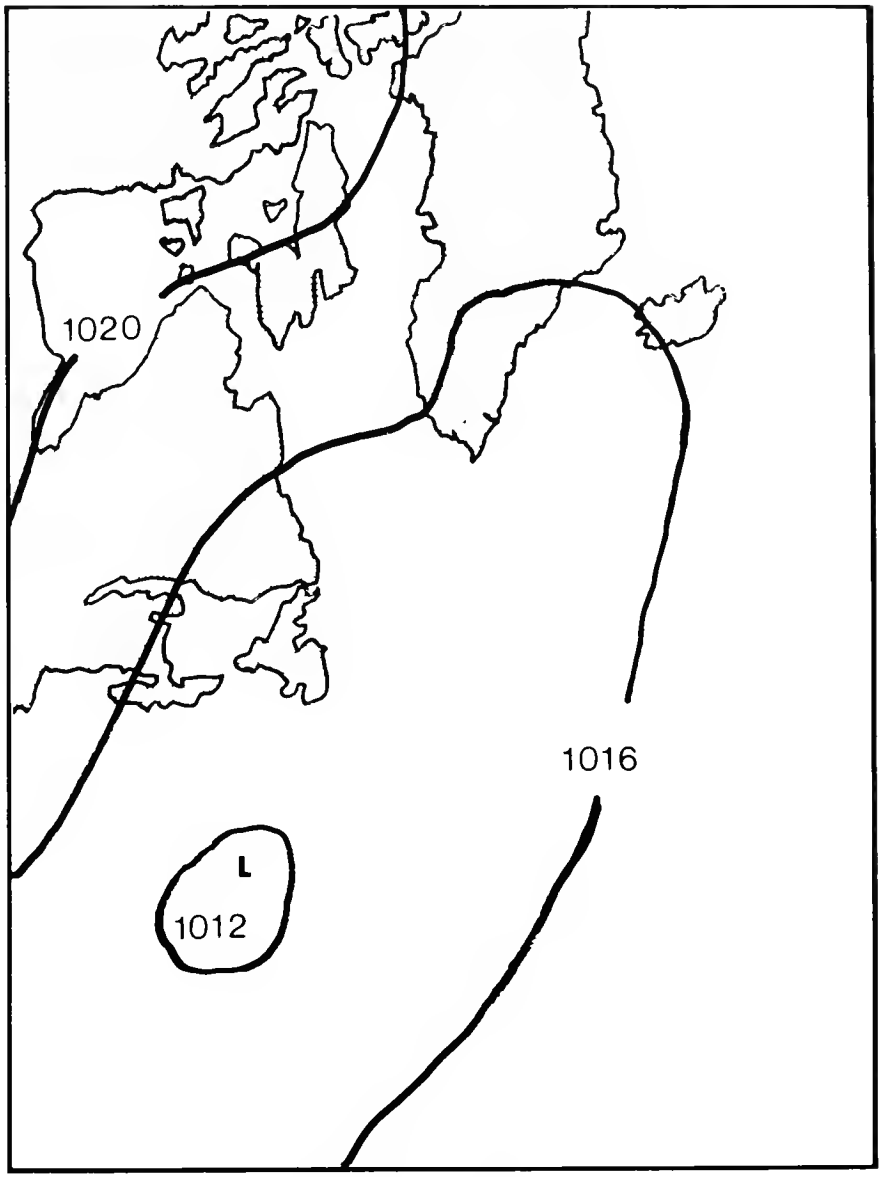

March 1984

Figure 3

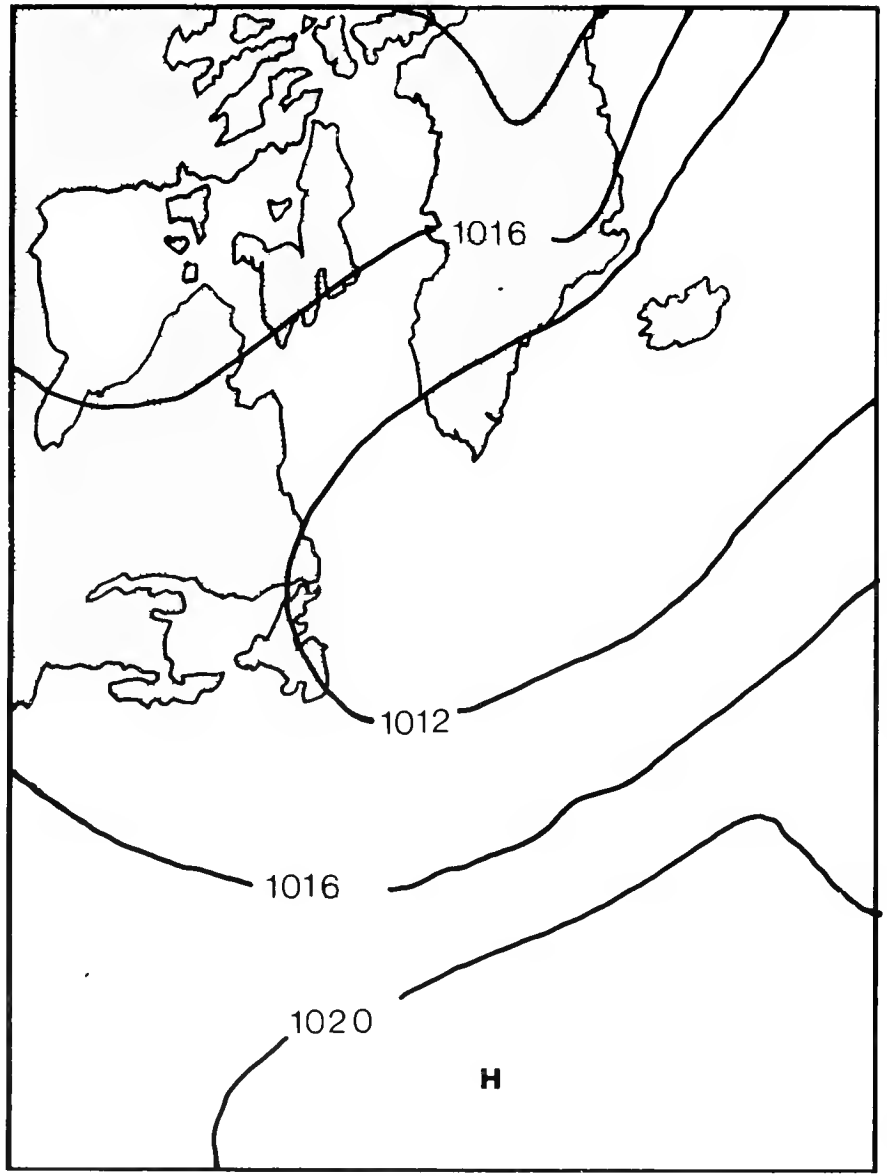

Normal

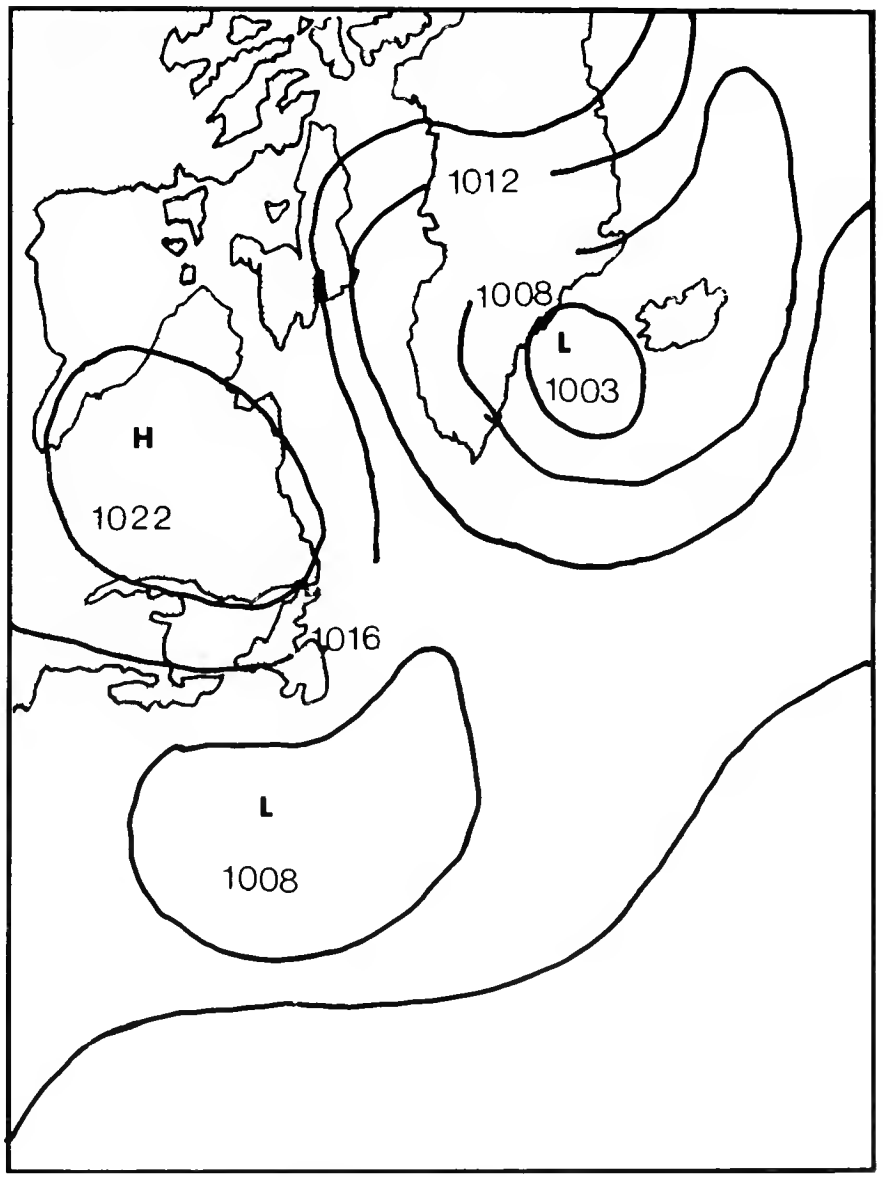

April 1984

Figure 4

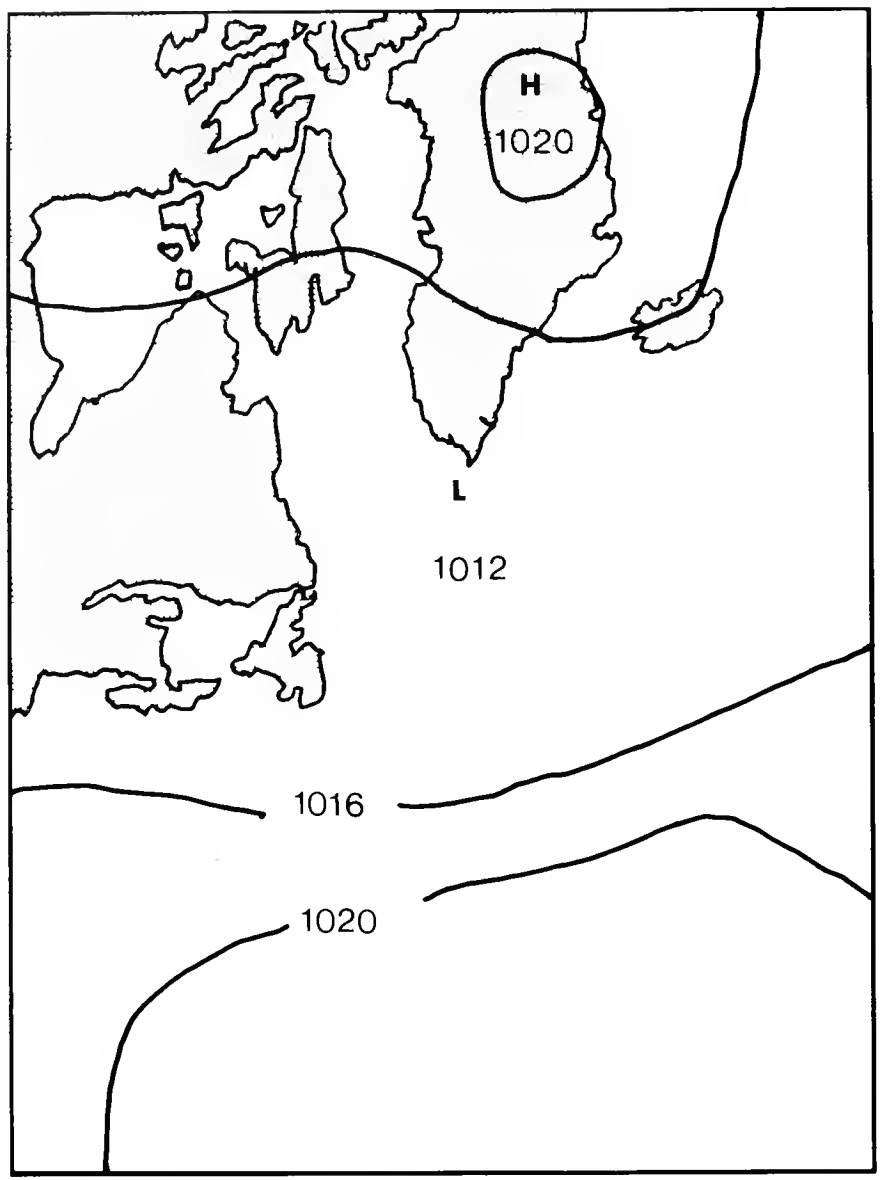

Normal

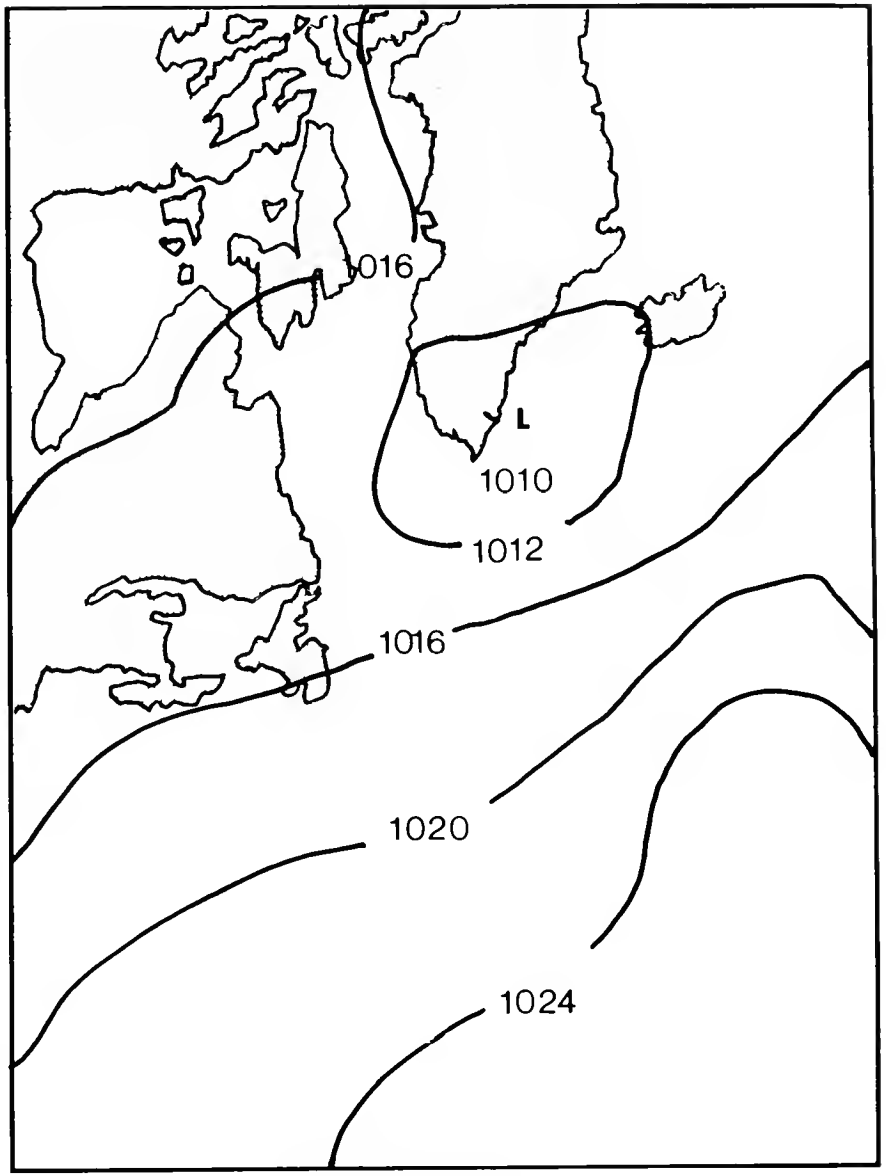

May 1984

Figure 5

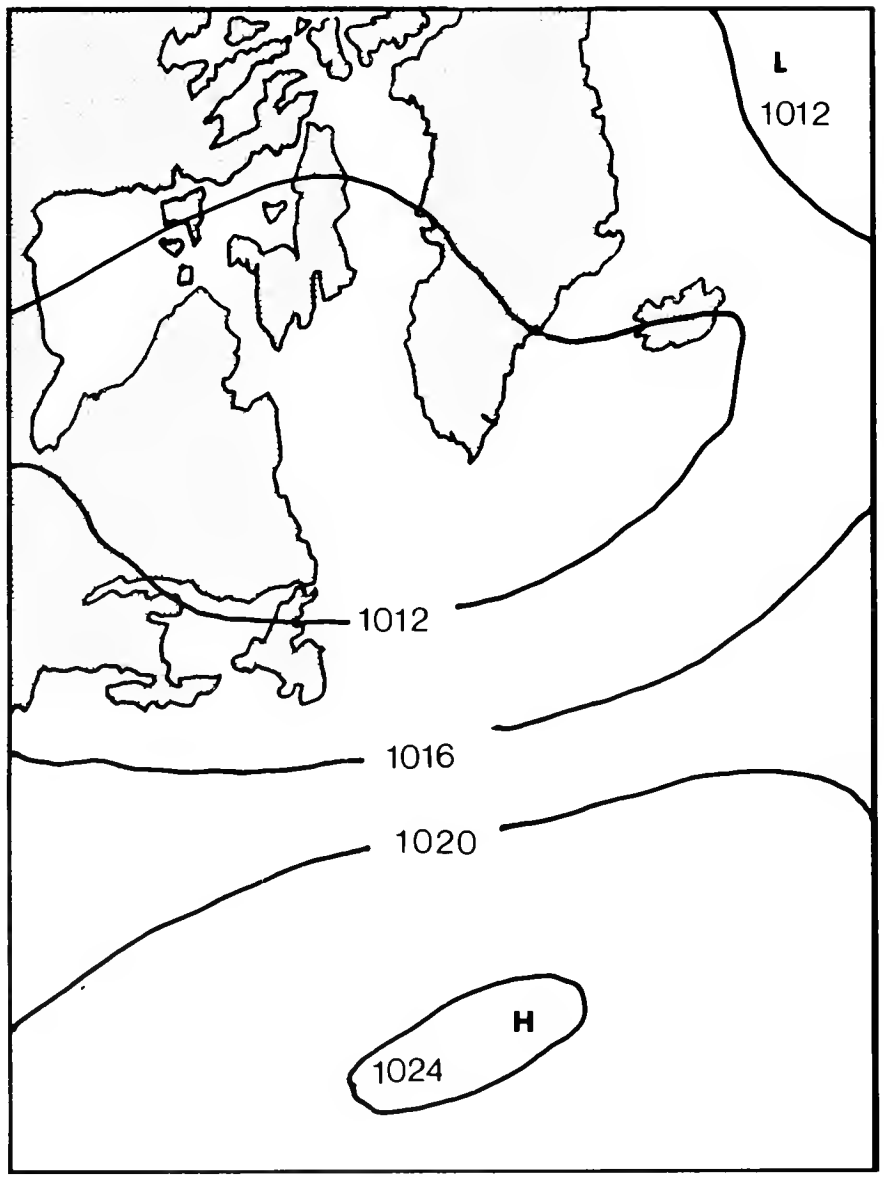

Normal

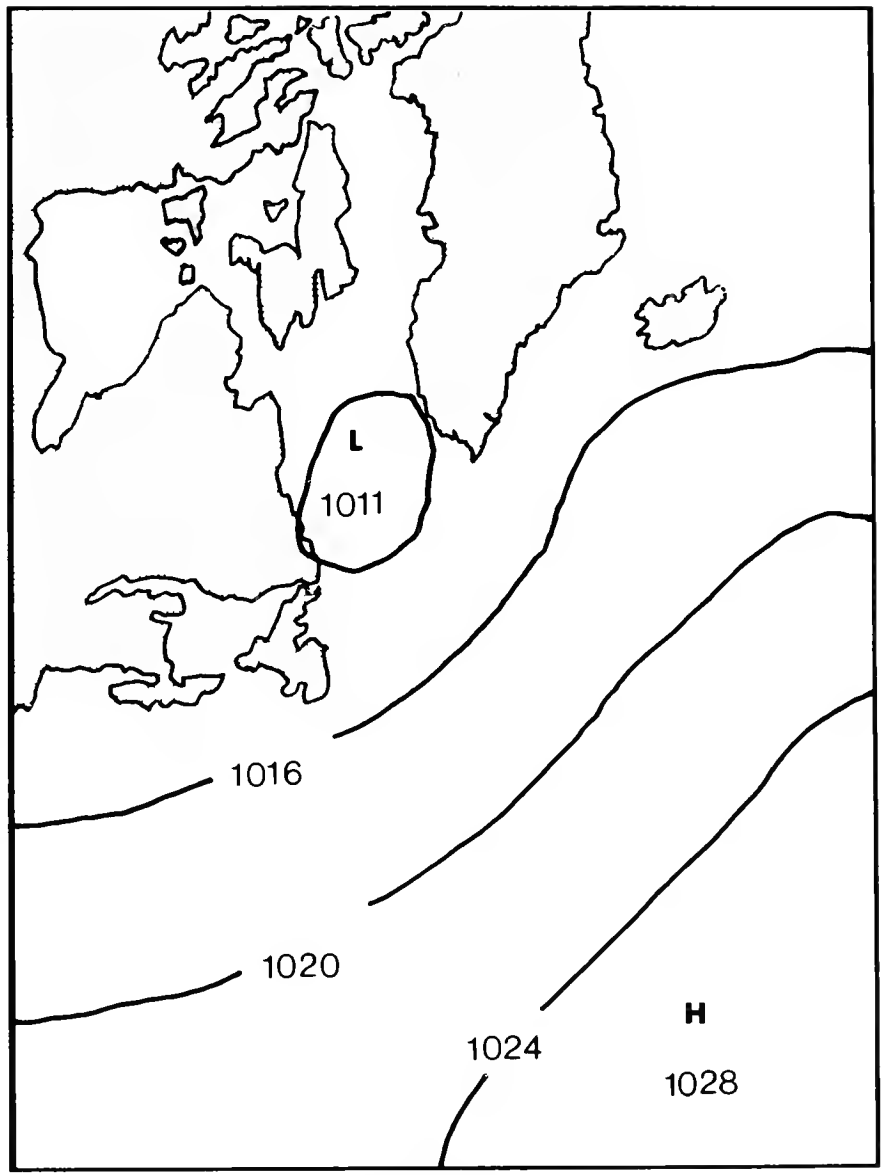

June 1984

Figure 6

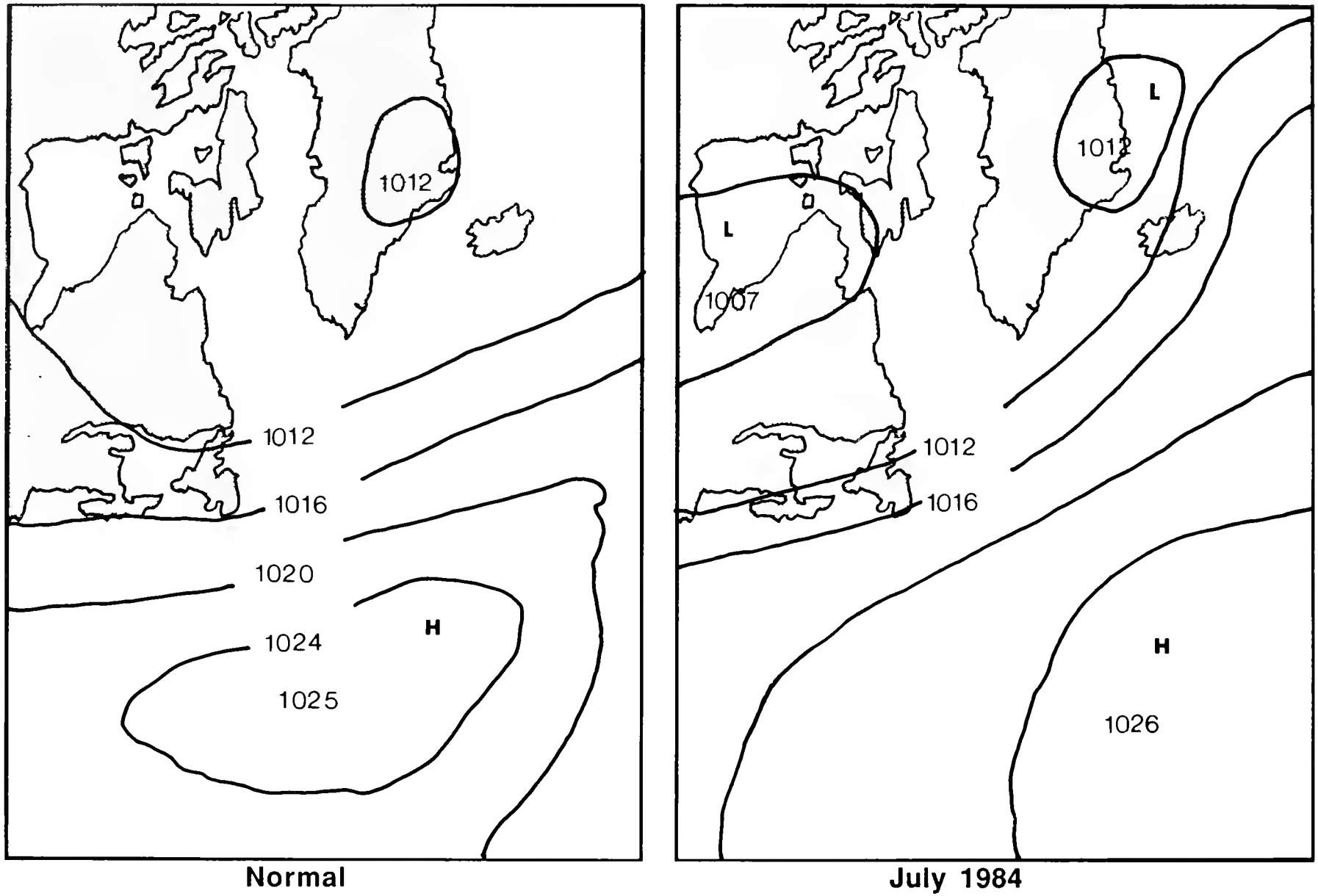
1012
1012
1016
1020
H
1024
1025
Normal
L
1012
L
1007
1012
1016
H
1026
July 1984

Figure 7

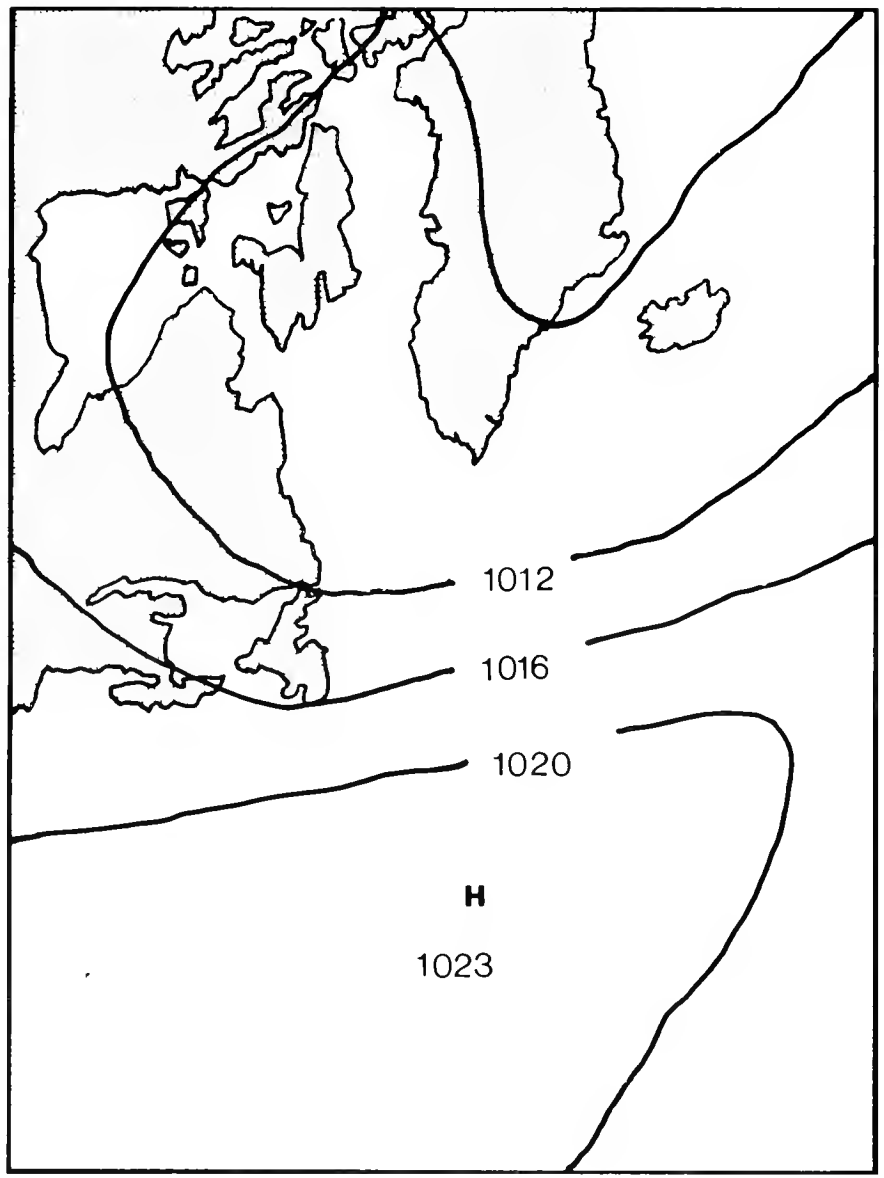

Normal

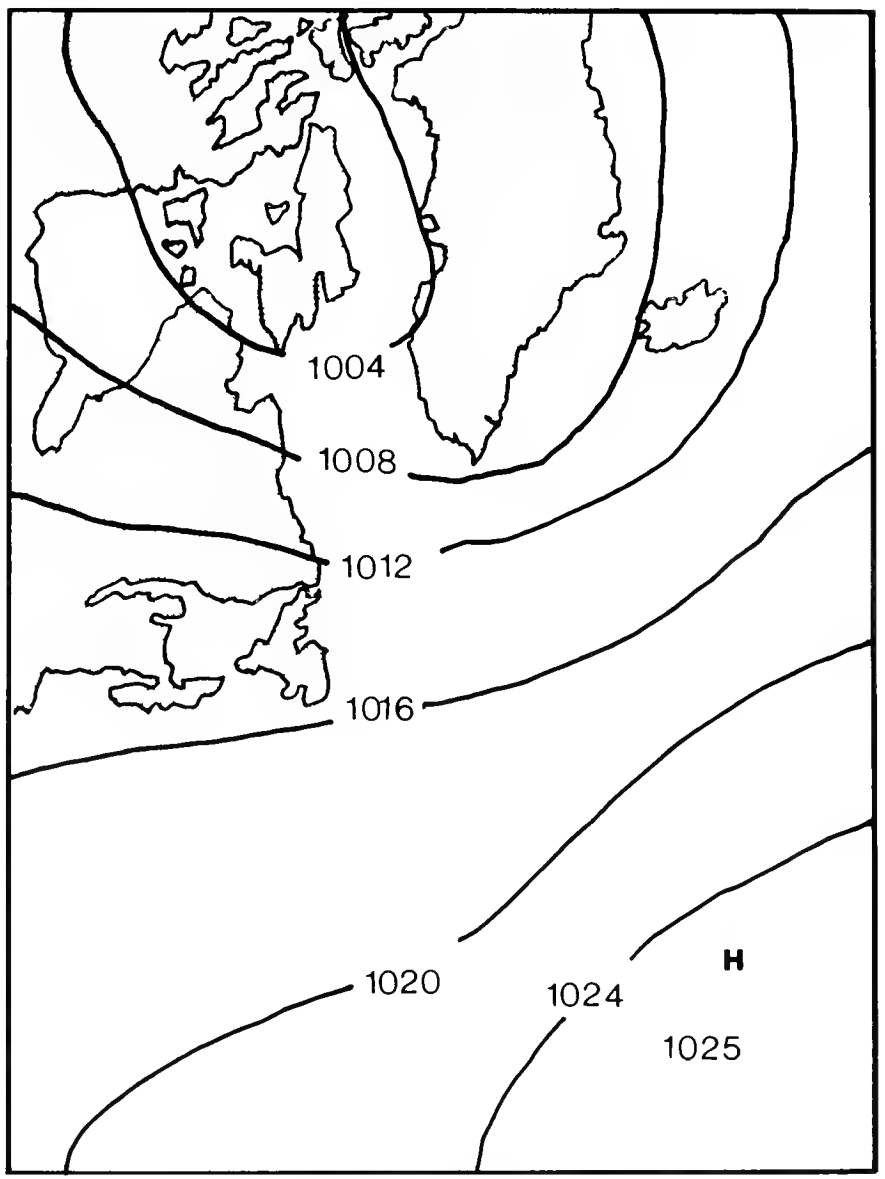

August 1984

Figure 8

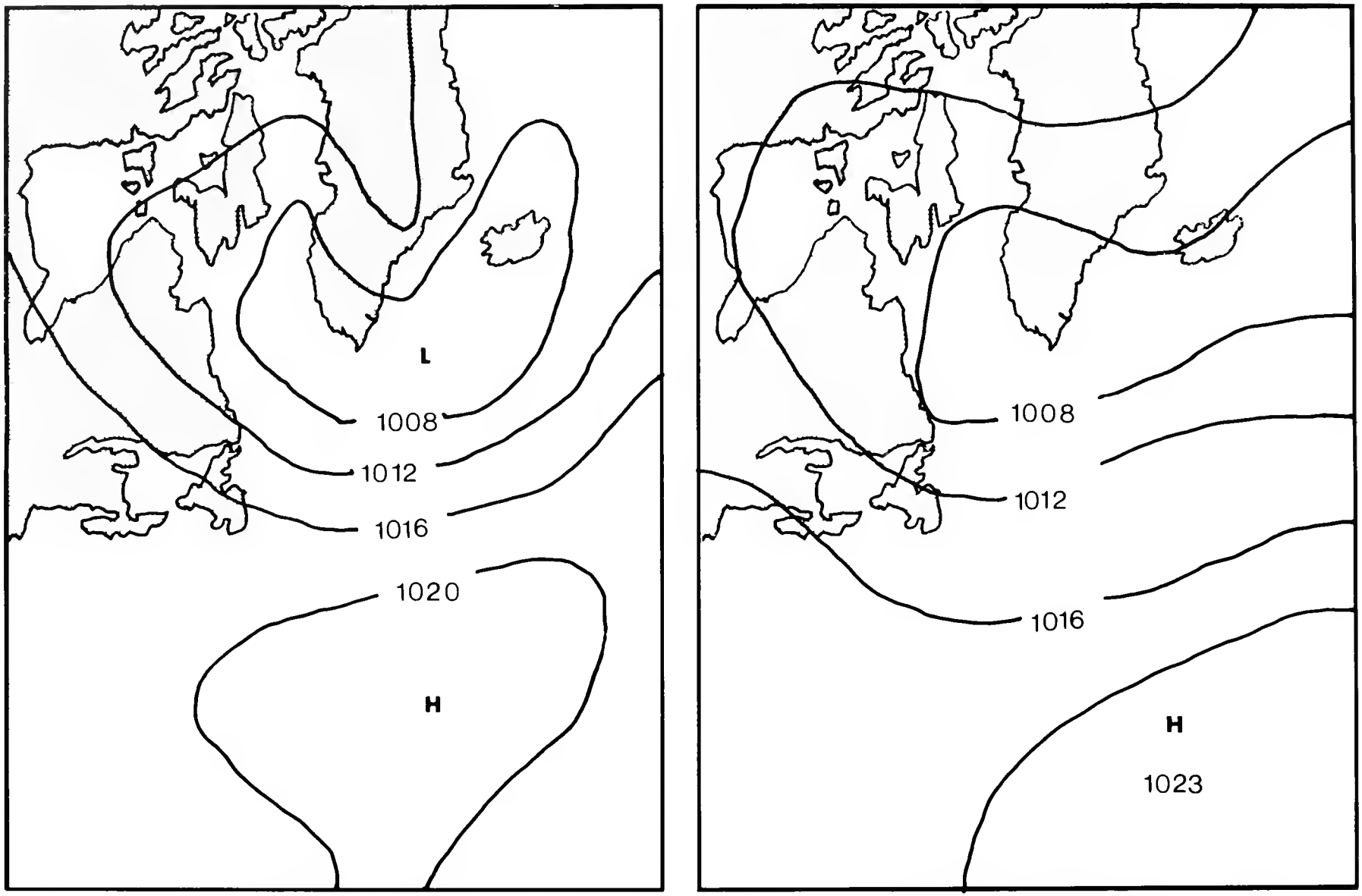
L
1008
1012
1016
1020
H
Normal
1008
1012
1016
H
1023
September 1984

Figure 9

Ice Conditions 1984 Season

October - November 1983: Temperatures were near normal and no sea ice formed south of 58°N during October and November (Figures 10 and 11). By the end of November, Hudson Strait and the mouth of Ungava Bay were closed by sea ice with the southern part of Ungava Bay remaining ice-free. Iceberg sightings south of 52°N reported to International Ice Patrol during October were near the entrance to the Straits of Belle Isle and no sightings were reported south of 52°N during November.

December 1983: Early in the month, sea ice along the coast of Labrador was as far south as Lake Melville. By mid-month (Figure 12), sea ice was approaching, and by the end of the month had closed the Straits of Belle Isle. Seven icebergs were reported to International Ice Patrol south of 52°N during December, all in the vicinity of the Straits of Belle Isle.

January 1984: By mid-month (Figure 13), ice along the coast was south of Cape Bonavista. The Iceland Low was deeper than normal during January, and the distribution of pressure funnelled in cold continental air (Figure 1), causing air temperatures to be well below normal (Table 5). No new iceberg sightings were reported to International Ice Patrol south of 52°N during January.

February 1984: Sea ice was as far south as Cape St. Francis throughout the month with a seaward penetration late in the month over the Grand Banks nearly reaching 46°N (Figure 14). the Iceland Low was again deeper than normal, but pressure patterns allowed warmer marine air to flow over the Maritimes (Figure 2), raising temperatures above normal. The first pre-season International Ice Patrol deployment took place 31 January - 3 February. Reconnaisance flights sighted 50 icebergs south of 52°N, one of which was south of 49°N. The International Ice Patrol received only one ship sighting south of 52°N during February.

March 1984: Sea ice remained near Cape St. Francis throughout the month with heavy coverage over the Grand Banks (Figure 15). Average surface winds during the month were almost opposite the normal pattern (Figure 3), with the easterly and northeasterly flow holding the sea ice and icebergs toward the Newfoundland and Labrador coasts. The second pre-season deployment, 7-13 March, resulted in 54 sightings south of 52°N, 18 of which were south of 48°N. A second deployment was made 21-30 March with the 1984 Ice Patrol season officially opening on 23 March. Figure 22 shows the limits of all known ice south of 48°N. At the end of the month, 156 icebergs were on plot at the International Ice Patrol office in Groton, Connecticut.

April 1984: Sea ice continued to persist along the coast as far south as Cape St. Francis throughout the month (Figure 16). The unusual high pressure system over Labrador in April (Figure 4), coupled with low pressure over Iceland, brought northerly flow into the Maritimes and lower than normal temperatures prevailed (Table 5). Under the influence of northerly winds and retreat of the sea ice westward, April was the heaviest iceberg month with 1043 icebergs sighted, of which 953 passed south of 48°N. The first ICERECDET deployment for the month was extremely busy, reporting large numbers of icebergs daily while participating in both an airborne radar iceberg detection experiment and ice patrols over a two week period. On 15 April 1984, a memorial wreath was dropped at the site of the HMS TITANIC sinking (41°16'N 51°W) to commemorate the nearly 1500 lives lost on 15 April 1912. At the end of the month, 156 icebergs were on plot at the International Ice Patrol.

May 1984: Sea ice in Davis Strait retreated to the west under the warm air temperatures of May, and at the same time receded northward along the the east coast of Greenland (Figure 17). In contrast, near normal weather conditions resulted in a light westerly flow over the Newfoundland and Labrador coasts that did little to affect sea ice, which remained as far south as Cape St. Francis throughout the month. In May, 1037 icebergs were sighted, of which 484 passed south of 48°N. At the end of the month, 198

Table 6. Explanation of Sea Ice Symbology used in Figures 10-21

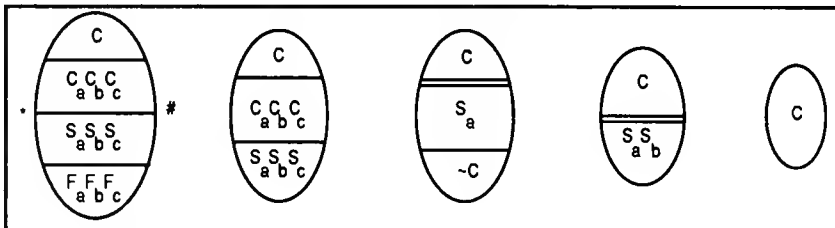

C = Total ice concentration in the area in tenths.

$C_a C_b C_c$ = Concentration of thickest (C_a), 2nd thickest (C_b), and 3rd thickest (C_c).

$S_a S_b S_c$ = Stage of development of thickest (S_a), 2nd thickest (S_b), and 3rd thickest (S_c).

~C = Concentration of ice within areas of strips and patches.

$F_a F_b F_c$ = Floe size of thickest (F_a), 2nd thickest (F_b), and 3rd thickest (F_c).

Stage of Development		Floe Sizes	
0	No stage of development	0	Pancake ice
1	New ice	1	Brash, small ice cake
2	Nilas, ice rind	2	Ice cake
3	Young ice	3	Small floe
4	Grey ice	4	Medium floe
5	Grey-white ice	5	Big floe
6	First-year ice	6	Vast floe
7	Thin first-year ice	7	Giant floe
8	Thin first-year ice, 30-50 cm	8	Growlers and floebergs
9	Thin first-year ice, 50-70 cm	9	Icebergs
1·	Medium first-year ice	/	Undetermined or unknown
4·	Thick first-year ice		
7·	Old ice		
8·	Second-year ice		
9·	Multi-year ice		
▲	Icebergs		
•	A trace of ice thicker than S_a		
#	Fourth type, if $C_a C_b C_c$ do not add up to C		

icebergs were on plot at the International Ice Patrol. Icebergs on plot at the International Ice Patrol were widely distributed by mid-month and a second two-week ICERECDET was conducted. By month's end, several drifted outside the Ice Patrol area (west of 57°W longitude) and others extended the southernmost limits south of 40°N latitude (Figure 27).

June 1984: As seen in Table 5, June was colder than normal and sea ice remained in the western part of Davis Strait and off the Straits of Belle Isle (Figure 18). The number of icebergs on plot decreased during June, although the limits of all known ice remained well to the south and east, held there by widely scattered icebergs (Figures 28 and 29). The southernmost iceberg on plot for the season came on 6 June at 40°01'N 45°51'W. There were 555 icebergs sighted in June, of which 227 drifted south of 48°N and several of these drifted outside the Ice Patrol area (east of 39°W or west of 57°W longitude). At the end of the month, 149 were on the International Ice Patrol plot and widely scattered.

July 1984: Under the influence of warm but near-normal weather during July, the sea ice retreated north of 54°N by mid-month. Although the number of icebergs on plot at the International Ice Patrol decreased throughout the month, the limits of all known ice continued to be much farther south and east than normal due to widely scattered icebergs at the limits (Figures 30 and 31). Of the 975 icebergs sighted and reported to the International Ice Patrol in July, 335 passed south of 48°N. Both numbers are greater than those of June, with the increase due to the release of icebergs by the retreating ice pack.

August 1984: With air temperatures somewhat above normal, sea ice continued to retreat in August (Figure 20). Increasing sea surface temperatures accelerated iceberg melt and caused the limits of all known ice to move north (Figures 32 and 33). Of the 251 icebergs sighted in August, 93 passed south of 48°N and 46 remained on plot at the end of the month.

September 1984: Sea ice continued to retreat rapidly, and by 18 September had disappeared from Davis and Hudson Straits (Figure 21) and completely melted in Baffin Bay to conclude this ice year. By the end of the 1984 International Ice Patrol season on 7 September, 124 icebergs had been sighted in September with only 9 drifting south of 48°N and 24 remaining on plot at the end of the season (Figure 34).

Figure 10

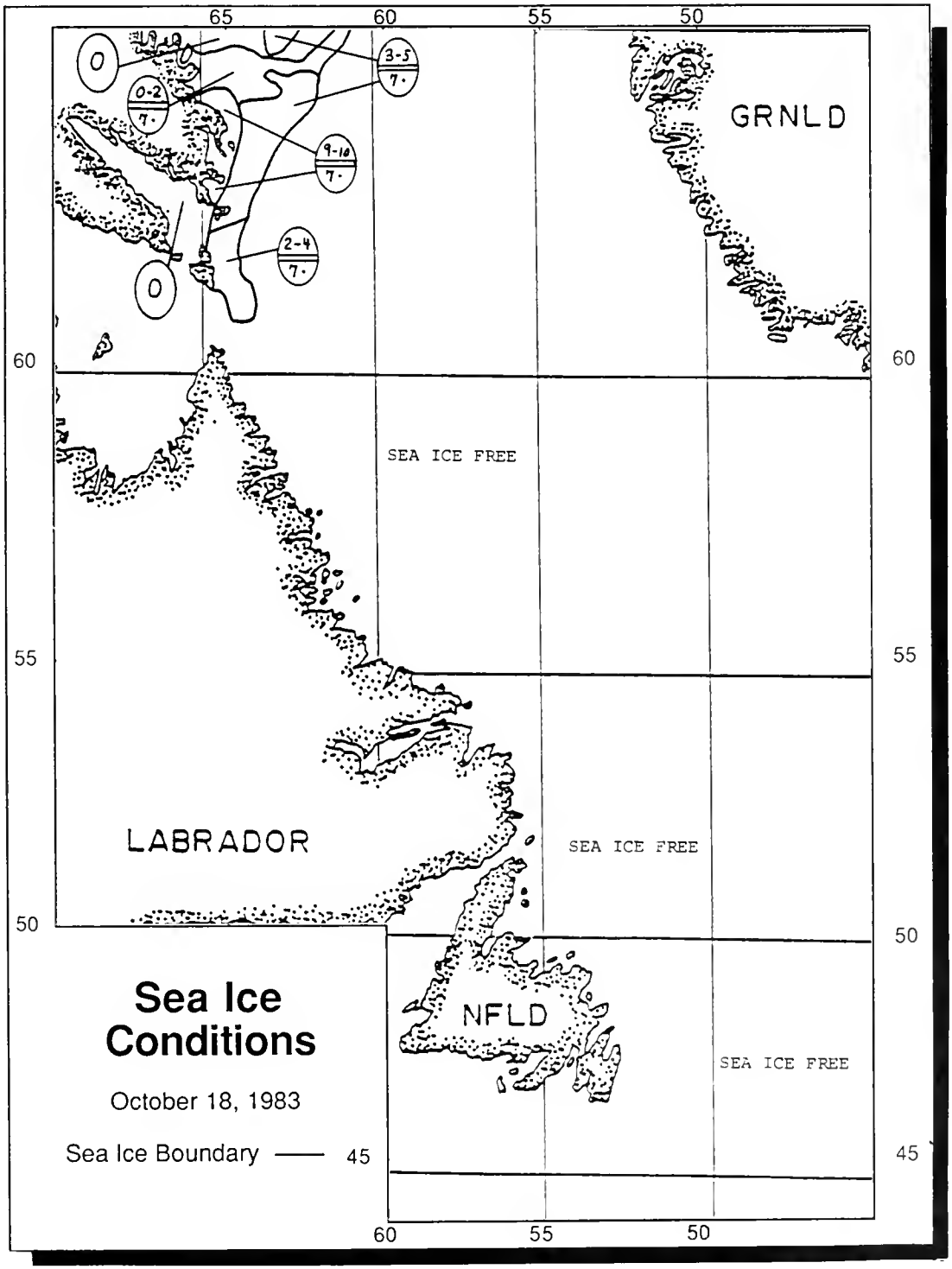
65
60
55
50
0
0-2
7·
3-5
7·
9-10
7·
2-4
7·
0
GRNLD
60
SEA ICE FREE
55
LABRADOR
SEA ICE FREE
50
NFLD
SEA ICE FREE
45
Sea Ice Conditions
October 18, 1983
Sea Ice Boundary —— 45

Figure 11

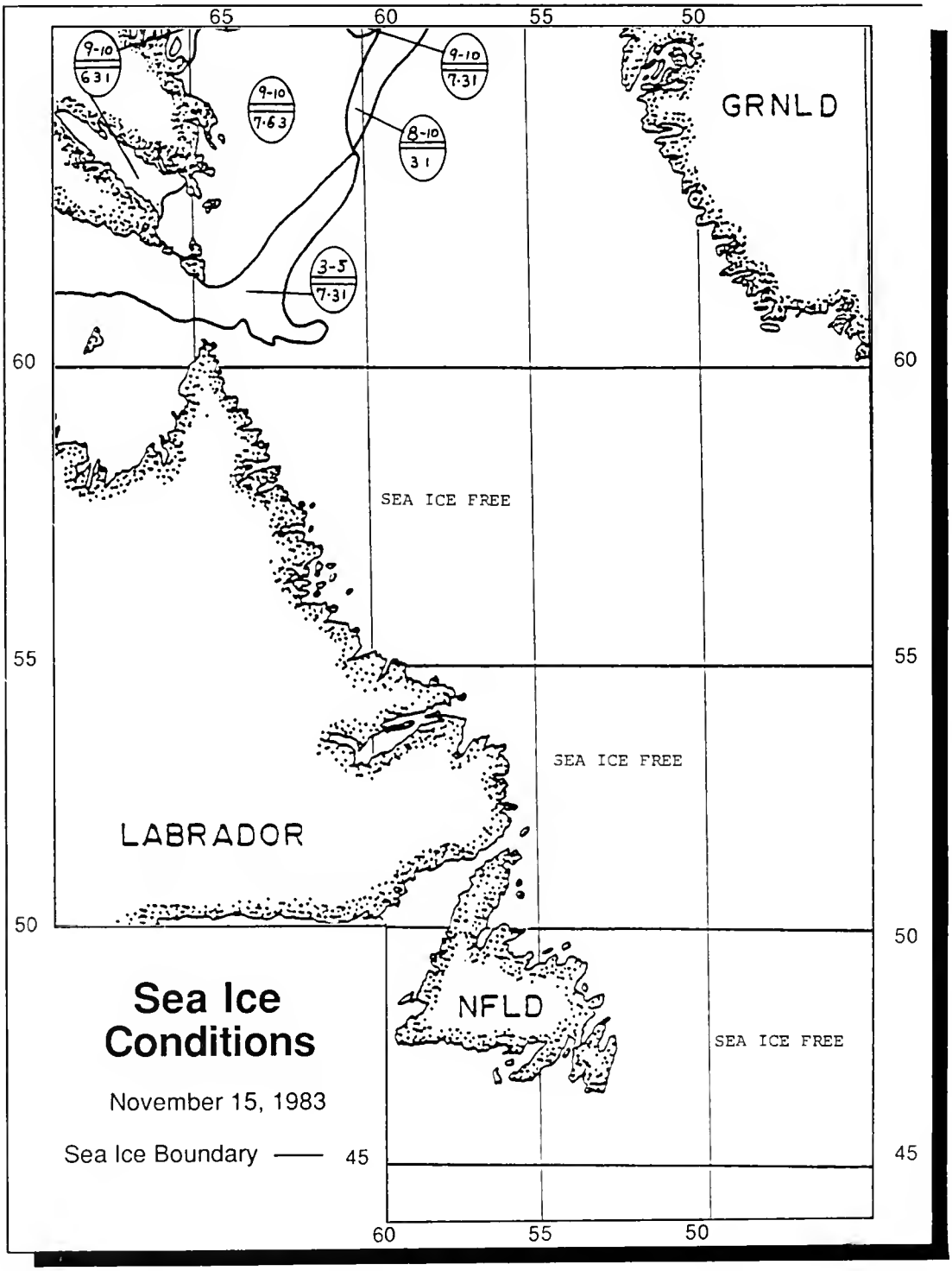
65
60
55
50
9-10
6 3 1
9-10
7·63
9-10
7·31
8-10
3 1
3-5
7·31
GRNLD
60
SEA ICE FREE
55
SEA ICE FREE
LABRADOR
50
NFLD
SEA ICE FREE
45
Sea Ice Conditions
November 15, 1983
Sea Ice Boundary —— 45
60
55
50

Figure 12

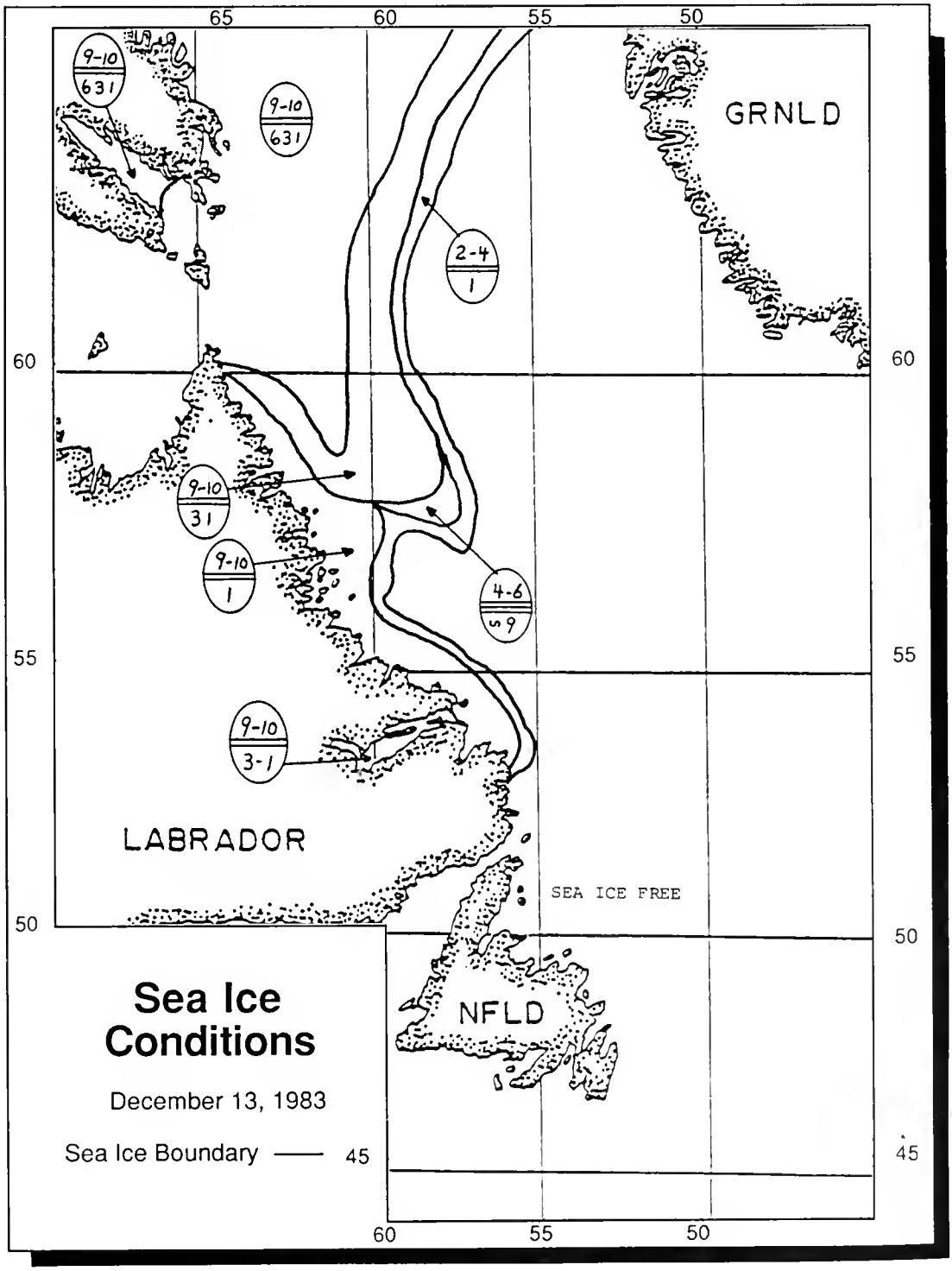
65
60
55
50
9-10
631
9-10
631
GRNLD
2-4
1
60
60
9-10
31
9-10
1
4-6
s 9
55
55
9-10
3-1
LABRADOR
SEA ICE FREE
50
50
NFLD
Sea Ice
Conditions
December 13, 1983
Sea Ice Boundary
45
45
60
55
50

Figure 13

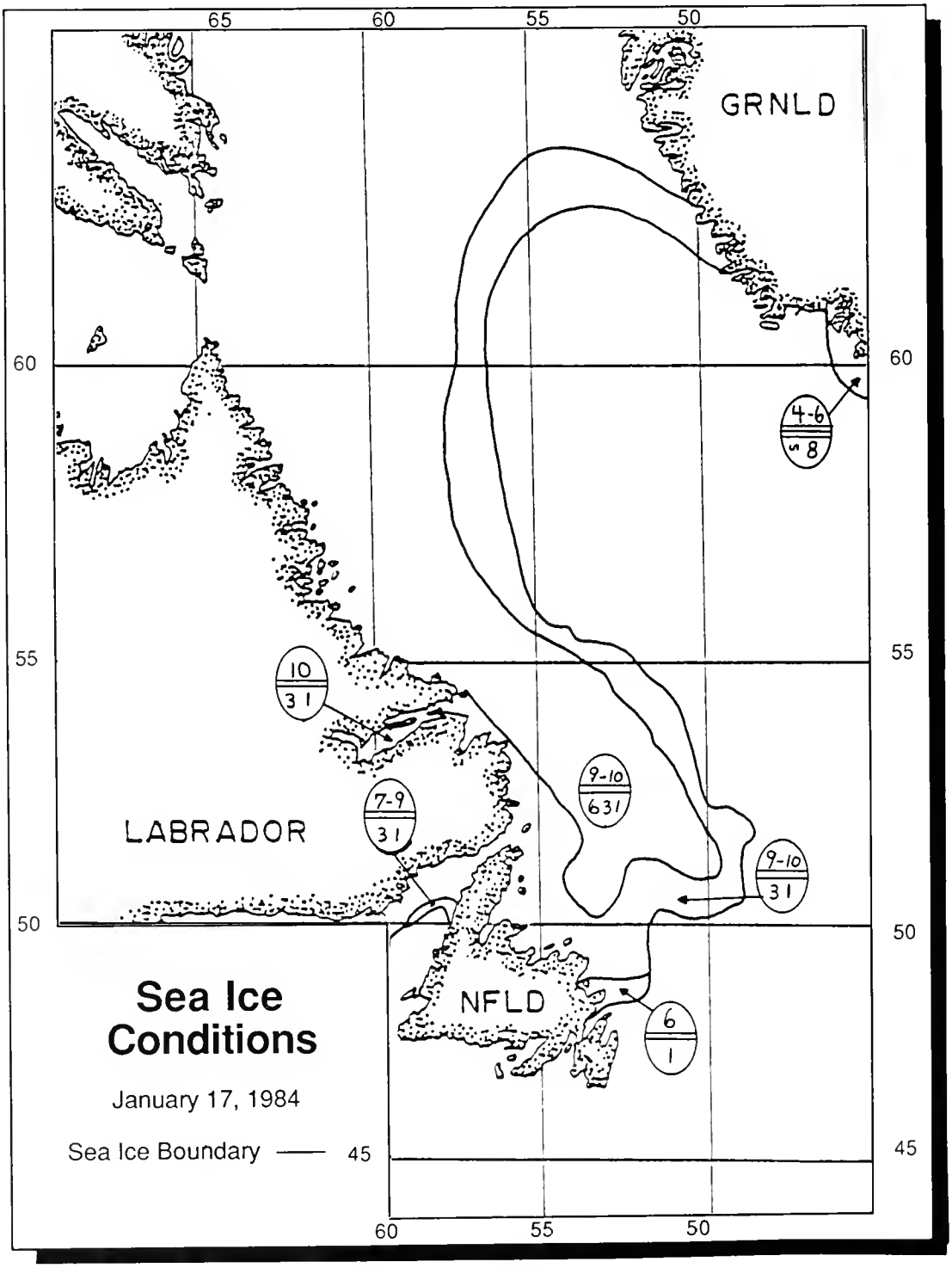
65
60
55
50
GRNLD
60
55
50
45
4-6
8
10
31
7-9
31
9-10
631
9-10
31
LABRADOR
NFLD
6
1
Sea Ice Conditions
January 17, 1984
Sea Ice Boundary —— 45

Figure 14

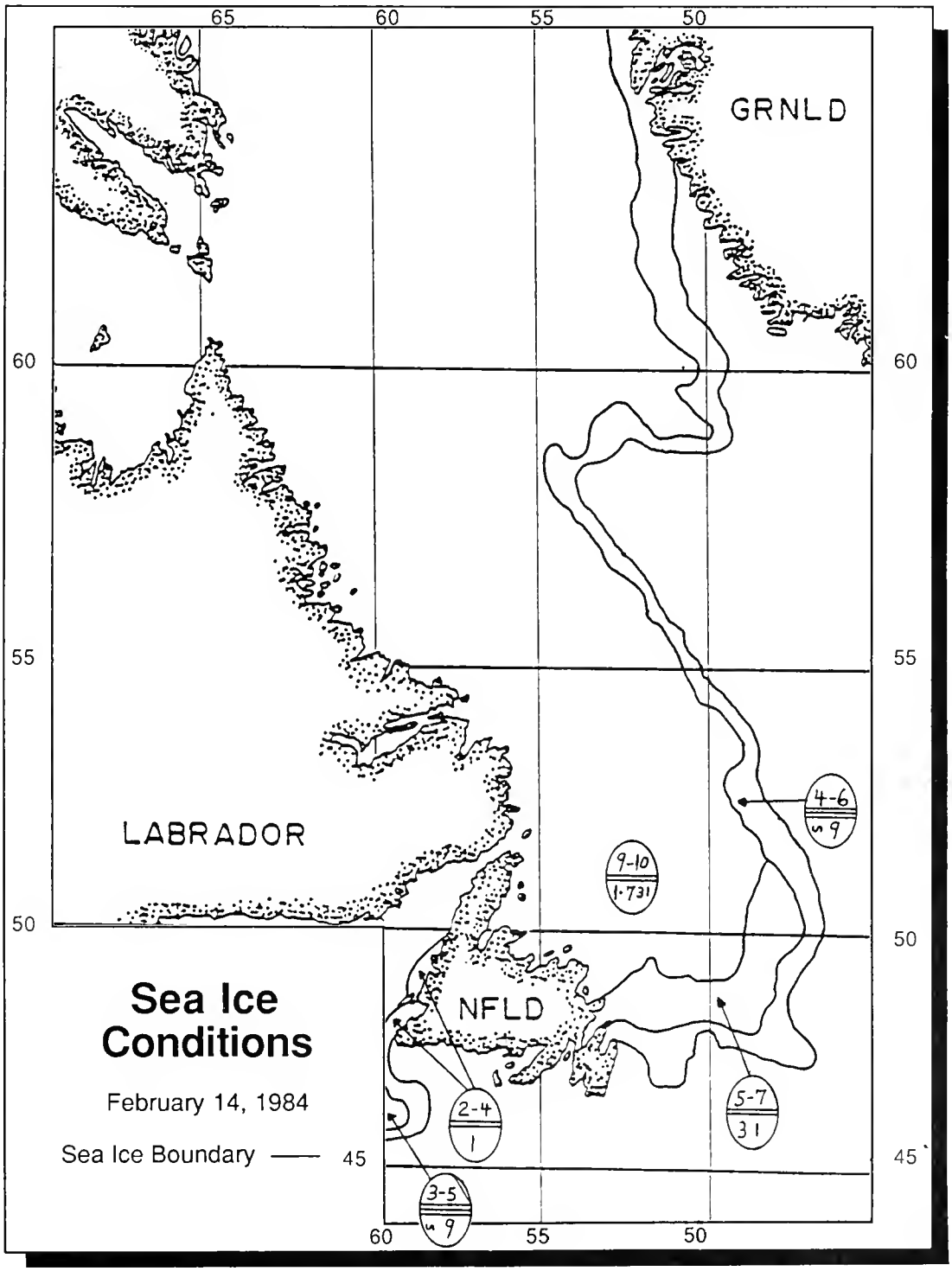
65
60
55
50
GRNLD
60
55
50
45
LABRADOR
NFLD
4-6
s 9
9-10
1·731
2-4
1
5-7
31
3-5
s 9
Sea Ice Conditions
February 14, 1984
Sea Ice Boundary

Figure 15

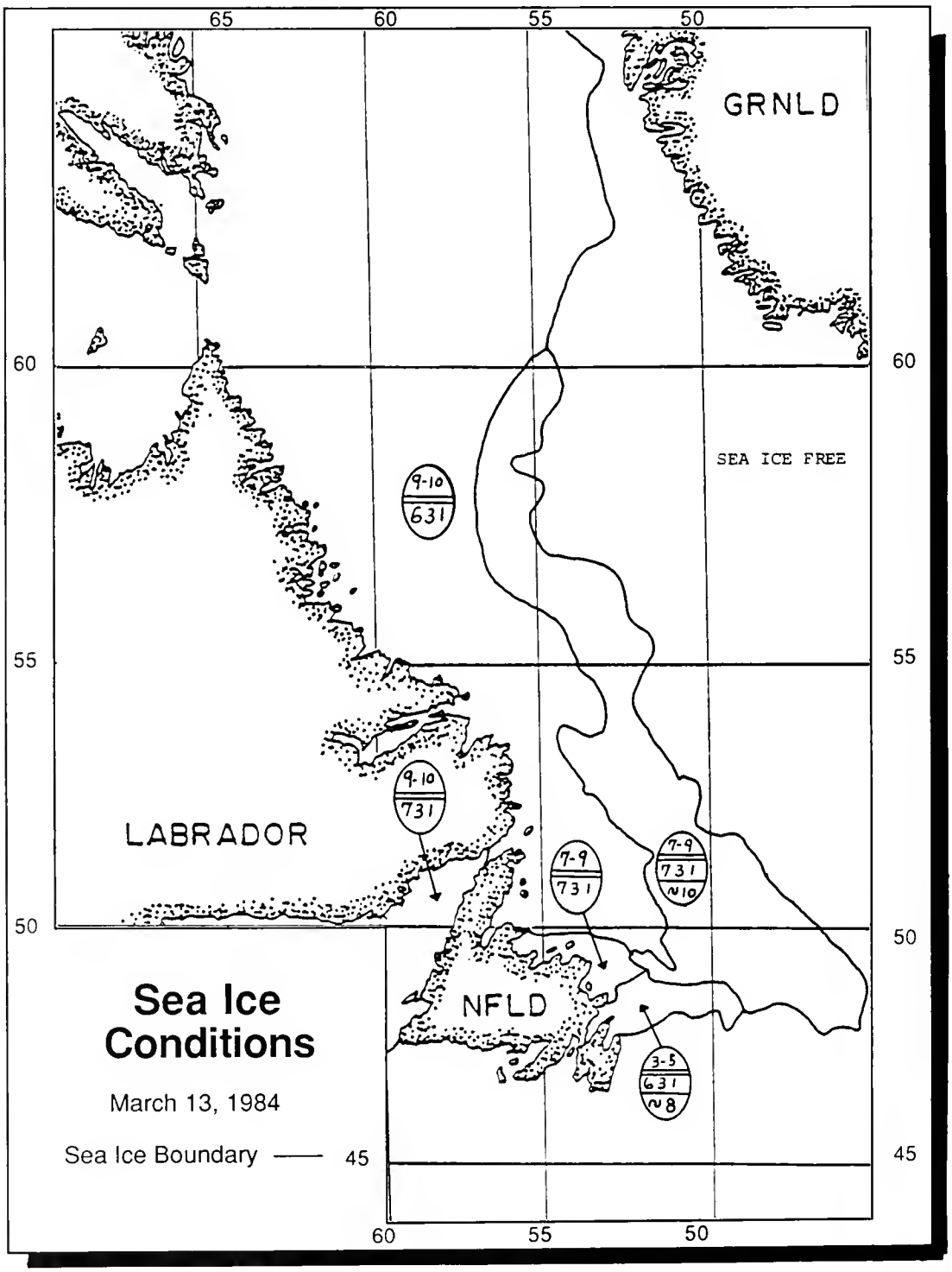
65
60
55
50
GRNLD
60
SEA ICE FREE
9-10
631
55
9-10
731
LABRADOR
7-9
731
7-9
731
N10
50
NFLD
3-5
631
N8
45
Sea Ice
Conditions
March 13, 1984
Sea Ice Boundary
45
60
55
50

Figure 16

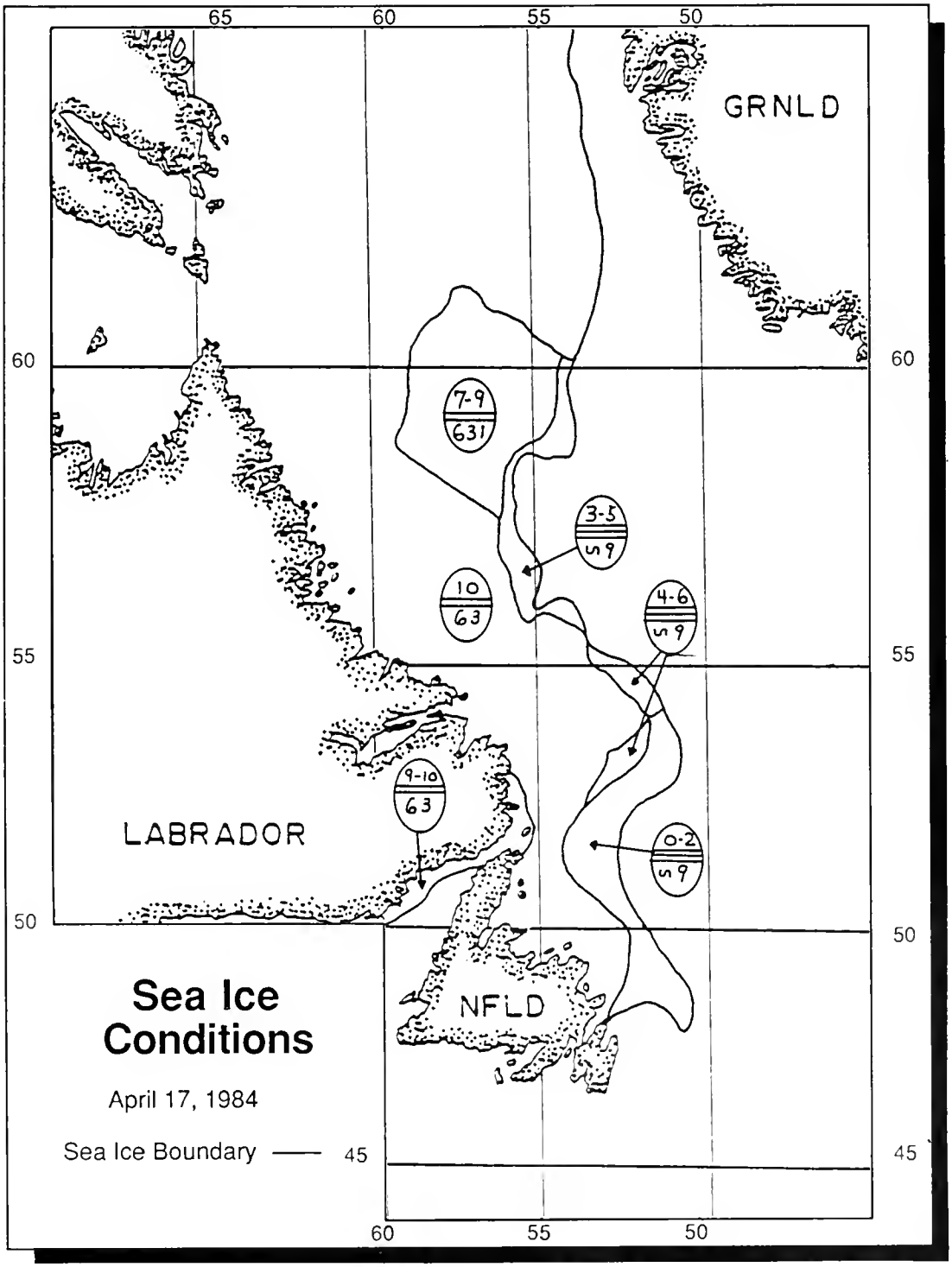
65
60
55
50
GRNLD
60
7-9
631
3-5
9
10
63
4-6
9
55
9-10
63
LABRADOR
0-2
9
50
NFLD
Sea Ice
Conditions
April 17, 1984
Sea Ice Boundary
45
60
55
50

Figure 17

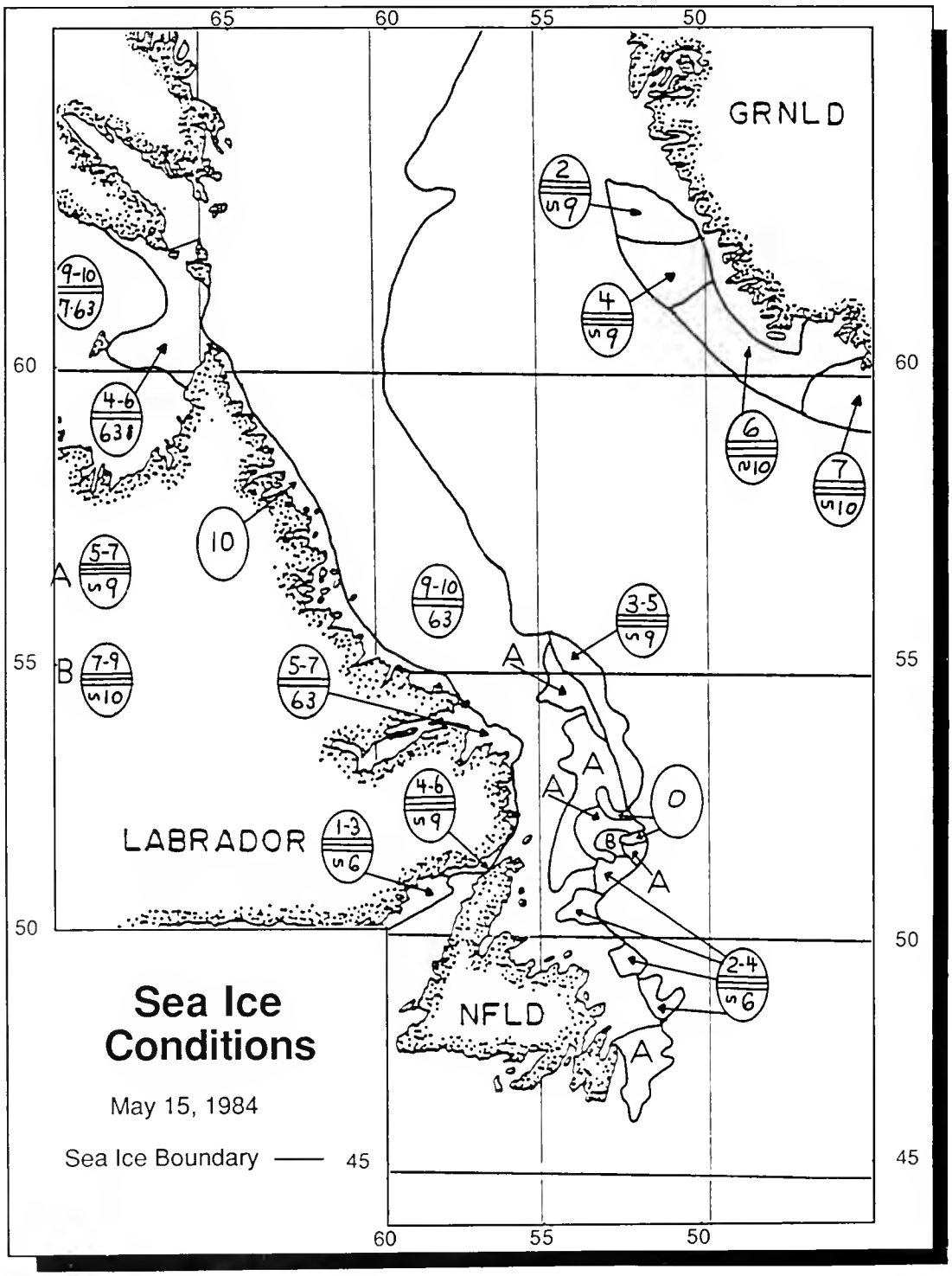
65
60
55
50
GRNLD
LABRADOR
NFLD
60
55
50
45
Sea Ice Conditions
May 15, 1984
Sea Ice Boundary
9-10 / 7-63
4-6 / 63
5-7 / S9
A
B
7-9 / S10
10
5-7 / 63
9-10 / 63
4-6 / S9
1-3 / S6
2 / S9
4 / S9
6 / S10
7 / S10
3-5 / S9
A
A
A
O
B
A
2-4 / S6
A

Figure 18

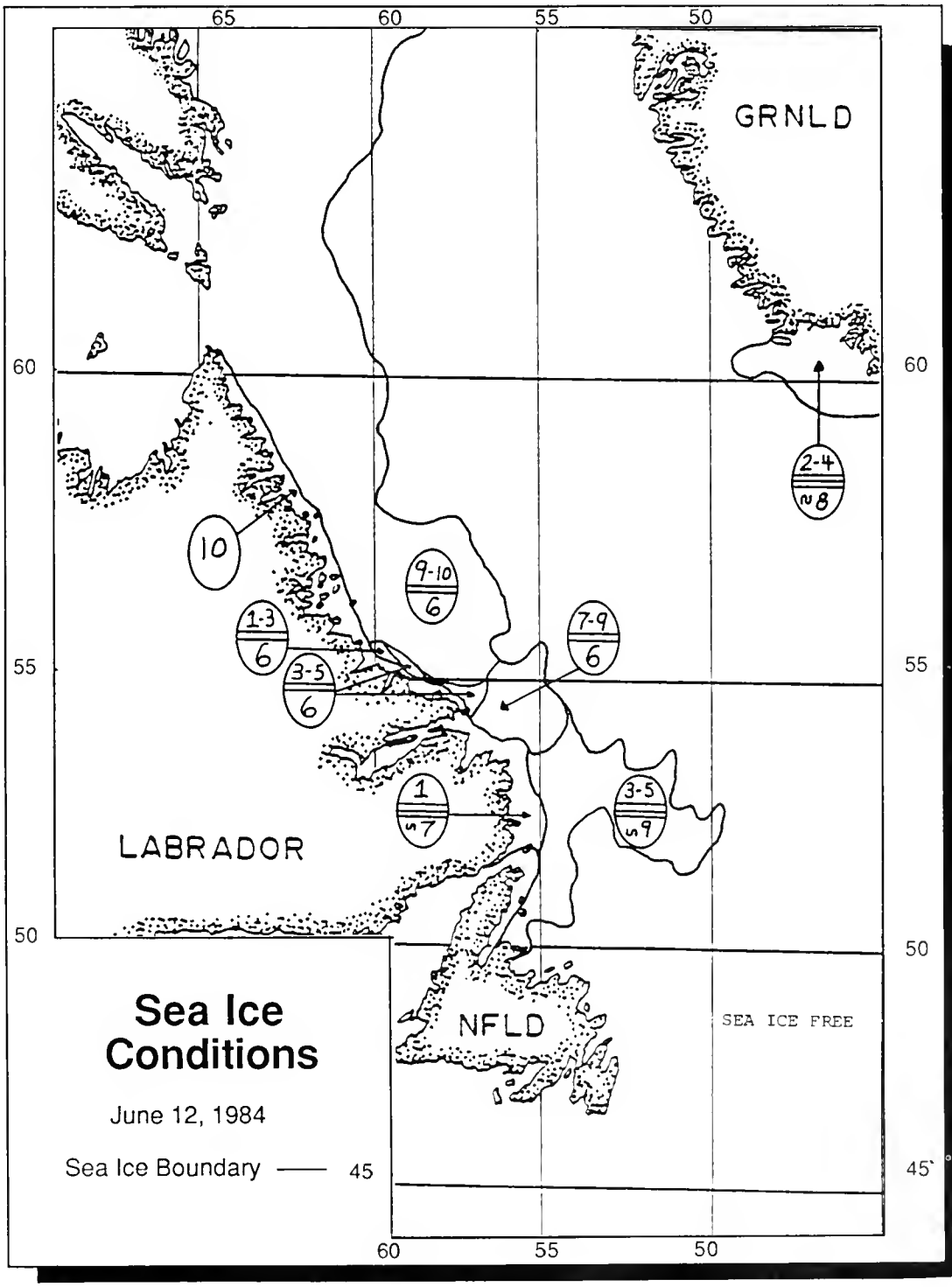
65
60
55
50
GRNLD
60
55
50
45
LABRADOR
NFLD
SEA ICE FREE
10
1-3
6
3-5
6
9-10
6
7-9
6
2-4
≈8
1
≈7
3-5
≈9
Sea Ice Conditions
June 12, 1984
Sea Ice Boundary —— 45

Figure 19

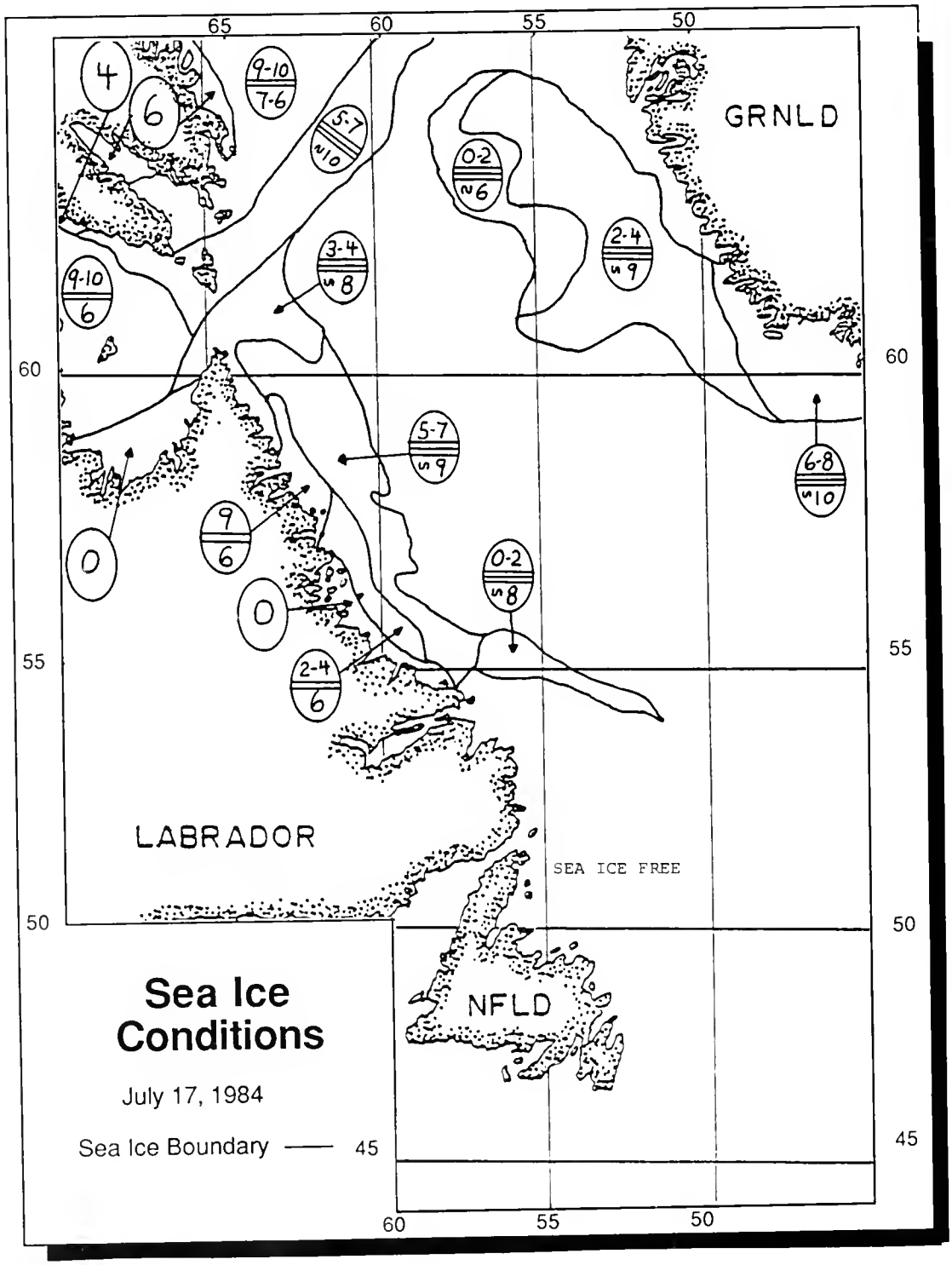
65
60
55
50
GRNLD
LABRADOR
SEA ICE FREE
NFLD
60
55
50
45
Sea Ice Conditions
July 17, 1984
Sea Ice Boundary —— 45

Figure 20

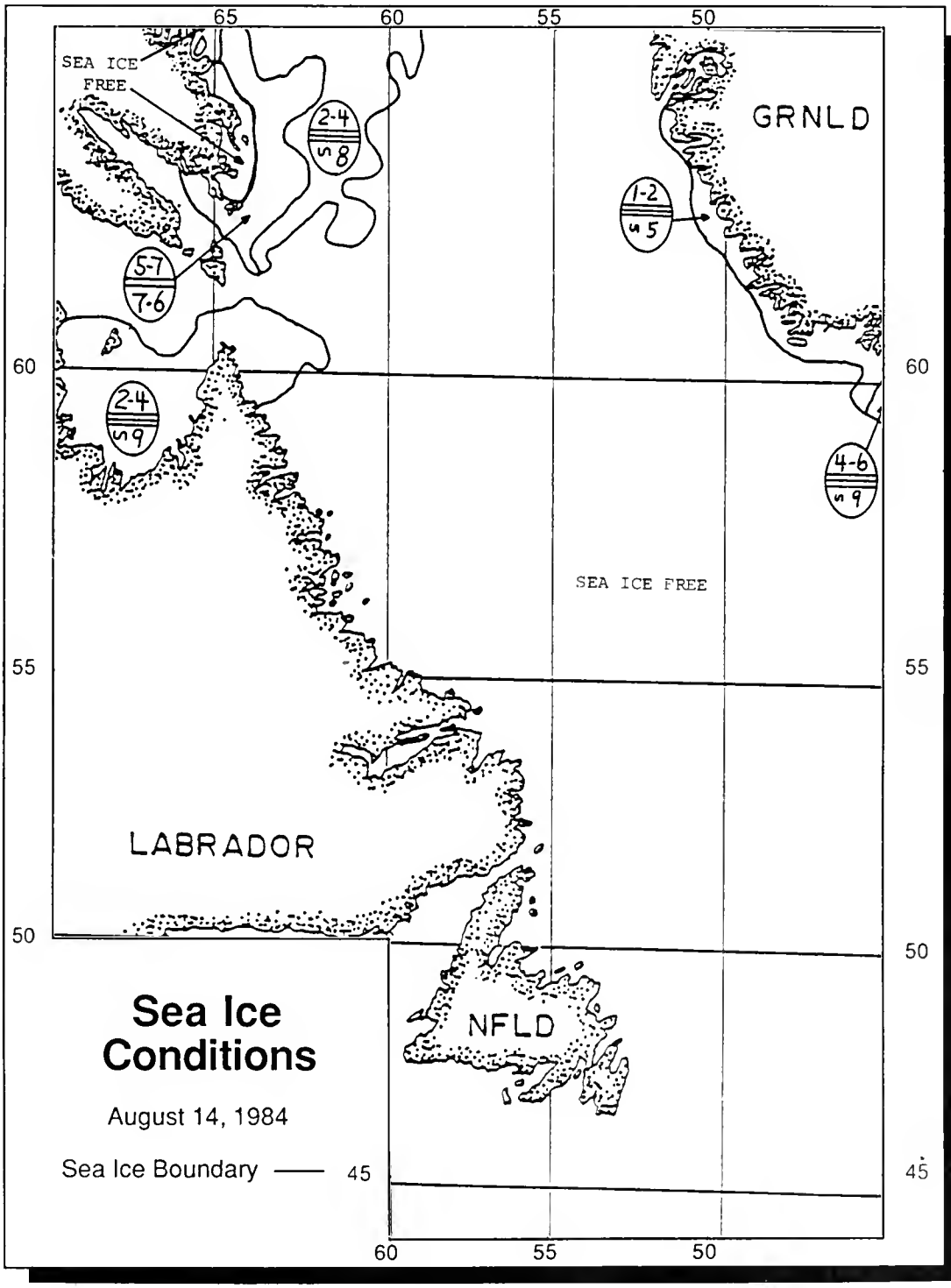
65
60
55
50
SEA ICE FREE
GRNLD
2-4
s 8
1-2
s 5
5-7
7-6
60
2-4
s 9
4-6
s 9
SEA ICE FREE
55
LABRADOR
50
NFLD
Sea Ice Conditions
August 14, 1984
Sea Ice Boundary
45

Figure 21

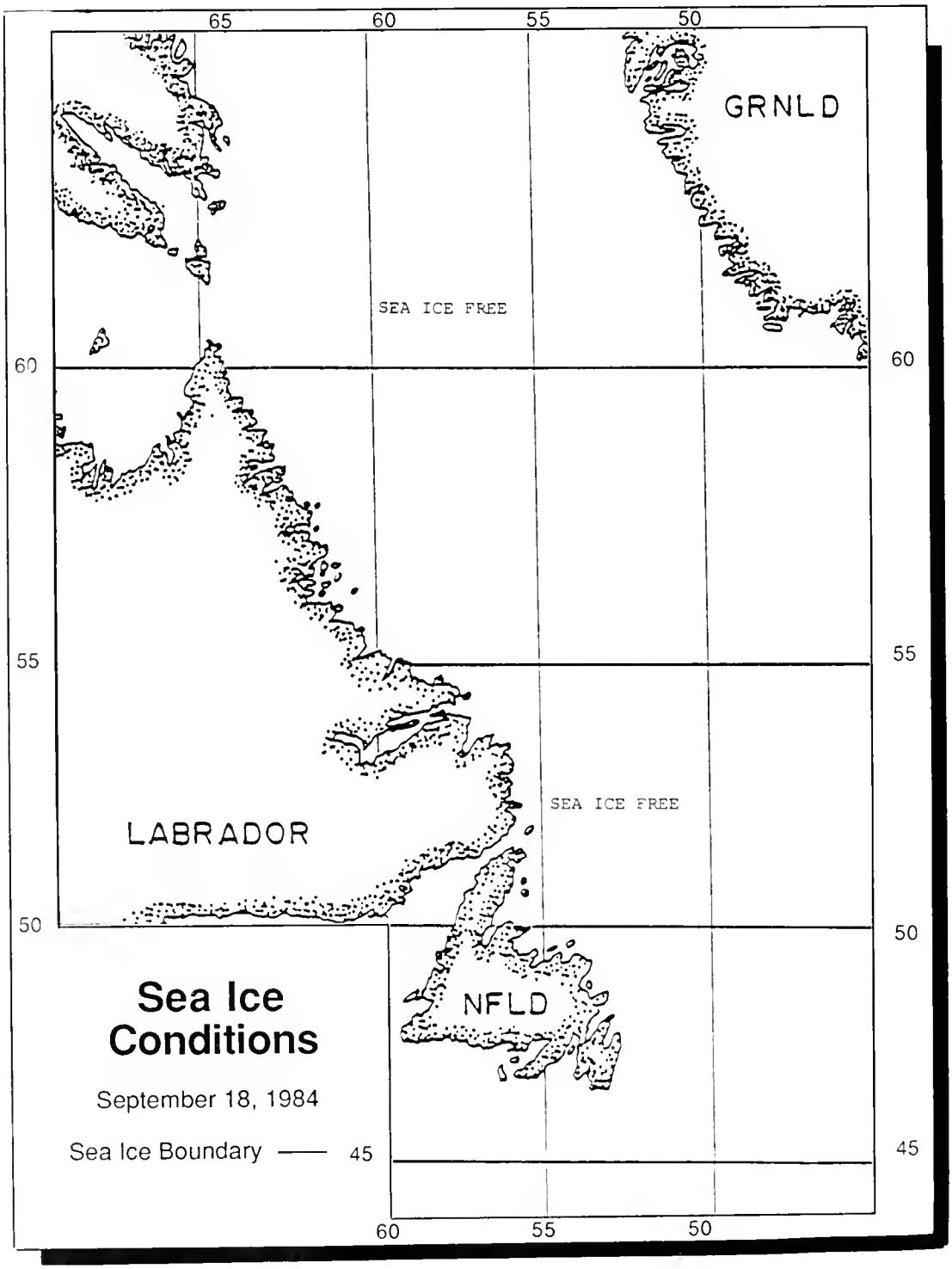
65
60
55
50
GRNLD
SEA ICE FREE
60
60
55
55
LABRADOR
SEA ICE FREE
50
50
NFLD
Sea Ice Conditions
September 18, 1984
Sea Ice Boundary —— 45
45
60
55
50

Figure 22

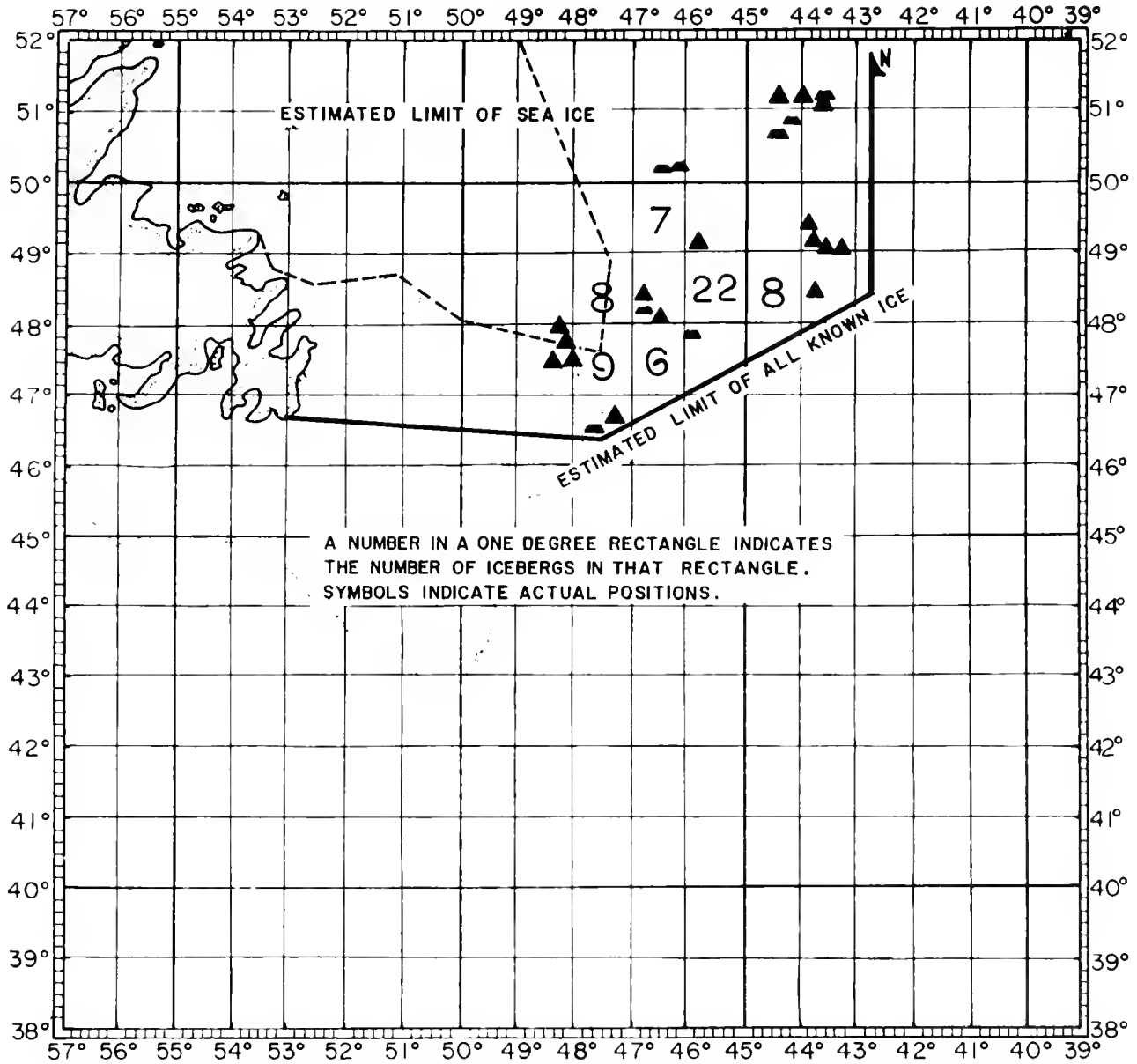

▲ BERG

▬ GROWLER

X RADAR TARGET/CONTACT

FOR 1200 GMT 23 MAR 84
BASED ON OBSERVED AND
FORECAST CONDITIONS

Figure 23

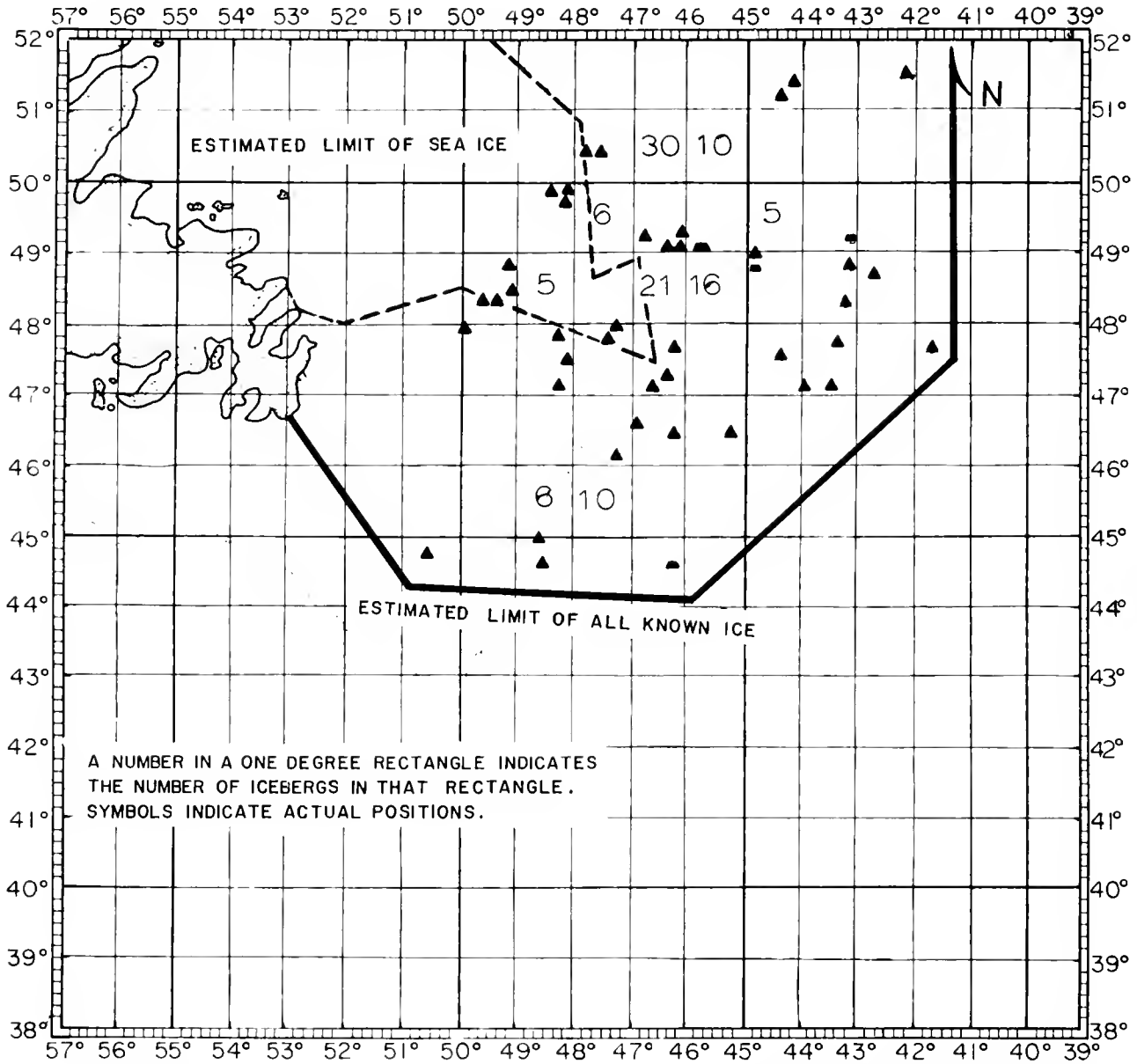

▲ BERG

● GROWLER

X RADAR TARGET/CONTACT

FOR 1200 GMT 30 MAR 84
BASED ON OBSERVED AND
FORECAST CONDITIONS

Figure 24

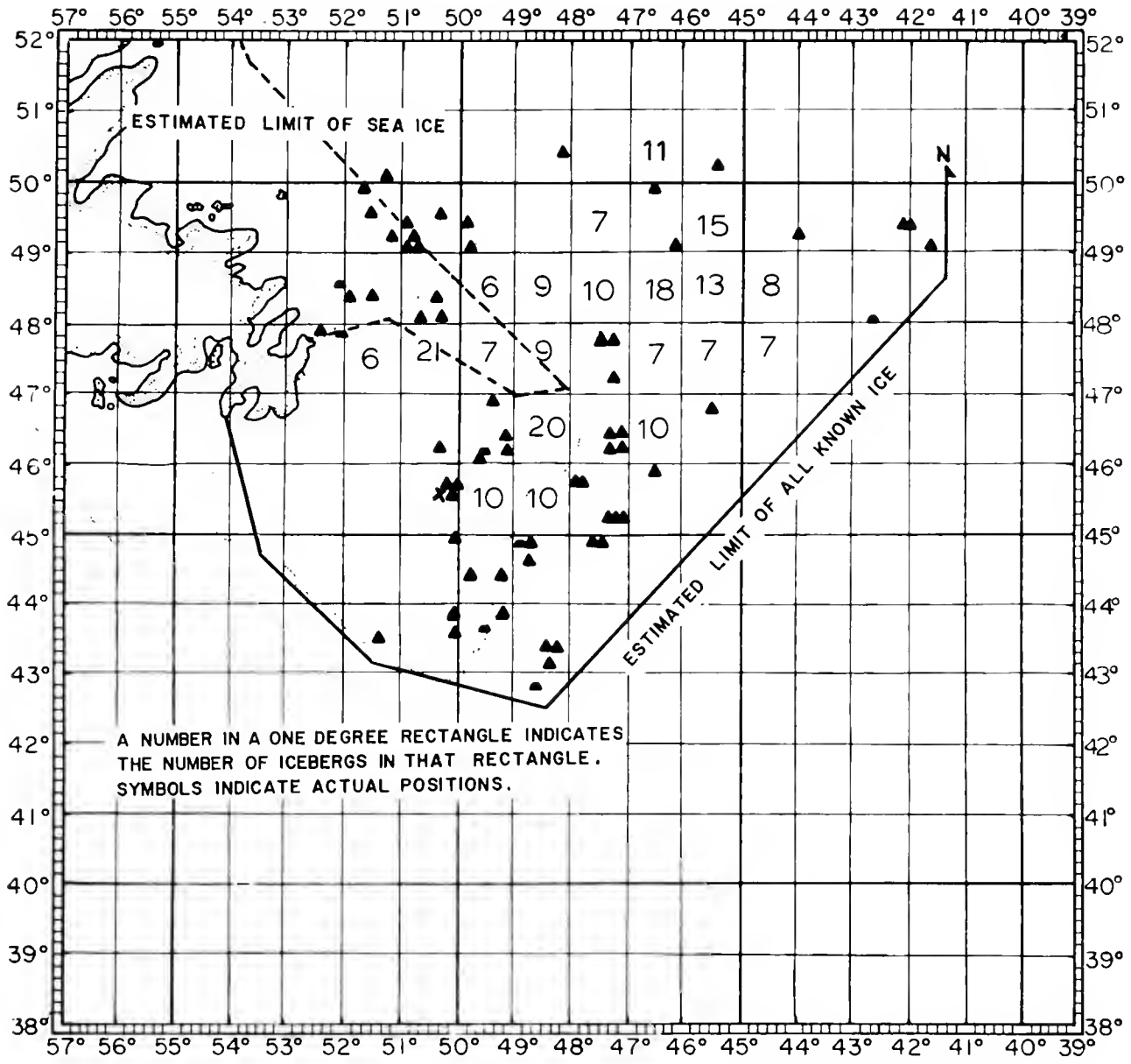

▲ BERG

● GROWLER

X RADAR TARGET/CONTACT

FOR 1200 GMT 15 APR 84
BASED ON OBSERVED AND
FORECAST CONDITIONS

Figure 25

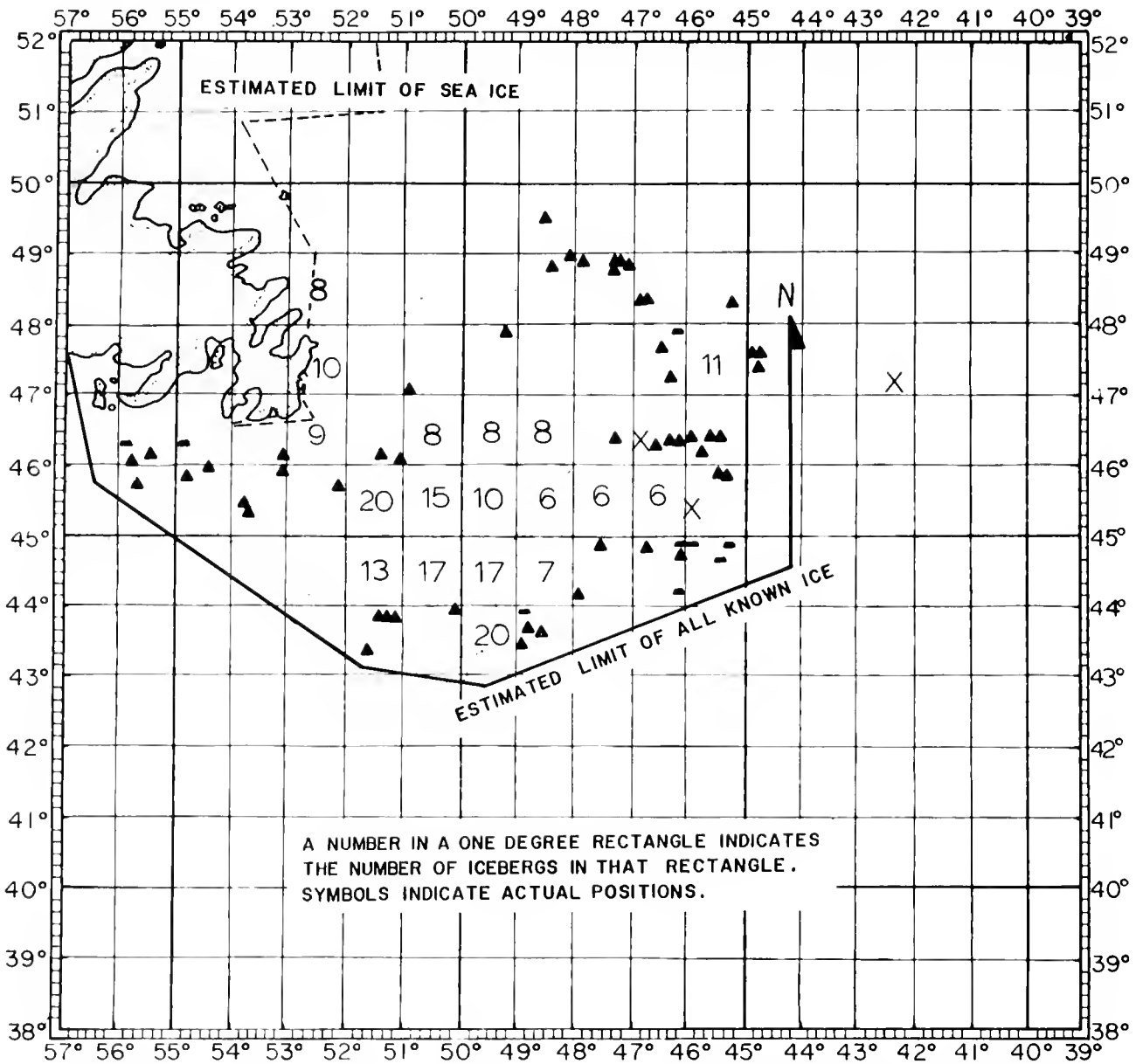
ESTIMATED LIMIT OF SEA ICE
ESTIMATED LIMIT OF ALL KNOWN ICE
A NUMBER IN A ONE DEGREE RECTANGLE INDICATES THE NUMBER OF ICEBERGS IN THAT RECTANGLE. SYMBOLS INDICATE ACTUAL POSITIONS.
N
8
10
9
8
8
8
11
20
15
10
6
6
6
13
17
17
7
20
BERG
GROWLER
RADAR TARGET/CONTACT
FOR 1200 GMT 30 APR 84
BASED ON OBSERVED AND
FORECAST CONDITIONS

Figure 26

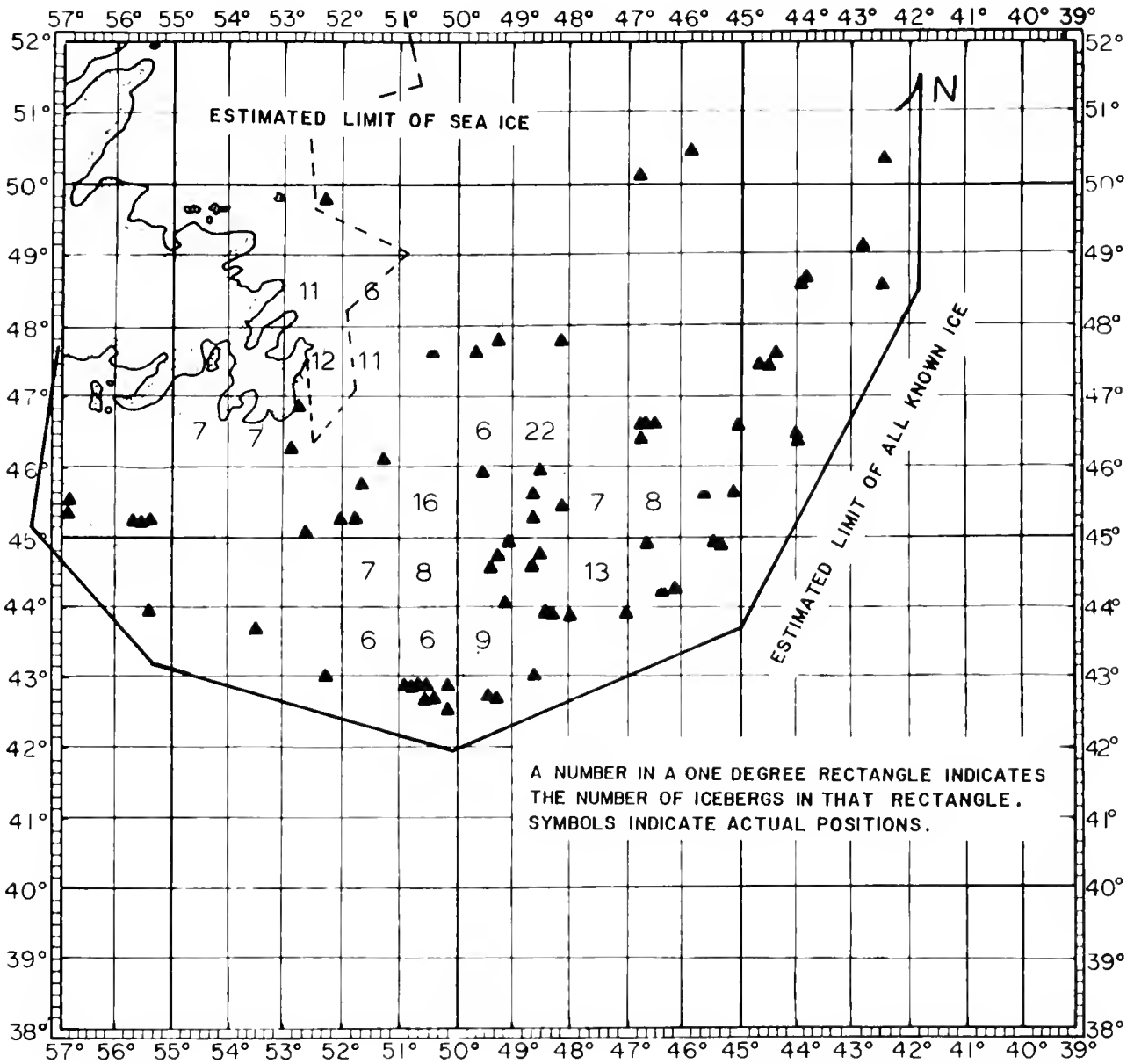
ESTIMATED LIMIT OF SEA ICE
N
ESTIMATED LIMIT OF ALL KNOWN ICE
A NUMBER IN A ONE DEGREE RECTANGLE INDICATES THE NUMBER OF ICEBERGS IN THAT RECTANGLE. SYMBOLS INDICATE ACTUAL POSITIONS.
11
6
12
11
7
7
6
22
16
7
8
7
8
13
6
6
9
BERG
GROWLER
X RADAR TARGET/CONTACT
FOR 1200 GMT 15 MAY 84
BASED ON OBSERVED AND
FORECAST CONDITIONS

Figure 27

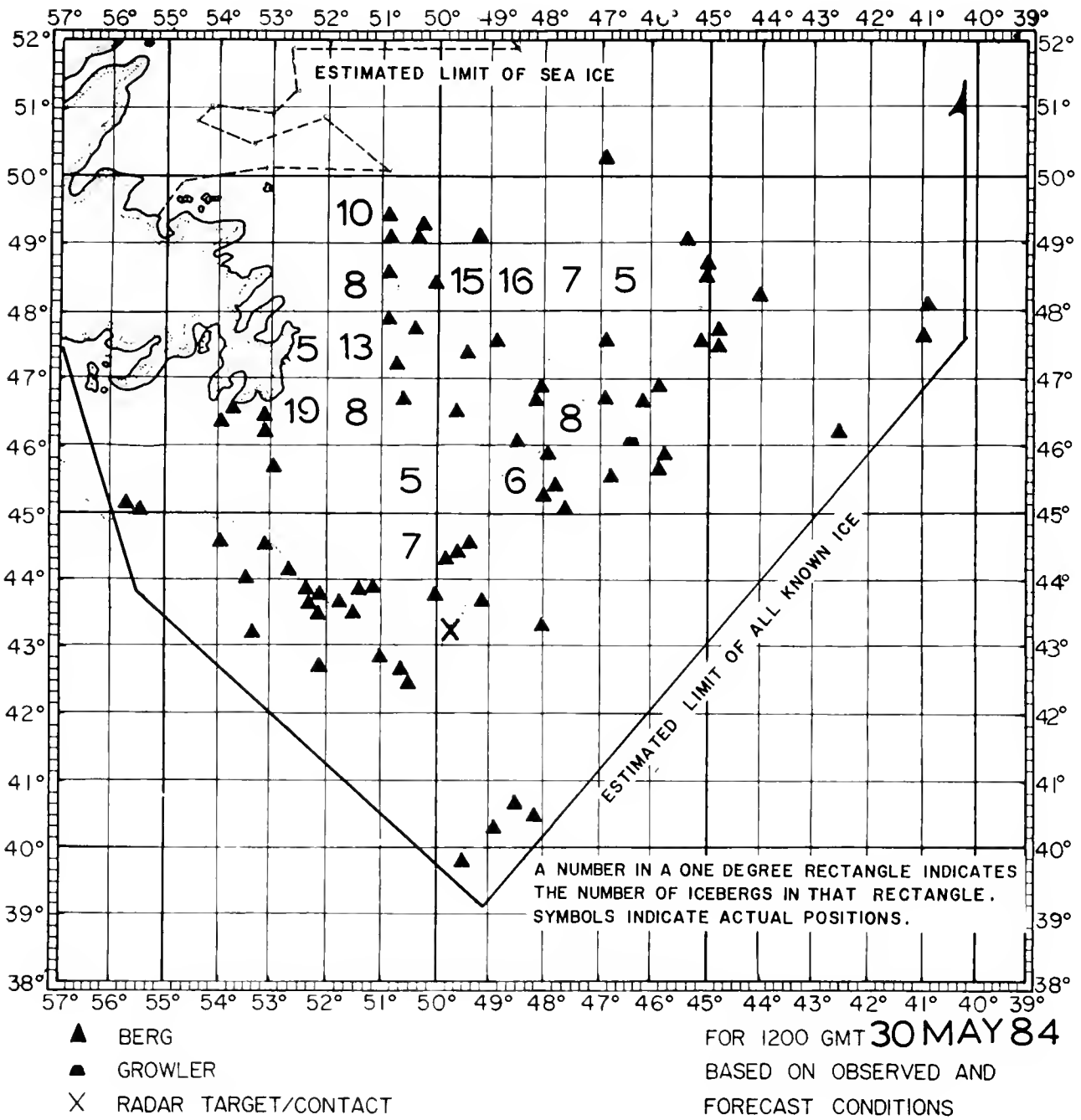
ESTIMATED LIMIT OF SEA ICE
ESTIMATED LIMIT OF ALL KNOWN ICE
A NUMBER IN A ONE DEGREE RECTANGLE INDICATES THE NUMBER OF ICEBERGS IN THAT RECTANGLE. SYMBOLS INDICATE ACTUAL POSITIONS.
BERG
GROWLER
RADAR TARGET/CONTACT
FOR 1200 GMT 30 MAY 84
BASED ON OBSERVED AND FORECAST CONDITIONS

Figure 28

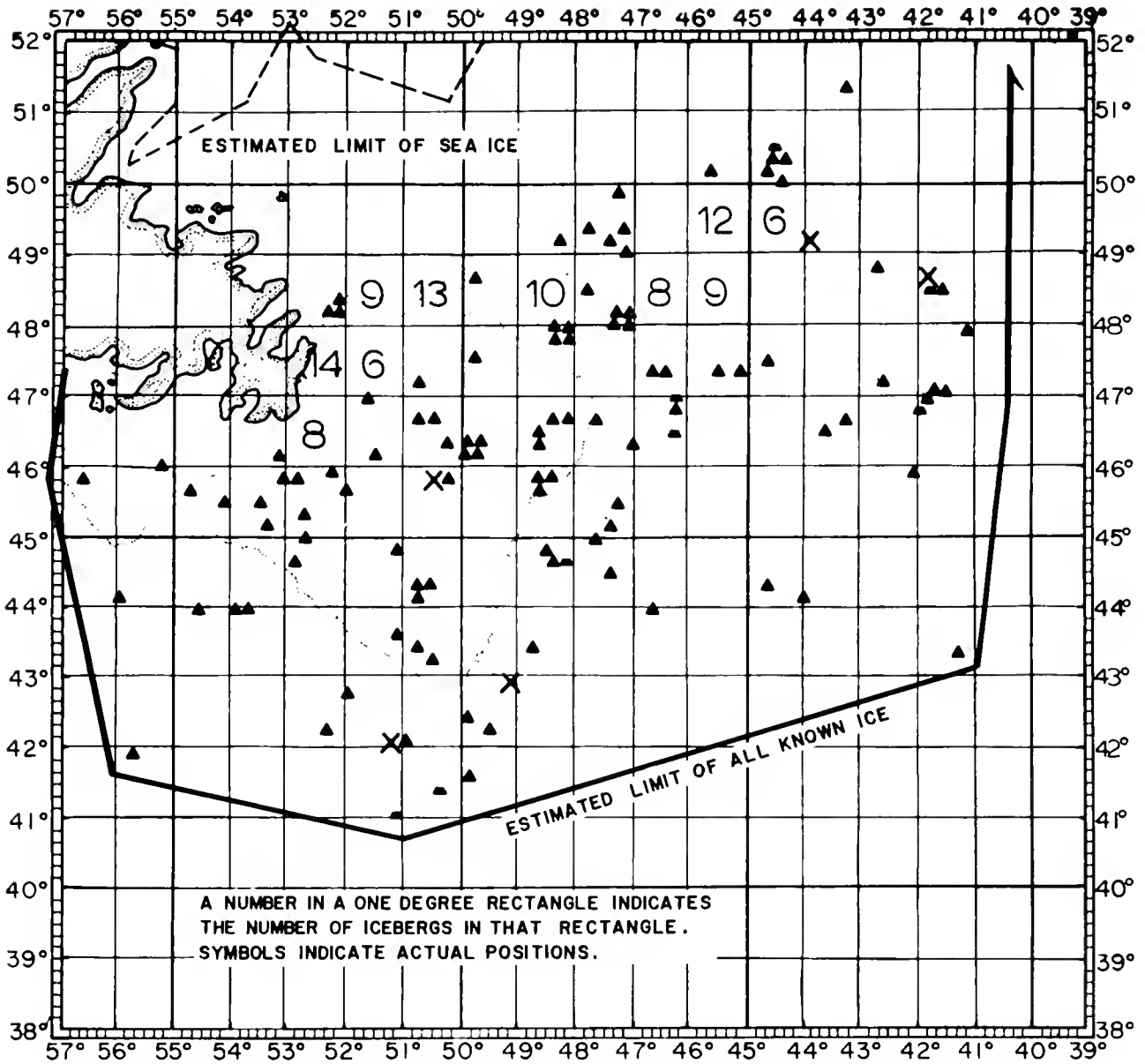
ESTIMATED LIMIT OF SEA ICE
ESTIMATED LIMIT OF ALL KNOWN ICE
A NUMBER IN A ONE DEGREE RECTANGLE INDICATES THE NUMBER OF ICEBERGS IN THAT RECTANGLE. SYMBOLS INDICATE ACTUAL POSITIONS.
12 6
9 13 10 8 9
14 6
8
BERG
GROWLER
RADAR TARGET/CONTACT
FOR 1200 GMT 15 JUN 84
BASED ON OBSERVED AND
FORECAST CONDITIONS

Figure 29

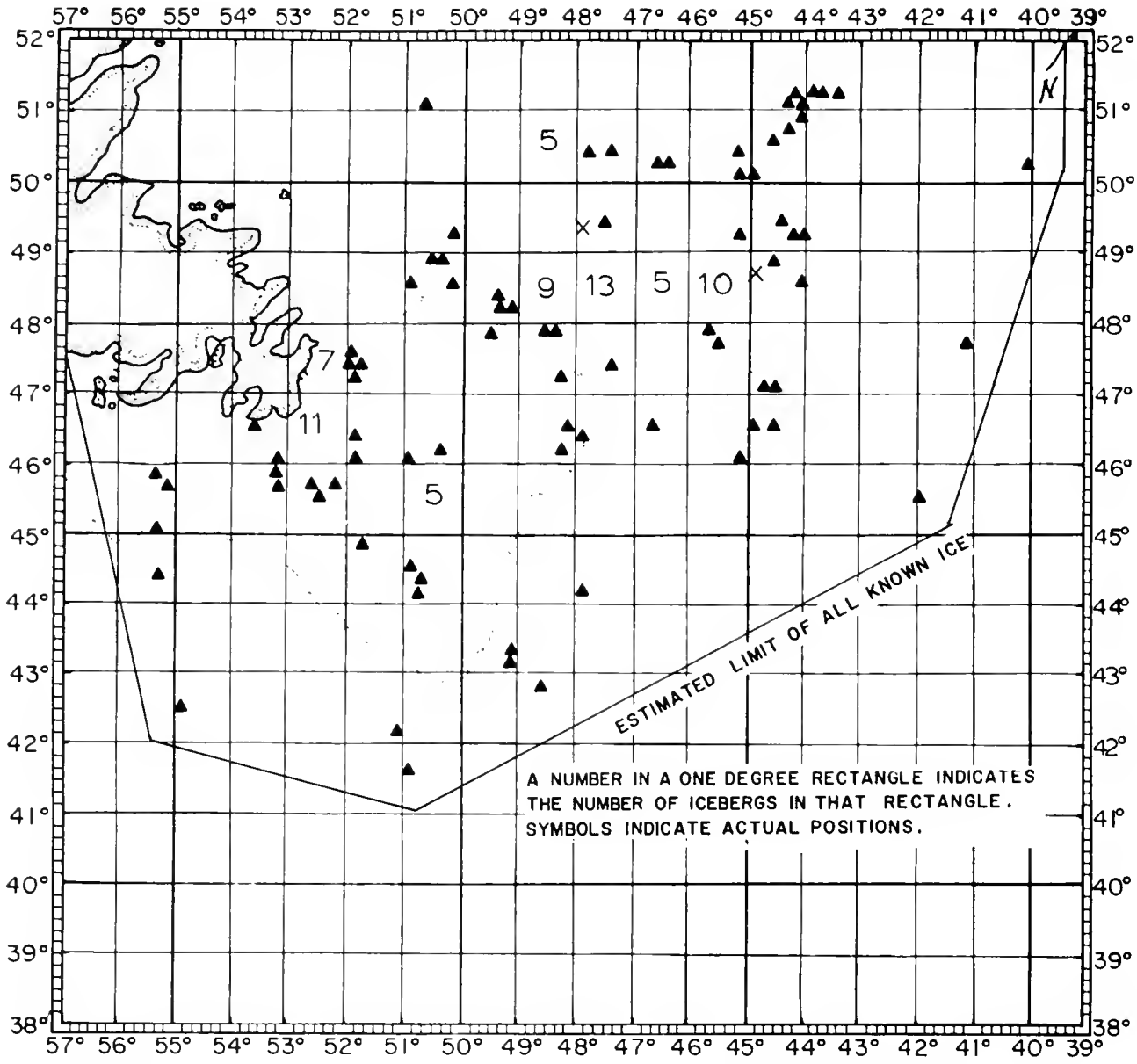
57° 56° 55° 54° 53° 52° 51° 50° 49° 48° 47° 46° 45° 44° 43° 42° 41° 40° 39°
52° 51° 50° 49° 48° 47° 46° 45° 44° 43° 42° 41° 40° 38°
N
5
9
13
5
10
7
11
5
ESTIMATED LIMIT OF ALL KNOWN ICE
A NUMBER IN A ONE DEGREE RECTANGLE INDICATES THE NUMBER OF ICEBERGS IN THAT RECTANGLE. SYMBOLS INDICATE ACTUAL POSITIONS.
BERG
GROWLER
RADAR TARGET/CONTACT
FOR 1200 GMT 30 JUN 84
BASED ON OBSERVED AND FORECAST CONDITIONS

Figure 30

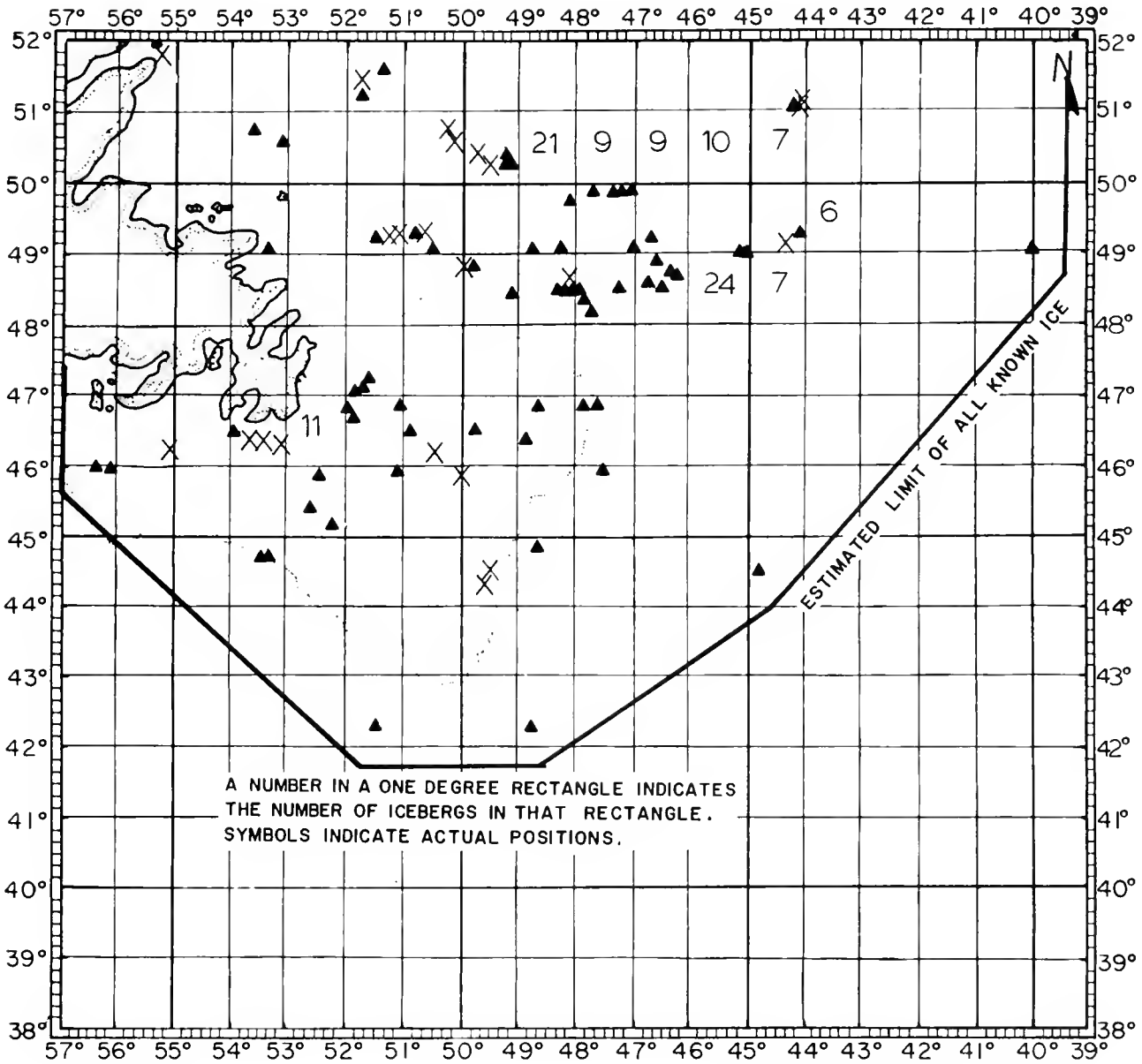
57° 56° 55° 54° 53° 52° 51° 50° 49° 48° 47° 46° 45° 44° 43° 42° 41° 40° 39°
52° 51° 50° 49° 48° 47° 46° 45° 44° 43° 42° 41° 40° 38°
N
21
9
9
10
7
6
24
7
11
ESTIMATED LIMIT OF ALL KNOWN ICE
A NUMBER IN A ONE DEGREE RECTANGLE INDICATES THE NUMBER OF ICEBERGS IN THAT RECTANGLE. SYMBOLS INDICATE ACTUAL POSITIONS.
BERG
GROWLER
RADAR TARGET/CONTACT
FOR 1200 GMT 15 JUL 84
BASED ON OBSERVED AND FORECAST CONDITIONS

Figure 31

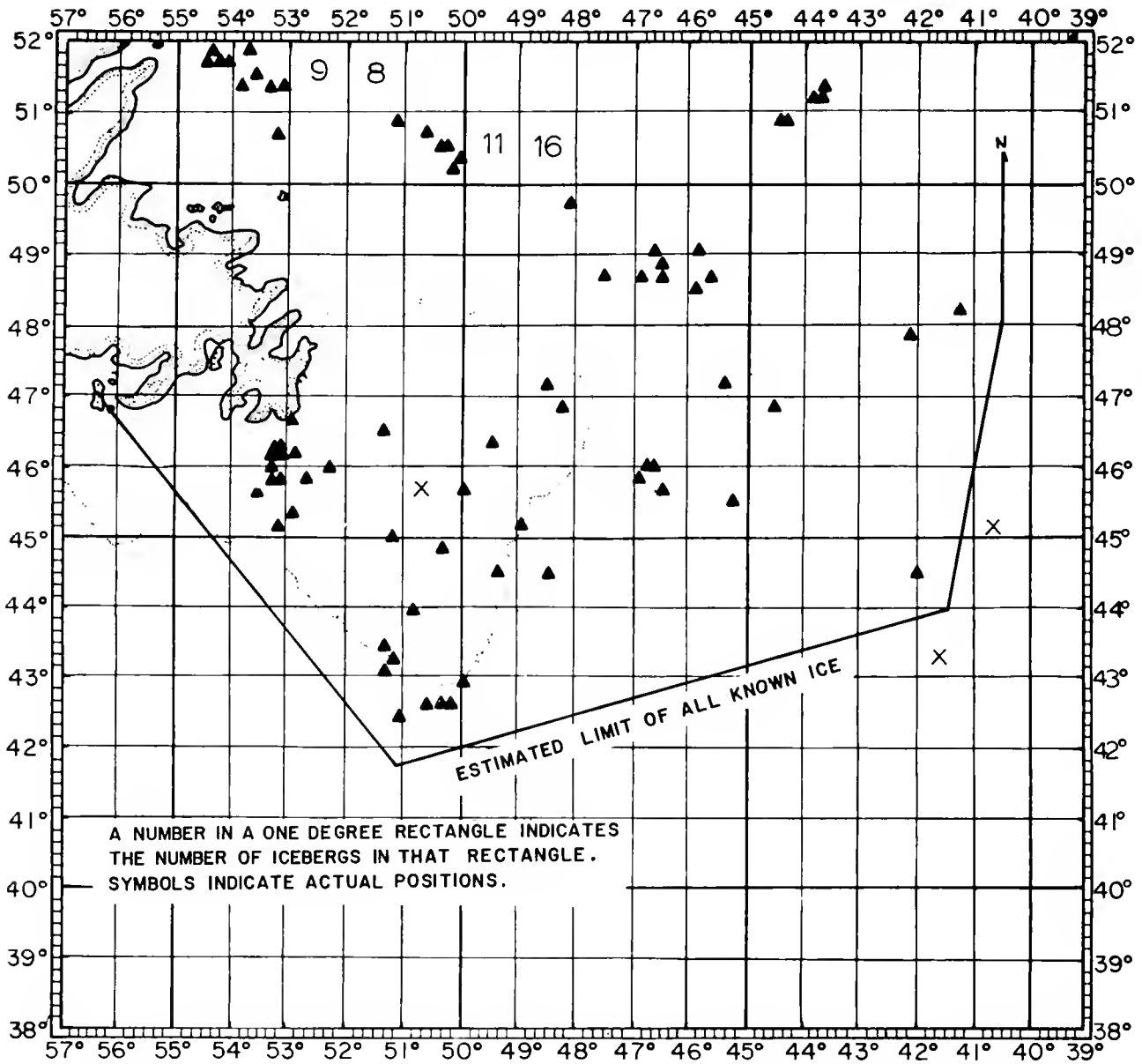
57° 56° 55° 54° 53° 52° 51° 50° 49° 48° 47° 46° 45° 44° 43° 42° 41° 40° 39°
52° 51° 50° 49° 48° 47° 46° 45° 44° 43° 42° 41° 40° 38°
9
8
11
16
N
ESTIMATED LIMIT OF ALL KNOWN ICE
A NUMBER IN A ONE DEGREE RECTANGLE INDICATES THE NUMBER OF ICEBERGS IN THAT RECTANGLE.
SYMBOLS INDICATE ACTUAL POSITIONS.
BERG
GROWLER
RADAR TARGET/CONTACT
FOR 1200 GMT 30 JUL 84
BASED ON OBSERVED AND
FORECAST CONDITIONS

Figure 32

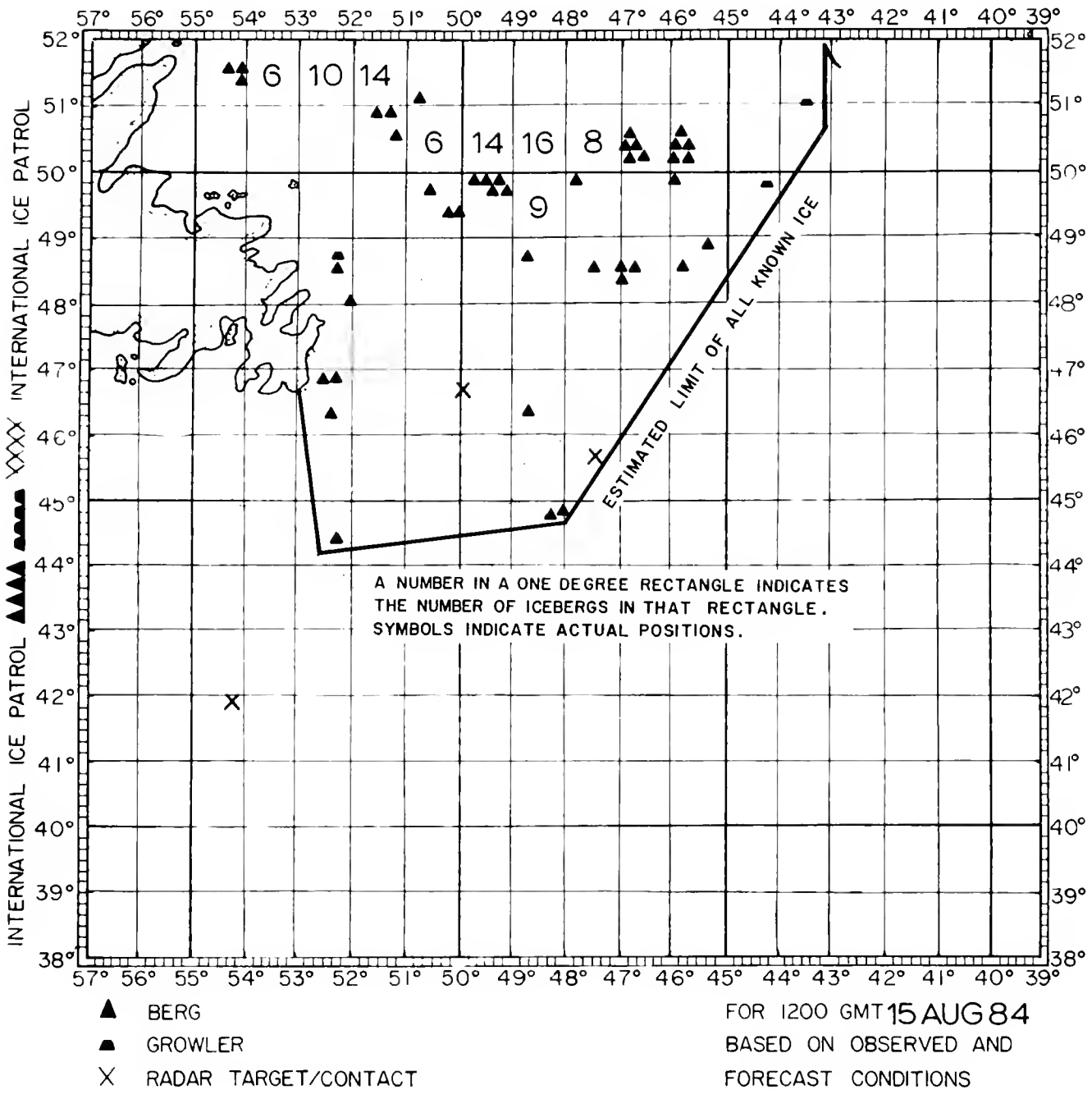
57° 56° 55° 54° 53° 52° 51° 50° 49° 48° 47° 46° 45° 44° 43° 42° 41° 40° 39°
52° 51° 50° 49° 48° 47° 46° 45° 44° 43° 42° 41° 40° 39° 38°
6 10 14
6 14 16 8
9
ESTIMATED LIMIT OF ALL KNOWN ICE
A NUMBER IN A ONE DEGREE RECTANGLE INDICATES
THE NUMBER OF ICEBERGS IN THAT RECTANGLE.
SYMBOLS INDICATE ACTUAL POSITIONS.
INTERNATIONAL ICE PATROL XXXX INTERNATIONAL ICE PATROL
BERG
GROWLER
RADAR TARGET/CONTACT
FOR 1200 GMT 15 AUG 84
BASED ON OBSERVED AND
FORECAST CONDITIONS

Figure 33

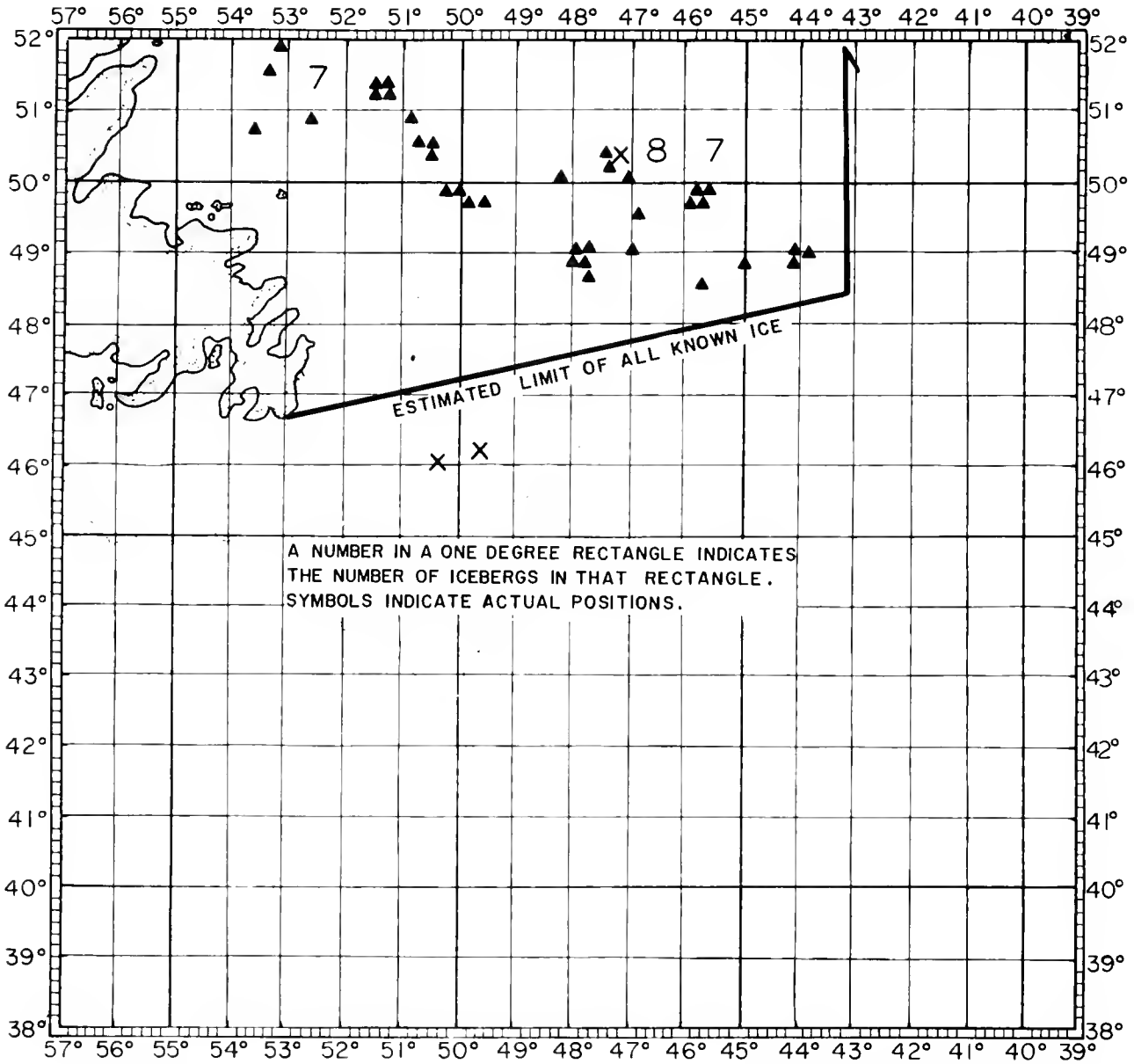
57° 56° 55° 54° 53° 52° 51° 50° 49° 48° 47° 46° 45° 44° 43° 42° 41° 40° 39°
52° 51° 50° 49° 48° 47° 46° 45° 44° 43° 42° 41° 40° 38°
7
8
7
ESTIMATED LIMIT OF ALL KNOWN ICE
A NUMBER IN A ONE DEGREE RECTANGLE INDICATES THE NUMBER OF ICEBERGS IN THAT RECTANGLE.
SYMBOLS INDICATE ACTUAL POSITIONS.
▲ BERG
▬ GROWLER
X RADAR TARGET/CONTACT
FOR 1200 GMT 30 AUG 84
BASED ON OBSERVED AND
FORECAST CONDITIONS

Figure 34

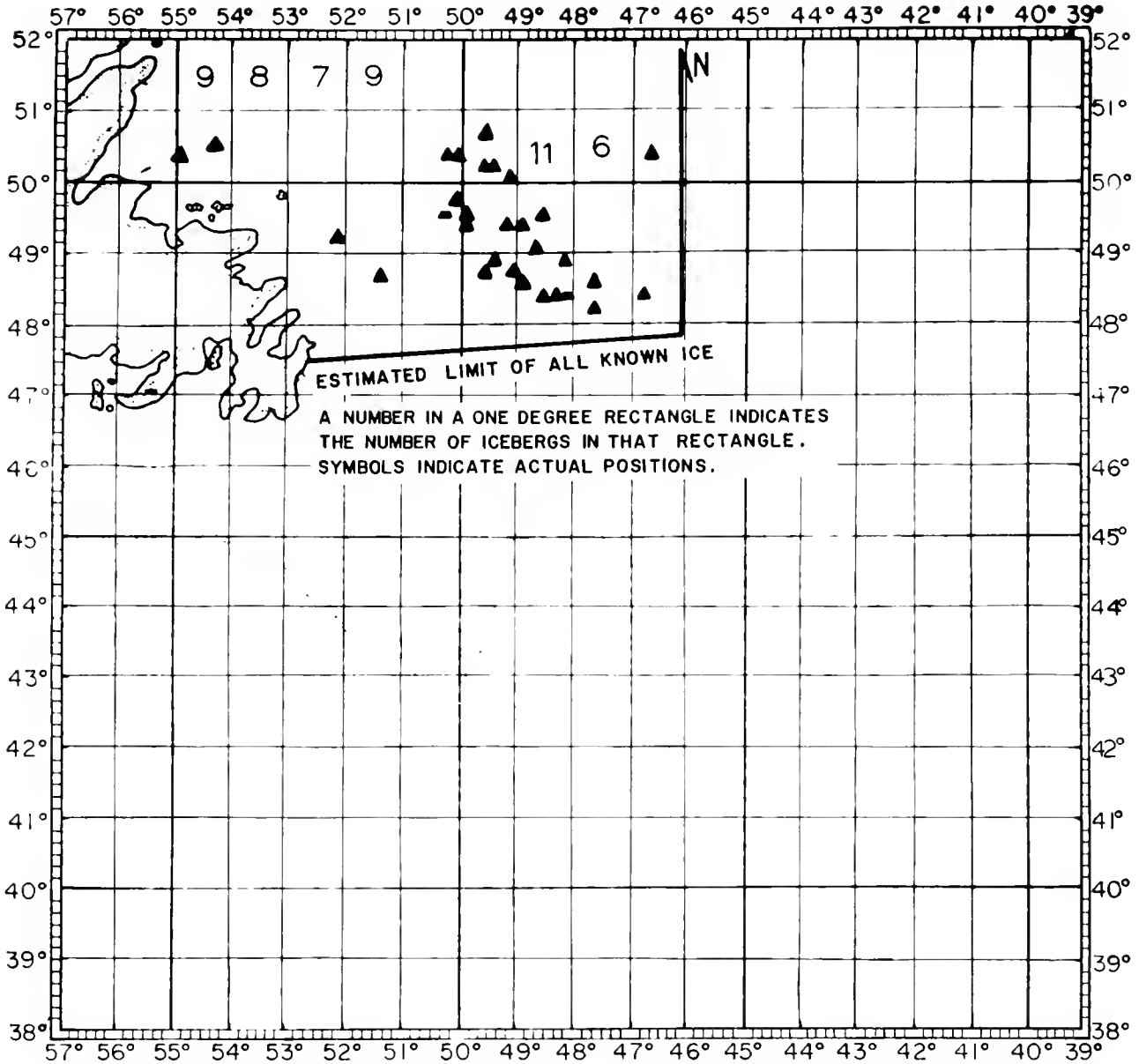

▲ BERG

▬ GROWLER

X RADAR TARGET/CONTACT

FOR 1200 GMT 07 SEP 84
BASED ON OBSERVED AND
FORECAST CONDITIONS

Discussion of Iceberg and Environmental Conditions

The number of icebergs that pass south of 48°N in the International Ice Patrol area each year is the measure by which International Ice Patrol has judged the severity of each season since 1912 (Table 1). With 2202 icebergs south of 48°N, 1984 is the record year with the previous maximum in 1972 being 1587. This record number and the near-record for 1983 (1348, fourth highest on record) are partially the result of International Ice Patrol's increased iceberg detection capability due to the introduction of the AN/APS-135 Side-Looking Airborne Radar (SLAR) to ice reconnaisance flights. The impact of SLAR on International Ice Patrol iceberg detection is examined in Appendix C.

During the period 2-7 April 1984, the International Ice Patrol participated in an airborne radar iceberg detection evaluation called Bergsearch '84. This experiment was sponsored by the Environmental Studies Revolving Funds (ESRF) administered by the Canada Oil and Gas Lands Administration (COGLA). The AN/APS-135 SLAR was tested along with two APS-94 SLAR's and the two synthetic aperture radars (SAR's) to assess the capabilities of these modern airborne imaging radars in the detection of icebergs in open water. The Ice Patrol conducted 71 passes on five sorties over iceberg-infested waters while ground truth was provided by the M/V POLARIS and visual confirmations were made by a King Air aircraft. The detection data were taken with light to moderate sea conditions of less than 4 meters and included target type (icebergs, sea ice, ships), iceberg size, aircraft altitude, aspect angle relative to the wind (sea), and depression angle. Since the emphasis was placed upon determining the detection of smaller pieces of ice (growlers and small icebergs), the analysis, which was conducted by CANPOLAR Consultants Ltd. under contract to ESRF, dealt with primarily icebergs less than 30 meters long. Because the Ice Patrol has been using the new SLAR for two seasons, this evaluation was of considerable interest. Preliminary results indicate that the APS-135 SLAR has a detection probability of approximately 65% for 10-30m icebergs, and better than 95% for icebergs over 30m in length at sea states moderate and less (Rossiter, 1984). Also, the repeatability of sighting these icebergs fluctuates less than +/- 10%. As suspected, the detectability of icebergs appears to decrease with increasing sea state, particularly for smaller targets. For growlers (<100m^2), the detection probability is very small (<5%), for they are often substantially submerged, hidden in the sea return or shadowed by the image of a parent iceberg. Of the 2202 icebergs sighted this past season, 83% were small, medium, large, or very large icebergs. Other sightings, which were not visually confirmed, may have been undersized from the SLAR imagery as growlers, since

the experiment illustrated that iceberg shape and size cannot be readily measured. In patrolling the southern, southeastern, and southwestern limits of the Grand Banks with SLAR during 1983 and 1984, the iceberg detection capability has improved greatly (see Appendix C) over prior visual search years. SLAR has provided a more efficient Ice Patrol, since visual reconnaisance flights were conducted only 50% of the time, covering much smaller search areas with visibility partially obscured by fog or low clouds. Since the SLAR capability of detecting and identifying icebergs is unknown for more severe weather conditions, future experiments will need to be conducted.

Since the number of icebergs calved each year by Greenland's glaciers is in excess of 10,000 (Knutson, 1978), a sufficient number of icebergs exist in Baffin Bay during any year. Therefore, annual fluctuations in the generation of Arctic Icebergs is not a significant factor in the number of icebergs passing south of 48°N annually. The factors that determine the number of icebergs passing south of 48°N each season can be divided into those affecting iceberg transport (currents, winds, and sea ice) and those affecting iceberg deterioration (wave action, sea surface temperature, and sea ice).

Sea ice acts to impede the transport of icebergs by winds and currents and also protects icebergs from wave action, the major agent of iceberg deterioration. Although it slows current and wind transport of icebergs, sea ice is itself an active medium, for it is continually moving toward the ice edge where melt occurs. Therefore, icebergs in sea ice will eventually reach open water unless grounded. The melting of sea ice itself is affected by snow cover (which slows melting) and air and sea water temperatures. As sea ice melt accelerates in the spring and early summer, trapped icebergs are rapidly released and then become subject to normal transport and deterioration.

Under the influence of northerly winds over Davis Strait and the Labrador Sea, a large number of icebergs entered the International Ice Patrol area in April, making it the heaviest iceberg month of the 1984 season. Light westerly flow during May, which did little to assist the southward transport of icebergs, and the persistance of sea ice off Newfoundland and Labrador throughout the month resulted in a reduced number of icebergs entering open water. The sea ice remained south of 52°N until mid-June, retarding iceberg drift and preserving the icebergs longer than normal (see SST chart for June 1984 in Appendix B).

During late June and early July, the sea ice retreated dramatically and the number of icebergs south of 48°N significantly increased in July. The sharp decrease in the number of icebergs in August and September was the result of the increase in air temperatures (Table 5) and the warming of surface waters on the Grand Banks, both of which accelerated iceberg melt.

References

Rossiter, J.R., L.D. Arsenault, A.L. Gray, E.V. Guy, D.J. Lapp, R.O. Ramseier, E. Wedler, (1984); Detection of Icebergs by Airborne Imaging Radars, Proceedings of the 9th Canadian Symposium on Remote Sensing, St. John's, Newfoundland

Knutson, K.N. and T.J. Neill, (1978); Report of the International Ice Patrol Service in the North Atlantic Ocean for the 1977 Season, CG-188-32, U.S. Coast Guard, Washington, DC.

Acknowledgements

Commander, International Ice Patrol acknowledges the assistance and information provided by the Canadian Department of the Environment, the U.S. National Weather Service, the U.S. Naval Weather Service, and the U.S. Coast Guard Research and Development Center.

We extend our sincere appreciation to the staffs of the Canadian Coast Guard Radio Station St. John's, Newfoundland/VON and the Gander Weather Office and to the personnel of U.S. Coast Guard Air Station Elizabeth City and the USCGC HORNBEAM for their excellent support during the 1984 International Ice Patrol season.

Appendix A

International Ice Patrol SST and Ice Reports for 1984

Ship's Name	Country of Registry	Ice Reports	SST Reports
Acadian Gail	Canada	2	
Achilles	Singapore	5	4
Admiral Farhi Engin	Turkey	1	
Aegis Britannic	Panama		1
Aeneas	Trinidad	2	
Agip Abruzzo	Italy	2	7
Akizuki Maru	Japan		8
Akranes	Iceland	3	
Albright Explorer	United Kingdom	9	1
Alexander Schroeder	Germany	1	
Alrazak	France		1
Ambassador	United Kingdom	7	
Anangel Ares	Greece	2	2
Anboto	Liberia	4	
Andes Traders	United Kingdom	2	
Angela Smith	Netherlands	5	
Aquarius	Italy	1	
Arctic Link	United Kingdom	1	1
Arctic Lynx	Canada	1	
Arctic Shiko	Canada	3	
Atlantic Champagne	France	2	
Atlantic Cinderella	Sweden	1	1
Atlantic Sage	Sweden	1	
Atlantic Service	France	1	
Bartlett	Chile	1	
Batna	Algeria	1	3
Benvorlich	United Kingdom	1	
Berljot	Norway	1	
Besor	Liberia	1	
Bischofstor	Germany	12	
Boujniba	Morocco		2
Breslau 2	Panama	1	
Belocean	United Kingdom		6
Bridgewater	Germany	3	
Brittania	United Kingdom	4	
Brunto	Norway	5	
Calanda	Switzerland	1	
Canadian Explorer	United Kingdom	3	
Canforces Tracker	Canada	2	
CapeCornwall	Japan		3
Cape Lance	Registry Unknown	2	2
Cape Roger	Canada	2	
Cape Syros	Greece	1	
Caribou	Liberia	3	2
Carsten Russ	Panama	4	2
Cast Caribou	Liberia	1	
Cast Husky	United Kingdom	1	
Cast Muskox	United Kingdom	6	
Cast Polar Bear	Liberia	2	15
Cast Salmon	Poland	1	
Century Hope	United Kingdom	1	
Chemspan	Trinidad	1	1
City of Perth	United Kingdom	4	7
Clymene	United Kingdom	8	
Colditz	Germany	5	
CrownPromise	Liberia		3
Cyrena	France	1	

Appendix A (cont'd.)

International Ice Patrol SST and Ice Reports for 1984

Ship's Name	Country of Registry	Ice Reports	SST Reports
Dart Britain	Colombia	1	
Dart Continent	Czechoslovakia	2	
Dart Europe	Belgium	1	
Dart Tiritian	United Kingdom	3	
Dauogulf	Phillipines		1
Dilderdijk	Netherlands Antilles	1	
Dole Vega	Brazil		4
Eastern Harjel	Colombia		3
Eastern Shell	Czechoslovakia	1	
Edough	Algeria		7
Elareg	Canada	1	
Eleusis	Burundi	1	1
Elisabeth	Liberia	3	
Elmina	Greece		1
Erika Bolten	Panama	3	4
Europe	Belguim	1	
GB Falcon	Norway	1	
Falkoen	Sweden	1	
Fanny	United Kingdom	1	
Farnes	Liberia	4	
Federal Danube	Belguim	1	
Federal Maas	Belguim	1	
Federal Ottawa	Belguim	1	
Federal Pioneer	Union of Soviet Socialist Republics	3	
Federal Schelde	Liberia	1	
Federal Thames	Belguim	1	
Finnrose	Finland	1	1
Fivestar	Liberia	5	4
Fogo Isle	Canada	1	
Fort Kipp	Great Britain		1
Fort Ramezay	Canada	1	
Fort Steele	Great Britain		12
Fossnes	Norway		3
Frank Schroder	Germany	1	
Frimaro	Cuba		1
Gaviota	Germany	1	
General Dabrowski	Poland	3	
General Luma	Phillipines	1	
Golarl Petrosun	Liberia	2	2
Gulf Mackenzie	Canada	2	
Halifax	Greece		2
Hampton Lion	Liberia	3	
Helate	Panama	1	1
Helen Schulte	Netherlands	1	3
Heritage	Greece		2
Hohn	Germany	1	
USCGC HORNBEAM	United States of America	7	14
Hudson	Canada	15	8
Hual Traveller	Norway		3
Hunter Bow	Liberia	1	
Husky	Panama	1	
Hydrolock	United Kingdom	1	
Iguazu	Liberia		2
Imperial Quebec	Canada	2	
Ingua Pilot	Panama	1	
Invincible	United Kingdom	4	
Irving Elm	Canada	1	

Appendix A (cont'd.)

International Ice Patrol SST and Ice Reports for 1984

Ship's Name	Country of Registry	Ice Reports	SST Reports
Irish Spruce	Ireland	1	
Irving Forest	United Kingdom	1	
Irving Nordic	Canada	1	
Irving Ours Polaire	Canada	2	
Islander	Malta	2	
Ivan Derbenev	Union of Soviet Socialist Republics	1	
Jena	Germany	4	
John M	Germany	5	1
Joseph Roty	France	1	
Judson	Canada		1
Juventia	Panama	5	
Kemano	United Kingdom	1	
Kansas Getty	Bahamas		10
Kapetan Yannis	Greece		3
Katerina	France	1	
Koeln Express	Germany	1	
Konkar Indo Kitable	Greece	7	
Kurashima Maru	Japan		3
Labrador	Canada	1	
Lady Saunders	Canada	1	
Lake Anne	Norway	2	
Lake Biwa	Chile	3	1
Lakeanina	Norway	1	
Lalberte	Liberia		2
Lantau	Singapore	1	
Leon Et Pierre	Belguim	1	
Lokvihar	India	8	1
Lorena	Spain	1	
Louis L. D.	France	2	15
Louis S. St-Laurent	Canada	1	
Lousdrecht	Netherlands	1	
Ludoluf Oldendorff	Singapore	2	
Lumaaq	Canada	1	
Madeleine	Great Britain	3	
Maersk Triton	Liberia	1	
Mahone Bay	Canada	1	
Malabar	Registry Unknown	1	2
Manchester Challenge	United Kingdom	33	3
Marinz L	Greece	1	
Masovia	Liberia	6	
Mega Bay	Norway	1	
Mela	Indonesia	3	
Meltimi	Greece	6	7
Mesange	Canada	1	
Michalis	Greece	1	2
Mihalis	Greece	2	
MimiM	Greece		2
Minerva	Brazil	1	
Mosbrook	Norway	2	
Moutsqina	Greece	3	
Myuta	Panama	1	
N. M. Engin	Turkey	1	
Nautic Pioneer	Liberia	1	
Navimar 1	Canada	2	
Nihonkaimaru	Japan	1	
Noble Supporter	Liberia		7
Nordstrand	Burundi		1

Appendix A (cont'd.)

International Ice Patrol SST and Ice Reports for 1984

Ship's Name	Country of Registry	Ice Reports	SST Reports
USCGC NORTHWIND	United States of America	69	25
Nyuta	Panama	1	
Olinda	Singapore	1	
Oriental Ruby	Japan		9
Pacific Challenge	United Kingdom	1	
Pacific Courage	United Kingdom	4	
Pacific Freedom	Liberia	1	
Pacific Friendship	Liberia	1	
Pacific Progress	United Kingdom	1	
Palmstar Orchid	Singapore	1	
Pampero	Panama	2	8
Panama	Denmark		9
Parita	Finland		4
Penmen	France	3	9
Perth	United Kingdom	1	
Permnitz	Germany	4	
Pharos	Germany	3	
Philippeld	France	1	
Pokkinen	Finland	1	
Polar Circle	Canada	2	
Polaris	Togolese Republic	5	
Precious	Liberia	2	2
Premwitz	Germany	1	
Princess	Panama	1	
Primorsk	Union of Soviet Socialist Republics	1	
Queen Elizabeth II	United Kingdom	3	
Rannoe	Finland	6	
Rebeka	Romania	3	
Regina	Switzerland	2	
Reynolds	United Kingdom	7	
Rich Alliance	Panama	1	
Rigoletto	Sweden		3
Roman Pazinski	Poland		3
Rubens	United Kingdom	6	
Ryokomaru	Japan	1	
Satu Mar	Singapore	2	
Schnoorturm	Great Britain	1	
Seaforth Atlantic	Canada	1	
Sealand Independence	United States of America	1	
Sealand Leader	United States of America	1	
Sealand Vokager	United States of America	1	
Sealve	Sweden		1
Sekirex	Japan	2	
Shanadith 2	Registry Unknown	1	
Shenandoah	Greece	1	
Shinrei Maru	Japan	1	
Smeliy	Union of Soviet Socialist Republics	1	
USNS SOUTHERN CROSS	United States of America	18	13
Steam Bollard	Liberia	2	
Stefan Batory	Poland	7	
Stefan Starzynski	Poland	3	
Stolt Castle	Liberia	3	1
Stolt Sydness	Liberia	2	2
Stovetrader	Sweden	1	5
String Bridge	Panama		6
Studlasfoss	Iceland		2

Appendix A (cont'd.)

International Ice Patrol SST and Ice Reports for 1984

Ship's Name	Country of Registry	Ice Reports	SST Reports
Takeshimamaru	Japan		1
Temse	Belguim	1	1
Tatucareer	Panama	1	
Terra Nova	Greece	3	
Texaco Massachusetts	United States of America	2	1
Transocean Transport	Phillipines	2	1
Ungava Transport	Canada	1	
United Venture	Singapore	1	
Varjakka	Finland	2	18
Vasiliki	Greece	1	1
Vasya Korokbo	Ukranian Soviet Socialist Republics	1	
Velizh	Union of Soviet Socialist Republics	1	
Vera Maretskaya	Union of Soviet Socialist Republics	1	
Vergo	Canada		8
Victor Bugaey	Union of Soviet Socialist Republics	1	
Vissani	Panama	1	
Vitosha	Bulgaria	1	1
Viva	Norway	1	
Vladimir Timofeyev	Union of Soviet Socialist Republics	1	
Watergeus	Netherlands	3	
Western Viking	Panama	2	
Western Harbour	United States of America	3	
Wilfred Templeman	Canada	1	
World Agamemnon	Greece		4
World Dawn	Panama	1	
Willow Peak	Chile	1	
Yevgenit Vaktangov	Union of Soviet Socialist Republics	1	1
Yukona	Liberia	4	1
Yukona	Union of Soviet Socialist Republics	1	
Zagreb	Canada	1	
Ziemia Bilostocka	Poland	3	
Zim Genova	Israel	1	
Zimberia	Israel		1

Appendix B

Oceanographic Conditions on the Grand Banks During the 1984 International Ice Patrol Season

Lieutenant Iain Anderson, USCG

Introduction

For the first time since 1978, International Ice Patrol conducted hydrographic measurements on the Grand Banks (the data report is still to be published). The cruise was divided into two parts; the first dedicated to a hydrographic survey, and the second to iceberg drift and deterioration. Due to an inoperative Ocean Sampling System (OSS), the hydrographic section of the cruise was conducted using Nansen casts.

During the 1984 season, eleven satellite-tracked TIROS Oceanographic Drifters (TOD) were deployed in the IIP operating area. Nine of the TODs were deployed from an HC-130 aircraft during regular ice reconnaisance flights. The remaining two TODs were deployed from the USCGC HORNBEAM, the vessel used to conduct the IIP cruise. The two TODs deployed from HORNBEAM had been recovered after the 1983 season and were reconditioned and then deployed.

TIROS Oceanographic Drifters

Eleven TODs were deployed during the 1984 IIP season (Table B-1). All of the TODs were deployed with window-shade drogues attached to the TOD by a 30m tether. Each TOD was equipped with a sea surface temperature sensor, a drogue tension sensor, and a battery voltage monitor. The position (determined by Doppler shift of the TOD transmitted frequency at the receiver of a polar orbiting satellite) and sensor information from each buoy was obtained through Service ARGOS.

As of 1 October 1984, six of the eleven TODs were still drifting in the IIP region (Figure B-1). One of the TODs (TOD #4513) failed on deployment and another (TOD #4514) failed after nine days. Several of the parachute release mechanisms failed to operate properly at deployment. TOD #4509 and #4531 were observed being dragged across the sea surface by an air-filled parachute during the post-deployment overflight. The apparent source of the problem was insufficient voltage in the gel cells used to supply power to the parachute cutters after the salt-water-activated switch closed. The actual fate of the parachutes is uncertain. We assume that when the drogue fully deployed or when the parachute collapsed, it settled into the water and, at worst, became a near-surface drogue.

There are no significant differences in the velocity distributions for TODs with confirmed parachute releases and those without, suggesting the parachute, if it remained attached did not affect the drift of the TOD (Figure B-2). TOD #2633 and TOD #2632 were deployed from HORNBEAM on 6 July and 17 July, respectively.

Table B-1.
TIROS Oceanographic Drifters Deployed in the 1984 Ice Patrol Season

TOD#	Date Deployed	Position Deployed	Avg Pos/Day	Last date data received*	Deployed
4511	22 MAR(082)	48°17.6'N 50°00.0'W	8.2	1 OCT+	C-130
4509	23 MAR(083)	49°53.4'N 45°50.3'W	6.8	1 OCT	C-130
4510	25 MAR(085)	49°00.0'N 47°58.2'W	8.3	20 SEP	C-130
4512	27 APR(118)	47°51.6'N 47°30.0'W	7.2	14 JUL	C-130
4514	28 APR(119)	48°15.0'N 52°20.0'W	10.4	7 MAY	C-130
4513	10 JUN(162)	47°29.7'N 47°28.8'W	---	------	C-130
4531	13 JUN(165)	48°32.0'N 48°01.0'W	7.9	1 OCT	C-130
2633	06 JUL(188)	48°20.0'N 48°30.0'W	7.8	1 OCT	SHIP
2632	17 JUL(199)	48°37.4'N 46°06.1'W	8.3	1 OCT	SHIP
4528	05 AUG(210)	50°59.4'N 51°01.2'W	9.7	1 OCT	C-130
4530	06 AUG(211)	46°46.8'N 46°54.4'W	9.3	1 OCT	C-130

* Within IIP region

+Picked up by fishermen on 1 AUG 84

The drogue sensors indicated the drogues were never attached to the buoys, although the drogues were attached when deployed and are assumed to have remained attached at least through 1 August. TOD deployment position selection is based on the location of areas of high iceberg concentrations and areas of most unreliable drift prediction. The analysis includes data through 1 October 1984. The drift tracks of the TODs will be discussed below in chronological order according to deployment.

TOD #4511 was deployed on 22 March 1984 (Julian Date 082) near the 200m contour at 48°18'N 50°00'W. This position was about 1/2 mile south of the sea ice edge. Its initial movement was to the east at about 19 cm/s. On 27 March (087), TOD #4511 turned and moved nearly south for five days onto the Grand Banks (averaging 16.5 cm/s). This was not the motion anticipated. We had anticipated the deployment position would have placed TOD #4511 in the Labrador Current, but the TOD motion indicated the deployment position was south of the main current stream. The movement continued generally to the southwest through the Avalon Pass (with anticyclonic motion) at an average velocity of 11 cm/s until 10 July (192) near 46°03'N 54°01'W. TOD #4511 then moved generally north into St. Mary's Bay and was picked up by a fisherman on about 1 August (214). (It was recovered by the Canadian Coast Guard in late October and was returned to the International Ice Patrol.)

TOD #4509 was deployed on 23 March (083) north of Flemish Cap at 49°53'N 45°50'W. It drifted with a slow cyclonic motion at an average velocity of 11 cm/s until 21 April (112). It then began a series of cyclonic and anticyclonic motions centered about 40 km south of its deployed position that lasted until about 2 June (154). TOD #4509 then travelled in a northerly direction at an average velocity of 63 cm/s until 7 June (159). From 8 June to 28 September (160-272), it remained trapped in an anticyclonic eddy. The motion was centered about 52°N 46°W. The radius of the motion ranged from 30 to 120 km at an average velocity of 27 cm/s. Canadian METOC sea surface temperature (SST) charts do not indicate the presence of an eddy near 52°N 46°W for the period TOD #4509 was moving anticyclonically (Figure B-3).

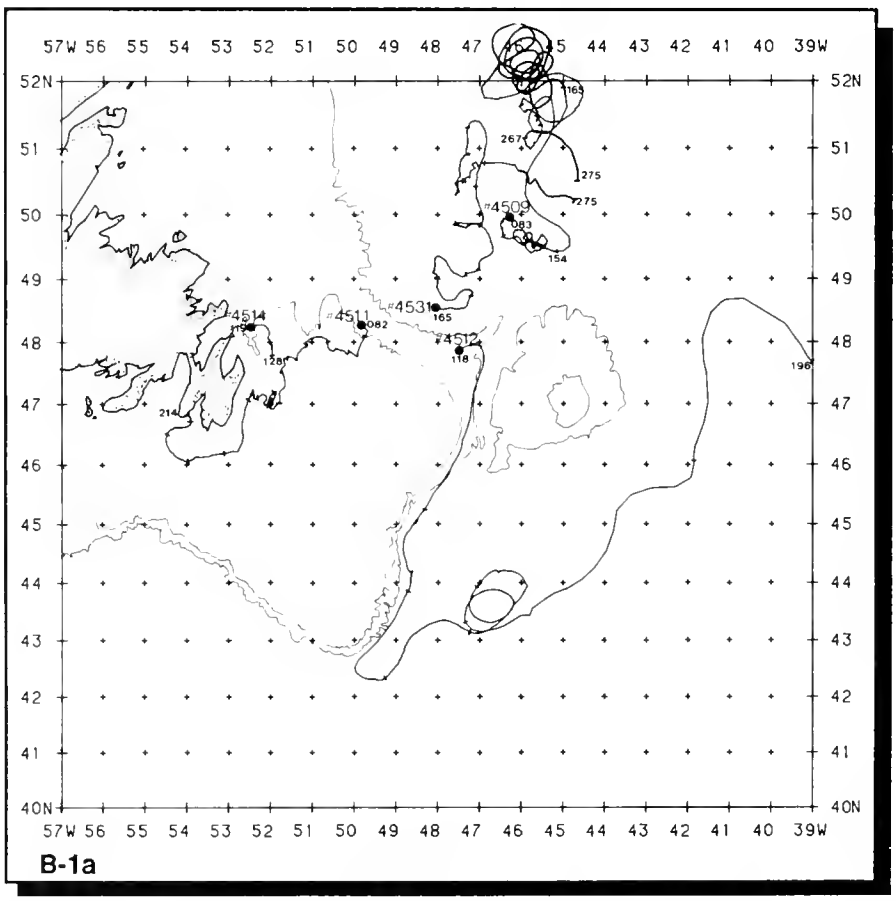

Figure B-1. Drift Tracks for International Ice Patrol's 1984 TODs. The • indicates the deployment position. Tick marks on the drift tracks are 10 days apart. Note the eddies contained in all of the drift tracks and the role of bathymetry in influencing the TOD motion.

TOD #4510 was deployed north of the Flemish Pass on 25 March (085) in position 49°N 47°58.2'W. This deployment position was in about one tenth sea ice cover. It proceeded east around the top of the Flemish Cap and followed the 2000m contour south around the eastern side of Flemish Cap at an average velocity of 17 cm/s until 4 May (125). On 4 May (125), TOD #4510 sharply altered its drift track and began drifting north and then northwest after crossing 49°N at an average velocity of 46 cm/s. Sea surface temperature charts and the drift indicate that TOD #4510 entered the North Atlantic Current on 4 May (125). The SST data from the TOD also confirms that TOD #4510 entered the North Atlantic Current. The drift pattern of TOD #4510 from 4 May (125) until it crossed 52°N on 22 May (143) is similar to those described in previous years (Anderson, 1983a and Summy, 1982). TOD #4510 remained above 52°N until 8 September (252). While above 52°N, TOD #4510 was caught in an anticyclonic eddy that was centered near 53°30'N 48°00'W before heading south on 29 August (241). From 1 September until 20 September (245-264), TOD #4510's motion was anticyclonic, apparently caught in the same eddy as TOD #4509. No signal was received from TOD #4510 after 20 September (264).

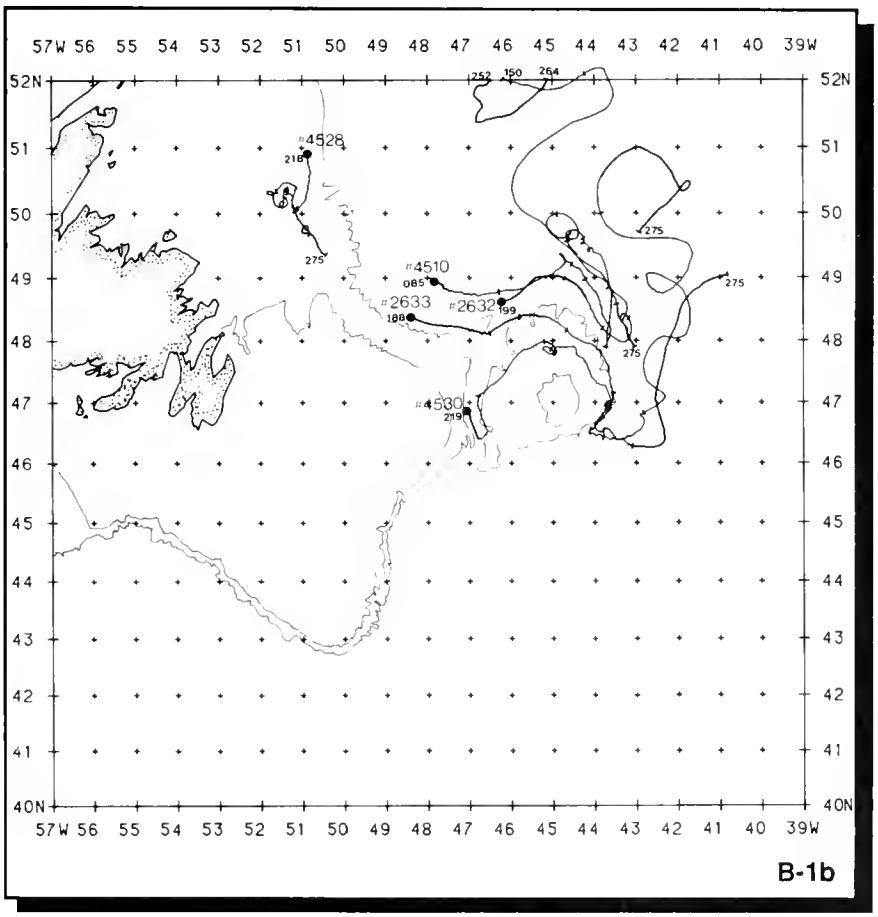

B-1b

TOD #4512 was deployed at the northern end of the Flemish Pass on 27 April (118) in position 47°51.6'N 47°30.0'W. TOD #4512 essentially followed the bathymetry south to the Tail of the Bank at an average velocity of 33 cm/s. On 24 May (145), TOD #4512 was caught up in the North Atlantic Current and began moving northeast. It was caught in a cyclonic eddy between 6 June and 27 June (158-179) (average velocity in eddy was 35 cm/s; radius of motion about 90 km). The METOC SST charts indicated the presence of two warm core (anticyclonic) eddies in the area where TOD #4512 exhibited cyclonic motion (Figure B-3). It continued drifting to the northeast at an average velocity of 74 cm/s. TOD #4512 exited the International Ice Patrol region at 46°41'N 39°00'W on 14 July (196).

TOD #4514 was deployed in the northern area of the Avalon Channel on 28 April (119) in position 48°15'N 52°20'W. It drifted slowly to the southwest at an average velocity of 14 cm/s until 7 May (128). No further

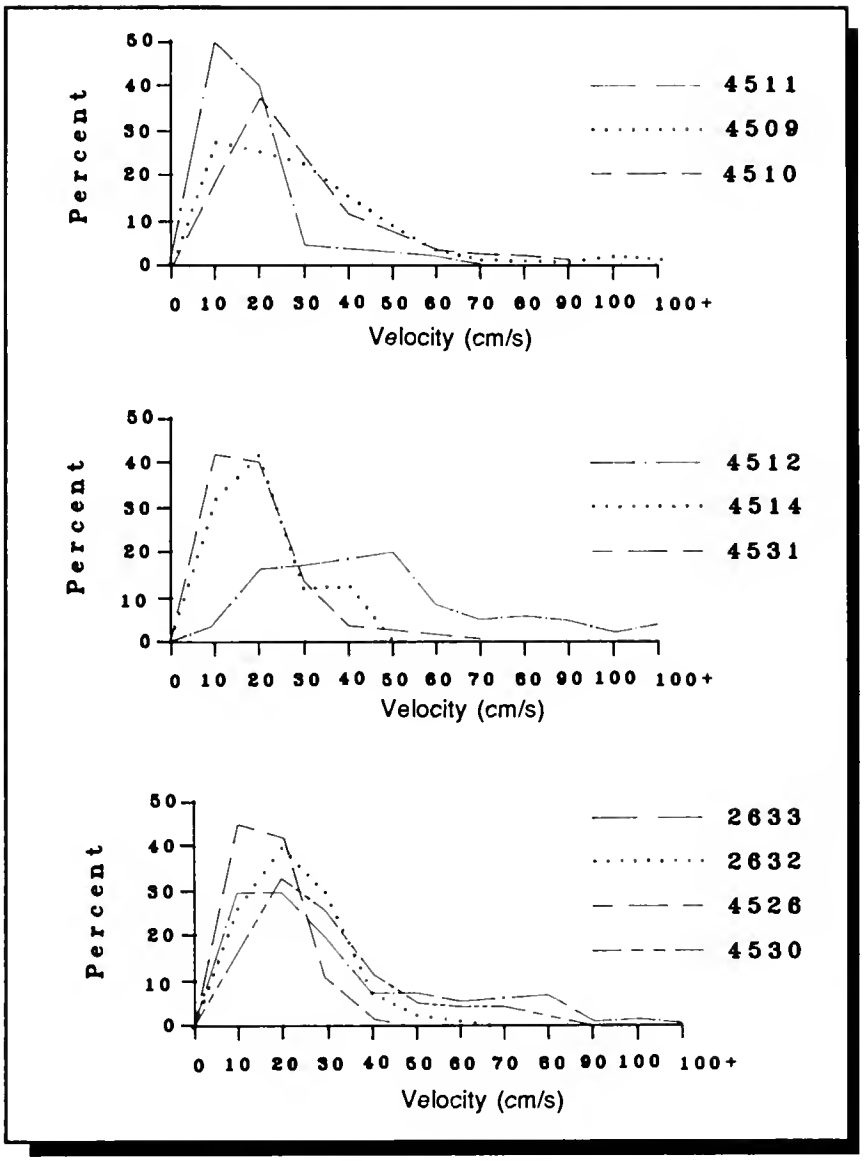

Figure B-2. *Velocity distributions for International Ice Patrol's 1984 TODs. TOD #4512's velocity distribution is significantly different from all others because it remained in the Labrador Current and the North Atlantic Current for the duration of its drift in the International Ice Patrol area.*

signal was received from TOD #4514 after that date, but this short drift illustrated much less than the 49 cm/s average velocity used by the historical current file in this section of the Avalon Channel.

TOD #4531 was deployed about 110 km northwest of the northern end of the Flemish Pass (48°32'N 48°01'W) on 13 June (165). It moved slowly (average velocity 12 cm/s) northward until 30 August (241). It then travelled southward roughly paralleling its northbound leg, about 8 km west of the northbound leg, at 12 cm/s until 18 September (262). After this date, TOD #4531 drifted east, then southeast at 29 cm/s until 1 October (275). The section of the drift after 18 September (262) was nearly perpendicular to the historical current field for that area.

The next two TODs were deployed from USCGC HORNBEAM during the IIP cruise. TOD #2633 was deployed from USCGC HORNBEAM during the IIP cruise. TOD #2633 was deployed on 6 July (188) at hydrographic station #23 in position 48°20'N 48°30'W. It drifted eastward over the top of the Flemish Cap and roughly followed the bathymetry south on the eastern side of the Cap until 28 August (241). It then began drifting northward at an average velocity of 39 cm/s in the North Atlantic Current. As of 1 October (275), TOD #2633 appeared to be caught in the circulation of an anticyclonic (warm core eddy) centered near 50°30'N 43°00'W. TOD #2632 was deployed on 17 July (199) next to the iceberg used in the drift and deterioration experiment described below. TOD #2632 drifted northeast and then southeast roughly following the bathymetry around the top of Flemish Cap until 11 August (224). TOD #2632 then drifted northwest at about 19 cm/s until 5 September (249) and then drifted southeast at 16 cm/s through the same general area it had just traversed. This drift helps illustrate the large temporal variability of the flow field in the Grand Banks region.

TOD #4528 was deployed on 5 August (218) in an area of high iceberg concentration at 50°59.4'N 51°01.2'W. It drifted southward at an average velocity of 15 cm/s until 17 August (230). It then apparently became caught in a weak cyclonic eddy and remained entrapped until 13 September (257). TOD #4528 continued drifting south at 12 cm/s until 1 October (275). The southward velocities indicate that TOD #4528 was not in the Labrador Current, yet the METOC SST charts indicate it should have been on the western edge (Figure B-3). This suggests the METOC SST charts alone cannot always be used to identify the location of the Labrador Current.

Figures 3 (a-g)
Canadian METOC Sea Surface Temperature Charts for the indicated periods. Sea Surface Temperatures (C°)

The final TOD of the 1984 season, TOD #4530, was deployed on 6 August (219) in the center of the Flemish Pass in position 46°46.8'N 46°54.4'W. It drifted south at 10 cm/s until 8 August (221). It then drifted north around the top of the Flemish Cap and continued to follow the bathymetry south down the east side of the Cap until 23 September (267). The average velocity around the Cap was 22 cm/s. Kollmeyer (1966) had reported the presence of a north flowing counter current in the Flemish Pass. This drift was similar to that found by Shuhy (1981). After 23 September (267), TOD #4530 began drifting with the North Atlantic Current towards the northeast at an average velocity of 64 cm/s.

The 1984 TOD's clearly demonstrate the variability of the flow field in the vicinity of the Grand Banks. The differences in TOD tracks #4510, #2633, #2632, #4530, and #4531 indicate that the axis of the North Atlantic Current migrates east and west in the area northeast of the Flemish Cap. The velocity distribution of TOD #4512 is significantly different from the remaining distributions (Figure B-2). It was the only TOD that remained in either the Labrador Current or the North Atlantic Current for its duration in the International Ice Patrol operating area. Considering the variability of the flow field, TOD's are essential to International Ice Patrol's ability to successfully predict the movements of icebergs in the Grand Banks area.

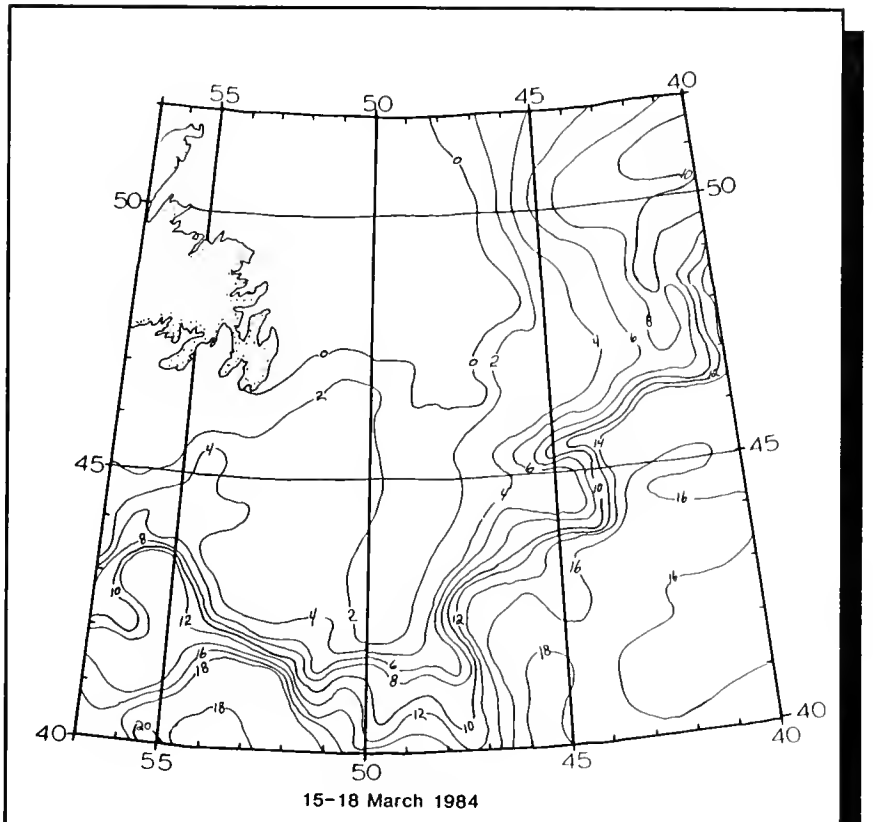

Figure 3-a

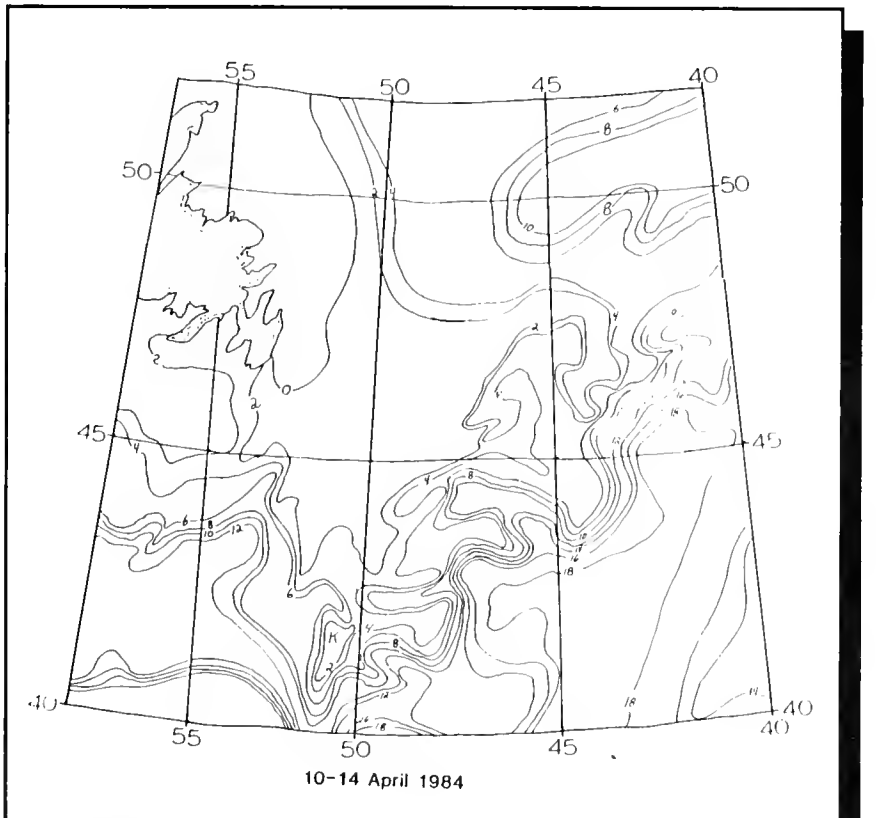

Figure 3-b

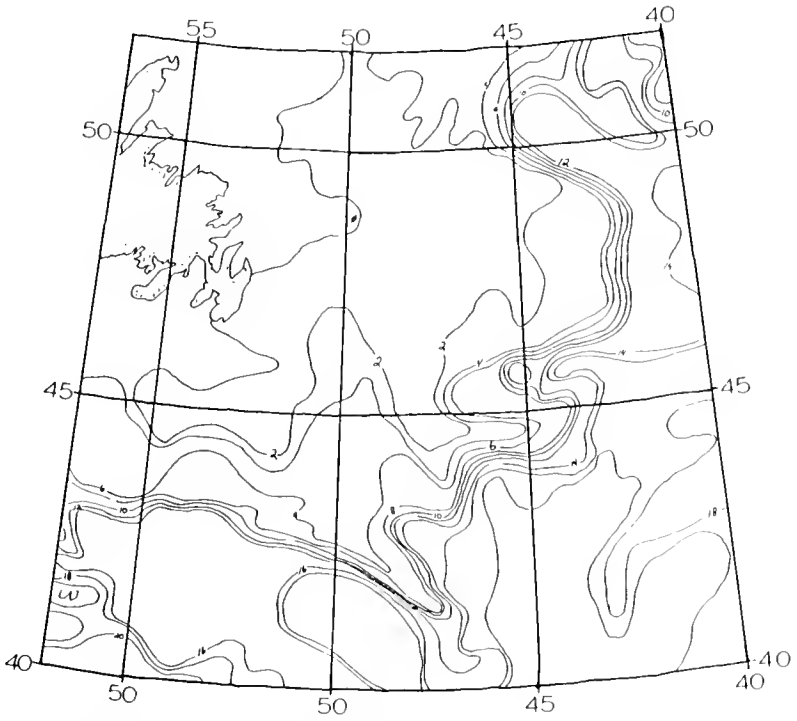

Figure 3-c 10-14 May 1984

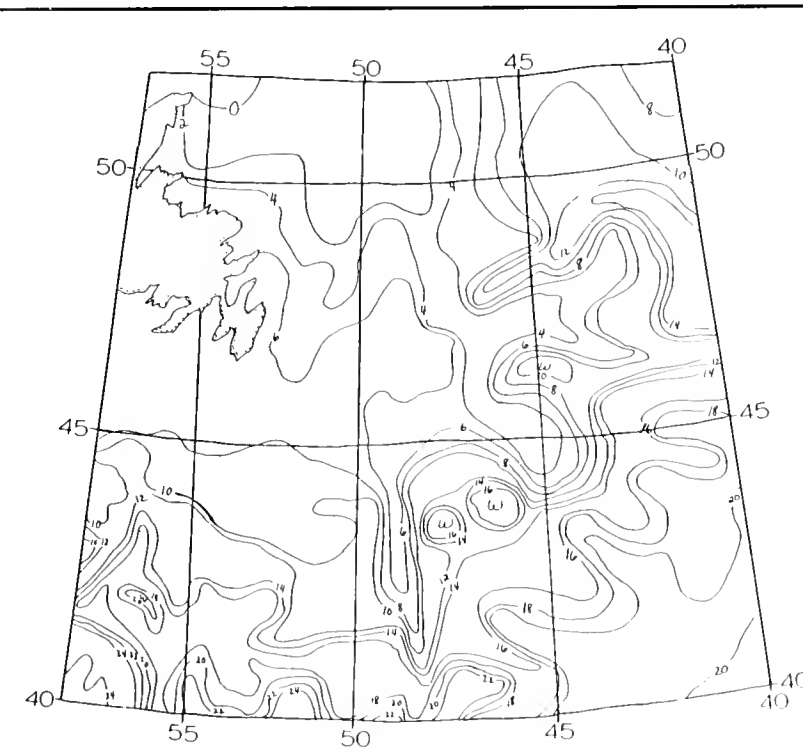

11-14 June 1984

Figure 3-d

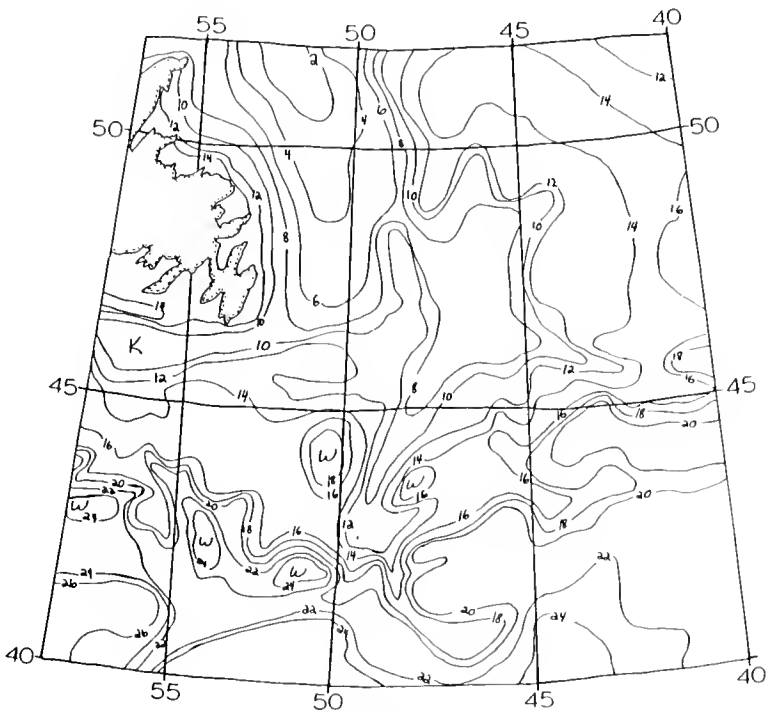

13-16 July 1984

Figure 3-e

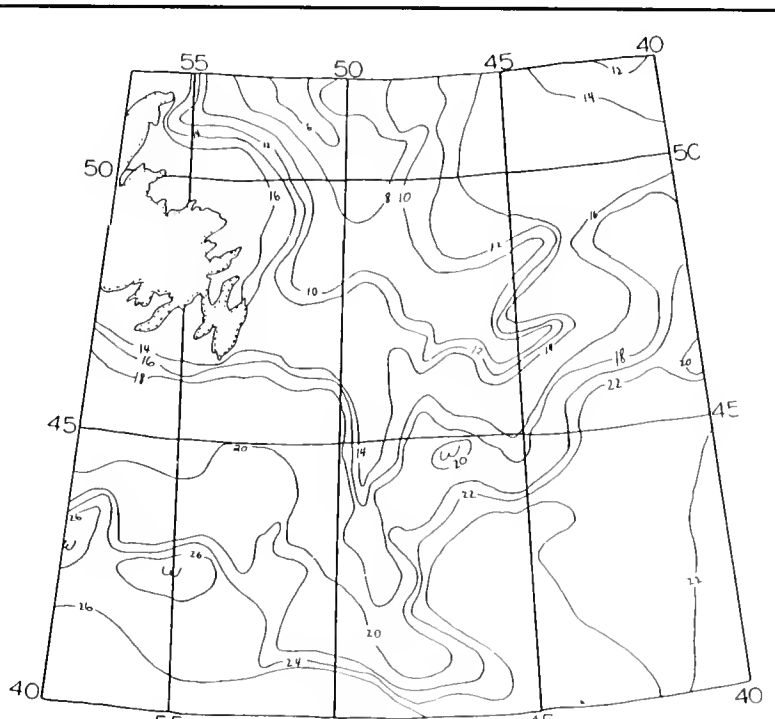

10-13 August 1984

Figure 3-f

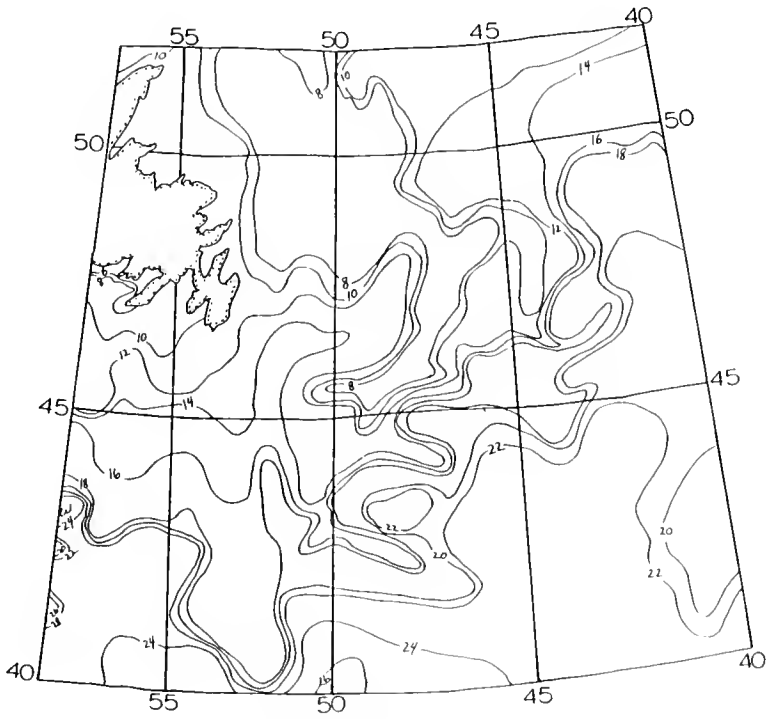

Figure 3-g

Hydrographic Survey

A two part oceanographic cruise was conducted from USCGC HORNBEAM (WLB-394). The first part was a hydrographic survey conducted between 1 and 11 July 1984 (Figure B-4). One of the objectives of this year's cruise was to compare TOD drift with geostrophic current. The International Ice Patrol has assumed TOD drift tracks can be used to calculate geostrophic currents since first using TODs in 1976. The Ice Patrol uses a computer program to remove wind driven current based on Ekman dynamics from TOD drifts and computes a "quasi-geostrophic" current. This current information is used to modify the time-invariant historical geostrophic current field used to predict iceberg motion. Another objective of the cruise was to determine how accurately Fleet Numerical Oceanography Center (FNOC) environmental products compared with actual conditions. We were interested in the magnitude of the errors in the products we received from FNOC.

Seventy-five of a planned 100 hydrographic stations were occupied during the first phase (Figure B-5). Water samples were collected using Nansen bottles at all standard depths to 500m (Table B-2). Nansen bottles were used because the Coast Guard's Ocean Sampling System (a Conductivity, Temperature, Depth instrument) was inoperative. A minimum of two protected deep sea reversing thermometers were attached to each Nansen bottle sampling above 200m. An unprotected deep sea reversing thermometer was also used on bottles sampling 200m and deeper. The conductivity ratios and corresponding salinities of all water samples were determined at sea, while corrected temperature values were determined after returning to Groton. The dynamic height contours relative to the 500 decibar pressure surface for the survey area are shown in Figure B-6. In previous surveys, dynamic heights were computed from CTD or STD data relative to the 1000 decibar surface and then contoured at 0.02 dynamic meter intervals (Kollmeyer, 1966; Scobie and Schults, 1976). Due to the inherent errors associated with Nansen casts (as compared to CTD data) and the spacing of the station lines, the data from this cruise were contoured at 0.05 dynamic meter intervals. All of the water samples from the 500m bottles had nearly the same temperature and salinity values, indicating the water at 500m was nearly homogeneous for the entire survey area. Historical IIP data shows the geopotential surfaces below 500 decibars are mainly isosteric and contribute only a small fraction to surface dynamic height variations, making relative measurements to 500 decibars valid for examining circulation in this area.

TOD #2633 was deployed immediately after occupying station #23 (48°20'N 48°30'W) on 6 July (188). The anticipated drift was through the survey area. For the first three to four days, TOD #2633, for the most part, followed the observed geostrophic flow (Figure B-6). The geostrophic current in this section of the hydrographic survey was well-defined. For the

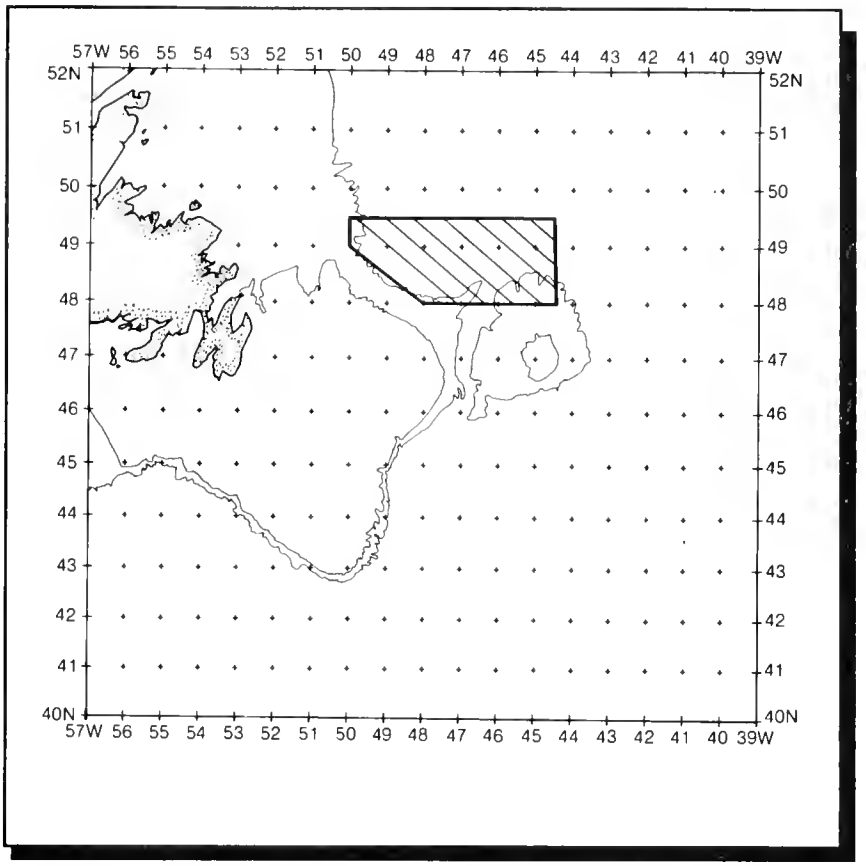

Figure B-4. *The location of the hydrographic survey conducted by International Ice Patrol from the USCGC HORNBEAM, 1-11 July 1984*

period of 6 -10 July (188-192) (when the buoy followed the geostrophic flow), the thermocline depth was about 20m for the area through which the buoy drifted. For this period, the drogue was below the middle of the thermocline.

East of 46°30'W, the observed geostrophic current field became less distinct. By the time TOD #2633 crossed 46°W on 20 July (202), the hydrographic data was 10 days old. The observed currents east of 46°W were weak. The current field of that particular area has a high degree of variability (Soule, 1964; Scobie and Schultz, 1976). For the period of 24 July - 1 August (206-214), TOD #2633 more closely followed the wind current (Figure B-7). The thermocline depth varied between 35m and 40m, indicating the drogue was above the middle of the thermocline, and thus, in the surface mixed layer. To illustrate this effect, the buoy motion is compared with a calculated wind driven current based on McNally (1981). He used 1.5% of the wind speed directed 30° to the right of downwind. Measured winds from HORNBEAM were used to calculate the wind driven current when available. Otherwise, FNOC winds were used.

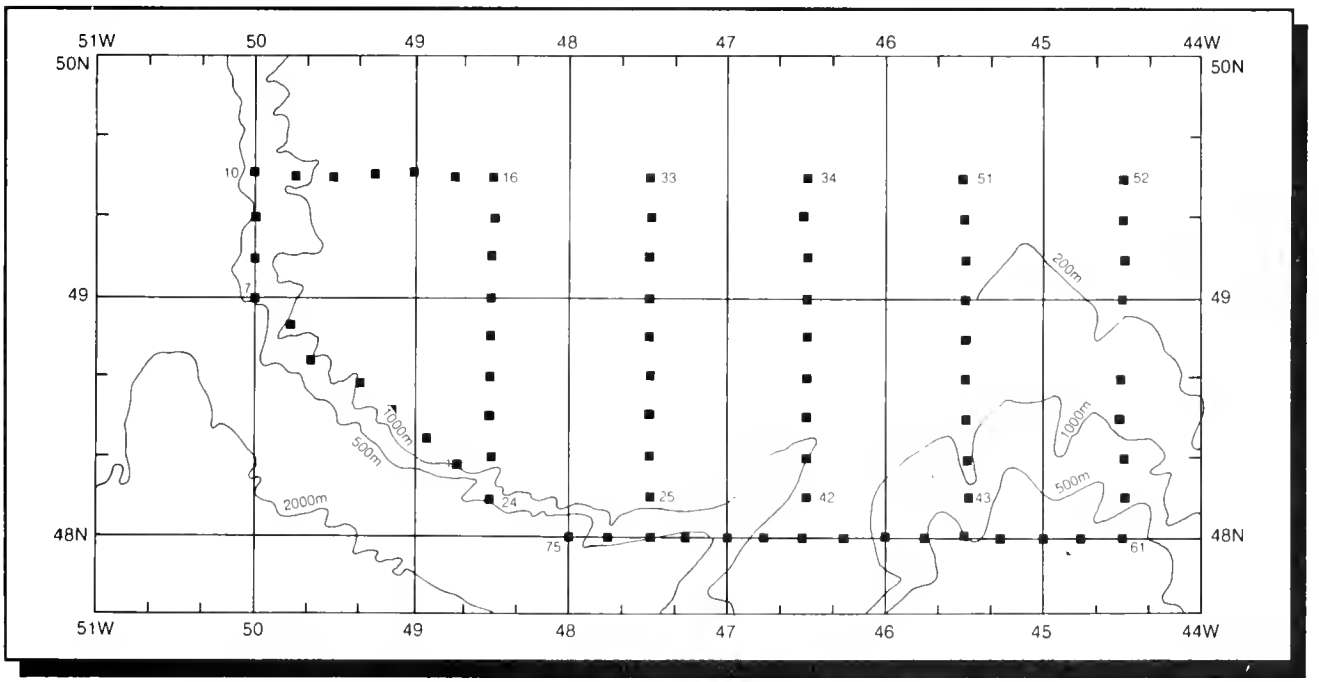

Figure B-5. *Hydrographic cast stations taken from USCGC Hornbeam 1-11 July 1984*

Table B-3. Measured vs FNOC Winds

Date	Direction+ Difference	Speed+ Difference	Speed Difference/ Measured Wind Speed*	Speed Difference/ FNOC Wind Speed*
7 JUL	40°	-6.5 M/S	162%	-62%
8 JUL	82°	-0.5 M/S	10%	-9%
10 JUL	-10°	-2.0 M/S	29%	-22%
11 JUL	0°	-2.5 M/S	28%	-22%
15 JUL	-32°	-2.0 M/S	22%	-18%
16 JUL	-43°	-5.5 M/S	110%	-52%
16 JUL	4°	0.0 M/S	0%	0%
17 JUL	-96°	-2.0 M/S	36%	-27%
18 JUL	30°	-3.0 M/S	40%	-29%
18 JUL	-20°	-2.5 M/S	50%	-33%
20 JUL	-23°	-6.0 M/S	120%	-55%
21 JUL	-11°	-1.0 M/S	22%	-18%
22 JUL	-27°	0.5 M/S	-7%	+7%
AVG	-8.2°	-2.5 M/S	48%	-26%
STD**	43°	2.2 M/S	51%	21%

+ Observed - FNOC; * Times 100; ** Standard Deviation

Table B-2

Standard Depths Sampled

0m	75m	300m
10m	100m	400m
30m	150m	500m
50m	200m	

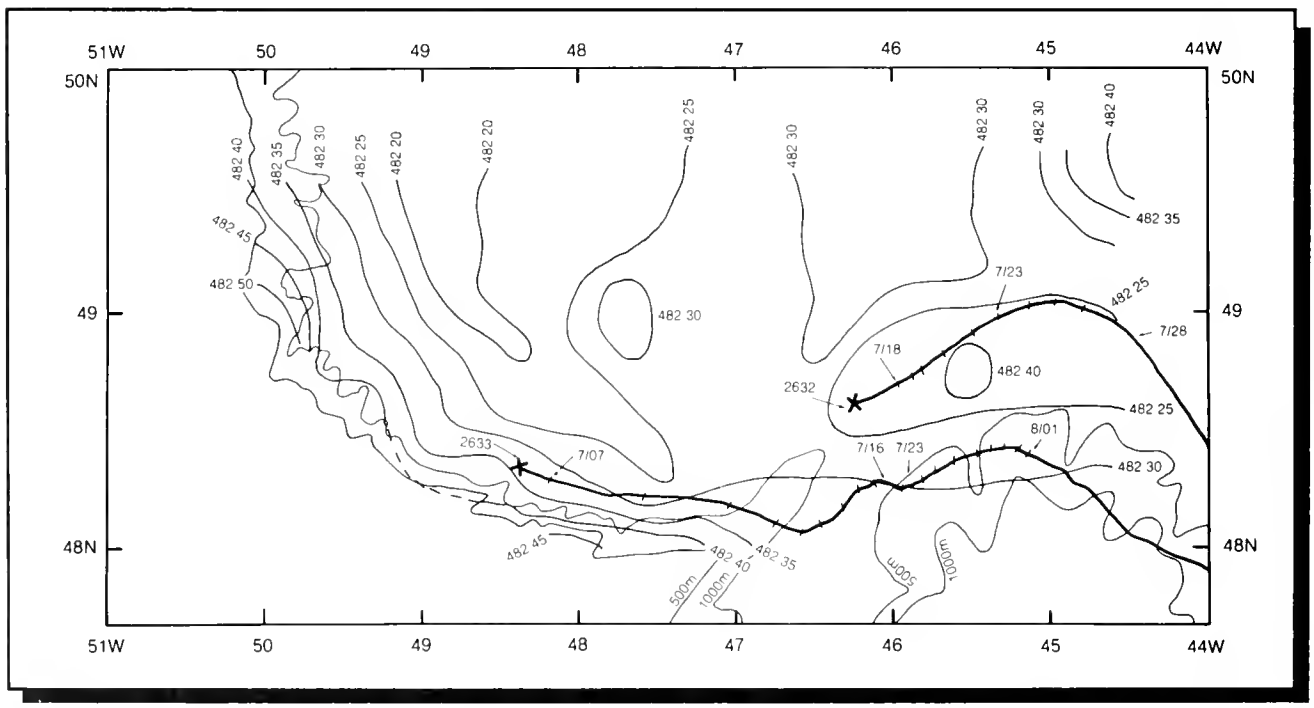

Figure B-6. *Dynamic heights calculated from the hydrographic survey of 1-11 July 1984 relative to the 500 decibar surface. The contouring interval is 0.05 dynamic meters. The 500m and 1000m depth contours are plotted. The heavy dark lines are the drift tracks of TODs #2633 and 2632 with the* **X** *indicating deployment positions.*

TOD #2632 was deployed as part of an iceberg drift and deterioration study and it remained in the survey area until 28 July (210). The drogue of TOD #2632 remained above the middle of the thermocline (35-40m) for the period of 17-28 July (199-210). The drift of TOD #2632 within the survey area can be almost totally explained by the wind driven current.

During both phases of the cruise, wind speed and direction measurements were taken aboard HORNBEAM every hour. The anemometer was approximately 15m above the water. The FNOC Marine Layer Wind product used by IIP represents winds 19.5m above the sea surface. Twelve hour average measurements for 0000Z and 1200Z (+/- 6 hours) were determined and compared to the analysis wind products received from FNOC. It should be noted that a comparison is being made between point source winds (HORNBEAM) and spatially averaged winds (FNOC). The data show that wind velocity computed by FNOC was consistently higher than that measured (Table B-3). The FNOC winds are used in the

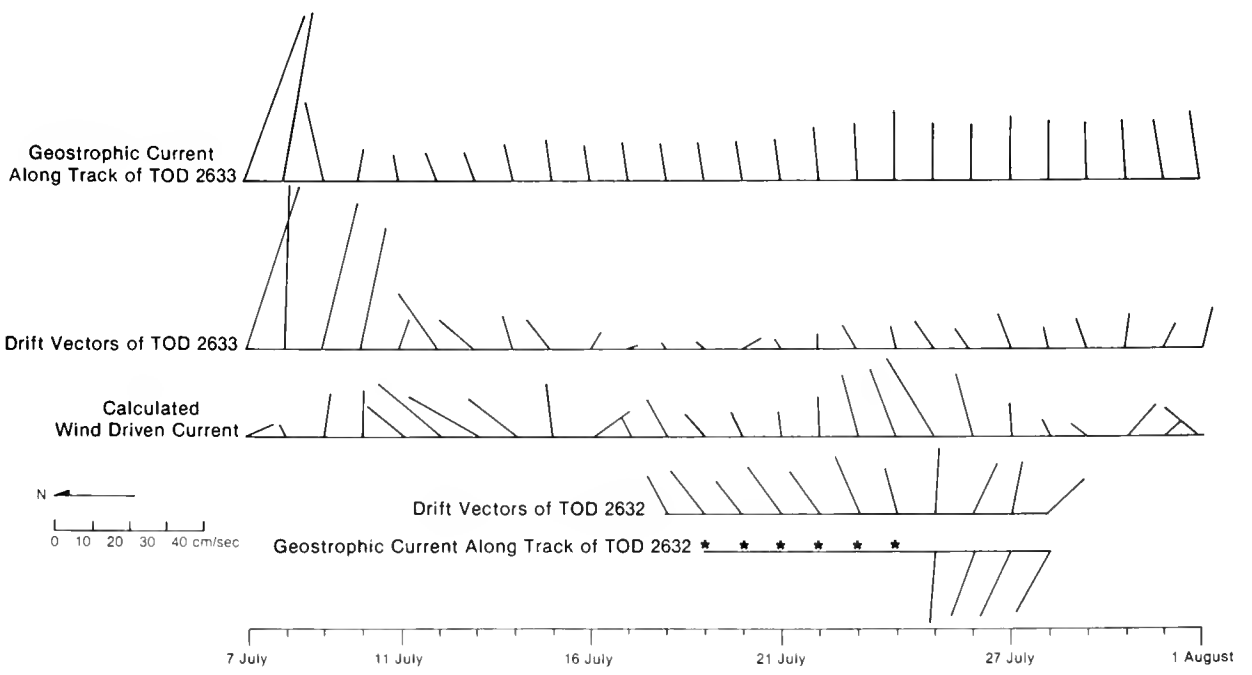

TOD Drift, Measured Geostrophic Current, and
Calculated Wind Driven Current

Figure B-7. *The geostrophic current shown for each TOD track was calculated from data obtained1-11 July 1984. The TOD drift vectors are a 24-hour average centered around 1200 GMT of each day. The wind driven current was calculated based on McNally (1981) and used 1.5% of the wind speed directed 30° to the right of downwind. Observed winds from the HORNBEAM were used in the calculations when available (7-11 and 16-21 July). FNOC winds were used for the remaining calculations. The * indicates an area where accurate geostrophic currents could not be calculated.*

Iceberg Drift and Deterioration

process described above to create a "quasi-geostrophic" current from the TOD drift data. This apparent over-estimate of the wind velocity would adversely affect the calculation of the Ekman wind current subtracted from the TOD motion. This study of the FNOC winds was not meant to be exhaustive but was an effort to identify possible sources of error in our calculations of the Ekman wind driven current.

The second part of the cruise was an iceberg drift and deterioration study conducted between 16 and 22 July 1984. The primary objective of the second phase was to evaluate the iceberg deterioration model being used by IIP. The iceberg deterioration model was used operationally during both the 1983 and 1984 seasons. The model is described in detail in Anderson (1983b). We hoped to locate a group of icebergs of various sizes and follow them and observe their deterioration. By following the melting icebergs, obtaining drift data was only a matter of recording the iceberg position periodically.

A medium iceberg approximately 120m long by 115m wide by 37m high was located on the afternoon of 16 July in position 48°41.9'N 46°20.4'W (Figure B-8). We were able to follow this iceberg until the morning of 22 July before we had to depart the area. At our departure, the iceberg was about 40m long, 28m wide, and 12m high (Figure B-8). The dimensions given here and discussed below will be maximum dimensions in each phase regardless of shape. Unfortunately, we were not able to locate a group of icebergs to observe.

Most of the size measurements of the iceberg were determined using a reticulated laser range finder. Due to extremely poor visibility (less than 200m) during

Table B-4 Actual vs Modelled Iceberg Deterioration

Date/Time July/Zulu	Actual Length	Predicted Length	Predicted Deterioration Due to: Insolation	Buoyant Convection	Wind-Forced Convection	Wave Erosion
16/1400	120m	120.0m	----	----	----	----
16/1800	137m	117.7m	.01m	.03m	.20m	2.08m
17/0600	114m	110.3m	.01m	.10m	.63m	6.54m
17/1800	102m	105.1m	.01m	.10m	.66m	4.46m
18/0600	87m	99.2m	.01m	.10m	.66m	5.09m
18/1800	90m	92.3m	.01m	.11m	.68m	6.06m
19/0600	91m	85.5m	.01m	.11m	.68m	5.95m
19/1800	87m	79.6m	.01m	.11m	.72m	5.08m
20/0600	67m	73.8m	.01m	.11m	.72m	4.98m
20/1800	----	69.0m	.01m	.11m	.72m	3.99m
21/0600	60m	64.7m	.01m	.12m	.79m	3.41m
21/1800	53m	60.4m	.01m	.12m	.79m	3.41m
22/0600	40m	54.9m	.01m	.13m	.84m	4.49m

Figure B-8. *Photographs of the iceberg observed during the drift and deterioration portion of the 1984 International Ice Patrol cruise.*
Top: *1426Z 16 July 1984, 115-120m across base, maximum height 37m.*
Bottom: *1400Z 21 July 1984, 45-50m across base maximum height 13m.*

the last two days of the study, measurement estimates of the dimensions of the iceberg were made by bringing HORNBEAM alongside the iceberg. The estimates were made using the frame numbers on the HORNBEAM. Photographs of the iceberg were taken and the range to the iceberg and the focal length of the lens recorded so measurement estimates could later be made from the pictures. The position of the iceberg, wave height and period, and wind force and direction were recorded hourly. SST was recorded several times per day.

The observed environmental information was used as inputs into IIP's deterioration model (Table B-4). An assumed relative motion of 25 cm/s was used in calculating wind force convective melting. Calculated remaining length was plotted against the maximum observed length (Figure B-9). The results show the model gives fairly good predictions for this one case.

There were several major calving events observed. The IIP model does not include calving. El-Tahan, et al. (1984) used a time integrated scheme at the iceberg waterline wave-cut notch to model calving. (The loss due to calving is estimated to be of the same order as wind driven convection.) The iceberg we observed showed some weakness in the above scheme. El-Tahan, et al. (1984) assume the iceberg remains in a constant

Figure B-9. *Observed vs remaining length predicted by International Ice Patrol's deterioration model. The observed wave height and sea surface temperature (SST) were used as the model inputs. The tick marks on the observed length indicate observed instances of iceberg rollover.*

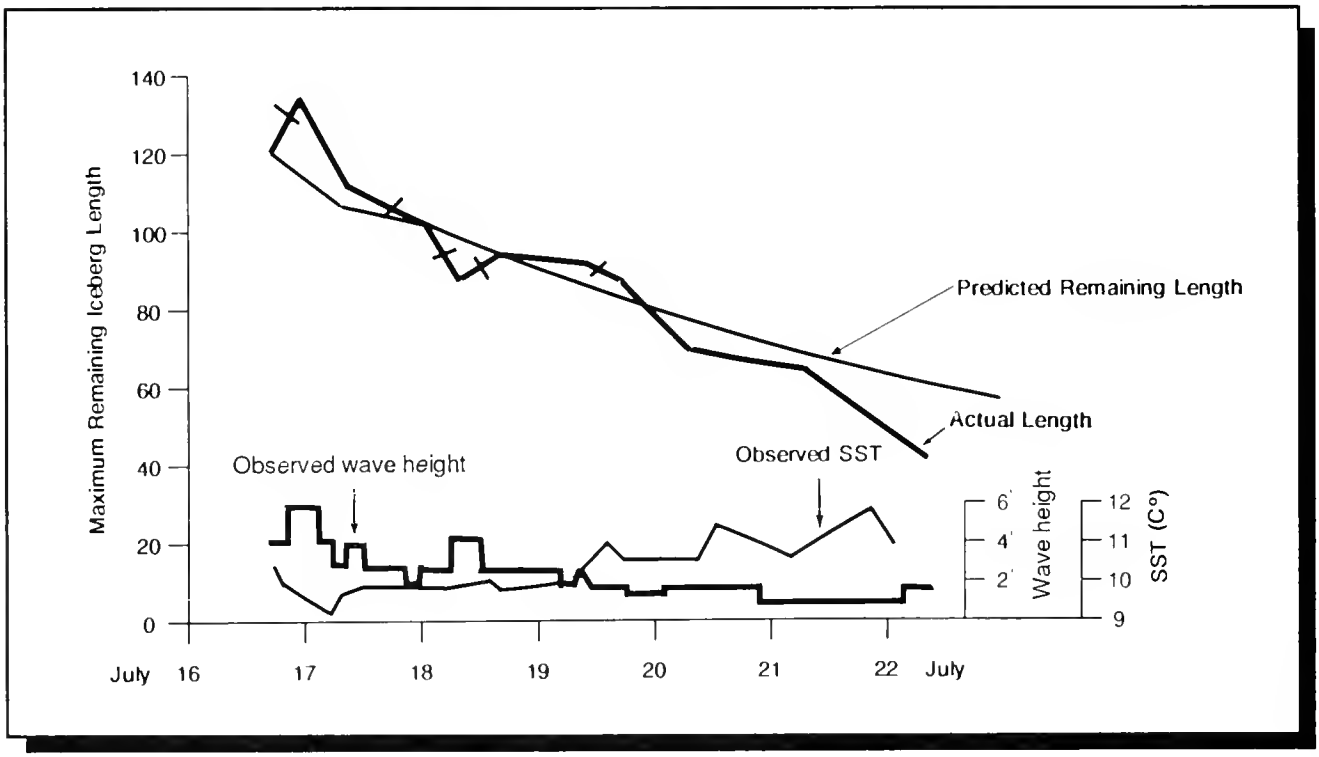

attitude to the wave field. The iceberg we observed rolled at least seven times in five days. Each time it rolled, a different section of the iceberg was exposed to wave erosion, therefore requiring their integration scheme to start over. Since iceberg rollover cannot be modelled, calving will not be included in our model until an acceptable scheme is available. This will allow the predictions from our model to remain on the conservative side.

Radar ranges and bearings to the iceberg and HORNBEAM's position as determined by LORAN-C were recorded every hour. The geographical position of the iceberg was then determined.

On 17 July, TOD #2632 was deployed within 400m of the iceberg in position 48°37.4'N 46°06.1'W. The TOD drifted to the northeast at a speed slower than the iceberg. After five days, the TOD was located 16.5 nm away and bearing 252°T from the iceberg (Figure B-10). This is approximately upwind (using the average wind for the period) of the iceberg, indicating the difference between the iceberg and the TOD may be due to the different leeway of the iceberg and the drift buoy.

The initial sighting position of the iceberg was entered into IIP's iceberg drift model and allowed to drift until 0000Z 22 July. FNOC winds and unmodified historical currents were used as the environmental inputs to the model. The maximum difference between the actual and predicted position of the iceberg was 7.2 nm and occurred 30 hours after the sighting. The error after five days was only 4.3 nm (Figure B-11). This preliminary analysis of the drift data is encouraging because the accumulated error was so small. Further analysis of this and other iceberg drift data still needs to be done.

Conclusions

The cruise has answered part of the question posed concerning the TOD's ability to follow the geostrophic flow. The data indicates that a TOD will follow the geostrophic flow as long as the drogue is below the thermocline. For next season, IIP intends to lengthen the drogue tethers on the buoys to 50m to place the drogues consistently below the surface layer and the thermocline in the area north of 43°N (Scobie and Schultz, 1976). This plan would eliminate the step of removing wind-driven current from the TOD motion to calculate geostrophic current.

The comparisons of FNOC winds conducted in both 1983 and

Figure B-10. *Actual iceberg and TOD drift from 17-22 July.. The predicted iceberg motion is from the International Ice Patrol drift model. The model drift was begun on 16 July and all predicted motion is from this initial sighting. Tick marks are at 0000Z each day.*

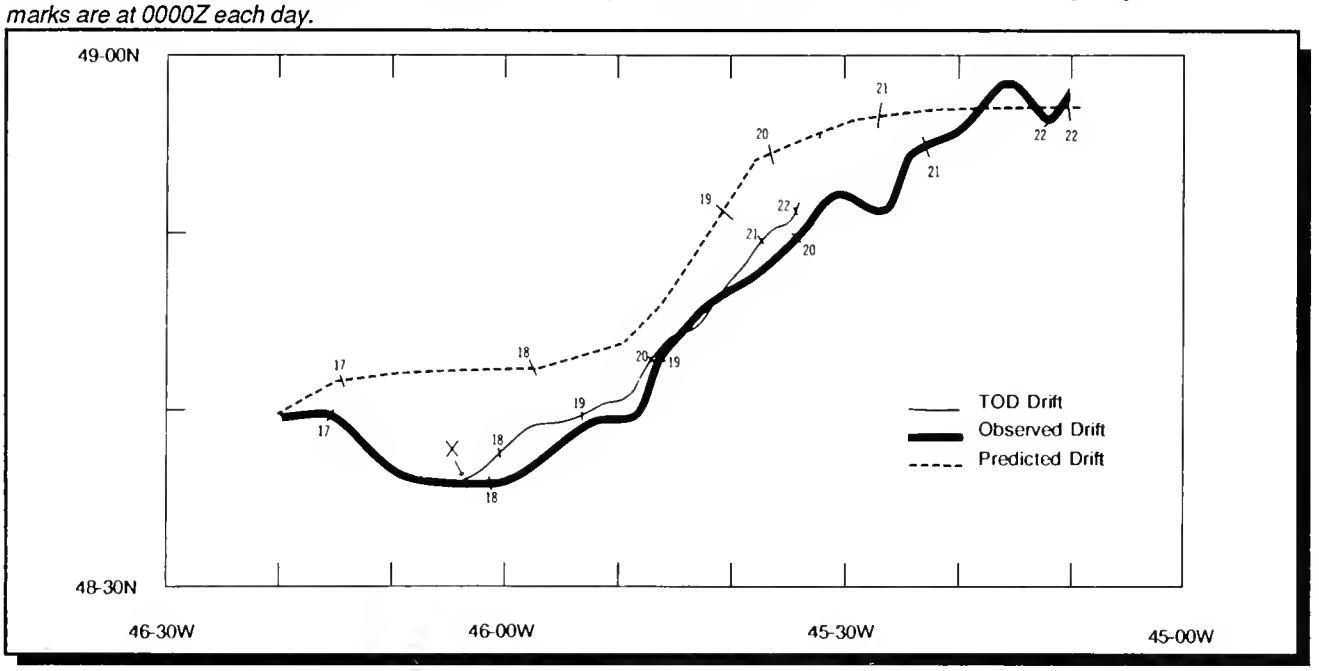

Figure B-11. *The iceberg Drift model error plotted vs total distance the iceberg drifted. The iceberg was drifted continuously by the model from its initial sighting position on 16 July 1984.*

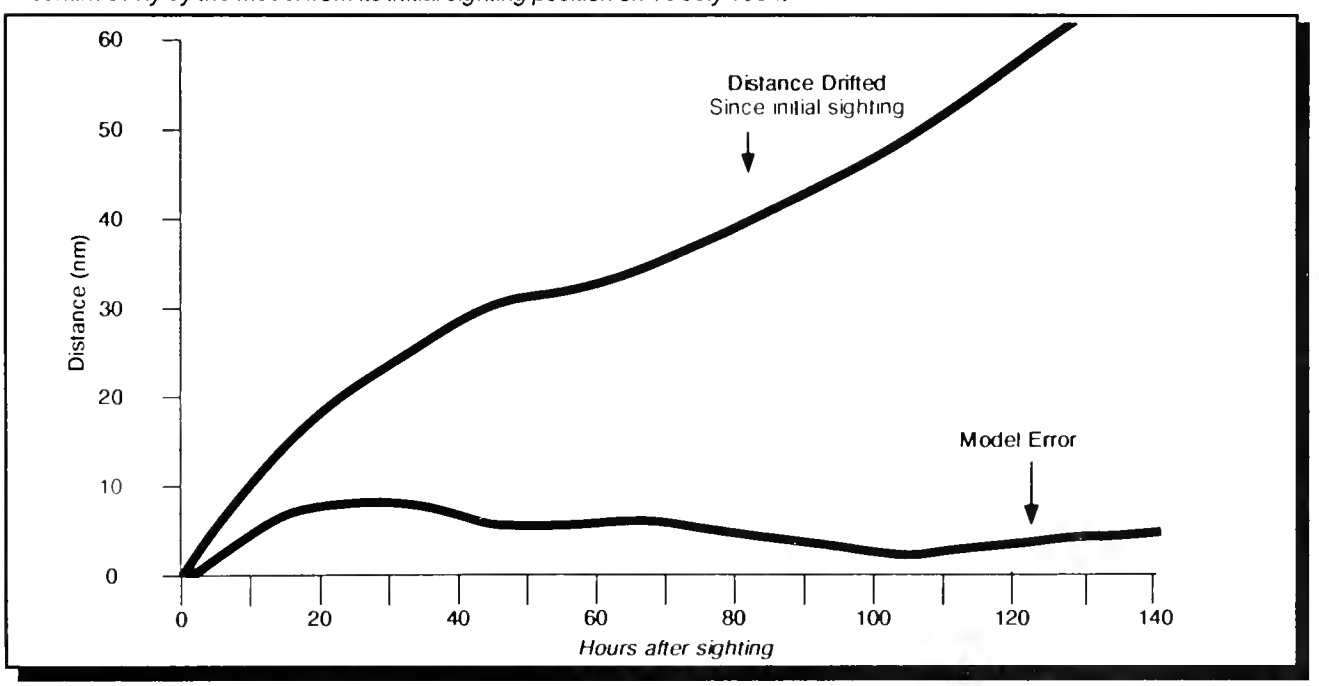

1984 have indicated that the FNOC velocities are consistently too large. This was an added error source in computing geostrophic current motion using the existing method. By using a 50m tether and eliminating the step of removing the wind driven current, the new TOD motion should more closely measure the geostrophic current in our operating area.

IIP intends to continue using TODs to modify the historical current field on a real-time basis. The experiment of a TOD following the geostrophic current will be repeated on future hydrographic cruises using a CTD system rather than Nansen bottles to measure the water column characteristics.
The results from the iceberg deterioration study are very encouraging, but our data set of one is not large enough to draw any conclusions. The deterioration model will be used in its present form, and a total deterioration percentage of 175% of the original length will be used as the point where deletion from the active iceberg list will be considered.

IIP does not plan to make further changes to our iceberg drift model before next season. IIP plans to evaluate the drift model using the drift data obtained from HORNBEAM, data from TIROS Arctic Drifters aboard icebergs during the 1983 season, and other sources. This analysis should allow IIP to evaluate the estimates of the model's error.

References

Anderson, I. (1983a); "Oceanographic Conditions on the Grand Banks During the 1983 International Ice Patrol Season", *Report of the International Ice Patrol Service in the North Atlantic Ocean,* CG-188-38, p. B1-B16.

Anderson, I. (1983b); "Iceberg Deterioration Model", *Report of the International Ice Patrol Service in the North Atlantic Ocean,* CG-188-38, p. C1-C8.

El-Tahan, M.; S. Ventatech; and H. El-Tahan (1984): "Validation and Quantitative Assessment of the Deterioration Mechanisms of Arctic Icebergs", *Proceedings of the Third International Offshore Mechanics and Arctic Engineering Symposium,* p. 18-25.

Kollmeyer, R.C.; T.C. Wolford; and R.M. Morse (1966): "Oceanography of the Grand Banks Region of Newfoundland in 1965), *U.S. Coast Guard Oceanographic Report No. 11,* CG-373-11, p. 157.

McNally, (1981); "Satellite Tracked Drift Buoy Observations of the Near-Surface Flow in the Eastern Mid-Latitude North Pacific", *Journal of Geophysical Research,* Vol. 86(C9), p. 8022-8030.

Scobie, R.W. and R.H., Schultz (1976); "Oceanography of the Grand Banks of Newfoundland, March 1971 - December 1972", *U.S. Coast Guard Oceanographic Report No. 70,* CG 373-70, p. 298.

Shuhy, J.L. (1981); "Oceanographic Conditions on the Grand Banks During the 1981 International Ice Patrol Season", *Report of the International Ice Patrol Service in the North Atlantic Ocean,* CG-188-36, p. A1-A3.

Soule, F.M. (1964); *The Normal Topography of the Labrador Current and its Environs in the Vicinity of the Grand Banks During the Iceberg Season,* WHOI Publication 64-36, p. 17.

Appendix C

Effects of Side Looking Airborne Radar (SLAR) on Iceberg Detection During the 1983 and 1984 International Ice Patrol Seasons

Lieutenant (jg) Neal Thayer, USCGR

Introduction

The AN/APS-135 Side-Looking Airborne Radar (SLAR) was introduced to International Ice Patrol (IIP) reconnaissance flights at the beginning of the 1983 IIP season, the first continuous operational use of SLAR by IIP. The AN/APS-135 is a replacement for the AN/APS-94D SLAR which was occasionally used by IIP on an experimental basis starting in 1976. With this more powerful AN/APS-135 SLAR, visual reconnaissance was replaced by SLAR as the main search method, and reconnaissance coverage of the IIP region was significantly increased. Since the IIP region is an area of frequent heavy fog and bad weather, the all-weather capability offered by SLAR increased both the number of days that IIP could conduct reconnaissance flights and the amount of reconnaissance coverage of search areas under conditions of intermittent visibility. In addition, longer flights became possible with SLAR, and regular reconnaissance of the eastern part of the region began. This increased capability is evident in that prior to the 1983 season, it was necessary to maintain an Ice Reconnaissance Detachment (ICERECDET) in Newfoundland continuously during the IIP season, while in 1983 and 1984, ICERECDET's were deployed every other week with the same number of flight hours as in previous years.

The introduction of SLAR constitutes a major change in the IIP iceberg detection techniques. An important question arises from this change. What effect does SLAR have on the number of icebergs south of 48°N, the traditional indicator of the severity of an iceberg season? This question is addressed in Part b. of the following section using the IIP data base for the years 1960 through 1984, data contained in the IIP historical data file. Part a. is a brief discussion of the effect on the number of icebergs estimated south of 48°N due to the introduction of the iceberg drift prediction model (IBERG) to International Ice Patrol operations in 1979.

Discussion

In 1900, the U.S. Naval Hydrographic Office began estimating the number of icebergs passing south of 48°N as a measure of the severity of each iceberg year. The International Ice Patrol, with its beginning in 1914, continued to keep records of this number. Prior to 1983, the mean annual number of icebergs south of 48°N was 364, with a range from 0 in 1966 to a record of 1584 in 1972. The number of icebergs south of 48°N was 1348 in 1983, representing the fourth highest number on record, and 2202 in 1984, the new record. Given the increased iceberg detection capability offered by SLAR, it seems possible that these elevated figures for 1983 and 1984 are primarily the result of SLAR reconnaissance. As a result, comparing the 1983 and 1984 numbers of icebergs south of 48°N directly with those of previous years might provide a misleading indication of the severity of these two seasons.

a. Iceberg Drift Prediction Model

In investigating the effect of SLAR, it was first necessary to assess the possible impact of the IBERG drift and deterioration model on the number of icebergs estimated south of 48°N, with its introduction to IIP operations in 1979. Any significant effect on the number of icebergs estimated south of 48°N would necessitate treating the IBERG and pre-IBERG data separately in the SLAR analysis. The IBERG impact was analyzed by comparing the number of icebergs south of 48°N with the number of sightings south of 48°N. Table C-1 shows the number of non-growler sightings south of 48°N from the International Ice Patrol historical data file for 1960 through 1984. Since the number of icebergs estimated south of 48°N does not include growlers, growler sightings were removed from the data. The ratio of non-growler sightings south of 48°N to icebergs estimated south of 48°N has three groups of values with significantly different ranges: prior to 1965 (9.9 to 16.4), 1965 through 1978 (0 to 39.8), and after 1978 (90.5 to 800). The change in this value in 1965 is not explicable through any change in methods mentioned in International Ice Patrol records. After 1979, the change in this ratio was due to the introduction of the iceberg drift prediction model (IBERG) to International Ice Patrol operations. It is important to note that the ratio increased dramatically in 1979, and that in 1980, the "sense" of the ratio changed; that is, the number of icebergs south of 48°N became greater than the number of sightings received. With the introduction of this model, the number of icebergs south of 48°N became an estimate based on both sighting reports received south of 48°N and icebergs drifted south of 48°N by the model. The model also made it possible to more accurately determine if a report was a resight of an iceberg or an original sighting. Since some resighting was done before IBERG, the net effect of introducing the model should be to increase the number of icebergs south of 48°N, due to the icebergs drifted across 48°N by the model. Examination of Table C-2 ,however, shows no significant change in the relationship between icebergs south of 48°N and the iceberg sighting ratio, a measure of iceberg season severity discussed in Part b. Therefore, IBERG and pre-IBERG data will be combined in the following analysis of the effect of SLAR on IIP iceberg detection.

b. Icebergs South of 48°N

In this section we seek to evaluate the impact of SLAR on the 1983 and 1984 seasons by establishing an alternate indicator of the severity of an iceberg season.

Over the years, ships transitting the IIP region have furnished regular sea surface temperature (SST) reports and sighting reports for any icebergs encountered. These ship reports provide a sample of iceberg population data which is independent of IIP detection techniques. Since the number of iceberg reports received is dependent on both iceberg density in the shipping lanes and the amount of maritime traffic, the number of reports alone cannot be used to indicate the severity of an iceberg year. Ships making SST reports, assumed to be the most consistent iceberg reporters, make their SST reports in numbers independent of iceberg density and provide a measure of the annual traffic. Therefore, by dividing the number of ship iceberg reports by the number of ship sea surface temperature reports, a term representing iceberg density, independent of traffic, is obtained. (Regression analysis of SST reports versus icebergs estimated south of 48°N for 1970-82 yield an F value of .004, clearly demonstrating independence, assuming normal distribution.) We will call this term the iceberg sighting ratio.

Although the iceberg sighting ratio is independent of the

amount of traffic, it is sensitive to the marine traffic patterns in the IIP region. Throughout the iceberg season, typically March through June, ship traffic passes through the area south of the Grand Banks between latitudes 48°N and 44°N. Late in the season, when the Straits of Belle Isle become ice-free, a large amount of traffic transits the northern part of the International Ice Patrol area, north of 50°N. This paper assumes that this traffic pattern does not vary widely from year to year and gives a consistent annual sample of the iceberg population in the IIP area. The number of icebergs encountered by ships in the southern traffic lanes is assumed to have a direct relationship to the number of icebergs south of 48°N that year, dependent on the amount of traffic. It is further assumed that the number of icebergs sighted and reported by ships in the northern traffic lanes is related to the number of icebergs passing south of 48°N and that this relationship does not vary widely from year to year. These assumptions regarding the relationship of iceberg sightings to the number of icebergs south of 48°N have two weaknesses. First, during especially light or heavy iceberg years, the normal traffic pattern is disturbed. Presumably, even though shipping tracks may be displaced to the north or south during these years, the relationship between iceberg density and the probability of iceberg sighting by individual ships should not be greatly affected, since ships will tend to travel through waters of "normal" (i.e., low) iceberg density even in abnormal years. Second, as icebergs drift south from the northern lanes, they are subject to varying environmental conditions (sea surface temperatures, wave heights, winds and currents) that affect iceberg deterioration and transport. The fraction of the icebergs sighted in the northern lanes that eventually reach 48°N varies with these changing environmental conditions. However, since these environmental conditions usually follow predictable seasonal patterns and long-term variations from seasonal norms (e.g., 1972 and 1966) are rare, it is reasonable to assume that the relationship between the number of sightings in the northern lanes and the number of icebergs south of 48°N does not vary widely.

Table C-2 contains totals of ship iceberg and SST reports, numbers of sightings south of 48°N from the International Ice Patrol historical data file (which contains information for 1960 through 1984), and the computed iceberg sighting ratio for each year. It is important to point out that ships often report more than one iceberg sighting on a single report. The term "ship iceberg reports" in Table C-2 represents the total number of

Table C-1 Icebergs South of 48°N: Estimated vs Sightings

Year	South of 48° N Icebergs Est.	South of 48° N Sightings, All Sources	Ratio (Est Sighting X100)	Year	South of 48°N Icebergs Est.	South of 48°N Sightings, All Sources	Ratio (Est Sighting X100)
1960	253	1538	16.4	1972	1548	3978	39.8
1961	117	1286	9.1	1973	850	2980	28.5
1962	120	1072	11.2	1974	682	3355	20.3
1963	25	163	15.3	1975	101	331	30.5
1964	369	3712	9.9	1976	151	454	33.3
1965	76	277	27.4	1977	22	84	26.2
1966	0	13	0.0	1978	75	341	22.0
1967	441	1448	30.5	1979	152	168	90.5
1968	226	719	31.4	1980	24	3	800.0
1969	57	171	33.3	1981	63	26	242.3
1970	85	324	26.2	1982	188	70	268.6
1971	73	222	32.9	1983	1348	620	217.4
				1984	2202	1106	198.3

Table C-2 Icebergs South of 48° N vs. Iceberg Sighting Ratio

Year	South of 48 °N Icebergs Estimated	Sightings, All Sources	Ship Iceberg Reports	SST Reports	Iceberg Sighting Ratio % (Berg RPT/SST)
1960	253	1538	1008	7436	13.6
1961	117	1286	928	8342	11.1
1962	120	1072	1077	7916	13.6
1963	25	163	251	4633	5.4
1964	369	3712	1362	9147	14.9
1965	76	277	227	6347	3.6
1966	0	13	51	1592	3.2
1967	441	1448	524	3194	16.4
1968	226	719	384	2271	16.9
1969	57	171	139	1985	7.0
1970	85	324	439	1014	43.3
1971	73	222	162	159	101.9
1972	1584	3978	1151	432	614.0
1973	850	2980	842	381	191.4
1974	682	3355	540	215	179.5
1975	101	331	197	260	77.9
1976	151	454	312	297	59.3
1977	22	84	316	257	117.1
1978	75	341	399	478	68.4
1979	152	168	183	397	46.6
1980	24	3	40	215	34.8
1981	63	26	39	302	17.4
1982	188	70	92	434	21.2
1983	1348	620	148	334	44.3
1984	2202	1106	586	353	166.0

ship iceberg reports received by International Ice Patrol throughout the IIP area for any given year, while "sightings south of 48°N" is the total number of sightings south of 48°N from all sources recorded as individual icebergs at IIP. Icebergs estimated south of 48°N are the total number determined by the International Ice Patrol to have actually passed south of 48°N during the season and reported in the annual Ice Bulletin.

There is an abrupt change in the iceberg sighting ratio in 1970, which could be attributed to the disestablishment of Coast Guard Radio Station Argentia in 1969. Since 1970, the International Ice Patrol has broadcast daily ice bulletins and facsimile charts to ships from Coast Guard Communications Station Boston, but has no direct communications with vessels transitting the Grand Banks. This lack of direct contact is believed to be the cause of the significant decrease in the number of SST reports received by the International Ice Patrol. Sea surface temperature reports decreased by a factor of 14 in the mean annual number between the two periods. Therefore, these two periods will be treated independently in this analysis.

Table C-2 also shows that the previous record year of 1972 still holds the record as the most severe iceberg year on record if the iceberg sighting ratio is used as the evaluating criterion. Using this criterion, 1984 is unquestionably a severe iceberg year, but not as severe as 1972. Although the 1983 number of 1348 icebergs south of 48°N makes it appear as a very severe year, the iceberg sighting ratio suggests that it is a light year. Comparison to 1975, the median year with respect to icebergs south of 48°N, indicates that 1983 would have fewer icebergs south of 48°N than that year and that 1984 would have more.

Figures C-1 and C-2 show plots of the iceberg sighting ratio versus icebergs south of 48°N for the periods 1960 through 1969 and 1970 through 1982 and the linear regression fits of those data. In Figure C-2, the iceberg sighting ratio has been adjusted by removing iceberg sighting and SST reports received from Coast Guard vessels from the data. Coast Guard vessels, when deployed in the IIP area, typically contribute a significant number of iceberg and SST reports to IIP. They do not operate within the normal traffic pattern described above, often actively search for icebergs and have operational requirements to submit regular SST reports, all of which might bias the Coast Guard component of the iceberg sighting ratio. The number of reports contributed by individual vessels, including Coast Guard vessels, was not recorded in the International Ice Patrol Bulletin prior to 1972 so this adjustment could not be made to earlier data. Using the regression fit shown and the

Figure C-1

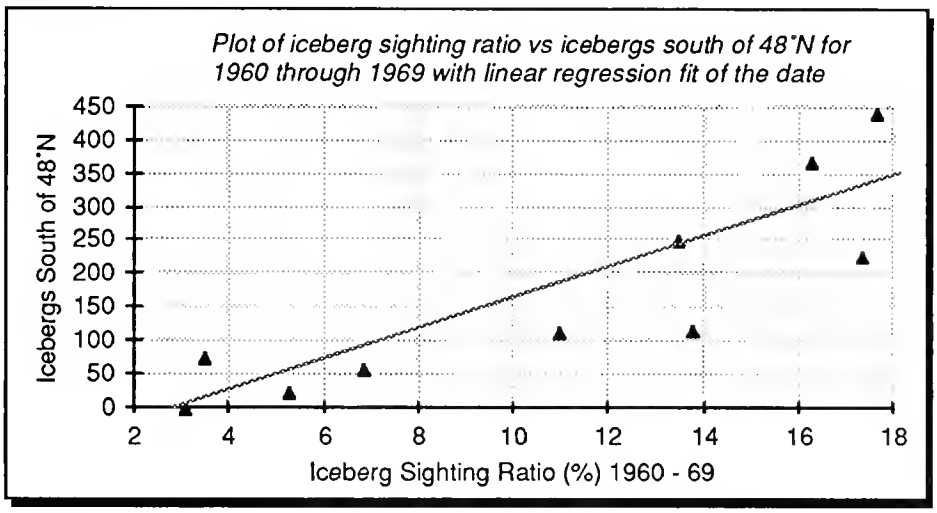

Figure C-2

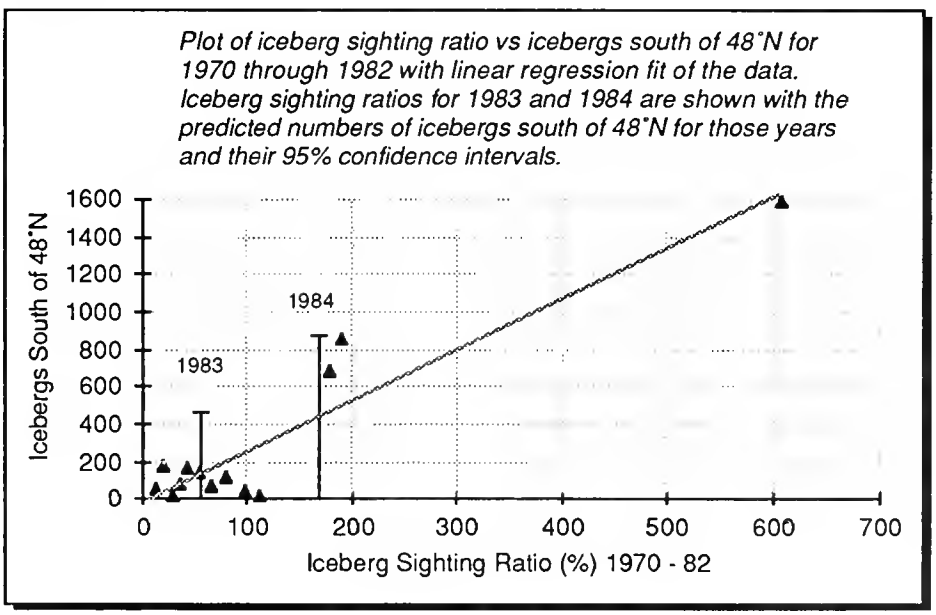

Conclusion

iceberg sighting ratios for 1983 and 1984, the solved-for values are 102 (+/- 483 at the 95% confidence level) and 430 (+/- 417 at the 95% confidence level), respectively. The data clearly shows the existence of a SLAR effect for both years, since the number of icebergs estimated south of 48°N each year far exceeds the values predicted by the iceberg sighting ratio, even at the upper limits of the 95% confidemce interval (Figure C-2). Given the small number of observations (n=13) used in performing this analysis and the large confidence intervals (due in part to the scatter of the data), this estimate only demonstrates that the effect of SLAR on iceberg reconnaisance exists and should not be used to compare the SLAR and pre-SLAR data numerically.

In addition to improved iceberg detection with SLAR, the increase may also be partly caused by misidentification of non-iceberg targets as icebergs, due both to unfamiliarity with the new technology and the inherent ambiguities of SLAR imagery.

It is important to note that data presented throughout this appendix was collected and analyzed over the years by a constantly changing International Ice Patrol staff, using techniques that undoubtedly varied somewhat with the turnover in personnel. Therefore, this data should be examined with that caution in mind.

The effect of introducing the iceberg drift prediction model (IBERG) to International Ice Patrol operations on 1979 was analyzed by examining the relationship of icebergs estimated south of 48°N to iceberg sighting reports south of 48°N for 1960 through 1984. These values had a close linear relationship for the years 1965 through 1978 and their ratio showed a marked increase with the introduction of the model. But since the relationship of the number of icebergs estimated south of 48°N due to the iceberg sighting ratio appeared to be unchanged after 1979, we assume that the effects of the side-looking airborne radar (SLAR) on the number of icebergs estimated south of 48°N are much greater than those of the IBERG model.

The introduction of SLAR to IIP in 1983 significantly changed the nature of IIP iceberg reconnaissance. Reconnaissance no longer depended on visibility, complete coverage of search areas was possible under conditions of intermittent visibility, and longer flights made it possible to search the outlying areas of the IIP region.

These improvements, together with possible misidentification of non-iceberg SLAR targets due to inexperience and the limitations of SLAR imagery resulted in elevated estimates of icebergs south of 48°N in 1983 and 1984. This conclusion is supported by relating pre-SLAR numbers of icebergs south of 48°N with the corresponding values for 1983 and 1984. These values were compared using the ratio of the ship iceberg reports and the ship SST reports, an iceberg density function called the iceberg sighting ratio. The apparent increase in iceberg detection due to SLAR is by an order of magnitude in 1983 and by half that in 1984, with large confidence intervals at the 95% confidence level.

The analysis of the effect of SLAR reconnaissance presented here provides only a preliminary investigation of the issue. In no way can an evaluation of two years of SLAR data identify the long-term effect of SLAR on IIP operations. Neither can it adequately place the 1983 and 1984 iceberg seasons in the context of the previous years of IIP history. It is clear that SLAR has increased the number of icebergs detected by IIP and that with several more years of SLAR data, and with the research currently being conducted on iceberg detection and identification by SLAR, we should be able to address this issue with more confidence.

☆ U. S. GOVERNMENT PRINTING OFFICE: 1986--600-846--20,197

U.S. Department
of Transportation

**United States
Coast Guard**

Report of the International Ice Patrol in the North Atlantic

1985 Season
Bulletin No. 71
CG-188-40

U.S. Department of Transportation
United States Coast Guard

Commandant
United States Coast Guard

MAILING ADDRESS G-OIO
U. S. COAST GUARD
WASHINGTON, D.C. 20593-0001
(202) 267-1458

17 MAR 1987

Bulletin No. 71

REPORT OF THE INTERNATIONAL ICE PATROL SERVICES IN THE NORTH ATLANTIC OCEAN

Season of 1985

CG-188-40

FOREWORD

Forwarded herewith is bulletin No. 71 of the International Ice Patrol describing the Patrol's services, ice observations and conditions during the 1985 season.

CLYDE E. ROBBINS
Chief, Office of Operations

DISTRIBUTION - SDL No. 124

	a	b	c	d	e	f	g	h	i	j	k	l	m	n	o	p	q	r	s	t	u	v	w	x	y	z
A	1*	1*		1	1	1*	1*	1*																		
B		1*	1		10					2				2	5		1									
C	1*																1*									
D																							60			
E																										
F																										
G																										
H																										

NON-STANDARD DISTRIBUTION:
*A;abfgh LANTAREA only
*B;b LANTAREA (5); B;b PACAREA (1)
*C:aq LANTAREA only
SML CG-4

International Ice Patrol 1985 Annual Report

Contents

Introduction

This is the 71st annual report of the International Ice Patrol Service in the North Atlantic. It contains information on ice conditions and Ice Patrol operations for 1985. The U.S. Coast Guard conducts the International Ice Patrol Service in the North Atlantic under the provisions of Title 46, U.S. Code, Sections 738, 738a through 738d; and the International Convention for the Safety of Life at Sea (SOLAS), 1974 regulations 5-8. This service was initiated shortly after the sinking of the RMS TITANIC on April 15, 1912.

Commander, International Ice Patrol under Commander, Coast Guard Atlantic Area, directed the International Ice Patrol from offices located at Groton, Connecticut. The unit analyzes ice and environmental data, prepares the daily ice bulletins and facsimile charts, and replies to any requests for special ice information. It also controls the aerial Ice Reconnaisance Detachment and any surface patrol cutters when assigned, both of which patrol the southeastern, southern, and southwestern limits of the Grand Banks of Newfoundland for icebergs. The International Ice Patrol makes twice-daily radio broadcasts to warn mariners of the limits of iceberg distribution.

During the 1985 season, International Ice Patrol reconnaissance was conducted by U. S. Coast Guard HC-130 aircraft equipped with Side-Looking Airborne Radar (SLAR), operating from Gander, Newfoundland. No U. S. Coast Guard cutters were deployed as surface patrol vessels this year. There were 1,063 icebergs estimated south of 48°N this year, the traditional measure of the severity of an IIP season.

Vice Admiral P.A. Yost was Commander, Atlantic Area from the start of the 1985 season, 14 March until its end on 29 August 1985. Commander Norman C. Edwards, Jr., U.S. Coast Guard, was Commander, International Ice Patrol during the Ice Patrol season.

Summary of Operations, 1985

From 14 March to 29 August 1985, the International Ice Patrol (IIP), a unit of the U.S. Coast Guard, conducted the International Ice Patrol Service, which has been provided annually since the sinking of the RMS TITANIC on April 15, 1912. During past years, Coast Guard ships and/or aircraft have patrolled the shipping lanes off Newfoundland within the area delineated by 40°N - 52°N, 39°W - 57°W, detecting icebergs and warning mariners of these hazards. During the 1985 Ice Patrol season, Coast Guard HC-130 aircraft flew 72 ice reconnaissance sorties, logging over 507 flight hours. The AN/APS-135 Side-Looking Airborne Radar (SLAR), which was introduced into Ice Patrol duty during the 1983 season, again proved to be an excellent all-weather tool for the detection of both icebergs and sea ice as demonstrated during the BergSearch '84 experiment (Rossiter, *et al.*, 1984). On IIP reconnaissance flights alone, the SLAR provided 53 percent of the 1985 sightings.

A deployment was made from 20-25 February to determine the pre-season iceberg distribution. Based on this trip, regular deployments started on 12 March with the 1985 season opening on 14 March. From that date until 29 August 1985, an aerial Iceberg Reconnaissance Detachment (ICERECDET) operated from Gander, Newfoundland one week out of every two. The season officially closed on 29 August 1985.

During the 1985 season, an estimated 1,063 icebergs drifted south of 48°N latitude. Table 1 shows monthly estimates of the number of icebergs that crossed 48°N.

No U. S. Coast Guard cutters were deployed to act as surface patrol vessels this year. The USCGC EVERGREEN and USCGC NORTHWIND were deployed to conduct oceanographic research for the Ice Patrol during the periods 10 April - 10 May and 1-9 August. On board EVERGREEN, the IIP iceberg drift and deterioration models were evaluated (See Appendices C and D), hydrographic equipment was evaluated, and a joint IIP/USCG Research and Development Center study of surface craft and iceberg target detection performance by the AN/APS-135 SLAR was conducted (Robe, *et al.*, 1985). The NORTHWIND hydrographic cruise was cancelled because of main diesel engine problems on board NORTHWIND.

Other research conducted at IIP during 1985 included an analysis of eddy formation in the vicinity of the Grand Banks (Appendix E), an evaluation of iceberg/ship SLAR target discrimination (Appendix B), and a comparison of ocean fronts detected on National Weather Service satellite imagery and IIP SLAR imagery (Appendix F).

Table 1. Icebergs South of 48°North

	Avg 1900-85	Total 1900-85	Avg 1946-85	Total 1946-85	1985
OCT	1	112	0	5	3
NOV	1	121	0	15	11
DEC	1	100	1	20	7
JAN	2	196	2	76	2
FEB	11	945	12	494	57
MAR	42	3628	38	1526	129
APR	110	9476	116	4631	208
MAY	131	11230	104	4147	205
JUN	70	6025	63	2507	247
JUL	26	2219	26	1023	123
AUG	7	625	6	236	39
SEP	3	297	1	51	32
Annual Total	405	34974	368	14631	1063

As explained in the 1984 Ice Patrol Bulletin (Thayer, 1984), the methodology and technology of iceberg reconnaissance and data analysis have changed significantly over the past 40 years. A change is evident in the source distribution of iceberg sightings in that SLAR accounted for 78% of the USCG iceberg sightings in 1984 (49% of sightings from all sources) but only accounted for 53% of USCG sightings in 1985 (13% of all sightings) (Table 2). (An increased emphasis on icebergs by Canadian Atmospheric and Environmental Service flights and an increased contribution by the commercial shipping community account for other changes in the overall figures.) With icebergs more widely dispersed than normal during much of the 1985 IIP season, it was frequently necessary to search the eastern part of the IIP area. To conserve fuel during these long searches, high altitude legs were flown to and from the search areas. Although SLAR was not operated during these high altitude legs, icebergs could still be sighted in large numbers during good weather. These high-altitude flights were much more frequent during 1985 than 1984. The large number of USCG visual sightings on these flights, together with the changes in reconnaissance procedures described below, greatly decreased the percentage of USCG iceberg sightings that were SLAR-only during 1985.

Further evaluation of SLAR's capability confirms its usefulness in detecting icebergs (Robe, *et al.*, 1985) and the necessity for specific SLAR iceberg reconnaissance procedures to assist with iceberg/ship target discrimination (Appendix B). Specific changes in SLAR reconnaissance procedures were made to maximize visual confirmation of SLAR targets and aid target identification during 1985. These changes consisted of selecting daily search areas for optimal visibility, subjecting SLAR films to more post-flight analysis and making more use of supporting data from other sources.

Table 3 — Aircraft Deployments from 10/1/84 to 9/30/85

Ice Reconnaisance Detachment Deployments	No. of Hours Flown
Pre-season	29.6
In-season	631.0
Post-season	11.3
Total	671.9

Note: In-season ICERECDET flights include transit and logistics flights to and from Gander during the Ice Patrol season. A significantly large number of logistic flights, 14 sorties and 86.1 hours were conducted. There were 72 sorties dedicated solely to ice reconnaisance with a total of 507.8 flight hours. They are summarized as follows:

Month	Number of Sorties	Flight Hours
FEB	4	23.6
MAR	5	38.7
APR	12	85.8
MAY	15	107.5
JUN	13	87.3
JUL	11	83.9
AUG	11	75.7
SEP	1	5.3
TOTAL	72	507.8

Table 2 — Sources of IIP Iceberg Reports by Size

Sighting Source	Growler	Small	Med.	Large	Radar Target	Total	% of Total
Coast Guard SLAR	65	194	182	113	10	564	13.3
Coast Guard Visual	60	155	177	107	0	499	11.8
Canadian SLAR	17	56	115	21	229	438	10.3
Canadian Visual	19	239	187	65	4	514	12.1
Commercial Radar	7	30	114	33	124	308	7.3
Commercial Visual	122	300	808	279	15	1524	36.0
Mobil Oil Canada, LTD	12	81	98	18	18	227	5.4
Lighthouse/Shore	0	2	13	9	0	24	0.6
Other	4	52	47	28	5	136	3.2
Total	306	1109	1741	673	405	4234	100

Iceberg Reconnaissance and Communications

During the 1985 Ice Patrol year (from 1 October 1984 through 30 September 1985), 98 aircraft sorties were flown in support of the International Ice Patrol. These included pre-season flights, ice observation and logistics flights during the season, and post-season flights. Pre-season flights determined iceberg concentrations north of 48°N, necessary to estimate the time when icebergs would threaten the North Atlantic shipping lanes in the vicinity of the Grand Banks of Newfoundland. During the active season, ice observation flights located the southwestern, southern, and southeastern limits of icebergs. Logistics flights were necessary due to aircraft maintenance problems. Post-season flights were made to retrieve parts and equipment from Gander and to close out all business transactions from the season.

U.S. Coast Guard aircraft, deployed from Coast Guard Air Station Elizabeth City, North Carolina, conducted all the aircraft missions. SLAR-equipped HC-130 aircraft were utilized exclusively for aerial ice reconnaissance, and HC-130 and HU-25A aircraft were used on logistics flights. Table 3 (left) shows aircraft utilization during the 1985 season.

During the 1984 season, only 5% of the deployed days were spent on the ground in Gander. In 1985, this figure climbed to 14%. After an aircraft mishap in Groton in March, IIP relied on a single SLAR-equipped HC-130 for much of the 1985 season. The increased use of this one aircraft and its SLAR resulted in an increased number of maintenance problems.

U.S. Coast Guard Communications Station Boston, Massachusetts, NMF/NIK, was the primary radio station used for the dissemination of the daily ice bulletins and facsimile charts after preparation by the Ice Patrol office in Groton. Other transmitting stations for the 0000Z and 1200Z ice bulletins included Canadian Coast Guard Radio Station St. John's/VON, Canadian Forces Radio Station Mill Cove/CFH, and U.S. Navy LCMP Broadcast Stations Norfolk/NAM; Thurso, Scotland; and Keflavik, Iceland.

Canadian Forces Station Mill Cove/CFH as well as AM Radio Station Bracknell/GFE, United Kingdom are radiofacsimile broadcasting stations which used Ice Patrol limits in their broadcasts. Canadian Coast Guard Radio Station St. John's/ VON provided special broadcasts.

The International Ice Patrol requested that all ships transitting the area of the Grand Banks report ice sightings, weather, and sea surface temperatures via U.S. Coast Guard Communications Station Boston, NMF/NIK. Response to this request is shown in Table 4, and Appendix A lists all contributors. Commander, International Ice Patrol extends a sincere thank you to all stations and ships which contributed.

Table 4. Iceberg and SST Reports

Number of ships furnishing Sea Surface Temperature (SST) reports	103
Number of SST reports received	505
Number of ships furnishing ice reports	497
Number of ice reports received	673
First Ice Bulletin	140000Z MAR 85
Last Ice Bulletin	291200Z AUG 85
Number of facsimile charts transmitted	169

Environmental Conditions 1985 Season

Weather in Labrador and East Newfoundland during the 1985 International Ice Patrol season tended to be colder and dryer than normal during the winter and warmer and wetter than normal during the summer (Table 5). The weather stations listed in Table 5 were selected to give a cross-section of weather conditions throughout the province. The colder than normal months of December 1984 through March 1985 caused an early accumulation of sea ice which expanded south of 43°N and persisted longer than normal. This sea ice forced oil drilling rigs off the Grand Banks and protected the icebergs moving into the region.

January: With the Iceland Low southwest of its normal position and deeper than normal (Figure 1), the maritimes experienced a strong northerly flow that brought lower than normal temperatures.

February: The Iceland Low was deeper than normal (Figure 2), causing northwest winds to bring in cold continental air, resulting in below normal temperatures and precipitation in Newfoundland and Labrador (Table 5).

March: During March, the Iceland Low was southwest of its normal position (Figure 3), bringing more continental air than normal into the maritimes and lowering temperatures (Table 5).

April: Surface pressure was near normal during April (Figure 4). With a westerly flow returning to Newfoundland, temperatures and precipitation were normal (Table 5).

May: The Iceland Low was farther west and deeper than normal during May (Figure 5), bringing more marine air into St. John's and greater than normal precipitation (Table 5).

June: Flow, normally southwesterly over Newfoundland, was southerly in June (Figure 6), bringing greater than normal precipitation to Gander (Table 5).

July: Direction of surface winds was normal in July, but the stronger than normal pressure gradient (Figure 7) caused greater southerly flow, bringing above normal precipitation.

August: August temperatures and precipitation were above normal (Table 5). The shape of the isobars in Figure 8 were near normal, but the pressure gradient between a deeper Iceland Low and the Bermuda High caused increased southwest flow bringing in more warm, moist air than normal (Table 5).

September: With the Iceland Low deeper than normal (Figure 9), a westerly flow dominated, bringing warmer, drier air over the maritimes resulting in above normal temperatures (Table 5).
Ice Conditions, 1985 Season

Table 5. Environmental Conditions for 1985 International Ice Patrol Season

	Station	Temp°C Monthly Mean	Temp°C Diff. from Norm.	Total Precipitation (mm)	% of Normal Precipitation	% of Normal Snowfall
OCT 1984	Nain	0.8	1.8	74.2	118.2%	217.9%
	Goose	2.1	0.6	38.7	50.5%	62.8%
	Gander	3.8	2.2	59.4	56.7%	141.0%
	St. John's	5.0	1.9	80.7	55.5%	59.1%
NOV	Nain	-4.6	-1.4	141.1	245.8%	263.3%
	Goose	-3.8	0.0	117.0	155.6%	206.8%
	Gander	1.0	0.8	73.6	68.6%	118.9%
	St. John's	2.8	0.6	100.6	61.9%	50.5%
DEC	Nain	-17.2	-6.5	67.8	119.6%	111.3%
	Goose	-17.2	-4.2	112.5	154.7%	194.6%
	Gander	-4.3	-0.5	68.2	63.0%	80.4%
	St. John's	-2.0	-0.5	109.2	67.7%	52.7%
JAN 1985	Nain	-12.6	-3.2	210.7	338.7%	291.0%
	Goose	-15.6	-0.8	134.0	180.1%	293.9%
	Gander	-7.4	-1.7	96.0	88.0%	122.5%
	St. John's	-5.9	-1.3	111.6	71.6%	102.6%
FEB	Nain	-16.2	-1.1	124.3	248.1%	189.9%
	Goose	-14.5	0.0	25.1	41.4%	66.7%
	Gander	-7.4	-0.6	91.4	91.7%	108.9%
	St. John's	-5.9	-1.4	96.3	68.7%	97.5%
MAR	Nain	-12.0	-1.5	124.3	224.4%	193.3%
	Goose	-9.3	-1.1	56.5	78.3%	146.6%
	Gander	-5.8	-2.7	51.0	46.3%	57.3%
	St. John's	-5.1	-3.2	102.3	77.6%	78.6%
APR	Nain	-8.1	-3.2	119.6	257.2%	253.6%
	Goose	-3.2	-1.5	52.8	86.3%	101.2%
	Gander	-0.6	0.3	86.6	92.9%	112.1%
	St. John's	-0.1	1.1	96.2	83.2%	125.4%
MAY	Nain	-1.0	0.4	52.2	103.0%	42.6%
	Goose	2.8	-2.6	66.5	104.2%	100.0%
	Gander	5.7	0.5	37.2	53.1%	88.5%
	St. John's	4.4	1.0	168.6	165.6%	81.1%
JUN	Nain	6.9	0.5	22.4	35.1%	58.1%
	Goose	11.0	0.3	85.8	92.2%	91.9%
	Gander	11.8	0.0	124.2	154.7%	0.0%
	St. John's	10.4	0.5	88.9	103.9%	0.0%
JUL	Nain	10.8	0.3	89.6	106.0%	0.0%
	Goose	15.5	0.3	235.3	223.9%	*
	Gander	17.7	1.2	107.8	156.2%	*
	St. John's	17.5	2.0	108.8	130.9%	*
AUG	Nain	10.2		46.0		*
	Goose	14.6	4.7	153.3	148.5%	*
	Gander	14.9	0.7	110.0	113.1%	*
	St. John's	13.9	1.4	100.9	83.0%	*
SEP	Nain	8.0		60.5		*
	Goose	9.9	0.8	81.6	96.6%	*
	Gander	11.0	4.6	75.6	93.1%	*
	St. John's	11.0	4.9	54.2	48.4%	*

* No snowfall recorded during this month

Figure 1.

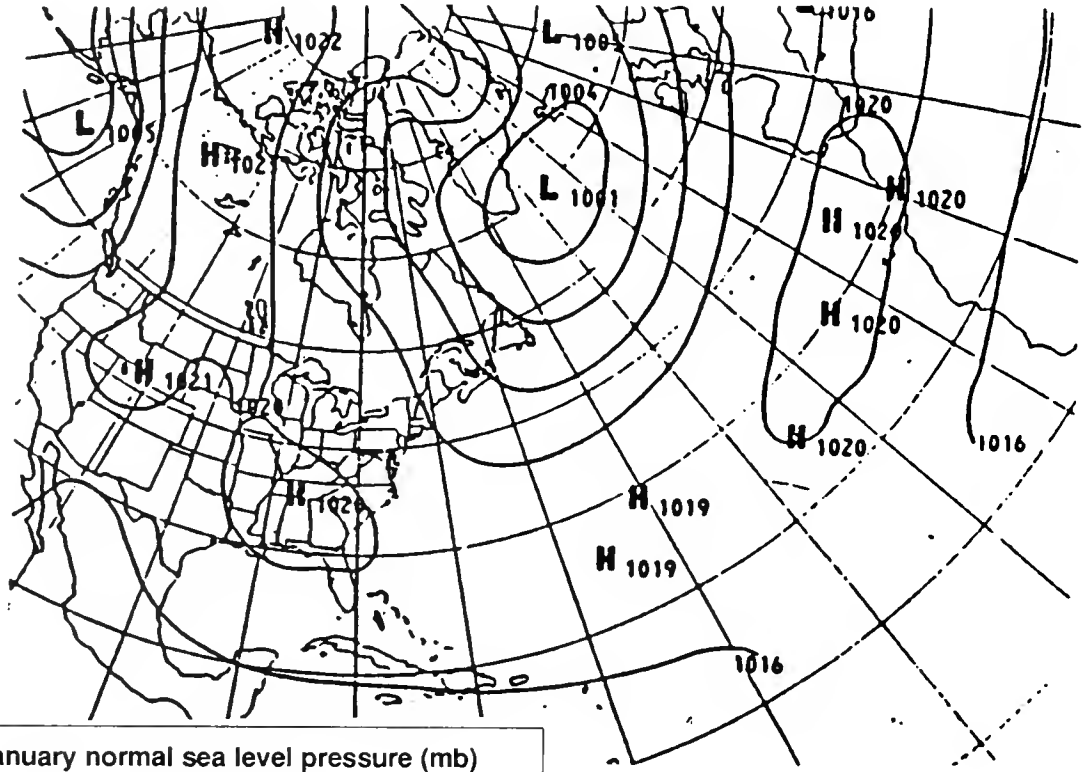

January normal sea level pressure (mb)
(1948 — 1970)

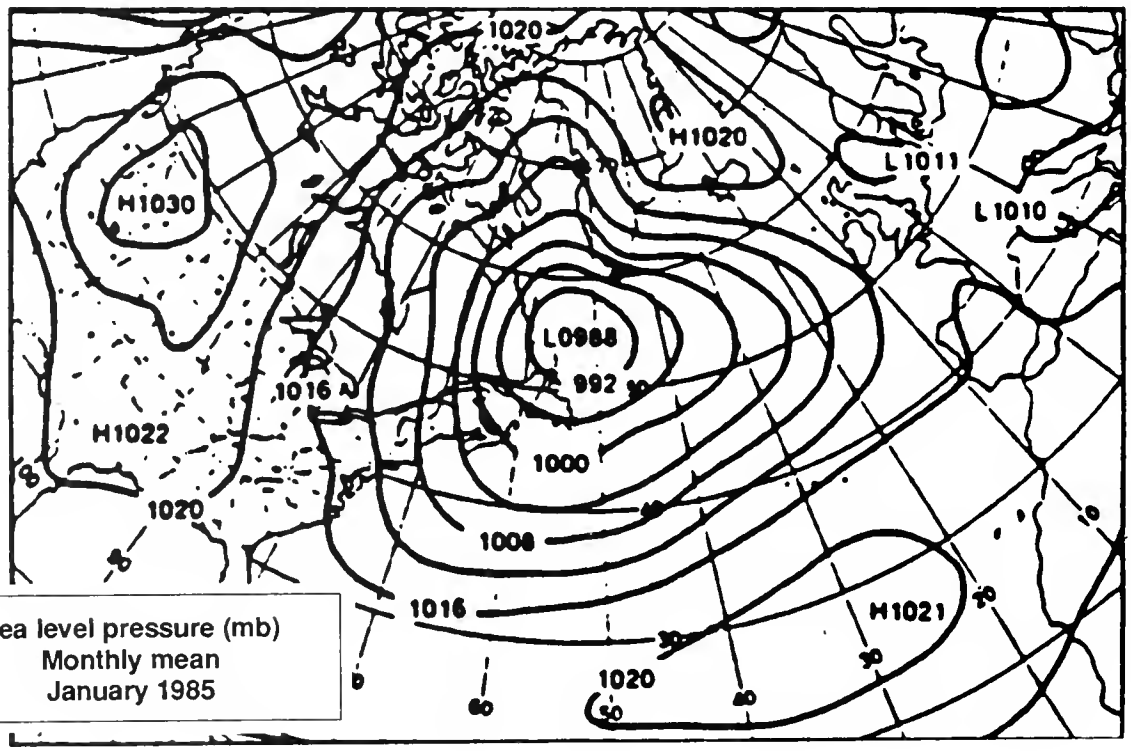

Sea level pressure (mb)
Monthly mean
January 1985

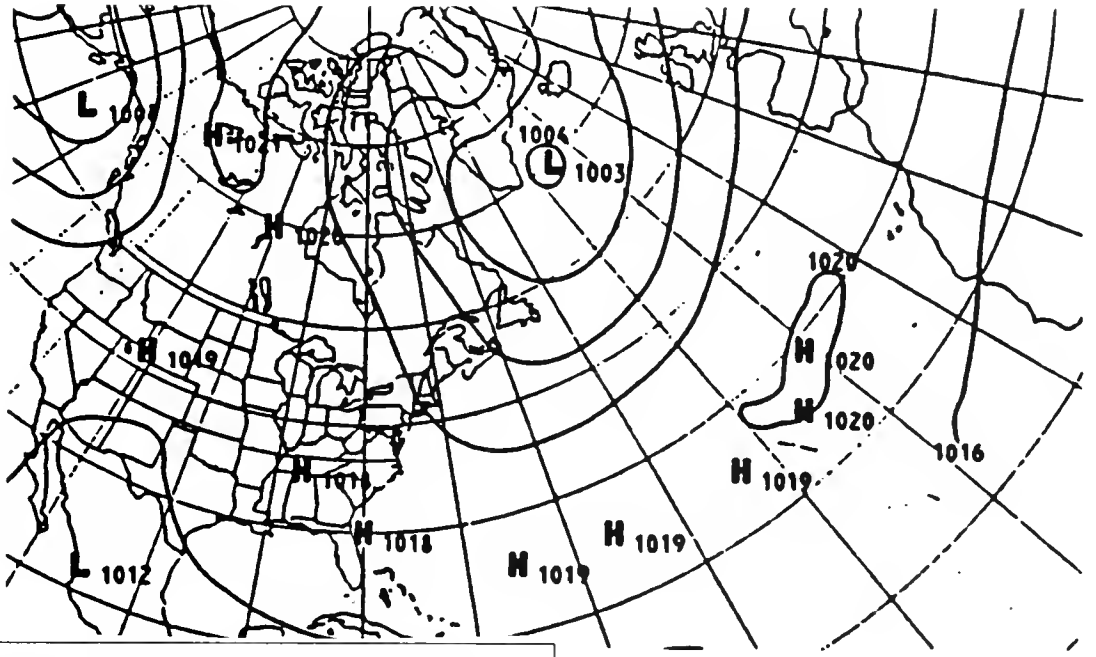

February normal sea level pressure (mb)
(1948 — 1970)

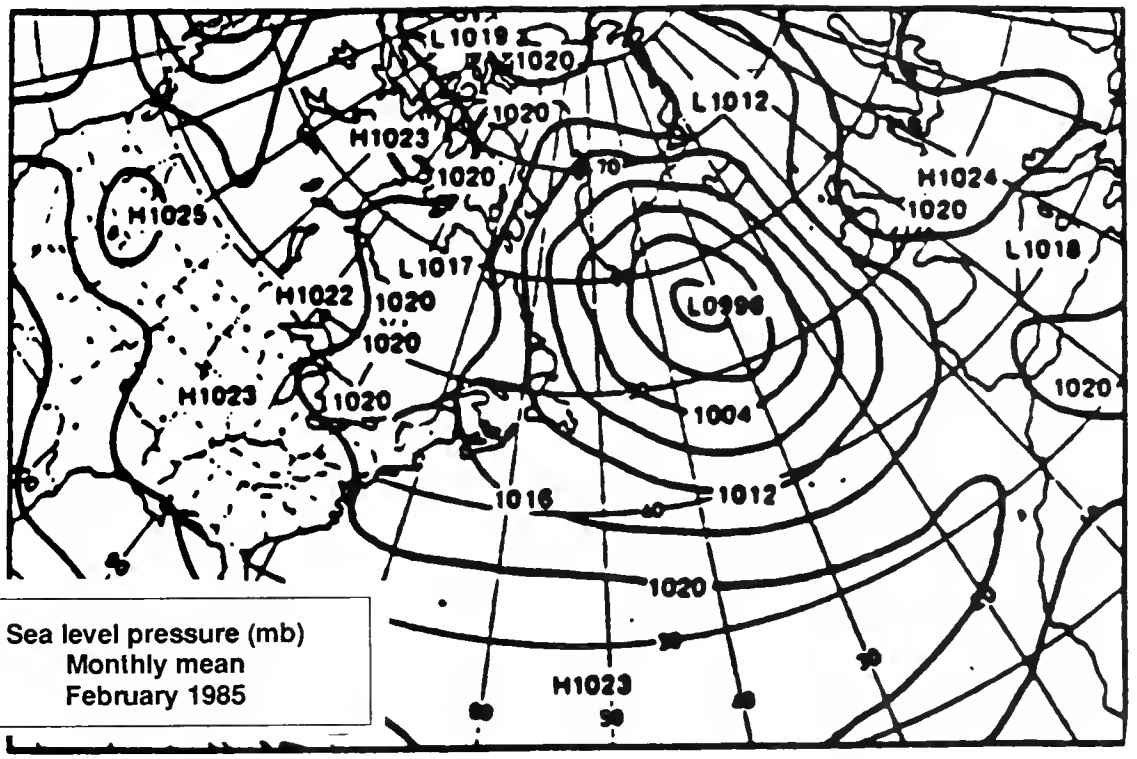

Sea level pressure (mb)
Monthly mean
February 1985

Figure 3.

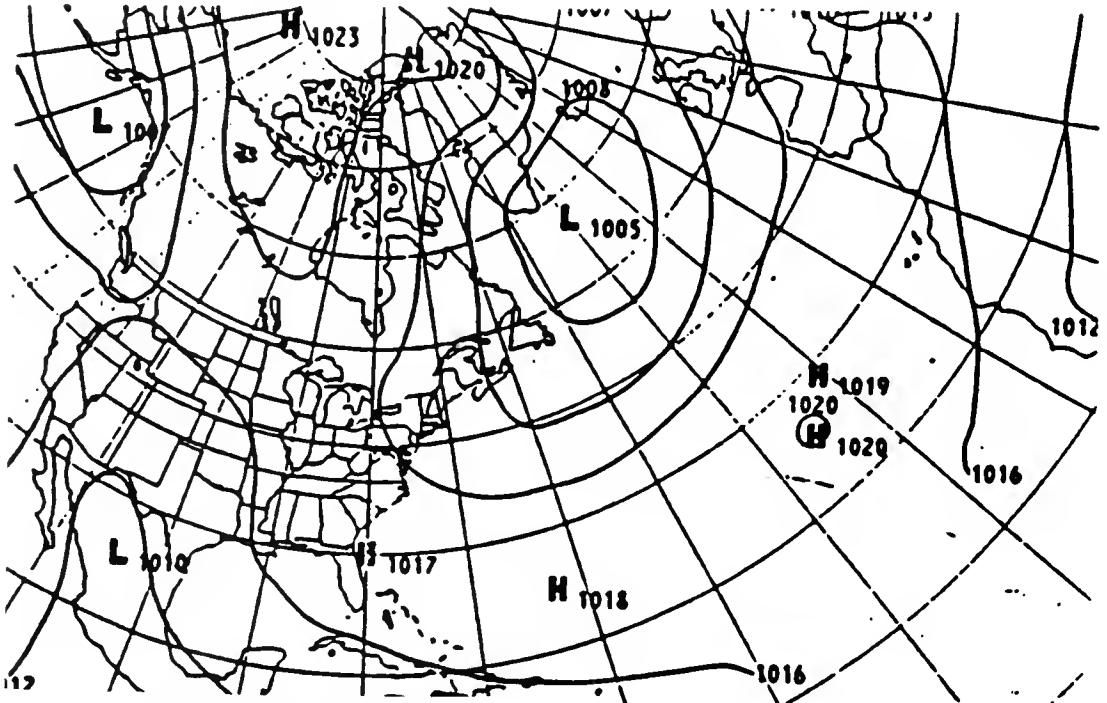

March normal sea level pressure (mb)
(1948 — 1970)

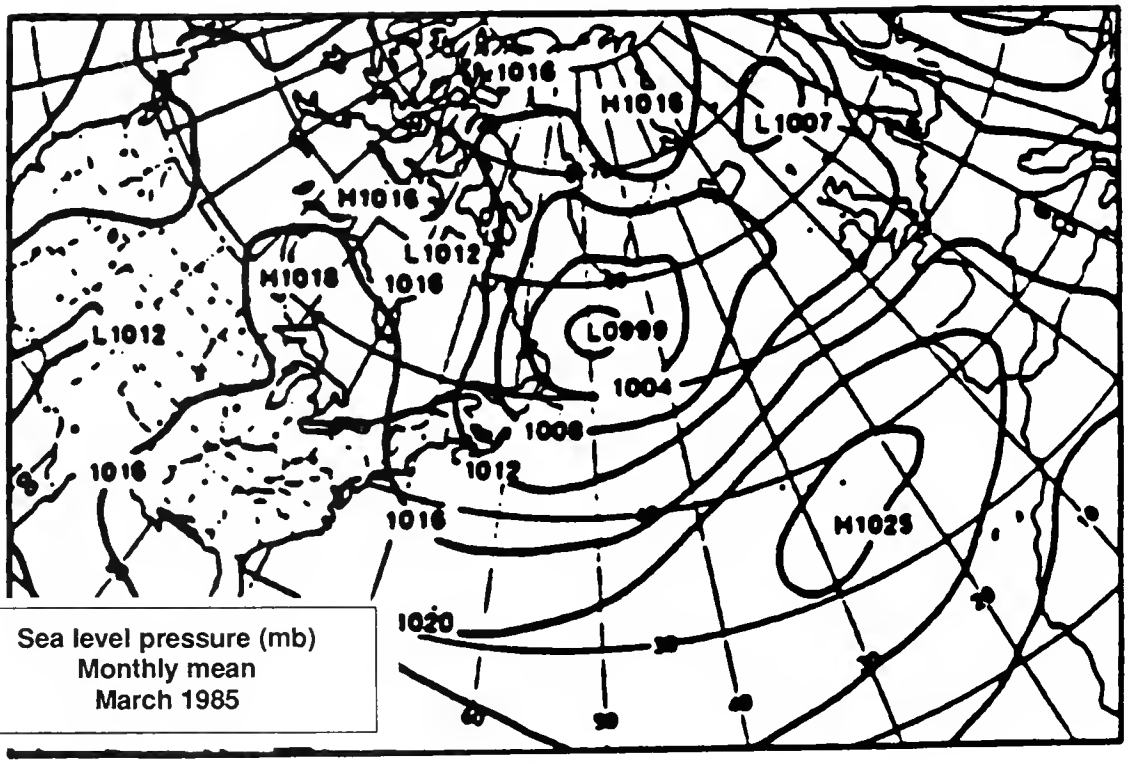

Sea level pressure (mb)
Monthly mean
March 1985

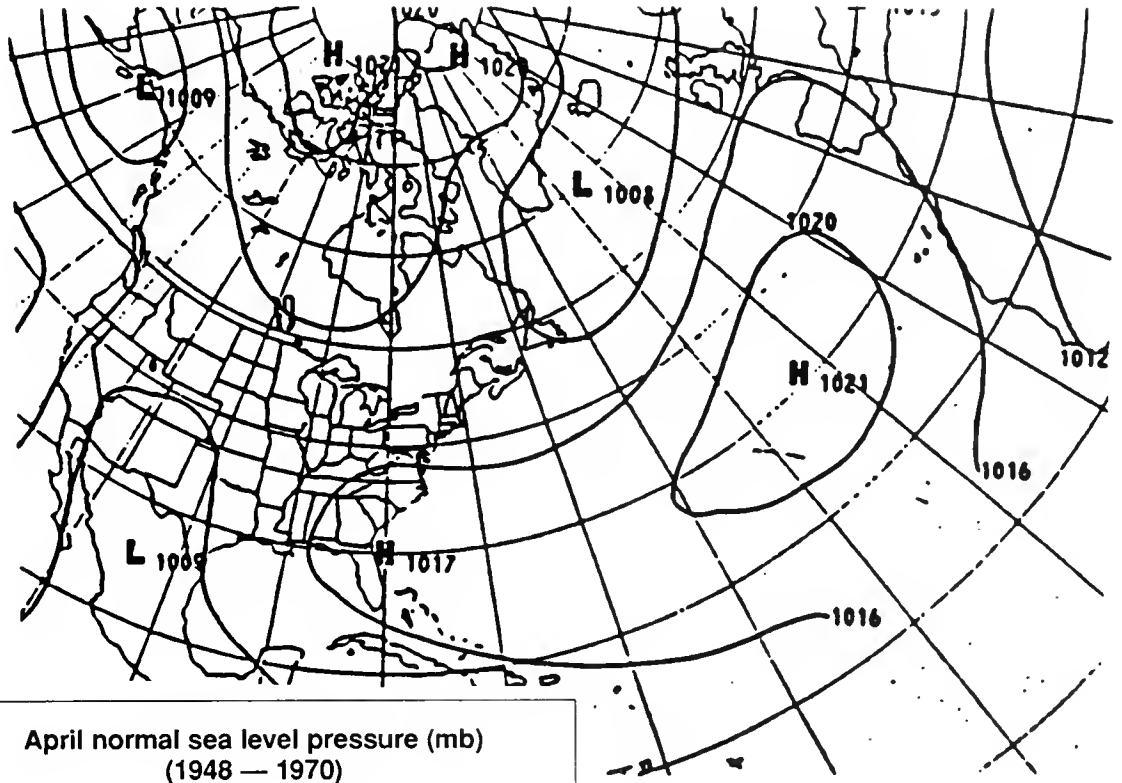

April normal sea level pressure (mb)
(1948 — 1970)

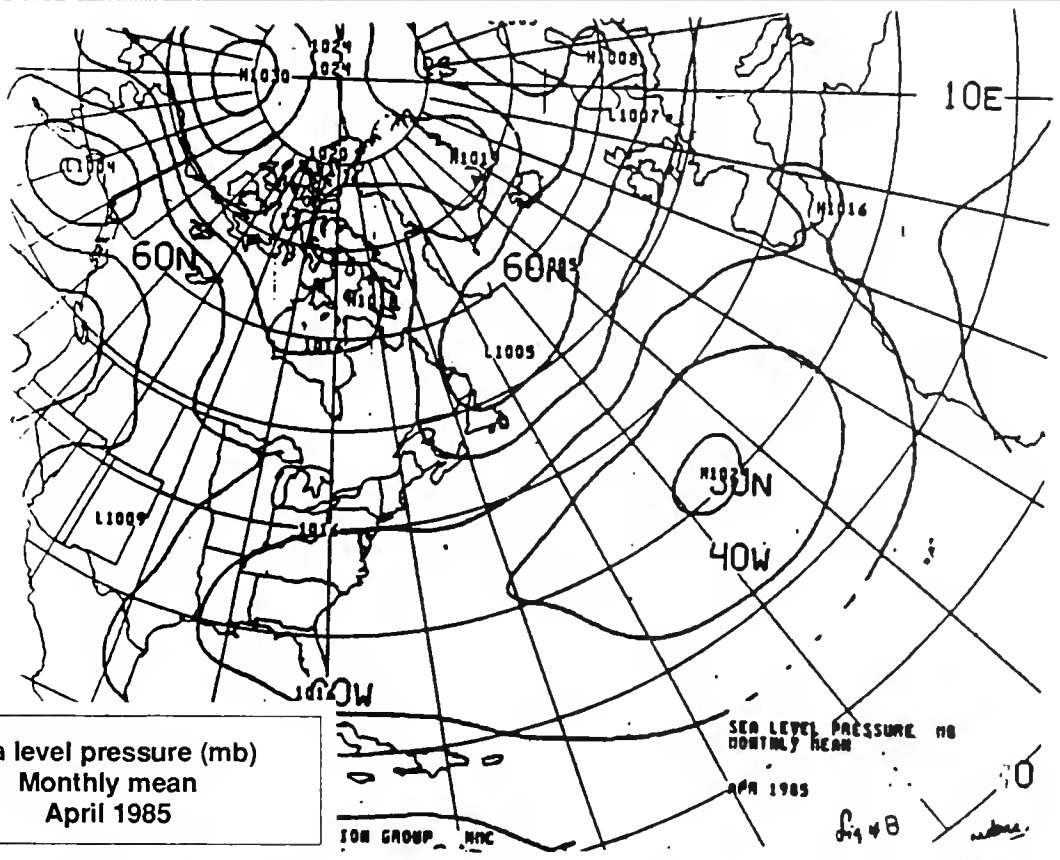

Sea level pressure (mb)
Monthly mean
April 1985

Figure 5.

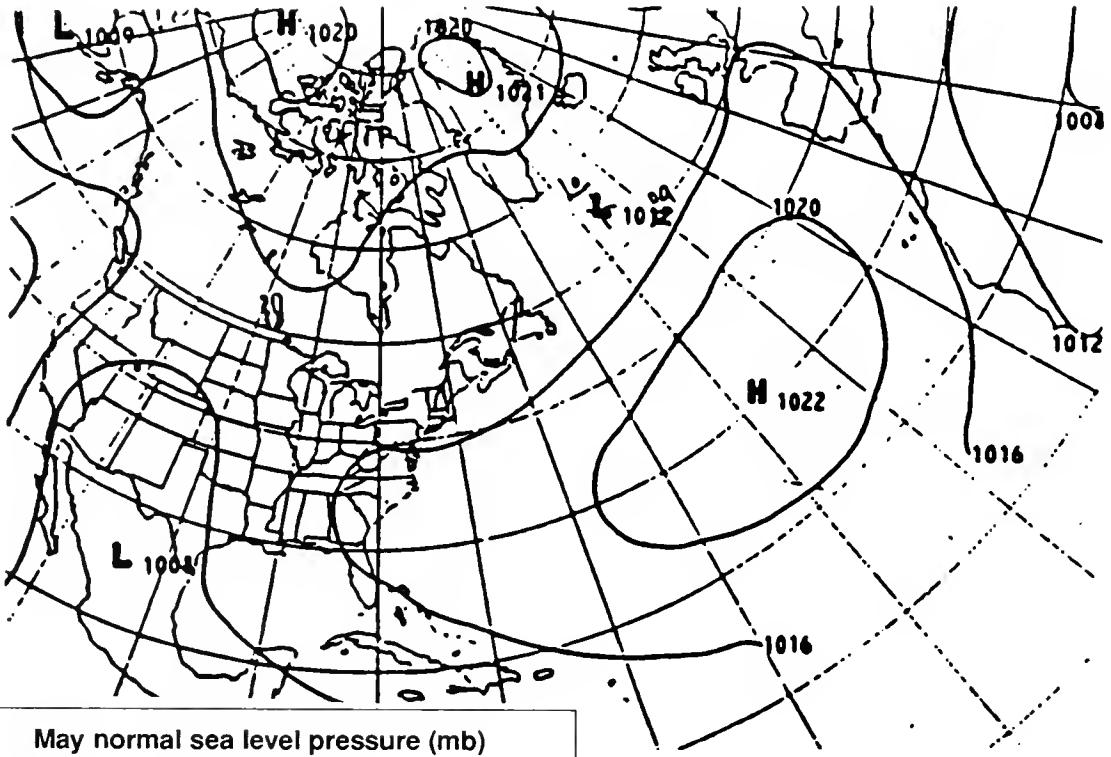

May normal sea level pressure (mb)
(1948 — 1970)

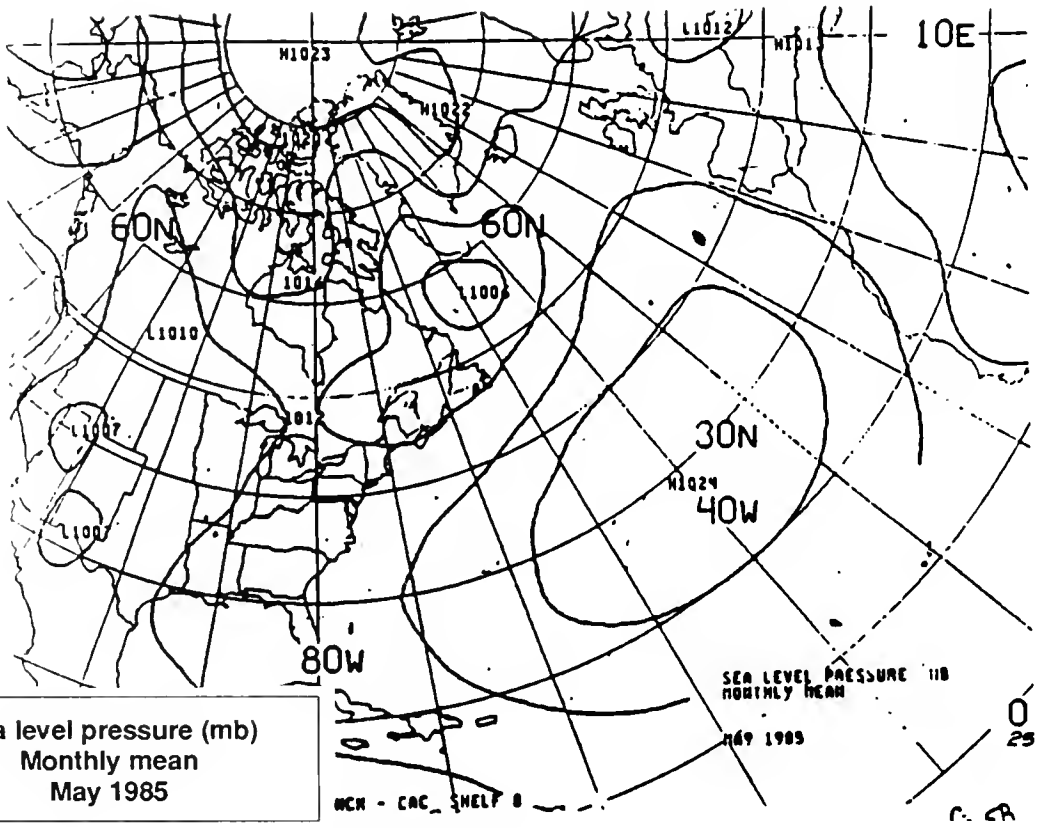

Sea level pressure (mb)
Monthly mean
May 1985

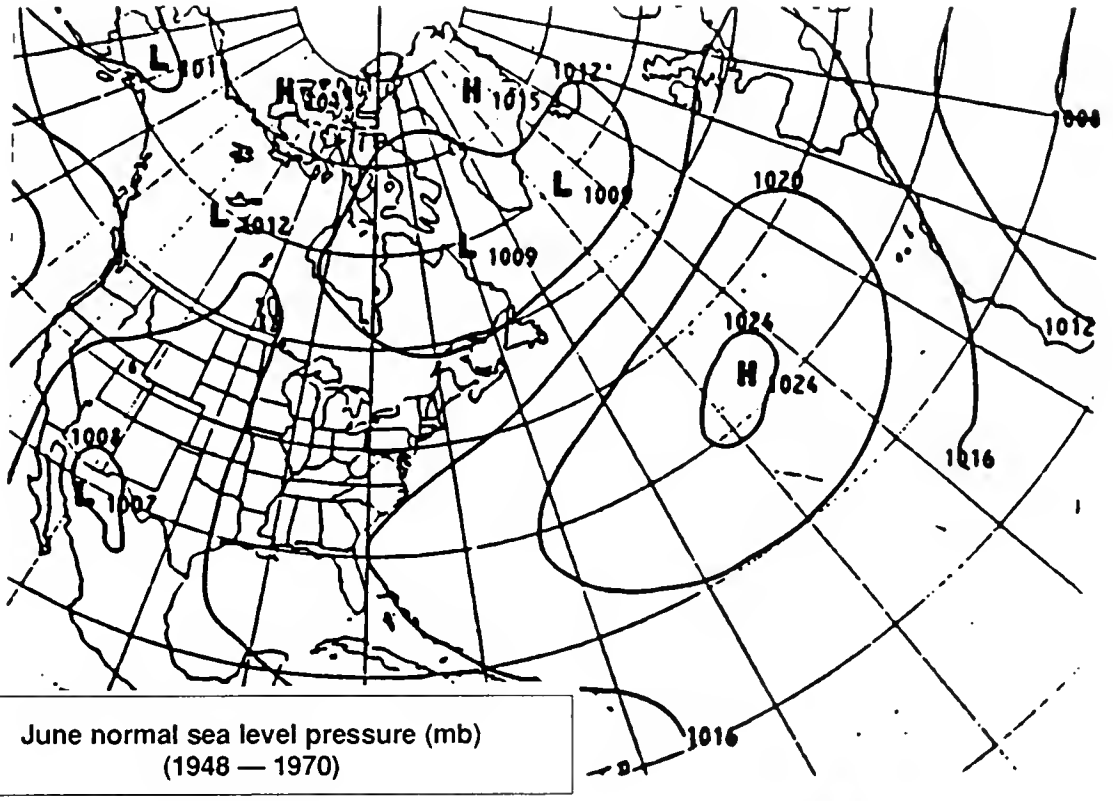

June normal sea level pressure (mb)
(1948 — 1970)

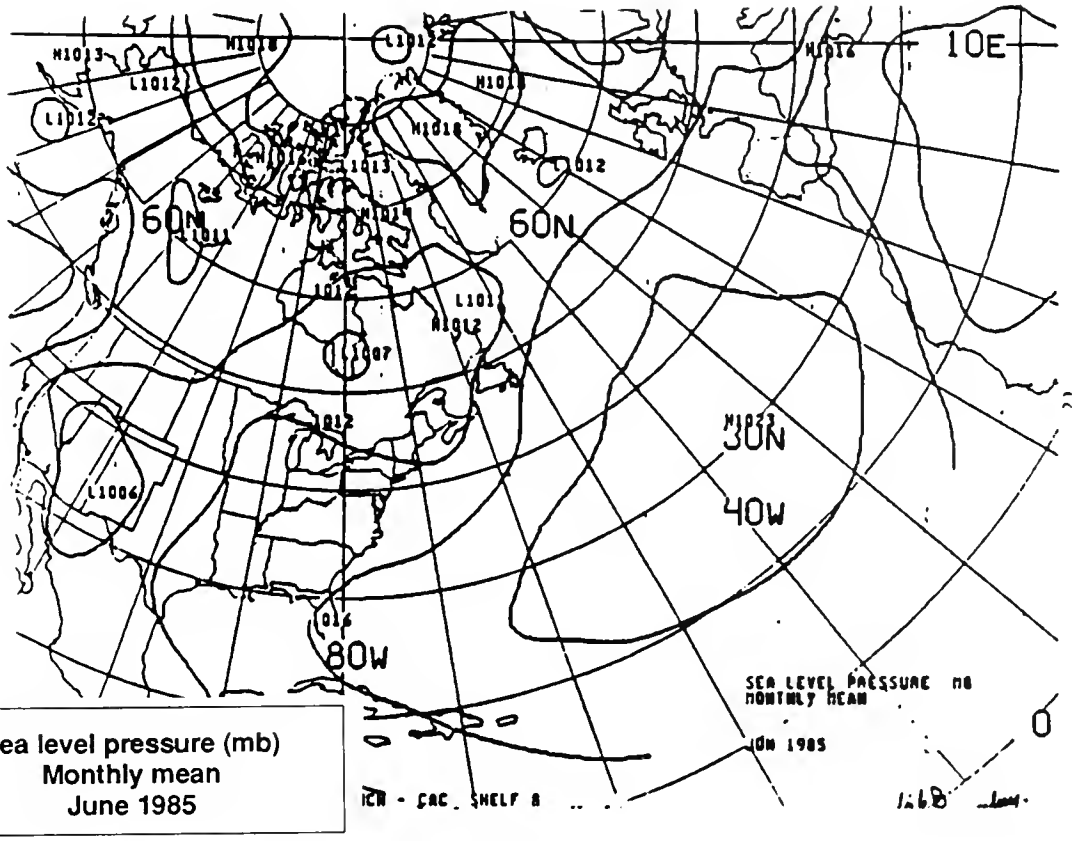

Sea level pressure (mb)
Monthly mean
June 1985

Figure 7.

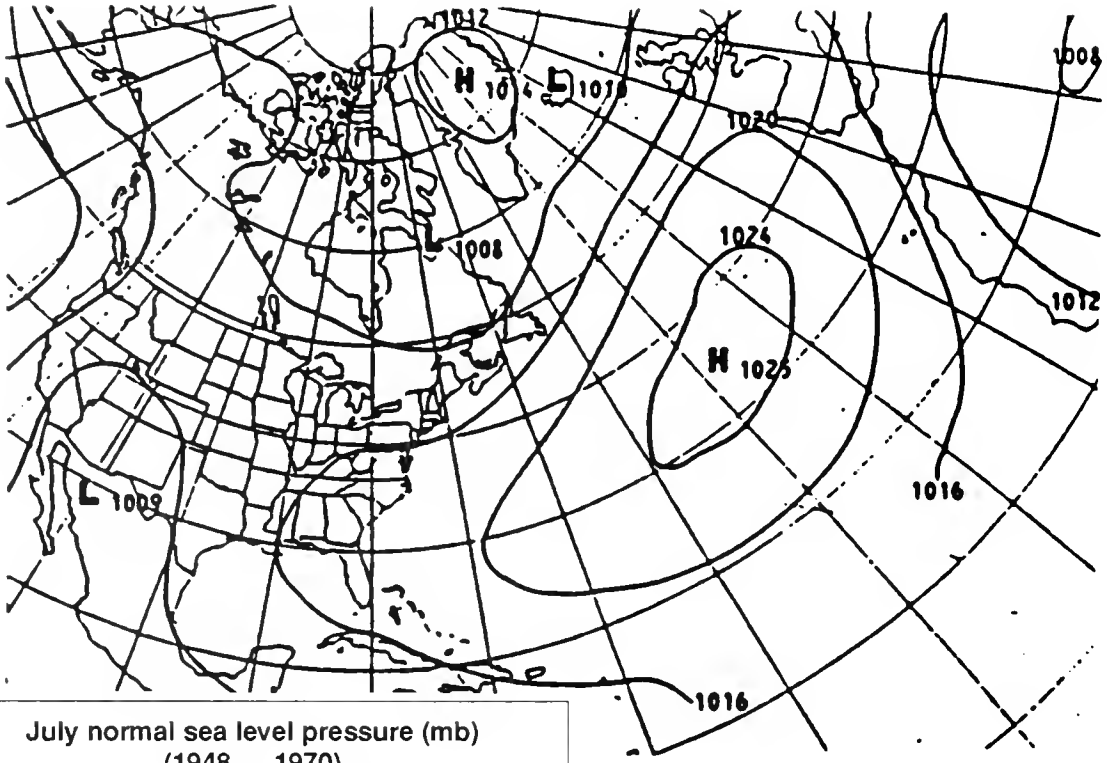

July normal sea level pressure (mb)
(1948 — 1970)

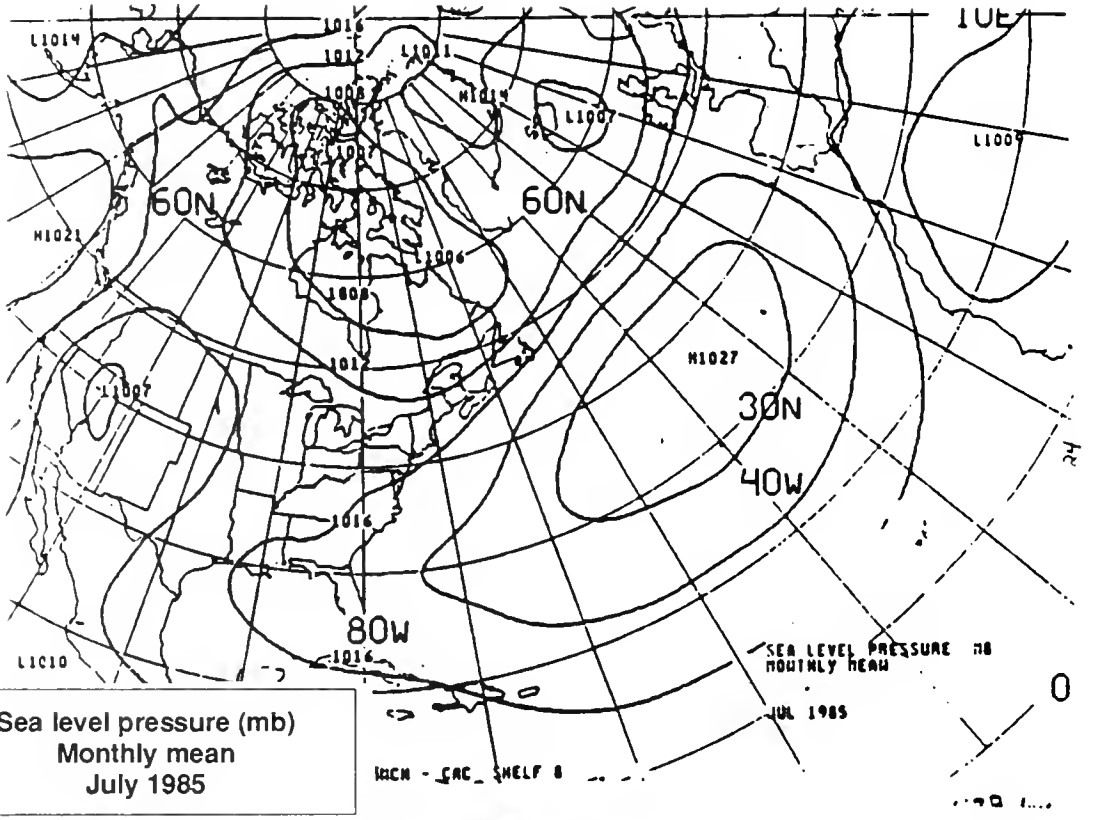

Sea level pressure (mb)
Monthly mean
July 1985

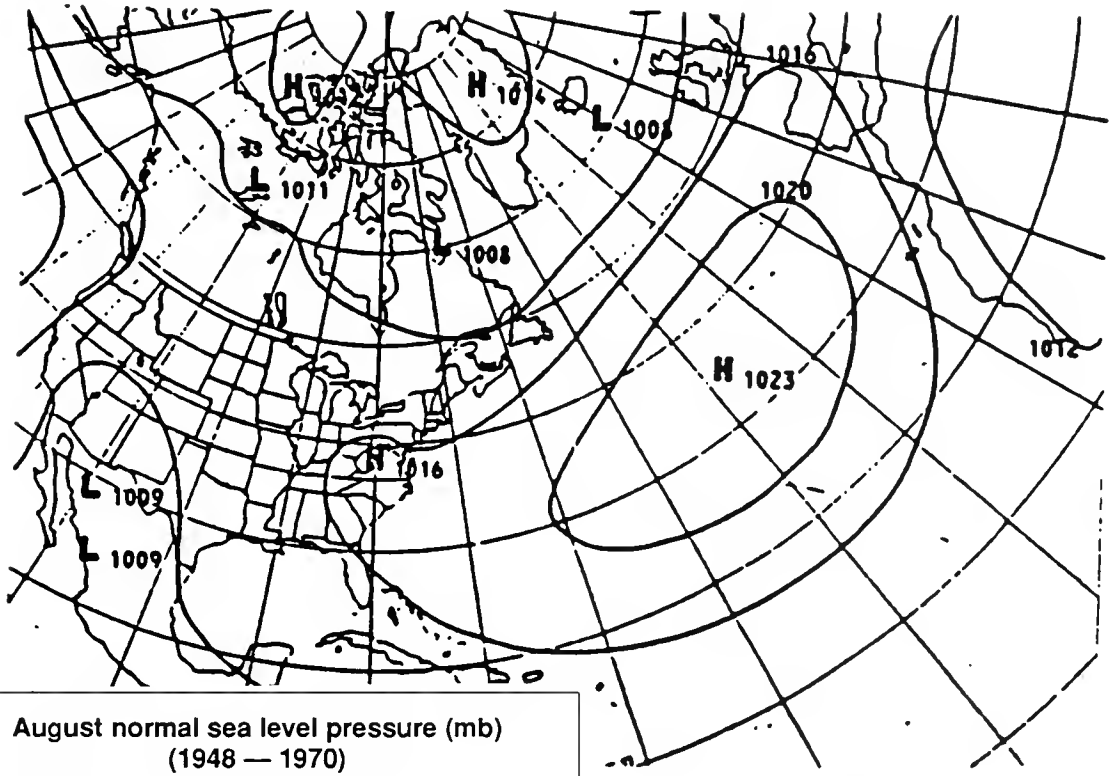

August normal sea level pressure (mb)
(1948 — 1970)

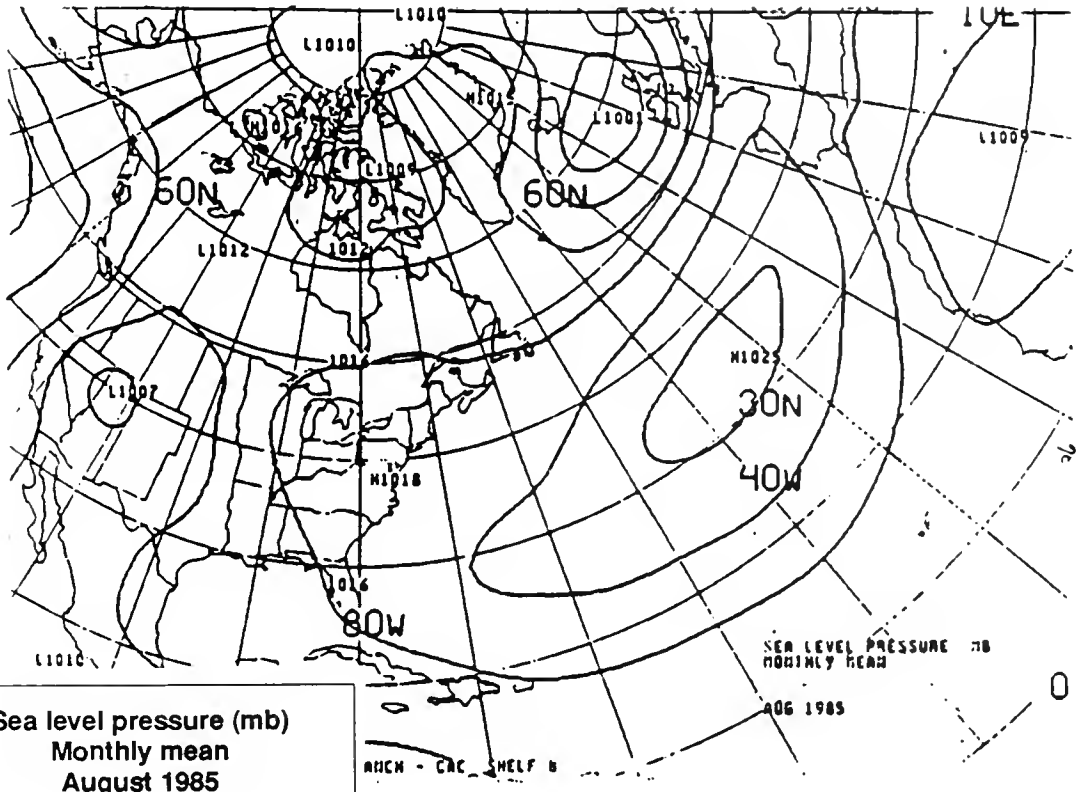

Sea level pressure (mb)
Monthly mean
August 1985

Figure 9.

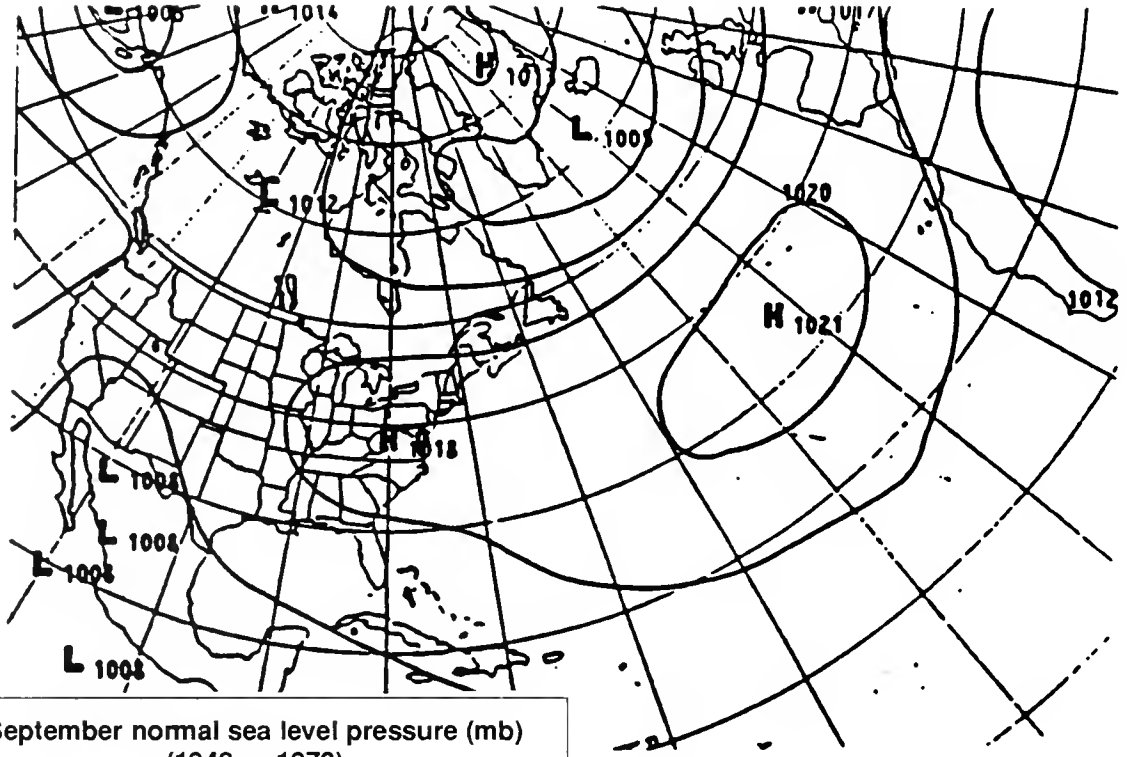

September normal sea level pressure (mb)
(1948 — 1970)

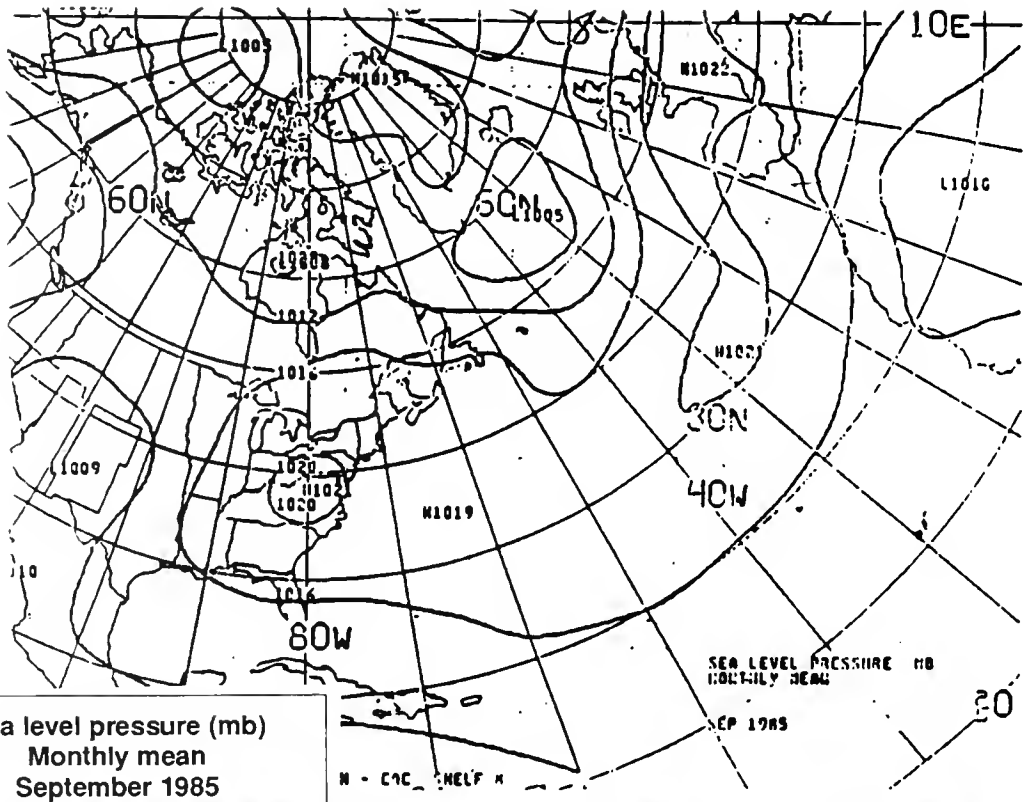

Sea level pressure (mb)
Monthly mean
September 1985

Figure 10. 16 October 1984

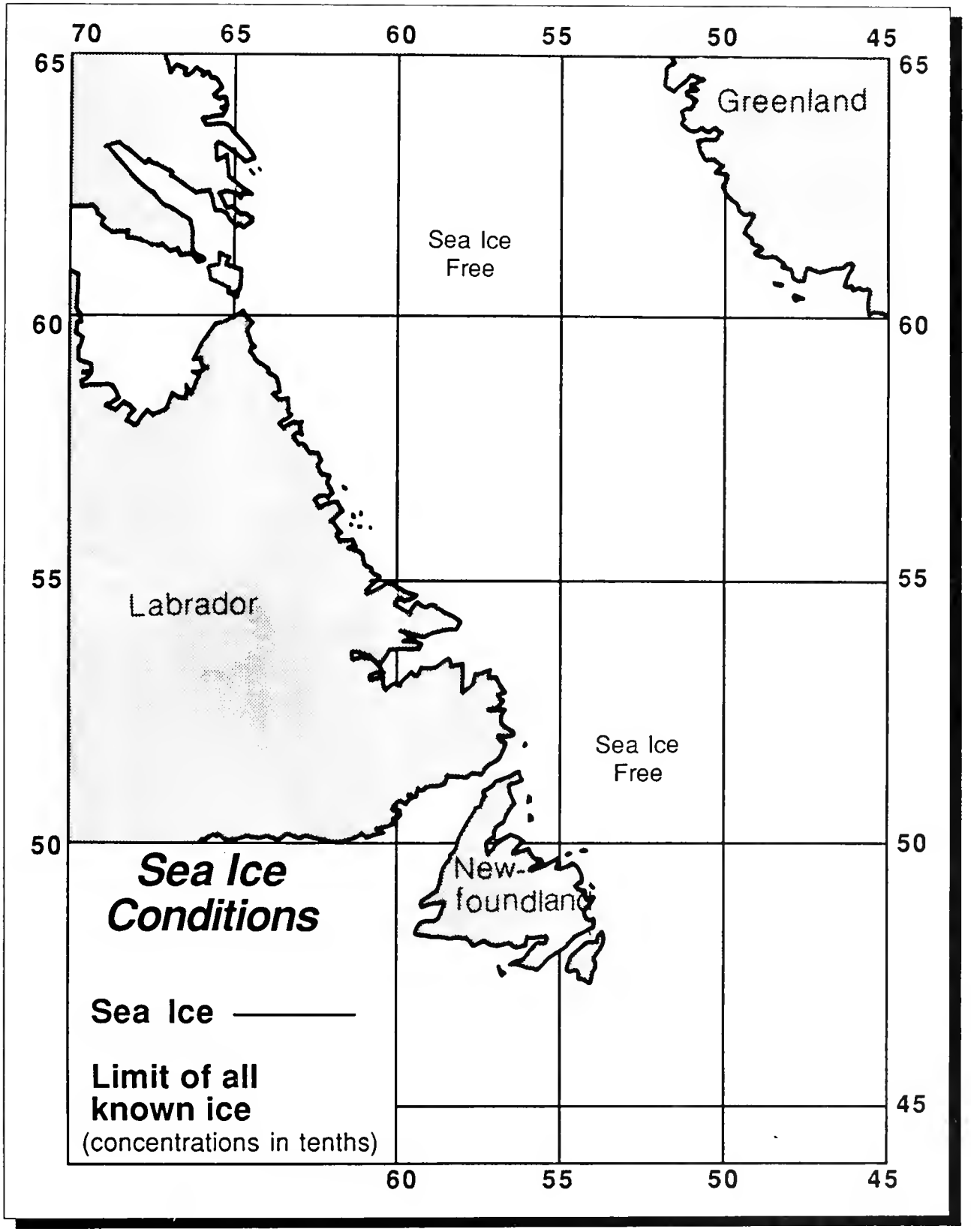

Figure 11. 13 November 1984

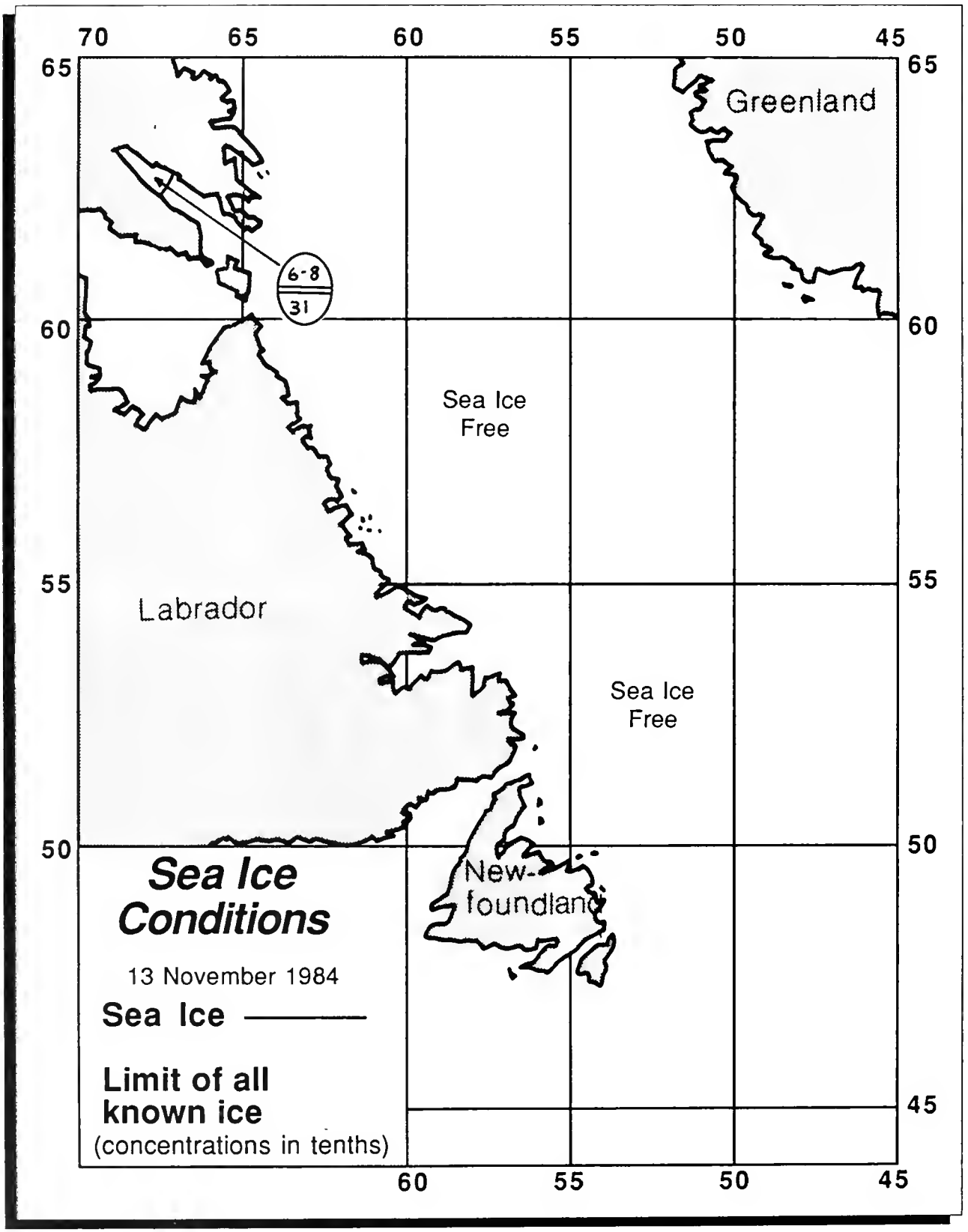

Figure 12. 18 December 1984

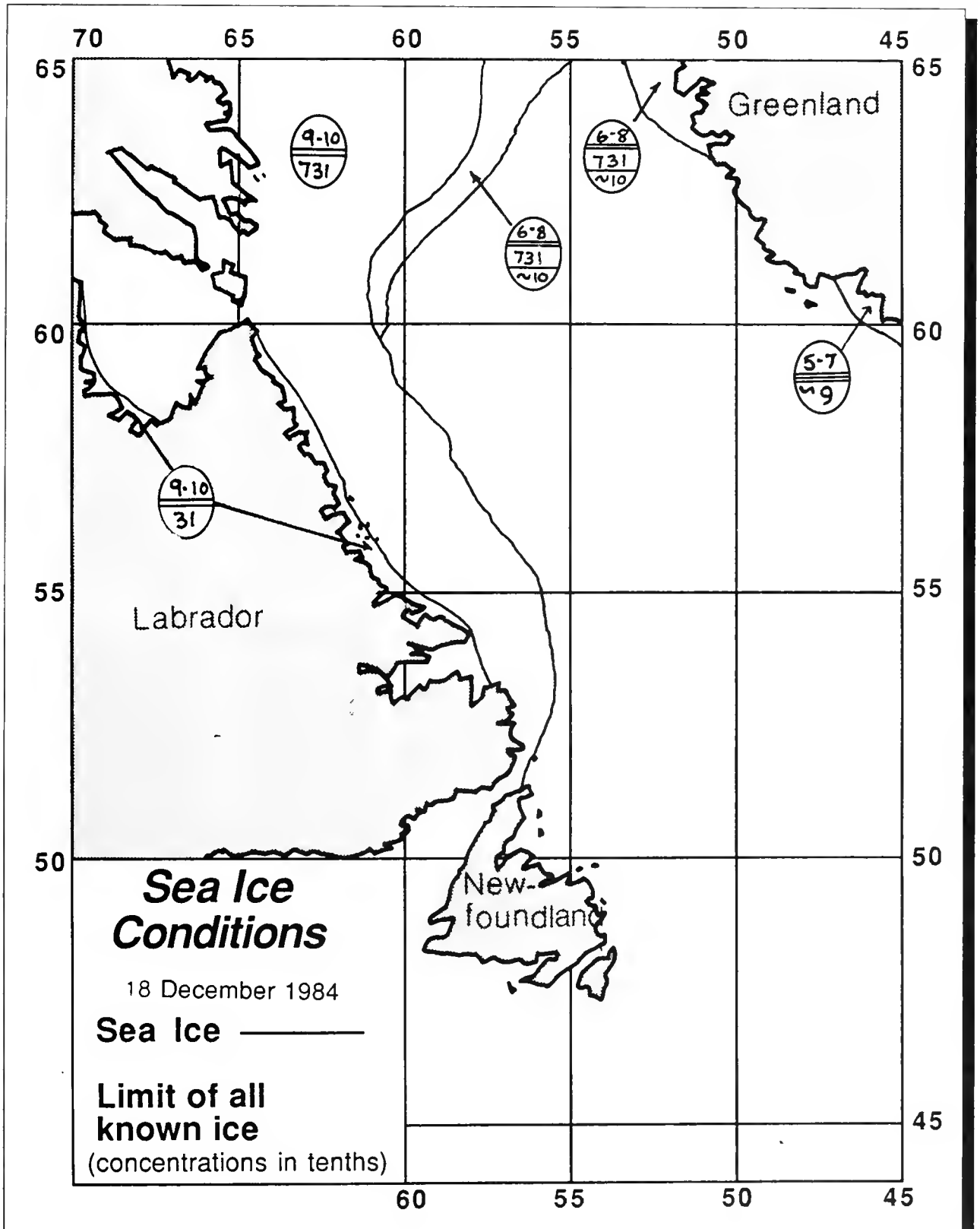

Figure 13. 15 January 1985

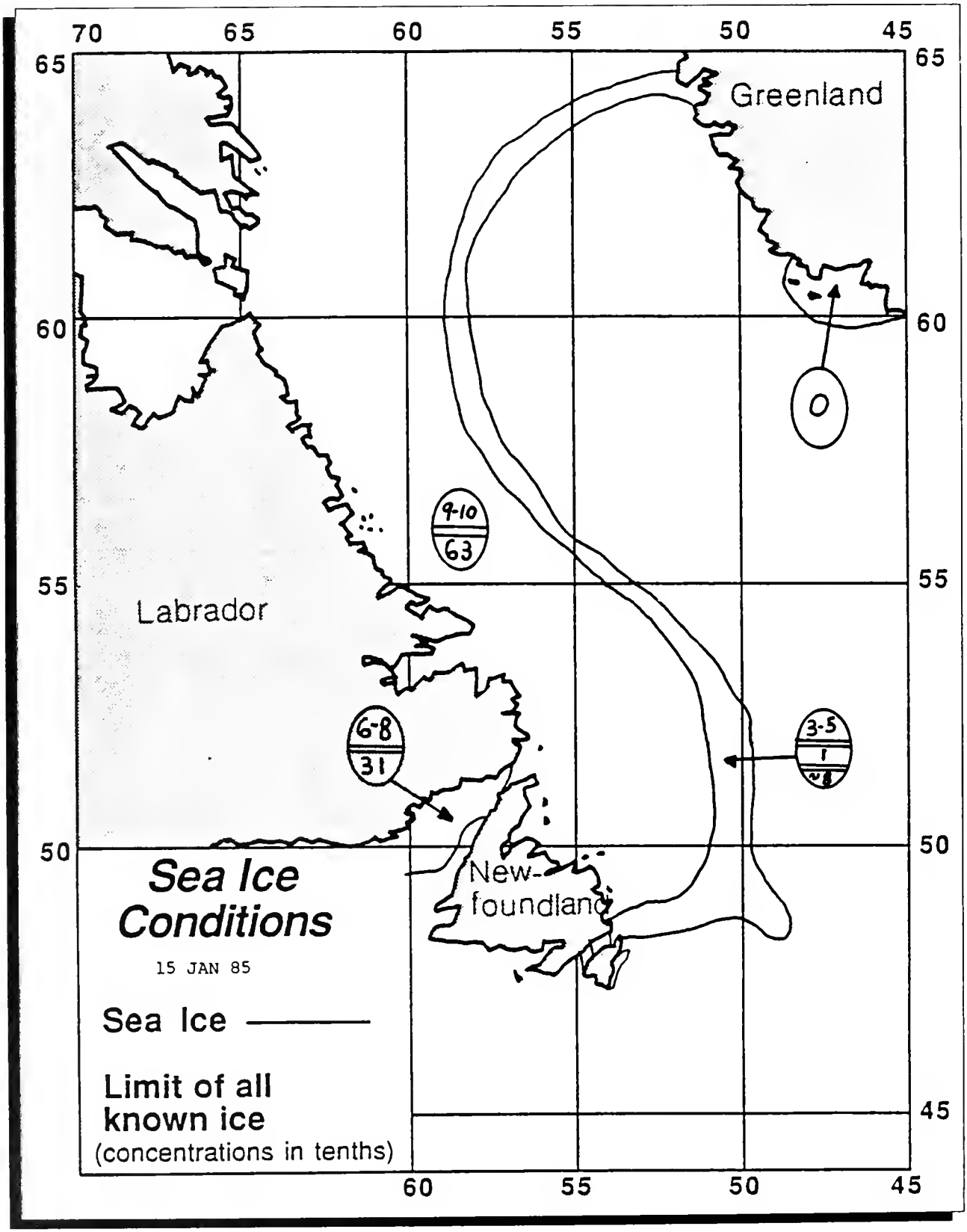

Figure 14. 12 February 1985

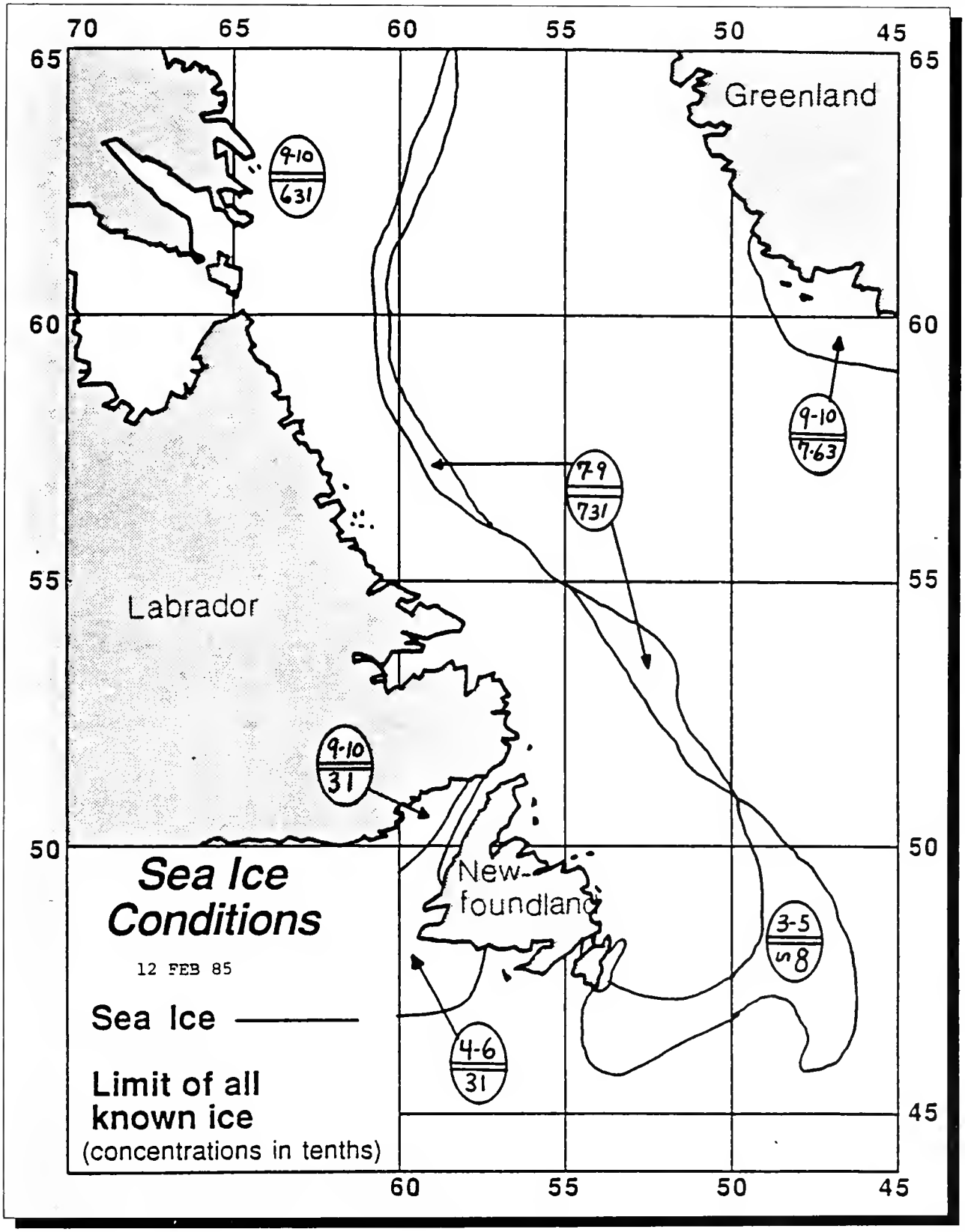

Figure 15. 12 March 1985

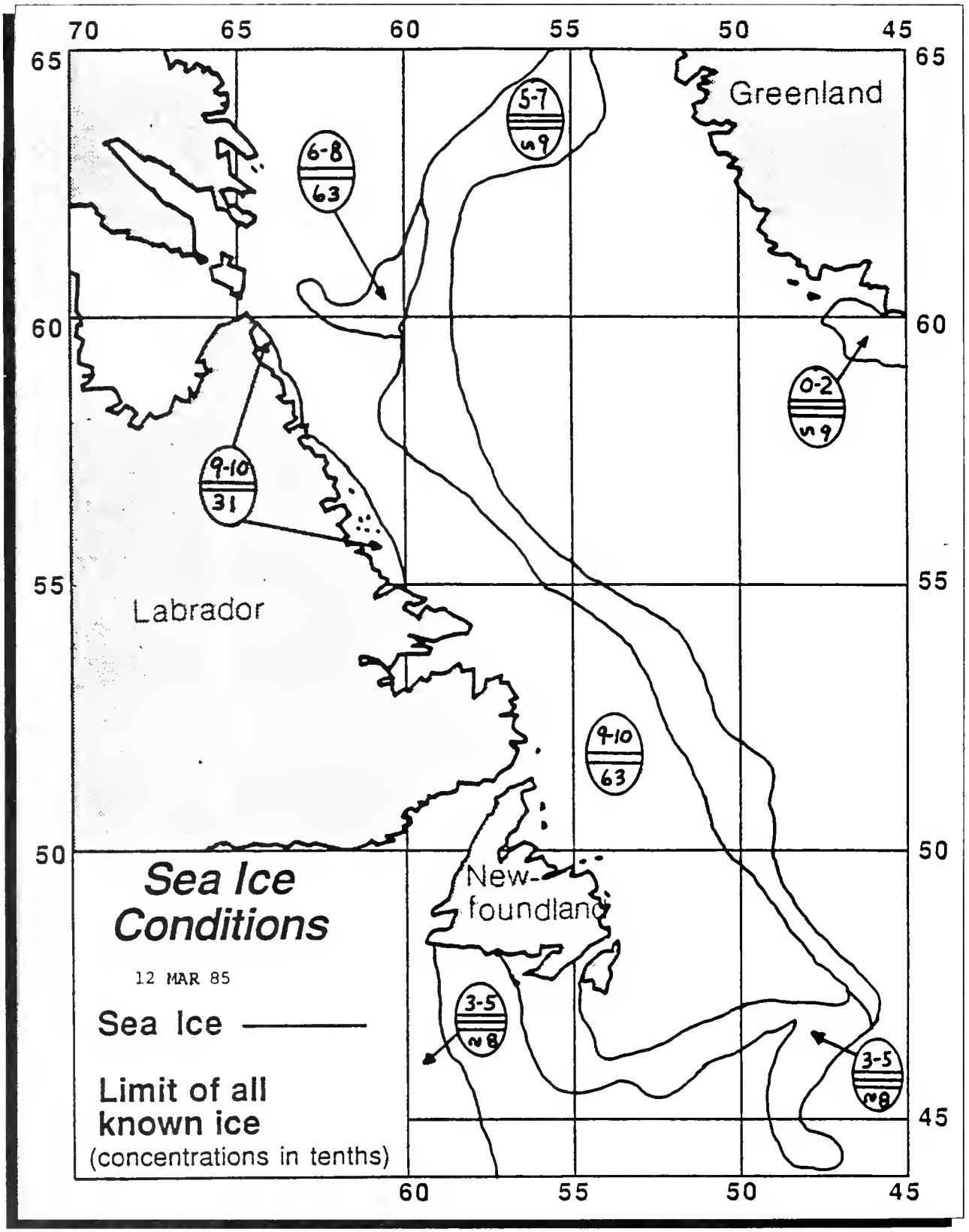

Figure 16. 16 April 1985

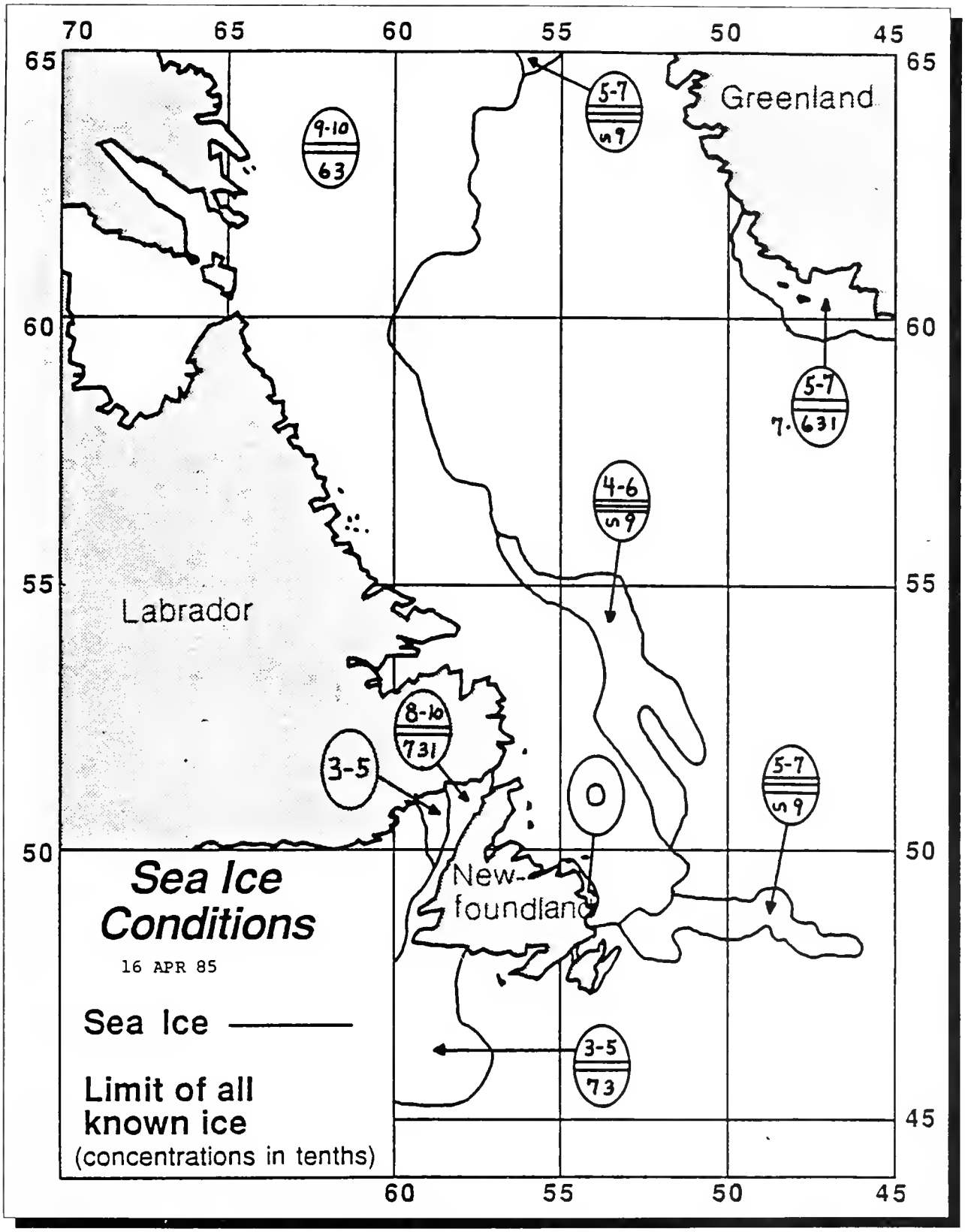

Figure 17. 14 May 1985

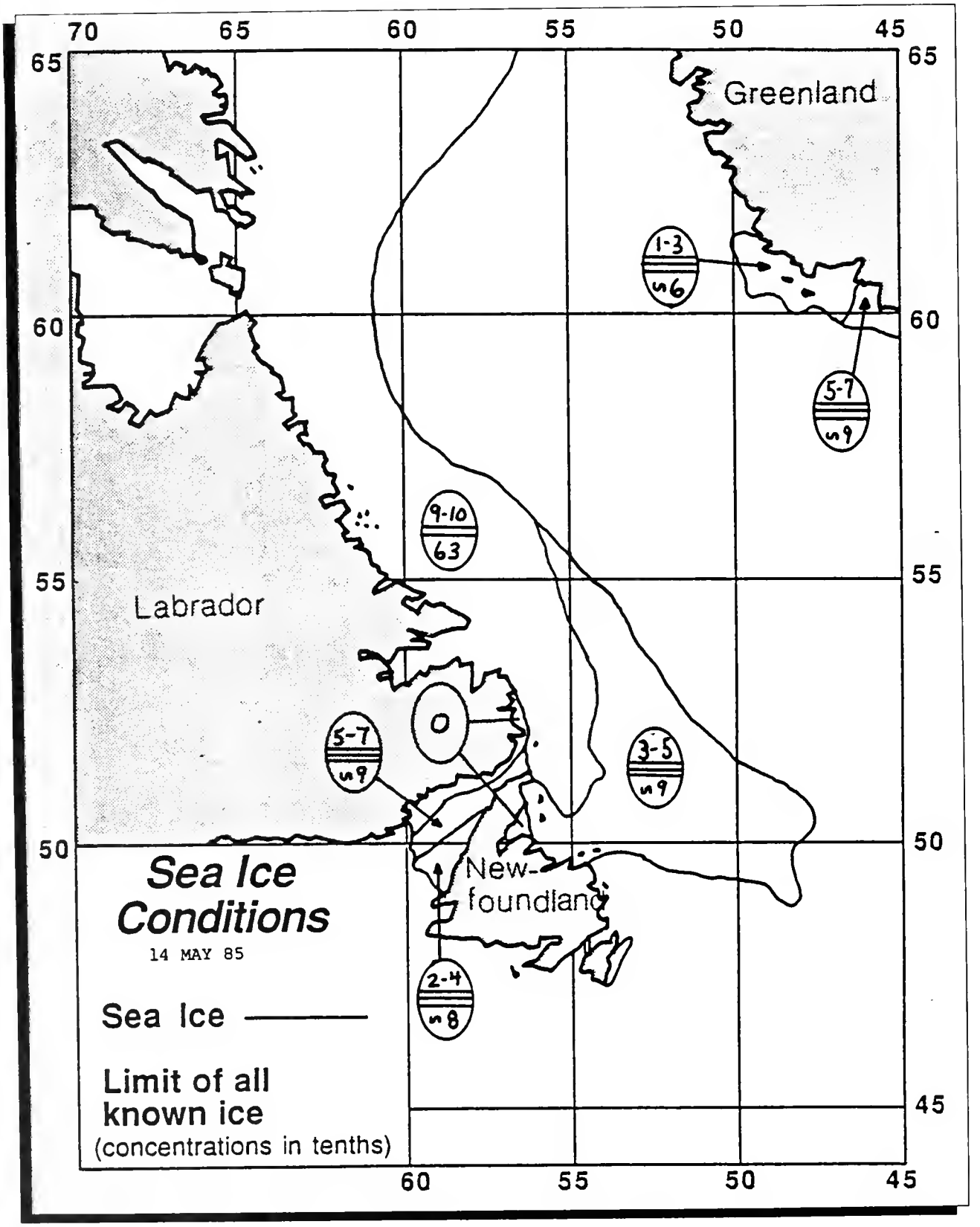

Figure 18. 18 June 1985

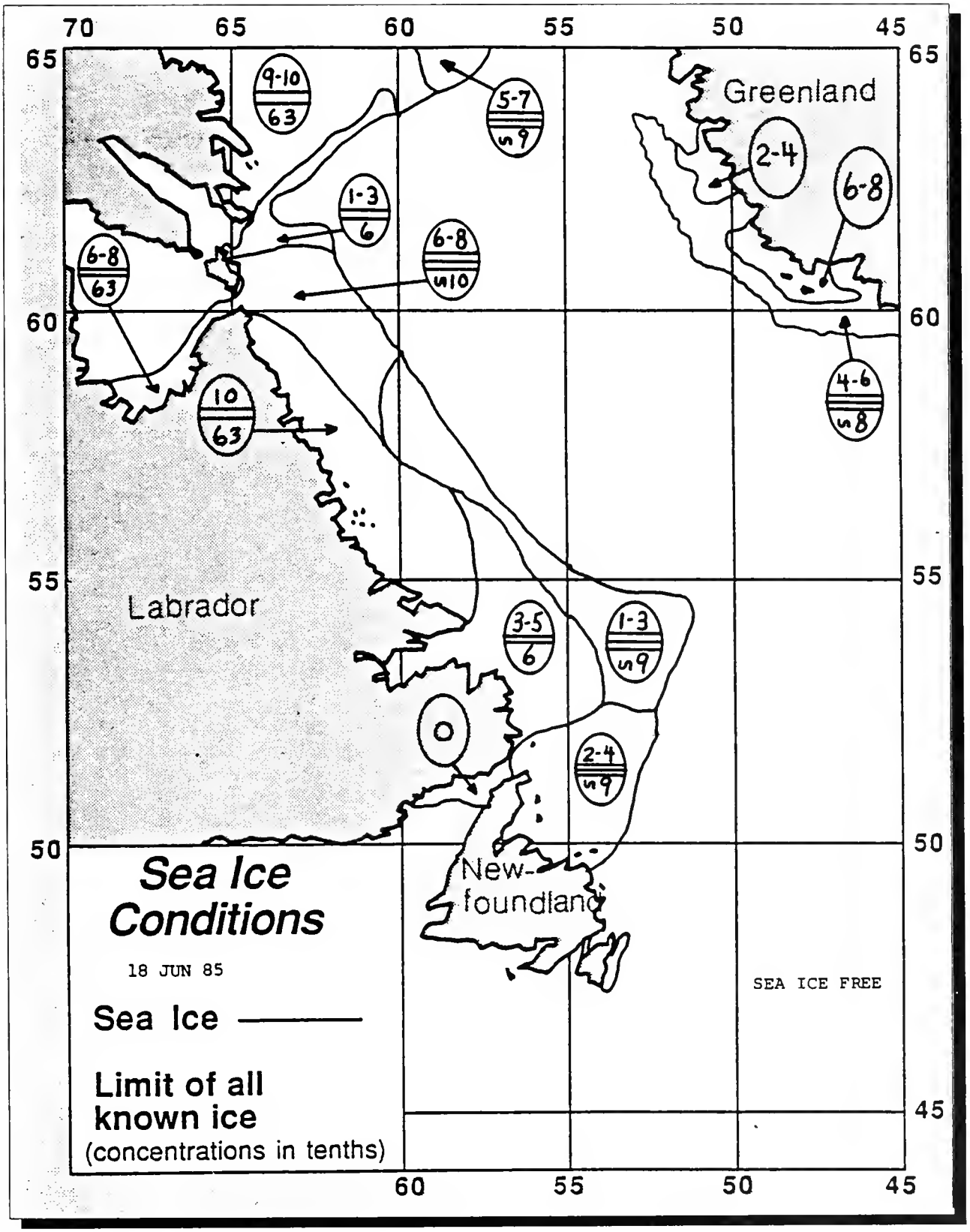

Figure 19. 16 July 1985

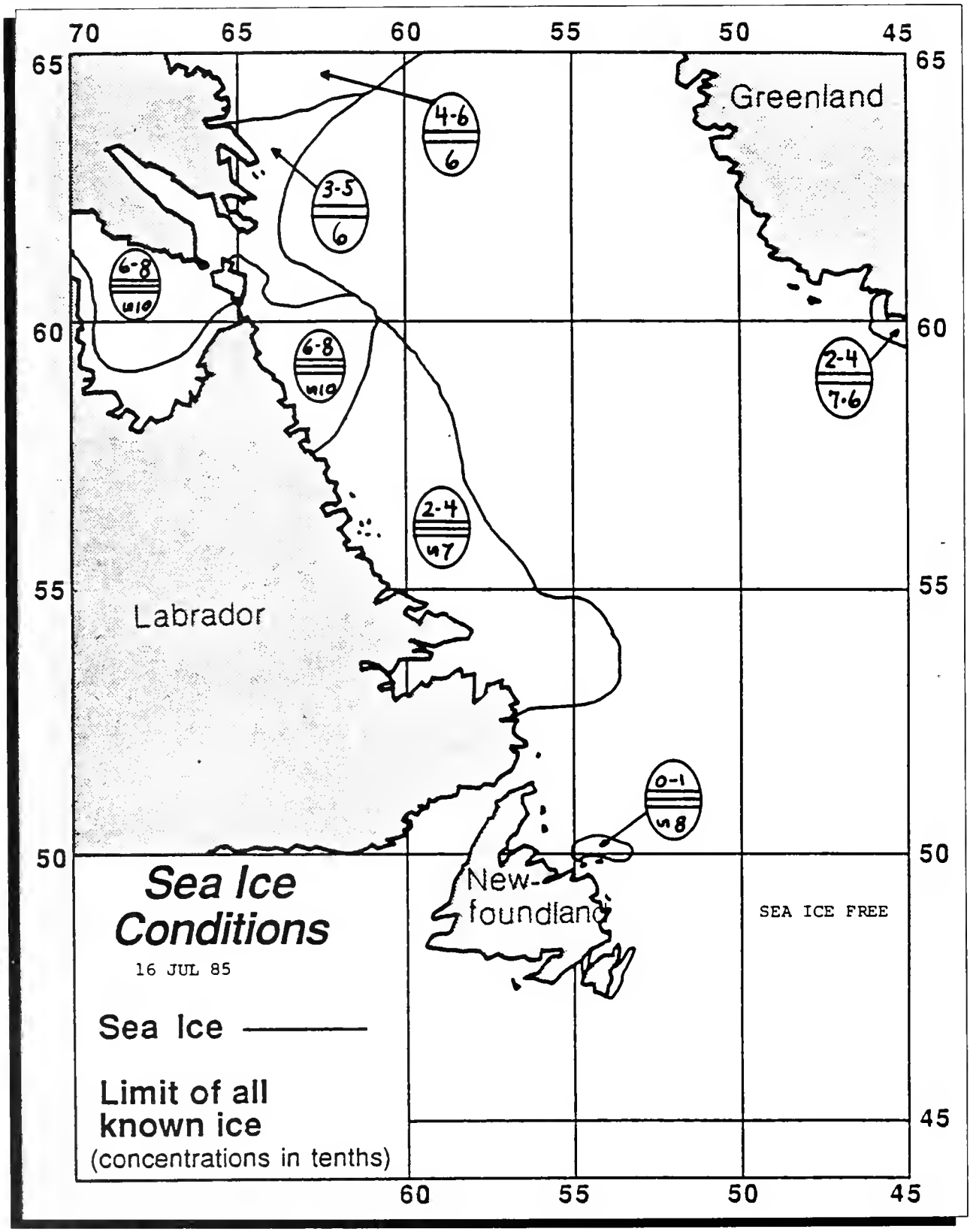

Figure 20. 13 August 1985

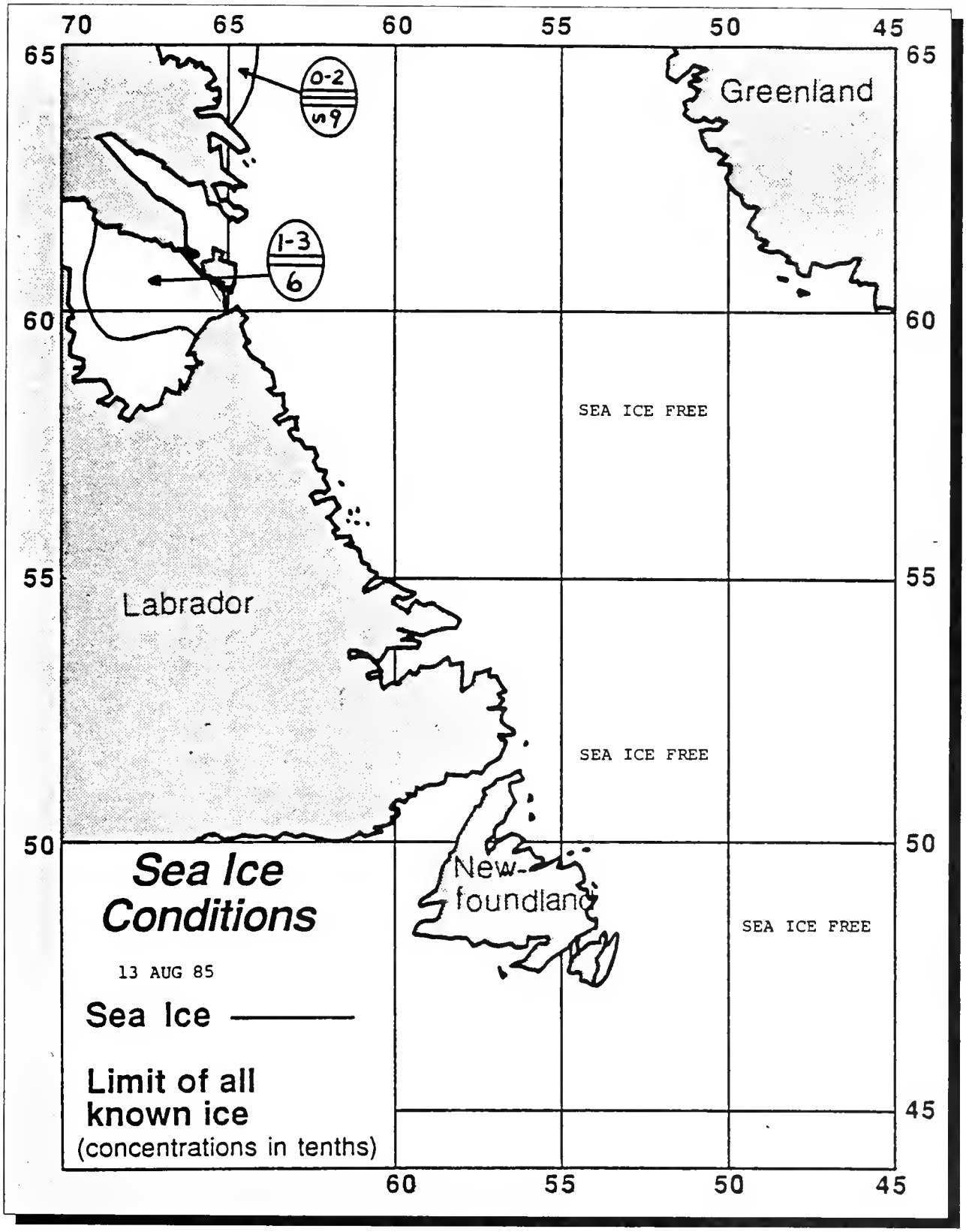

Figure 21. 17 September 1985

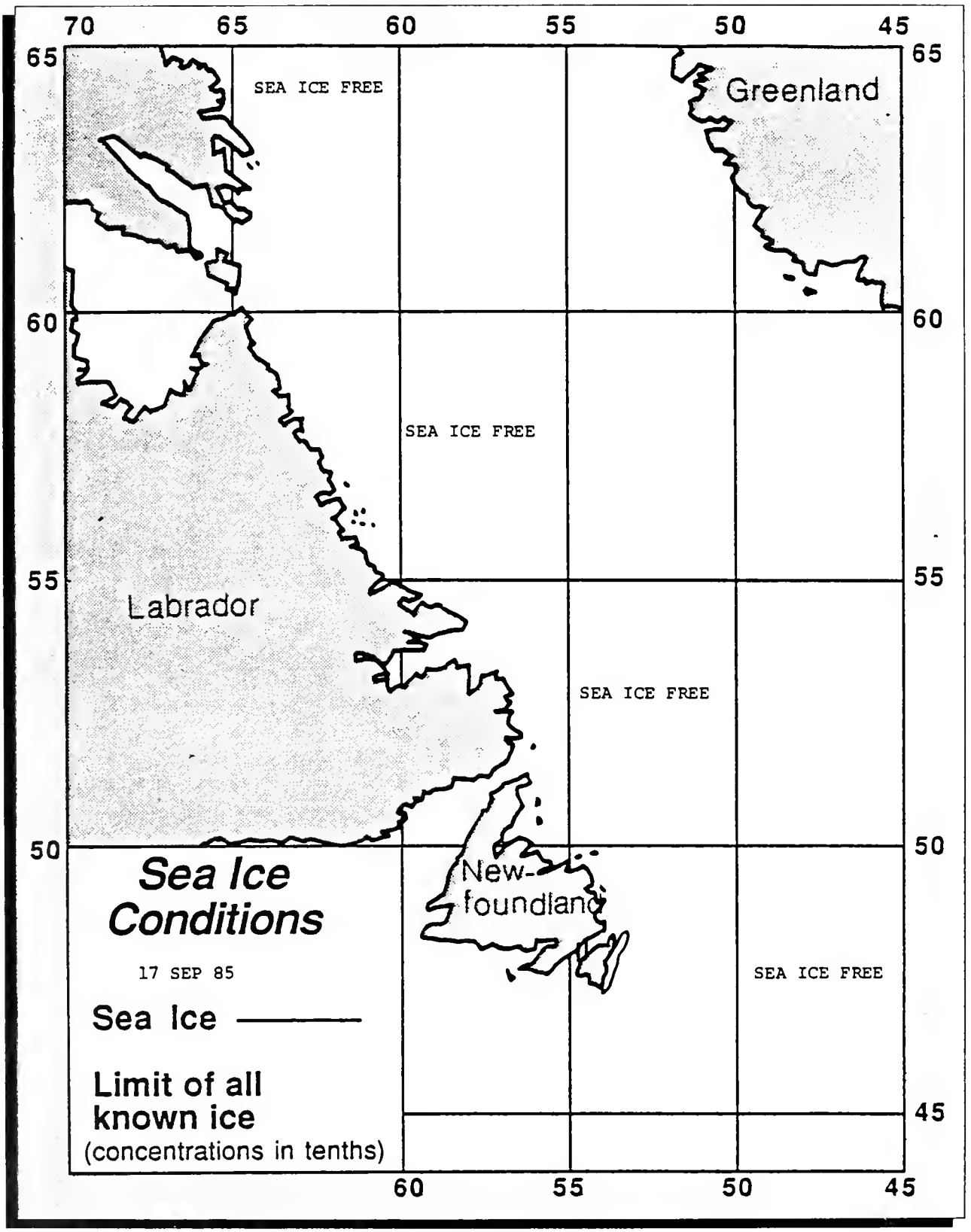

Figure 22. 15 March 1985

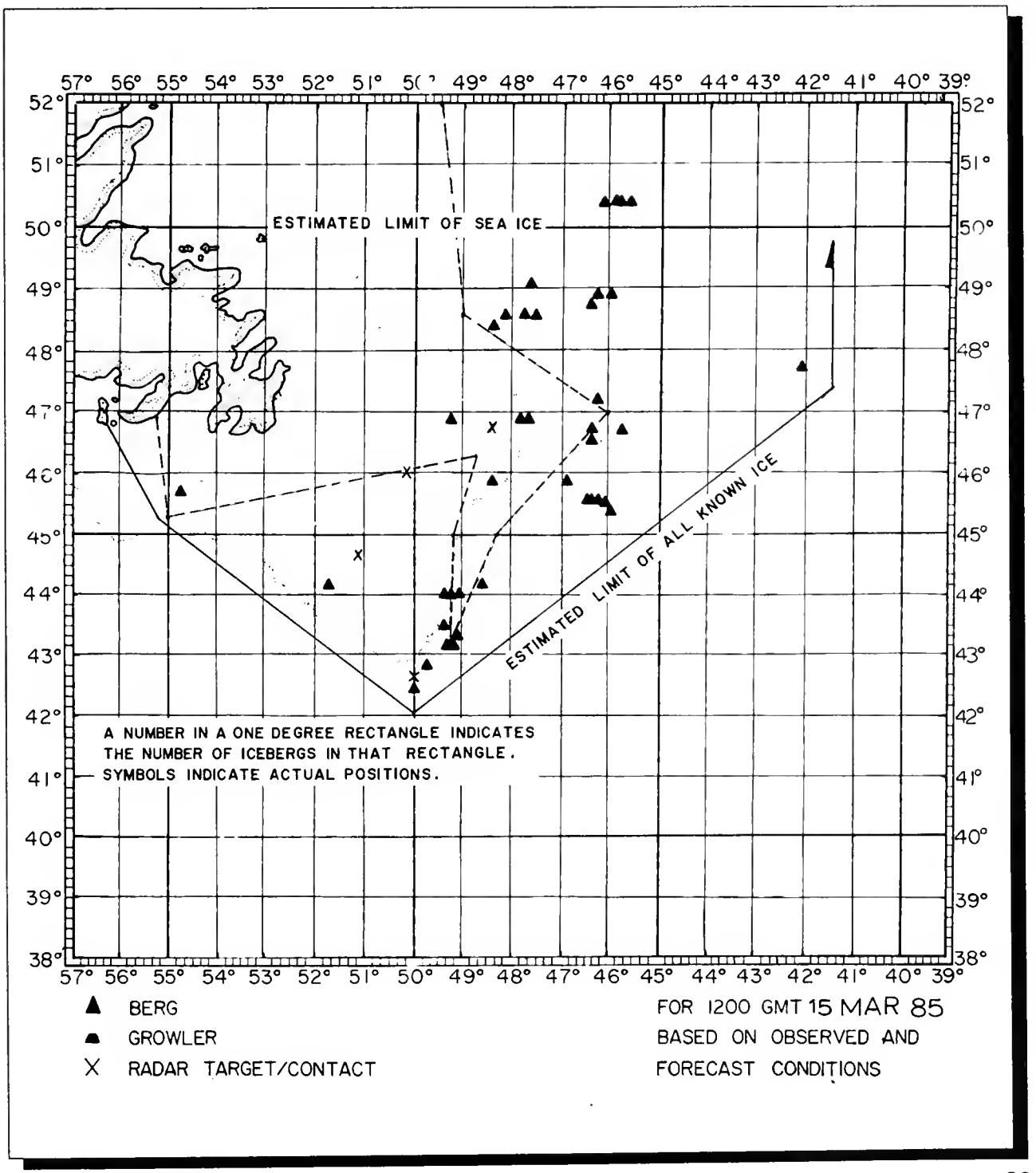

Figure 23. 30 March 1985

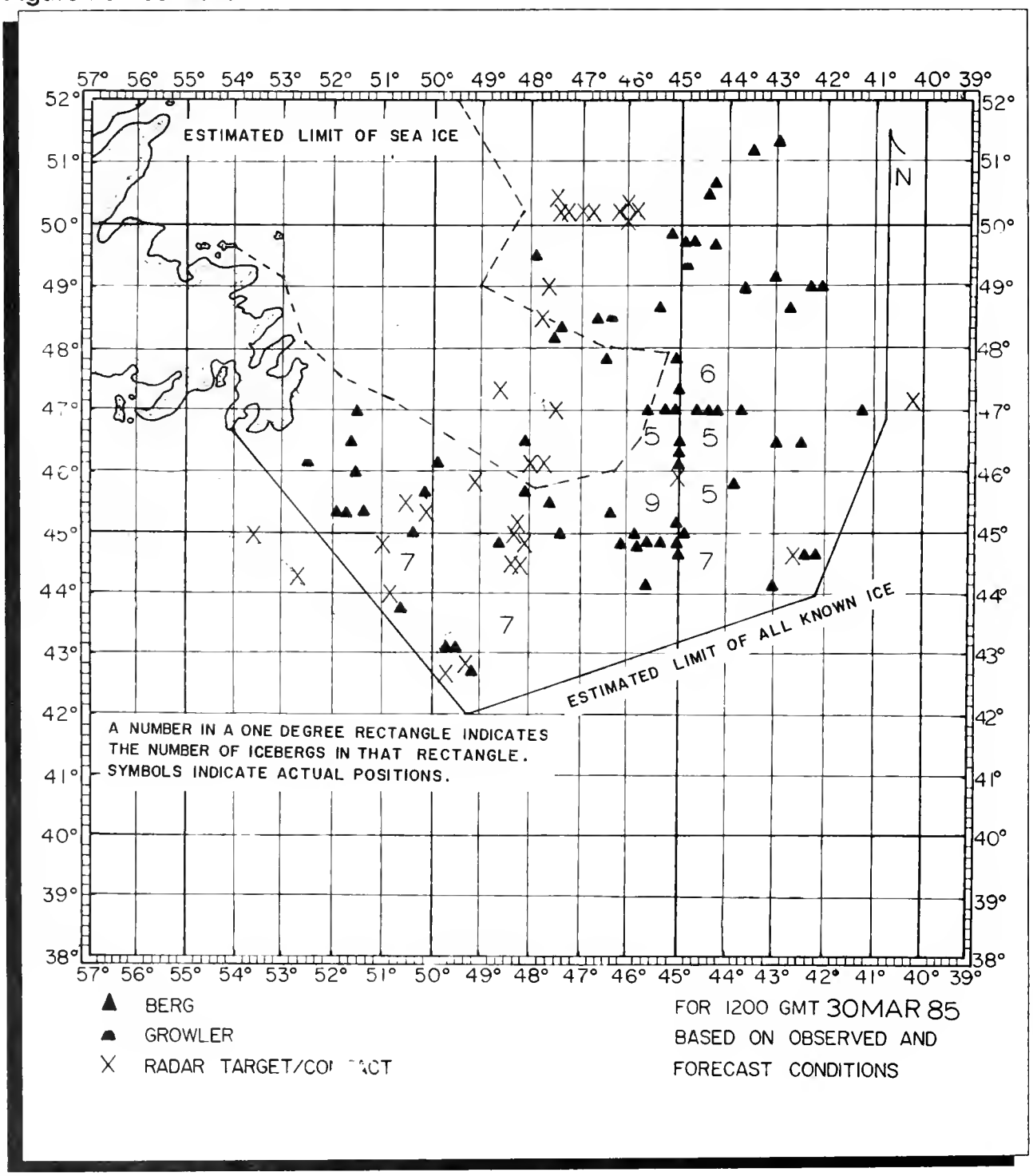

Figure 24. 15 April 1985

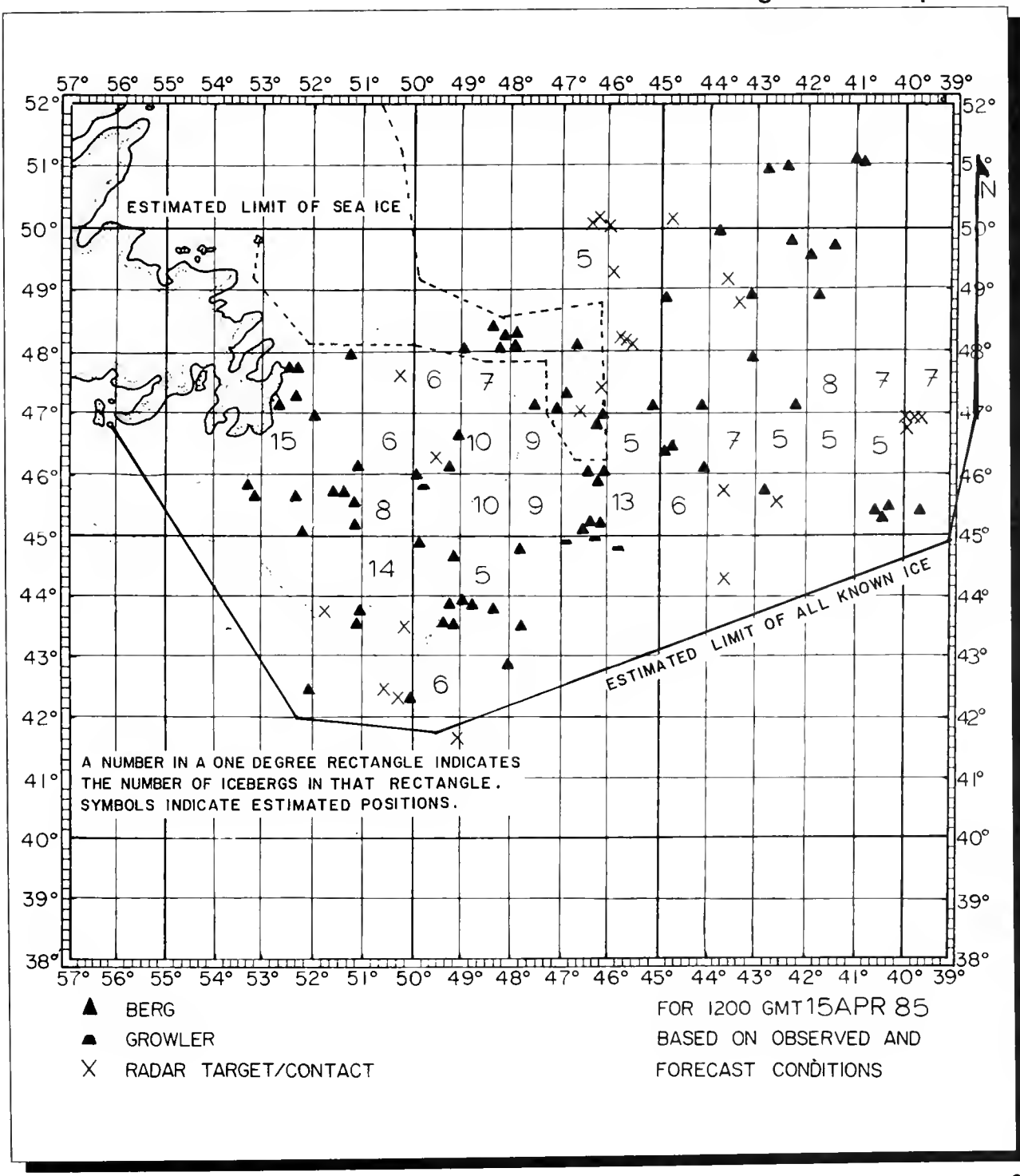

Figure 25. 30 April 1985

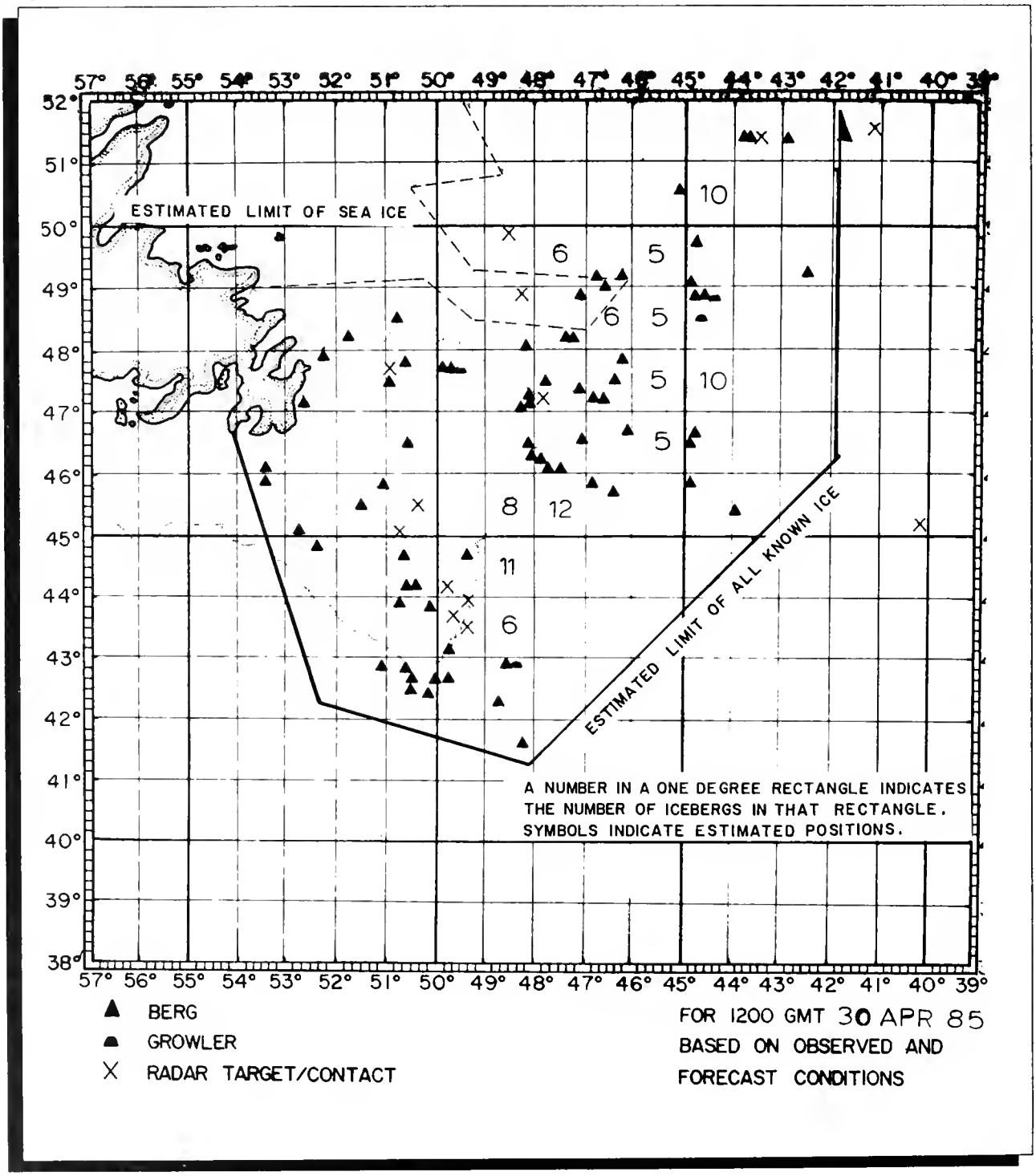

Figure 26. 15 May 1985

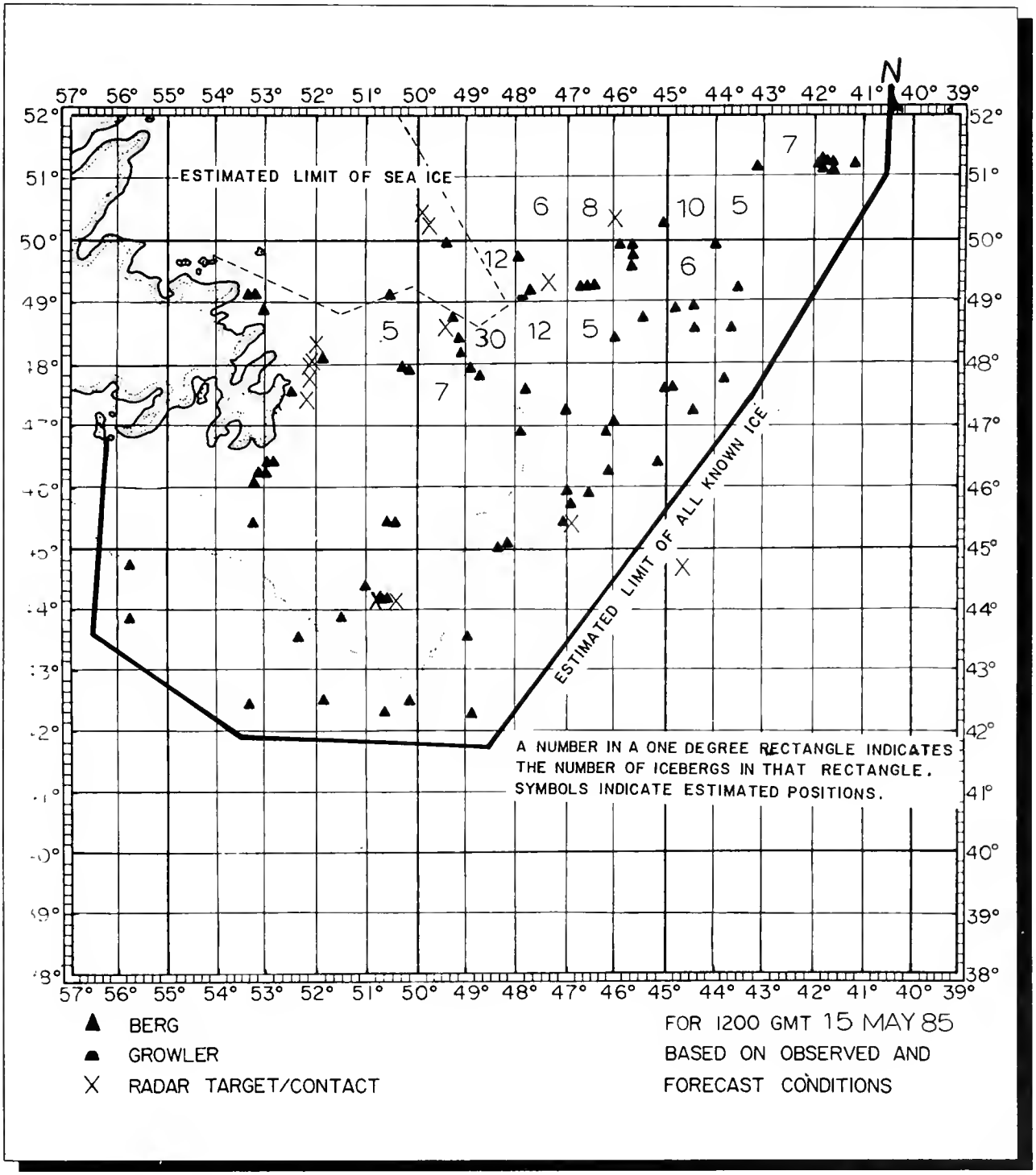

Figure 27. 30 May 1985

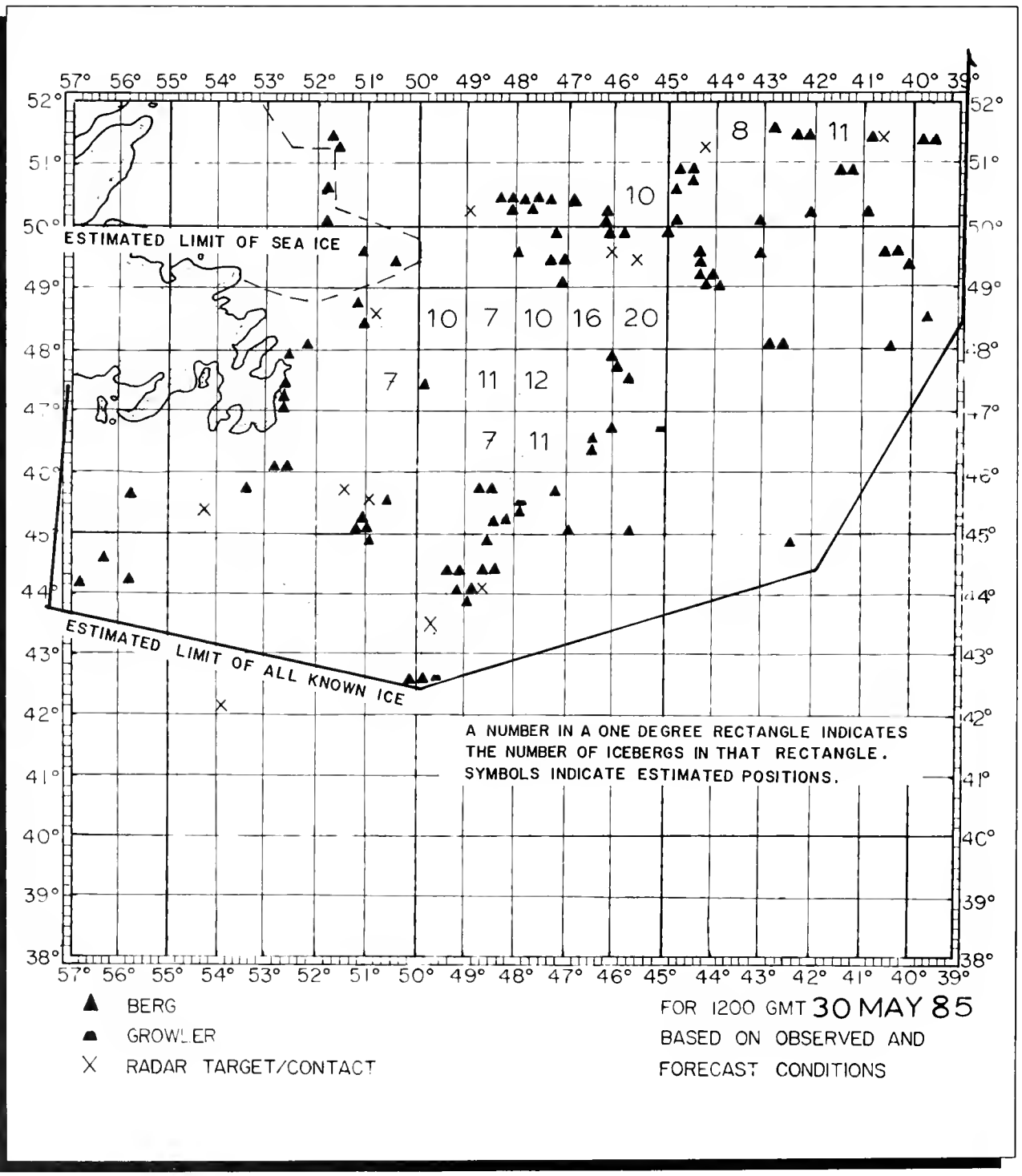

Figure 28. 15 June 1985

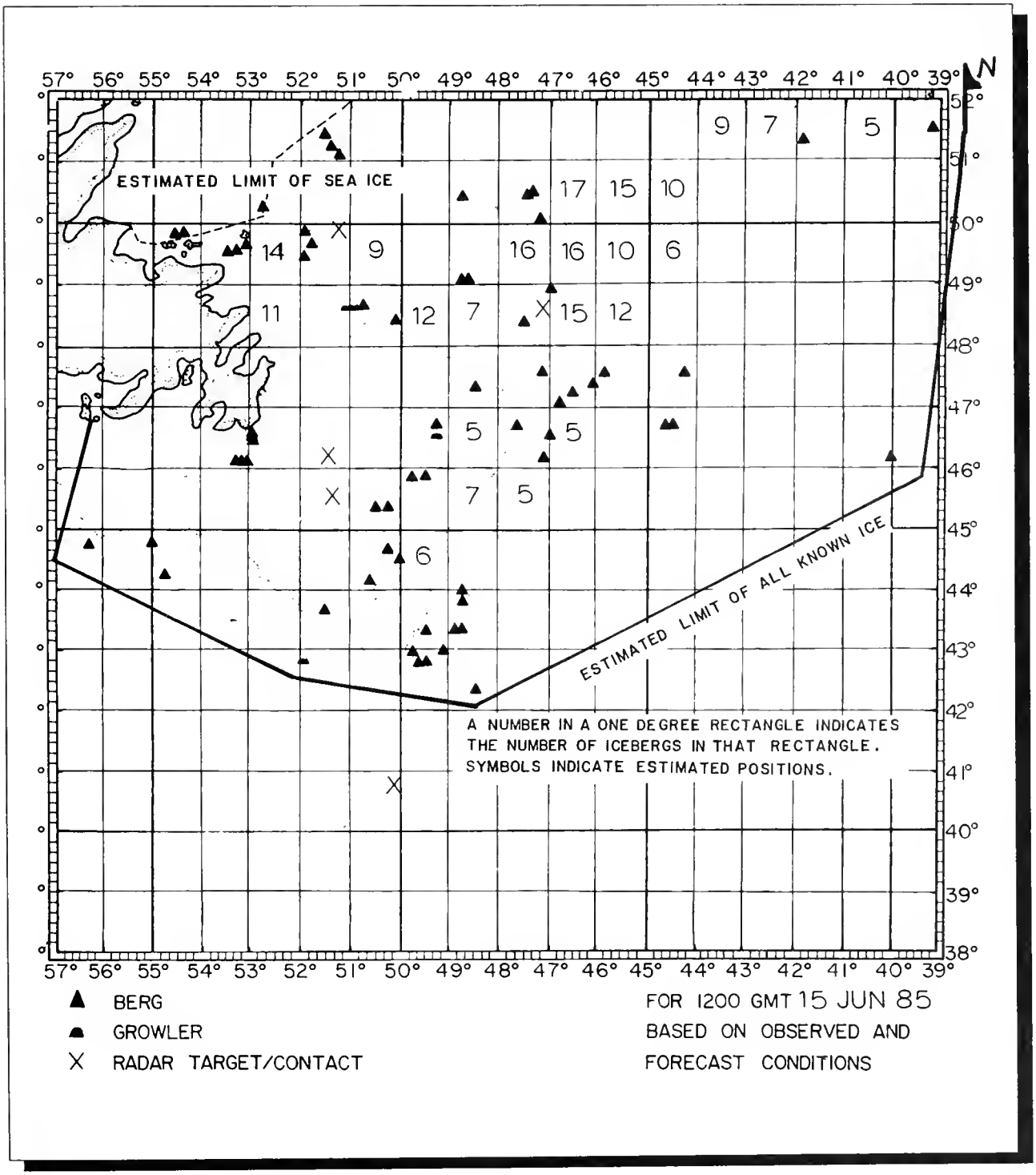

Figure 29. 30 June 1985

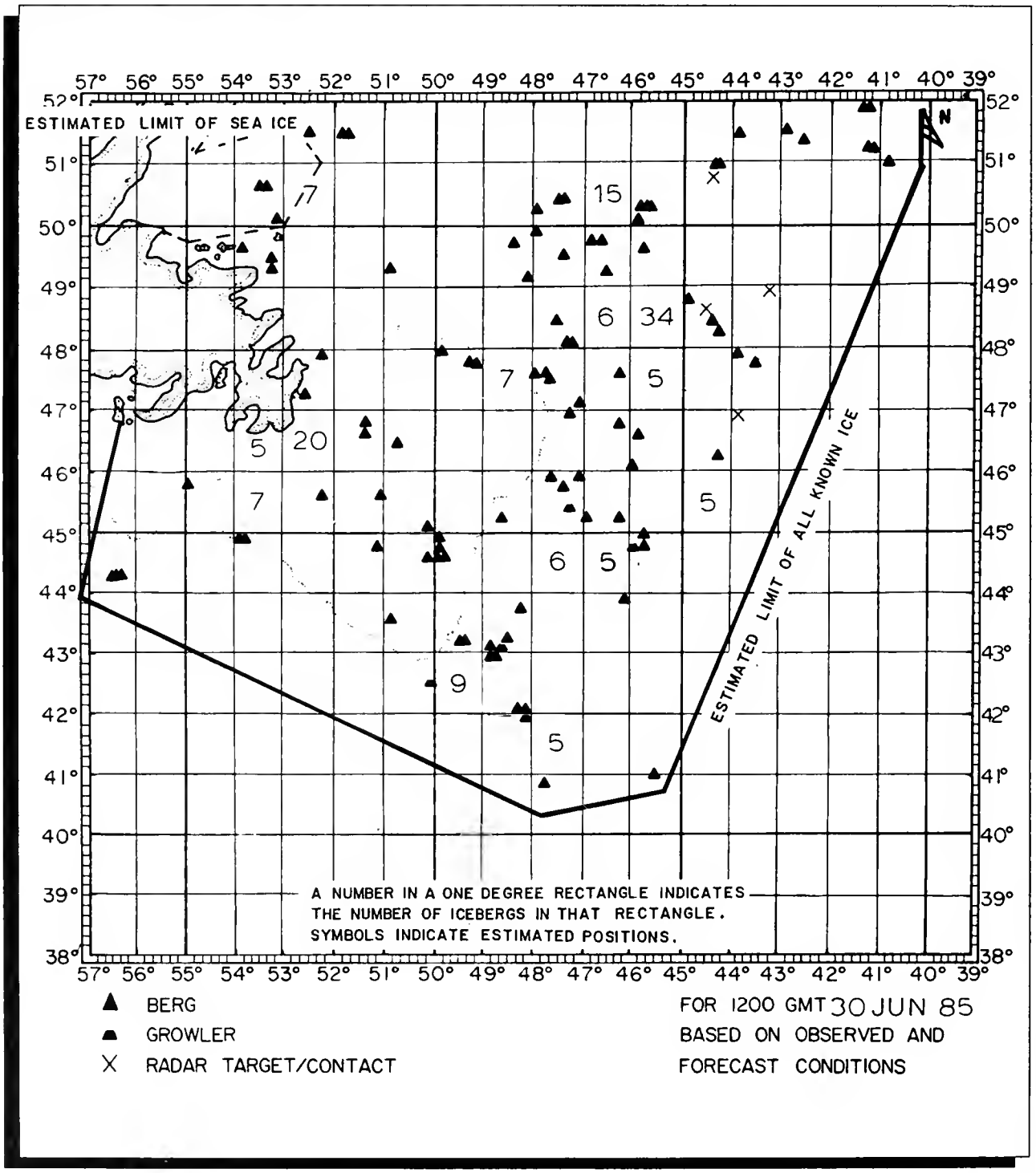

Figure 30. 15 July 1985

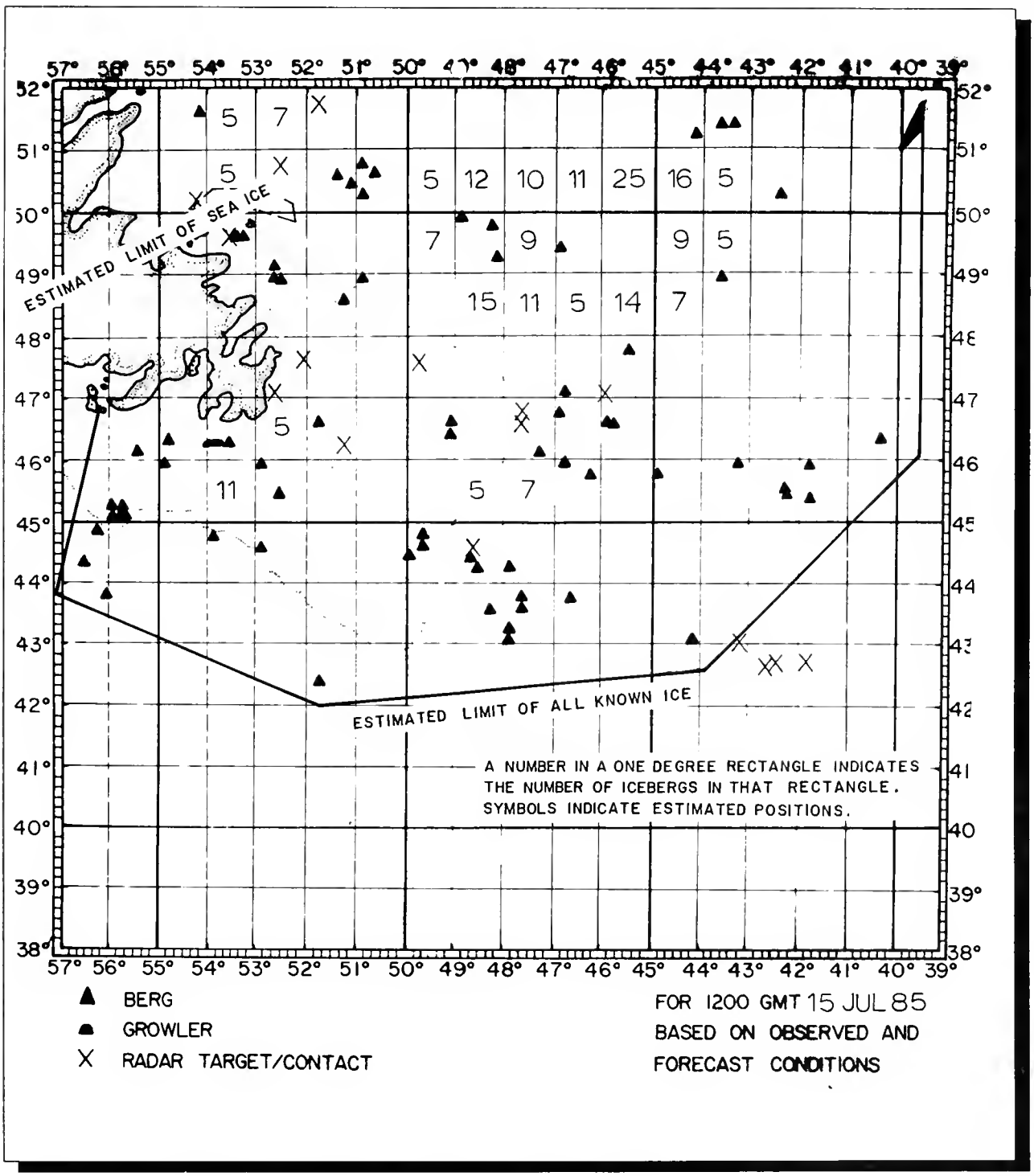

Figure 31. 30 July 1985

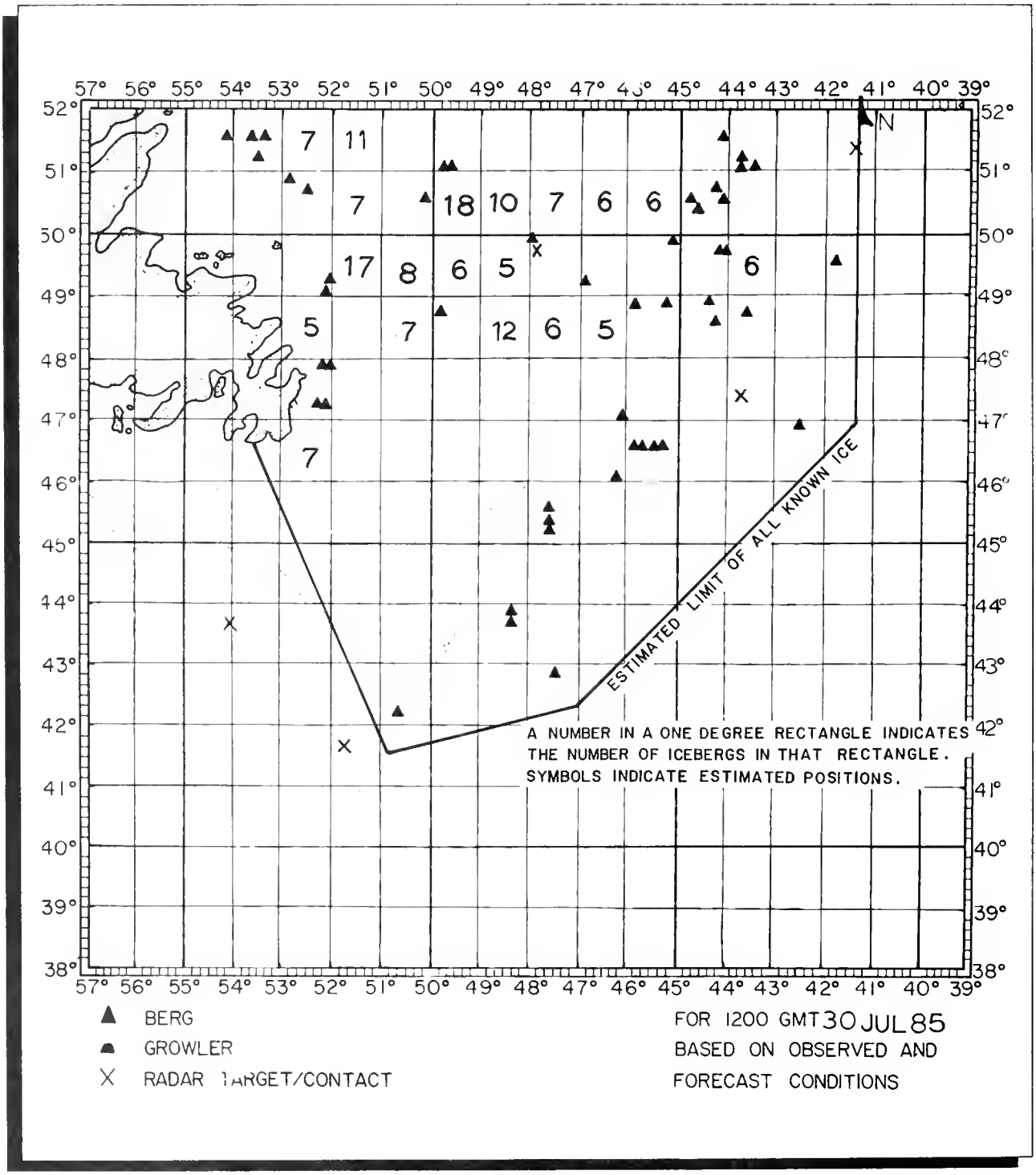

Figure 32. 15 August 1985

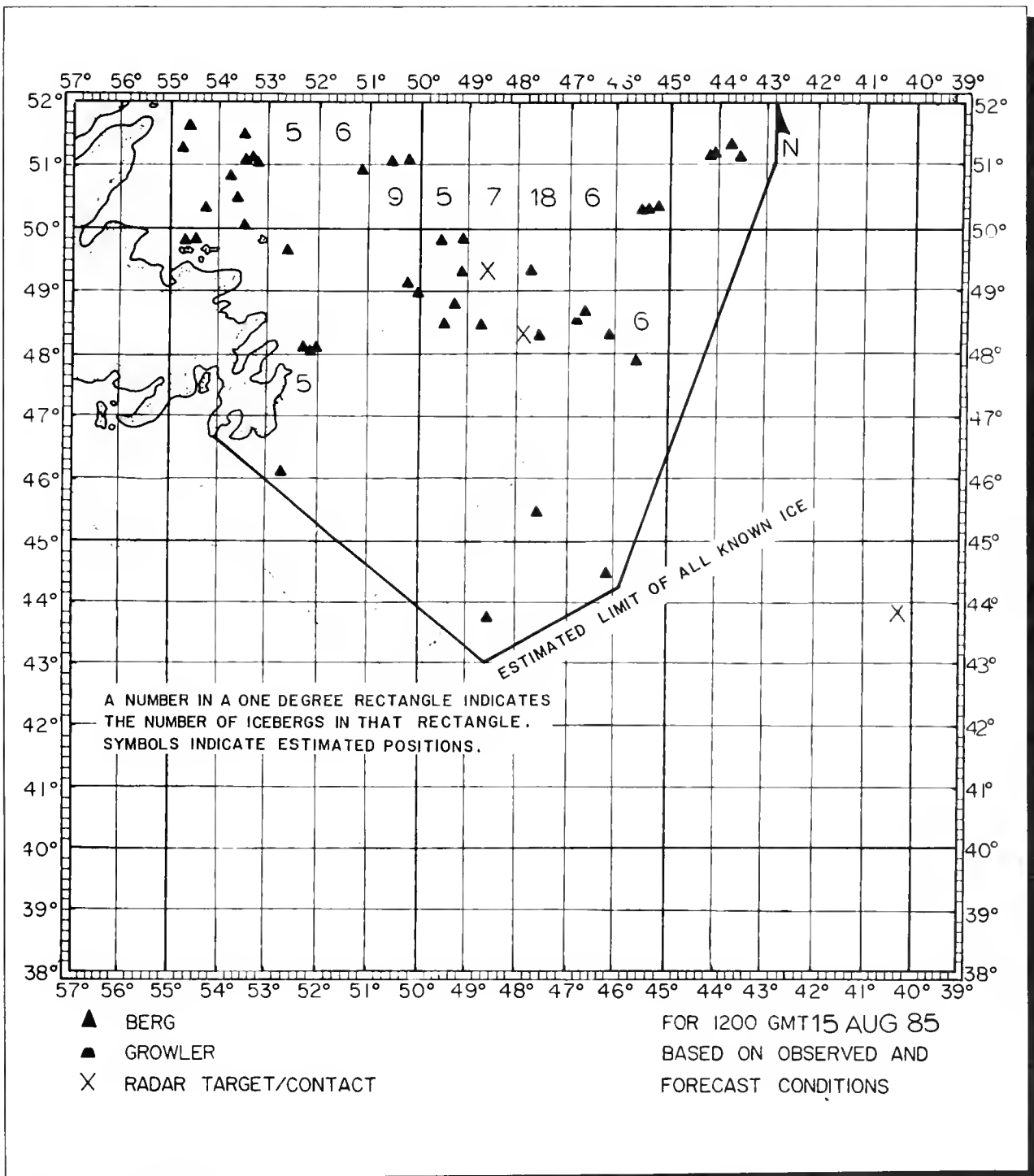

Figure 33. 29 August 1985

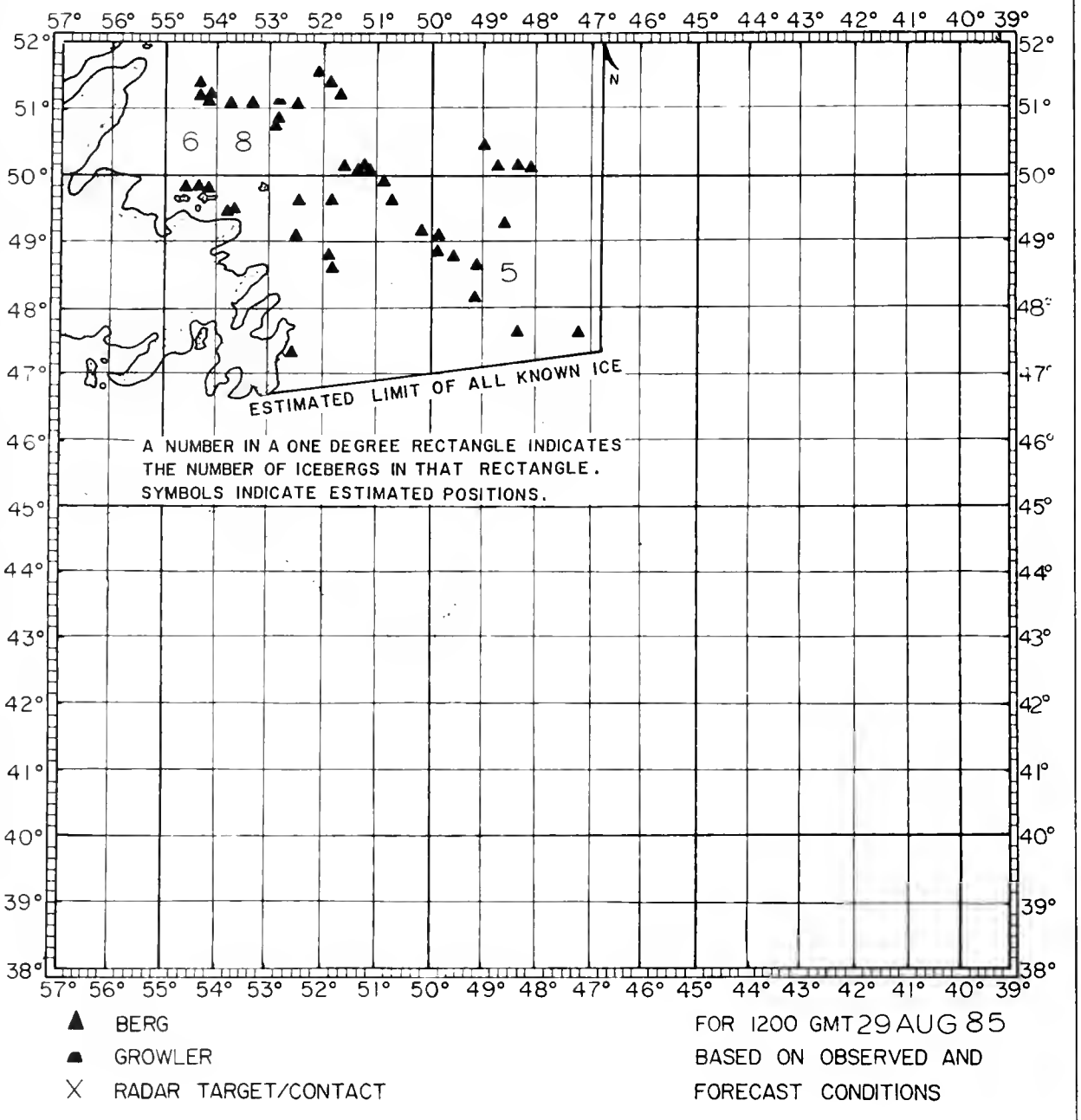

Ice Conditions 1985 Season

October - November 1984: Ice formation was delayed in October by warm temperatures (Figure 10 and Table 5). By mid-November, some ice was forming in the Foxe Basin and Frobisher Bay (Figure 11). Freeze-up continued gradually through November and by the end of the month, Ungava Bay and Hudson Strait were completely covered by light ice. Much of Hudson Bay remained ice-free. There were 14 icebergs south of 48°N during October and November, which is unusually high.

December 1984: By mid-month, sea ice had formed south along the Labrador coast and closed the Strait of Belle Isle (Figure 12). It held this position through the rest of the month with some formation beginning in the Gulf of St. Lawrence. The colder temperatures experienced in December (Table 5) and the northerly flow over the region contributed to the advance of ice. During December, 7 more icebergs were sighted south of 48°N.

January 1985: By January 15, the southern limit of sea ice had reached the vicinity of Cape Freels (Figure 13). On January 22, the sea ice had reached Cape Bonavista and a tongue of ice was being carried south in the Labrador Current to approximately 48°N 49°W. With continued low temperatures and northerly winds, sea ice formed rapidly, expanding to the Grand Banks. This provided protection for icebergs moving south and also retarded their drift so that only two icebergs drifted south of 48°N during January.

February 1985: On 12 February, a broad expanse of ice was as far south as Cape Race and extended out to 47°W from that point. A tongue of three- to five-tenths first year ice was estimated to extend approximately to 46°N 47°W (Figure 14) which terminated oil drilling operations on the Grand Banks for over 30 days. Sea ice formation progressed rapidly throughout the month and by 26 February an expanse of nine- to ten-tenths first year ice covered the area from midway between Cape St. Francis and Cape Race to approximately 45°N 46°W. Due to the number of sightings in early February, an IIP pre-season flight was made 20-25 February, during which 64 icebergs were sighted, 57 of which were south of 48°N.

March 1985: A long tongue of ice started forming in the Labrador Current during early March and by 12 March had reached 43°N 48°W (Figure 15). The first regular season ICERECDET, planned for 12 March, was delayed until 17-27 March by an aircraft mishap in Groton on 12 March. There were 129 icebergs estimated to have drifted south of 48°N during March and there were 168 icebergs on plot at IIP on 29 March (Figure 23).

April 1985: With near normal temperatures (Table 5) and westerly/southwesterly flow (Figure 4), the sea ice had receded somewhat by 16 April and a small shore lead had opened along the northeast coast of Newfoundland (Figure 16). While on an iceberg reconnaissance flight on 15 April, HC-130 CG-1504 dropped a memorial wreath at position 41°56'N 50°14'W to commemorate the tragic sinking of the RMS TITANIC 73 years earlier. During April, normally a heavy iceberg month, an estimated 208 icebergs drifted south of 48°N and 176 icebergs were on plot on 30 April (Figure 25).

May 1985: Sea ice retreated in May with a region of three- to five-tenths coverage remaining as far south as Cape Freels on 14 May (Figure 17). With the receding ice edge releasing icebergs to open water, May was a heavy iceberg month, with 205 icebergs estimated to have drifted south of 48°N. This large population of icebergs provided a good supply of experimental subjects for the detection , drift and deterioration experiments (Appendices B, C and D). There were 272 icebergs on plot on 30 May (Figure 27).

June 1985: The retreat of sea ice continued in June (Figure 18). By 25 June only strips and patches remained south of Cape Bauld. The shipping season for the Strait of Belle Isle was

delayed opening 2-3 weeks this year due to ice persisting longer than normal in the Strait. June was the heaviest iceberg month with 893 icebergs plotted by IIP during the month and 247 icebergs estimated south of 48°N. The largest number of icebergs on plot during any single day in 1985 was on 14 June (Figure 28), when there were 292 on plot. There were 242 icebergs on plot on 30 June (Figure 29).

July 1985: On 16 July, the Strait of Belle Isle was ice-free as was much of Davis Strait (Figure 19). The melt proceeded rapidly and by 30 July sea ice only extended as far south as Cape Mugford on the Labrador Coast. July also was a heavy iceberg month with 765 icebergs plotted during the month. However, only 123 icebergs were estimated to have passed south of 48°N and 227 icebergs remained on plot on 30 July (Figure 31).

August 1985: With warmer than normal temperatures (Table 5) and favorable winds, the sea ice continued to melt rapidly and the iceberg population decreased dramatically. On the 6-14 August ICERECDET deployment, only 30 icebergs were detected south of 50°N and the eastern limits of all known ice shifted 4 degrees west (Figure 32). On 13 August, Newfoundland and Labrador were nearly ice-free with some ice remaining in Hudson Strait and along the east coast of Baffin Island (Figure 20). August was a light iceberg month with only 32 icebergs south of 48°N. As a result of the final ICERECDET on 20-28 August, the limit of all known ice shifted another 4 degrees west and north and the 1985 Ice Patrol season was closed on 29 August with 64 icebergs on plot at IIP, only three of which were south of 48°N (Figure 33).

September 1985: Labrador and the Davis Strait was entirely sea ice free by 17 September (Figure 21). There were an additional 32 icebergs sighted south of 48°N during September.

Table 6.
Explanation of Sea Ice Technology Used in Figures 10-21

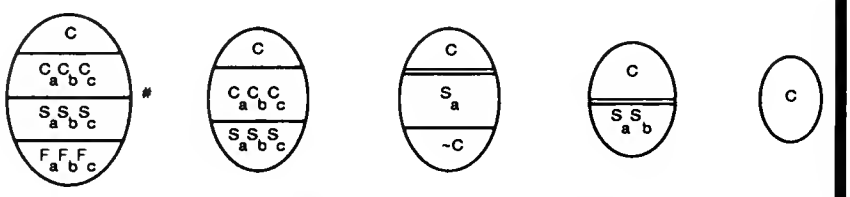

C = Total ice concentration in the area in tenths.

$C_a C_b C_c$ = Concentration of thickest (C_a), 2nd thickest (C_b), and 3rd thickest (C_c).

$S_a S_b S_c$ = Stage of development of thickest (S_a), 2nd thickest (S_b), and 3rd thickest (S_c).

~C = Concentration of ice within areas of stripe and patches.

$F_a F_b F_c$ = Floe size of thickest (F_a), 2nd thickest (F_b), and 3rd thickest (F_c).

Stage of Development

0 No stage of development
1 New ice
2 Nilas, ice rind
3 Young ice
4 Grey ice
5 Grey-white ice
6 First-year ice
7 Thin first-year ice
8 Thin first-year ice, 30-50 cm
9 Thin first-year ice, 50-70 cm
1· Medium first-year ice
4· Thick first-year ice
7· Old ice
8· Second-year ice
9· Multi-year ice
▲ Icebergs
· A trace of ice thicker than S_e
Fourth type, if $C_a C_b C_c$ do not add up to C

Floe Sizes

0 Pancake ice
1 Brash, small ice cake
2 Ice cake
3 Small floe
4 Medium floe
5 Big floe
6 Vast floe
7 Giant floe
8 Growlers and floebergs
9 Icebergs
/ Undetermined or unknown

Discussion of Icebergs and Environmental Conditions

The number of icebergs that pass south of 48°N in the International Ice Patrol area each year is the measure by which International Ice Patrol has judged the severity of each season since 1912 (Table 1). With 1063 icebergs south of 48°N, 1985 is the seventh highest year on record.

Since the number of icebergs calved each year by Greenland's glaciers is in excess of 10,000 (Knutson and Neill, 1978), a number of icebergs exist in Baffin Bay during any year. Therefore, annual fluctuations in the generation of arctic icebergs is not a significant factor in the number of icebergs passing south of 48°N annually. The factors that determine the number of icebergs passing south of 48°N each season can be divided into those affecting iceberg transport (currents, winds, and sea ice) and those affecting iceberg deterioration (wave action, sea surface temperature, and sea ice).

Sea ice acts to impede the transport of icebergs by winds and currents and also protects icebergs from wave action, the major agent of iceberg deterioration. Although it slows current and wind transport of icebergs, sea ice is itself an active medium, for it is continually moving toward the ice edge where melt occurs. Therefore, icebergs in sea ice will eventually reach open water unless grounded. The melting of sea ice itself is affected by snow cover (which slows melting) and air and sea water temperatures. As sea ice melt accelerates in the spring and early summer, trapped icebergs are rapidly released and then become subject to normal transport and deterioration.

With sea ice extending south over the Grand Banks later than usual during the 1985 season, icebergs were protected longer than normal, making it possible for the icebergs to reach farther south than normal.

References

Knutson, K.N. and T.J. Neill, (1978); *Report of the International Ice Patrol Service in the North Atlantic Ocean for the 1977 Season*, CG-188-32, U.S. Coast Guard, Washington, DC.

Robe, R.Q., N.C. Edwards, Jr., D.L. Murphy, N.B. Thayer, G.L. Hover, and M.E. Kop, (1985); *Evaluation of Surface Craft and Ice Target Detection Performance by the AN/APS-135 Side-Looking Airborne Radar (SLAR)*, CG-D-02-86, U.S. Coast Guard, Washington, DC.

Rossiter, J.R., L.D. Arsenault, A.L. Gray, E.V. Guy, D.J. Lapp, R.O. Ramseier, and E. Wedler, (1984); *Detection of Icebergs by Airborne Imaging Radars*, Proceedings of the 9th Canadian Symposium on Remote Sensing, St. John's, Newfoundland, August 1984.

Thayer, N.B. (1984); *Effects of Side-Looking Airborne Radar (SLAR) on Iceberg Detection During the 1983 and 1984 International Ice Patrol Seasons*; from Report of the International Ice Patrol in the North Atlantic, 1984 Season, CG-188-38, U.S. Coast Guard, Washington, DC.

Acknowledgements

Commander, International Ice Patrol acknowledges the assistance and information provided by the Canadian Department of the Environment, the U.S. National Weather Service, the U.S. Naval Weather Service, and the U.S. Coast Guard Research and Development Center.

We extend our sincere appreciation to the staffs of the Canadian Coast Guard Radio Station St. John's, Newfoundland/VON and the Gander Weather Office and to the personnel of U.S. Coast Guard Air Station Elizabeth City and the USCGC EVERGREEN for their excellent support during the 1985 International Ice Patrol season.

Appendix A

International Ice Patrol Ice and SST Reports for 1985

Ship's Name	Country of Registry	Ice Reports	SST Reports
Aberdeen	Panama	3	
Abitibi Concord	Germany	7	
Acadia Forest	Liberia	1	
Aeneas	Singapore	2	
Akizuki Maru	Japan		3
Albright Explorer	United Kingdom	2	
Alcona	United States of America	1	
Alexander Henry	Canada	2	2
Alexandros F	Greece	1	1
Alfanourious	Liberia	1	1
Alfred Needler	Canada	4	
Algonquin	Korea	1	27
Altamira	Spain	3	
Altay	Union of Soviet Socialist Republics	1	
Altis	Greece	1	
Ambassador	United Kingdom	16	
Ambrose Shea	Canada	2	
Amstelwal	Netherlands	3	4
Anagell Horizon	Greece	1	
Anka D	Cyprus	1	
Annoula	Greece	4	7
Arctic	Canada	2	
Arctic Link	United Kingdom	1	
Arctic Viking	Canada	2	
Astron	Canada	2	
Atlantic Conveyer	United Kingdom	1	
Atlantic Link	United Kingdom	4	15
Atlantic Saga	Sweden	1	
Atlantic Service	France	2	
Atlantic Star	United Kingdom	2	1
August Thyssen	Liberia	2	
Australian Reefer	Bahamas		2
Azalea	Korea	2	1
Badak	Liberia	1	5
Bahia Portete	Columbia		1
Balder Hesnes	Canada	3	
Balder Vigra	Canada	1	
Balu	Sri Lanka		1
Bandazul	Spain	1	
Bart Atlantica	United Kingdom	1	
Bartlett	Canada	4	
Batna	Algeria	4	4
Beinir	Canada	1	
Belle Etoile	Mauritius	4	10
Bernhard Oldendorf	Panama		1
Bernier	United Kingdom	4	
Bilderdyk	Netherlands Antilles	1	
Bissaya Barrero	Portugal	6	
Boltentor	Canada	4	
Bonavista Bay	Canada	3	
Boxy	Sweden	3	
Bridgewater	Germany	7	

Appendix A (cont'd.)

International Ice Patrol Ice and SST Reports for 1985

Ship's Name	Country of Registry	Ice Reports	SST Reports
Bulkness	United Kingdom	3	
Canada Marquis	Canada	1	
Canadian Explorer	Canada	10	1
Cape Roger	Canada	4	
Capetan Costis	Cyprus		9
Cast Huskey	United Kingdom	3	
Cast Muskox	United Kingdom	5	
Cast Otter	United Kingdom	5	
Cast Polar Bear	Liberia	4	6
Cavallo	Canada	1	
Chandidis	India	2	
Chateaugay	Liberia	1	
Chignecto Bay	Canada	5	
Chili	United Kingdom		2
City of Perth	United Kingdom	5	
C. Mehmet	Turkey		4
Chippewa	Liberia	2	
Commandant Guy	France	1	
Concord	United States of America		8
Condata	Honduras		1
Conta Belgica	Korea	2	
Corner Brook	Korea	2	
Danaos	Greece	4	
Daphne	Netherlands	1	
Dart Americana	United Kingdom	3	1
Dart Atlantica	United Kingdom	1	
Dart Britain	United Kingdom	3	
Diana	Brazil	1	
Dock Express	Netherlands	1	
Dora Oklendorff	Singapoore	1	
Donny	Sweden	2	
Dr D. K. Samy	Liberia	1	
Dry Sack	Spain	2	
Eastern Unicorn	Panama	8	9
Eeklo	Belgium	4	
El Aalim	Liberia	1	
Elisat	Italy	1	
Elizabeth	Liberia	1	
Esso Aberdeen	United Kingdom	2	1
Eulima	Norway	1	
Europe	Belgium	6	
USCGC EVERGREEN	United States of America	8	69
Evimeria	Greece	1	2
Fairlift	Netherlands Antilles	2	
Fair Spirit	Liberia	2	
Faith	Singapore		1
Falcoen	Sweden	1	
Falcon	Norway	5	
Farnes	Liberia	2	
Federal Asahi	Japan		4
Federal Danube	Belgium	4	

Appendix A (cont'd.)

International Ice Patrol Ice and SST Reports for 1985

Ship's Name	Country of Registry	Ice Reports	SST Reports
Federal Ottawa	Belgium	8	
Federal Rhine	Liberia	1	
Federal Saguenay	Liberia	1	
Federal St. Laurent	Liberia	2	
Federal Thames	Belgium	1	
Fermita	Norway		3
Filiatra Lagacy	Greece		5
Filispoint	Greece	1	
Fina America	Belgium	2	
Finn Fighter	Finland	1	
Finn Fury	Finland	2	
Finnrose	Finland		2
Finn Oceanis	Finland	2	
Fiona Mary	Panama	1	
Firmes	Liberia	12	
Fjord Bridge	Panama	2	1
Flora	Greece	1	1
Fogo Isle	Canada	1	
Fort Providence	United Kingdom	1	1
Fortune Ace	Panama	1	1
Fred J. Agnich	Canada	1	
Frithjof	Germany	2	7
Fuji Reefer	Japan	1	1
Garbarus Bay	Canada	9	
Genoa	Singapore	1	1
Germanic	Federal Republic of Germany	3	
Godafoss	Iceland	1	
Golden Rio	Liberia	1	10
Graiglas	United Kingdom	1	
Grand Eagle	Panama	9	
Gripo	Finland	3	7
Gulf Grain	Liberia	3	1
Hassho	Panama	1	
Heide	Germany	1	
Helene	Federal Republic of Germany	1	1
Helen Schulte	Cyprus	1	2
Hercules Bulker	Liberia	3	
Hofsjoull	Iceland	1	1
Hokusetmaru	United States of America	1	1
Hual Trapper	Liberia	1	
Hudson	Canada	6	3
Hugo	Finland	1	
Imperial Bedford	Canada	2	
Imperial Quebec	Canada	2	
Imperial St. Clair	Canada	2	
Inma	Spain	1	

Appendix A (cont'd.)

International Ice Patrol Ice and SST Reports for 1985

Ship's Name	Country of Registry	Ice Reports	SST Reports
Irenes Galaxy	Panama	1	
Iroquois	Korea		8
Irving Nordic	Canada	4	
Irving Ours Pollaire	Canada	1	
Ivan Der Benev	Union of Soviet Socialist Republics	2	
Iver Libra	Liberia		1
Jackamn	Chile	1	
Jade Kim	Panama	2	
Jan Wilhelm	Germany		1
James Transport	Canada	3	
Jason	Panama	1	
Je Bernier	Canada		2
Jennifer Jane	Cyprus	2	
Jenny	United Kingdom	1	
Jljet	Yugoslavia	1	
Joao Ferreira	Portugal	2	
John	Greece		4
John A. MacDonald	Canada	4	
John M.	Federal Republic of Germany	1	
Johnson Chemstream	Singapore	1	
Jugoagent	Yugoslavia	2	14
Juventia	Panama	1	
Kaladia	India	3	
Kapitan Chukhchinche	Union of Soviet Socialist Republics	4	
Keenaviga	United Kingdom	1	
Khiko	Panama	1	
Klippergracht	Netherlands	1	
Koeln Express	Germany	10	
Korea Pacific	Korea		4
Kyoushi Waru	Japan	2	
Lake Anina	Liberia		2
Lake Biwa	United States of America	1	
Lake Shell	Canada	1	
La Pampa	United Kingdom	7	
La Richardais	France	2	3
Lamara	Singapore	1	
Larrado	Canada	2	
Laurentian	France	9	
Laurentian Forest	Panama	2	
Lena	Philippines		8
Leninsk	Union of Soviet Socialist Republics	1	
Leros Challenger	Malta		1
Leventes	Liberia	1	
Liberian Badak	Liberia		1
Liquid Bulker	Panama		4
Liria	Spain	1	1
Lok Nayak	India	1	1
Lorme	Canada	1	
Louis S. St. Laurent	Canada	1	
Ludolf Oldedorff	Singapore	1	

Appendix A (cont'd.)

International Ice Patrol Ice and SST Reports for 1985

Ship's Name	Country of Registry	Ice Reports	SST Reports
Mahone Bay	Canada	1	
Maiakamd	Pakistan		4
Manchester Challenge	United Kingdom	10	2
Manga	United Kingdom	1	
Manila Triumph	Philippines	1	
Maratha Shogun	India	2	
Margit Gorthon	Sweden	3	
Maria	Germany	1	
Marine Reunion	Liberia	1	
Marine Star	United Kingdom		1
Marques Debolarque	Spain		1
Marshal Grechko	Union of Soviet Socialist Republics	3	
Meshill	Norway	2	
Meerdrecht	Netherlands	1	
Meerkatze	Germany	6	
Megastar	Sri Lanka	2	
Mela	Panama	1	4
Mesarige	Canada	1	
Metro Star	Canada	1	
Mini Lot	Panama		1
Mightious	Panama	1	1
Miyashima Maru	Japan	1	1
Mljet	Mongolia	2	
Mobil Engineer	Sweden		4
Mobil Oil Co.	Bolivia	1	
Monana D.	Liberia		6
Montcalm	United States of America	1	
Monty Python	Malta		1
Mosel Oreck	Liberia	1	
Moshrouk	Norway	1	
Mouthaina	Greece	3	
M. Soveron	Singapore	1	
Musashi	Greece	2	
Musson	Union of Soviet Socialist Republics	1	
Nancy Bartlet	Canada	1	
Navtroll	Liberia	1	2
Neckarore	Liberia	1	
Noble Supporter	Panama	1	
Nordertor	Liberia	1	12
Nordheide	Canada	3	
Nordic Sun	Singapore	4	
Nordkap	Liberia	3	
Norshwisn	Cyprus	1	7
Northern Lynx	Liberia	1	
USCGC NORTHWIND	United States Of America	7	6
Nosira Lin	United Kingdom	1	51
Nosira Madeleine	United Kingdom	3	
Nürnberg Express	Germany	4	
Ocean King	Greece	1	
Osolemio	Liberia		5
Overseas Argonaut	United Kingdom	1	2

Appendix A (cont'd.)

International Ice Patrol Ice and SST Reports for 1985

Ship's Name	Country of Registry	Ice Reports	SST Reports
Pacific Challenger	United Kingdom	1	
Pacific Courage	United Kingdom	1	
Pacific Defender	Liberia		9
Pacific Express	Liberia	1	
Pacifico Mexicano	Panama	1	
Pan Crystal	Korea	1	
Pantazis	Greece	1	
Pavel Vavilov	Union of Soviet Socialist Republics	1	
Pawnee	United Kingdom		12
Petrodvorets	Union of Soviet Socialist Republics	4	
Philippeld	France	1	
Placentia Bay	Canada	1	
Planeta	Germany	1	
Polar Bear	Liberia		2
Polar Circle	Canada	2	
USCGC POLAR SEA	United States of America	1	
Port St. Jean	Canada	2	
Premnitz	Germany	2	
President Quezon	Philippines	1	
Priimorsk	United Kingdom	2	
Prins Maurits	Netherlands	2	
Pristina	Yugoslavia	1	
Proteus	United Kingdoom	1	
Puhos	Finland	3	5
Quadra	Canada	4	
Queen Ellizabeth II	United Kingdom	2	
Quest	Canada	1	
Reginas	Greece	1	
Ruebens	United Kingdom	1	
Rio Frio	Netherlands	1	
Rio Plaata	Liberia	1	
Saar lore	Liberia	2	
Salvia Star	Philppines	2	
Saskatchewan Pioneer	Canada	1	
Scandinavia Maru	Japan	1	
Schnoorturm	Canada	4	
Seaforth Atlantic	Canada	3	
Seaforth Atlantic Cartwright I	Canada	1	
Sea Fortune	Panama	3	
Sealand Express	United States of America	1	
Sealand Independence	Mexico	1	
Seijin Maru	Japan		5
Selkirk Settler	Canada	1	
Senhora Das Candeias	Portugal	4	
Sentinel 2	France	1	
Silverland	Sweden		2
Sir Robert Bond	Canada	7	
Sir W. Alexander	Canada	1	
Sitia Glory	Panama	2	
Skaftefell	Iceland	1	
Stefan Batory	Poland	9	2
Stefan Starzynski	Poland	4	

Appendix A (cont'd.)

International Ice Patrol Ice and SST Reports for 1985

Ship's Name	Country of Registry	Ice Reports	SST Reports
Stolt Castle	France	1	
Stolt Excellence	Liberia	1	
Stratus	Liberia		4
Stuttgart Express	Germany	3	
Suvretta	Panama	1	
Tadeusz Kosciuszzko	Poland	1	
Takapu	Canada	1	
Teamhada	Singapore		2
Techno St.. Laurent	Canada	1	
Terra Nordica	Canada	4	
Thuleland	Singapore	1	
Tina	Cyprus		1
Toanui	Canada	2	
Tobruk	Poland	1	
Tokiarrow	United Kingdom	1	
Torrent	Liberia	1	
Trans Reefer	Panama		1
Traquair	United Kingdom		9
Travemar Africa	Spain	1	6
Trinity Bay	Canada	9	
Tsukubamaru	Japan	1	1
Tuber	Canada	1	
Tuifias	Sweden	1	
Tulsidas	India	1	
Uniwersytet Slasky	Poland	1	
Uority Dolgarufiy	Union of Soviet Socialist Republics	1	
Vamand Wave	United Kingdom	1	
Vanil	Sweden	1	5
Varjakka	Finland		2
Vimieiro	Portugal	1	
Vascaya	Norway	1	
Wanderer	United Kingdom		4
Warnemundie	Union of Soviet Socialist Republics	3	
Wilfred Templeman	Canada	2	
Wise	Cyprus		6
World Agamemnon	Greece		1
World Argonaut	Greece	1	
World Nancy	Panama	1	
Yannis	Greece	1	
Yukona	Liberia	3	1
Zeepaard	Bahamas	1	
Ziemia Opolska	Poland	2	
Ziemia Zamojska	Poland	3	4

Appendix B

Iceberg / Ship Target Discrimination with Side-Looking Airborne Radar

LTJG N. B. Thayer, USCGR
CDR N. C. Edwards, USCG

Introduction

Since 1983, the International Ice Patrol (IIP) has been using a Motorola AN/APS-135 Side-Looking Airborne Multi-Mission Radar (SLAMMR) as its primary method of iceberg reconnaissance in the North Atlantic. The ability to detect icebergs with a side-looking airborne radar (SLAR) in poor or zero visibility, plus the ability to search larger areas, has resulted in a significant increase in the number of icebergs tracked by IIP.

Because SLAR can be used with the sea surface obscured by clouds, IIP frequently conducts reconnaissance flights when visual confirmation of SLAR targets is not possible. Without visual confirmation, distinguishing between icebergs and vessels is sometimes difficult.

Without visible cues on the SLAR film (target movement, wakes, brash, radar shadows, strength of return) which improve target identification, it is difficult to distinguish between targets with similar radar return, e.g., small icebergs and vessels. IIP has planned its search legs and the track spacing equal to one-half the total SLAR sweep width (i.e., 25 nm). This type of search plan gives 200% coverage between parallel legs and provides two views of each target within the search area. Despite these efforts to maximize cues, it is still sometimes difficult to distinguish vessels from small and medium icebergs. For example, fishing vessels often drift or move slowly, producing no wake and showing little or no movement between looks. In addition, the search legs going to and from the search area as well as the outlying legs of the search itself do not afford double SLAR coverage. As a result, approximately 35% of the search area is seen only once on SLAR, eliminating the chance to detect movement and decreasing the probability of picking up other cues from SLAR images.

This study measures the error rate in SLAR target identification, using single looks at individual iceberg and ship targets without visual cues.

Methods

To conduct this study, it was necessary to find a source of SLAR targets with visual confirmation. The best source of targets with positive identification of both target size and type was the BERGSEARCH '84 (Rossiter, *et al.*, 1984) data and the 1985 SLAR experiment conducted by IIP and the Coast Guard Research and Developoment Center (Robe, *et al.*, 1985). These two sources provided SLAR film from 7 days of IIP operations with shipboard ground truth data, 160 ship and iceberg targets in all. All of the film used in this study was collected at an altitude of 8,000 feet on the 50 km SLAR range scale, standard conditions during IIP iceberg reconnaissance.

The films were duplicated and the duplicate films were examined for suitable targets for the study. All targets without obvious cues were used. Although targets were not selected for ambiguity, all of those used were quite ambiguous, since they were all single targets without accompanying visual cues. With the limited number of vessels and icebergs involved in the two source experiments, some targets were used more than once, but separate SLAR passes

provided different looks so that each image was used only once.

To isolate individual targets and at the same time give the SLAR interpreters a surrounding piece of film to examine for background, each target was cut from a duplicate film and mounted on a 2 1/4" photo slide mount. Each target was randomly assigned a 2-3 digit identification number and each slide mount was labelled with that number, the lateral range to the target from the aircraft, and the sea conditions (from ship ground truth).

These 74 slides (35 icebergs and 39 ships) were taken to U. S. Coast Guard Air Station Elizabeth City, North Carolina, for viewing by the Coast Guard Avionics Technicians who are the IIP's SLAR interpreters, operators and technicians during ice reconnaissance flights. Four experienced technicians separately viewed the slides on a light table using an optical magnifier, conditions approximating the normal IIP post-flight analysis. Each technician was asked to identify each target as either a ship or an iceberg.

Results

Table B-1 presents the raw test results, divided into the two target types: ships and icebergs. The "correct" column under each target type represents the number of times each observer identified that target correctly, while "incorrect" represents the number of times that type of target was misidentified.

The data was subjected to Chi-square analysis (Lapin, 1975) to identify statistically significant differences in the error rates between the observers, and to look for differences in how the two target types were treated. The analysis revealed that there was too much difference in error rate and target treatment between the four observers to allow combining all the data. Also, observers 1 through 3 showed a bias toward icebergs, i.e., a tendency to identify ships as icebergs. This is a reflection of their IIP experience, since observers are taught to be conservative and identify doubtful targets as icebergs. Observers 1 and 3 were sufficiently similar in their treatment of the targets to allow combining their data. Finally, observer 4 showed no bias toward icebergs.

The results from observers 1 and 3 probably offer the most representative sample, since the bias they show toward icebergs reflects their IIP experience. Actually, while selection of different subsets of the data can be made based on bias shown or statistical judgements, the error rate for all targets is in the range of 40-45%, as shown in Table B-2.

While these data sets cannot be combined or compared for statistical reasons, selecting any one of them yields essentially the same result, i.e., that the observers correctly identified all targets 55-60% of the time. Applied directly to all IIP SLAR detections, a possible 45% error rate would have alarming implications. The targets used in this study, however, represent only a subset of IIP SLAR targets. There are characteristics that limit the size of that subset and mitigate the 45% figure.

First, the sizes of icebergs in BERGSEARCH '84 and the

Table B-1. Target Identification

	Iceberg		Ship	
Observer	Correct	Incorrect	Correct	Incorrect
1	31	4	15	24
2	23	12	7	32
3	28	7	15	24
4	20	15	24	15
TOTAL	102	38	61	95

Table B-2. Error Rates

Obser-ver(s)	Error Rate (Ships & Icebergs)
1-4	45%
1,3	40% (Iceberg Bias)
4	40% (No Bias)

Table B-3. Iceberg Size Distribution (SLAR) 1984 - 1985

Year	Growler	Small	Medium	Large	Radar	Total
1984	370 (25%)	441 (30%)	418 (29%)	211 (14%)	21 (1%)	1461
1985	65 (11%)	194 (34%)	182 (32%)	113 (20%)	10 (1%)	564
1960-1982	8393 (15%)	21353 (37%)	15461 (27%)	4854 (8%)	7711 (13%)	57772

1985 IIP experiment range from growler through medium. The targets selected for this study were small and medium icebergs (ground truthed by on-scene vessels) and ship targets of similar radar return. Small and medium icebergs represent 59% of the icebergs recorded by IIP SLAR in 1984 and 66% in 1985, as shown in Table B-3. These percentages are comparable to the pre-SLAR value of 64% for the period 1960 through 1982.

The second mitigating factor is the ambiguity of the targets used, i.e., the absence of cues. Since the methods of this study eliminated these cues, the targets used represented the most ambiguous available.

In order to assess the impact of these results on IIP iceberg reconnaissance, it is necessary to estimate the proportion of IIP SLAR targets that are cueless. It can be conservatively assumed that 40% of SLAR targets are cueless, based on IIP operational experience. Indications that this is a reasonably conservative assumption are that the data set used for this study in which 74 of 160 targets (46%) were cueless, and the fact that 65% of IIP search flight mileage offers 200% search coverage, which is assumed to greatly increase the probability of cues being present. A further assumption is that the presence of cues results in 100% correct identification

Applying a worst-case error rate of 45% to the (estimated) cueless 40% of the small and medium icebergs detected by SLAR, yields an estimated SLAR error of 161 and 68 misidentified icebergs in 1984 and 1985, in the small and medium size range.

Conclusions

The probability of correctly identifying ambiguous (cueless) iceberg and ship SLAR targets is just above chance (55-60%). Therefore, the International Ice Patrol uses search tactics to maximize cues and visual confirmation during SLAR reconnaissance.

Based on this limited study of cueless SLAR targets, the SLAR error rate and iceberg bias of SLAR operators could inflate the number of icebergs that IIP reports. This inflation is insignificant when compared with the increased efficiency that SLAR provides iceberg reconnaissance. Even though visual searches provide unquestionable identification, they were historically flown only on 50% of the deployment time and each visual flight covered one-third less area than a SLAR flight does.

An important issue not addressed by this study is the SLAR identification error rate for unambiguous targets, i.e., targets with cues. If this error is quantified by further study, a better estimate of the overall error rate would be possible.

References

Lapin, L. 1975. *Statistics: Meaning and Methods.* Harcourt, Brace and Janovich. New York.

Robe, R.Q., N. C. Edwards, Jr., D. L. Murphy, N. B. Thayer, G. L. Hover, M. E. Kop. 1985. *Evaluation of Surface Craft and Ice Target Detection Performance by the AN/APS-135 Side-Looking Airborne Radar (SLAR),* CG-D-02-86. U. S. Coast Guard, Washington, DC

Rossiter, J. R., L. D. Arsenault, A. L. Gray, E. V. Guy, D. J. Lapp, R. O. Ramseier, E. Wedler. 1984. *Detection of Icebergs by Airborne Imaging Radars,* Proceedings of the 9th Canadian Symposium on Remote Sensing, St. John's, Newfoundland, Canada

Appendix C

Oceanographic Conditions on the Grand Banks During the 1985 IIP Season

LT I. Anderson, USCG

Introduction

During the 1985 International Ice Patrol (IIP) season, twelve satellite-tracked TIROS Oceanographic Drifters (TODs) were deployed in the IIP operating region. Ten of the TODs were deployed from an HC-130 aircraft during regular ice reconnaissance flights. The data from these TODs are discussed below. The remaining two TODs were deployed and recovered five times each from the USCGC EVERGREEN as part of an iceberg drift and deterioration study. This is the first time IIP has deployed TODs with the expressed intent of recovery. The tracks of the two ship-deployed TODs are discussed in Appendix D.

Two oceanographic cruises were planned during the 1985 IIP season. The first cruise was on the USCGC EVERGREEN (WMEC 295) from 10 April until 10 May 1985. The objectives of obtaining iceberg drift, deterioration and detection data were met. The results of the EVERGREEN cruise drift data are discussed in Appendix D and the detection data results are discussed in Appendix B. The iceberg deterioration data will be discussed below. The second cruise planned for USCGC NORTHWIND (WAGB 282) was cancelled because of ship's main engine problems.

TIROS Oceanographic Drifter Tracks

IIP uses TODs to provide real time current information to update the historical current field used by our iceberg drift model. TODs are deployed in areas of high iceberg density and in areas of high variability in the current field in order to improve drift prediction.

All ten of the air-dropped TODs have a 3 meter long spar-shaped hull with a 1 meter diameter flotation collar and are equipped with a sea surface temperature (SST) sensor, a drogue tension sensor, and a battery voltage monitor. Each TOD is deployed with a 2 meter by 10 meter window shade drogue attached to the TOD by either a 30 or 50m tether (Table C-1). An average of 7.4 positions per day from each TOD were obtained through Service ARGOS. The distribution of the positions and sensor data points are evenly distributed in time except for the period between 0000Z and 0400Z where virtually no data is received. This null data period is due to the orbits of the NOAA/TIROS N-series satellites.

Table C-1. 1985 IIP TIROS Oceanographic Drifters

TOD #	Date Deployed	Deployment Position		Tether Length	Par. Rel.	Deploy SST	Date Left IIP Area	Ave/ Day
4526	10 APRIL	46°15.6N	46°28.8W	30M	NO	-0.8	22 JULY	7.2+
4536	7 MAY	45°42.0N	48°09.6W	50M	NO	-0.6	5 AUG *	6.4
4527	30 MAY	46°34.8N	47°22.8W	30M	NO	0.0	17 SEP**	7.1
4537	3 JUNE	47°40.0N	48°00.0W	50M	NO	---	---------	---
4548	26 JULY	47°00.6N	47°17.4W	50M	NO	10.2	8 AUG *	7.7
4529	28 JULY	48°21.0N	46°48.0W	30M	NO	10.0	17 OCT	7.9
4550	29 JULY	50°30.0N	50°29.4W	50M	YES	8.3	2 OCT	7.6
4546	10 AUGUST	47°00.0N	47°30.0W	50M	NO	---	--------	---
4541	11 AUGUST	48°17.4N	47°00.6W	50M	NO	12.6	11 SEP	8.7
4544	26 AUGUST	50°07.2N	50°29.4W	50M	YES	8.8	***	6.6

PAR. REL..: Visually confirmed release of parachute at deployment

+: INCLUDES DATA FROM 3 JUNE ONLY
*: PICKED UP BY FISHING VESSELS. 4536 HAS BEEN RETURNED TO IIP AND 4548 IN MURMANSK, USSR

**: TOD FAILED ON 17 SEPTEMBER WHILE IN IIP REGION
***: STILL IN IIP REGION AS OF 30 OCTOBER 1985

Figure C-1. Drift tracks for International Ice Patrol's 1985 TODs.
Tracks presented include data through 30 October 1985. The symbol ( ) indicates deployment position of the TOD. The julian dates beside the tick marks correspond to events discussed in the text.

Figure C-1a

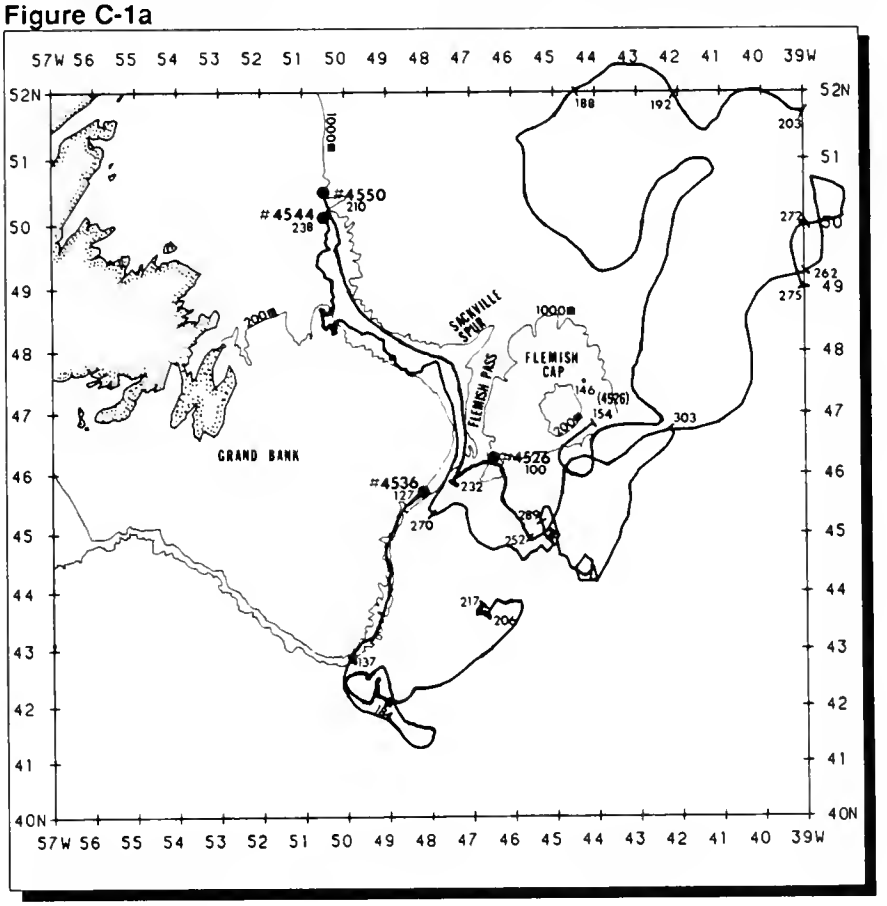

Figure C-1b

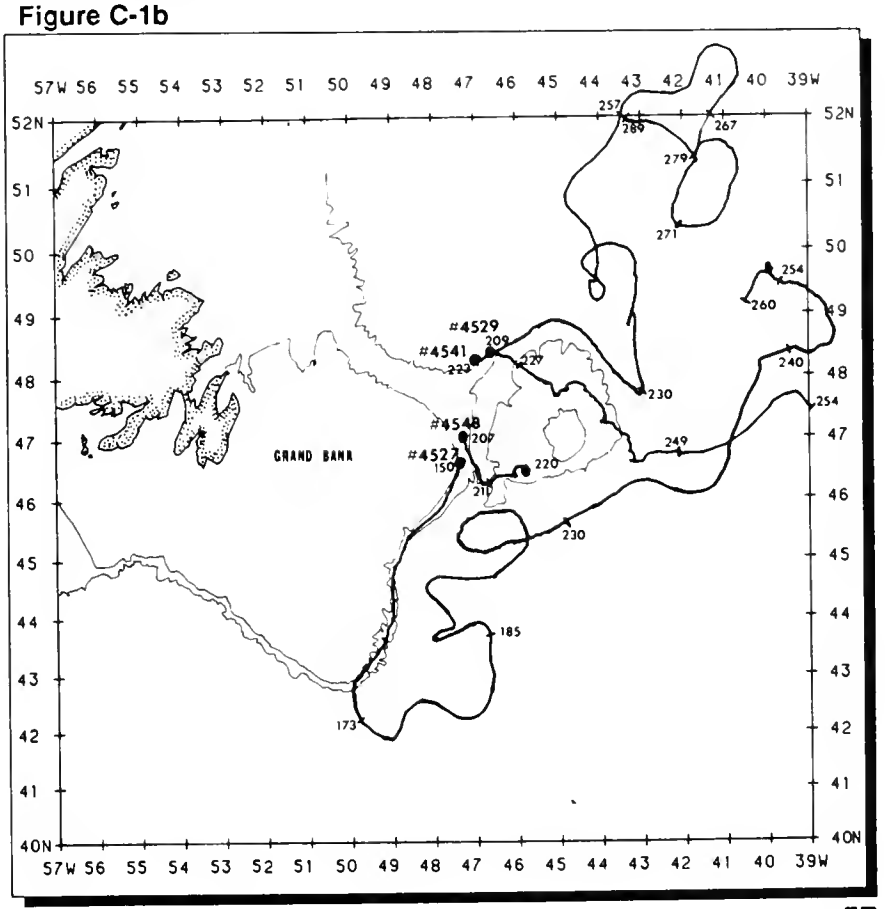

As of 30 October, only one of the TODs (#4544) remained in the IIP region (Figure C-1). Two of the TODs (#4537 and #4546) failed on deployment. TOD #4526 was deployed on 10 April. Between 11 April and 3 June, only one position was received. After 3 June, TOD #4526 performed without problem. Two TODs (#4536 and #4548) were recovered by fishing vessels. Four of the TODs (#4529, #4541, #4544 and #4550) are still drifting and providing data while two other TODs failed after 110 days (#4527) and 178 days (#4526).

Only two of the parachute release mechanisms (TODs #4550 and #4544) were observed to operate following deployment. The actual fate of the remaining TOD parachutes is uncertain. We assume that when the parachute collapsed, it settled into the water and, at worst, ended up acting as a near-surface drogue. TOD #4536 was observed from CG-1504 on 18 July, more than two months after deployment, with the parachute wrapped abound the TOD hull. The parachute was still attached to the TOD when it was recovered by a fishing vessel on 5 August. There are no significant differences in the velocity distributions for TODs with confirmed parachute releases and those without, suggesting the parachute, even if it remains attached to the TOD does not significantly affect the drift of the TOD (Figure C-2).

The below discussions include TOD data through 30 October

1985. The drift tracks of the TODs will be discussed below in chronological order according to when they were deployed. The number in parenthesis following dates are Julian dates and correspond to the dates on Figure C-1.

TOD #4526

TOD #4526 was deployed on 10 April (100) in the Flemish Pass in position 46°15.6'N 46°28.8'W (Figure C-1). Between 11 April and 3 June (154), only one position was received from TOD #4526. This position on 26 May (146) at 47°35.4'N 44°15.0'W indicated TOD #4526 drifted north around Flemish Cap. From 3 June (154) to 7 June, TOD #4526 drifted from 46°48.6'N 44°07.2'W in a southwesterly direction at an average velocity of 27 cm/s until it entered the North Atlantic Current. On 7 June (158), the sea surface temperature reading from TOD #4536 increased from 3°C to 5°C. Although TOD #4526 briefly drifted north of the IIP region between 7 July (188) and 11 July (192), the drift track of TOD #4526 after 7 June corresponds well with the isotherm pattern as depicted by the Canadian METOC SST charts (Figure C-3). An average velocity of 51 cm/s was maintained while TOD #4526 was in the North Atlantic Current until exiting the IIP region to the east on 22 July (203).

During June when TOD #4526 was drifting north of Flemish Cap in the North Atlantic Current, the 8°C isotherm apparently indicated the western edge of this branch of the North Atlantic Current. TOD #4526 continued to return data as it drifted across the Atlantic until its failure on 5 October. Throughout the period from 3 June until 5 October, the drogue sensor indicated the drogue was disconnected.

Figure C-2. Velocity distributions for International Ice Patrol's 1985 TODs

Figure C-2a

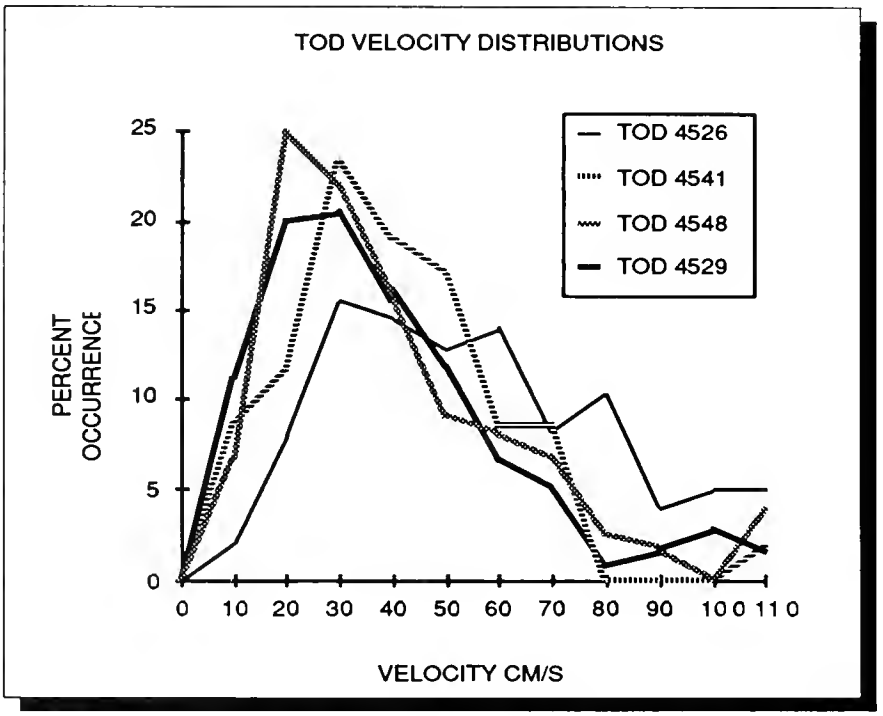

Figure C-2b

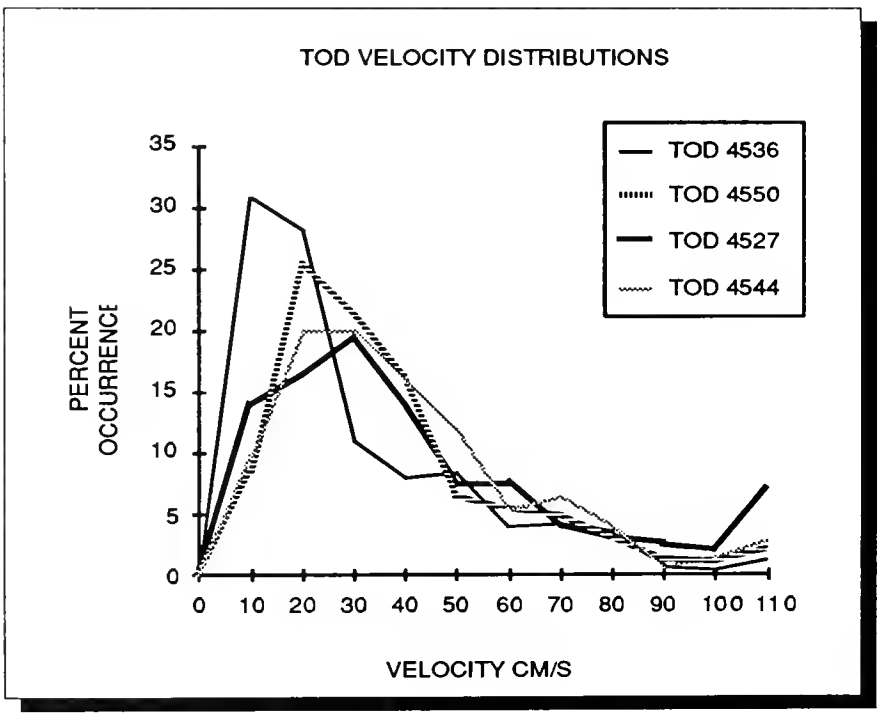

TOD #4536

TOD #4536 was deployed on 7 May (127) in 500m of water on the eastern edge of the Grand Bank south of Flemish Pass in position 45°42.0'N 48°09.6'W (Figure C-1). TOD #4536 was carried south by the Labrador Current roughly following the 500m contour at an average velocity of 44 cm/s until passing south of the Tail of the Bank on 17 May (137). Between 17 May and 3 July (184), TOD #4536 meandered along the front between the Labrador Current and the North Atlantic Current at an average velocity of 32 cm/s. The location of the front is particularly evident near 42°N 47°W along the 10°C isotherm in the METOC SST chart of 14-17 June (Figure C-3). The large amount of time (47 days) that TOD #4536 spent in this relatively slow moving area explains the shift of the velocity distribution curve to the left (Figure C-2).

On 3 July (184), the water temperature increased from 9°C to 11°C and the velocity increased significantly from about 20 to 60 cm/s indicating TOD #4536 had been caught up in the North Altlantic Current. It remained in the North Atlantic Current until 25 July (206). From 25 July until 5 August (217), TOD #4536 drifted slowly at an average velocity of 10 cm/s.

On 5 August, TOD #4536 was picked up by a fishing vessel working out of New Bedford, Massachusetts and the TOD was subsequently returned to the Ice Patrol. The exact date TOD #4536 was picked up by the fishing vessel is not certain. The drogue was attached to the TOD when it was recovered.

TOD #4527

TOD #4527 was deployed between the 200m and 500m contours along the eastern Grand Bank in position 46°34.8'N 47°22.8'W on 30 May (150) (Figure C-1). It drifted south with the Labrador Current at an average velocity of 29 cm/s along the edge of the shelf until entering the North Atlantic Current on about 22 June (173). It remained in the North Atlantic Current travelling in a generally northeasterly direction at 47 cm/s until 4 July (185). Between 4 July and 18 August (230), TOD #4527 meandered generally northward at 26 cm/s completing one large cyclonic circle south of the Flemish Cap. This period of time was spent between the Labrador Current and the North Atlantic Current.

On 18 August (230), TOD #4527 re-entered the North Atlantic Current and was carried again to the northeast at 74 cm/s. On 28 August (240), TOD #4527 began a slow cyclonic motion that followed the isotherm pattern at an average velocity of 27 cm/s (Figure C-3). TOD #4527 exited and re-entered the IIP region during this section of the drift. It continued this motion until the TOD failed on 17 September (260). The drogue sensor indicated the drogue remained attached until 11 September (254).

TOD #4529

TOD #4529 was deployed on the north side of Sackville Spur in about 1000m of water on 28 July (209) in position 48°21.0'N 46°48.0'W (Figure C-1). It drifted around the top of Flemish Cap at an average velocity of 21 cm/s until 18 August (230) when it was caught up in the North Atlantic Current. TOD #4529 was carried in a generally northerly direction at 36 cm/s until it exited the IIP region on 14 September (257). This northward drift corresponds well with the 12°C isotherm as depicted on the 15-19 August METOC SST chart

Table C-2.
1984 IIP TIROS Oceanographic Drifters Grounding in Europe

TOD #	Deployment Date	Deployment Position	Grounding Date	Grounding Position
4512	27 APR 84	47°51.6N 47°30.0W	27 SEP 85	49°36.6N 01°38.4W
4528	5 AUG 84	50°59.4N 51°01.2W	12 OCT 85	57°03.0N 06°29.4W
4530	6 AUG 84	46°46.8N 46°54.4W	28 AUG 85	50°01.2N 05°15.6W

Figure C-3. Canadian METOC Seas Surface Temperature Charts for the indicated periods

(Figure C-3). The SST sensor on TOD #4529 indicated between 11°C and 13°C during this time period.

TOD #4529 drifted to the northeast before turning south and re-entering the IIP region on 24 September (267). After re-entry, TOD #4529 drifted south until 28 September (271) when it turned cyclonically completing an ellipse with a major axis length of about 140 km on 6 October (279). The average velocity during the elliptical drift was 39 cm/s. TOD #4529 then drifted slowly to the northwest exiting the IIP region on 17 October (289). As of 30 October, TOD #4529 was still transmitting and the drogue sensor indicated the drogue was still attached.

TOD #4550

TOD #4550 was deployed in about 750m of water north of the Grand Bank on 29 July (210) in position 50°30.0'N 50°29.4'W (Figure C-1). It drifted southeast and then south with the Labrador Current through the Flemish Pass following the bathymetry until 20 August (232). During this bathymetrically guided drift period, the average velocity was 34 cm/s. TOD #4550 meandered in a southeasterly direction at an average velocity of 18 cm/s until 9 September (252). The SST values returned from TOD #4550 rose from 12°C to 17°C between 9 and 10 September indicating TOD #4550 had been caught up in the North Atlantic Current.

The North Atlantic Current carried TOD #4550 to the northeast at an average velocity of 97 cm/s until it

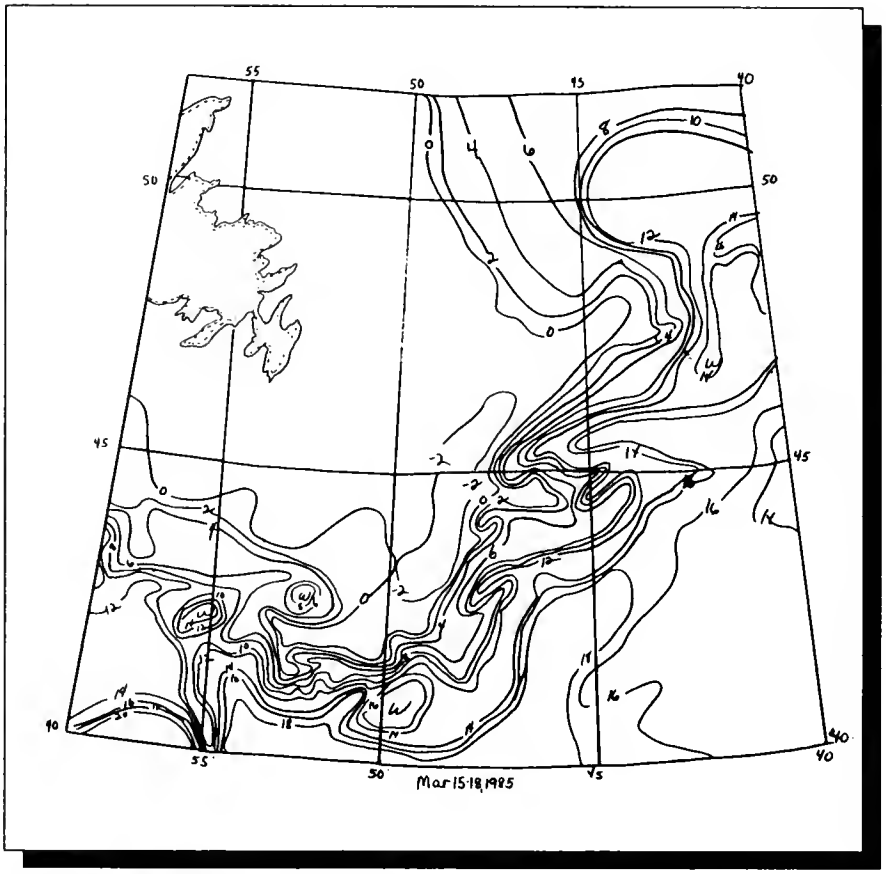

Figure C-3a. March 15-18, 1985

Figure C-3b. April 12-15, 1985

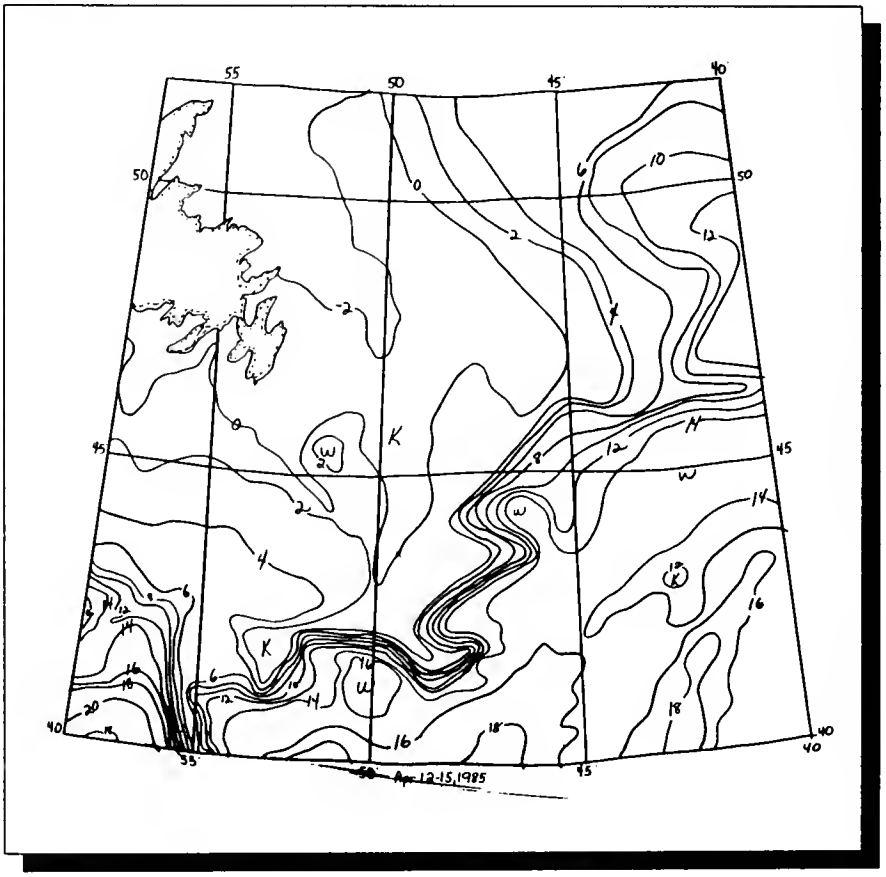

Figure C-3c. May 10-13, 1985

Figure C-3D. June 14-17, 1985

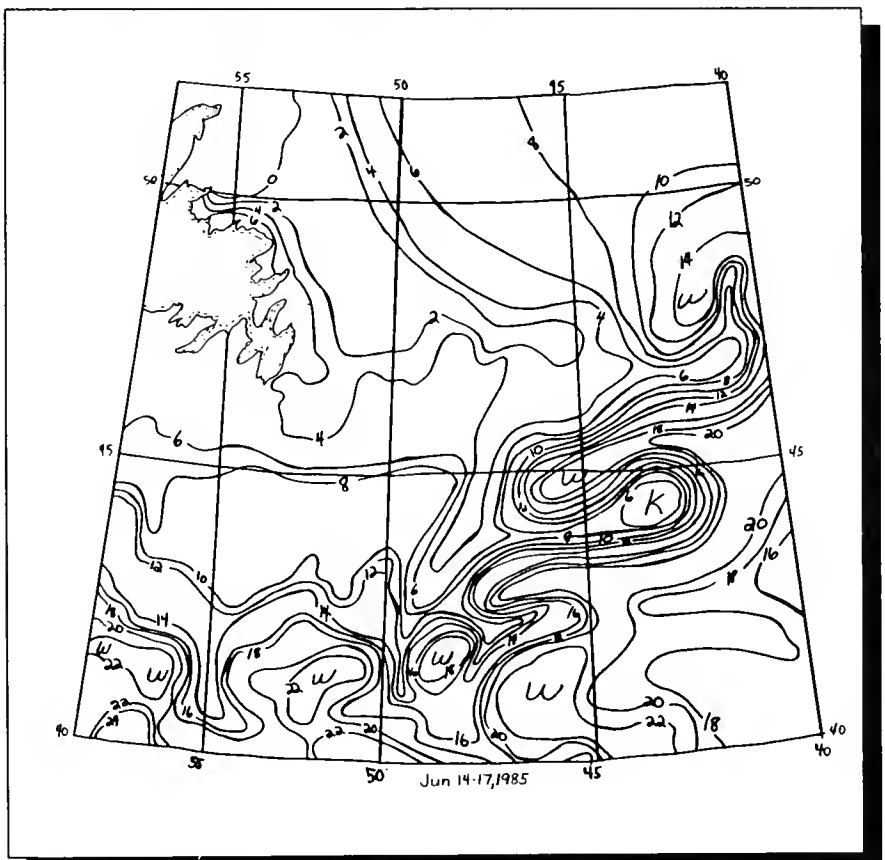

exited the IIP region on 19 September (262). TOD #4550 re-entered the IIP region briefly between 29 September (272) and 2 October (275). The drogue sensor indicated the drogue became disconnected from the TOD on 6 October. TOD #4550 is still transmitting.

TOD #4541

TOD #4541 was deployed north of Sackville Spur in about 1000m of water on 11 August (223) in position 48°17.4'N 47°00.6'W (Figure C-1). The drogue sensor indicated the drogue became disconnected on 15 August (227). TOD #4541 drifted to the southeast across the top of Flemish Cap, crossing isobaths, at an average velocity of 27 cm/s until 6 September (249). Between 6 and 8 September, the SST readings from TOD #4541 rose from 12°C to 16°C indicating TOD #4541 had entered the North Atlantic Current. From 6 September until TOD #4541 left the IIP region on 11 September (254), it drifted in an easterly direction at 70 cm/s. As of 30 October, TOD #4541 was still transmitting.

TOD #4544

To determine the drift of the last concentration of icebergs for the season, TOD #4544 was deployed north of the Grand Banks in 500m of water on 26 August (238) in position 50°07.2'N 50°29.4'W (Figure C-1). TOD #4544 drifted with the Labrador Current, following the bathymetry, through the Flemish Pass at an average velocity of 34 cm/s until 27 September (270). The drogue sensor indicated the drogue was attached only between 28 and 30 August.

From 27 September (270) until 16 October (289), TOD #4544 drifted in a southeasterly direction at 26 cm/s until it was caught in the North Atlantic Current. Between 16 October (289) and 30 October (303), TOD #4544 drifted with the North Atlantic Current at 53 cm/s. As of 30 October, TOD #4544 was still transmitting from within the IIP region.

TOD Results and Conclusions

The variability of the flow in the IIP region is again well-depicted by this year's TOD drift tracks. The areas northeast and south of Flemish Cap, in particular, illustrate the variability that exists in the IIP region making drift prediction so difficult without near-real-time inputs. As shown in previous years, the bathymetry of the Grand Bank and Flemish Cap plays a major role in guiding the drifts of TODs (Anderson, 1984). The only TOD (#4541) not apparently guided bathymetrically in this area apparently had lost its drogue.

TODs continue to supply IIP with needed real-time current information that is required to improve iceberg drift prediction. IIP intends to continue using TODs operationally. The data from all future TODs will be entered into the Global Telecommunications System (GTS). The historical current file east and north of Flemish Cap will be examined for possible changes based upon accumulated TOD drift tracks.

As a footnote, three of the TODs released in 1984 have grounded in Europe. TOD #4512 ran aground near Cherborg, France on 27 September 1985 and was taken to Brest, France, TOD #4528 grounded on the island of

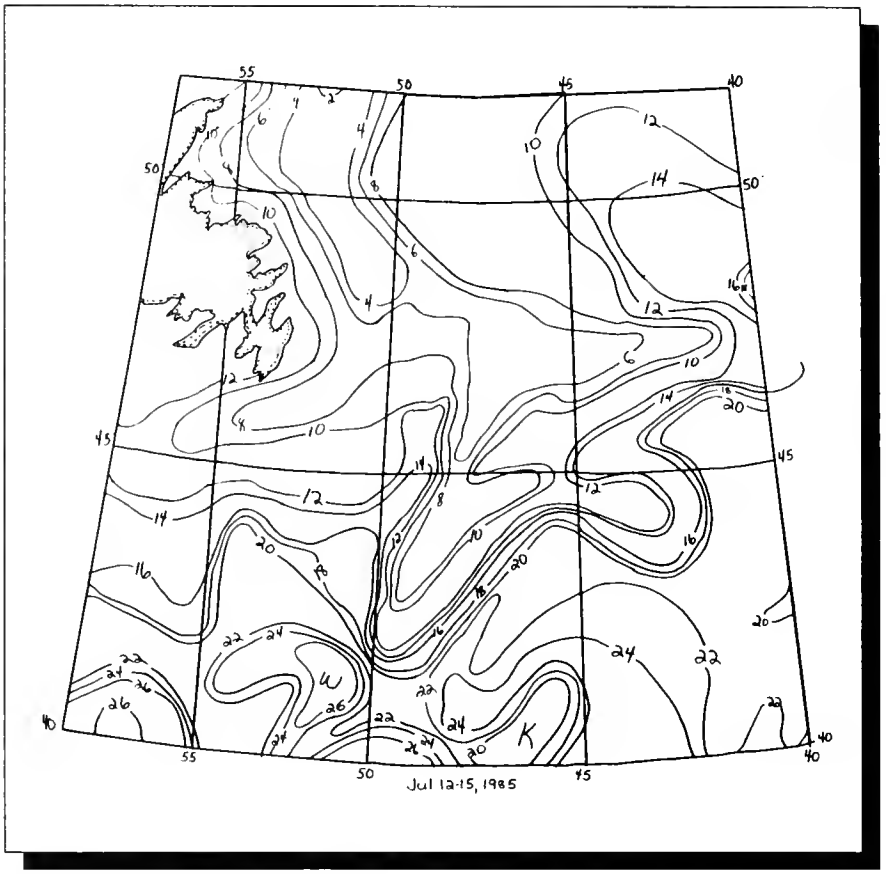

Figure C-3e. July 12-15, 1985

Figure C-3f. August 16-19, 1985

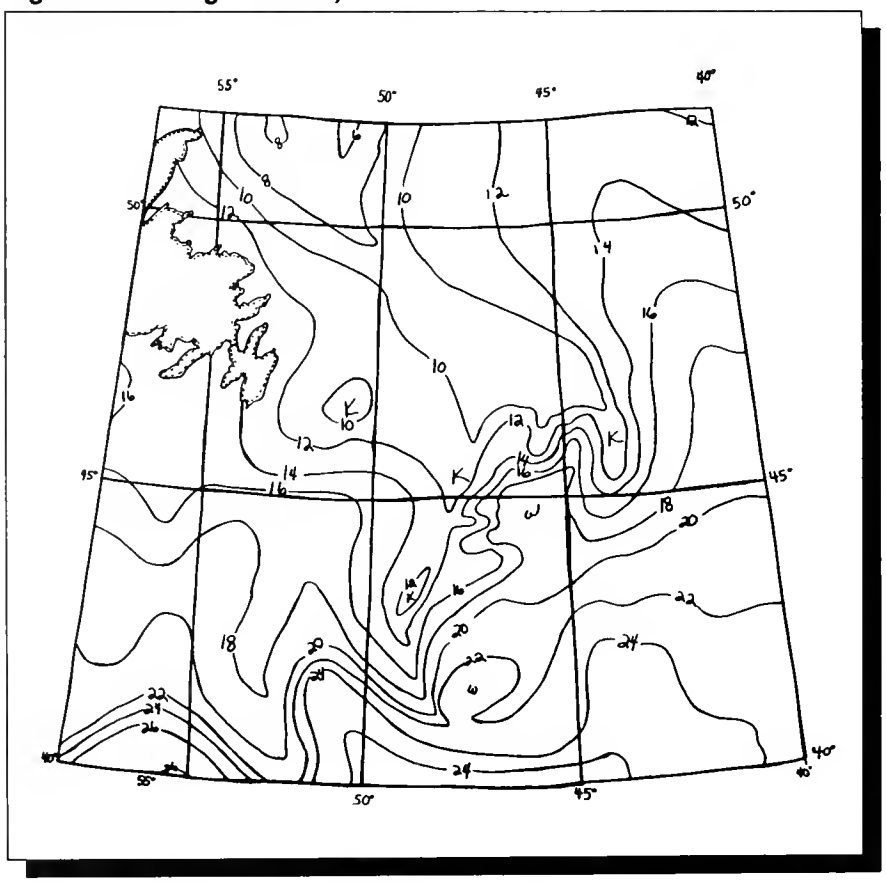

Rhum in the Sea of The Herbides off Scotland on 12 October 1985, and TOD #4530 ran aground near Helston, England (near Lands End) on 28 August 1985 (Table C-2). With the cooperation of the Royal Navy and the Military Airlift Command, TOD #4530 is being returned to Ice Patrol.

1985 Iceberg Deterioration Observations

In 1983 International Ice Patrol began using a computer model to predict iceberg deterioration. The model, based on White, *et al.*, 1980, uses melting due to insolation, vertical buoyant convection, wind-forced convection, and wave erosion to reduce the length of each iceberg. The details of the equations used by IIP to model these four processes can be found in Anderson, 1983.

During the EVERGREEN cruise, measurements of the observed icebergs were made using a reticulated laser range finder. Measurements were made twice a day separated by 12 hours, weather and other operations permitting. Photographs of the iceberg were taken in conjunction with the measurements. Length and mass estimates were made from the measurements and photographs. These methods can lead to a large error in mass estimation, since none of the underside of the iceberg was observed. Sea surface temperature (SST), significant wave height and period data were also collected. The observed environmental data were used as the inputs for the deterioration model in the discussions that follow. In the operational use of the model, the required environmental data is received

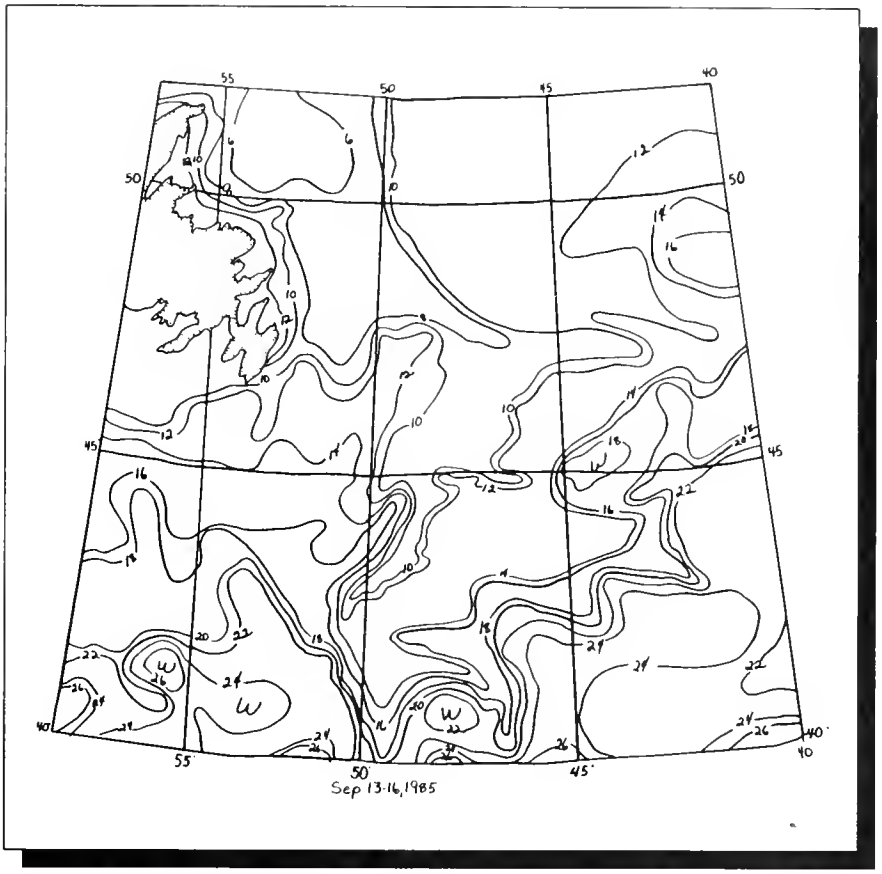

Figure C-3g. September 13-16, 1985

Figure C-4. Iceberg #1, 19 April 1985, 0930Z. Est length,129 m.

from Fleet Numerical Oceanography Center (FNOC) in Monterey, CA. FNOC provides SST data in °C and wave heights in feet. For consistency, the following discussion uses the same units.

Due to IIP's reconnaissance methods, iceberg length (not mass) is the characteristic used to evaluate deterioration. Each of the four sizes of icebergs used by IIP is assigned a characteristic length based on our size definitions (Table C-3). Before each iceberg is eliminated from our list of active icebergs because of deterioration, it is allowed to melt to 175% of its original length. This figure, although selected arbitrarily, is used conservatively to ensure the iceberg has melted before elimination. In order to reduce this figure and still ensure complete deterioration before an iceberg is eliminated, field measurements of the deterioration of three icebergs were observed during the 1985 EVERGREEN cruise, one during the first phase and two during the second phase. Comparisons of these observations to the predictions of the deterioration model are discussed below.

The two icebergs observed during the second phase of the EVERGREEN cruise were used as targets for a side-looking airborne radar (SLAR) detection and identification experiment conducted between 27 April and 5 May 1985. In order for the iceberg to be tracked during the SLAR experiment, it had to be detectable up to at least 5 nm (9 km) on EVERGREEN's surface search radar.

Table C-3. Characteristic Length of Iceberg Sizes

Size	IIP Definitions	Melt Model Length
Growler	less than 16 m.	16
Small	greater than 16 m but less than 60 m	60
Medium	greater than 60 m but less than 122 m	120
Large	greater than 122 m	225

Figure C-5. Observed Vs. Model Predicted Iceberg Length

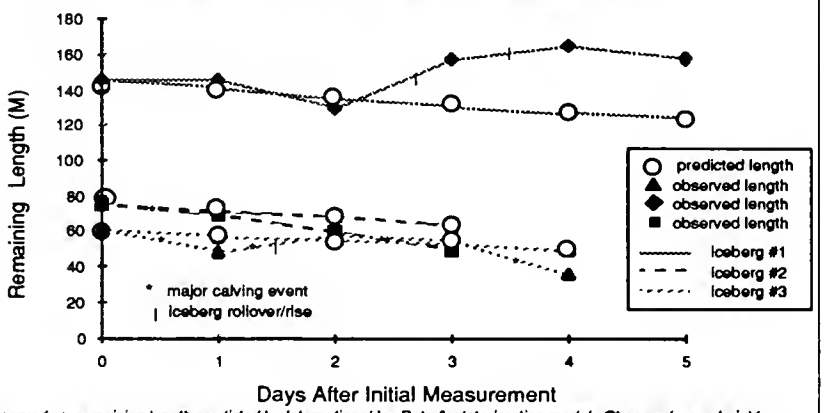

Observed vs. remaining length predicted by International Ice Patrol's deterioration model. Observed wave height and sea surface temperature were used as the model inputs. The tick marks indicate observed instances of iceberg rollover or rise while the asterisks indicate observed major calving events.

Fig. C-6. Iceberg #2 at 1000Z 28 April 1985. Est length 73m.

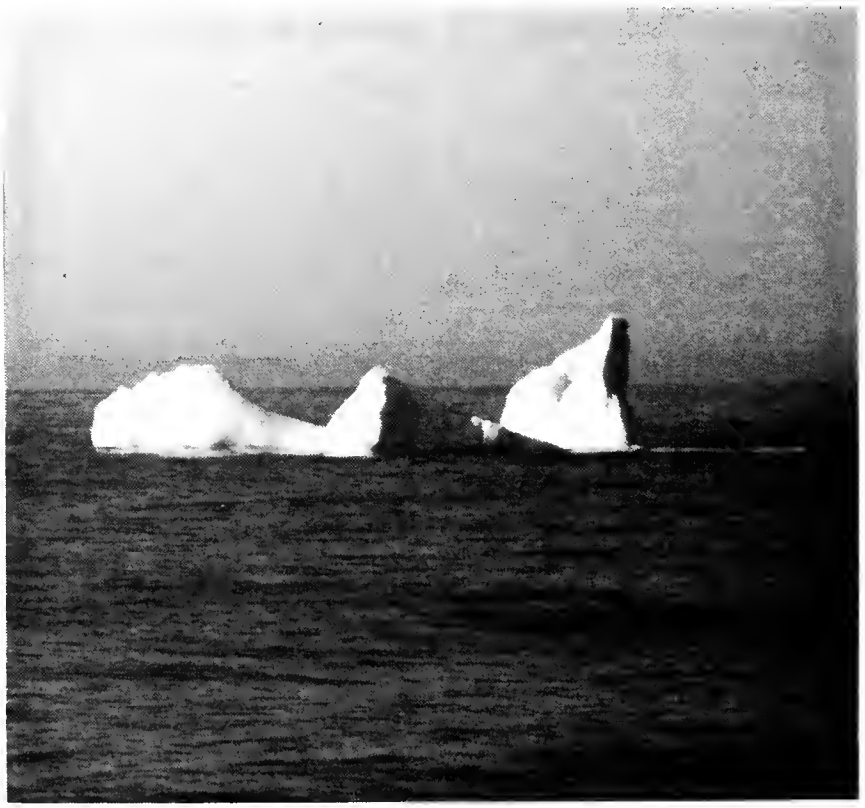

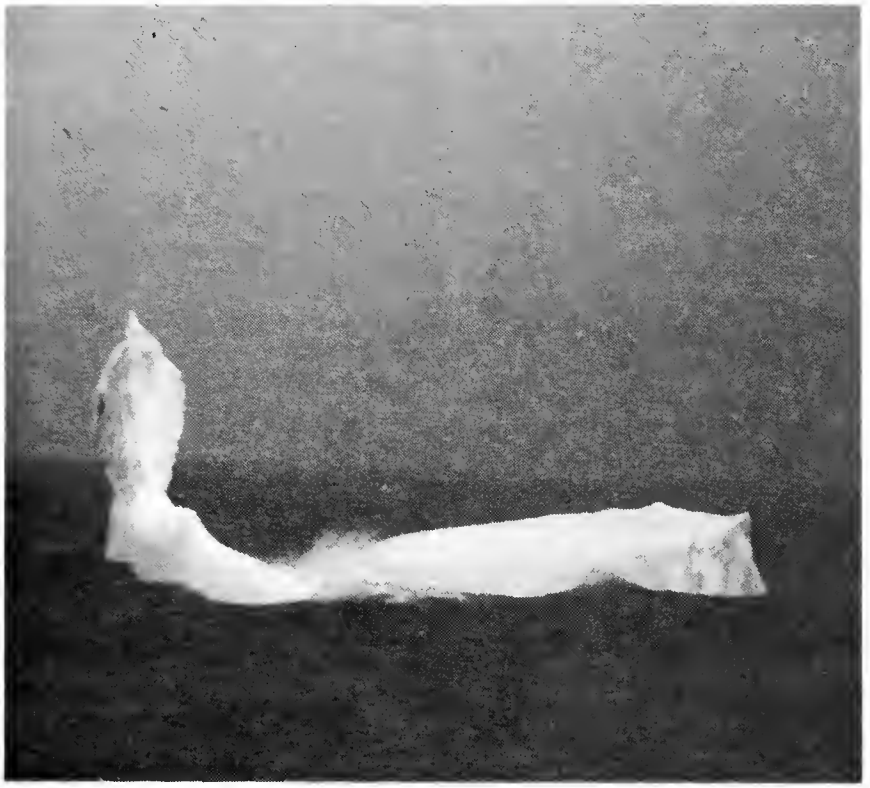

Figure C-7. Iceberg #3 at 2145Z 2 May 1985. Est length 48m.

Figure C-8. Observed vs. FNOC sea surface temperature (SST). *The rise in observed SST between 30 April and 1 May was due to change in location of EVERGREEN*

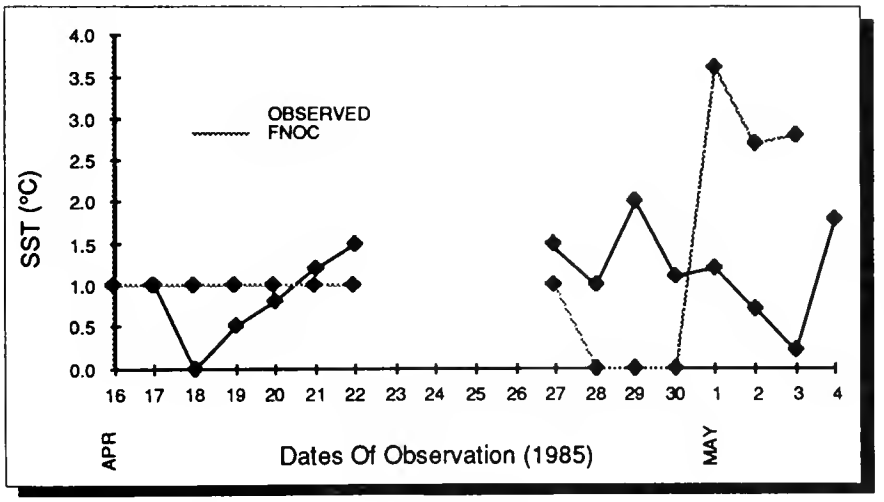

Iceberg #1

A large pinnacled iceberg with an initial length and estimated mass of about 150m and 800,000 metric tons was located in Lilly Canyon in position 44°57'N 49°03'W along the eastern edge of the Grand Bank on 16 April during the first phase of the cruise (Figure C-4). Subsequent position calculations showed that this iceberg was intermittently grounded, never drifting more than about 10 nm from the original sighted position. Poor visibility prevented the collection of size data on 16 April. Data on this iceberg were collected 17-22 April. The model-predicted waterline length matched the observed length fairly closely until the iceberg rolled on 19 April (Figure C-5).

During the evening of 19 April, the iceberg rolled, increasing the maximum observed waterline from 129m to 157m. Due to continued deterioration on 19 April, part of the iceberg rose as it tilted, allowing the iceberg to increase in length again. Although the iceberg increased in length between 17 and 22 April, it was observed to lose approximately 15% of its mass during the same period. Throughout the observation period, only a few minor calving events were observed. The average wave height and period were 5 feet and 4 to 5 seconds and the SST averaged 1.2°C.

Iceberg #2

A medium drydock iceberg was located south of Flemish Cap in position 46°12'N 46°14'W on 27 April during the second phase of the EVERGREEN cruise (Figure C-6). The initial length of the iceberg was approximately 75m. Due to the highly irregular shape, no quantitative estimates of the mass were made. Due to fog, no measurements were made on 29 April. The iceberg was observed until 30 April when it no longer was an acceptable target for the SLAR experiment.

During the observation period, there were no observed incidents of iceberg roll over. Major calving events were observed on 27 April and 30 April. The event of 30 April caused a considerable loss of mass. The model predicted a slower deterioration than was actually observed (Figure C-5). SST averaged about 1.5°C while the average wave height and period were 3 feet and 4 seconds for the observation period.

Iceberg #3

The last iceberg observed during the EVERGREEN cruise was a small drydock iceberg located in position 45°12'N 48°28'W on 1 May (Figure C-7). The initial length and mass were 60m and 35,000 metric tons respectively. Although this iceberg was never observed to have rolled over, there were frequent major calving events. A calving between 2 and 3 May caused a rise in the iceberg resulting in an increase in water-line length. The model does a fair job of predicting the deterioration rate until day 4 (5 May) when a major calving event significantly reduced the size of the iceberg (Figure C-5). On 5 May, the iceberg calved 7 large pieces of ice with the largest being 20m in length and having a mass of about 4,000 metric tons. The mass of the iceberg after this event was reduced to about 8,000 metric tons. The average significant wave height for the duration of the obser-vations was 4 feet with a 5- to 6-second period. SST averaged about 1.0°C.

Observed vs. FNOC Environmental Model Inputs

Comparisons were made between the observed and FNOC SST and wave height data. Six hour averages before the synoptic hour of the observed data were used in the comparisons below. The FNOC SST is reasonably close to the observed data (Figure C-8). The largest difference was 0.4°C. The magnitude of this difference is consistent with past comparisons (Anderson, 1983). The change in FNOC SST between 30 April and 1 May was due to EVERGREEN's change in position as iceberg #2 deteriorated substantially and iceberg #3 was located (Figure C-5). The largest error of 2.5°C occurred during the observation of iceberg #3 on 1 May.

The highest waves observed during the EVERGREEN cruise were 8 feet on 18 April (Figure C-9). FNOC predicted the wave height for EVERGREEN's position on 18 April to be 25 feet. The observed wave heights never were greater than one half of the wave height predicted by FNOC with the average error being about 10 feet. These differences between the predicted and observed wave heights are consistent with comparisons made by IIP in previous years (Anderson, 1983).

Figure C-9.
Observed vs. FNOC predicted wave heights.

Note the consistent over-estimation of wave height by FNOC for the observed period.

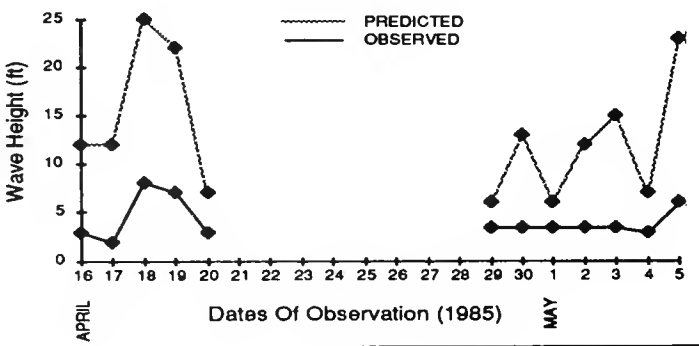

Iceberg Deterioration Discussion and Conclusions

Of the four physical processes used in the IIP model to predict deterioration, wave erosion is responsible for the vast majority of the predicted erosion. This equation is dependent on SST, wave height, and period. (Calving of growlers from an iceberg is not directly modelled but is dependent on wave erosion.) The SST and wave heights experienced by the three icebergs observed in 1985 were not significantly different.

The amount of wave-induced erosion of an iceberg of a given length under the same environmental conditions is dependent on the shape of the iceberg and the amount of surface area exposed to wave action. The shape of an opening, large or small, in an iceberg can concentrate the wave energy on a small area creating faster erosion and subsequent calving. If an iceberg has a large exposed waterline-to-mass ratio, as did icebergs #2 and #3, wave erosion with associated calving is a more effective deterioration force than on an iceberg (like iceberg #1) with a relatively small exposed waterline-to-mass ratio.

The model-predicted deteriorations for icebergs #2 and #3 were less than the observed rate over the entire observation period. The instances where the observed icebergs deteriorated much more rapidly than predicted by the model are correlated with observed calving events and no associated rollover or rise of the iceberg (Figure C-5). The model-predicted deterioration for iceberg #1 was greater than that observed over the entire observation period. Iceberg #1 had no observed major calving events. The major reason for the model's poor performance with iceberg #1 was the increase in maximum length due to rollover. Before the iceberg rolled over, the model-predicted deterioration closely matched the observed deterioration, and after it stabilized on day 4, the observed deterioration again closely matched the model-predicted deterioration.

Under operational conditions, the required environmental data for the deterioration model are supplied by FNOC. On their own, the observed errors in the wave height data would increase the modelled deterioration rate significantly. Part of this increase is, however, offset by the increased period of the bigger waves. (Wave height is in numerator while wave period is in the denominator of the wave erosion equation (Anderson, 1983).) During the largest error in FNOC wave height (17 feet), the deterioration rate would have been increased by about 25 percent.

Given accurate environmental data, the iceberg prediction model used by IIP predicts the deterioration reasonably well. Because of errors introduced by our present methods of operation (FNOC data errors and SLAR sizing errors), IIP will continue its conservative approach and will require that an iceberg deteriorate175% of its original length before it is eliminated. Future IIP cruises will continue to gather iceberg drift and deterioration data to further evaluate the performance of the models.

References

Anderson, I. (1983); *Iceberg Deterioration Model*, Appendix C of the Report of the International Ice Patrol Service in the North Atlantic. Bulletin No. 69., CG-188-38, International Ice Patrol, Avery Pt., Groton, CT 06340-6096

Anderson, I. (1984); *Oceanographic Conditions on the Grand Banks During the 1984 International Ice Patrol Season*, Appendix B of the Report of the International Ice Patrol Service in the North Atlantic. Bulletin No. 70., CG-188-39. International Ice Patrol, Avery Pt., Groton, CT 06340-6096.

White, F. M., M. L. Spaulding, and L. Gominho (1980); *Theoretical Estimates of the Various Mechanisms Involved in Iceberg Deterioration in the Open Ocean Environment*, U. S. Coast Guard Research and Development Center Report CG-D-62-80, 126pp.

Appendix D

An Evaluation of the International Ice Patrol Drift Model

D. L. Murphy
LT I. Anderson, USCG

Introduction

Since 1979, International Ice Patrol (IIP) has been using an iceberg drift model as an integral part of its iceberg tracking operations. During the season of maximum iceberg threat, typically March through August, IIP conducts aerial reconnaissance of its operations area (40° - 52°N, 39° - 57°W) on alternate weeks. During the week that the IIP Ice Reconnaissance Detachment (ICERECDET) is deployed to Gander, Newfoundland (IIP field operations base), daily flights are conducted on five consecutive days, each covering only a small portion of the IIP operations area. As a result of this reconnaissance schedule, IIP must often rely on the model predictions to set the limits of iceberg danger during periods when no ice reconnaissance is being conducted. In addition, the model drift predictions are used to help recognize icebergs that have been previously sighted, either by the ICERECDET or merchant vessels. Lacking this ability to recognize iceberg resights has the effect of inflating the numbers of icebergs south of 48°N, the traditional indicator of the severity of an iceberg season.

Despite the reliance that IIP places on the accuracy of the drift model results, relatively little testing of the model has been possible, primarily because adequate iceberg drift data, with accompanying environmental data, are expensive and often difficult to obtain. Moreover, only in the last few years has navigation in the operations area been accurate and reliable enough to permit the collection of good data.

Mountain (1980) tested the model using the tracks of two large tabular icebergs, a large pinnacle iceberg, and a freely-drifting satellite-tracked buoy. The drift durations were from 3 to 25 days. The results were quite variable, ranging from a small 9km error for the 3-day drift to a constant 90-150km drift error in the 25-day case. Although he recognizes the limitations of this small data set, he suggests that the primary cause of the model error is due to inaccurate inputs, i.e., winds and currents.

This report describes the results of four case studies in which the performance of the IIP iceberg drift model was examined at four different locations (Figure D-1) in the IIP operations area. The objectives were twofold: first, to test the accuracy of the drift predictions of the operational IIP iceberg drift model, and second, to investigate how the accuracy changes when on-scene measured wind and current data are used to drive the model.

Model Description

Mountain (1980) describes the details of the IIP operational drift model; thus, only a brief outline is presented here. The fundamental model balance is between iceberg acceleration, air and water drag, the Coriolis acceleration and a sea surface slope term. The resulting differential equations are solved using a fourth-order Runge-Kutta algorithm. The model is driven by a water current which combines a depth- and time-independent geostrophic flow with a depth- and time-dependent current driven by the local wind (time-dependent Ekman flow).

When used operationally, the IIP drift model employs a mean geostrophic current field based on many years of hydrographic surveys (Scobie and Schultz, 1976). It is on a grid of 20 minutes of latitude by 20 minutes of longitude, except for the Labrador Current, which is defined on a more detailed grid of 10 minutes of longitude. Wind data, on a 1 degree of latitude by 2 degrees of longitude grid, are provided to the model every 12 hours from the surface-wind analysis of the U. S. Navy Fleet Numerical Oceanography Center (FNOC).

Finally, the model requires as input the mass and cross-sectional area of the drifting iceberg. Obviously, IIP reconnaissance operations do not permit precise measurement of each detected iceberg. Often, IIP locates icebergs using the side-looking airborne radar

(SLAR) with no visual confirmation. As a result, IIP can only classify icebergs into the broad categories of growler, small, medium, and large, and assume characteristic mass and cross-sectional areas for each category. When visual confirmation is available, it is possible to distinguish between tabular and non-tabular icebergs, resulting in somewhat different mass and cross-sectional areas. Regardless of the size and shape of the iceberg, both the air and water drag coefficients are set to 1.5.

Currently, IIP estimates that the model drift error is 10nm (~18.5km) for the first 24-hour period and an additional 5nm (~9km) for each additional 24 hours of drift, up to a maximum error of 30nm (~56km). The accuracy of this error estimate is evaluated in this report.

In 1983 IIP began using observed-current data derived from the trajectories of freely-drifting satellite-tracked buoys to modify the mean geostrophic field (Summy and Anderson, 1983) during operational model runs. The modifications are both temporary and localized in that they are only applicable during the period that a buoy is in that specific region, after which the currents revert back to the mean geostrophic currents. It is not the intent of the present report to address this practice directly, but rather to compare the drift-model accuracy using two sets of input data: mean geostrophic data with FNOC wind and on-scene measured data. In doing so, the importance of using on-scene data becomes clear.

Figure D-1. Area of Study

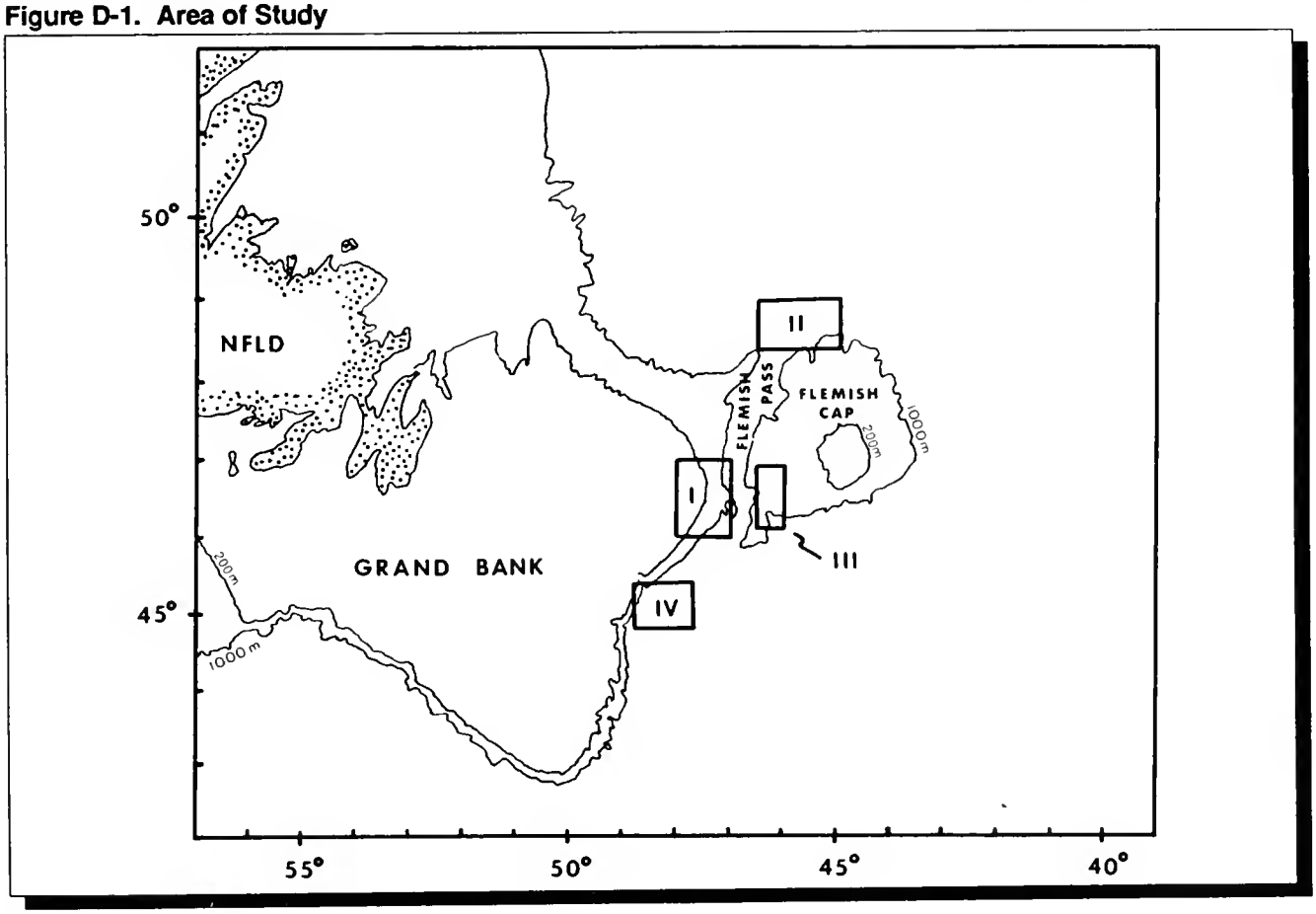

Figure D-2. Iceberg and TOD trajectories for Case I (1983)

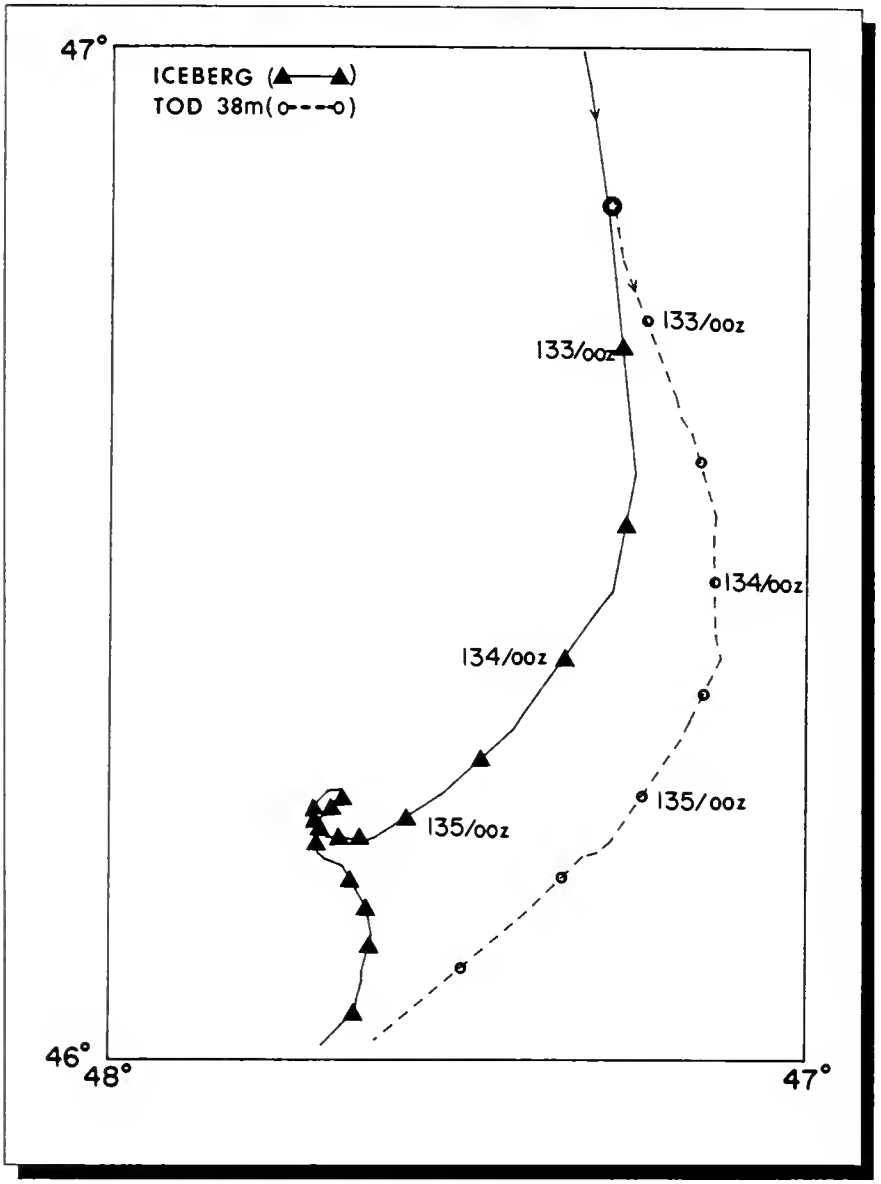

Data Description

The data used in this study were collected from 1983 through 1985. All of the cases were drifts of short duration, with a maximum drift period of 4.5 days. In all four cases, the drifting iceberg was close to at least one freely-drifting TIROS Oceanographic Drifter (TOD), from which local currents were determined. The TOD hull was a 3m spar and was fitted with a 2m x 10m window-shade drogue at the end of a tether. The drogue depths presented here refer to the depth of the center of the drogue. The TOD's were tracked by the NOAA/TIROS series satellites and the data provided to IIP by Service ARGOS, with a position accuracy well within 500m (Bessis, 1981).

In three of the cases (II, III, and IV), a surface vessel near the iceberg was collecting local wind data. The data for each case are discussed separately. The numbers in parentheses after each date are Julian year dates, that is, dates numbered sequentially from 1 January.

Case I

This case consists of a 2.5-day drift of a large tabular iceberg with a TIROS Arctic Drifter (TAD) aboard. The TAD, which is essentially a TOD with different packaging, had been deployed onto the iceberg on 27 March 1983 (86) by IIP, in cooperation with the U. S. Coast Guard Research and Development Center (R&DC).

The test period began at 1600Z on 12 May 1983 (132) when a TOD, drogued at 38m, was air-deployed from a HC-130 aircraft at a location approximately 1km from the iceberg, which at the time was moving southward in the Labrador Current (Figure D-2).

The test period ended on 15 May (135) shortly before the iceberg grounded for a 4-day period. The iceberg was last sighted with the TAD aboard on 21 May (141) by Mobil Oil Company, Canada (Anderson, 1983). On this date the iceberg was still classified as large, with estimated dimensions of 150mx110mx30m. During the test period, the maximum separation between the TAD (iceberg) and the TOD was less than 25km. No on-scene wind data were available.

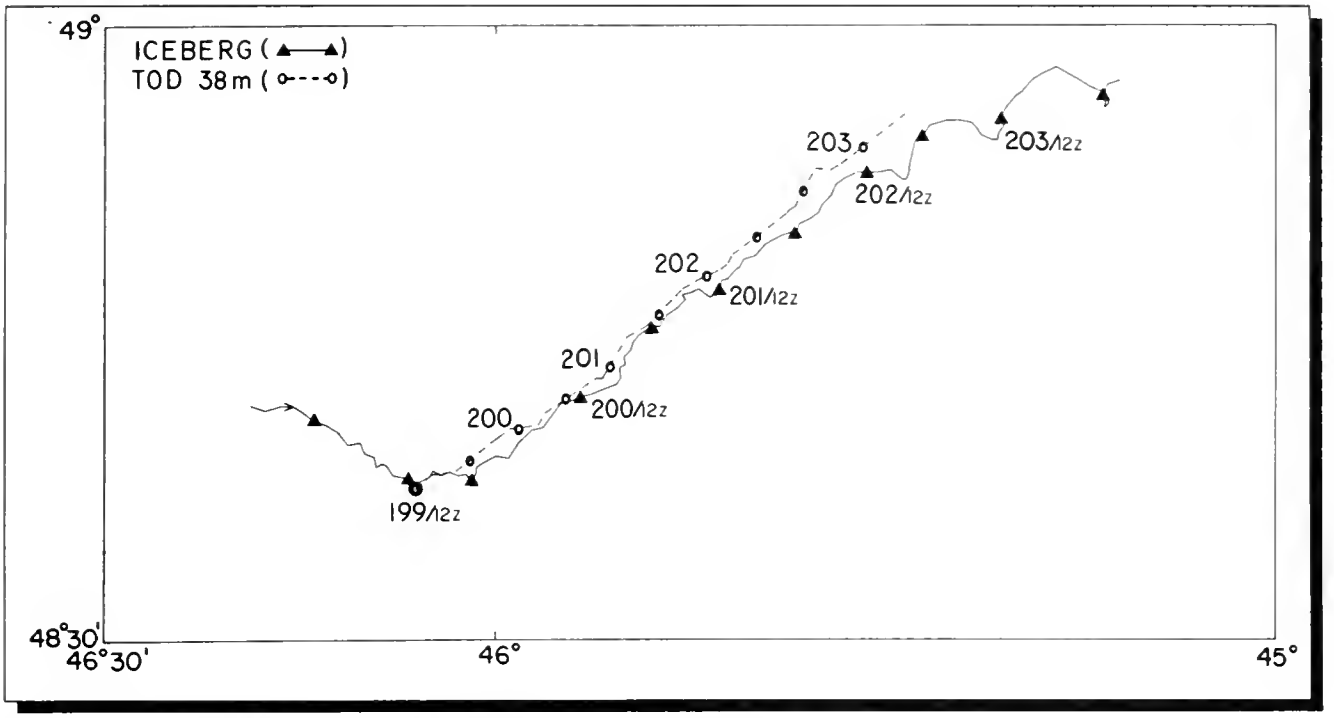

Figure D-3. Iceberg and TOD trajectories for Case II (1984)

Case II

This case is a 4.5-day segment of an iceberg track obtained in 1984 by USCGC HORNBEAM. The test period began 17 July (199) at 1300Z when HORNBEAM deployed a TOD drogued at 38m approximately 500m from a medium (120mx115mx37m) pinnacle iceberg in the region north of Flemish Cap. Although the iceberg was rapidly deteriorating, it was in the medium size range (>60m) for most of the drift period. Only in the last 24-30 hours of drift was it at or slightly below the medium/small border. Hourly iceberg positions were recorded using radar ranges and bearings and the HORNBEAM's LORAN C position (Figure D-3). Hourly wind speed and direction were measured using the shipboard anemometer (Figure D-4). The maximum separation between the iceberg and the TOD was less than 25km.

Case III

The third case is a 3.5-day [27 - 30 April 1985(117-120)] track of a medium (75mx56mx18m) drydock iceberg south of Flemish Pass obtained by USCGC EVERGREEN. Over the drift period, the target iceberg was deteriorating but only on the last day of drift did it fall into the upper part of the small range. Again, hourly iceberg position (Figure D-5) and wind data (Figure D-6) were collected using shipboard radar and anemometer, respectively.

Figure D-4. Hourly wind vectors for Case II

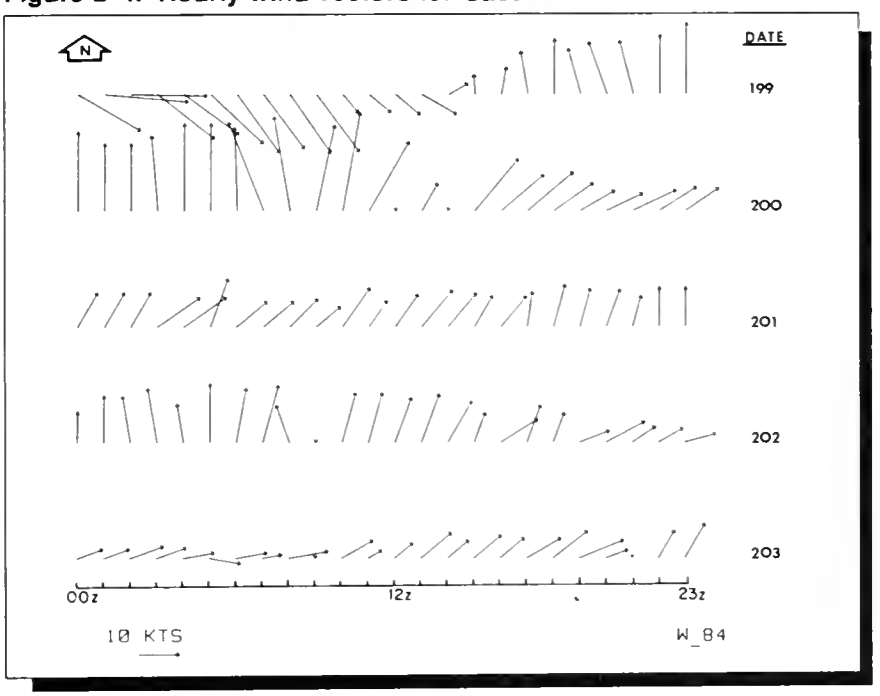

Two TOD's provided the current data. They were deployed, one drogued at 38m and the other at 58m, 300m from the iceberg on 27 April (117). Approximately halfway through the drift period, both buoys were retrieved and redeployed close to the iceberg to minimize the separation between the iceberg and the TOD's. Upon redeployment, the drogue at 38m was set to 8m. The maximum separation between the iceberg and the TOD's, which occurred during the first part of the drift period, was approximately 35km.

Case IV

A 4-day drift [1-5 May 1985(121-125)] of a small (60mx40mx10m) drydock iceberg provides the data for Case IV. As in Case III, the area of study was south of Flemish Pass, and EVERGREEN tracked the target (Figure D-7) and obtained the wind data (Figure D-8). Two TOD's, one drogued at 8m and the other at 58m, were deployed on 1 May (121); they were retrieved and redeployed at the iceberg on 4 May (124). The maximum separation between the iceberg and the TOD's was approximately 30km. On the last day of the experiment, there was a major calving event that left two small icebergs. At this time the parent (larger) iceberg had a maximum waterline length of 37m.

Test Runs

Table D-1 summarizes the runs made during the model tests. For each case, the first run used the mean surface geostrophic current field from the IIP data base and wind data from FNOC. This set of inputs is referred to as system currents and system winds. The remaining runs for each case differed from the first run only in that available on-scene environmental data (observed) were used to drive the model.

The observed currents were obtained from the TOD trajectories by linearly interpolating to positions at 0000Z and 1200Z each day, and then calculating the 12-hour averaged current. When wind data were available, 12-hour averages were computed for use in the model. When no observed wind data were available, FNOC data were employed.

For each run, the model computed a predicted iceberg position at 0000Z and 1200Z on each date. The range and bearing from the actual to the predicted iceberg position were computed for these times.

Table D-1. Model Test Runs Summary

Case	Size	Run Number	Inputs Winds	Currents	
I	Large	1	SYS	SYS	
I	Large	2	SYS	OBS	(38m)
II	Medium	1	SYS	SYS	
II	Medium	2	OBS	OBS	(38m)
III	Medium	1	SYS	SYS	
III	Medium	2	OBS	OBS	(38m/8m)
III	Medium	3	OBS	OBS	(58m)
IV	Small	1	SYS	SYS	*
IV	Small	2	OBS	OBS	(8m)
IV	Small	3	OBS	OBS	(58m)

Summary of the test runs. SYS=system, OBS=observed.The numbers in parentheses indicate the depth of the drogue center.

* Note: The observed currents for this case were a combination of data from buoys drogued at different depths: 38m for the first half of the period and 8m for the second half.

Figure D-5. Iceberg and TOD trajectories for Case III

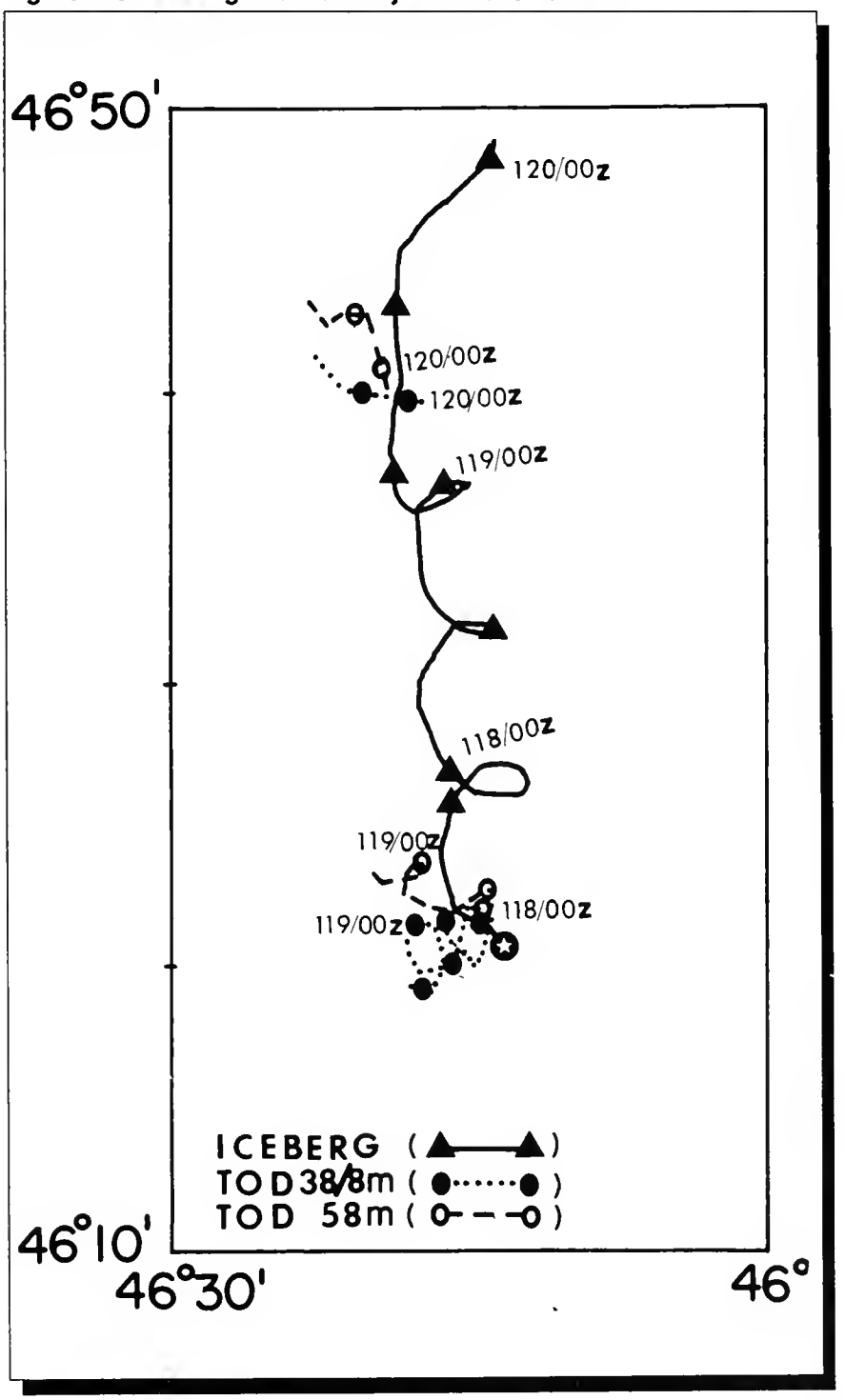

Results

Figures D-9 through D-12 show the magnitude of the drift errors as a function of elapsed time for each of the four cases. The IIP error estimate of 10nm for the first 24-hour period and an additional 5nm for each additional 24-hours of drift, up to a maximum error of 30nm, is also plotted.

In Case I (Figure D-9), the system inputs result in drift errors that increase rapidly and persistently; after approximately 2.5 days they exceed 40nm (~75km). The magnitude of this error is 52% of the total predicted drift. When observed currents drive the model, the errors are substantially reduced so that they are nearly consistent with the currently-used IIP error estimate. In Case I, both the iceberg and the buoy were in the southward-flowing Labrador Current with typical current speeds of 0.4-0.5 m/s.

In Case II (Figure D-10), the errors for the system/system run were less than 12nm (~22km) or 22% of the total predicted drift for the entire 104-hour drift period, well below the IIP error estimate. Using observed current and wind data improves the results; after 104 hours the error is 2.5nm (~4.6 km). The drift test was conducted north of Flemish Cap with typical current speeds of 0.2 m/s, approximately half that observed in Case I.

Figure D-6. Hourly wind vectors for Case III

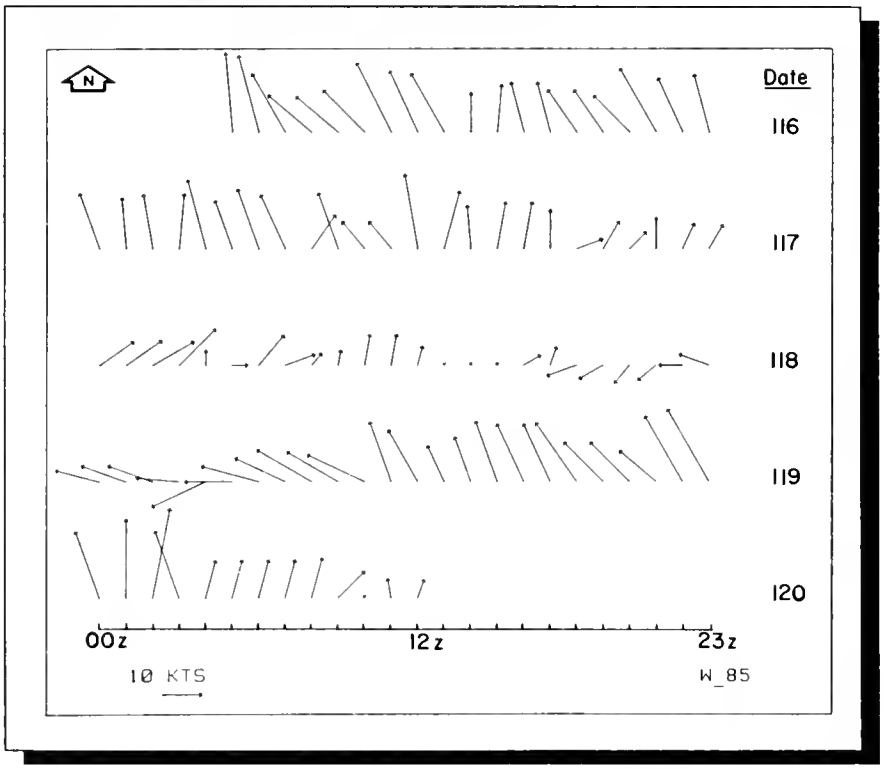

The Case III system/system run (Figure D-11) produced errors that increased persistently, exceeding the IIP error estimate after about 36 hours of drift. At the end of the drift period, the error was over 30nm (~56km), which is 73% of the total predicted drift. In the early part of the drift period (<48hrs.), the use of the observed current and wind data produced no improvement in the results; indeed, at one point, the results were less accurate than the system/system case. This result is not surprising because the iceberg moved rapidly to the north while both buoys remained close to the deployment area. When the buoys were retrieved and redeployed at the iceberg (~60 hrs.), the model results computed using observed data improved somewhat.

Using the observed data to drive the model in Case IV (Figure D-12) made an enormous improvement in the results. The system/system run produced errors between 30-45nm (~56-83km) while, for the observed data, the errors were approximately half those values. For most of the drift period, the currents measured at 58m provided more accurate model results than those measured at 8m. At 84 hours this situation reversed, and the 8m data produced better results. This is an expected result because as this small iceberg deteriorated, its motion should have been more consistent with the 8m currents than the 58m currents. However, the data are few and the difference between the results (8m vs. 58m) is small so there is no certainty that the reversal is meaningful.

Conclusions

No firm conclusions can be drawn from this small data set, but there is some consistency in the results that is worthy of note.

In all four cases, using on-scene measured data improved the model accuracy over the runs made using geostrophic currents and FNOC winds. The accuracy improvement was substantial in two cases: Case I and Case IV. Thus, the results of this study support the IIP practice of using TOD drift data to modify the geostrophic current. The more widespread the use of TOD's, the more we can rely on the model results. No attempt was made to separate the improvements due to on-scene current data and on-scene wind data because of the small amount of data. However, Case I, for which there were no on-scene wind data, showed considerable improvement when on-scene current data were used in the model predictions.

In three of the four cases (Case II excepted), the observed drift error was larger than the IIP estimated error when the system

Figure D-7. Iceberg and TOD trajectories for Case IV

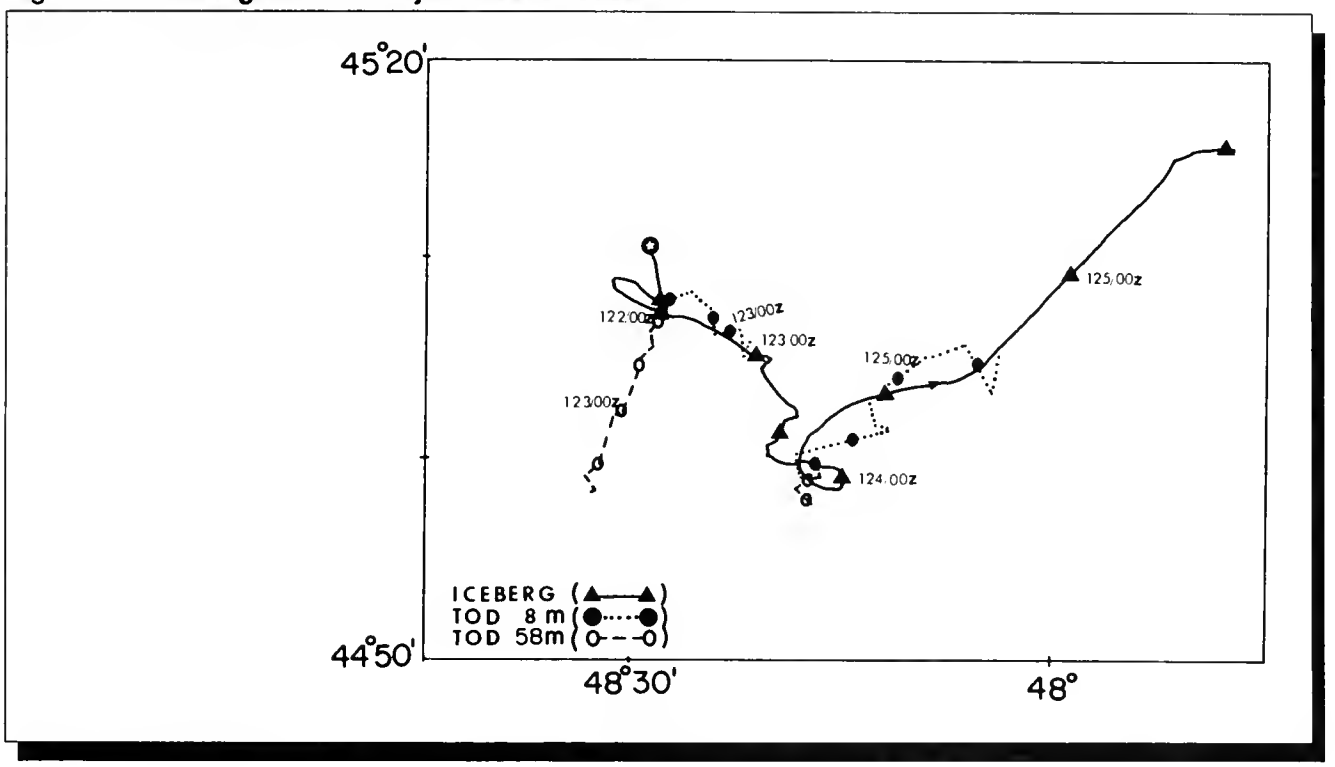

winds and currents were used. For these three cases, the drift errors were 52-73% of the total predicted drift; for Case II the drift error was 22% of the total predicted drift. While it is tempting to suggest that the estimated position error be linked to the total length of the predicted drift (distance along the predicted path), no clear guidance can be given based on these results. The limited data show that if there is a TOD providing current information in the vicinity of a drifting iceberg, the model will probably produce positions that are within the IIP error limits. If only geostrophic data are available, the errors can be substantially larger, even for drifts of short duration. This issue is particularly important when an iceberg is being used to set the limits of iceberg threat.

The importance of collecting current data as close as possible to the tracked iceberg cannot be overemphasized. Early in Case III, when the TOD's and the iceberg separated rapidly, there was no improvement in the model errors when observed inputs were entered. Later in the drift period (after the buoys were redeployed), the model errors were smaller when the observed data were used.

Finally, the results of this study provide some guidance on the deployment of IIP operational TOD's. Although TOD drift data directly north of Flemish Cap are useful, the results of Case II showed that the model performed within the error estimates using the geostrophic currents. The TOD's deployed in the Labrador Current (Case I) and south of Flemish Pass (Cases III and IV), on the other hand, provided bigger payoffs.

References

Anderson, I., 1983. *Oceanographic Conditions on the Grand Banks During the 1983 International Ice Patrol Season.* Appendix B of Report of the International Ice Patrol in the North Atlantic. Bulletin No. 69. CG-188-38. International Ice Patrol, Avery Point, Groton, CT 06340-6096, 73 pp.

Bessis, J.L., 1981, *Operational Data Collection and Platform Location by Satellite*, Remote Sensing of the Environment, Vol II

Mountain, D.G., 1980. *On Predicting Iceberg Drift*, Cold Regions Science and Technology, Vol 1 (3/4): 273-282.

Scobie, R.W., and R.H. Schultz, 1976. *Oceanography of the Grand Banks Region of Newfoundland March 1971 - December 1972.* Report No. 373-70. U. S. Coast Guard, Washington, DC, 298 pp.

Summy, A.D., and I. Anderson, 1983. *Operational Use of TIROS Oceanographic Drifters by International Ice Patrol (1978-1982).* Proc. 1983 Symposium on Buoy Technology. Marine Technology Society, Gulf Coast Section, Bldg. 2204, NSTL, MS 39529, p. 246-250.

Figure D-8. Hourly wind vectors for Case IV

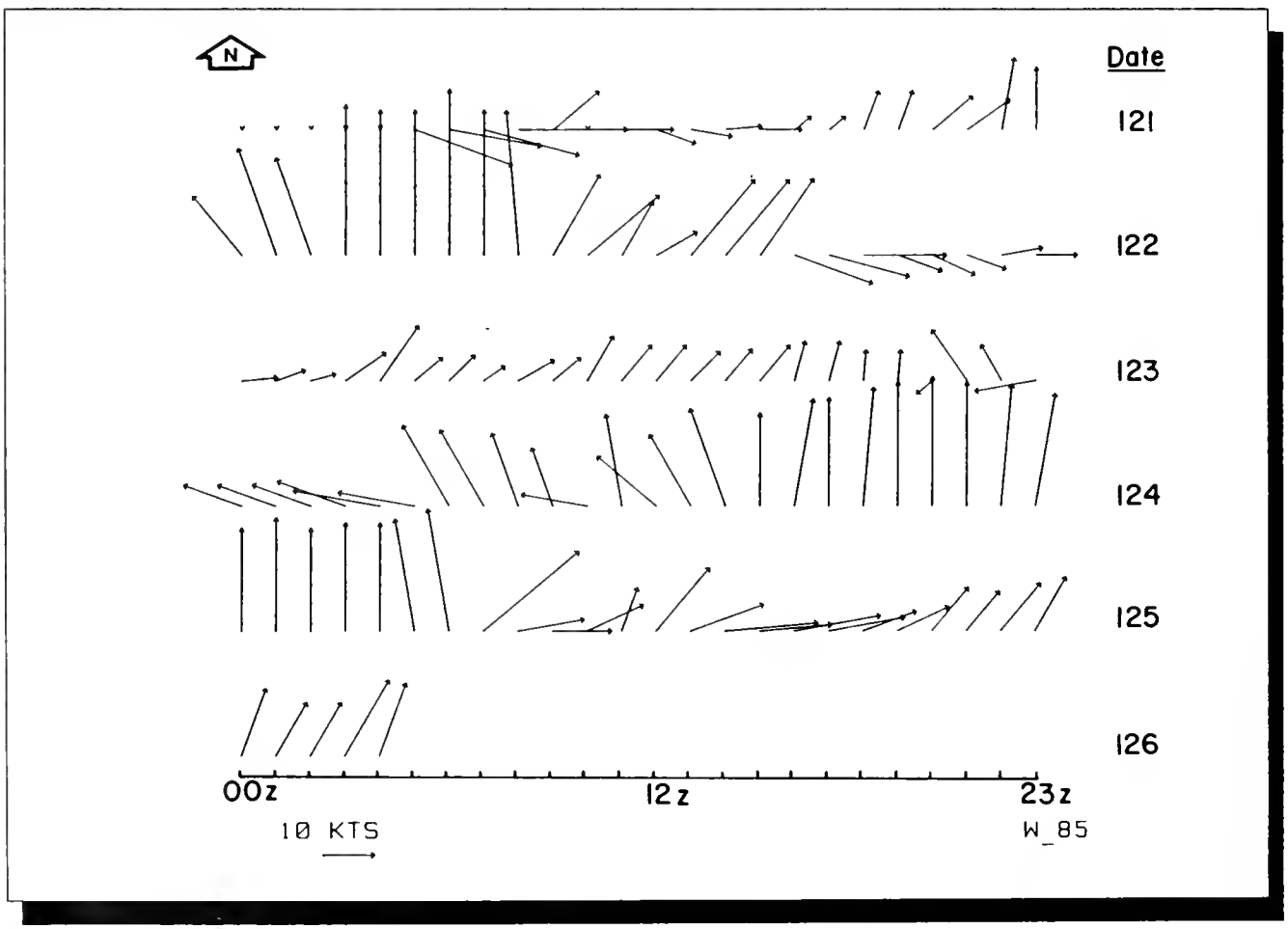

Figure D-9. Case I model errors

Figure D-10. Case II model errors

Figure D-11. Case III model errors

Figure D-12. Case IV model errors

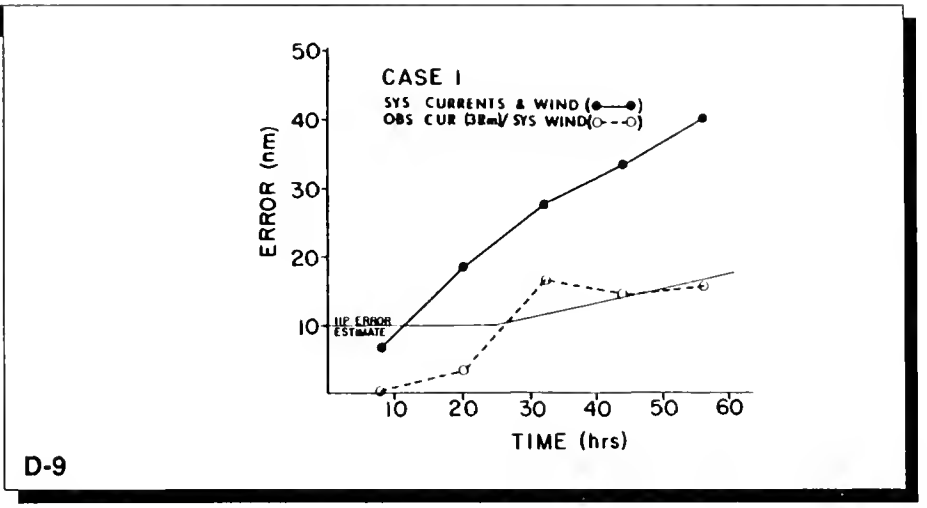

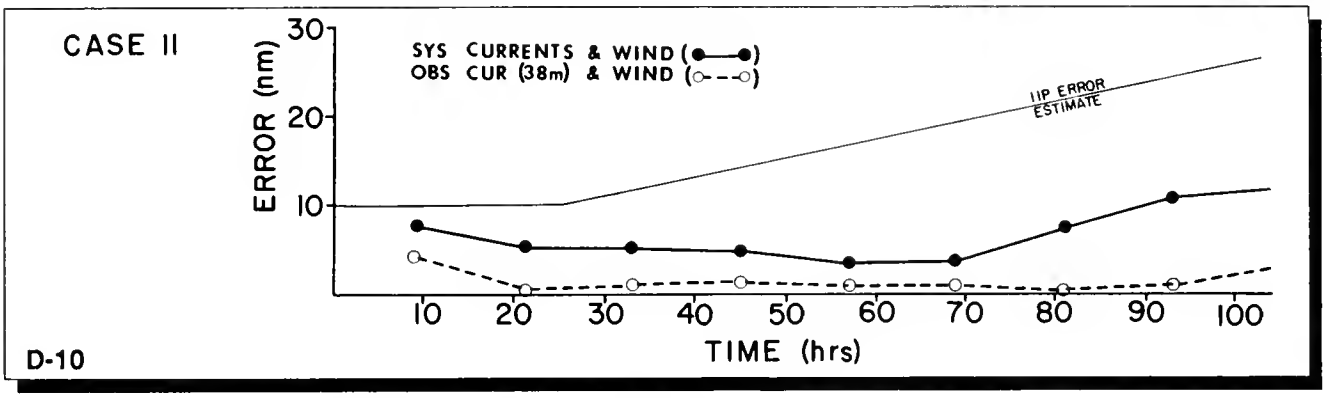

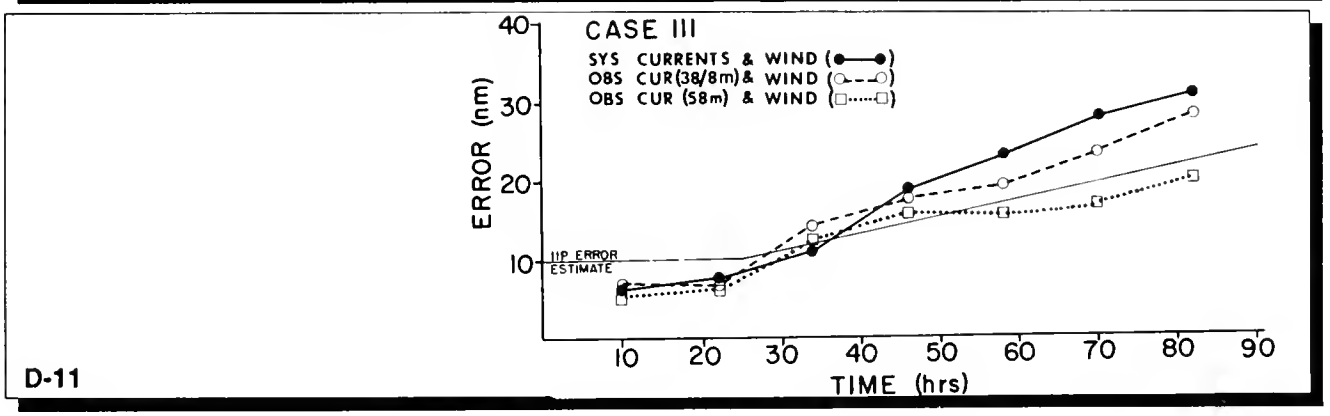

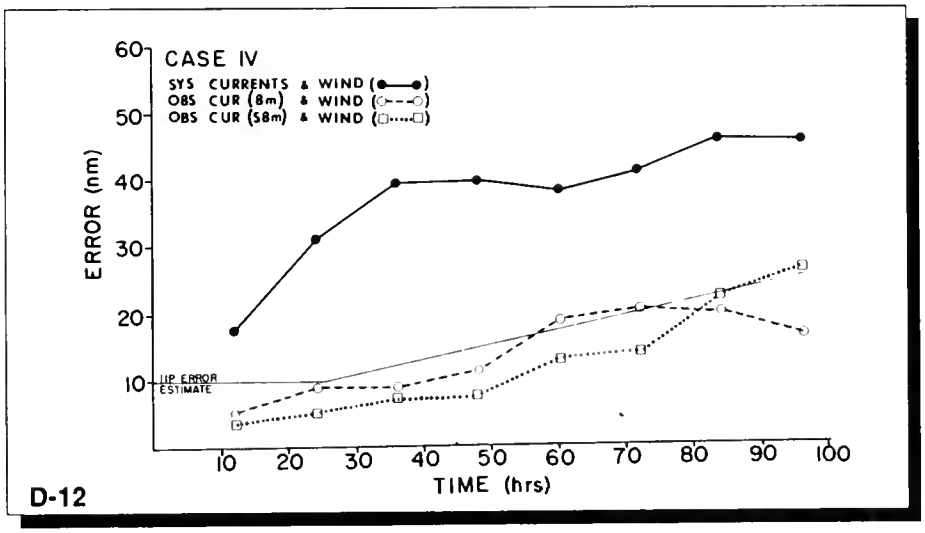

Appendix E

An Analysis of Eddy Formation in the Vicinity of the Grand Banks of Newfoundland

LT F. J. Williams, USCG
D. L. Murphy

Introduction

The International Ice Patrol conducted a study of the eddy population in the Newfoundland Basin region based on data from the period from November 1981 to December 1984 to investigate the importance and basic character of eddy motion in the southern portion (40°N - 45°N and 40°W - 55°W) of our patrol area. This area (Figure E-1) contains the confluence of three surface currents and is bathymetrically dominated by the Grand Banks of Newfoundland, the Newfoundland Seamount Range and the Newfoundland Ridge.

A similar study was conducted by Voorheis, Aagaard and Coachman in 1973. They researched hydrographic data collected during IIP cruises in an attempt to establish an eddy population. The present study encompasses a larger geographic area and also introduces infrared (IR) imagery. Voorheis, *et al.* looked for eddies in hydrographic data along standard IIP transects. The present study uses data collection specifically designed to locate eddies.

Ocean frontal analysis charts maintained by National Weather Service (NWS) and Naval Eastern Oceanographic Center (NEOC), and Canadian Forces METOC Center sea surface temperature data formed the data base for the investigation. Analysts produce these charts from satellite IR imagery gathered predominantly from the GOES and NOAA 6 and 9 satellites. The research area is dominated by cloud and fog cover and so does not always present ideal conditions for use of IR imagery, but these charts represent the only complete data set displaying eddies. An explanation of the methodology is given in Williams (1985). Data analyzed include the number of eddies in the area, their average life span and size, the area of formation, generation and deterioration patterns, and their movement through the area. Eddies included in the study are only those in the southern portion of the area that had an IR signature. Other eddies may affect the operations area, but are not included.

Eddy Population

Eighty-five percent of the time at least one eddy was active in the research area, and on several occasions two or more were present. During the 38 months of the experiment the NWS and NEOC charts indicated 46 eddies in the area. The life of the eddies ranged from two to 218 days with an average life span of 42 days. Voorheis, *et al.* (1973), indicates an average life span of 30 to 120 days.

Areas of Formation

The positions of formation of the eddies as shown in Figure E-2 indicate that they formed in two major areas: over the Newfoundland Ridge and over the Newfoundland Seamount Range. Of the 46 observed eddies, 12 (26%) were first sighted directly over the Newfoundland Seamount Range and 34 (74%) were first sighted west of the Newfoundland Ridge. These areas are both dominated by large, relatively shallow bathymetric features. Huppert and Bryan (1976) have demonstrated that the Atlantis II Seamounts are instrumental to eddy

Figure E-1. The research area, showing major ocean currents and bathymetry

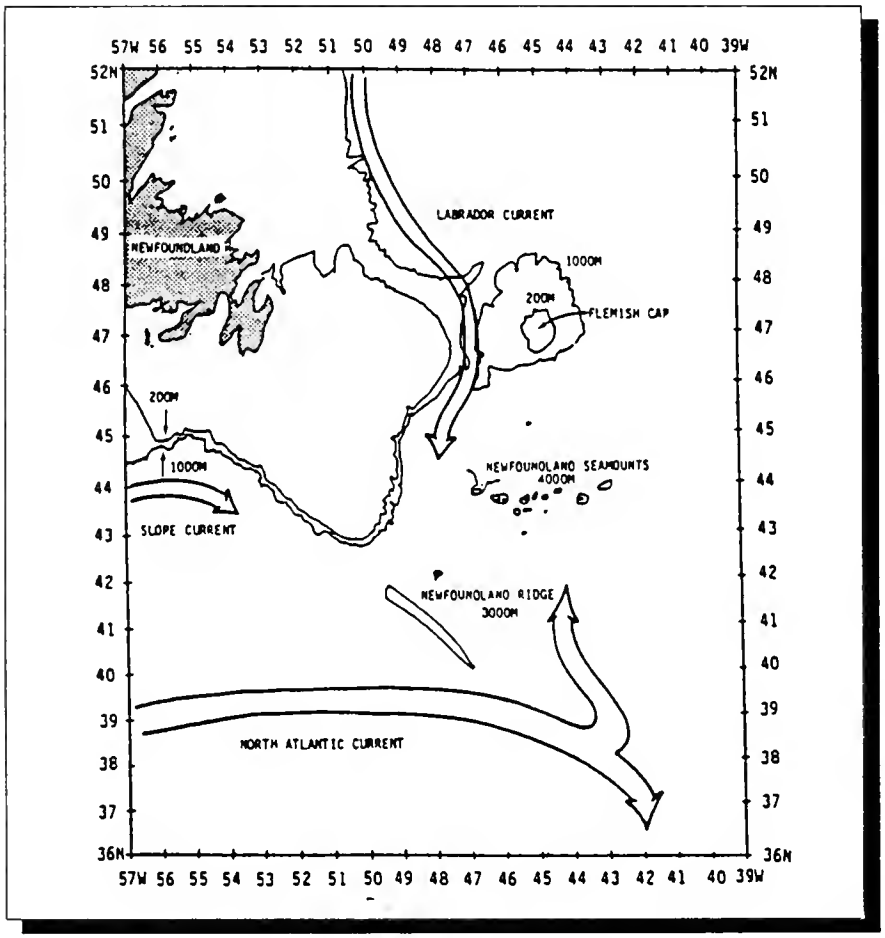

formation. Voorheis *et al.* (1973) suggest eddies in the Newfoundland Basin are bathymetrically generated. The formation of eddies in this study near the bathymetric features support the theory that interaction of the ocean currents with the topography of the Seamounts or the Ridge is important to eddy generation. Figure E-2 indicates that except for these two regions the remainder of the area appears to be relatively eddy free.

Generation and Deterioration

IR signatures indicate that twenty-one of the eddies (46%) formed from pinched-off meanders, eight (17%) from interactions between currents. Seventeen eddies (37%) had no identifiable source. It is possible that the cloud cover hid the meander from which the eddy formed and that by the time visibility improved, the eddy was in place and the generative process was unobserved. Seven of these eddies were in the Seamount area and ten were near the Ridge.

Translation Through the Area

Twenty-one eddies showed a net westward drift throughout their lives. Only three displayed a net eastward drift. The remaining 22 showed no net drift.

Of the 22 showing no net drift, 18 had a fully-observed life span of fifteen days or less and so may not have had the opportunity to drift at all. Three were seen in periods of heavy clouds and so were carried in the original reported position for a month and deleted from the NWS charts. The other four showing no net drift display an oscillatory drift, both east and west alternately. This motion is also displayed by many of the longer-lived eddies that show definite westward net drift. The motion may be explained by positioning errors due to the analysis of the satellite data.

These same factors may have influended the three eddies that displayed a net eastward drift. Joyce (1984), working in an area bounded by 40°N - 45°N and 55°W - 75°W (immediately to the west of this study area), demonstrated that eddies interacting with the Gulf Stream display a predominantly westward drift. The present study shows similar results because of the 21 eddies showing westward drift, 12 interacted with the North Atlantic Current (NAC) during their life spans. Of the three that drifted east, one showed no interaction with the parent current. Interactions with the NAC then could not have caused the net eastward drift of the eddies.

Figure E-2. Initial reported positions of eddies in this study. *Symbols indicate the source(s) of each eddy report, numbers indicate sequence of formation.*

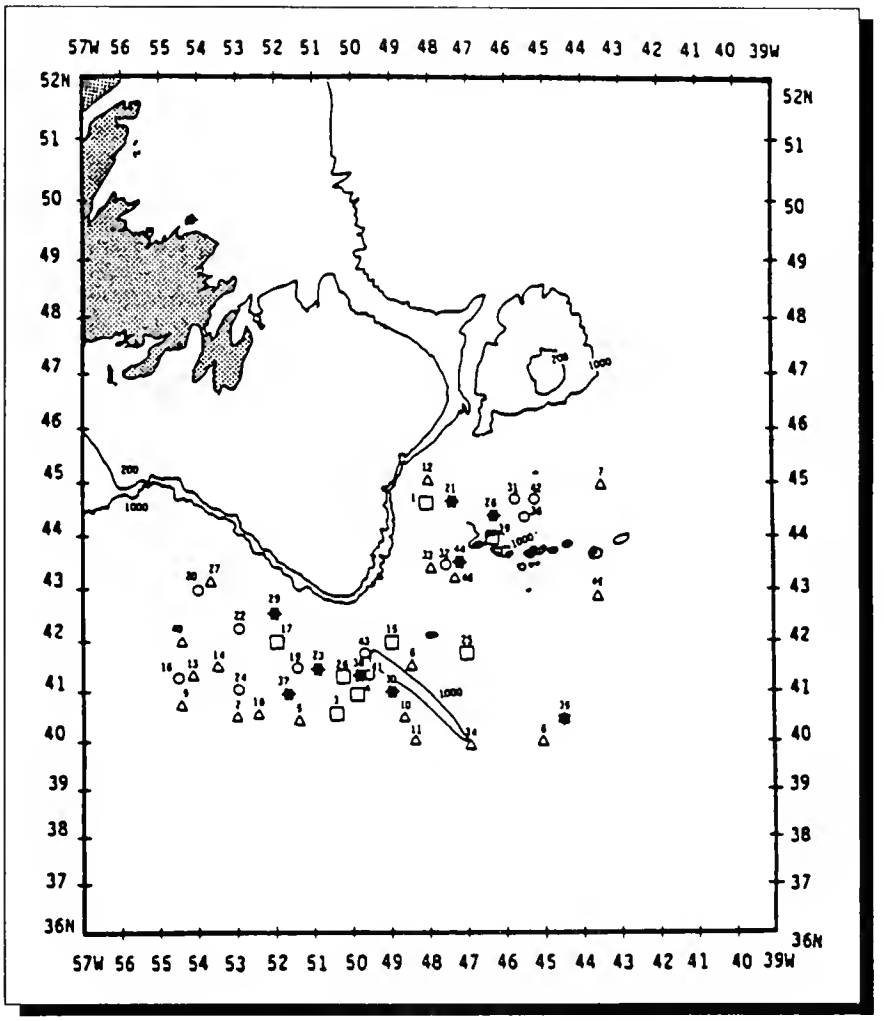

predominantly westward drift. The present study shows similar results because of the 21 eddies showing westward drift, 12 interacted with the North Atlantic Current (NAC) during their life spans. Of the three that drifted east, one showed no interaction with the parent current. Interactions with the NAC then could not have caused the net eastward drift of the eddies.

Eddy Size

The eddies varied in shape from roughly circular to elongated ellipses and many had irregular circumferences. To estimate the average size, all eddies were assumed to be of circular form of diameter equal to the average of the major and minor axes. The mean characteristics are shown in Table E-1.

Comparison of Eddy Characteristics in Two Areas

The following discussion centers on whether or not the area of formation had any effect on eddy characteristics.

The duration of eddies over the Seamounts ranged from six to 115 days with an average duration of 46 days. The same statistics for the 34 eddies formed near the Ridge show a range of two to 218 days with an average of 41 days. These figures indicate that the area of formation has no significant effect on the life span of the eddy. In general, eddies in this area have a shorter life span than the two to three year spans reported by Joyce (1984), Richardson (1980) and Richardson (1983) in other areas of the Gulf Stream system.

The area of the Seamounts showed eddy activity 63% of the time; the Ridge, 69% of the time. Both areas have equal potential for eddy activity.

The areas of formation shows no apparent affect on the migration of the eddy through the area. The eddies that formed over the Seamounts showed a westward migration in six of twelve eddies while five showed no significant migration. The remaining eddy showed eastward migration. Those formed in conjunction with the Ridge topography showed westward migration in 16 of 34 eddies and

was cold core. Eight cold core eddies formed in the area of the Ridge. There are two possible explanations for this: either the cold-core eddies form more as an interaction with the NAC in the Newfoundland Ridge/Tail of the Bank area, or they drifted southeast out of the Seamount area hidden by cloud cover before they were reported.

A much higher percentage of Seamount eddies had an unidentified generation mechanism. Seven out of twelve or 58% had an unknown source of origin as compared with ten out of 34 or 23% of the Ridge eddies.

Labrador Current Eddies

Perhaps one of the most interesting results of this study is the location of five cold-core eddies in the area north of the Gulf Stream in the normal domain of warm-core NAC eddies. A possible explanation for the presence of these eddies is the Labrador Current. No studies have been conducted on the generation of eddies by this current, but Hayes and Robe (1978) showed that the Labrador Current extends to the bottom and that the flow is variable and quite often influenced by the position of the NAC. If we make the assumption that the bottom features may cause the bifurcation noted in the current's flow, it is reasonable to assume the varied bathymetry can also cause meander and eddy generation in much the same way as it does in the NAC. Research dedicated to the generation of eddies by the Labrador Current is necessary.

Conclusions

For the three-year period, this study evaluated data from several different sources and identified a total of 46 eddies in the research area. The research area was eddy free only 15% of the study period. This clearly indicates that eddies are frequently in the area and that they are important to the dynamics of the area. The eddies were concentrated near the Newfoundland Seamount Range and the Newfoundland Ridge. Except for these two areas, the research area showed no sign of eddy activity. This distribution suggests that the topography features had an influence on the formation of the eddies. This indicates that, at least in some areas, the NAC is influenced by the bottom in the Newfoundland Basin area.

The study also suggests that the Labrador Current is capable of generating eddies. Five cold-core eddies were found in an area where they could not have been generated by the NAC. Kollmeyer, *et al.* (1965) documented the existence of a cold-core eddy spawned by the Labrador Current and recognized its importance as a cold trap for icebergs. However, no systematic study of Labrador Current cold-core eddies has yet been conducted. This is a subject that requires further investigation.

In their movement, the eddies followed the pattern predicted by Joyce (1984) and drifted predominantly to the west. This was true even for those eddies that showed a considerable interaction with the eastward-flowing NAC. The most common method of formation was pinched-off meanders. Absorption back into the parent current by similar meanders was the most common method of deterioration.

The area of formation had no apparent effect on the characteristics of the eddies. Those formed over the Seamounts displayed features similar to those formed over the Ridge. All were of equivalent size and duration.

The study indicates that the average eddy in the southern IIP operations area will be a warm core eddy approximately 116 km in diameter. It will form over the Seamounts or over the Ridge, normally from a pinched-off meander, and will migrate to the west after formation. It will remain on plot for about 42 days and will normally be absorbed back into the parent current. We can expect to see an eddy similar to the one described here in the southern IIP operations area about 80% of the time.

Table E-1. Average Characteristics of Eddies in study area

Eddy Type	Number of Observations	Average Size	Average Life (days)
Warm Core	38	117	49
Cold Core	8	94	21

Table E-2. A Comparison of Characteristics of the Eddies near the Newfoundland Ridge and the Newfoundland Seamounts

Warm Core			
Newfoundland Ridge	26	127	47
Newfoundland Seamounts	11	105	55
Cold Core			
Newfoundland Ridge	8	100	23
Newfoundland Seamounts	1	55	6

These figures are in general agreement with Voorheis *et al.* (1973). The only difference in the conclusions is the rotation of the eddies. Their data indicated cold core eddies are more numerous. The present study indicates warm core eddies dominate. It is difficult to address this difference, but IR positively indicates the temperature differences in water masses. Additional long term analyses may resolve this discrepancy.

References

Hayes, R.M. and R.Q. Robe, 1978. *Oceanography of the Grand Banks Region of Newfoundland, 1973.* U.S. Coast Guard Oceanographic Report No. 13, CG-373-13, United States Coast Guard, Washington, DC 20593.

Huppert, H.E. and K. Bryan, 1976. "Topographically Generated Eddies". *Deep-Sea Research*, 23, 655-679.

Joyce, T.M., 1984. "Velocity and Hydrographic Structure of a Gulf Stream Warm-Core Ring". *Journal of Physical Oceanography*, 14(5), 936-941.

Kollmeyer, R.C., R.M. O'Hagan, R.M. Morse, D.A.McGill, and N. Corwin, 1965. *Oceanography of the Grand Banks Region and the Labrador Sea in 1964.* U.S. Coast Guard Oceanographic Report 10, CG 373-10. United States Coast Guard, Washington, DC 20593.

Lai, D.Y. and P.L. Richardson, 1977. "Distribution and Movement of Gulf Stream Rings". *Journal of Physical Oceanography*, 7(9), 670-683.

Richardson, P.L., 1980. "Gulf Stream Ring Trajectories". *Journal of Physical Oceanography*, 10(1), 90-104.

Richardson, P.L., 1983. "Eddy Kinetic Energy in the North Atlantic Ocean from Surface Drifters". *Journal of Geophysical Research*, 88(C7), 4355-4367.

Voorheis, G. M., K. Aagaard and L. K. Coachman, 1973. "Circulation Patterns Near the Tail of the Banks". *Journal of Geophysical Research*, 3(10), 397-405.

Williams, F.J., 1985. *Investigation into the Population and Motion of Eddies in the Southern International Ice Patrol Operations Area.* Master of Science Thesis. Old Dominion University, Norfolk, Virginia.

Appendix F

Detection of Ocean Fronts in the Gulf Stream / Labrador Current System by Side-Looking Airborne Radar

LTJG N. B. Thayer, USCGR
D. L. Murphy

Introduction

The Gulf Stream probably reaches its greatest complexity in the region south and southeast of Newfoundland where it interacts with complex bathymetry and the southward-flowing Labrador Current to produce an ever-changing system of fronts, eddies and associated features. This complex current system is responsible, in large part, for the distribution of icebergs in much of the International Ice Patrol's (IIP) operating area.

The IIP iceberg drift model, an integral part of the IIP operations, relies primarily on historically time-averaged currents. Using these currents can lead to substantial drift errors, particularly in regions with large current fluctuations. To address this problem, IIP uses the drift of satellite-tracked drift buoys, deployed by IIP aircraft, to provide near real-time current data to the model. Although this program is successful, the updates to the current field are limited temporally and spatially to the period for which a buoy is drifting through a specific region.

Remote sensing techniques hold the most promise for providing current data for future IIP operations. For example, satellite infrared imagery is used successfully under certain conditions to define ocean frontal boundaries and, thus, infer circulation patterns for several ocean areas. Unfortunately, infrared imagery is of limited operational use in the IIP area due to persistent fog and cloud cover. However, active microwave systems (radars) are capable of penetrating clouds and, under the right circumstances, detecting frontal features.

In 1985 IIP began investigating the feasibility of using imagery from a side-looking airborne radar (SLAR) to map ocean fronts in the IIP area. This report describes some of the preliminary results of that investigation.

Background

The International Ice Patrol deploys one week out of two to Gander, Newfoundland, during the icebergs season, typically March through August. Using U.S. Coast Guard HC-130 aircraft, IIP conducts iceberg reconnaissance flights within the area bounded by 40°-52°North and 39°-57°West. Reconnaissance flights are made each day during the deployments, each flight approximately 3,150 km long (1,700 nm), covering approximately 65,000 square km.

Since the spring of 1983, IIP has used SLAR as the main method of iceberg reconnaissance, replacing visual reconnaissance. SLAR is an X-band radar that scans the sea surface in a plane normal to the flight path. The radar image is displayed on a narrow CRT that produces a negative image on photographic film (Figure F-1). The standard altitude for IIP reconnaissance is 8,000 feet, with a SLAR swath width of 100 km, 50 km to each side of the aircraft with an unimaged swath directly below the aircraft of about 5 km. SLAR is largely unaffected by weather, with only heavy precipitation obscuring the view of the surface.

Review of IIP SLAR films for 1983-1985, representing some 200 flights, has revealed that SLAR is capable of detecting the fronts of the Gulf Stream and Labrador Current, with the water masses of different temperatures showing up as different shades on the SLAR film's negative image, warm water appearing dark and cooler water appearing light. These correspond to high radar backscatter and low radar

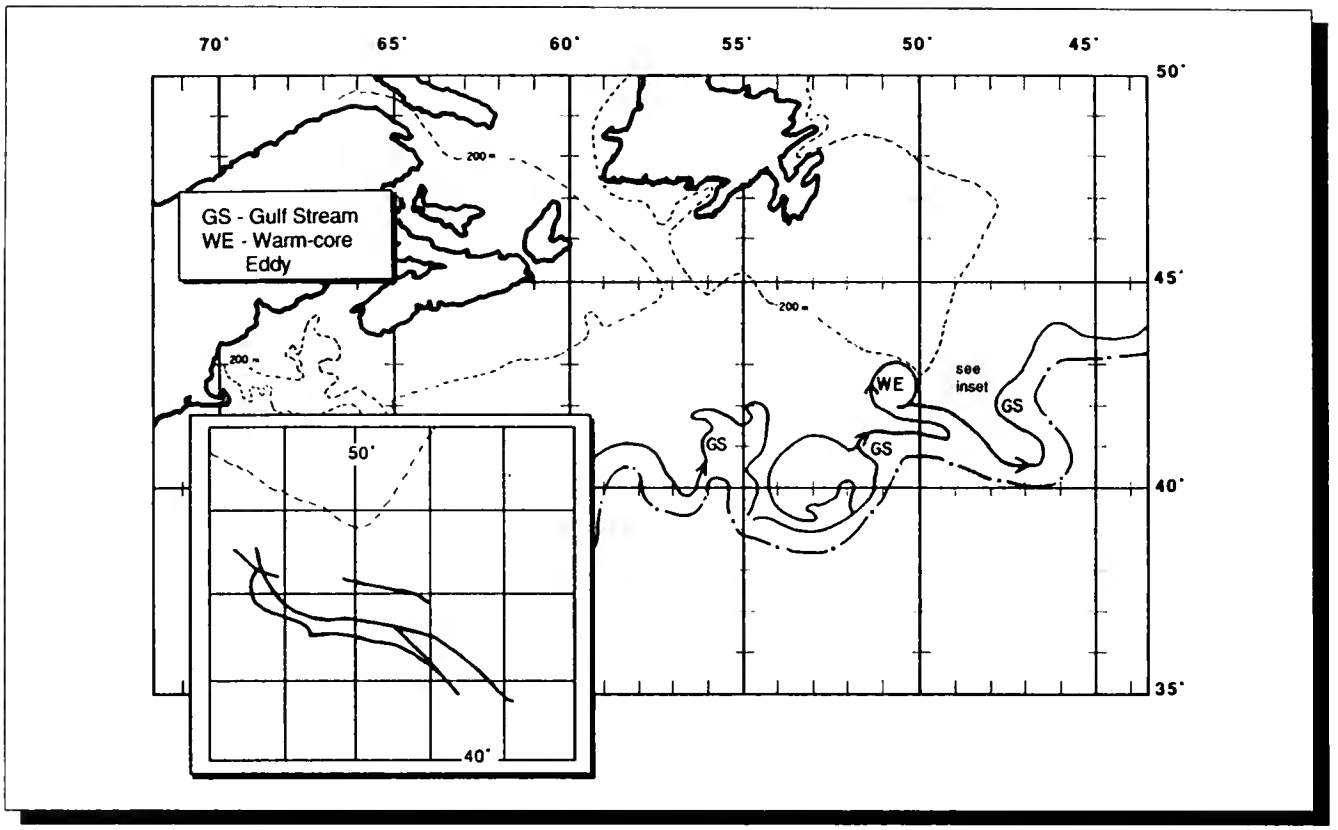

Figure F-1. Reproduced National Earth Satellite Service (NESDIS) product from April 26, 1985. Inset — NESDIS worksheet from 25-26 April 1985.

Figure F-2. A segment of SLAR film from the International Ice Patrol reconnaissance flight of April 28, 1985, with a photo mosaic of the same piece of film. Warm (rough) water appears dark.

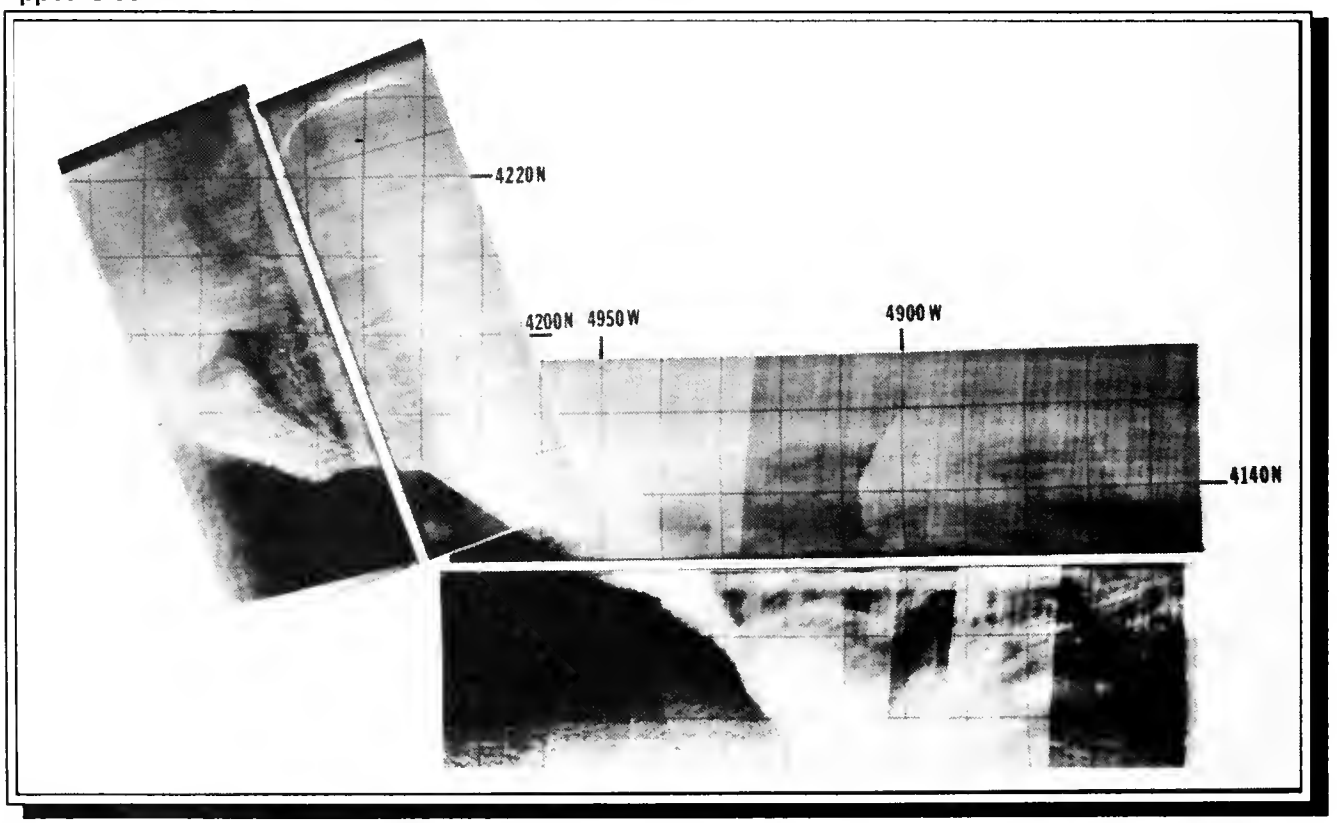

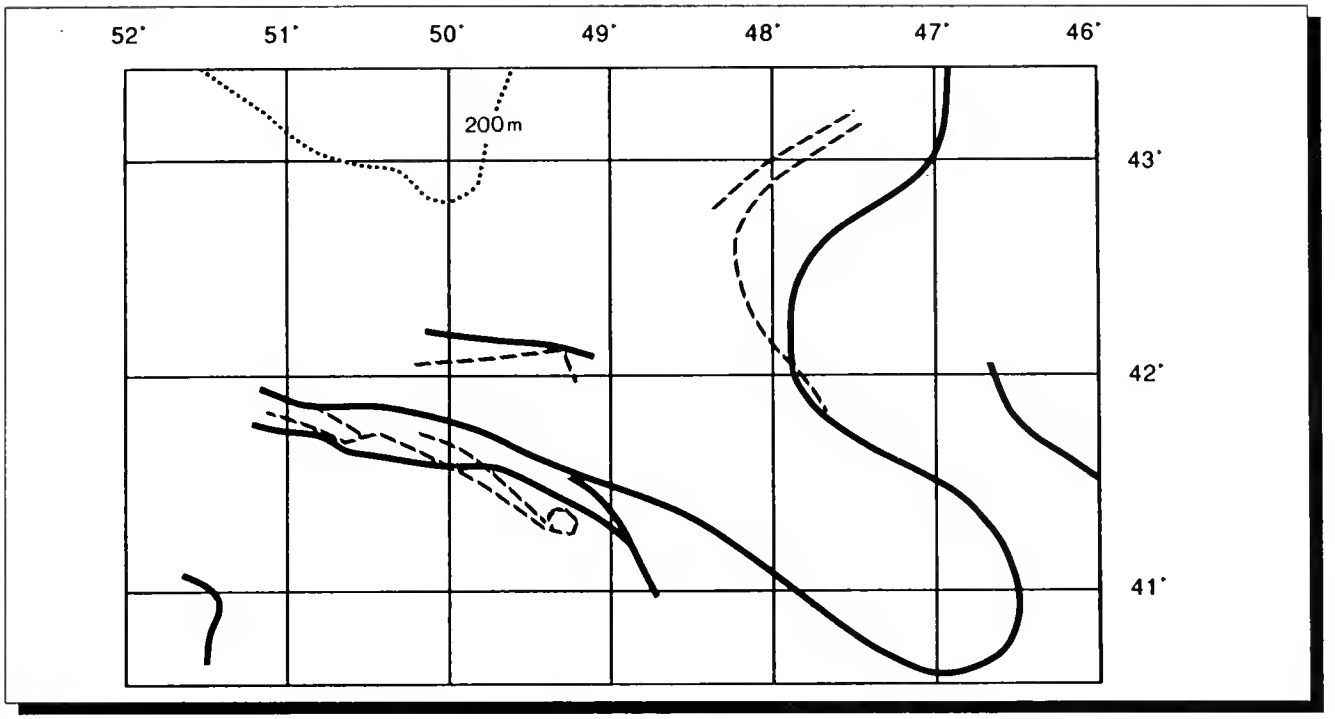

Figure F-3. Superimposition of the ocean features detected by NESDIS (solid line) on 25-26 April 1985 (see inset, Figure F-1) and features detected by IIP SLAR (dashed line) on 28 April 1985, some of which are visible in Figure F-2.

backscatter respectively. The imagery frequently shows very sharply delineated fronts in great detail.

Previous work using SLAR and satellite infrared in the Grand Banks area was done by LaViolette (1983), using an earlier Coast Guard SLAR and a NASA SLAR. The earlier SLAR's had lower power outputs and the images reproduced by LaViolette are apparently less sharp and less detailed than the ones produced by the present model, a Motorola AN/APS-135 Side-Looking Airborne Multi-Mission Radar (SLAMMR).

The most extensive body of work involving detection of ocean features with an active microwave system has been done with SEASAT synthetic aperture radar (SAR) (Beal, *et al.*, 1981). Some of the work done with SEASAT imagery has included comparison with satellite infrared imagery (Fu and Holt, 1982, 1983; Hayes, 1981).

Although the precise mechanism is uncertain, it is clear that the difference in backscatter is due to a difference in surface roughness. Visual inspection of the sea surface during IIP flights has shown that the dark and light areas on the SLAR film correspond closely to rough and smooth areas visible under conditions of light wind. Also, the SLAR films contain many images of internal wave trains, many of them closely linked to the bathymetry of the edge of the continental shelf. The alternate rough and smooth bands of internal waves detected by SEASAT SAR have been described in Alpers and Salusti (1983) and Hughes and Gower (1983), among others.

Discussions of the mechanism of detecting ocean features in radar imagery usually invoke Bragg scattering (Valenzuela, 1978; Brown, Elachi and Thompson, 1976), which defines a critical surface wavelength for maximum backscatter. For the X-band SLAR and the range of incidence angles encountered in IIP operations, the range of ocean wavelengths causing Bragg scattering is approximatley 2-30 cm. The relationship between the rough and smooth patches seen visually and the SLAR imagery reflects the relative spectral energy density in those patches, (i.e., the wave height at the Bragg wavelength).

Results

IIP SLAR imagery of ocean fronts has frequently been confirmed by the interpretations of Advanced Very High Resolution Radiometry (AVHRR) imagery by NOAA's National Environmental Satellite, Data and Information Service (NESDIS). A simplified reproduction of the NESDIS chart for 26 April 1985 is seen in Figure F-1, with an inset showing the interpreter's worksheet for the area outlined on the main chart. Figure F-2 is a SLAR image from 28 April, from the area outlined in Figures F-1

and F-3, showing a complex set of frontal features. The NESDIS worksheet and a SLAR interpretation are superimposed in Figure F-3, showing a very close match of the features.

In comparing the two images in Figure F-3, the similarities are apparent. The two fronts that converge to the east, the transverse north-south feature to the west and the area of sharp curvature on the western part of the southern front are present in both images, but differ somewhat in spatial orientation. The SLAR fails to detect the warm-core eddy shown on the final NESDIS chart (probably off the edge of the film), but SLAR shows an additional small-scale (10 km) eddy along the front. The differences between the SLAR interpretation and the NESDIS worksheet do not appear to be due to navigational displacement or rotation between the two, and are probably due to movement of the feature during the two day span between images.

Discussion

It is significant that by using the apparent SLAR temperature/backscatter relationship, the gradation of temperature from south to north is the same for both SLAR and AVHRR, i.e., a large area of warm water to the south (the Gulf Stream), a narrow band of cool water, a band of warm water and finally a band of cool water. Perhaps more important is that, giving the good match of location, shape and apparent temperature gradients across fronts, both SLAR and AVHRR appear to be detecting the same features.

The SLAR and satellite infrared imagery from 28 April and 26 April, respectively, show a good match of the features detected, both in location and overall shape. The particular SLAR image is a good illustration of how well the two sources can agree. Over the three years of SLAR operation at IIP, a large number of SLAR images of fronts have been collected. Of these, there have been a number of cases in which SLAR and AVHRR do not seem to agree both in location and shape of features. Williams (1985) examines the match and mismatch of SLAR and AVHRR images in eddies and associated features in the IIP region. Most frequently the difference seems to be one of placement rather than shape, reflecting a navigational discrepancy between the two sources.

Of the two, SLAR offers the greater positional accuracy. It makes use of the aircraft's Inertial Navigation System (INS), yielding an accuracy of ±5 km (Thayer SLAR/LORAN, unpub.). Positioning on the NESDIS chart is done using visible known land forms on the image, which may be obscured by cloud cover, making it less accurate, with errors possibly as much as 15-20 kilometers (personal communication, Jennifer Clark, NESDIS). Given the nature of the NESDIS product, i.e., the large area covered, more accurate positioning is unnecessary.

There are other cases in which there is considerable difference in overall shape between SLAR and the NESDIS product. This usually occurs when the area is obscured by clouds and NESDIS is estimating the location and shape of features based on information that is up to several days old.

In working with the original satellite imagery, the worksheets produced from it, and the final NESDIS product, it becomes apparent that NESDIS is able to take very complex, detailed imagery and produce from it remarkably accurate, coherent information. The imagery compared in Figure F-3 occupies approximately 1 square centimeter on the satellite image, from which the NESDIS interpreter was able to extract and correctly interpret several features.

Conclusions

Each system has its own application, capabilities and limitations. Satellite imagery is able to cover very large areas with a reasonable amount of detail. It is limited by cloud cover and offers limited navigational accuracy. SLAR, on the other hand, offers a very detailed look at an area, even through cloud cover, with good positioning. It can only cover small areas compared to a satellite and is limited by the operational constraints of IIP, with oceanographic applications of secondary importance to iceberg reconnaissance.

Although the mechanism involved in SLAR detection of temperature differences is not yet clear, both systems are able to detect the temperature gradients across the same fronts.

For the immediate future, SLAR will play an important role in IIP operations, locating frontal features for hydrographic research and for planning TOD deployments. Future research with SLAR should be directed toward providing real-time quantitative input for the IIP iceberg drift model. Another possible application of this technology is real-time mapping of current systems for other Coast Guard missions such as search and rescue and pollution response.

Acknowledgements

We wish to thank Jennifer Clark and her staff at NESDIS for providing satellite images and NESDIS worksheets.

References

Alpers, W., and E. Salusti, 1983. "Scylla and Charybdis Observed from Space". *Journal of Geophysical Research 88(C3)*: 1800-1808.

Beal, R. C., P. S. DeLeonibus and I. Katz, 1981. *Spaceborne Synthetic Aperture Radar for Oceanography.* Johns Hopkins University Press, Baltimore, MD.

Brown, W. E., Jr., C. Elachi and T. W. Thompson, 1976. "Radar Imaging of Ocean Surface Patterns". *Journal of Geophysical Research 81(15)*: 2657-2667.

Fu., L., and B. Holt, 1982. *SEASAT Views Oceans and Sea Ice With Synthetic Aperture Radar.* JPL Publication 81-120. Jet Propulsion Laboratory, Pasadena, CA.

Fu., L., and B. Holt, 1983. "Some Examples of Detection of Oceanic Mesoscale Eddies by the SEASAT Synthetic Aperture Radar". *Journal of Geophysical Research 88(C3)*: 1844-1852.

Hayes, R. M., 1981. "Detection of the Gulf Stream." In: *Spaceborne Synthetic Aperture Radar for Oceanography.* Johns Hopkins University Press, Baltimore, MD.

Hughes, B. A. and J. F. R. Gower, 1983. "SAR Imagery and Surface Truth Comparisons of Internal Waves in Georgia Strait, British Columbia, Canada." *Journal of Geophysical Research 88(C3)*: 1809-1824.

LaViolette, P. E., 1983. *The Grand Banks Experiment: A Satellite/Aircraft/Ship Experiment to Explore the Ability of Specialized Radars to Define Ocean Fronts.* NORDA Report #49, U. S. Naval Oceanographic Research and Development Activity, U. S. Navy, Washington, DC.

Sabins, F. F., Jr., 1978. *Remote Sensing: Principles and Interpretation.* pp 195-202. W. H. Freeman and Company, San Francisco, CA.

Valenzuela, G. R., 1978. *Theories for the Interaction of Electromagnetic and Oceanic Waves - A Review.* Boundary-Layer Meteor. 13: 61-85

Williams, F. J., 1985. "Investigation into the Population and Motion of Eddies in the Southern International Ice Patrol Operations Area." Master of Science Thesis, Old Dominion University, Norfolk,VA.

☆ U. S. GOVERNMENT PRINTING OFFICE; 1987--701-823--60028

U.S. Department
of Transportation

**United States
Coast Guard**

Report of the International Ice Patrol in the North Atlantic

**1986 Season
Bulletin No. 72**

CG-188-41

U.S. Department of Transportation
United States Coast Guard

Commandant
United States Coast Guard

MAILING ADDRESS
2100 2nd St., S.W.
Washington, D.C. 20593
(202)-267-1450

JAN 25 1988

Bulletin No. 72

REPORT OF THE INTERNATIONAL ICE PATROL SERVICES IN THE NORTH ATLANTIC OCEAN

Season of 1986

CG-188-41

FOREWORD

Forworded herewith is bulletin No. 72 of the International Ice Patrol describing the Patrol's services, ice observations and conditions during the 1986 season.

CLYDE E. ROBBINS
Chief, Office of Operations

DISTRIBUTION - SDL No. 126

	a	b	c	d	e	f	g	h	i	j	k	l	m	n	o	p	q	r	s	t	u	v	w	x	y	z
A																										
B		*1	*1		5					2				2	2		1									
C	*1																*1									
D																							60			
E																										
F																										
G																										
H																										

NON-STANDARD DISTRIBUTION: *B:b LANTAREA (5), B:b PACAREA (1), B:c First, Fifth, Seventh Districts Only, *C:aq LANTAREA only, SML CG-4

International Ice Patrol 1986 Annual Report

Contents

Appendices

Introduction

This is the 72nd annual report of the International Ice Patrol Service in the North Atlantic. It contains information on ice conditions and Ice Patrol operations for 1986. The U.S. Coast Guard conducts the International Ice Patrol Service in the North Atlantic under the provisions of U.S. Code, Title 46, Sections 738, 738a through 738d; and the International Convention for the Safety of Life at Sea (SOLAS), 1974, regulations 5-8. This service was initiated shortly after the sinking of the RMS TITANIC on April 15, 1912.

Commander, International Ice Patrol, under Commander, Coast Guard Atlantic Area, directed the International Ice Patrol from offices located at Groton, Connecticut. International Ice Patrol analyzes ice and environmental data, prepares the daily ice bulletins and facsimile charts, and replies to any requests for special ice information. It also controls the aerial Ice Reconnaissance Detachment and any surface patrol cutters when assigned, both of which patrol the southeastern, southern, and southwestern limits of the Grand Banks of Newfoundland for icebergs. The International Ice Patrol makes twice-daily radio broadcasts to warn mariners of the limits of iceberg distribution.

Vice Admiral P.A. Yost was Commander, Atlantic Area from the start of the 1986 season, March 27. Vice Admiral D.C. Thompson became Commander, Atlantic Area on May 27, 1986. Commander Norman C. Edwards, Jr., U.S. Coast Guard, was Commander, International Ice Patrol during the Ice Patrol season.

Summary of Operations, 1986

During the 1986 Ice Patrol season, from March 27 to July 3, 1986, the International Ice Patrol (IIP), a unit of the U.S. Coast Guard, conducted the International Ice Patrol Service, which has been provided annually since the sinking of the RMS TITANIC on April 15, 1912. During past years, Coast Guard ships and/or aircraft have patrolled the shipping lanes off Newfoundland within the area delineated by 40°N - 52°N, 39°W - 57°W, detecting icebergs and warning mariners of these hazards. During the 1986 Ice Patrol season, Coast Guard HC-130 aircraft flew 45 ice reconnaissance sorties, logging over 294 flight hours. The AN/APS-135 Side-Looking Airborne Radar (SLAR), which was introduced into Ice Patrol duty during the 1983 season, again proved to be an excellent all-weather tool for the detection of both icebergs and sea ice, providing 26.1 percent of all 1986 sightings.

Deployments were made February 1- 5 and March 11-20 to determine the pre-season iceberg distribution. Based on the latter trip, regular deployments started on March 25 with the 1986 season opening on March 27. From that date until July 2, 1986, an aerial Ice Reconnaissance Detachment (ICERECDET) operated from Gander, Newfoundland one week out of every two. The season officially closed on July 3, 1986.

During the 1986 ice year, an estimated 204 icebergs drifted south of 48°N latitude. Table 1 shows monthly estimates of the number of icebergs that crossed 48°N.

Six satellite-tracked oceanographic drifters were deployed to provide operational data for IIP's iceberg drift model. The drift data from these buoys are discussed in Appendix B.

No U. S. Coast Guard cutters were deployed to act as surface patrol vessels this year. The USCGC EVERGREEN was deployed to conduct oceanographic research for the Ice Patrol during the period April 22 through May 22. In 1986, research efforts were directed toward studying ocean frontal features associated with a warm core eddy between the Grand Bank and the North Atlantic Current. SLAR was used to map the surface roughness gradients across frontal boundaries. The study area was re-mapped weekly during the month of May. Based on the initial SLAR survey, a series of hydrographic transects were made of the eddy, and satellite-tracked drifting buoys were deployed in the area. The results of this study are presented in Appendix C.

Table 1. Icebergs South of 48° North *The three periods shown are ship reconnaissance (1900-45), aircraft visual reconnaissance (1946-82) and SLAR reconnaissance (1983-85)*

	Avg 1900-45	Avg 1946-82	Avg 1983-85	1986
OCT	2	0	1	0
NOV	2	0	4	0
DEC	2	0	3	0
JAN	3	7	4	0
FEB	10	8	74	3
MAR	46	32	118	40
APR	105	85	500	60
MAY	154	81	384	59
JUN	77	50	214	24
JUL	26	13	178	18
AUG	9	3	45	0
SEP	5	0	14	0
Total	441	279	1539	204

Table 2. Source of International Ice Patrol Iceberg Reports by Size

Sighting Source	Growler	Small	Medium	Large	Radar Target	Total	Percent of Total
Coast Guard SLAR	44	101	37	13	10	205	26.1
Coast Guard Visual	7	56	44	21	0	128	16.3
CanadianSLAR	1	16	14	1	65	97	12.4
Canadian Visual	0	20	16	1	0	37	4.7
Commercial Radar	8	10	10	1	31	60	7.6
Commercial Visual	5	33	112	26	0	176	22.4
Offshore Industry	0	3	0	1	2	6	0.8
Lighthouse/Shore	0	0	0	0	0	0	0.0
Other	1	31	35	9	0	76	9.7
Total	66	270	268	73	108	785	100.0

Table 2 shows the sightings reported to the International Ice Patrol in 1986, broken down by the source of the sighting and the size of iceberg sighted. It is important to note that the IIP side-looking airborne radar (SLAR) provided over 26% of the iceberg reports, the single largest source of icebergs sightings. Given that IIP SLAR reconnaissance usually takes place near the limit of all known ice, this sighting source becomes especially important.

Iceberg Reconnaissance and Communications

During the 1986 Ice Patrol year (from October 1, 1985 through September 30,1986), 63 aircraft sorties were flown in support of the International Ice Patrol. These included pre-season flights, ice observation and logistics flights during the season, and post-season flights. Pre-season flights determined iceberg concentrations north of 48°N to estimate the time when icebergs would threaten the North Atlantic shipping lanes in the vicinity of the Grand Banks of Newfoundland. During the active season, ice observation flights located the southwestern, southern, and southeastern limits of icebergs. Logistics flights were necessary due to aircraft maintenance problems. Post-season flights were made to retrieve parts and equipment from Gander and to close out all business transactions from the season.

U.S. Coast Guard aircraft, deployed from Coast Guard Air Station Elizabeth City, North Carolina, conducted all the aircraft missions. SLAR-equipped HC-130 aircraft were utilized exclusively for aerial ice reconnaissance, and HC-130 and HU-25A aircraft were used on logistics flights. Table 3 shows aircraft utilization during the 1986 season.

U.S. Coast Guard Communications Station Boston, Massachusetts, NMF/NIK, was the primary radio station used for the dissemination of the daily ice bulletins and facsimile charts after preparation by the Ice Patrol office in Groton. Other transmitting stations for the 0000Z and 1200Z ice bulletins included Canadian Coast Guard Radio Station St. John's/VON, Canadian Forces Radio Station Mill Cove/CFH, and U.S. Navy LCMP Broadcast Stations Norfolk/NAM; Thurso, Scotland; and Keflavik, Iceland. Canadian Forces Station Mill Cove/CFH as well as AM Radio Station Bracknell/GFE, United Kingdom, are radiofacsimile broadcasting stations which used Ice Patrol limits in their broadcasts. Canadian Coast Guard Radio Station St. John's/ VON provided special broadcasts.

The International Ice Patrol requested that all ships transiting the area of the Grand Banks report ice sightings, weather, and sea surface temperatures via the above communications/radio stations. Response to this request is shown in Table 4, and Appendix A lists all contributors. Commander, International Ice Patrol extends a sincere thank you to all stations and ships which contributed.

Table 3. Aircraft Use During the 1986 IIP Year (October 1, 1985 to September 30, 1986)

Aircraft Deployment	Hours Flown
Pre-season	63.1
Regular season	294.5
Post season	22.2
Total	379.8

Iceberg Reconnaissance Sorties by Month

Month	Sorties	Flight hours
Feb	2	13.7
Mar	9	40.7
Apr	7	50.9
May	14	99.1
Jun	10	74.4
Jul	3	15.2
Total	45	294.0

Table 4. Iceberg and SST Reports

Number of ships furnishing Sea Surface Temperature (SST) reports	49
Number of SST reports received	274
Number of ships furnishing ice reports	211
Number of ice reports received	437
First Ice Bulletin	270000Z MAR 86
Last Ice Bulletin	031200Z JUL 86
Number of facsimile charts transmitted	97

Environmental Conditions 1986 Season

January: The mean pressure distribution in Figure 1 shows a normal location for the Icelandic Low, with stronger than normal pressure gradients surrounding it. A westerly flow brought drier, somewhat warmer conditions to Newfoundland, while a northerly flow brought near-normal conditions to Labrador (Table 5).

February: The Icelandic Low was deeper than normal and was south and west of its normal mean February location (Figure 2). The two Newfoundland stations had colder and wetter conditions than normal (Table 5), the result of increased flow from the Labrador Sea, providing a combination of moisture and cooling from the pack ice. Labrador (Goose Bay) was at or above normal temperature and significantly drier than normal, the result of a stronger northerly flow.

March: March was significantly colder for all three stations, with precipitation below normal in Goose Bay and Gander and above normal in St. John's. This pattern was caused by a deeper than normal Icelandic Low, causing a colder, more westerly flow over the region (Figure 3). St. John's received moist marine flow from the Gulf of St. Lawrence while Gander and Goose Bay were under the influence of drier continental air.

April: The Icelandic Low was farther east than normal, setting up southerly, even southeasterly flow over Newfoundland and Labrador (Figure 4). April was much warmer at all three locations and significantly wetter in Newfoundland. These conditions were caused by the more southerly flow, bringing warm, moist marine air from the Atlantic, without the continental influence that normally moderates conditions.

May: The mean surface pressure distribution was close to normal during May (Figure 5). The below-normal precipitation was caused by the trough-like feature south of Newfoundland, causing flow south of the island rather than over it.

June: A more southerly flow over Newfoundland in June (Figure 6), brought moister, slightly warmer marine air, while Labrador received cooler, moister marine air from the Labrador Sea (Table 5).

July: Labrador and Newfoundland were cut off from their normal southerly/southwesterly flow (Figure7). As a result, all three stations were cooler than normal. The two Newfoundland stations received a northeasterly flow, bringing above normal precipitation, while Labrador had a westerly flow, bringing continental air and below normal precipitation.

NOTE: Temperature and precipitation data for Nain, Labrador, are compared to 1985 values in Table 5. The reporting station at Hopedale, Labrador, was closed in 1984 and the Nain station opened. An historical mean for Nain does not exist.

Table 5. Environmental Conditions for 1986 IIP Season

	Station	Temp °C Monthly Mean	Temp °C Diff. from Norm.	Total Precipitation (mm)	% of Normal Precipitation	% of Normal Snowfall
OCT 1985	Nain	1.3	-0.5	56.7	76.4%	
	Goose	1.8	-0.9	61.2	79.9%	90.7%
	Gander	4.5	-1.5	72.3	69.1%	229.5%
	St. John's	5.8	-1.1	85.9	59.0%	250.0%
NOV	Nain	-3.7	1.1	87.7	160.9%	
	Goose	-5.1	-1.3	24.3	32.3%	31.2%
	Gander	-1.2	-3.0	71.8	66.9%	74.2%
	St. John's	0.3	-3.1	103.7	63.8%	144.8%
DEC	Nain	-11.7	5.5	229.8	295.0%	
	Goose	-14.2	-1.2	32.7	45.0%	51.4%
	Gander	-5.3	-1.5	95.0	87.8%	98.4%
	St. John's	-3.2	-1.7	113.9	70.7%	124.0%
JAN 1986	Nain	-16.5	-3.9	125.3	59.5%	
	Goose	-15.6	0.8	76.6	103.0%	117.4%
	Gander	4.8	1.4	73.4	67.3%	39.4%
	St. John's	-2.7	1.2	117.3	75.3%	64.7%
FEB	Nain	-13.8	2.4	74.2	59.7%	
	Goose	-14.0	0.5	21.9	36.1%	47.4%
	Gander	-7.5	-0.7	124.8	125.2%	138.8%
	St. John's	-5.5	-1.0	184.9	132.0%	87.9%
MAR	Nain	-17.6	-5.6	20.7	16.7%	
	Goose	-12.9	-4.3	44.3	61.4%	65.3%
	Gander	-5.9	-2.4	85.3	77.7%	114.8%
	St. John's	-3.8	-1.5	175.3	132.9%	71.2%
APR	Nain	-3.3	4.8	44.8	37.5%	
	Goose	0.8	2.5	61.0	99.7%	27.2%
	Gander	4.1	3.2	130.0	139.5%	18.7%
	St. John's	4.2	3.0	129.2	111.8%	12.7%
MAY	Nain	3.5	2.5	31.4	60.1%	
	Goose	7.8	11.5	44.8	70.2%	32.6%
	Gander	7.1	0.9	45.0	64.3%	145.0%
	St. John's	6.1	0.7	43.4	42.6%	182.9%
JUN	Nain	3.6	-3.3	114.9	512.9%	
	Goose	9.2	-2.1	115.9	124.5%	43.2%
	Gander	12.1	0.3	96.8	120.5%	42.9%
	St. John's	11.9	1.0	130.2	152.1%	*
JUL	Nain	9.1	-1.7	59.1	66.0%	
	Goose	13.3	-2.5	87.8	83.5%	*
	Gander	14.0	-2.5	113.2	164.1%	*
	St. John's	13.0	-2.5	87.8	105.7%	*
AUG	Nain	11.2	1.0	68.7	149.3%	
	Goose	15.4	-3.9	122.4	118.6%	*
	Gander	16.0	0.4	61.8	63.5%	*
	St. John's	15.1	-0.2	60.6	49.8%	*
SEP	Nain	7.4	0.6	38.8	64.1%	
	Goose	7.7	-1.4	115.2	136.3%	*
	Gander	9.0	-6.6	138.5	170.6%	*
	St. John's	9.7	-6.2	118.1	105.4%	*

* No snowfall recorded during this month

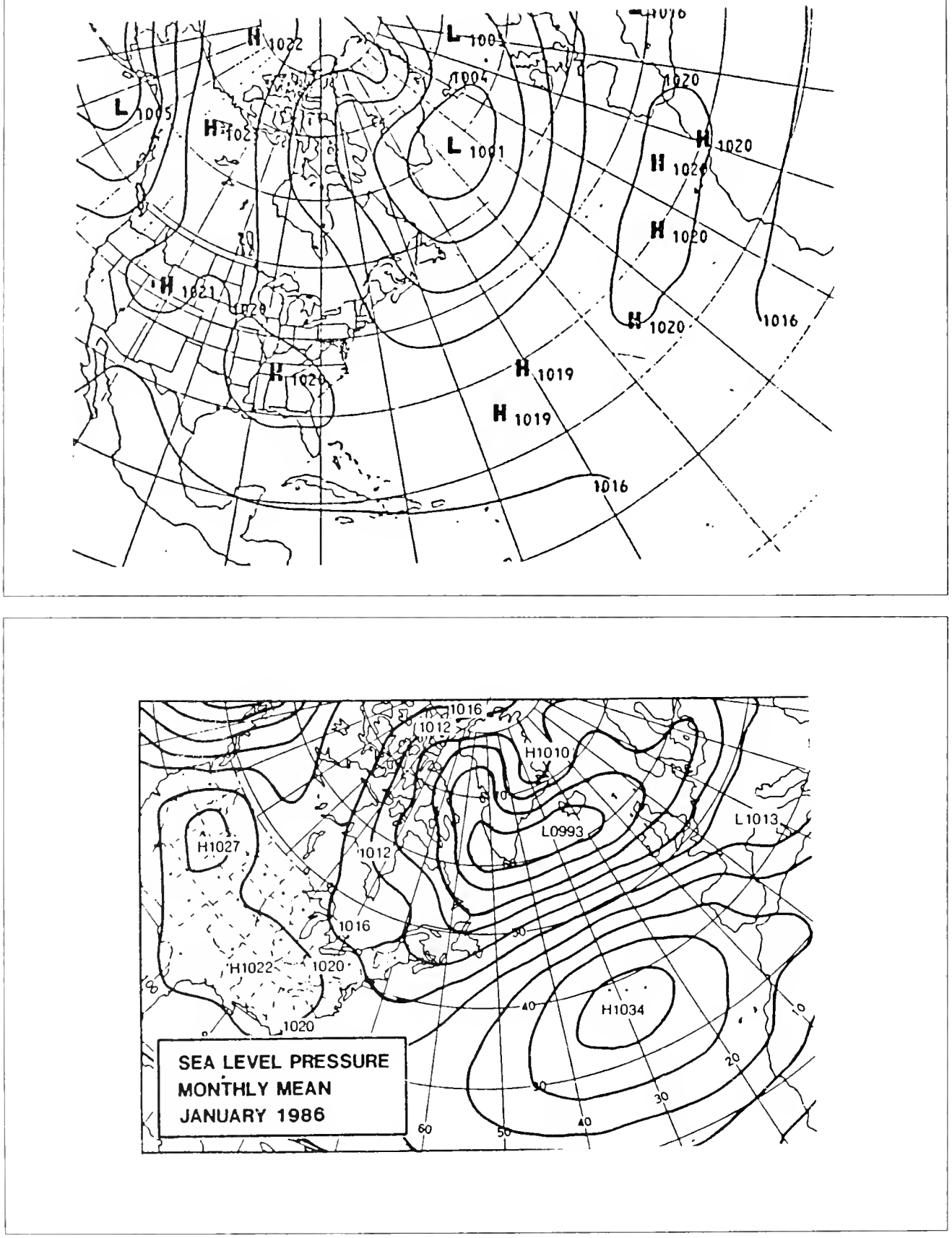

Figure 1. January 1986. Comparison of monthly mean surface pressure (bottom) with January historical average, 1948 - 1970 (top).

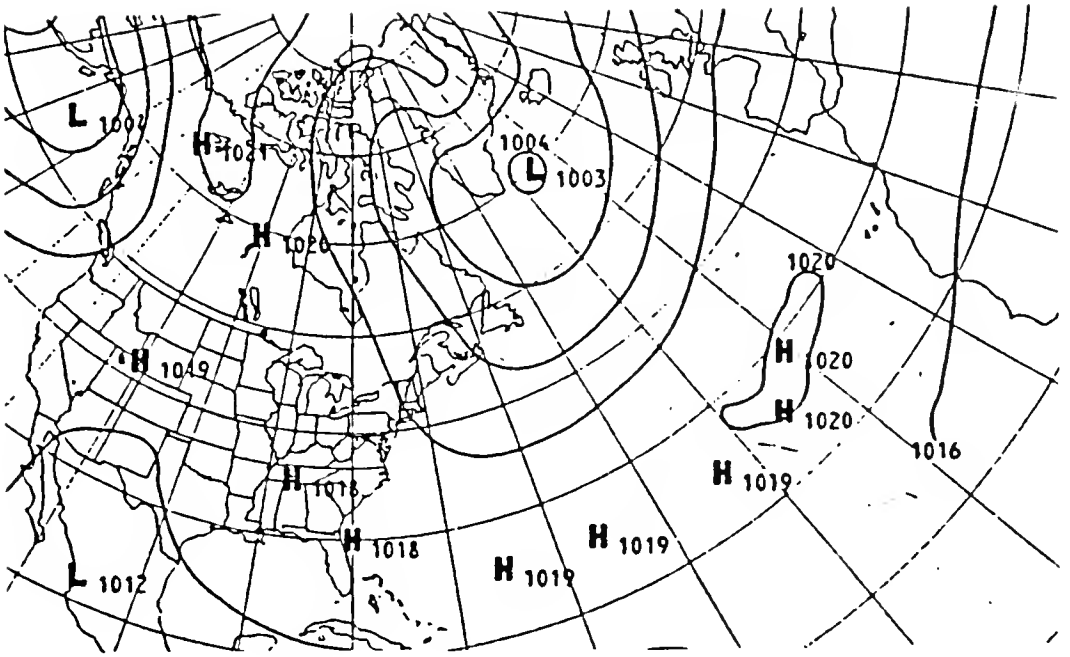

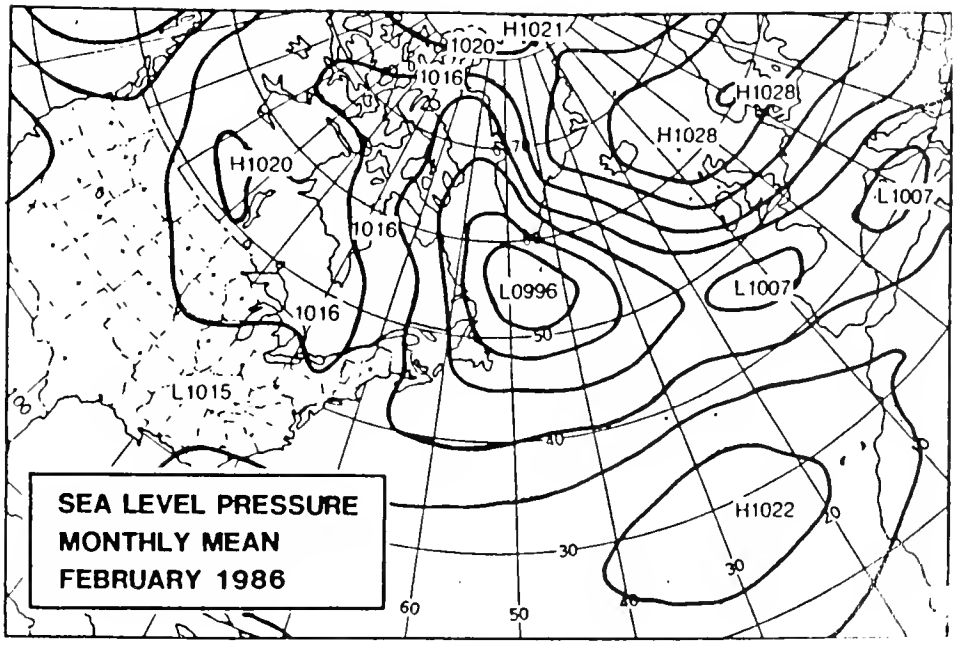

Figure 2. February 1986

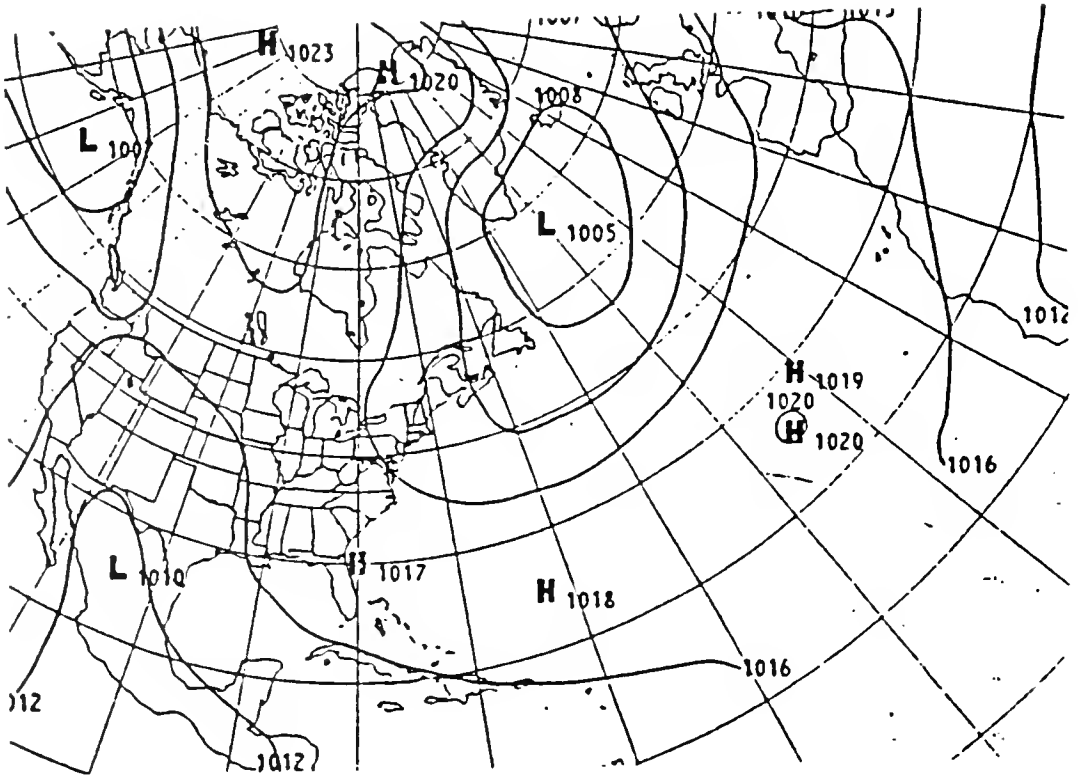

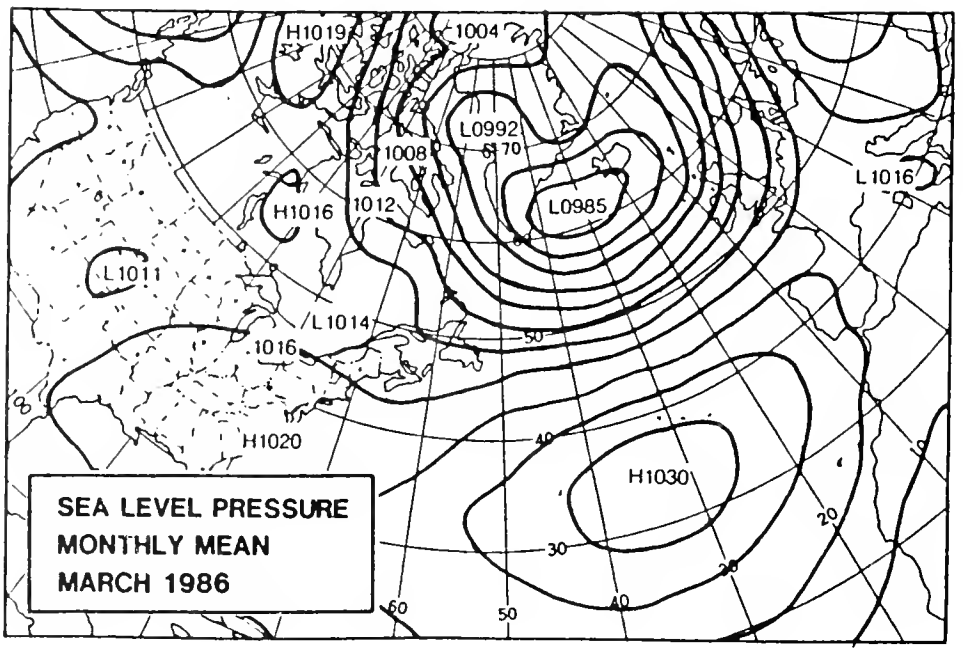

Figure 3. March 1986

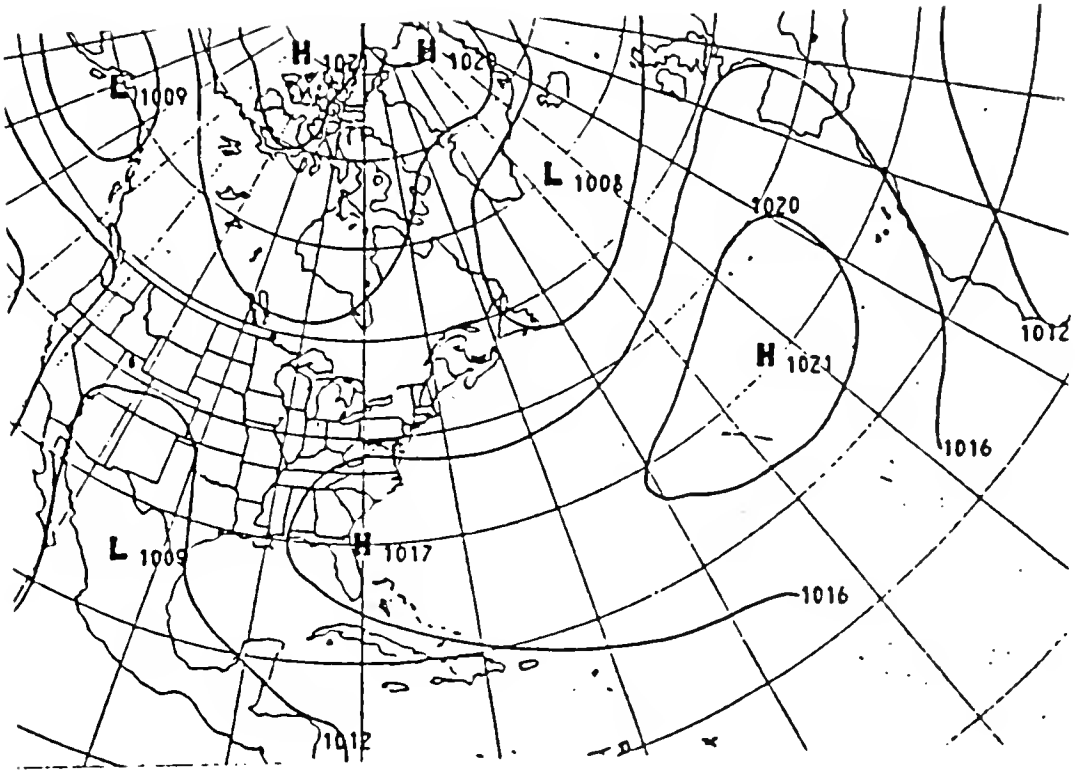

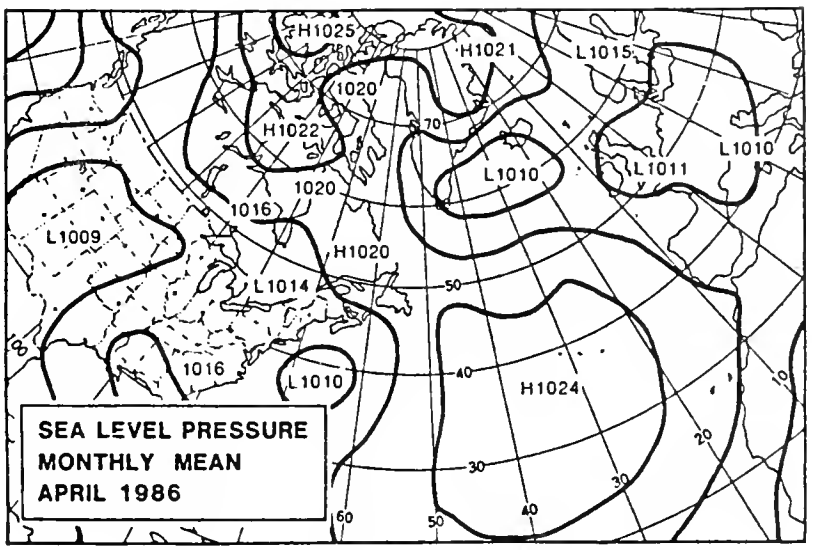

Figure 4. April 1986

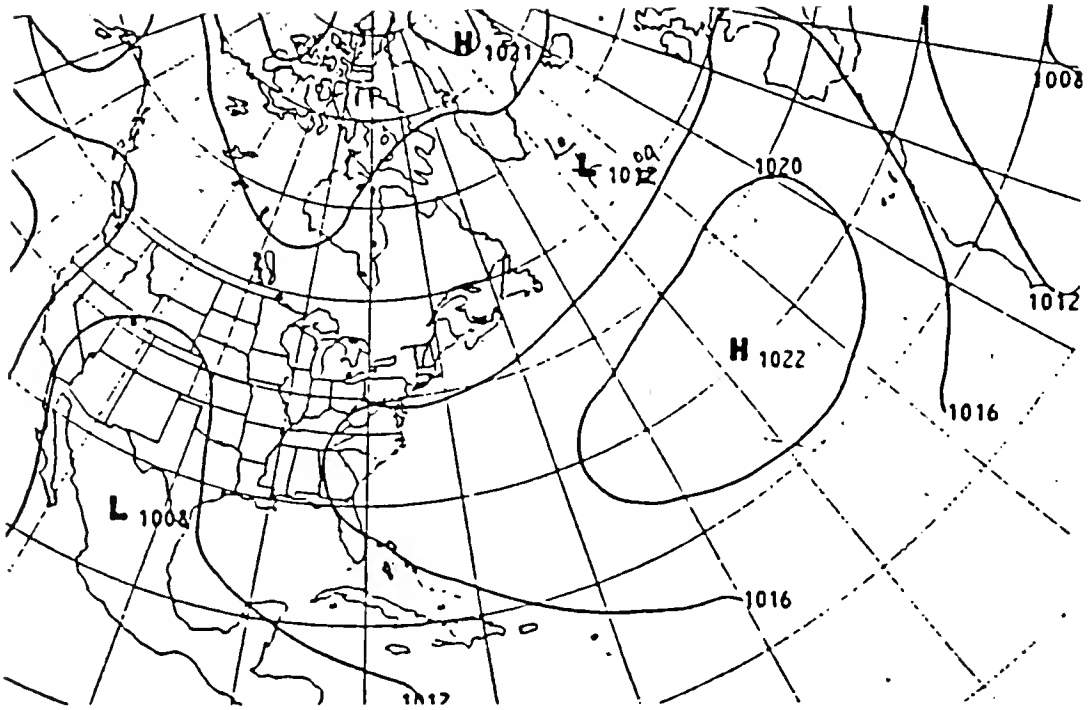

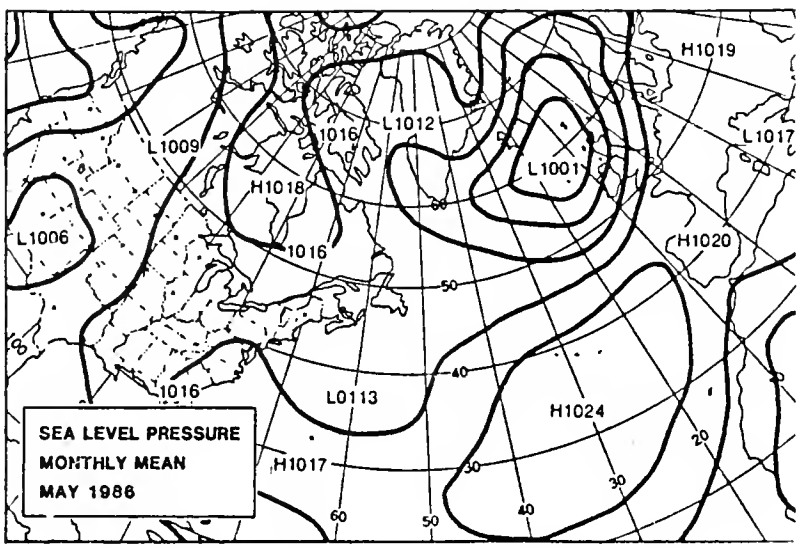

Figure 5. May 1986

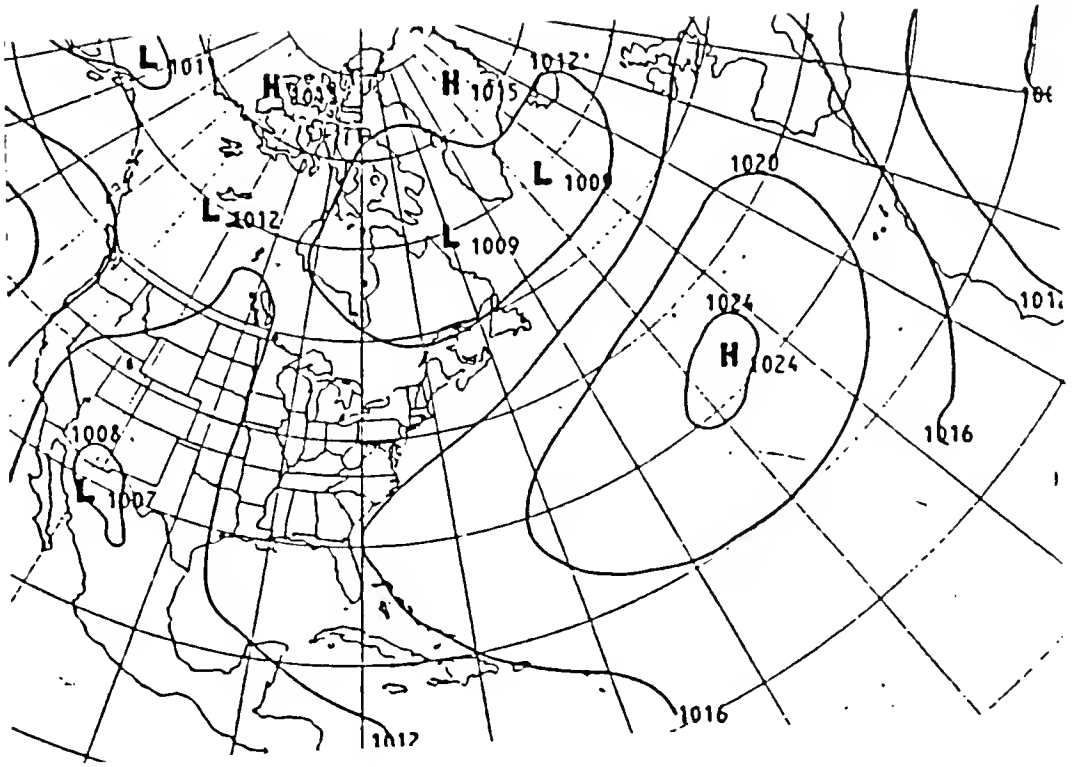

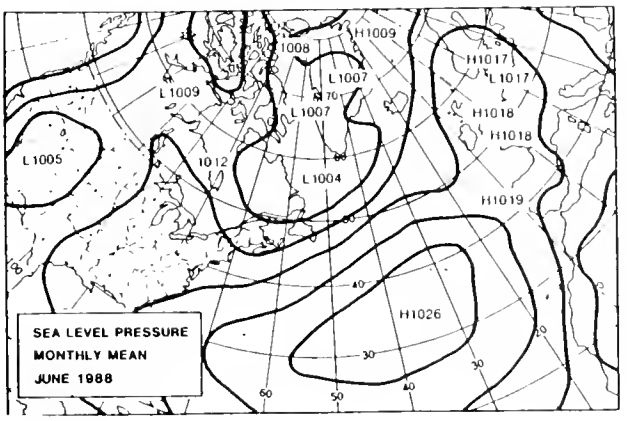

Figure 6. June 1986

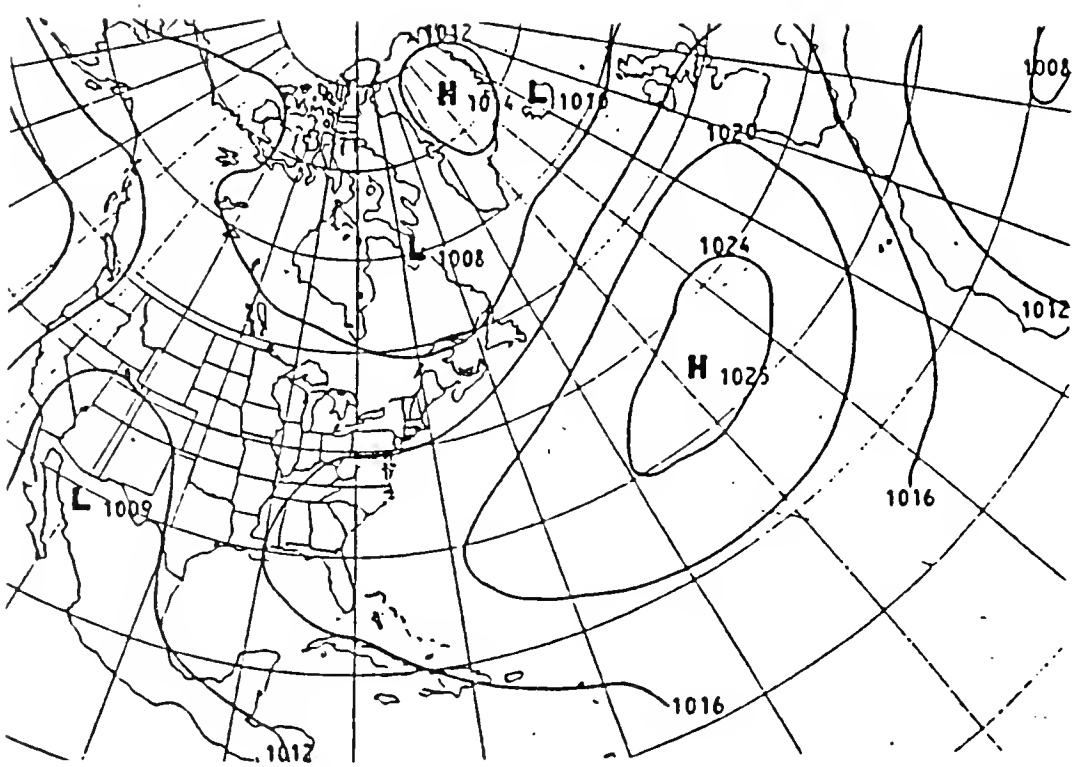

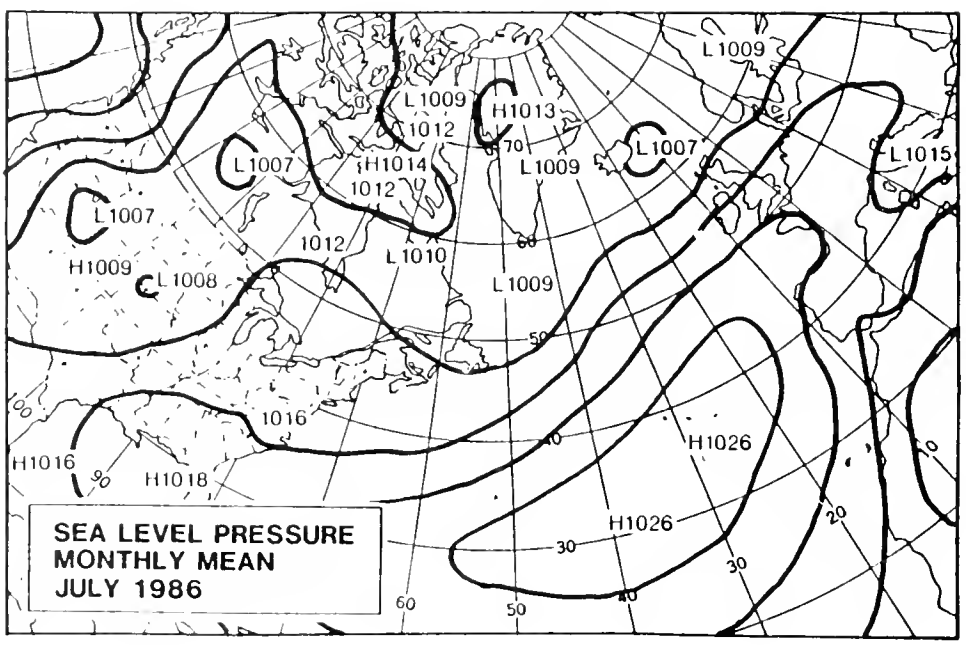

Figure 7. July 1986

Ice Conditions 1986 Season

October - November 1985: No sea ice was seen south of 65°N during these two months (Figures 8 and 9), however, sea ice formation was at or ahead of normal north of 65°N, due to below normal temperatures (Table 5). There were no icebergs added to plot south of 52°N in October or November.

December 1985: By mid-December (Figure 10), under the influence of continued below normal temperatures, Ungava Bay, Hudson and Davis Straits and the Labrador coast all showed 9 - 10 tenths coverage with new and young ice. Some sea ice formation was also taking place in the bays and coves of the northern Gulf of St. Lawrence. Consolidated first year ice extended as far south as Resolution Island in Hudson Strait. There were no icebergs added to plot south of 52°N in December.

January 1986: Mid-January showed the advance of new/young ice to the northern Avalon Peninsula in eastern Newfoundland (Figure 11). The boundary of first year ice was virtually unchanged from mid-December. There were no icebergs added to plot south of 52°N in January.

February 1986: Under the influence of a strong northerly flow in February (Figure 2), the sea ice advanced south along the Labrador coast and first year ice reached almost to the Avalon Peninsula by mid-month (Figure 12). Six icebergs were added to plot south of 52°N in February, 3 of which were south of 48°N.

March 1986: The ice edge continued to advance south (Figure 13), with a tongue of 9-10 tenths first year ice extending out to the vicinity of Flemish Pass by mid-March. The westerly flow over the region produced areas of somewhat lighter sea ice concentration along the east coasts of Baffin Island, Labrador and Newfoundland. During March, 42 icebergs were added to plot south of 52°N, 40 of which were south of 48°N. The high proportion south of 48°N was caused by icebergs being carried south and east of the ice pack by the Labrador Current. The 1986 International Ice Patrol season opened on March 27 (Figure 19).

April 1986: The sea ice deteriorated and retreated along the Labrador and Newfoundland coasts during April (Figure 14), normally a month of continued sea ice development in the area. This retreat was caused by the warm conditions and southerly flow (Figure 4) described previously. During April, 60 icebergs were added to plot south of 52°N, all of which were south of 48°N. At mid-month, the main concentration of icebergs on plot at IIP was in Flemish Pass and across the northern half of the Grand Bank (Figure 20). By April 30, icebergs were widely distributed across the area south of 48°N (Figure 21).

May 1986: The ice edge continued to retreat in May and by mid-month, the Strait of Belle Isle was ice-free (Figure 15). Of the 74 icebergs added to plot south of 52°N in May, 59 were south of 48°N, the most icebergs south of that latitude for any month in 1986. The southernmost iceberg of the 1986 season was on May 10 at position 41° 06'N 48°06'W. By May 16 (Figure 22), fewer icebergs were seen on the Grand Bank and south of Flemish Pass, while the number north of 48°N had increased. On May 30 (Figure 23), only 7 icebergs remained south of 48°N and the total number of icebergs on plot had greatly decreased since mid-month.

June 1986: The ice edge was north of Goose Bay by mid-June and continuing to retreat (Figure 16). With 151 icebergs added to plot, June was the heaviest month for new icebergs, but only 24 new icebergs were south of 48°N. At mid-month, the only icebergs remaining south of 48°N were concentrated along the Newfoundland coast near Cape Race (Figure 24). On June 30, no icebergs remained south of 48°N (Figure 25).

July - September 1986: The ice edge continued to retreat in July and August (Figures 17 and 18) and by mid-September, there was no sea ice south of 65°N. There were no icebergs reported south of 48°N during July, August and September. The 1986 International Ice Patrol season closed on July 3 (Figure 26).

Table 6. Explanation of Sea Ice Symbols Used in Figures 8 — 18

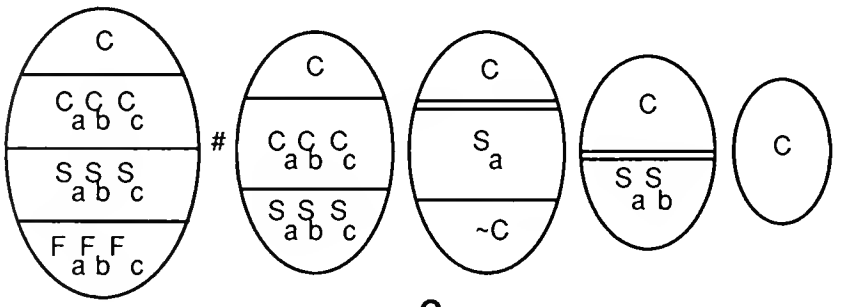

C

Total ice concentration in the area in tenths.

$C_a C_b C_c$

Concentration of thickest (C_a), 2nd thickest (C_b), 3rd thickest (C_c).

$S_a S_b S_c$

Stage of development of thickest (S_a), 2nd thickest (S_b), 3rd thickest (S_c).

$F_a F_b F_c$

Concentration of ice within areas of strips and patches.

~C

Floe size of thickest (F_a), 2nd thickest (F_b), 3rd thickest (F_c).

Stage of Development

0 No stage of development
1 New ice
2 Nilas, ice rind
3 Young ice
4 Grey ice
5 Grey-white ice
6 First-year ice
7 Thin first-year ice
8 Thin first-year ice, 30-50 cm
9 Thin first-year ice, 50-70 cm
1 · Medium first-year ice
4 · Thick first-year ice
7 · Old ice
8 · Second-year ice
9 · Multi-year ice
▲ Icebergs
* A trace of ice thicker than S_a
\# Fourth type, if $C_a C_b C_c$ do not add up to C

Floe Sizes

0 Pancake ice
1 Brash, small ice cake
2 Ice cake
3 Small floe
4 Medium floe
5 Big floe
6 Vast floe
7 Giant floe
8 Growlers and floebergs
9 Icebergs
/ Undetermined or unknown

Figure 8. October 15, 1985

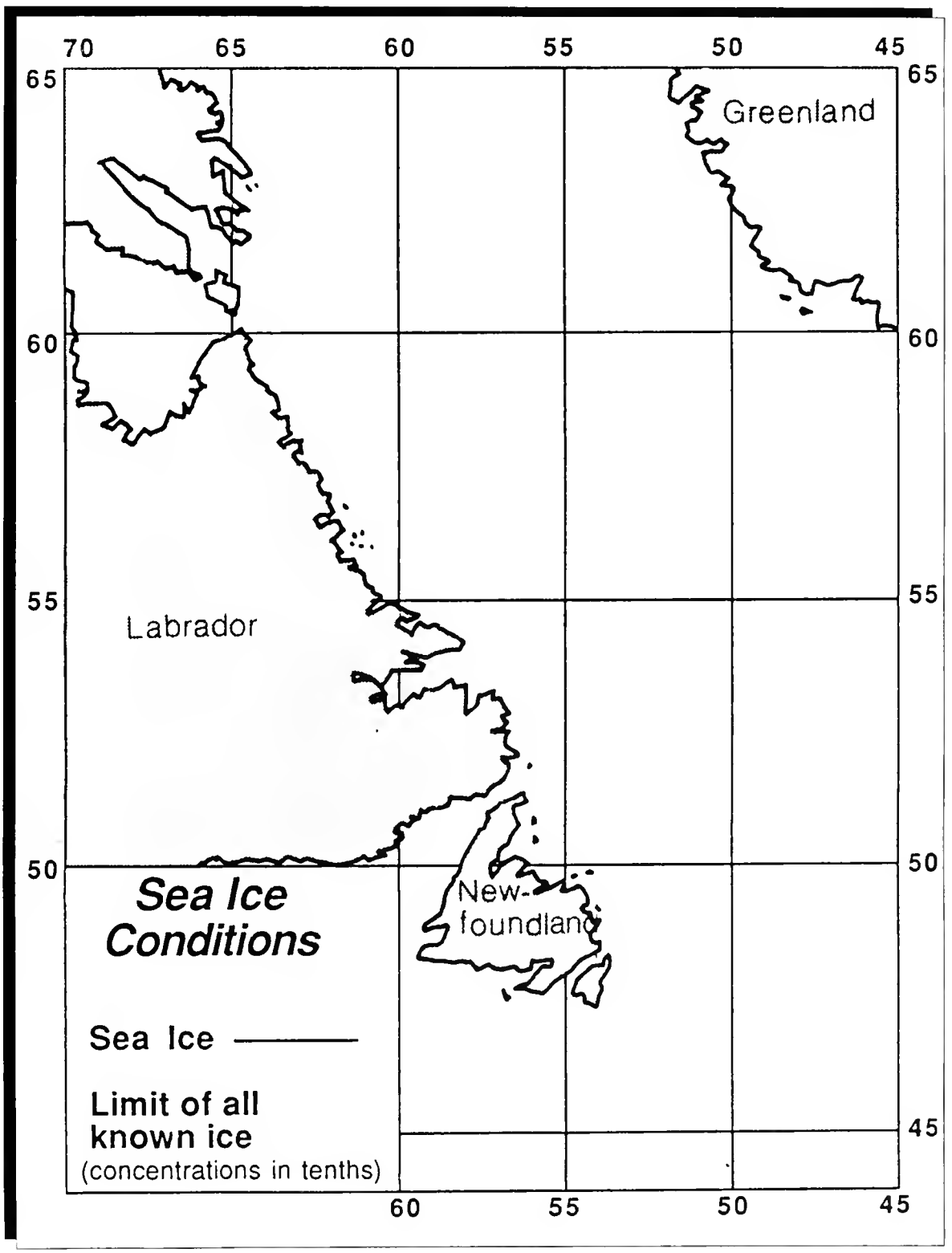

Figure 9. November 12, 1985

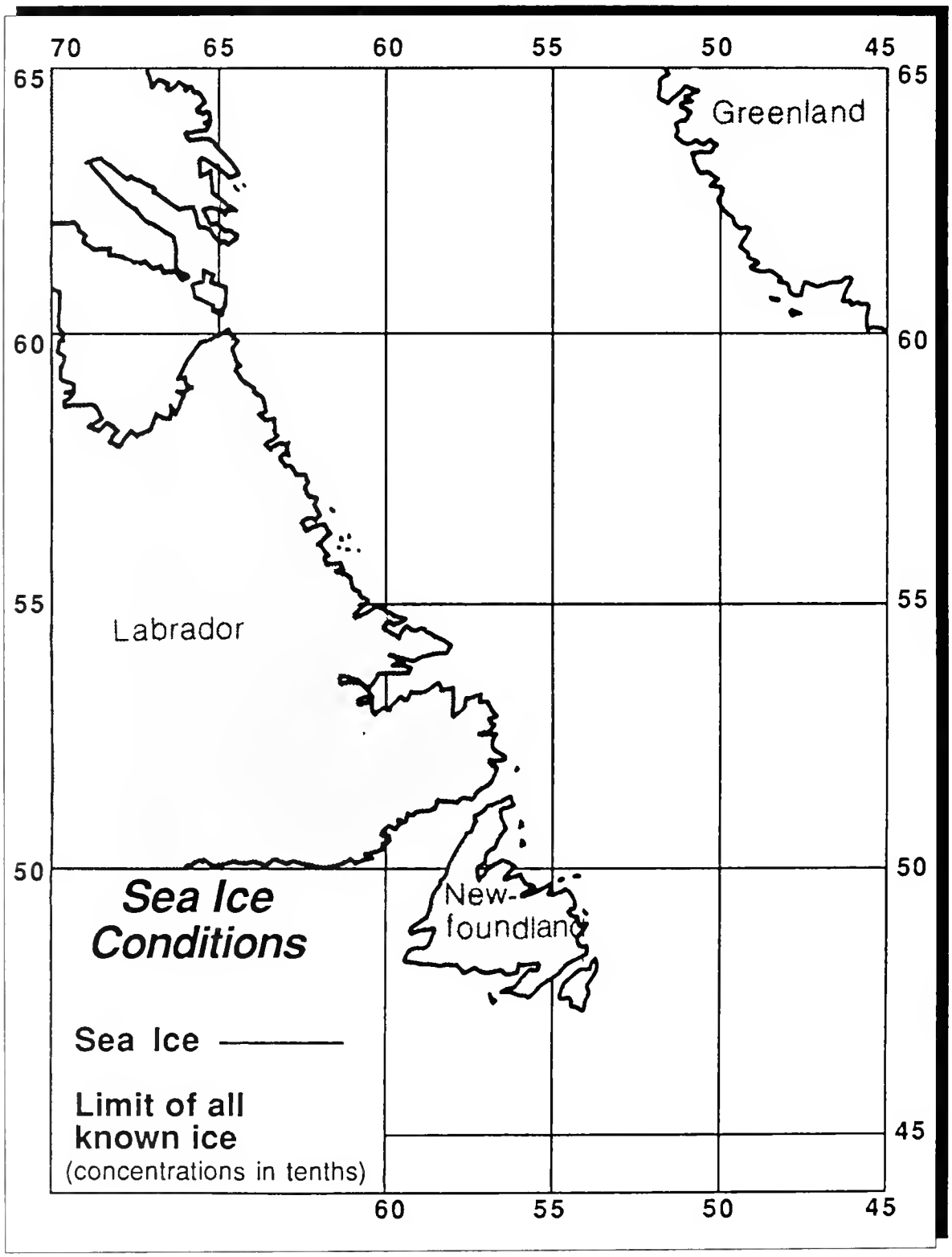

Figure 10. December 17, 1985

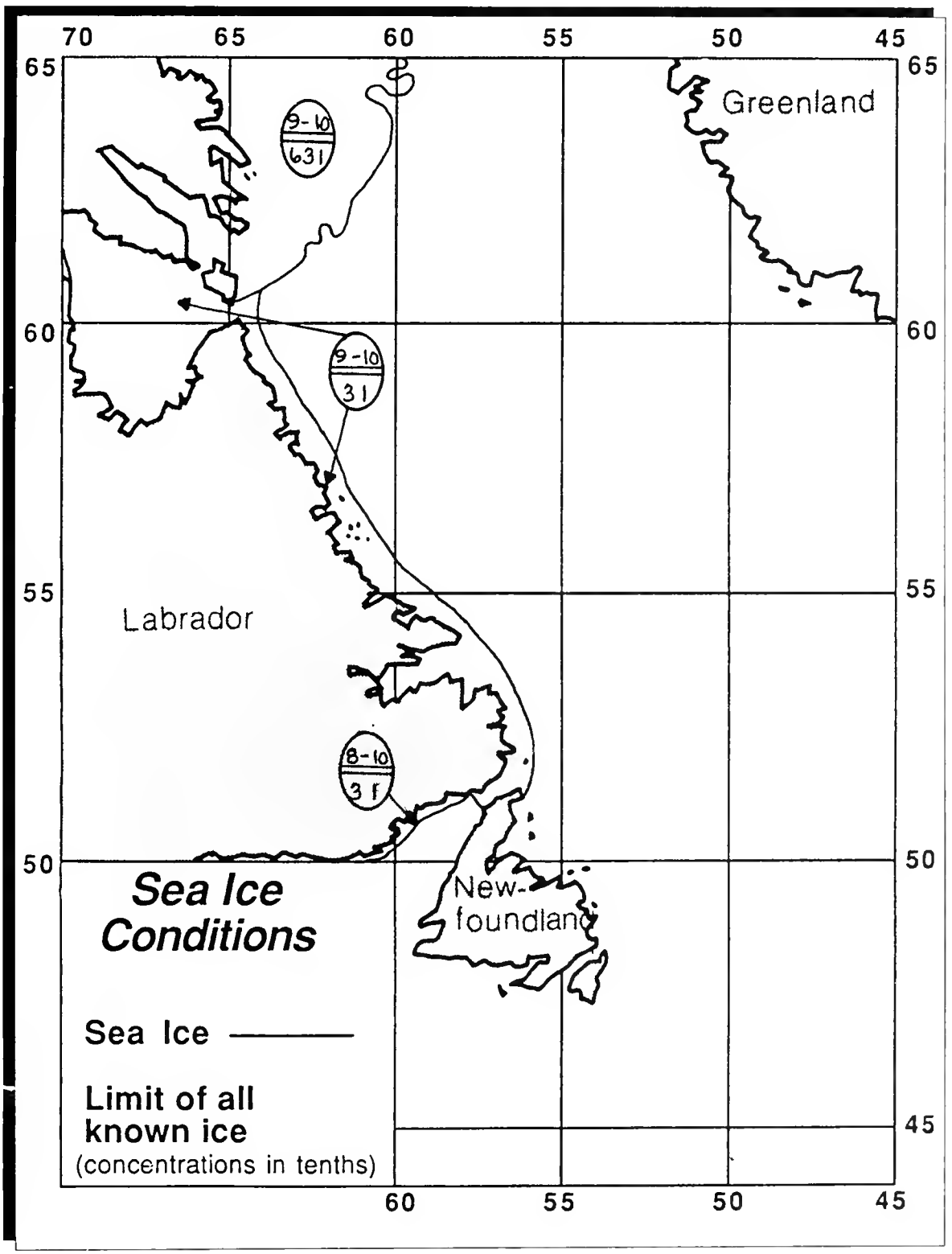

Figure 11. January 14, 1986

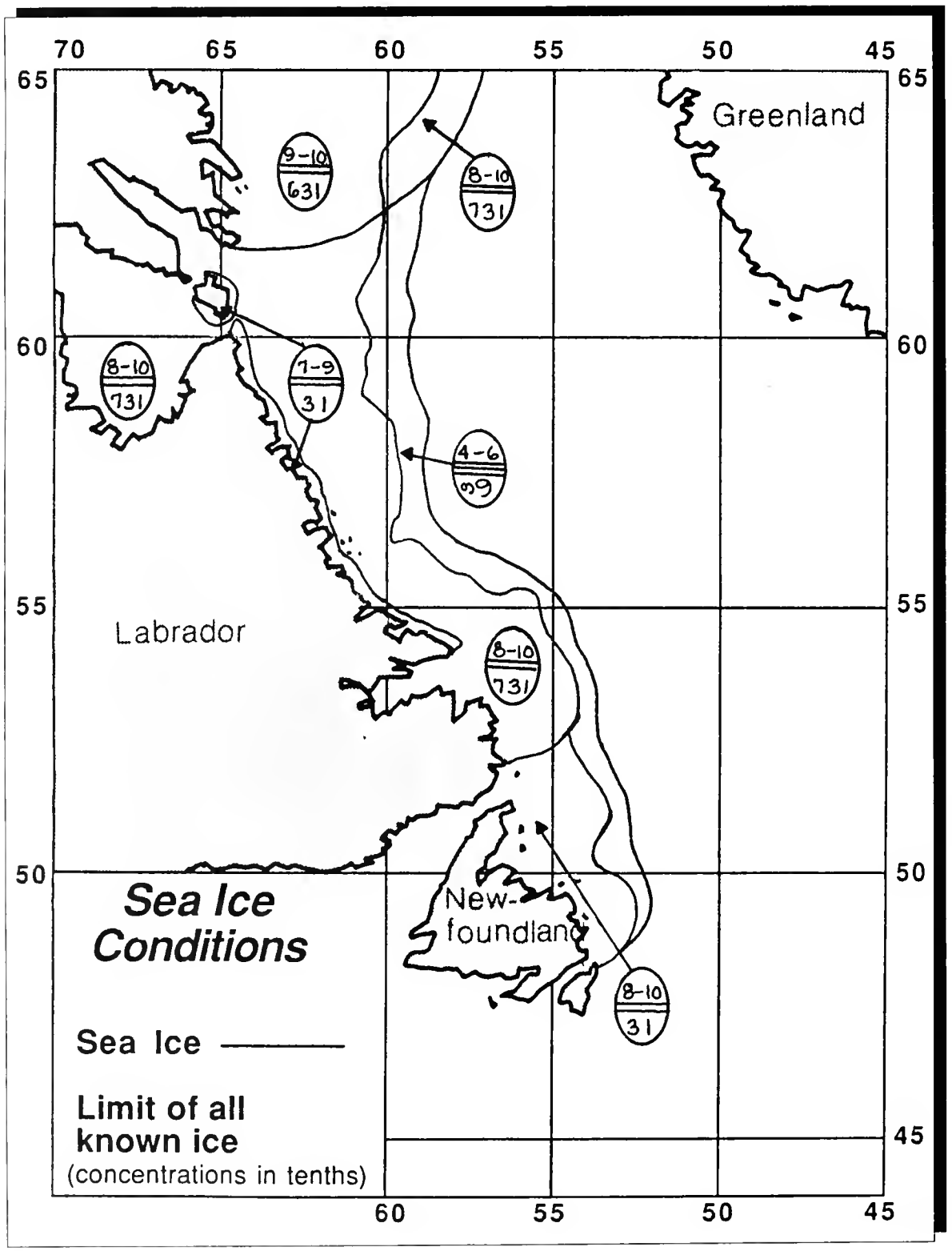

Figure 12. February 18, 1986

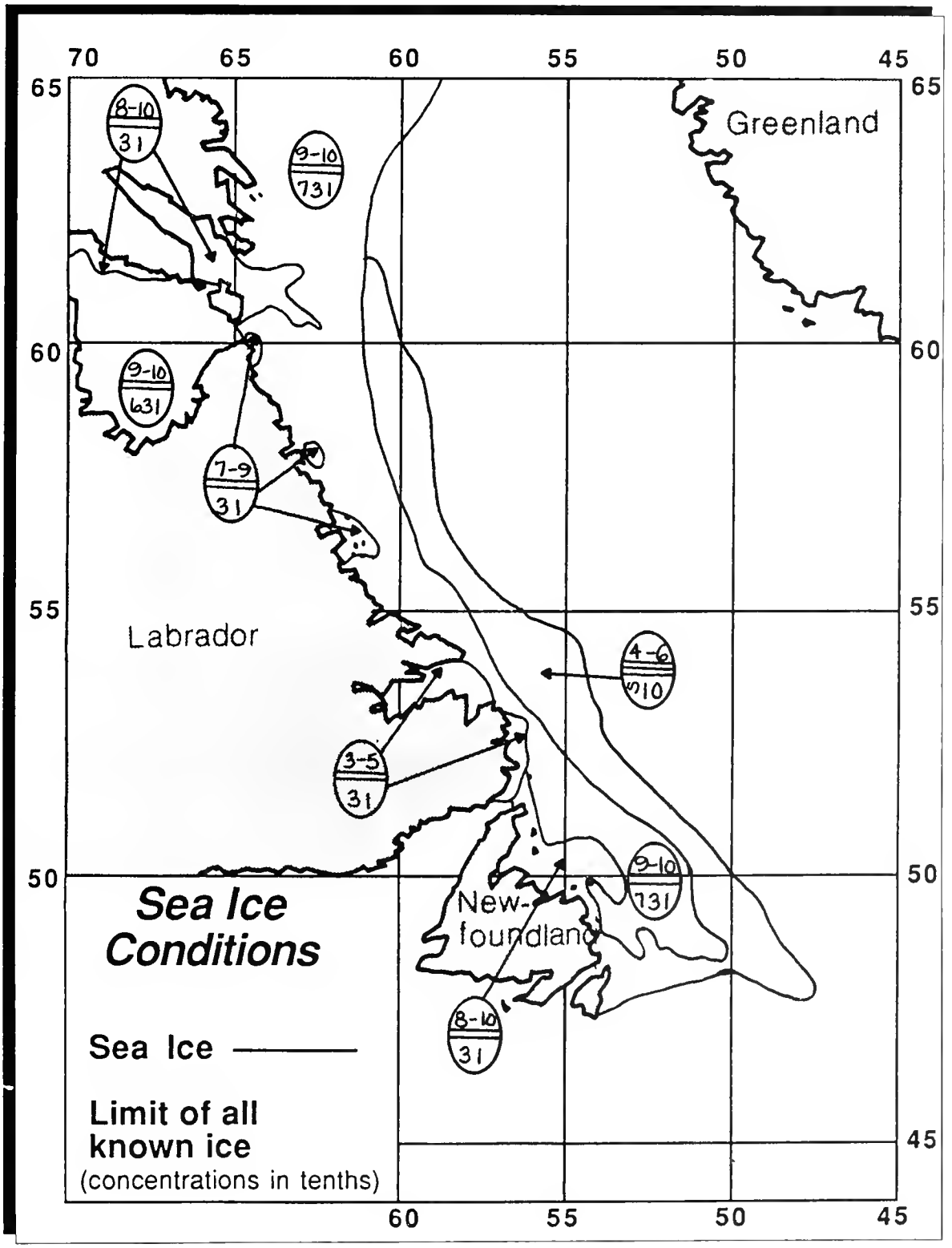

Figure 13. March 18, 1986

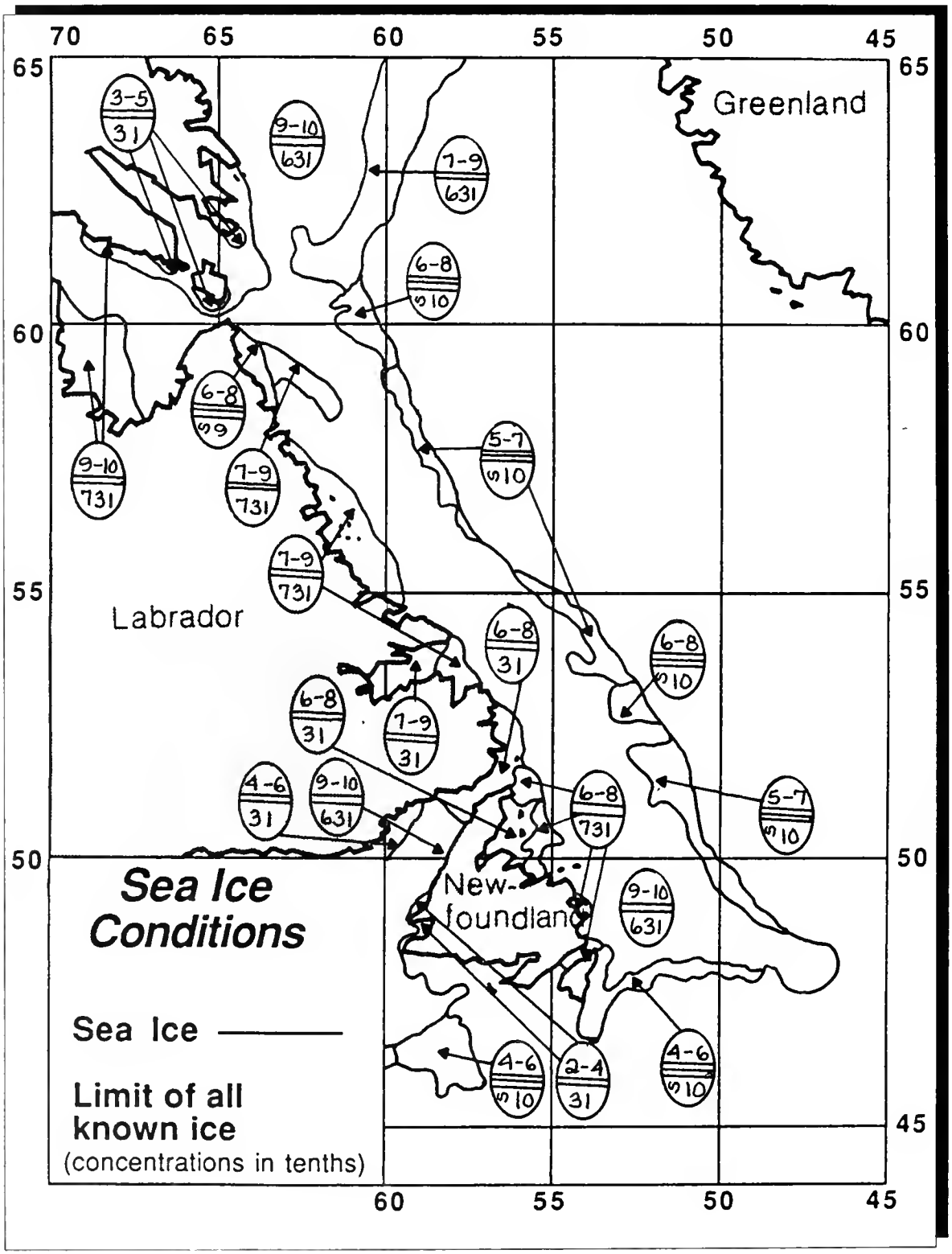

Figure 14. April 15, 1986

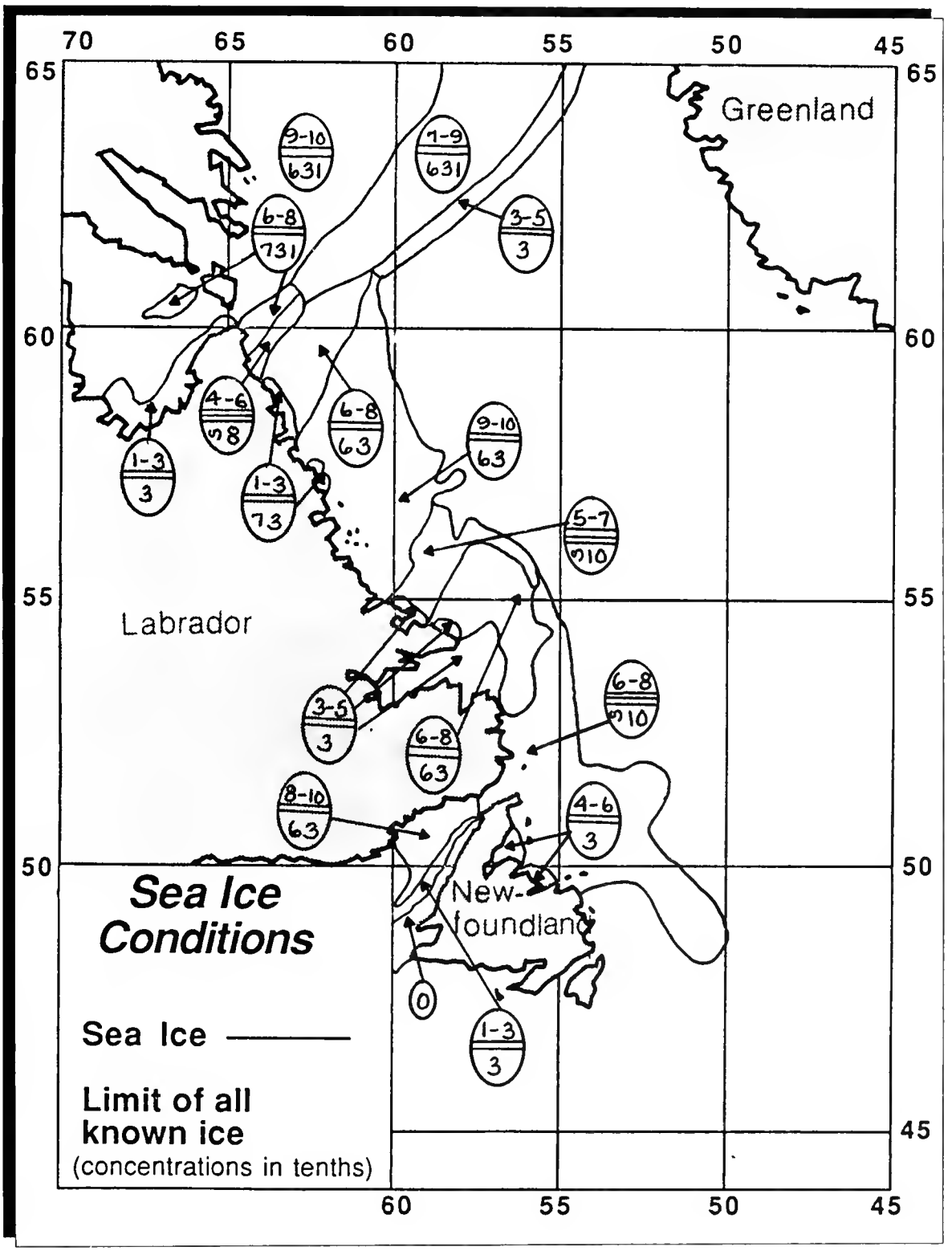

Figure 15. May 13, 1986

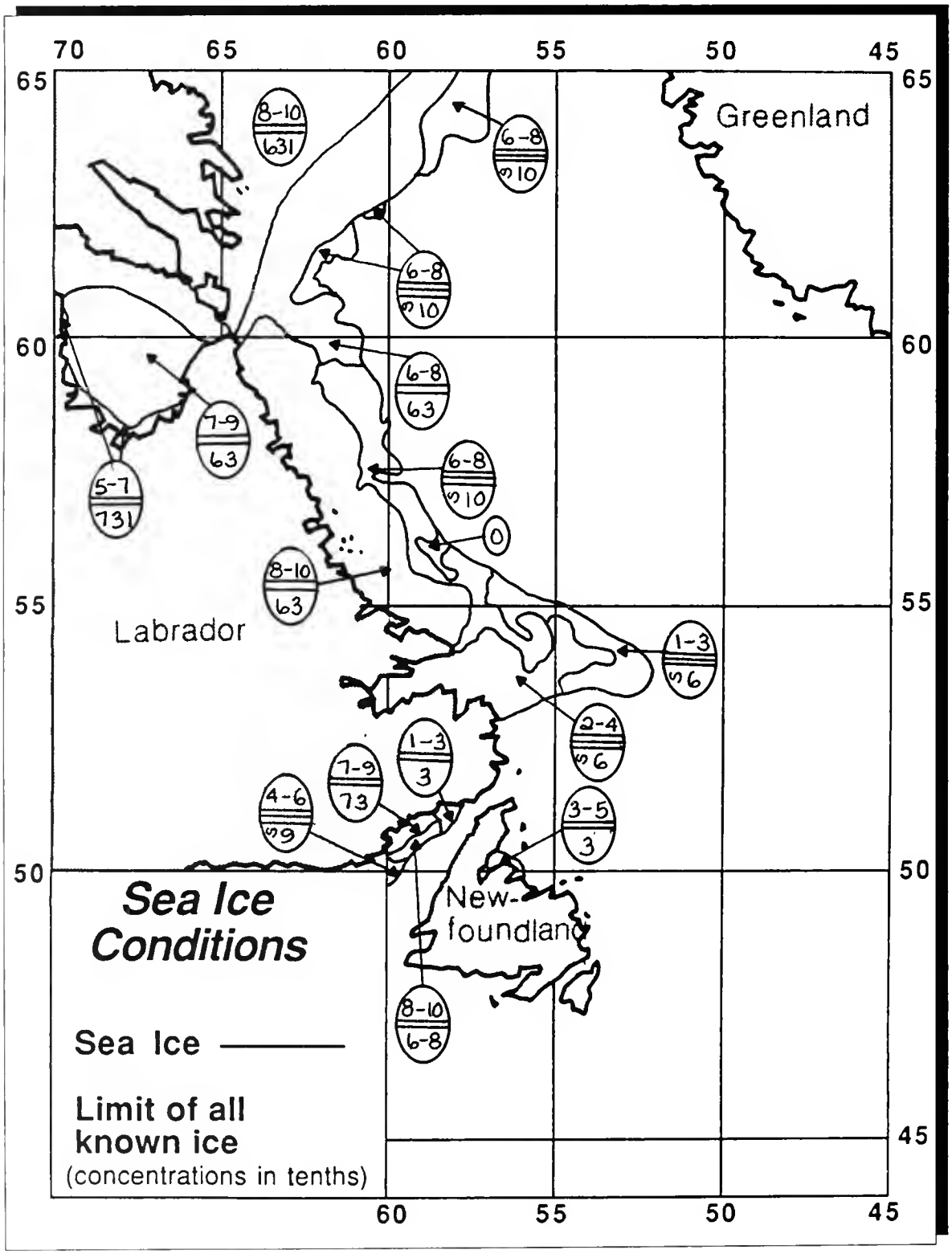

Figure 16. June 17, 1986

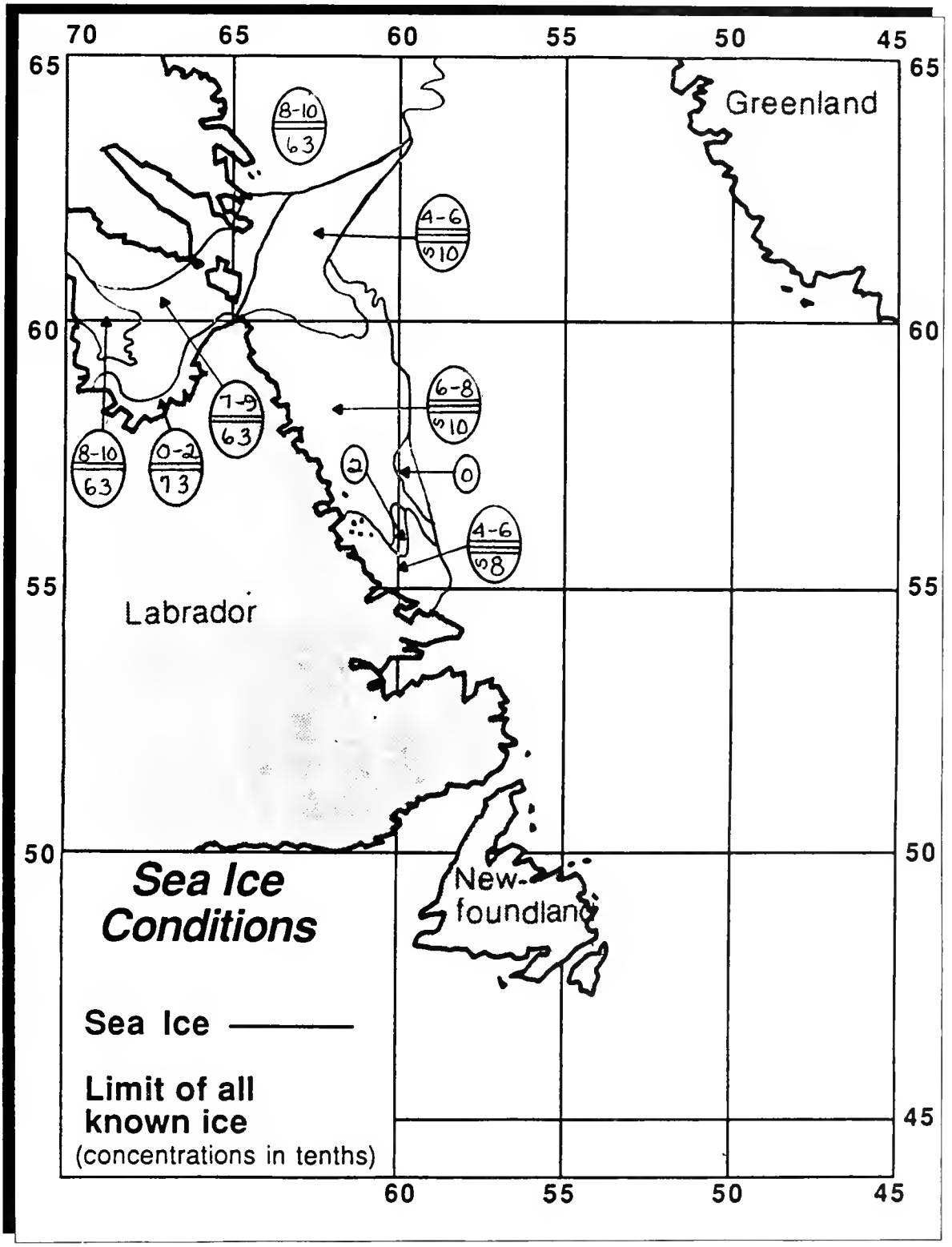

Figure 17. July 15, 1986

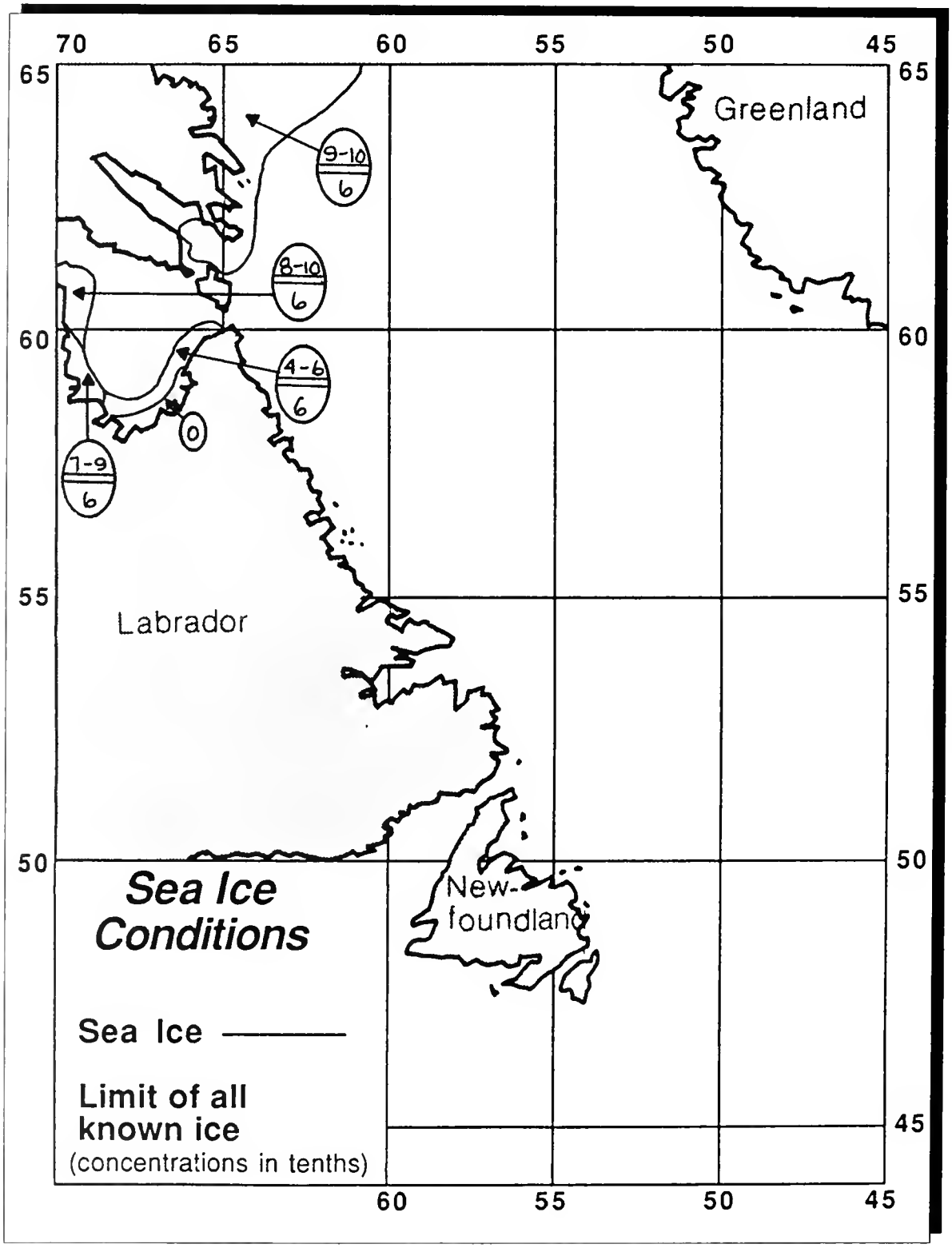

Figure 18. August 18, 1986

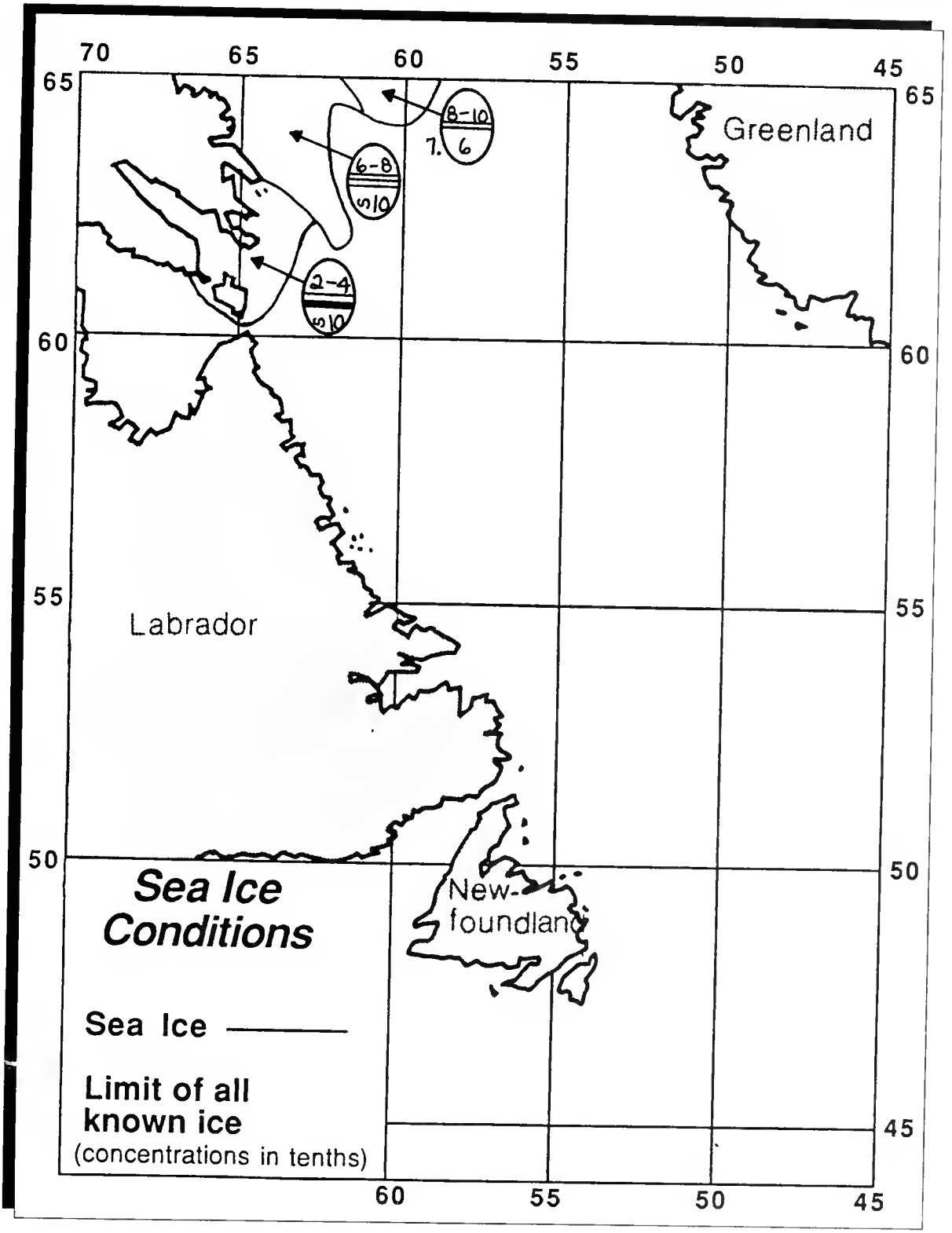

Figure 19. March 27, 1986

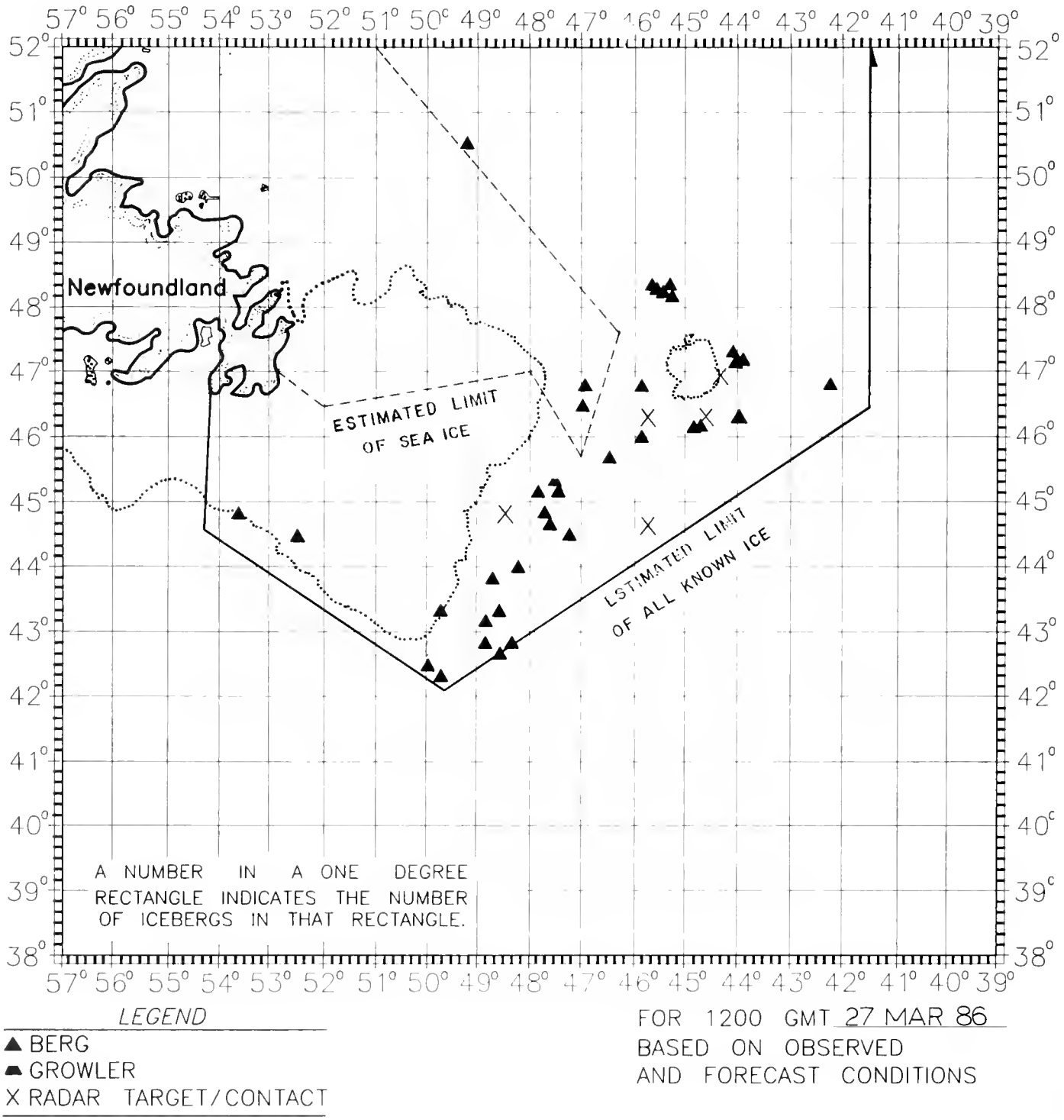

Figure 20. April 15, 1986

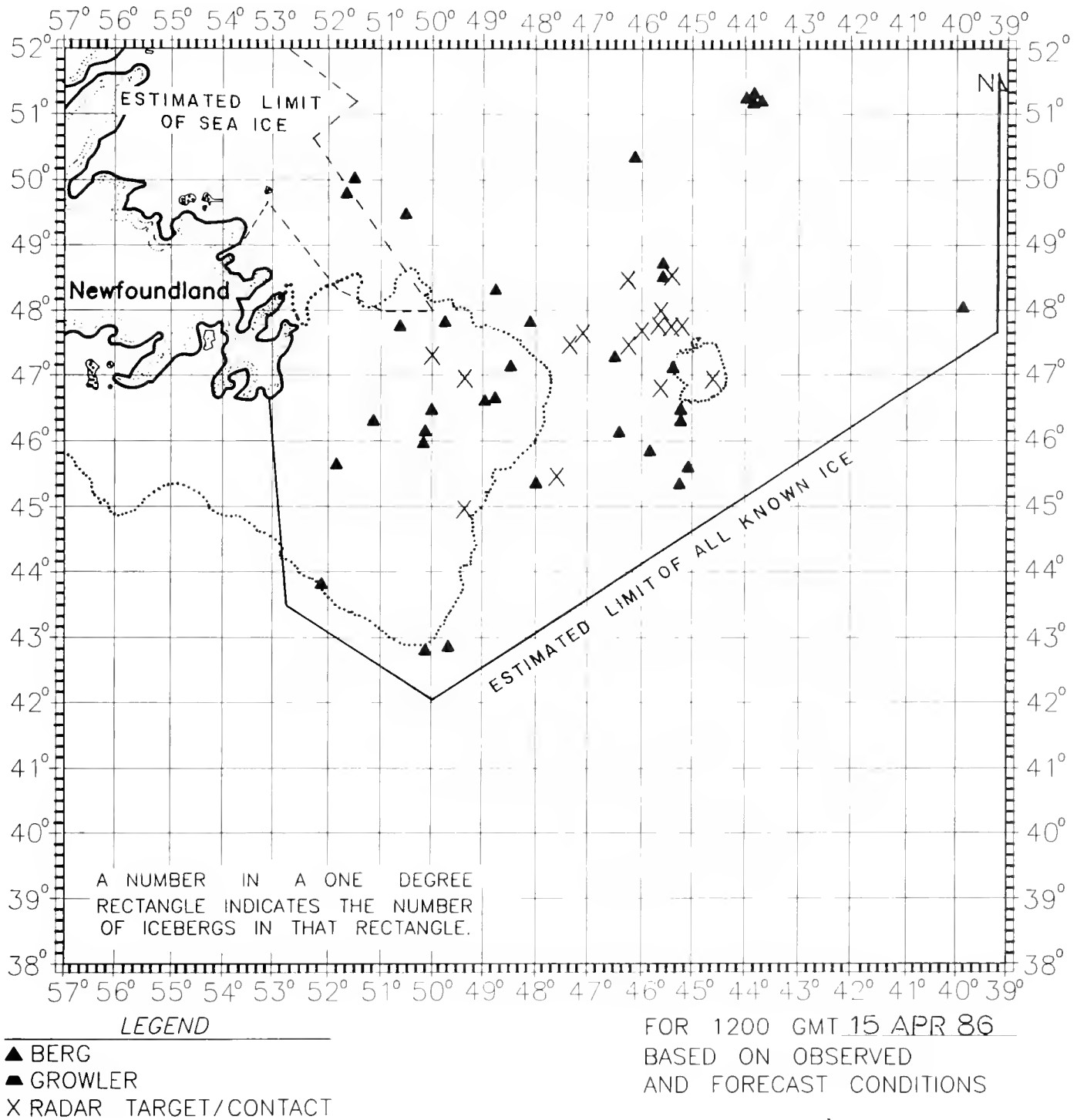

Figure 21. April 30, 1986

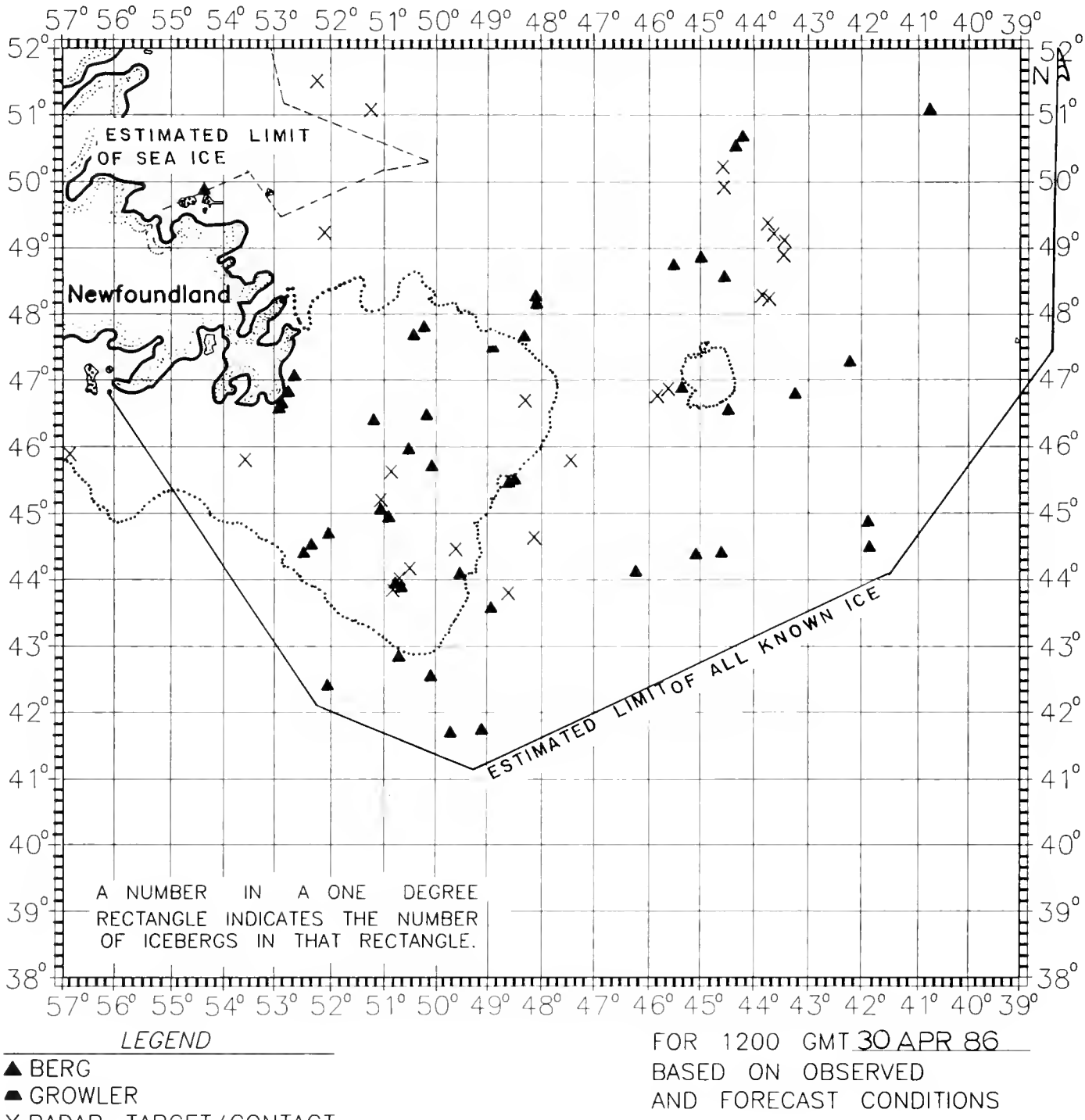

Figure 22. May 16, 1986

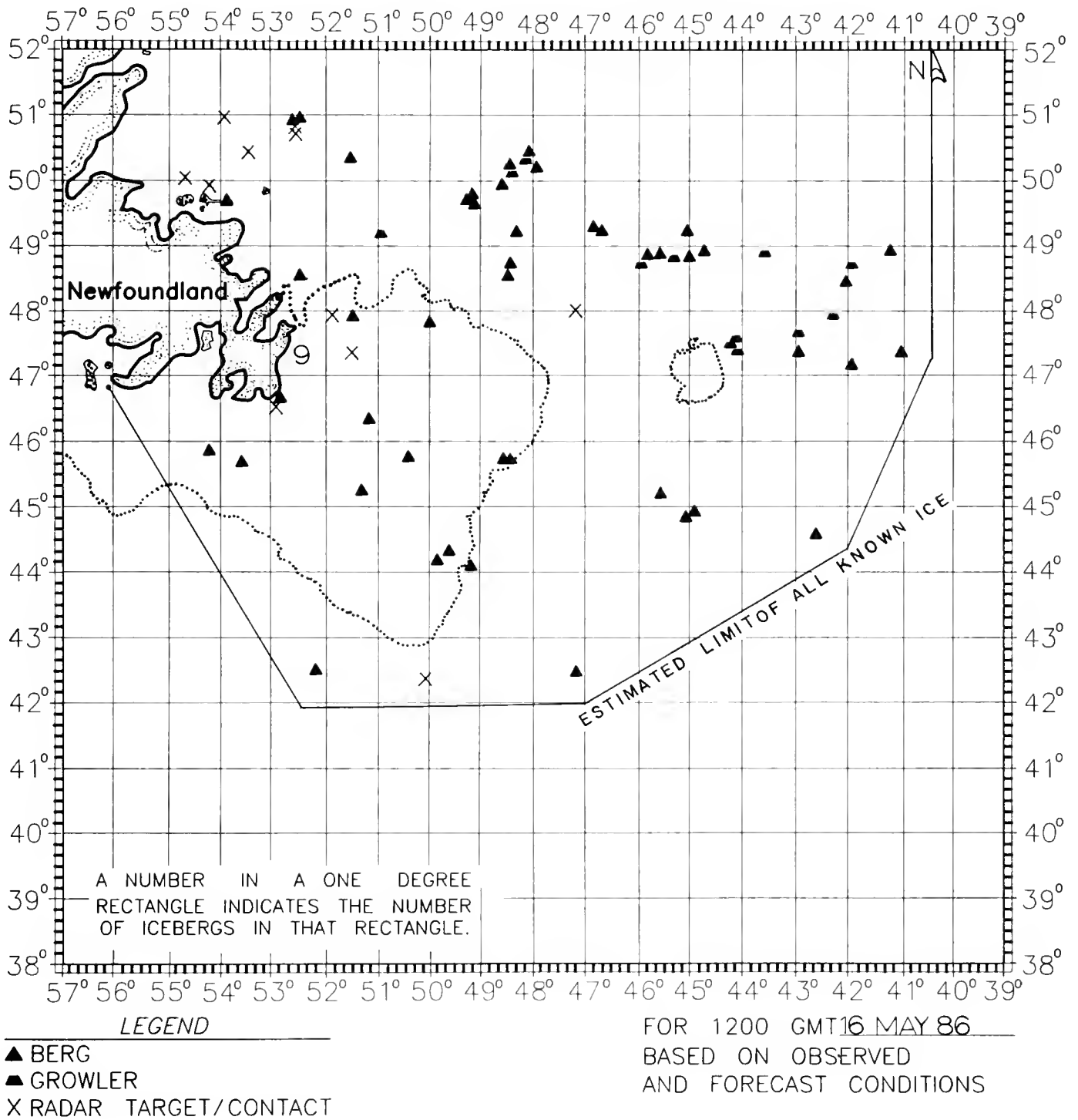

Figure 23. May 30, 1986

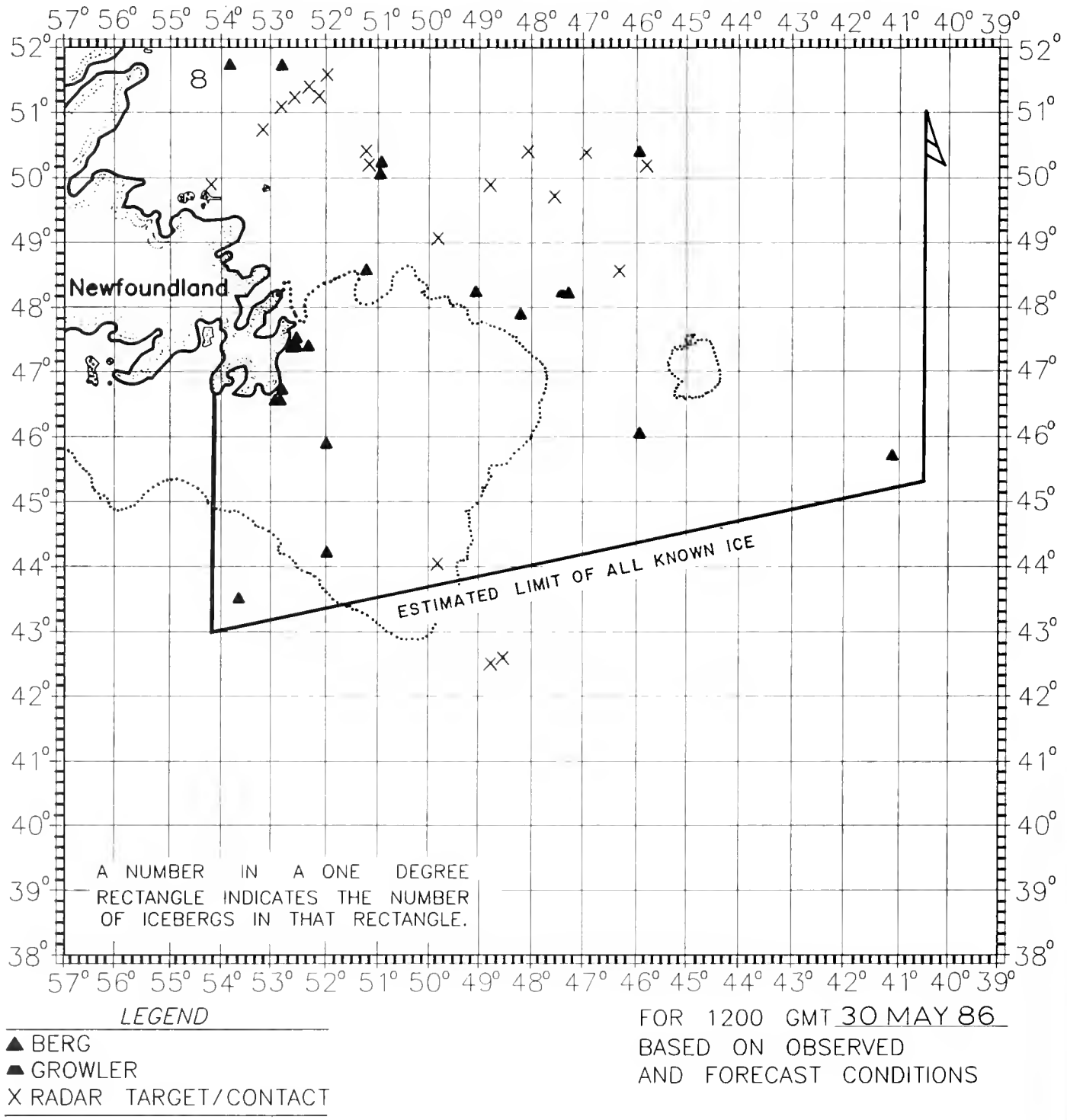

Figure 24. June 16, 1986

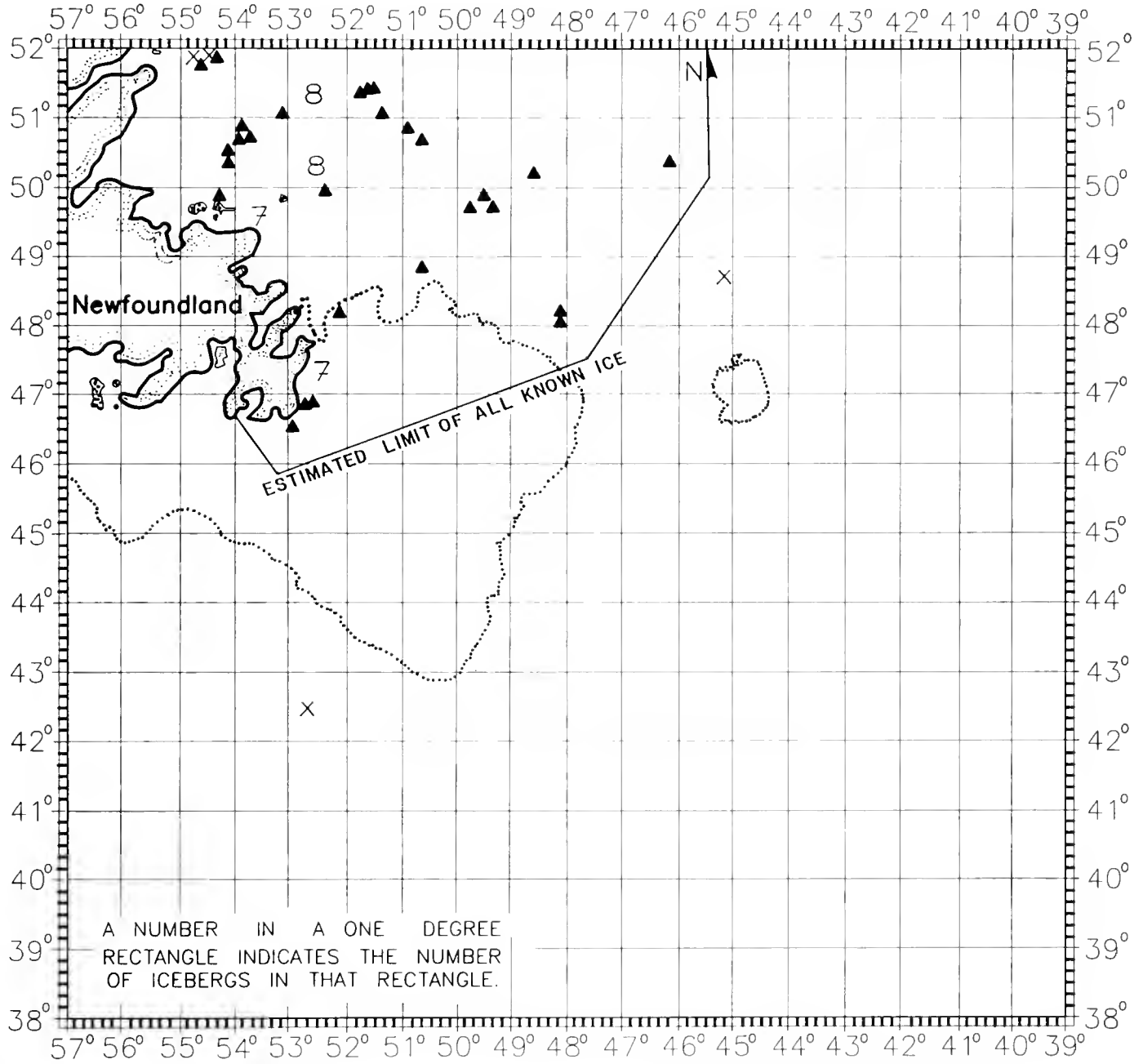

LEGEND

▲ BERG
▬ GROWLER
X RADAR TARGET/CONTACT

FOR 1200 GMT 16 JUN 86
BASED ON OBSERVED
AND FORECAST CONDITIONS

Figure 25. June 30, 1986

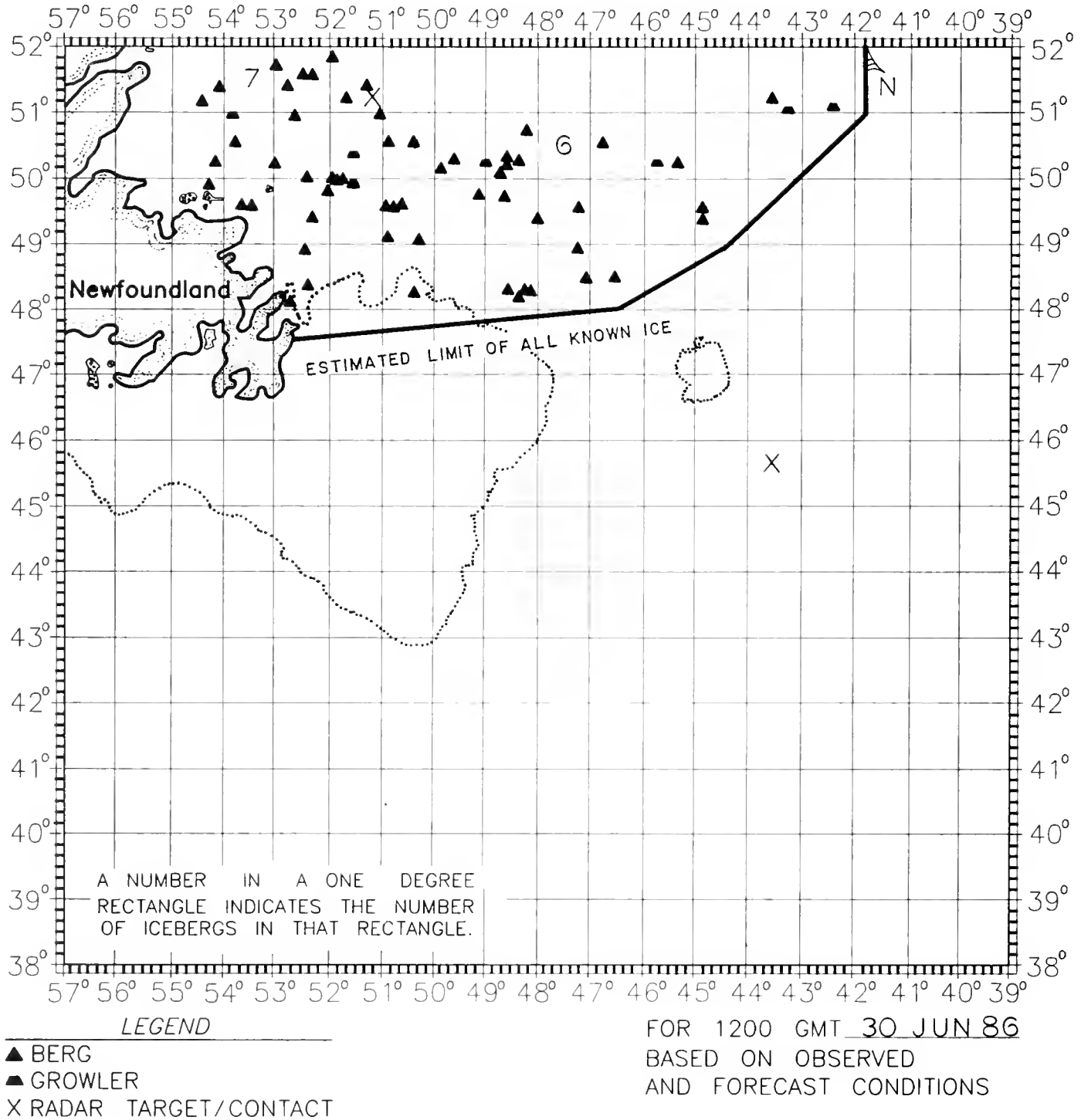

Figure 26. July 3, 1986

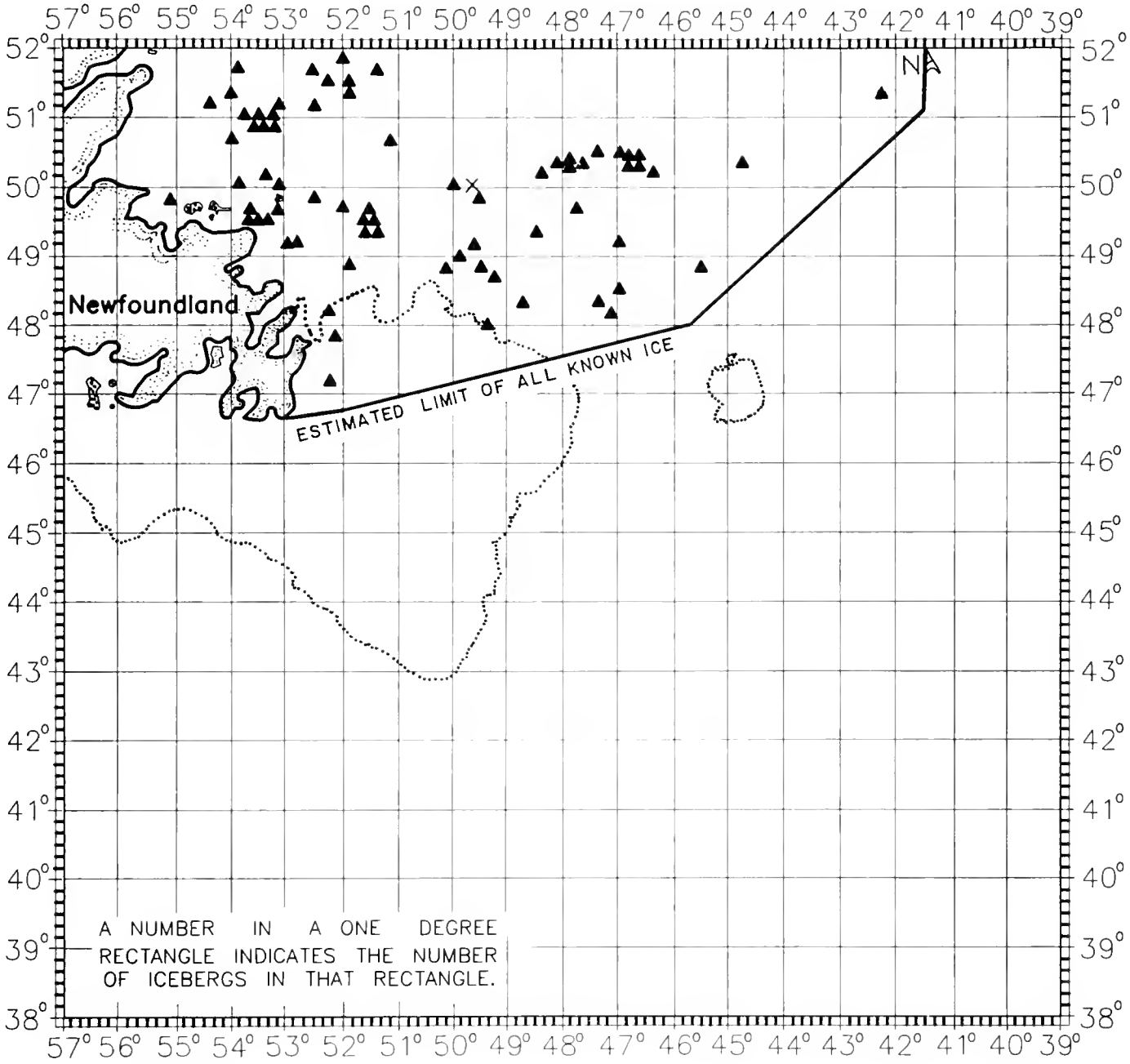

LEGEND

▲ BERG
▬ GROWLER
X RADAR TARGET/CONTACT

FOR 1200 GMT 03 JUL 86
BASED ON OBSERVED
AND FORECAST CONDITIONS

Discussion of Iceberg and Environmental Conditions

The number of icebergs that pass south of 48°N in the International Ice Patrol area each year is the measure by which International Ice Patrol has judged the severity of each season since 1912 (Table 1). With 204 icebergs south of 48°N, 1986 is the 49th most severe year on record, a relatively light year.

Since the number of icebergs calved each year by Greenland's glaciers is in excess of 10,000, a sufficient number of icebergs exist in Baffin Bay during any year. Therefore, annual fluctuations in the generation of Arctic icebergs is not a significant factor in the number of icebergs passing south of 48°N annually. The factors that determine the number of icebergs passing south of 48°N each season can be divided into those affecting iceberg transport (currents, winds, and sea ice) and those affecting iceberg deterioration (wave action, sea surface temperature, and sea ice).

Sea ice acts to impede the transport of icebergs by winds and currents and also protects icebergs from wave action, the major agent of iceberg deterioration. Although it slows current and wind transport of icebergs, sea ice is itself an active medium, for it is continually moving toward the ice edge where melt occurs. Therefore, icebergs in sea ice will eventually reach open water unless grounded. The melting of sea ice itself is affected by snow cover (which slows melting) and air and sea water temperatures. As sea ice melt accelerates in the spring and early summer, trapped icebergs are rapidly released and then become subject to normal transport and deterioration.

Acknowledgements

Commander, International Ice Patrol acknowledges the assistance and information provided by the Canadian Department of the Environment, the U.S. National Weather Service, the U.S. Naval Weather Service, and the U.S. Coast Guard Research and Development Center.

We extend our sincere appreciation to the staffs of the Canadian Coast Guard Radio Station St. John's, Newfoundland/VON, the Gander Weather Office, the personnel of U.S. Coast Guard Air Station Elizabeth City, and the USCGC EVERGREEN for their excellent support during the 1986 International Ice Patrol season.

It is also extremely important to recognize the efforts of the personnel of the International Ice Patrol:
CDR N.C. Edwards, Jr., Dr. D.L. Murphy, LT F. J. Williams, LT I. Anderson, LTJG N.B. Thayer, MSTCS G.F. Wright, MSTC D.A. Eichmann, MST1 M.G. Barrett, YN1 S.A. Cooper, MST1 K.O. Pelletier, MST1 R. J. Uebelacker, MST2 A.A. Anzelmo, MST2 D.A. Hutchinson, MST2 R.L. Franco, MST2 J.K. Silves, MST3 W.A. Henry, MST3 K.A. Martin, MST3 C.F. Weiller.

Appendix A
List of Participating Vessels

VESSEL NAME	FLAG	SST	ICE REPORTS
ABITIBI CONCORD	FEDERAL REPUBLIC OF GERMANY		1
ACADIAN GAIL	CANADA		1
ACHILLES	SINGAPORE		6
ACT 7	UNITED KINGDOM		3
AIME GAUDREAU	CANADA		1
AKRANES	ICELAND		1
AKTEA	EGYPT		1
ALBRIGHT	UNITED KINGDOM		1
ALRAZIQ	REPUBLIC OF LIBERIA	9	
AMBASSADOR	UNITED KINGDOM		1
AMBROSE SHEA	CANADA		6
AMERICA EXPRESS	FEDERAL REPUBLIC OF GERMANY	1	1
AMERSHAM	PANAMA		2
AMITIBICORD	FEDERAL REPUBLIC OF GERMANY		1
ANANGEL HORIZON	GREECE		1
ARC MINOS	GREECE		2
ARCTIC	CANADA		1
ARCTIC SHIKO	UNKNOWN		1
ARGO 2	PANAMA	1	
ARTHUR W. RADFORD	UNKNOWN		1
ATLANTIC SERVICE	FRANCE		1
ATLANTIC STAR	SINGAPORE		4
BADAK	LIBERIA		3
BAKAR	LIBERIA	3	
BARTLETT	CANADA		11
BARWA	LIBERIA	7	
BEAUSONGE	MAURITIUS		2
BELLE ETOILE	MAURITIUS	2	2
BHAVABHUTI	INDIA	1	1
BISCHORSTOR	PANAMA		1
BIYO MARU	JAPAN		1
BOEFJORD	PHILIPPINES		1
BONAVISTA	UNKNOWN		1
BONNY	BAHAMAS	8	3
BORIJINIBA	UNKNOWN	1	
BOWDRILL 3	CANADA		2
BOXY	SWEDEN		4
BRANT POINT	UNITED KINGDOM		4
BRISTOL MARU	JAPAN		1
BRITISH STEEL	UNITED KINGDOM		6
BUDAPESHT	SINGAPORE		1
CAMBRIDGE	PANAMA		1
CANADA MARITIME	SINGAPORE		2
CANADA MARQUIES	CANADA		1
CANADIAN EXPLORER	UNITED KINGDOM		7

VESSEL NAME	FLAG	SST	ICE REPORTS
CANMAR AMBASSADOR	CANADA		5
CANMAR (DART) EUROPE	BELGIUM		4
CANMAR VENTURE	UNITED KINGDOM		1
CANTIHOLANDIA	FEDERAL REPUBLIC OF GERMANY	1	
CAPE BALLARD	CANADA		1
CAPE NORTH	CANADA		5
CAPE RACE	UNITED KINGDOM	3	
CAPE ROGER	CANADA		3
CAPITAN CHUKACHIN	UNKNOWN		1
CARAVEL STAR	PANAMA		1
CAST CARIBOU	LIBERIA	14	7
CAST HUSKEY	UNITED KINGDOM		4
CAST MUSKOX	UNITED KINGDOM		1
CAST OTTER	UNITED KINGDOM		2
CAST POLAR BEAR	LIBERIA	9	5
CHARLOTTE CASTIAN	FEDERAL REPUBLIC OF GERMANY		1
CHEMICAL TRANSPORT	CANADA		2
CHESTNUT HILL	USA		1
CHIBA	UNITED KINGDOM		1
CHIGNECTO BAY	CANADA		3
CHIPPEWA	LIBERIA		1
COMFORT COVE	CANADA		2
CUNARD	UNKNOWN		1
DANIELA	BRAZIL		2
DANILOVGRAD	YUGOSLAVIA		2
DART ATLANTIC	UNITED KINGDOM		1
DART BRITIAN	UNITED KINGDOM		1
DONNY	SWEDEN		2
DORIS	FEDERAL REPUBLIC OF GERMANY		1
DUESSELDORE EXPRESS	FEDERAL REPUBLIC OF GERMANY		1
EASTERN SHELL	UNKNOWN		1
EASTERN UNICORN	PANAMA	1	1
ESPANA 1	FEDERAL REPUBLIC OF GERMANY	1	
EUROPE	BELGIUM		5
EVA	FRANCE	1	1
EVERGREEN	USA	15	1
FALCON	NORWAY		1
FALKNES	NORWAY		1
FARLAND	UNITED KINGDOM		1
FARNES	LIBERIA		1
FEDERAL DANUBE	BELGIUM		3
FEDERAL HURON	PANAMA	1	2
FEDERAL LAKES	USA		3
FEDERAL MAAS	BELGIUM		5
FEDERAL OTTAWA	BELGIUM		1

VESSEL NAME	FLAG	SST	ICE REPORTS
FEDERAL RHINE	LIBERIA		1
FEDERAL SCHELDE	LIBERIA	3	
FEDERAL THAMES	BELGIUM		2
FERNGOLF	LIBERIA		1
FERNWAVE	LIBERIA	1	
FINNARCTIS	UNITED KINGDOM		1
FINNFIGHTER	FINLAND		5
FINNPOLARIS	UNITED KINGDOM		2
FINNSNES	LIBERIA		1
FINNWHALE	UNKNOWN		1
FJELLNESS	PANAMA		1
FJORD MARINER	PANAMA		2
FORT VICTORIA	UNITED KINGDOM		1
GIZHIGA	USSR		1
GOLDEAN PIONEER	PHILIPPINES		1
GOLDEN GATE SUN	SINGAPORE	2	
GRENFELL	CANADA		1
GUNRUN MAERS	DENMARK	1	
HIBISCUS	MAURITIUS		1
HOLCAN ELBE	FEDERAL REPUBLIC OF GERMANY		2
HOLCAN MAAS	FEDERAL REPUBLIC OF GERMANY		2
HUDSON	CANADA		14
HUMBER ARM	LIBERIA		4
IBERITA	UNITED KINGDOM		2
IMPERIAL ACADIA	CANADA		3
IMPERIAL ST. CLAIR	CANADA		5
IVAN TEVOSYAN	UNKNOWN		1
IRVING CEDAR	UNITED KINGDOM		1
IRVING OURS POLARIS	CANADA		2
JACKMANN	CANADA		1
JADE KIM	PANAMA		2
JENNA	GERMAN DEMOCRATIC REPUBLIC		1
JOHANNA	FEDERAL REPUBLIC OF GERMANY		1
JOHN C. HELMSING	CYPRUS		2
JOKUFELL	ICELAND		1
JUGOAGEN	YUGOSLAVIA		
KAMENITZG	BULGARIA		1
KANGUK	CANADA		6
KHAIRPUR	PAKISTAN		1
KIISLA	FINLAND		1
K. OLSHANSKY	USSR		1
KRISTINA LOGOS	CANADA		1
L. ROSETTE	CANADA		4
LAKE ANINA	NORWAY		1
LAKE SHELL	CANADA		2

VESSEL NAME	FLAG	SST	ICE REPORTS
LAWRENCE H. GIANELLA	UNKNOWN	21	
LE CREDE NO. 1	CANADA		4
LENINSK	USSR		3
LEONARD J. COWLEY	UNKNOWN		5
LOK VIHAR	INDIA		1
LUCIEN PAQUIN	CANADA		2
LYRA	POLAND		1
M. W. NEAL	UNITED KINGDOM		1
MAGRITTE	BELGIUM		3
MAHONE BAY	CANADA		1
MANCHESTER CHALLENGE	UNITED KINGDOM		7
MARIA B.	UNKNOWN		2
MARIA OLDENDORFF	PANAMA	7	
MAVRO VETRANIC	INDIA	3	1
MELLA	PANAMA	5	2
MELISSA MARY	LIBERIA		2
MICHELLE C.	PANAMA	8	
MIJDRECHT	NETHERLANDS		1
MIRABELLA	NETHERLANDS ANTILLES		1
MONTCALM	FRANCE	1	1
MOSEL ORE	LIBERIA		5
MYRSINIDI	LIBERIA		4
NARWIK 2	POLAND		2
NAVIOS COURIER	LIBERIA	4	
NEDRILL	NETHERLANDS		1
NEWFOUNDLAND HAWK	CANADA		1
NORDSTAR	SINGAPORE		1
NORTH WIND	USA	71	
NORTHERN PRINCESS	UNKNOWN		1
NORTHERN SHELL	CANADA		2
NORTRANS ELMA	PANAMA	3	
OCEAN LINK	UNITED KINGDOM	3	
OFFSHORE HUNTER	UNKNOWN		2
OLYMPIC RAINBOW	GREECE		1
ONTADOC	CANADA		1
PARADISE SOUND	UNKNOWN		1
PASSAT	PANAMA		2
PAUL BUNYAN	USA		3
PAWEE	UNITED KINGDOM	2	
PEGGY	BAHAMAS	2	
PLACENTIA BAY	CANADA		5
POINT ARMUR	BAHAMAS	3	
PRINS FREDRIK HENDRIK	NETHERLANDS		1
PRINS MAURITS	NETHERLANDS		1
PRISTINA	YUGOSLAVIA		1

VESSEL NAME	FLAG	SST	ICE REPORTS
PUHOS	UNITED KINGDOM	7	3
RAINBOW HOPE	UNKNOWN		1
RANFORD	UNKNOWN		1
REED VOYAGER	PANAMA		4
ROBIN	FRANCE	1	1
SAAR PRE	LIBERIA		1
SAUNIERE	CANADA		1
SAYA	YUGOSLAVIA		1
SEA FORTH ATLANTIC	CANADA		2
SEA FORTH ISLAND	CANADA		1
SENTIS	UNITED KINGDOM		
SHOW OLYMPIA	PANAMA	5	1
SIR HUMPHREY GILBERT	CANADA		5
SIR ROBERT BOND	CANADA		21
SENHOR DOS MARANTES	PORTUGAL		1
SOUNION	CYPRUS		1
SPYROS ALEMOS	GREECE	1	
STAR	UNKNOWN		1
STEFAN BATONY	POLAND	4	4
STEPHANITOR	PANAMA		1
STOLT CASTLE	LIBERIA		1
STOLT TENACITY	LIBERIA		1
STOVE CAMPBELL	NORWAY	7	1
STUBBENHUK	FEDERAL REPUBLIC OF GERMANY		1
STUTTGART EXPRESS	FEDERAL REPUBLIC OF GERMANY		1
SUMMIT	LIBERIA	9	2
TELFAIR MARINER	LIBERIA		1
TEXACO BRAVE	CANADA		2
TOANUI	CANADA		1
TONGALA	UNITED KINGDOM		1
TRAWLER ZIDANI	UNKNOWN		1
TRINITY BAY	CANADA		1
TRONES	PANAMA		1
TUPPER	CANADA		1
VALCOURT	LIBERIA	1	
VARJAKKA	FINLAND	3	2
VASILI SURIKOV	USSR		1
VENTURA	FEDERAL REPUBLIC OF GERMANY		1
VESALIUS	BELGIUM		1
VIKING HARRIER	SINGAPORE		1
VIKING OSPREY	SINGAPORE	1	1
VJAZMA	USSR	3	1
VOLGA	UKRANIAN SSR		2
VOLNA	USSR		1
WHIDBEY ISLAND	UNKNOWN		1

VESSEL NAME	FLAG	SST	ICE REPORTS
WINNA	UNKNOWN		1
WORLD CONTAINER	PANAMA		2
YAMAHMEMARU	JAPAN	4	1
YAYAMARIA	JAPAN		1
YUKONA	CYPRUS		1
ZAMBIA	LIBERIA		8
ZEILA	UNKNOWN		1
ZIEMIA GNIEZMIESKA	POLAND		1
ZIEMIA KRAKOWSKA	POLAND		1
ZIEMIA OLSZTYNSKA	POLAND		1
ZIEMIA ZAMOJSKA	POLAND	6	
ZIM SAVANNAH	ISRAEL		1

Appendix B

TIROS Oceanographic Drifter Tracks on the Grand Banks During the 1986 International Ice Patrol Season

LT Iain Anderson, USCG

Introduction

During the 1986 International Ice Patrol season, nine TIROS Oceanographic Drifting buoys were deployed in the Ice Patrol operating region. Three of the nine drifters were used exclusively for data gathering in conjunction with the IIP-1-86 cruise and these data are discussed in Appendix C. Of the six buoys used operationally, five were deployed by HC-130 aircraft during regular ice reconnaissance flights. The sixth was deployed by USCGC EVERGREEN as part of IIP-1-86 cruise and was not recovered so that its track could be used operationally.

An oceanographic cruise was conducted using USCGC EVERGREEN (WMEC 295) from 22 April until 22 May 1986. The primary objective of the cruise was to provide surface truth data for an airborne radar study of an oceanic front south of Flemish Cap. The results of the cruise are discussed in Appendix C.

The International Ice Patrol uses drifting buoys for real-time current information for weekly updates to the historical current field used in its iceberg drift model (Summy and Anderson, 1983 and Summy, 1982). Drifters are deployed for operational use in areas of high iceberg density and in areas of high variability in the current field to improve drift prediction. All of the drifters except drifter 4547 were deployed to monitor the variability of the Labrador Current. Drifter 4547 was deployed near the end of the Ice Patrol season in the area of the highest remaining iceberg concentration.

All of the buoys deployed by Ice Patrol are three meters long and have a spar-shaped hull with a flotation collar. They are equipped with a sea surface temperature sensor, a drogue tension sensor, and a battery voltage monitor. The temperature sensor is located approximately one meter below the surface. Each drifter is deployed with a 2m by 10m window shade drogue attached to the drifter by a 50m tether. An average of nine positions per day was received from each operational drifter with position accuracy of approximately 300m (Bessis, 1981) The positions and sensor data points are evenly distributed in time except for the period between 00Z and 04Z when virtually no data are received. This null data period is due to the orbits of the NOAA series satellites.

As of 30 September 1986, no drifter remained transmitting in the Ice Patrol region (Table B-1). Two drifters (4542 and 4547) were recovered intentionally by Coast Guard cutters. Drifter 4557 was picked up by an unknown vessel. Drifter 4552 stopped transmitting 28 days after deployment. The remaining two drifters (4543 and 4549) are still drifting across the North Atlantic, providing data outside the Ice Patrol region.

All air-launched buoys deployed properly except 4552. Its parachute opened but the wooden frame holding the buoy broke apart in the air. Because of this the parachute did not cut free from the buoy after splashdown. The remainder of the air-dropped drifters deployed properly and the parachutes released from the drifter packages.

The following section describes the data from the satellite-tracked buoys used by Ice Patrol during the 1986 iceberg season. It is not intended as an exhaustive data analysis. The data are archived at the International Ice Patrol, Avery Point, Groton, CT 06340.

Buoy Trajectories

The tracks of the operational buoys are discussed below in chronological order based on the deployment date. The numbers in parenthesis following dates are year dates (numbered sequentially from 1 January through 31 December).

4543

Buoy 4543 was deployed on 26 March 1986 (85) from an HC-130 aircraft in the Flemish Pass at 46°59.3'N 47°19.6'W (Figure B-1a). After deployment, it moved southwesterly, following the bathymetry, with an average speed of 61 cm/s until it encountered an oceanic front on 30 March (89). (This front was the focus of IIP-1-86 cruise and is dis-

Table B-1. 1986 Buoy Summary

Number	Date	Deployment Method	Position	Status	No. of days in IIP Area/Total
4543	26 MAR	C-130	46°59.3'N 47°19.6'W	Still transmitting	110/188
4542a	16 APR	C-130	47°01.1'N 47°19.7'W	Recovered 3 MAY(1)	17/17
4542b	5 MAY	EVERGREEN	46°58.2'N 47°18.5'W	Recovered 17 MAY(1)	13/13
4557	12 MAY	EVERGREEN	45°10.2'N 47°18.8'W	Recovered 14 JUL(2)	63/63
4549	16 MAY	C-130	48°25.0'N 49°29.3'W	Still transmitting	52/137
4552	30 MAY	C-130	48°10.0'N 48°55.0'W	Stopped 27 JUN	28/28
4547	12 JUN	C-130	50°59.0'N 53°00.0'W	Recovered 26 AUG(3)	75/75

Notes:
(1) Recovered and /or redployed by USCGC EVERGREEN.
(2) Picked up by an unknown vessel.
(3) Recovered by USCGC NORTHWIND.

cussed in Appendix C.) It drifted in an easterly direction along the north side of the front at an average speed of 12 cm/s until 9 April (99) when the temperature increased from about 0.8°C to 2.8°C in one day. Buoy 4543 accelerated to 47 cm/s from 9 April through 19 April (109). After 19 April, it moved in a northerly direction at 31 cm/s until it became entrained in an anticyclonic (warm core) eddy north of Flemish Cap on 8 May (128). Based on the buoy trajectory, the eddy was centered near 50°N 46°W and had no substantial translation. The approximate diameter of the eddy as defined by the buoy track was 95 km. Buoy 4543 averaged 40 cm/s while completing five loops of the eddy. It departed the eddy on 25 June (175) and drifted northeasterly, passing east of 39°W (the eastern boundary of the Ice Patrol operations area) on 14 July (195). The drogue sensor indicated the drogue remained attached throughout the period described above. As of 30 September 1986, buoy 4543 was still transmitting as it moved eastward across the North Atlantic.

4542

Buoy 4542 was used twice during 1986. The two deployments are referred to as 4542(a) and 4542(b).

Buoy 4542(a) was deployed by an HC-130 on 16 April 1986 (106) in the Flemish Pass in position 47°01.1'N 47°19.7'W (Figure B-1b). It drifted south with the Labrador Current at an average speed of 32 cm/s until 25 April (115) when it encountered an oceanic front. It drifted in an easterly direction at an average speed of 63 cm/s along the front until 30 April (120). On that date, 4542(a) turned northwest, still along the front, and drifted at 46 cm/s until recovered by USCGC EVERGREEN on 3 May (123).

Buoy 4542(b) was redeployed from EVERGREEN on 5 May 1986 (125) in the Flemish Pass in position 46°58.2'N 47°18.5'W. It drifted south along the bathymetry at 37 cm/s until encountering the front again on 11 May (131). It then moved easterly along the front at an average speed of 53 cm/s until 13 May (133) when it turned north and slowed to 8 cm/s. Drifter 4542(b) was recovered by EVERGREEN on 17 May (137). The drogue remained attached to drifter 4542 throughout both deployments, and this fact was accurately reported by the drogue sensor.

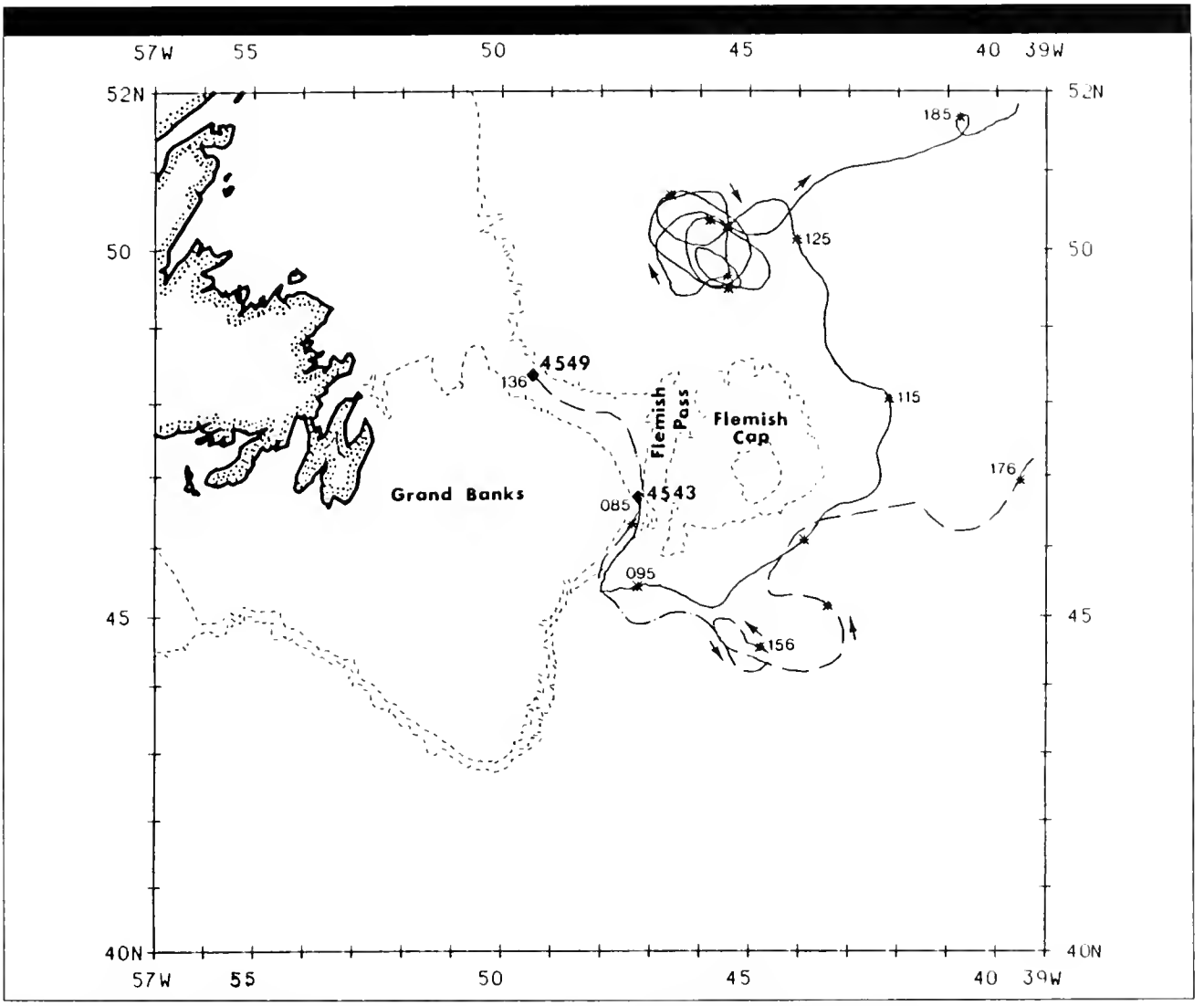

Figure B-1a Drift trajectories of buoys 4543 and 4549, marked with Julian dates.

4557

Buoy 4557 was deployed in a warm core eddy (45°10.2'N 47°18.8'W (Figure B-1b)) on 12 May 1986 (132) from USCGC EVERGREEN as part of an oceanographic study. It remained in the eddy for three revolutions as the eddy migrated to the east at about 4 km/day until 7 June (158). Based on the buoy track, the average diameter of the eddy was 70 km and within the eddy, drifter 4557 averaged 34 cm/s. Except for two short periods, the temperature reported by drifter 4557 was about 12°C while in the eddy. In the first, a 24-hour period on 25 May, the temperature decreased to about 7°C and then retumed to 12°C. The drifter motion was not affected, suggesting that the cold water encountered was only a surface feature. During the second, a 48-hour period beginning on 30 May, the temperature decreased to about 6°C and then returned to 12°C. The direction of the drifter was apparently unaffected but the average speed nearly doubled, to 65 cm/s.

After leaving the warm core eddy on 7 June (158), 4557 moved eastward until 10 June (161) when it entered a cyclonic (cold core) eddy. In a 24 hour period, the temperature dropped from 12°C to 7°C. Drifter 4557 maintained its cyclonic motion until 23 June (174), completing two loops in the eddy. While in the cyclonic eddy, 4557's speed ranged from 11 cm/s to 133 cm/s, averaging 76 cm/s. Between 19 June (170) and 23 June (174), the temperature again rose to 12°C but the motion of the drifter did not change. The motion of 4557 between 23 June and 26 June (177) was very sluggish with velocities averaging 12 cm/s and inconsistent direction. On 26 June, the temperature increased

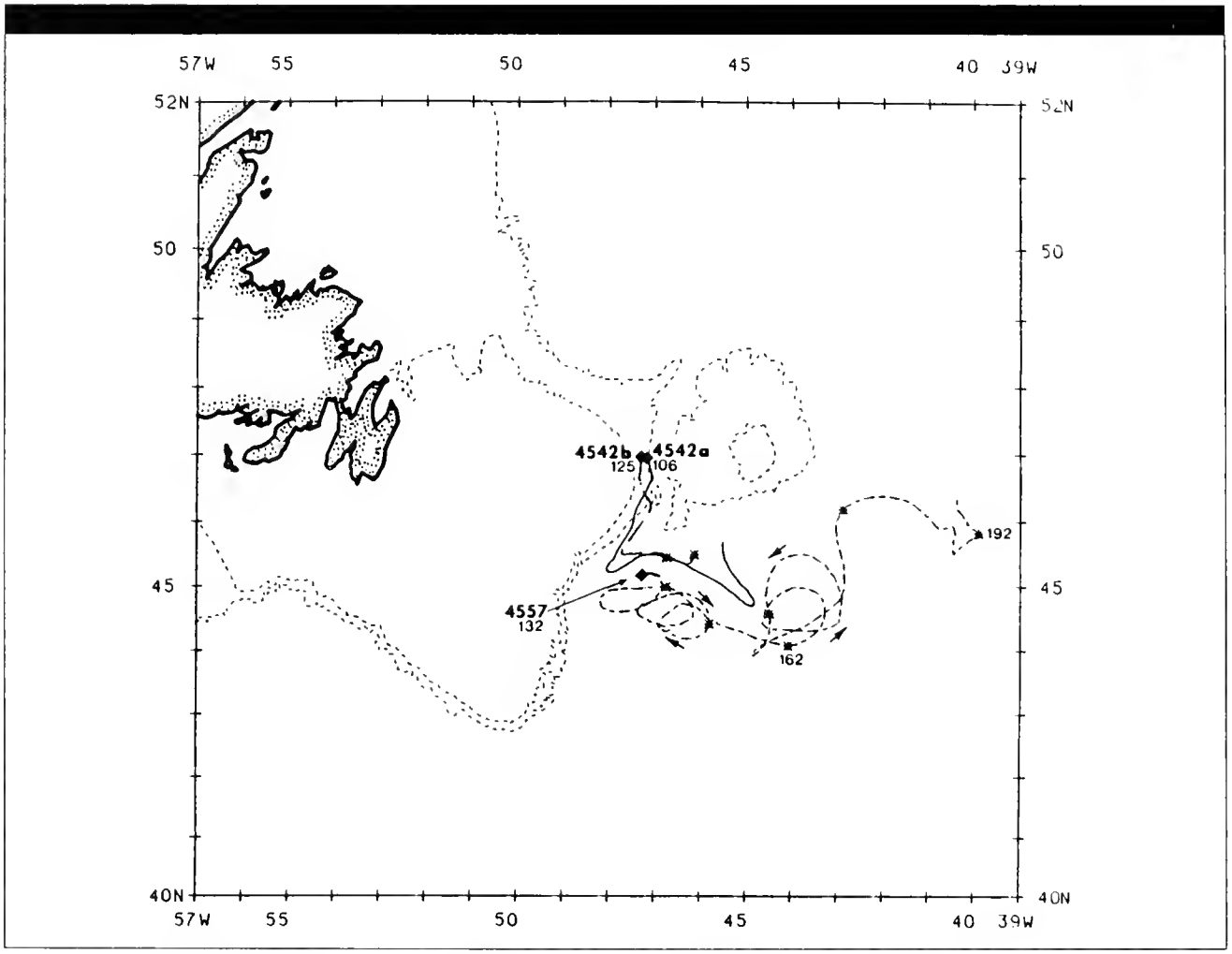

Figure B-1b Drift trajectories of buoys 4542 and 4557, marked with Julian dates.

by 2°C and 4557 was apparently caught in the North Atlantic Current and drifted towards the northeast at 45 cm/s. On 14 July (195), 4557 was picked up by an unknown vessel. The drogue sensor indicated the drogue was attached throughout its deployment.

4549

Buoy 4549 was deployed from an HC-130 north of the Grand Banks on 16 May (136) in position 48°25.0'N 49°29.3'W (Figure B-1a). It moved southward following the bathymetry at an average speed of 42 cm/s until it encountered an oceanic front on 29 May (149). The average speed of drifter 4549 increased to 65 cm/s as it travelled along the front. On 4 June (155), drifter 4549 began a small cyclonic loop. The average speed of drifter 4549 during the loop was 31 cm/s. On 13 June (164), it accelerated to an average of 96 cm/s and began a large cyclonic loop. This motion continued until 16 June (167). There was an increase from 7°C to 9°C when the motion stopped. The large cyclonic loop coincided temporally and spatially with the cyclonic eddy observed along the track of drifter 4557. Drifter 4549 moved to the north at an average speed of 30 cm/s until 19 June (170). It then accelerated to an average speed of 74 cm/s and drifted northeasterly, departing the Ice Patrol region on 27 June (178). The drogue sensor indicated the drogue was attached throughout its drift in the Ice Patrol region. As of 30 September 1986, the buoy was still transmitting.

4552

Buoy 4552 was deployed from an HC-130 north of the Grand Banks on 30 May 1986 (150) in position 48°10.0'N 48°55.0'W (Figure B-1c). It drifted south with the Labrador Current approximately following the bathymetry at an average speed of 40 cm/s until 15 June (166). It then nearly reversed direction and drifted in a northerly direction at about 25 cm/s until 27 June (178). No data were received after 27 June. There is no evidence in the data to suggest the reversal of direction was caused by the buoy being picked up by a vessel. The temperature sensor did not provide reliable data throughout the deployment. The drogue sensor indicated the drogue was attached throughout period

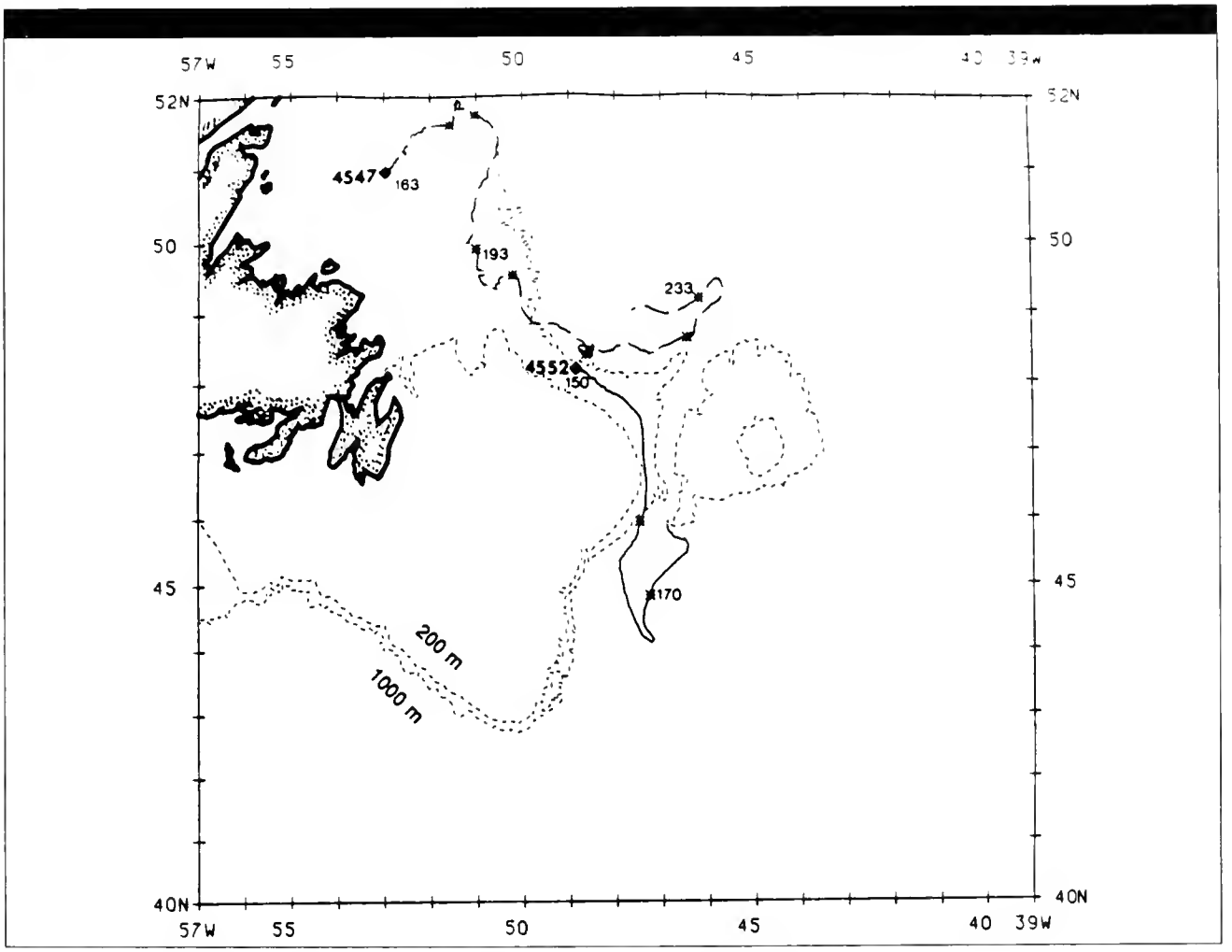

Figure B-1c Drift trajectories of buoys 4547 and 4552, marked with Julian dates.

described above. The fact that the parachute did not cut free after the buoy entered the water means that the buoy also had a near-surface parachute drogue. It is likely that the parachute wrapped around the buoy hull as happened with a 1985 buoy (Anderson, 1985). Although the track of 4552 should be viewed with caution, the fact that the parachute remained attched to the buoy is probably not an important factor.

4547

Buoy 4547 was deployed from an HC-130 on 12 June 1986 (163) in the northwestern section of the Ice Patrol region in position 50°59.0'N 53°00.0'W (Figure B-1c). After its deployment, 4547 drifted northeast at 16 cm/s until 1 July (182). On 1 July, it moved south then east with the Labrador Current until about 9 August (221). On this date, the temperature increased from about 9°C to 11°C and drifter 4557 moved northeast and then southwest at 21 cm/s until its recovery by USCGC NORTHWIND on 26 August (238).

The drogue sensor indicated the drogue became disconnected on the day after its deployment. When the buoy was recovered by NORTHWIND on 26 August 1986 (238) only about 10 meters of the tether still attached to the drifter. Inspection of the tether after recovery indicated the tether may have been cut. The prolonged low and inconsistent direction of the drift indicated early drogue loss during the deployment. This was another case where the drogue sensor reliably reported the drogue status.

Discussion

The tracks from this year's drifters illustrate the current variability of the Ice Patrol region. The presense of the oceanic front south of the Flemish Cap greatly influenced the movement of all drifters coming through Flemish Pass. In past years, drifters moving south through Flemish Pass have gone as far south as 42°N (Anderson 1984 and 1985). This year the farthest south a drifter travelled was about 44°N (4552). This difference can be attributed directly to the front.

Buoy 4543 entered an anticyclonic eddy north of Flemish Cap. Eddies in this location have been observed in previous years (Anderson 1983 and 1985). This eddy and the front south of Flemish Cap were dominant sources of departure from the Ice Patrol normal current field during the 1986 season.

The velocity distributions of the majority of this year's drifters are very similar except for the peaks at the high velocity end (greater than 100 cm/s) of the distribution for buoys 4557 and 4549 (Figure B-2). Drifter 4549's high velocity peak was the result of its entrainment in the North Atlantic Current. The high peak of drifter 4557 coincided with the time it spent in a cyclonic eddy. The main peak of the distribution of drifter 4547 is shifted to the left towards a lower speed than the others. This shift in the peak coincide with the loss of the drogue from drifter 4547.

Figure B-2 Frequency distribution of buoy drift velocities, by percent.

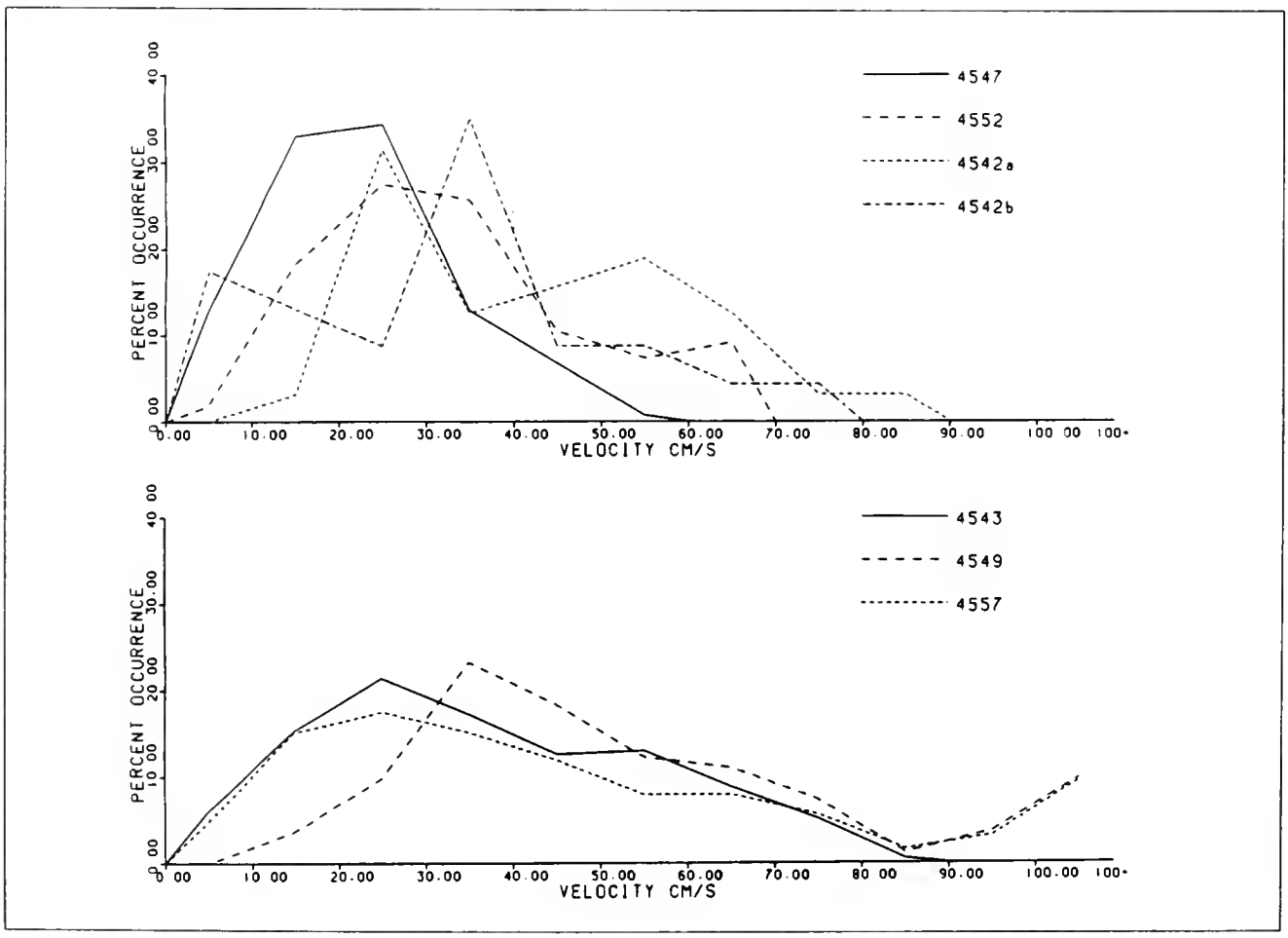

Conclusion

Ice Patrol has now been using satellite-tracked buoys for 5 years to provide near real-time current data for its iceberg drift prediction model. This year is a good example of the importance of this near real time input. Without weekly drifter data input, Ice Patrol would have been using historical mean currents to predict the motion of icebergs. Using historical currents, icebergs in the Labrador Current would have been drifted south to 43°N. After modification by drifter data to the current field, icebergs in the Labrador Current were drifted south to only 45°N. The lack of drifter data could have resulted in a 190 km drift error.

The drogue sensor appears to be providing more reliable data than in the past. All five recovered buoys (including those used exclusively for the cruise), verified the drogue sensor data, with four attached and one disconnected drogue.

Ice Patrol plans to continue using drifting buoys for near real-time current data to update the historical current field. In areas of high current variability, real-time data are essential to accurate drift prediction.

Acknowledgements

I am grateful to Dr. R. L. Pickett of the Naval Oceanographic Research and Development Activity and Dr. Brian Petrie of Bedford Institute of Oceanography for their comments on this manuscript.

References

Anderson, I., 1983. Oceanographic Conditions on the Grand Banks During the 1983 Ice Patrol Season. Appendix B, Report of the International Ice Patrol Service in the North Atlantic. Bulletin No. 69, CG-188-38, U. S. Coast Guard, Washington, DC 20593-7399, 73 pp.

Anderson, I., 1984. Oceanographic Conditions on the Grand Banks During the 1984 Ice Patrol Season. Appendix B, Report of the International Ice Patrol Service in the North Atlantic. Bulletin No. 70, CG-188-39. U. S. Coast Guard, Washington, D.C. 20593-7399, 74 pp.

Anderson, I., 1985. Oceanographic Conditions on the Grand Banks During the 1985 Ice Patrol Season. Appendix C, Report of the International Ice Patrol Service in the North Atlantic. Bulletin No. 71, CG-188-40. U. S. Coast Guard, Washington, D.C. 20593-7399, 90 pp.

Bessis, J. L., 1981. Operational Data Collection and Platform Location by Satellite. Remote Sensing of Environment, Vol II: p 93-111.

Summy, A.D., 1982. Oceanographic Conditions on the Grand Banks During the 1982 Ice Patrol Season. Appendix B, Report of the International Ice Patrol Service in the North Atlantic. Bulletin No. 68, CG-188-37. U. S. Coast Guard, Washington, D.C. 20593-7399, 35 pp.

Summy, A.D. and I. Anderson, 1983. Operational Uses of TIROS Oceanographic Drifters by International Ice Patrol (1978 - 1982). Proceedings: 1983 Symposium on Buoy Technology, National Data Buoy Center, NSTL Station, MS 39529, pp. 246-250.

Appendix C

Observations of an Oceanic Front South of Flemish Pass

Donald L. Murphy
LT Iain Anderson
LTJG Neal B. Thayer

Introduction

In April and May 1986 International Ice Patrol (IIP) conducted a study east of the Grand Banks of Newfoundland in which airborne radar imagery of the sea surface was compared with surface-truth data. Sea surface roughness was mapped using a real aperture, X-Band, Side Looking Airborne Radar (SLAR) aboard an HC-130 aircraft; surface-truth measurements consisted of hydrographic measurements made from USCGC EVERGREEN (WMEC 295) and the trajectories of satellite-tracked drifting buoys.

The primary goal of the experiment was to determine how well and how reliably the IIP SLAR could detect water-mass boundries. A knowledge of the location of the major boundries in the IIP operations area (40°-50°N, 39°-57°W) is useful in predicting the motion of icebergs, an important part of IIP's responsibility.

The study focused on a warm core eddy spawned from, and interacting with the North Atlantic Current (NAC). No attempt is made to describe the dynamics of the eddy because the data are insufficient for such an effort. Indeed, neither the remotely-sensed data nor the hydrographic data define the eddy boundries completely and unambiguously. Only from the drifting buoy data is it clear that the feature is an eddy. The treatment of the oceanographic data is undertaken solely to help understand the SLAR imagery.

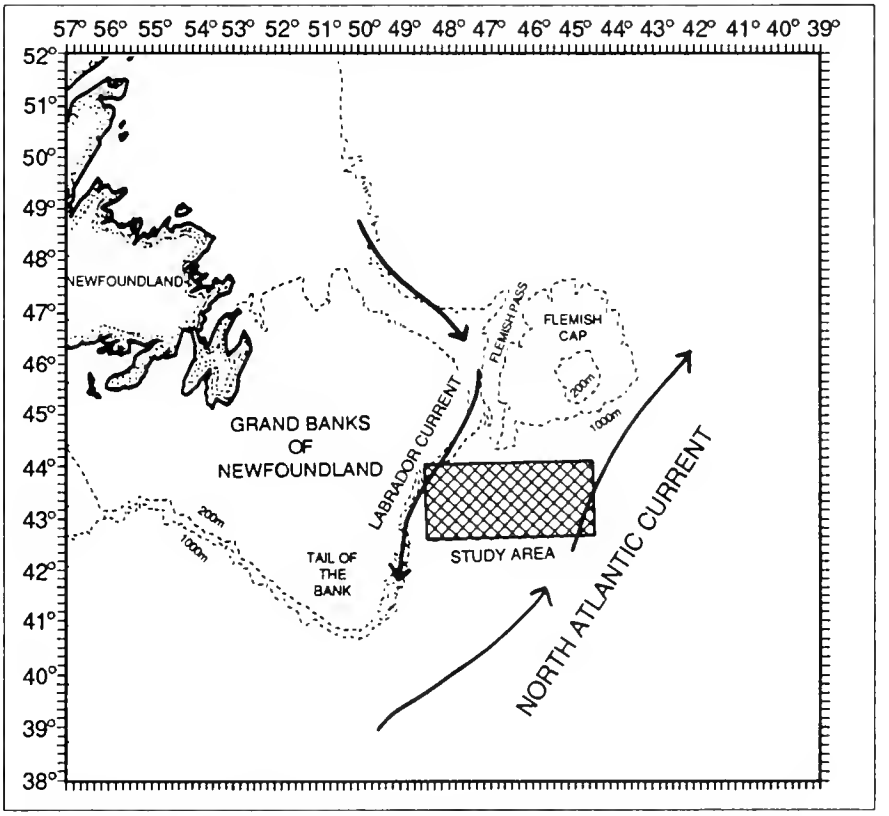

Figure C-1 Schematic of the major current systems near the Grand Banks of Newfoundland. The study area is shown by the shaded rectangle.

Background

Circulation in the North Atlantic Ocean east of the Grand Banks of Newfoundland is dominated by two major currents (Figure C-1): the southward-flowing, cold and relatively fresh (<2°C and <34.3 ppt) Labrador Current (LC) and the northeastward-flowing warm and more saline (>12°C and >35.5 ppt) NAC. The mean dynamic height field is reasonably well mapped, due in large part to the efforts of IIP, which conducted routine hydrographic surveys of the region from 1934 to 1978, excepting the years of World War II. From these data, maps of monthly mean dynamic height relative to the 1000 dbar level for April through June were developed by Soule (1964) and later updated by Scobie and Schultz (1976). Figure C-2, the mean dynamic topography for April, shows the narrow LC following along the eastern edge of the Grand Banks from Flemish Pass to the Tail of the Bank. The other months, May and June, show no

Figure C-2 Average dynamic topography for the month of April (from Scobie and Schultz, 1976).

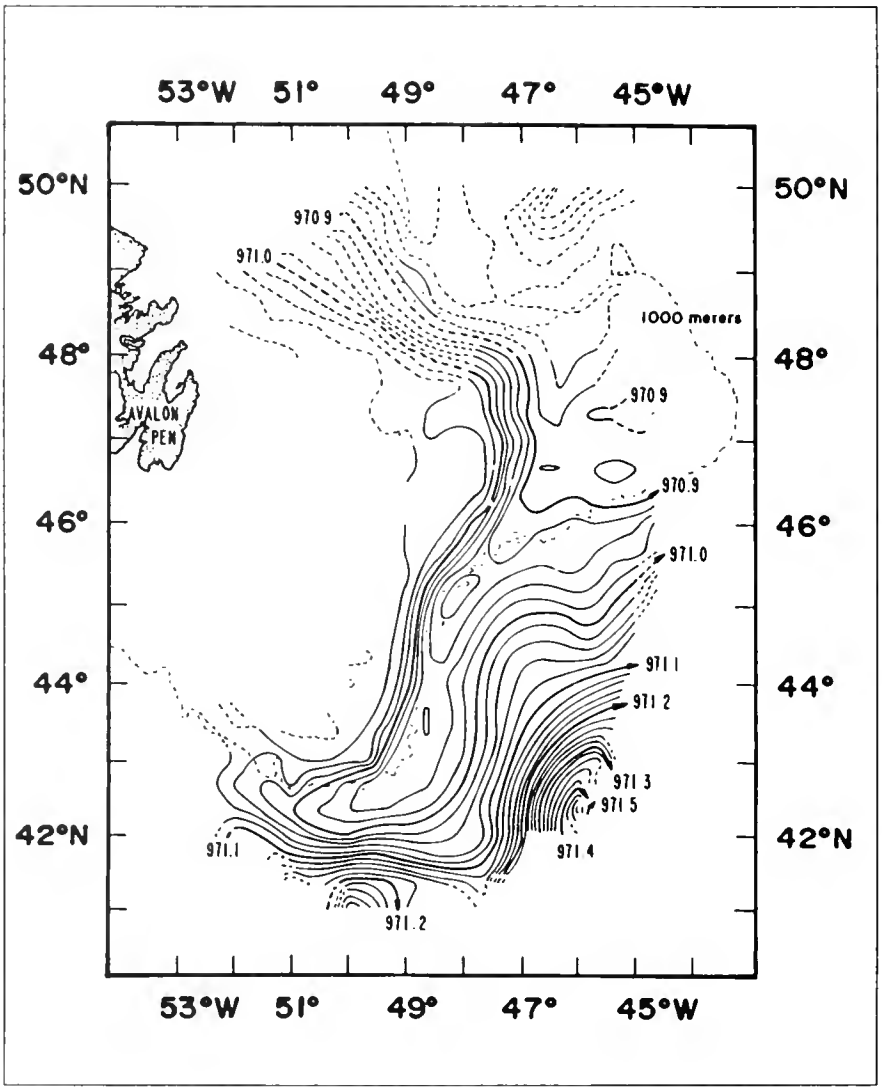

substantial departure from this distribution. Recognizing these similarities, IIP, in 1979, combined the monthly mean hydrographic fields and computed a single mean current field (Murray, 1979) for use in IIP's numerical iceberg drift model.

While the monthly mean dynamic topography represents the main features of the circulation, the averaging smooths out variations that may affect the circulation. For example, trajectories of satellite-tracked drifting buoys released in the LC (Anderson, 1983 and Anderson, 1984) suggest a much more complex flow pattern than the mean hydrography depicts. Figure C-3 summarizes the drift tracks of 17 buoys, deployed by IIP over a 10-year period (1976-1986), that passed through the study area. Although the tracks show the LC clearly, the most striking feature of the plot is the variability in the flow field. A further indication of variability in the area is shown by the map of standard deviation of dynamic height of the individual hydrographic surveys from the April mean (Figure C-4). The pattern of fluctuations in the standard deviation suggests that meanders and eddies of the NAC are major features, particularly in the eastern and southern areas where the standard deviation reaches 15 dyn-cm.

Little is known about the sizes and frequencies of NAC meanders or eddies in the study area, primarily because fog and clouds frequently prevent mapping of the ocean's features by satellite infrared (IR) imagery. Using the sparse IR data available, Williams (1985) studied the eddy population east of the Grand Banks. He found that eddies are frequently seen near the Newfoundland Seamounts and Ridge. He suggested that eddy generation is caused by the rapid changes in bottom topography, but there were insufficient data to form a complete history of an eddy.

Although IR mapping is limited by fog and clouds, satellite and airborne imaging radars, particularly the synthetic aperture radar (SAR) carried aboard SEASAT, are capable of all-weather detection of oceanic features such as fronts and internal waves (Fu and Holt, 1982; Hayes,1981). Using

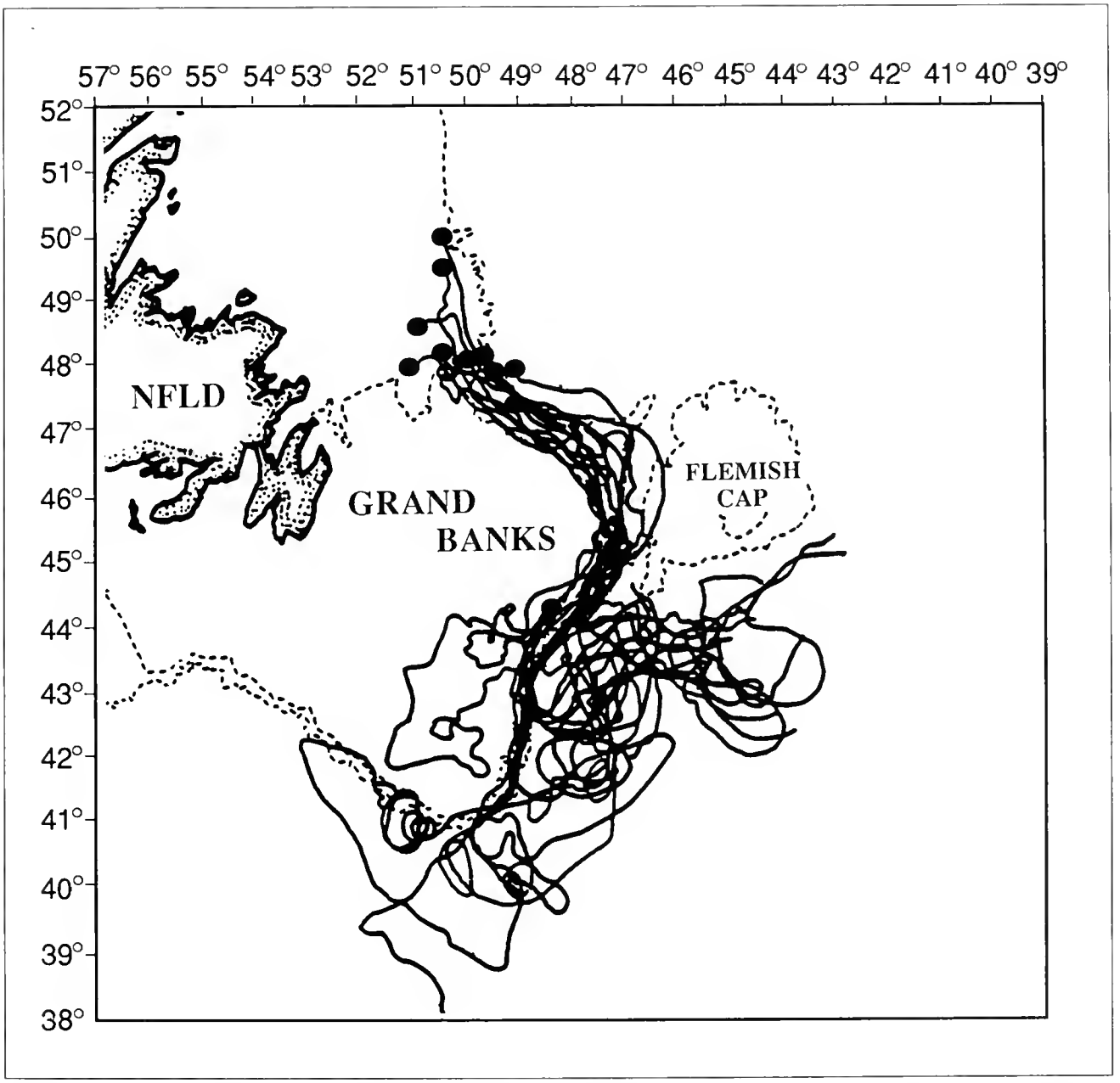

Figure C-3 Trajectories of 17 satellite-tracked buoys deployed by International Ice Patrol. The dots mark the launch positions.

SEASAT SAR data and a previous version of the IIP SLAR, LaViolette (1983) examined the ability of imaging radars to map oceanic features near the Grand Banks. He demonstrated that SLAR and SEASAT SAR showed similar features and that both radars could detect thermal fronts seen in the infrared imagery. He found, however, that in some cases the radar-defined fronts were not as sharp as those shown in the IR images. He recommended that since satellite SAR is currently unavailable and few aircraft-borne SAR's exist, SLAR-equipped aircraft should be used to improve the understanding of ocean processes.

Imaging radars map the sea-surface roughness through Bragg scattering (Robinson,1985), which for the 3-cm wavelength and incidence angles of the IIP SLAR, results in a sensitivity to ocean waves approximately 2-cm long. As a result, the IIP SLAR imagery of the ocean is essentially a map of the distribution of these 2 cm-long waves; the SEASAT SAR was sensitive to 30-cm wavelengths (Vesecky and Stewart, 1982). On both radars, differences in surface roughness are indicated on the

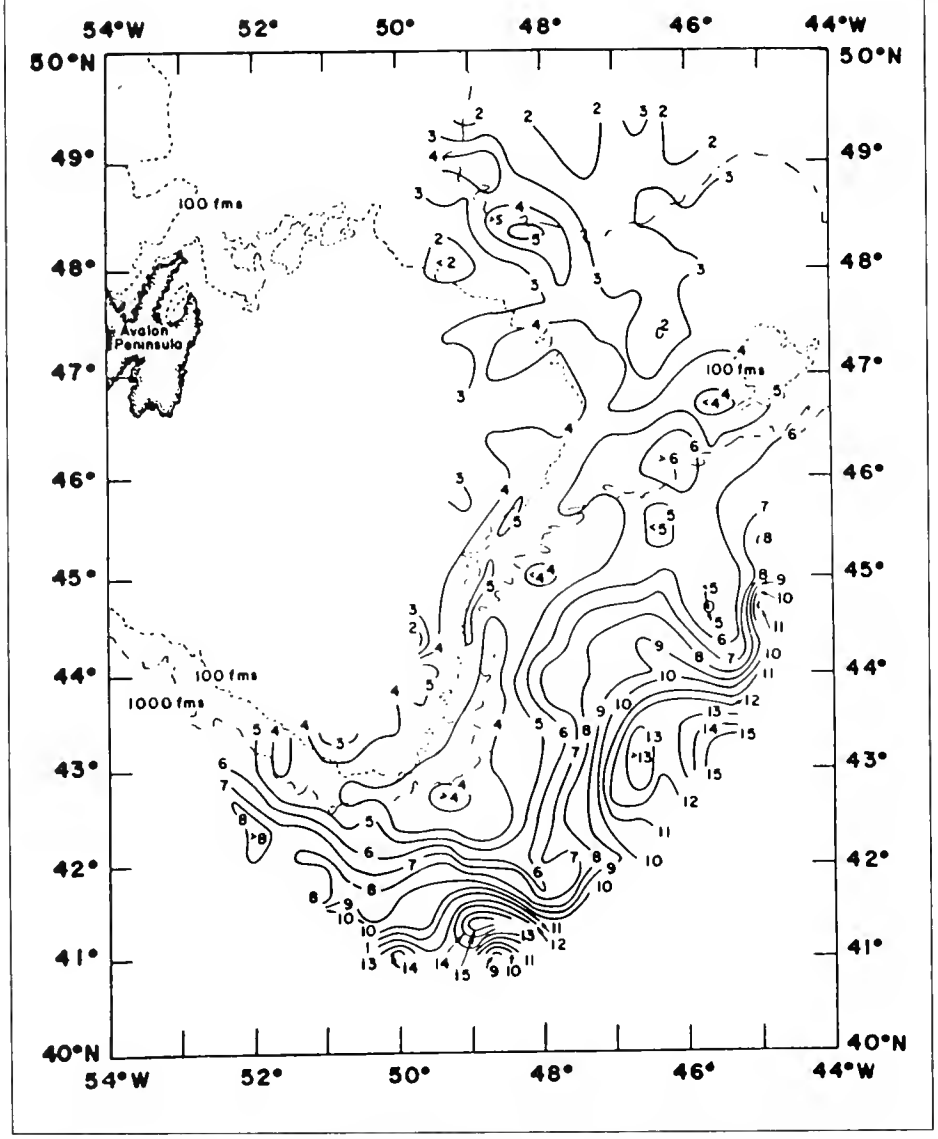

Figure C-4 Field of standard deviation of dynamic height of the individual surveys from the April normal. Contour interval is 1 dyn-cm (from Scobie and Schultz, 1976).

radar image as tonal changes. Thus, there are light and dark areas on the images that correspond to differences in the reflected radar energy.

Interpretation of the images requires an understanding of how wind stress, current gradients, etc. modulate short gravity waves on the ocean surface; but, our understanding is poor. Lichy *et al.* (1981), who tracked a warm core ring using SEASAT SAR data, found that within the warm water there was a more intense radar return than from the surrounding area.

This paper describes the results of a study of the circulation east of the Grand Banks of Newfoundland. Its goals were to collect surface-truth data for comparison of the remotely-sensed SLAR data and to investigate the effects of NAC meanders and eddies on the flow of the Labrador Current. Our intent was to locate a front using SLAR, examine the water property distribution and dynamics in the vicinity of the front with the ship, and compare the two. IIP's long-term goal is to use remote-sensing techniques to aid in iceberg movement prediction. IR imagery shows little promise near the Grand Banks because of clouds, but much can be learned from SLAR imagery. That information will help interpret future satellite SAR data and the occassional IR image.

Observational Program

Remote Sensing

SLAR imagery guided the hydrographic sampling program. The IIP SLAR is an X-band (3-cm wavelength), real-aperture radar that produces a continuous 9-inch (23 cm) analog (negative) image on a dry-process film. Because the IIP SLAR provides a negative image, areas of intense radar backscatter appear dark on the film. These dark areas mark regions where the sea surface is rough with 2-cm waves.

The aircraft, when flown at 8000 ft (2438 m), maps a 50 km wide swath on each side of the aircraft with a blind spot ~5 km wide directly under the aircraft (Figure C-5). Both of the antennas are vertically polarized. Navigational information from the HC-130's inertial navigation system (INS) is printed directly on the film.

Four aerial surveys, at approximately one-week intervals, mapped the features in the study area. The first survey (26 April 1986) covered 127,000 sq km and identified a site to conduct the hydrographic study. The three subsequent flights (2, 9, and 17 May 1986) each mapped 56,000 sq km with overlapping coverage.

On the last day of the experiment, the Advanced Very High Resolution Radiometer (AVHRR) on the NOAA 9 satellite provided the only usable IR image of the area.

Hydrography

Hydrographic sampling was divided into two phases. In the first, 26 April to 3 May, EVERGREEN occupied 68 stations in a 18x26 km grid. At each station water temperature and salinity profiles of the upper 1000 m of the water column were made using an internally-recording CTD. The station pattern was based on in-flight analyses of SLAR data. After reprovisioning, EVERGREEN returned to the study area for the second phase to repeat a similar pattern, but a winch failure after 28 CTD stations resulted in continuing the survey using only XBT's.

Over the ranges encountered in the study, the Neil Brown Internally-Recording CTD, has an accuracy of 0.01°C, 0.01 mmho and 0.5% of full scale in pressure up to 1000 dbar. Data were sampled at 5Hz, which for the 50m/min lowering rate resulted in conductivity, temperature and pressure data being collected every 0.2 dbar. Five scans of C,T, and P were averaged and recorded internally at approximately one dbar intervals. Salinity was computed using an algorithm based on Fofonoff (1985).

The primary method of navigation was LORAN-C, but when satellite-tracked buoys were aboard, their satellite-derived positions were also used to fix the ship's position.

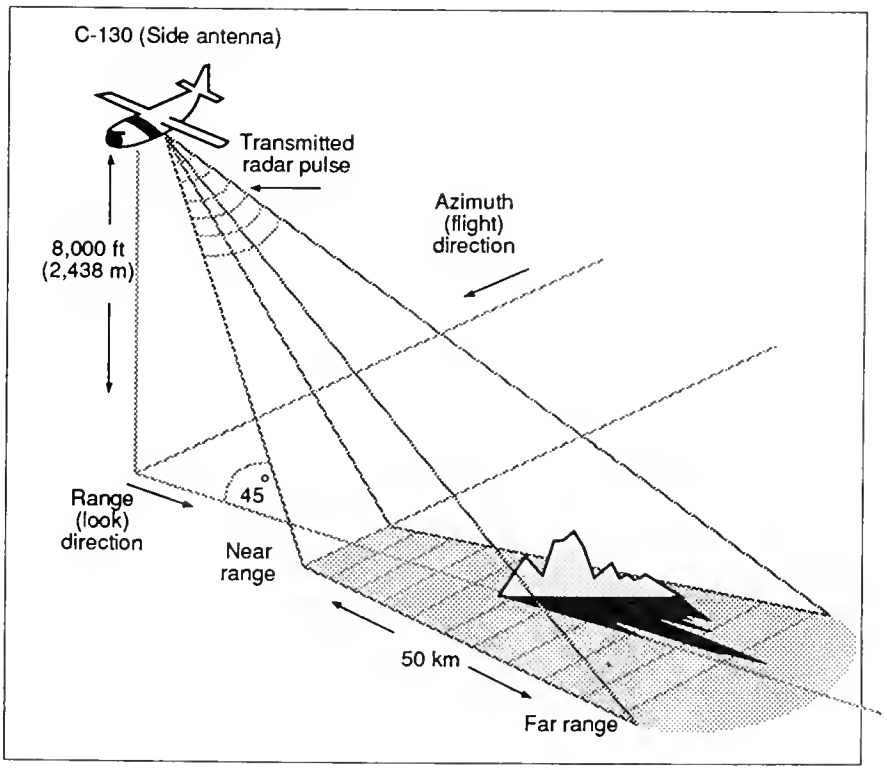

Figure C-5 Geometry of the International Ice Patrol Side-looking airborne radar (SLAR). Only one side is shown; the radar transmits and receives on both sides of the aircraft.

Drifting Buoys

In both phases, four satellite-tracked drifting buoys, each with a 2m x 10m window-shade drogue centered at 58m, were used to measure the currents. Tracked by System ARGOS, they provided 8-10 fixes (unevenly spaced in time) each day with a position accuracy of approximately 300m. The ARGOS system is described in detail by Bessis (1981). In addition to position, each buoy measured sea surface temperature at a depth of approximately 1m. All of the recovered buoys still had their drogues attached.

In the first phase, one buoy was deployed from an aircraft in the Labrador Current in Flemish Pass (47°N 47°20'W) and three were deployed by ship along the first hydrographic line (48°W). All four buoys were recovered after completion of the surveys.

As part of the second phase, EVERGREEN deployed a buoy in the Labrador Current in Flemish Pass (47°N 47°18'W) enroute to port. The buoy drifted into the study area at approximately the same time that the second hydrographic survey began. Three buoys were deployed during the surveys and before returning to port, three of the four buoys were recovered. The remaining buoy was left in the eddy. According to the drogue sensor on the buoy left in the eddy, its drogue remained in place until 7 July 1986.

Results

This section is divided into two parts. The first describes the SLAR imagery, with emphasis on the similarities and differences among the four surveys. Because some of the features on the SLAR film are difficult to reproduce photographically, the data are presented primarily in the form of digitized interpretations of the images. The second section compares the imagery with oceanic data that are derived from the hydrographic surveys and buoy tracks.

SLAR

Figure C-6, a photomosaic of the 26 April SLAR survey, shows what we interpret as the NAC, appearing as a dark region along the southern and eastern edge of the image. This is a negative image, thus the dark area represents high radar return. The area of the hydrographic study, enclosed by a box, is dominated by a sharply defined front that tends in the east-west direction. It appears to be the northern edge of a NAC meander or a newly-formed eddy that is interacting with the NAC. The SLAR imagery recorded changes in the shape and location of this feature over the subsequent three weeks (Figure C-7). In the following discussions this feature will be referred to as an eddy although the SLAR imagery is inconclusive. In no case was it possible to define all of the eddy boundaries because portions could not be located with certainty. In the cases when overlapping imagery permitted two determinations of sections of the eddy boundary , the positions agreed to about 5 km.

Although the tone of the images varied from survey to survey, the feature mapped in Figure C-7 was always characterized by greater radar return than the surrounding water. This is similar to the finding of Lichy *et al.* (1981), who found that within a warm core ring there was a more intense radar return than from the surrounding area; however, the differences were not as great as in the present SLAR data. Lichy *et al.* (1981) also

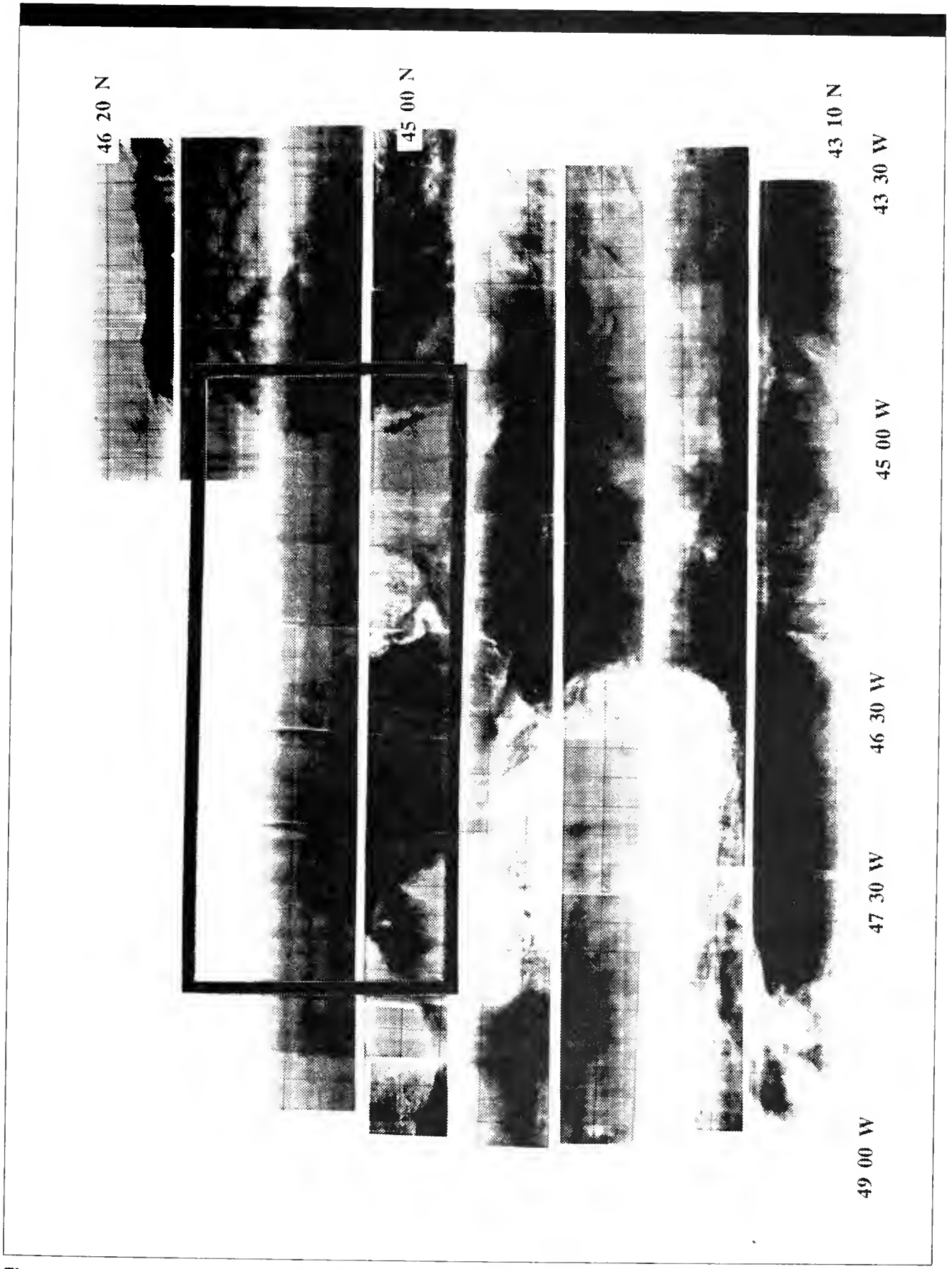

Figure C-6 Photomosaic constructed from the SLAR imagery of 26 April 1986.

Figure C-7 Digitized fronts depicted in the SLAR Imagery for: (a) 26 April; (b) 2 May.

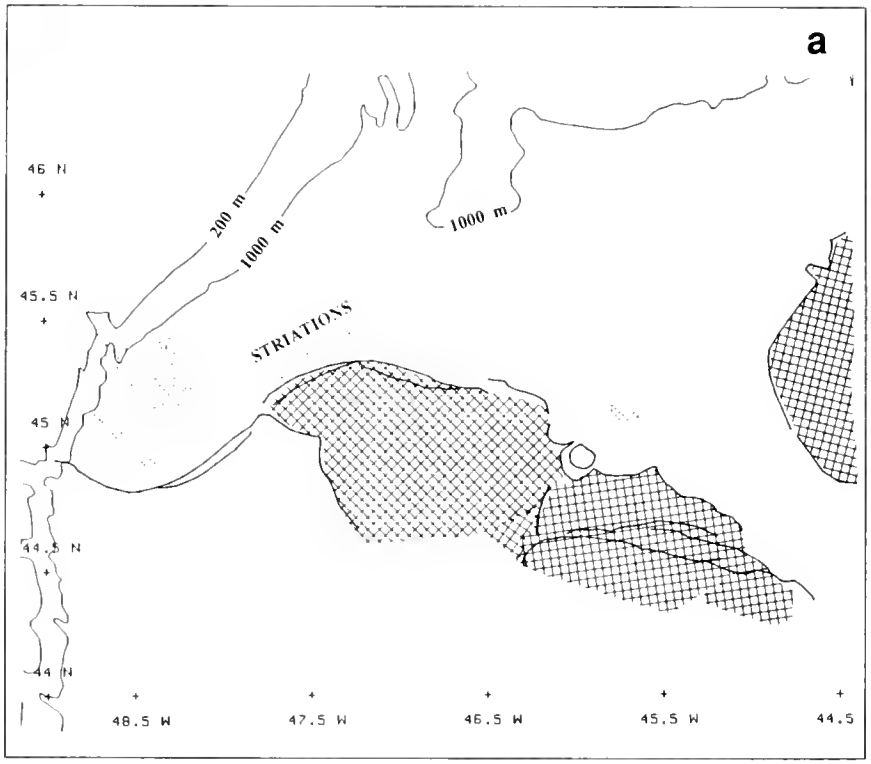

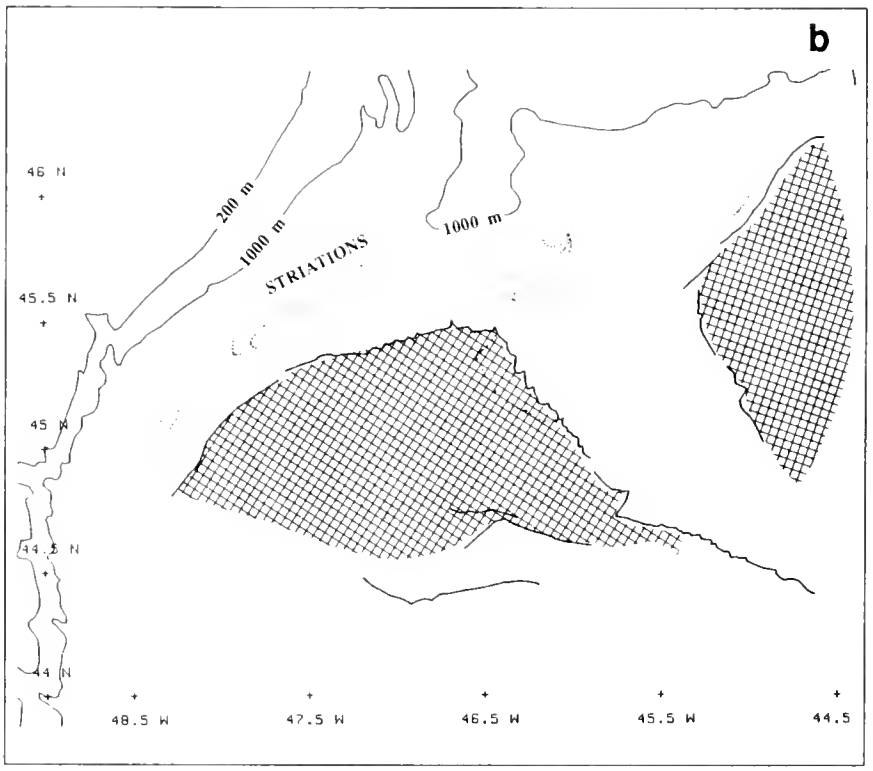

reported curved lines within the eddy. Such lines were never observed in the warm eddy water in the present study but in three of the four surveys (17 May excepted) there was a series of striations (lines) north of the eddy (Figure C-7). They were faint and patchy, but when they were present they were parallel to each other and approximately paralleled the northern boundary of the eddy. SEASAT SAR data also showed similar features, as reported by Cheney(1981) and Fu and Holt(1982), who suggested that the striations were parallel to the flow. There were no direct current observations in either study to confirm this.

Following the evolution of the eddy over the three-week period of observation was difficult for two reasons: first, the inability of the SLAR imagery to provide a closed boundary, and second, the complexity of an eddy interacting with the NAC and trapped against the Grand Bank and the Labrador Current. The location of the northern and eastern boundaries of the eddy was well-defined on both 26 April and 2 May SLAR surveys (Figures C-7a and b); however, in neither survey were the western and southern boundaries well defined. East of the eddy, the boundary of the NAC appeared to have moved about 30 km to the west during the six-day interval between the surveys.

The 9 May SLAR (Figure C-7c) survey provided the most complex and ambiguous images. The northernmost frontal location remained nearly unchanged. This survey provided the first good image of the southern portion of the eddy, as well as the best image of the striations north of the eddy. Unlike the patchy striations observed on the 26 April and 2 May surveys, they were widely distributed north of the eddy. Like the previous image, however, they were roughly parallel to the northern eddy boundary.

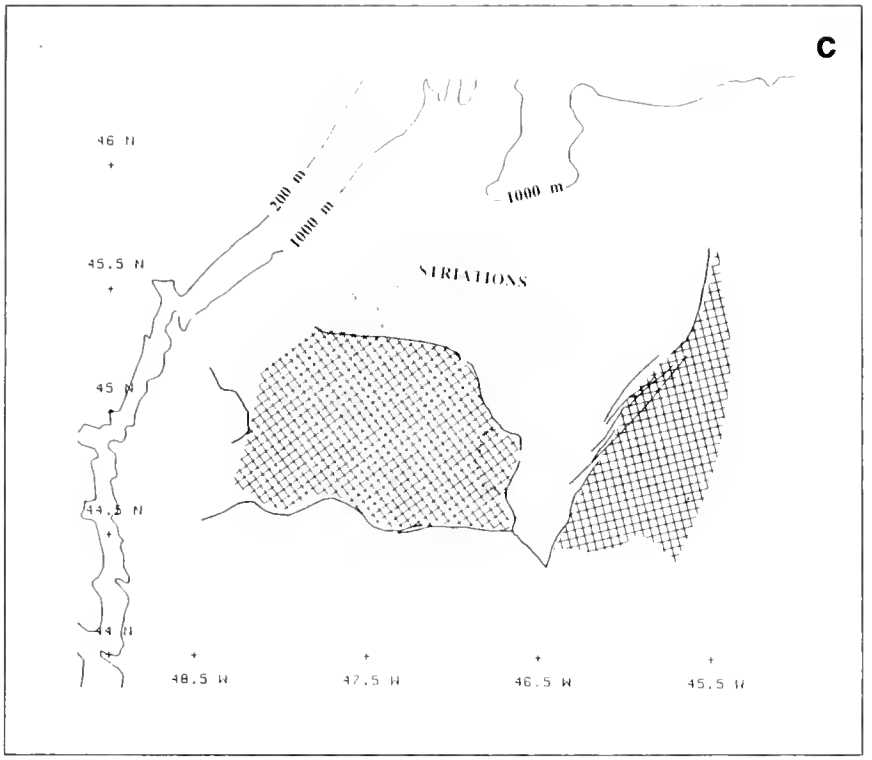

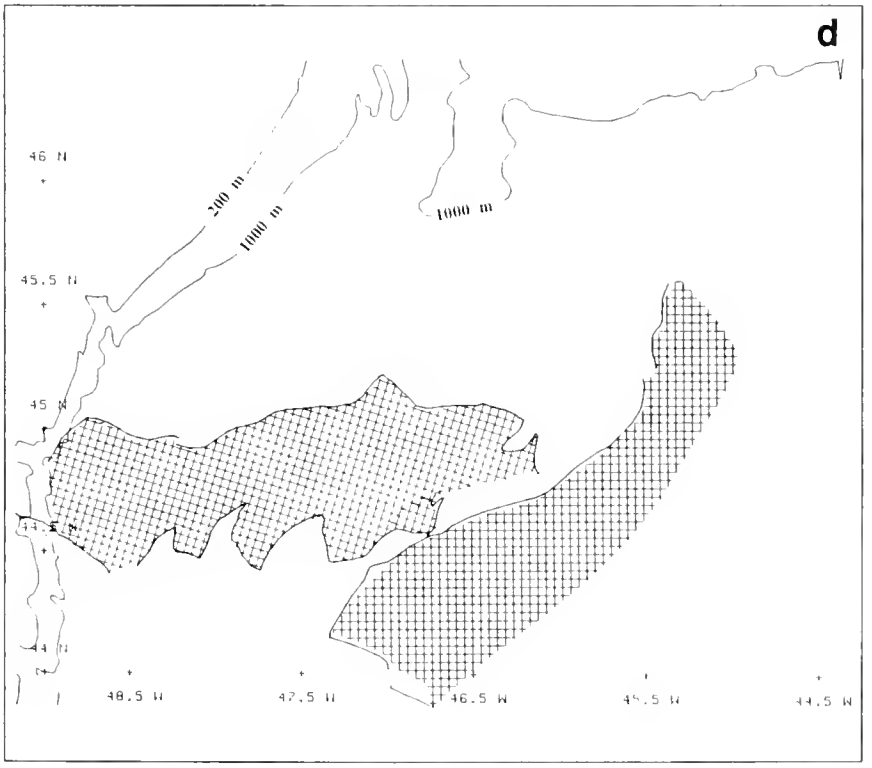

Figure C-7 Digitized fronts depicted in the SLAR imagery for: (c) 9 May; and (d) 17 May.

The 17 May SLAR survey, conducted on the last day of the experiment, provided the most remarkable image (Figure C-7d). It shows an eddy with a complex shape interacting with the NAC. Along the southern boundary of the eddy is a sawtooth-pattern with a peak-to-peak separation of 35km and a height of 20km. As on the other dates, not all of the boundaries are clearly defined, particularly the western boundary. As a result, it is difficult to estimate the size of the eddy based solely on the SLAR imagery; the best size estimate is 160 by 80 km.

The 17 May imagery gives no hint of striations on the cold water side of the front. This is the only date on which this occurred. May 17 was also the only cloud-free day during the three-week experiment. An AVHRR image from the NOAA 9 satellite, taken 8 hours before the SLAR image, shows an excellent agreement of the frontal boundaries (Figure C-8). In addition, the SLAR boundaries are as sharp as those seen on the IR imagery, unlike the results reported by LaViolette (1983).

Surface-truth

The SLAR imagery depicted a series of boundaries with intricate structure, most of which cannot be resolved by the coarsely spaced oceanographic survey and the tracks from a few buoys. This section deals only with the clearest and largest features.

First Oceanographic Survey

Near surface temperatures from the 26 April - 3 May survey (Figure C-9) supports the interpretation of the dark areas in the 26 April SLAR image as waters of NAC origin. The SLAR-detected front nearly coincides (Figure C-10a) with a sharp thermal front, represented in the figure as the 12°C (chosen as an indication of water of NAC origin) contour of sea

surface (0.5-1.0m) temperature The match is remarkably good in the western portion of the study area, but diminishes somewhat toward the east as the time separation between the imagery and hydrography approaches 4 to 5 days. Some of the mismatch is due to the coarse hydrographic grid, but most is due to the fact that the fronts were moving over the period of the hydrographic survey. A comparison of the 12°C surface temperature and the 2 May SLAR imagery (Figure C-10b) shows an excellent match in the eastern part of the study area. The easternmost hydrographic survey line was completed on 3 May.

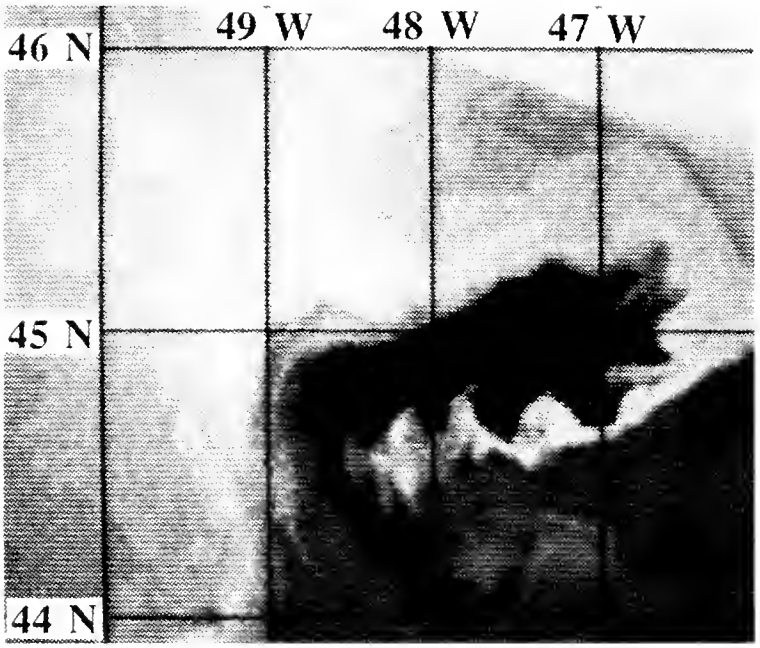

Figure C-8 Infrared image from the Advanced Very High Resolution Radiometer aboard NOAA 9 on 17 May.

The water-mass characteristics across the SLAR-detected front are best illustrated by Figure C-11, a temperature and salinity profile along section AC shown in Figure C-10a. It shows two sharp thermal fronts that coincide with those shown on the 26 April SLAR imagery. In the north, a surface temperature difference of 11°C exists between hydrographic stations on either side of the front, while in the south (C), the difference was 8°C. Between the two fronts is water of NAC origin. The isotherms dome sharply downward, with the 8°C isotherm reaching 320db. In the northern portion of the section (along AB) cold, low salinity water indicates the presence of Labrador Current water flowing eastward immediately to the north of the northern front. In this transect the core of the cold water was at 50 dbar, with a minimum temperature of -0.9°C; at this depth the salinity was 33.1 ppt. The cold-water core was seen at all 10 of the north-south sections of the first-phase hydrography. Typically, the lowest temperatures were found at 40m to 50m.

Figure C-12 shows the horizontal distribution of temperature at 58m, in which the 0°C contour is used to define the location of the core of the Labrador Current water. The 58m depth is chosen because it is the depth of the drogue center of the drifting buoys. Also plotted is the trajectory of a drifting buoy (ID 4542) deployed from an aircraft in Flemish Pass on 19 April. It arrived in the study area on 25 April, the day before the first SLAR survey and the beginning of the first hydrographic survey. The buoy track follows the 0°C contour remarkably well, recognizing that over the six-day period the front changed shape somewhat. The average buoy speed from A to B was 67 cm/s. Referring back to Figure C-11, the buoy passed almost exactly through station 20 and, with the center of the drogue at 58m, it was moving with the 0°C water. When the buoy reached its easternmost extent, it made a sharp cyclonic bend (radius = 20km) and then moved northwestward and eventually northward at about 50 cm/s before it was recovered on 3 May.

The easternmost hydrographic transect (line CD on Figure C-12) shows a water-property distribution (Figure C-13) that is consistent with the cyclonic bend in the trajectory of buoy 4542. Sub-zero water was found at both stations

65 and 67 but not in between. In both cases, this thin and narrow cold-water core was immediately adjacent to NAC water. The radius of the bend suggested in the hydrography is a function of the north/south station spacing (18 km), but it is approximately the same scale as the buoy track radius. The hydrographic section was taken three days after the buoy passed through the area. This probably explains the fact that the location of the bend in the buoy track and the zero degree water are not coincident.

The orientation of the SLAR-observed striations in the 26 April imagery (Figure C-14) north of the front is coincident with the direction of the buoy motion and the location of the Labrador Current as determined by hydrography.

None of the buoys deployed along the westernmost hydrographic section moved through the survey area, so their trajectories (Figure C-14) are of limited use. Buoy 4536 was deployed with its drogue in Labrador Current water about 4 km from a location that buoy 4542 moved through 48 hours earlier; however, while buoy 4542 moved rapidly to the east north of the eddy, 4536 moved sluggishly (20-30 cm/s) to the southwest , roughly parallel to a front shown on the 26 April imagery. Its subsequent northwestward movement was approximately parallel to the striations recorded by the SLAR four days earlier. There is no supporting hydrography, so it cannot be determined if the subsequent southward buoy motion along the 1000m bottom contour of the

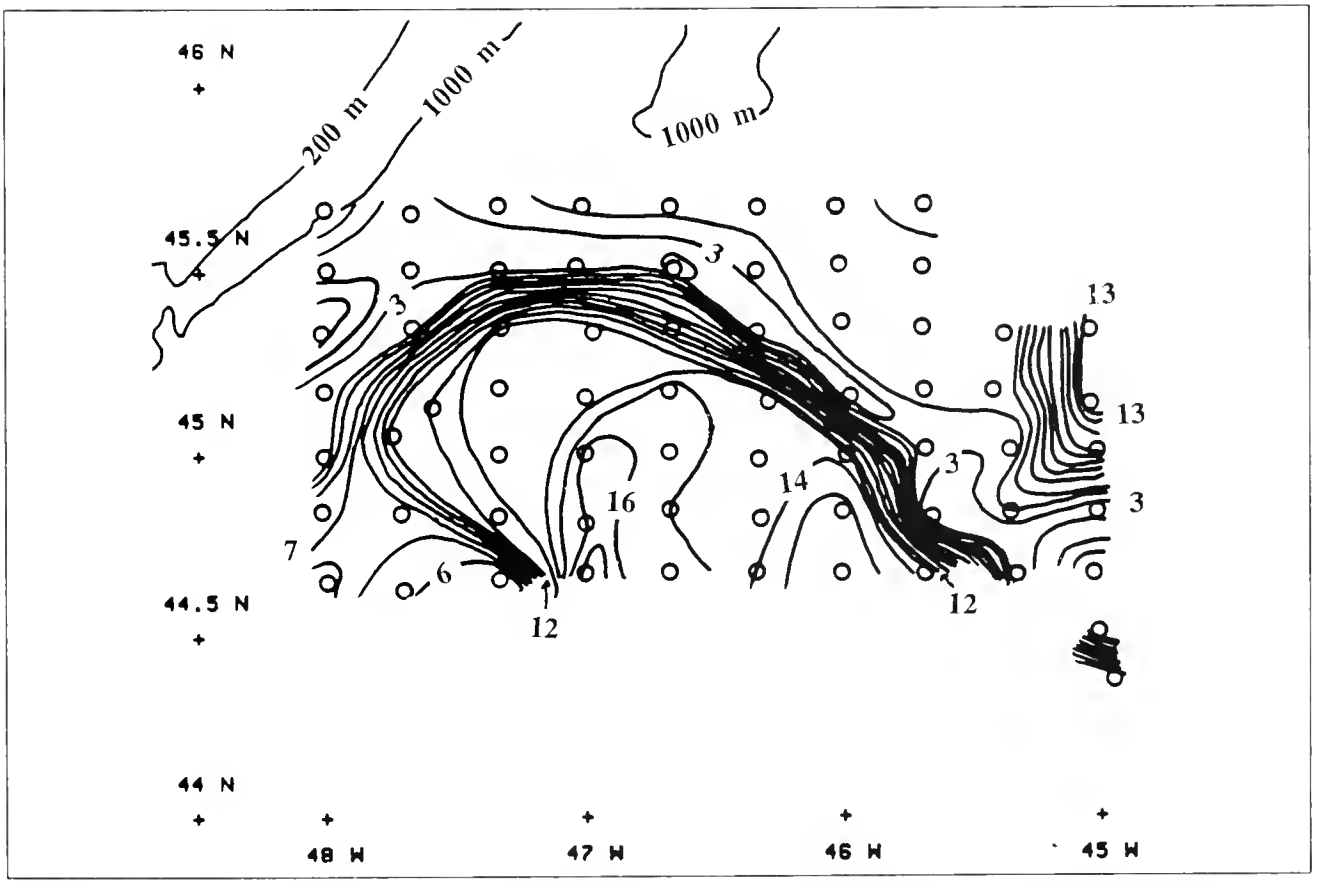

Figure C-9 Sea surface (0.5 - 1.0m) temperature (°C) distribution based on the first phase (27 April — 3 May) hydrography.

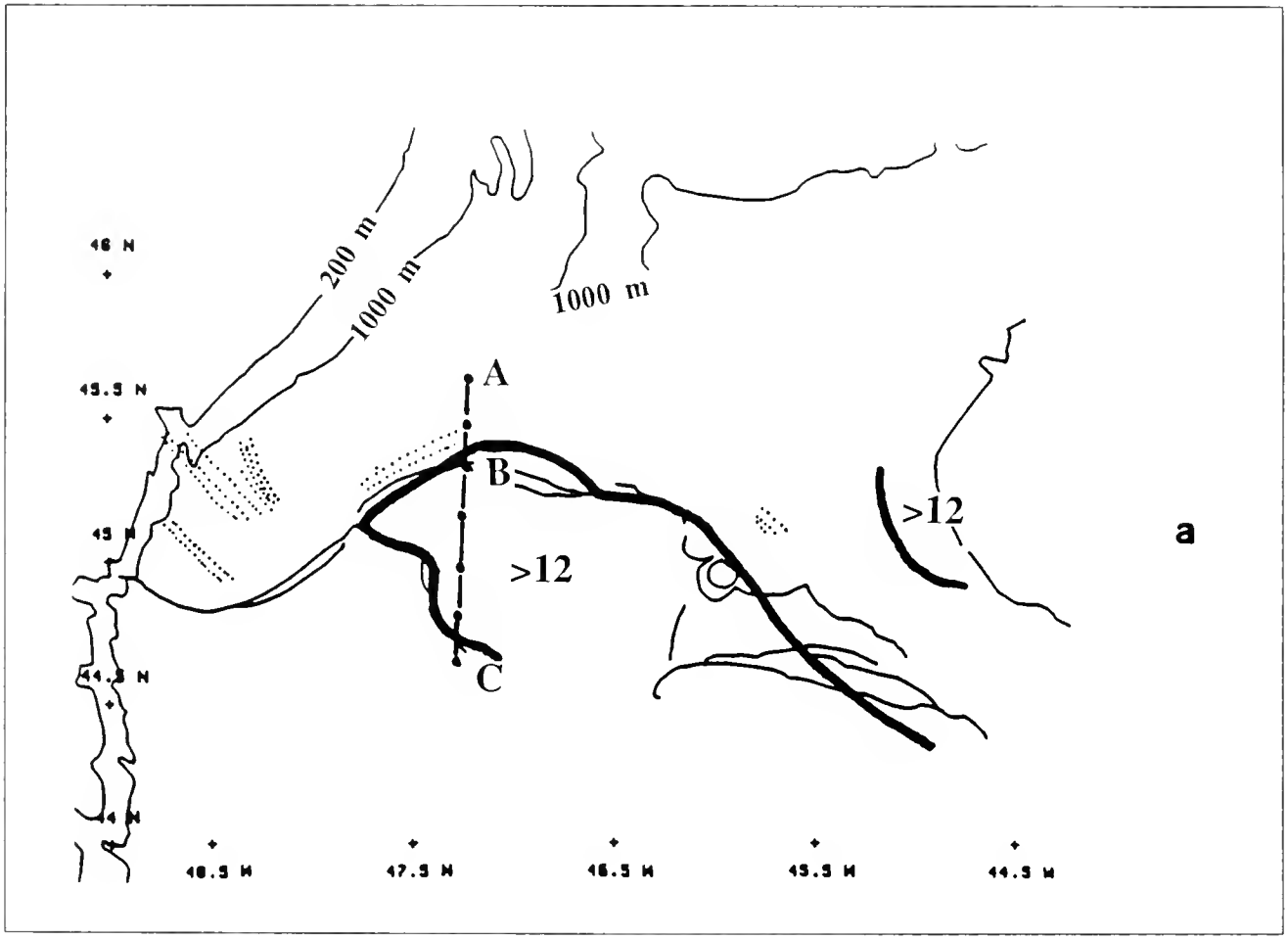

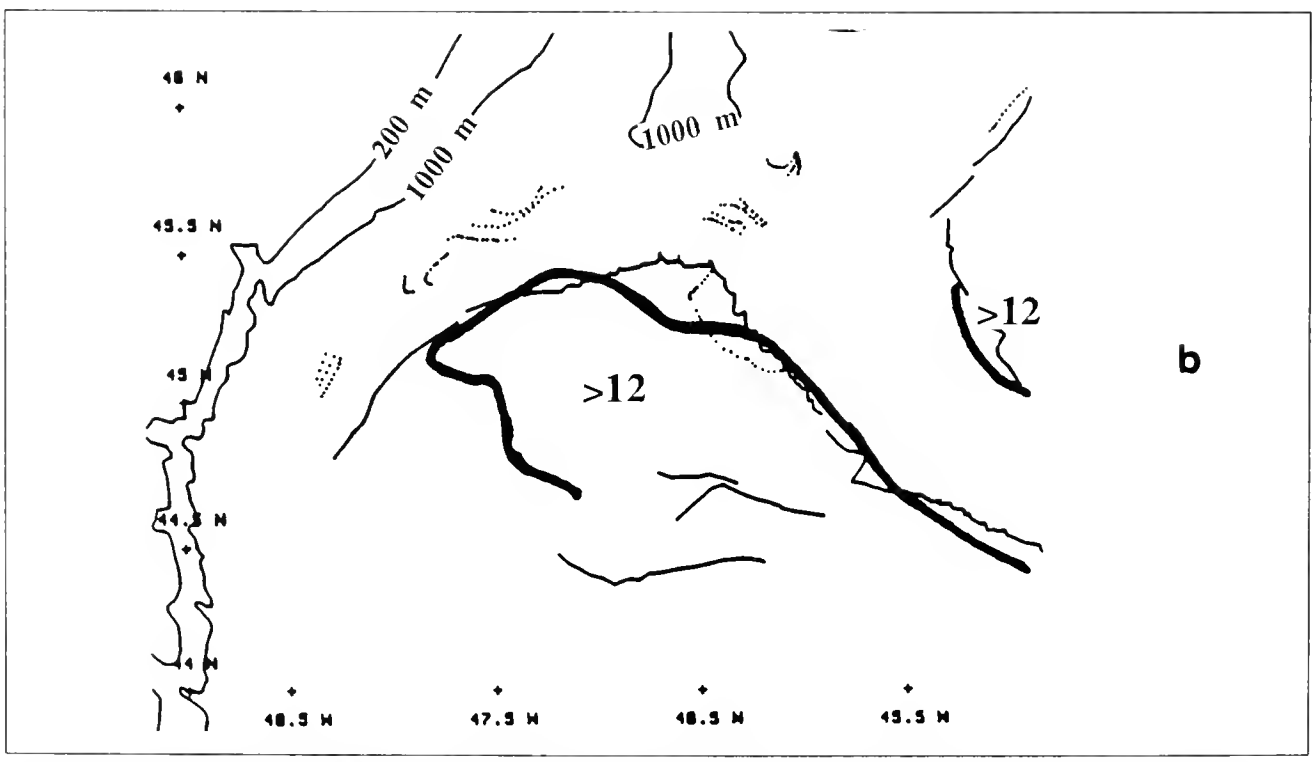

Figure C-10 Comparison between the sea surface temperature (0.5 m - 1m) from the first phase (27 April - 3 May) hydrography and the digitized fronts from SLAR imagery on (a) 26 April and (b) 2 May.

Grand Bank marked the motion of the Labrador Current. The buoy surface temperature reveals no significant thermal structure, with readings mainly in the 2-5°C range. The remaining two buoys exhibited a weak southwestward flow to the southwest of the eddy.

Although abbreviated, the second oceanographic survey, together with the associated buoy tracks, supports the intrepretation of the 9 May imagery as a warm core eddy. The dynamic topography of the 58 dbar surface relative to 1000 dbar (Figure C-15) shows that the SLAR imagery detined all but the western eddy boundary. As before, the area of high radar return was coincident with the warm water of the eddy. A temperature section (Figure C-16) through the eddy reveals downward sloping of the isotherms and the existence of a narrow and shallow core of cold water north of the eddy.

The three buoys released in the eddy (Figure C-17) started an anticyclonic circuit of the eddy. Two were recovered (as duplicating effort); the third remained in the eddy. North of the eddy, buoy 4542 moved rapidly (70 cm/s) eastward within the Labrador Current. On this occasion, however, it turned to the north before reaching 46°W.

Both the dynamic topography and the motion of buoy 4542 in the cold core of the Labrador Current support the interpretation of the striations observed in the SLAR imagery north of the eddy as flow lines oriented parallel to the flow direction.

Figure C-11 Temperature (a) and (b) salinity distribution along the north-south hydrographic section marked on Figure C-9. The letters B and C mark the approximate locations of SLAR detected fronts.

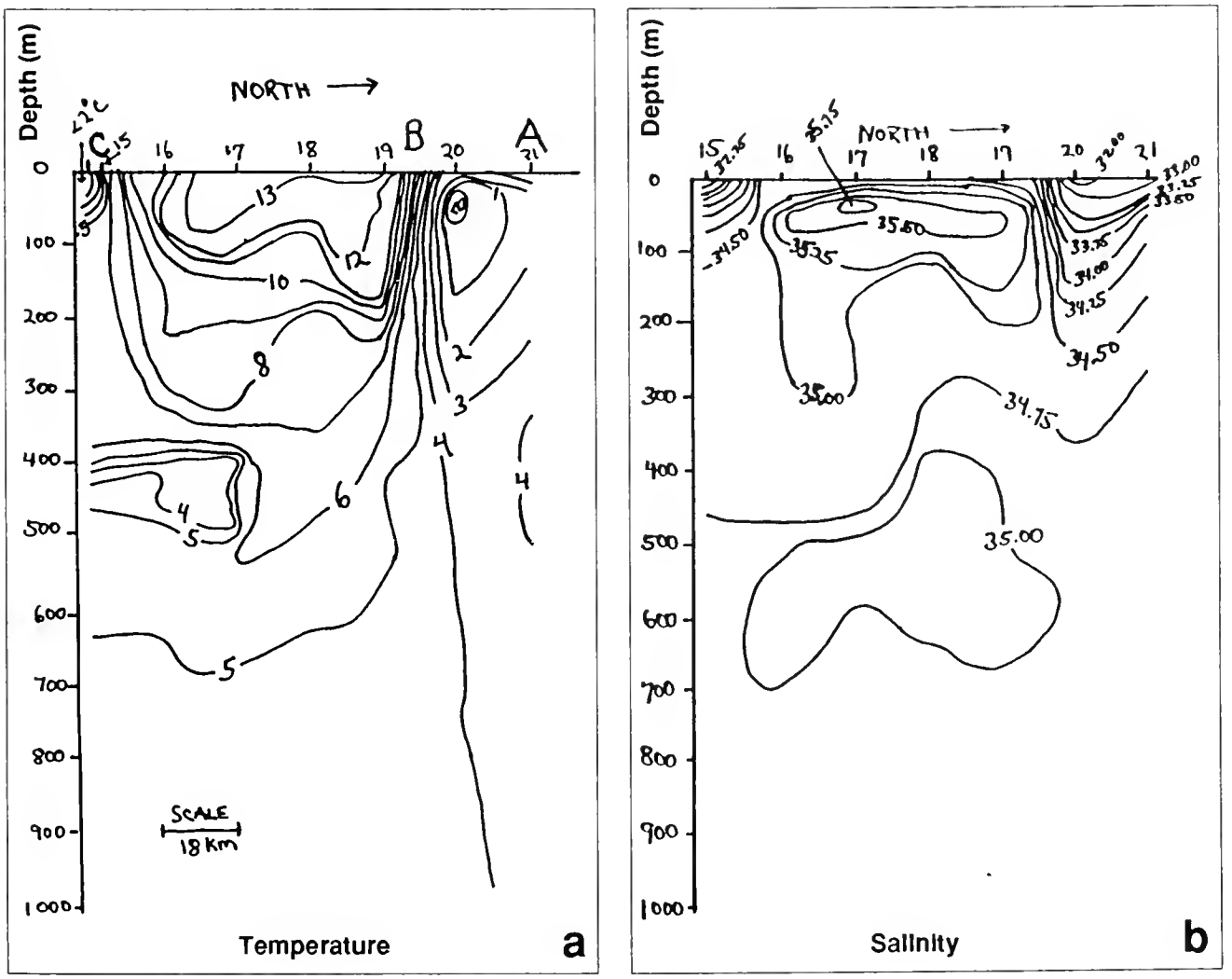

Figure C-12 Distribution of temperature at 58 db from the first-phase hydrography (27 April - 3 May) and the track of buoy 4542. The approximate position of the buoy at the beginning of each day is indicated.

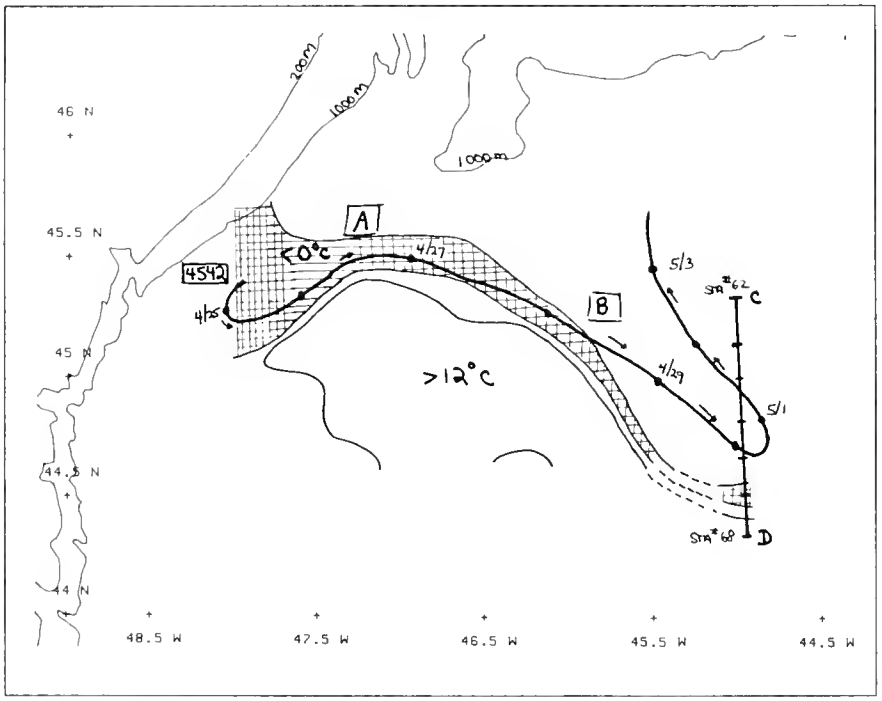

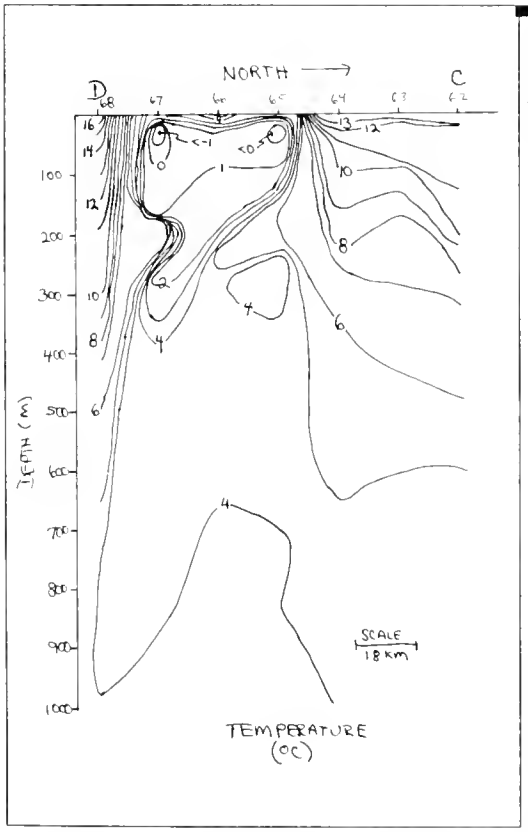

Figure C-13 Temperature distribution along the transect CD drawn on Figure 11.

Figure C-14 Comparison of the first-phase buoy tracks and the features from the 26 April SLAR survey.

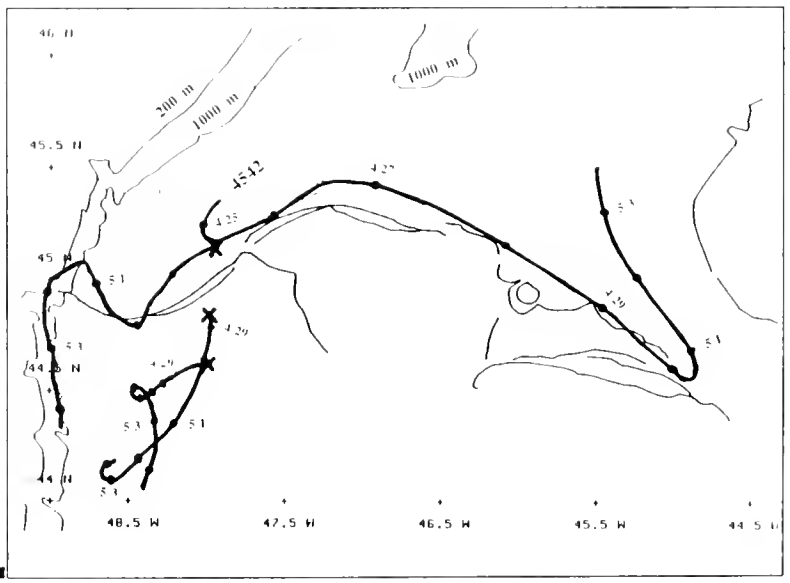

Subsequent History of the Eddy

The track of the buoy left in the eddy at the conclusion of the hydrography (#4557 on Figure C-18) provides the only data on the eddy after the conclusion of the survey. From 12 May to 9 June, it completed three anticyclonic revolutions of the eddy. Its motion indicates an eddy with a diameter of about 80 km with a southeastward translation of 110 km over the 28-day period, about 4 km/day. During the period the surface temperature was mostly in the 11-13°C range, but there were several intervals when it decreased substantially. For example, for a three-day period (31 May-2 June) the temperature decreased to 5-8°C. This suggests that the buoy was close to the eddy boundary. The drogue was moving persistently within eddy water at 58m, while the hull was at times moving through thin cold features.

On 6 June, IIP attempted a SLAR survey of the region to relocate and map the eddy, but the SLAR failed. On 9 June the buoy apparently departed the eddy. The anticyclonic motion ceased and the surface temperature decreased to 6-8°C for a period of a week.

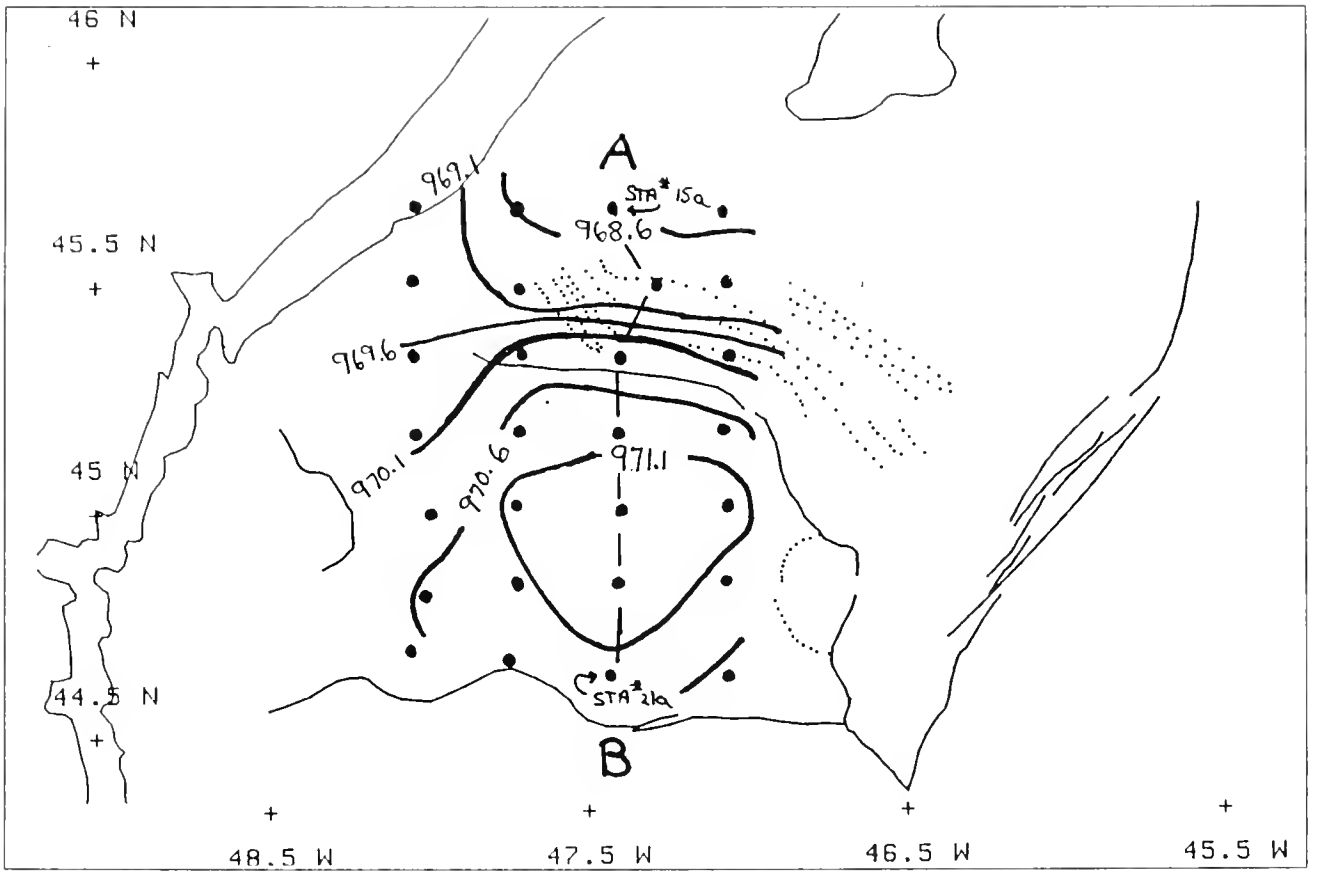

Figure C-15 Comparison between the digitized features from the 9 May SLAR survey and the dynamic topography of the 58 db surface relative to 1000 db (based on second-phase hydrography).

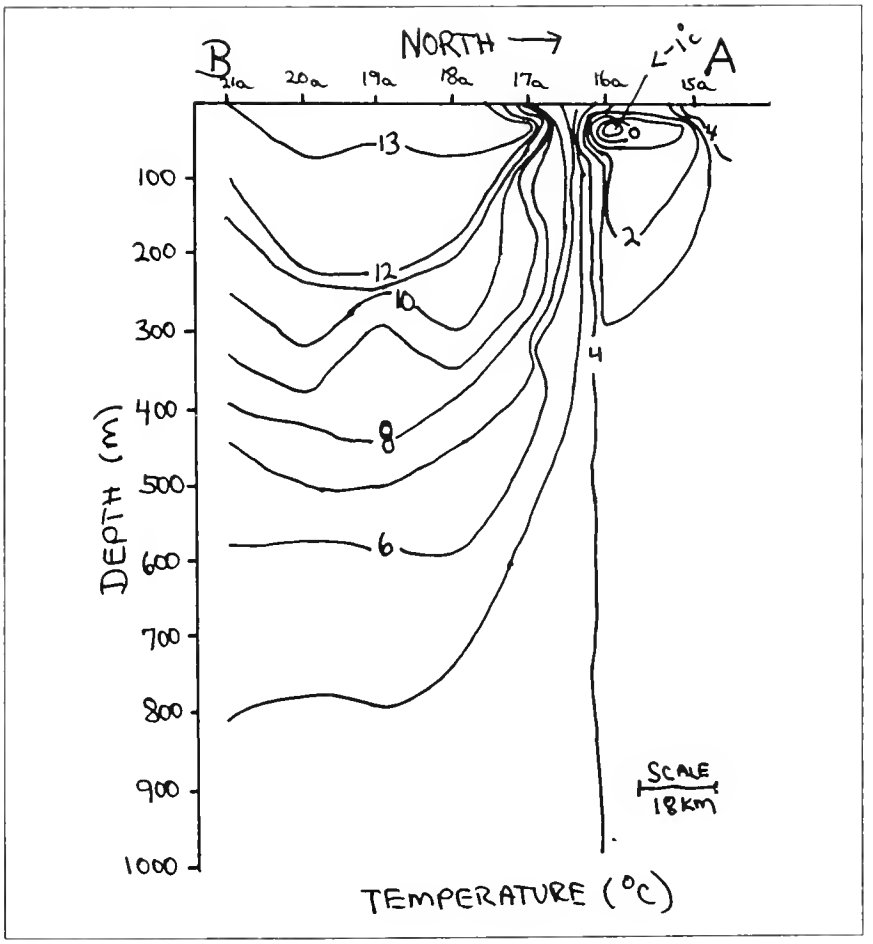

Figure C-16 Second-phase temperature section through the warm core eddy. The location of the section is marked by AB on Figure C-14.

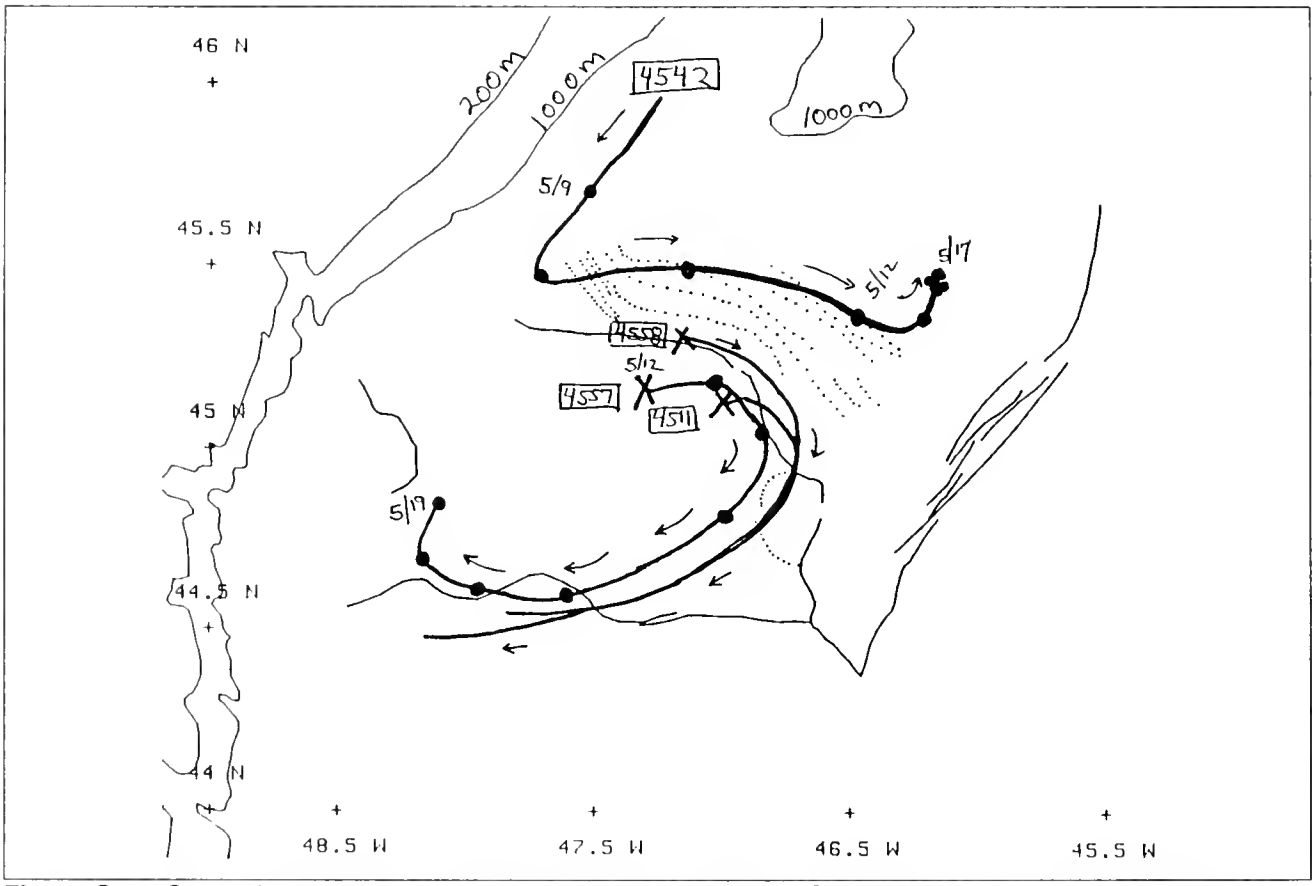

Figure C-17 Second-phase buoy tracks drawn on the digitized SLAR features from the 9 May survey.

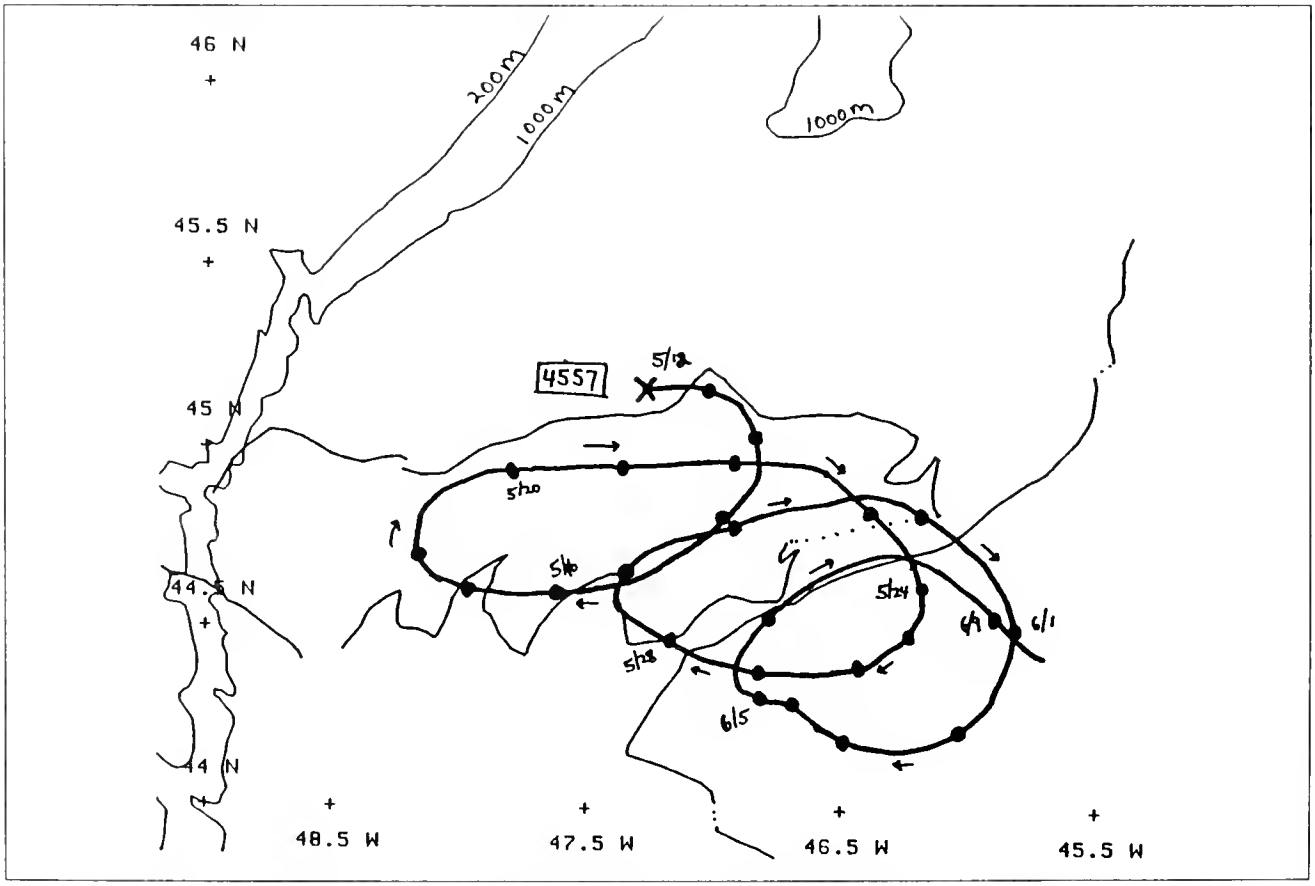

Figure C-18 Trajectory of buoy 4557 plotted on the 17 May SLAR-detected features.

Conclusions

A warm core eddy was found between the LC and NAC east of the Grand Banks of Newfoundland. The observed flow field differed substantially from that suggested by the mean sea-surface topography. During the period of the study, a portion of the Labrador Current left the slope of the Grand Banks north of 45°N and flowed eastward north of a warm core eddy.

The location of a portion of the eddy could be mapped by SLAR. The major cue was the strong signal indicating higher radar return from the warm water within the eddy. However, not all of the boundaries could be located with certainty.

The location and direction of the Labrador Current in the study area could be determined in some of the SLAR imagery using striations as flow lines. These are not reliable indicators, for on most days the striations were faint and patchy. On one day they were absent.

In one case where IR imagery could be compared to concurrently collected SLAR imagery, the match was excellent. The radar-detected fronts were as sharply defined as those in the AVHRR image.

The exact mechanism for the strong radar backscatter in the warm water is uncertain. It is probably due to increased wind stress over the warmer water. Cool air blowing over much warmer water results in an unstable boundary layer, greater wind stress, and a rougher sea surface.

The eddy was never well resolved in either of the hydrographic surveys: that was not the intent of the study. In fact, the best evidence for a closed circulation is the subsequent anticyclonic motion of the buoy left in the eddy after the completion of the hydrography. Exactly when the eddy separated from the NAC cannot be determined from the data. What is clear is the effect that the eddy had on the Labrador Current. The distribution of the unmistakable water mass characteristics of the Labrador Current and the eastward motion of buoy 4542 (on two separate occasions) show that a portion of this current left the slope of the Grand Bank at about 45°N. It moved eastward and then northward in close proximity to the eddy and finally along the boundary of the NAC.

The present study illustrates the importance of research that blends remote sensing with in-situ sampling, with the goal of studying ocean processes. Without the SLAR we could not have located the fronts as easily, nor recognized the spatial and temporal variability of the system. Without the in-situ sampling, the imagery would have been another opportunity for unfounded speculation.

SLAR imagery is difficult to interpret but can be used with other data to gain a better understanding of ocean processes. In addition, SLAR and SAR imagery portray similar features; thus, the more we learn about SLAR now, the better prepared we will be to interpret satellite SAR imagery when it becomes available.

The study results are important to IIP for several reasons. First, they provide a better recognition of the role of eddies in the circulation near the Grand Banks. This study reports a flow pattern that differs dramatically from the mean Labrador Current flow that IIP uses. The observed pattern provides a mechanism for the rapid eastward and even northward motion of icebergs in cold water (minimizing deterioration). There was no apparent cross-front movement. There is no confirmation that the observed flow field caused a major change in iceberg distribution south of Flemish Cap. Indeed, in 1986 only 204 icebergs were reported south of 48°N during the four-month season, giving little opportunity to recognize any iceberg distribution changes from normal. However, a better knowledge of the flow field leads to better iceberg reconnaissance planning. For example, IIP can focus its efforts on an area near the iceberg limit where a large concentration of icebergs is likely.

The IIP SLAR data suffer somewhat from the inability to record digital radar data aboard the aircraft. This is not important for the major features, such as the obvious tonal signal that marked

the eddy. However, for more subtle features like the striations, digital processing would have provided better definition.

The study also illustrates the importance of reliable and good navigation. Each of the major navigation systems used (inertial navigation, LORAN C, and System ARGOS) has different reliability, accuracy and availability. The coarse hydrographic sampling scheme was an accommodation to this problem, and even so, matching three navigational realizations of a physical feature was often difficult. The future offers a solution in the Global Positioning System, but for the next few years the problem will remain.

The use of aircraft-borne SLAR, and eventually satellite-borne SAR, in determining ocean circulation near the Grand Banks holds great promise for improving IIP operations. However, the work in interpreting radar imagery of the ocean surface has only started. Experiments such as that described here must be repeated several times with a broad range of ocean features. Ultimately, the combination of active microwave imagery and air-deployed buoys will permit IIP to gather the required near real-time data.

Acknowledgements

The officers and crews of USCGC EVERGREEN (WMEC 295) and CG-1503 and CG-1504 from Coast Guard Air Station Elizabeth City, N. C. enthusiastically supported our research; their efforts are greatly appreciated. The authors would also like to express their thanks to Frank Williams.

The foundation of the data collection and analysis reported here was provided by the Marine Science Technicians of International Ice Patrol. Without their efforts this work could not have been accomplished. They are: MSTCS G. Wright, MST1 K. Pelletier, MST1 M. Barrett, MST2 D. Hutchinson, MST2 W. Henry, MST3 C. Weiller, MST3 D. Beebe.

References

Anderson, I., 1983. Oceanographic Conditions on the Grand Banks During the 1983 International Ice Patrol Season. Appendix B to Report of the International Ice Patrol in the North Atlantic. Bulletin No. 69, CG-188-38, U.S. Coast Guard, Washington, D.C. 20593, 73pp.

Anderson, I.,1984. Oceanographic Conditions on the Grand Banks During the 1984 International Ice Patrol Season. Appendix B to Report of the International Ice Patrol in the North Atlantic. Bulletin No. 70, CG-188-39, U.S. Coast Guard, Washington, D.C. 20593, 74 pp.

Bessis, J. L., 1981. Operational Data Collection and Platform Location by Satellite. Remote Sensing of Environment, Vol II: p 93-111.

Cheney, R. E., 1981. A Search for Cold Water Rings, in Spacebome Synthetic Aperture Radar for Oceanography. The Johns Hopkins Oceanographic Studies,ed. by R.C. Beal. The Johns Hopkins University Press, Baltimore, MD, p. 161-170.

Fofonoff, N. P., 1985. Physical Properties of Seawater: A New Salinity Scale and Equation of State for Seawater. Journal of Geophysical Research, Vol 90(C2): p. 3332 - 3342.

Fu,L. and B. Holt, 1982. SEASAT Views Oceans and Sea Ice with Synthetic Aperture Radar. Publication 81-120, Jet Propulsion Laboratory, California Institute of Technology, Pasadena, California, 200pp.

Hayes,R.M., 1981. Detection of the Gulf Stream, in Spaceborne Synthetic Aperture Radar for Oceanography. The Johns Hopkins Oceanographic Studies, ed. by R.C. Beal. The Johns Hopkins University Press, Baltimore, MD, p. 146-160.

LaVoilette, P. E., 1983. The Grand Banks Experiment: A Satellite/Aircraft/Ship Experiment to Explore the Ability of Specialized Radars to Define Ocean Fronts. Report 49. Naval Ocean Research and Development Activity, NSTL Station, MS 39529, 126 pp.

Lichy, D. E., M. G. Mattie, and L. J. Mancini, 1981. Tracking of a Warm Core Eddy, in Spaceborne Synthetic Aperture Radar for Oceanography. The Johns Hopkins Oceanographic Studies, ed. by R.C. Beal. The Johns Hopkins University Press, Baltimore, MD, p. 171-182.

Murray, J. J., 1979. Oceanographic Conditions. Appendix B to Report of the International Ice Patrol in the North Atlantic. Bulletin No. 65, CG-188-34, U.S. Coast Guard, Washington, D.C. 20593, 31 pp.

Robinson, I. S., 1985. Satellite Oceanography: An Introduction for Oceanographers and Remote-Sensing Scientists. West Sussex, England: Horwood Limited. 455pp.

Scobie, R. W.and R. H. Schultz, 1976. Oceanography of the Grand Banks Region of Newfoundland March 1971-December 1972. Oceanographic Report No. CG-373-70, U.S. Coast Guard, Washington,D.C. 20593, 298 pp.

Soule, F. M., 1964. The Normal Dynamic Topography of the Labrador Current and its Environs in the Vicinity of the Grand Banks of Newfoundland During Iceberg Season. Report 64-36, Woods Hole Oceanographic Institution, Woods Hole MA, 9 pp.

Vesecky, J.F. and R. H. Stewart, 1982. The Observation of Ocean Surface Phenomena Using Imagery from the SEASAT Synthetic Aperture Radar: An Assessment. Journal of Geophysical Research, 87(C5):3397-3430.

Williams, F. J., 1985. Investigation of Eddy Population and motion in the Southern International Ice Patrol Operations Area (40-47N by 40-55 W). M.S. Thesis. Old Dominion University, 69 pp.

☆ U. S. GOVERNMENT PRINTING OFFICE: 1988--600-272--80097

U. S. Department
of Transportation
**United States
Coast Guard**

Report of the International Ice Patrol in the North Atlantic

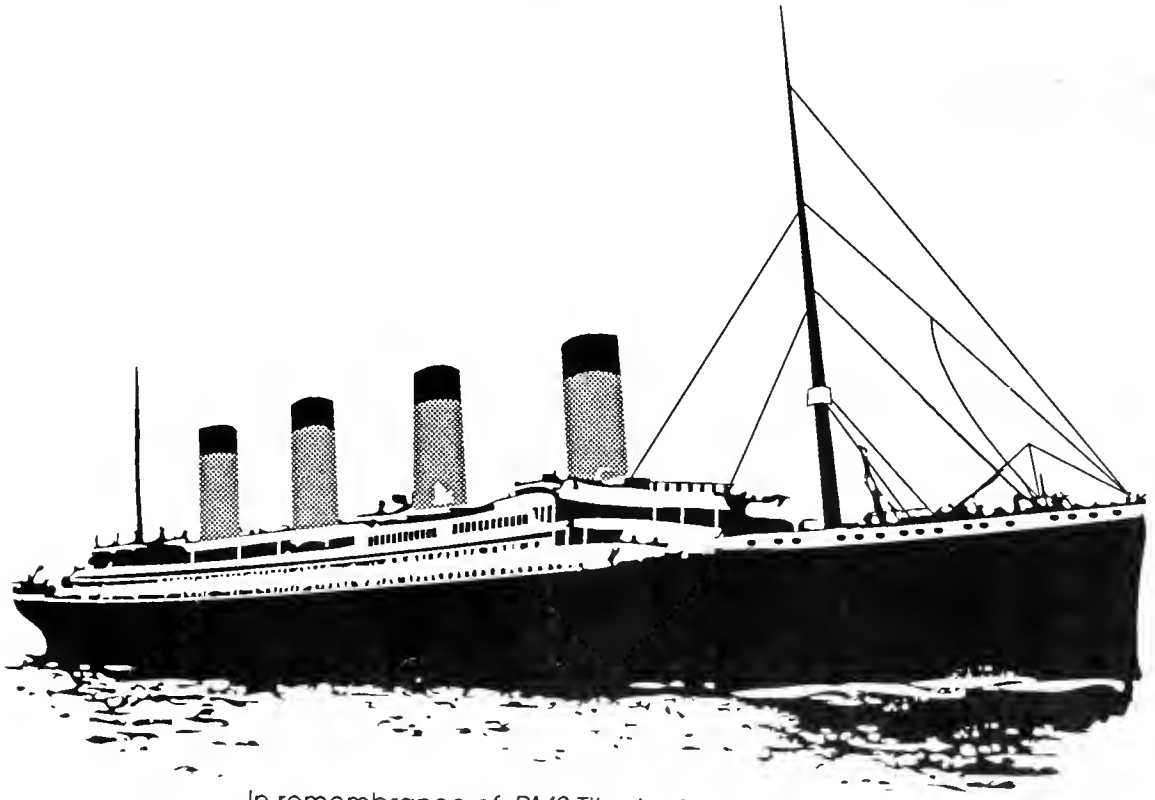

In remembrance of *RMS Titanic* April 14-15, 1912.

1987 Season
Bulletin No. 73
CG-188-42

Bulletin No. 73

REPORT OF THE INTERNATIONAL ICE PATROL SERVICES IN THE NORTH ATLANTIC OCEAN

Season of 1987

CG-188-42

FOREWARD

Forwarded herewith is bulletin No. 73 of the International Ice Patrol describing the Patrol's services, ice observations and conditions during the 1987 season.

R. T. NELSON
Chief, Office of Navigation Safety
and Waterway Services

DISTRIBUTION - SDL No. 126

	a	b	c	d	e	f	g	h	i	j	k	l	m	n	o	p	q	r	s	t	u	v	w	x	y	z
A																										
B	*3	*1	*1		2					1				2	2		1									
C	*1																*1									
D																							60			
E																										
F																										
G																										
H																										

Non-Standard Distribution: *B:a G-NIO only, *B:b LANTAREA (5), B:b PACAREA (1), B:c First, Fifth Districts Only, *C:a Elizabeth City only, *C:q LANATAREA only, SML CG-4

Introduction

This is the 73rd annual report of the International Ice Patrol Service in the North Atlantic. This report contains information on Ice Patrol operations, environmental conditions, and ice conditions for 1987. The U.S. Coast Guard conducts the International Ice Patrol Service in the North Atlantic under the provisions of U.S. Code, Title 46, Sections 738, 738a through 738d, and the International Convention for the Safety of Life at Sea (SOLAS), 1974, regulations 5-8. This service was initiated shortly after the sinking of the RMS TITANIC on April 15, 1912.

Commander, International Ice Patrol, working under Commander, Coast Guard Atlantic Area, directs the International Ice Patrol from offices located at Groton, Connecticut. The International Ice Patrol analyzes ice and environmental data, prepares the daily ice bulletins and facsimile charts, and replies to any requests for special ice information. It also controls the aerial Ice Reconnaissance Detachment and any surface patrol cutters when assigned, both of which patrol the southeastern, southern, and southwestern limits of the Grand Banks of Newfoundland for icebergs. The International Ice Patrol makes twice-daily radio broadcasts to warn mariners of the limits of iceberg distribution.

Vice Admiral D. C. Thompson was Commander, Atlantic Area, and LCDR S. R. Osmer was Commander, International Ice Patrol, during the 1987 ice season.

Summary of Operations, 1987

From March 12 to July 31, 1987, the International Ice Patrol (IIP), a unit of the U.S. Coast Guard, conducted the International Ice Patrol Service, which has been provided annually since the sinking of the RMS TITANIC on April 15, 1912. During past years, Coast Guard ships and/or aircraft have been patrolling the shipping lanes off Newfoundland within the area delineated by 40°N - 52°N, 39°W - 57°W, detecting icebergs, and warning mariners of these hazards. During 1987, Coast Guard HC-130 aircraft flew 53 ice reconnaissance sorties, logging over 368 flight hours. The AN/APS-135 Side-Looking Airborne Radar (SLAR), which was introduced into Ice Patrol duty during the 1983 season, again proved to be an excellent all-weather tool for the detection of both icebergs and sea ice.

Aircraft deployments were made on January 25 to February 4 and February 27 to March 6 to determine the pre-season iceberg distribution. For the first time, these pre-season surveys were made jointly with the Ice Branch of the Atmospheric Environment Service (AES) of Canada. This was the first season since 1978 that IIP has conducted a pre-season census of icebergs north of 52°N and the first pre-season census ever done using SLAR. Figures 1 and 2 show the iceberg distribution north of 52°N from these two surveys. This cooperative census with SLAR allowed a wider look at the pre-season iceberg distribution than in

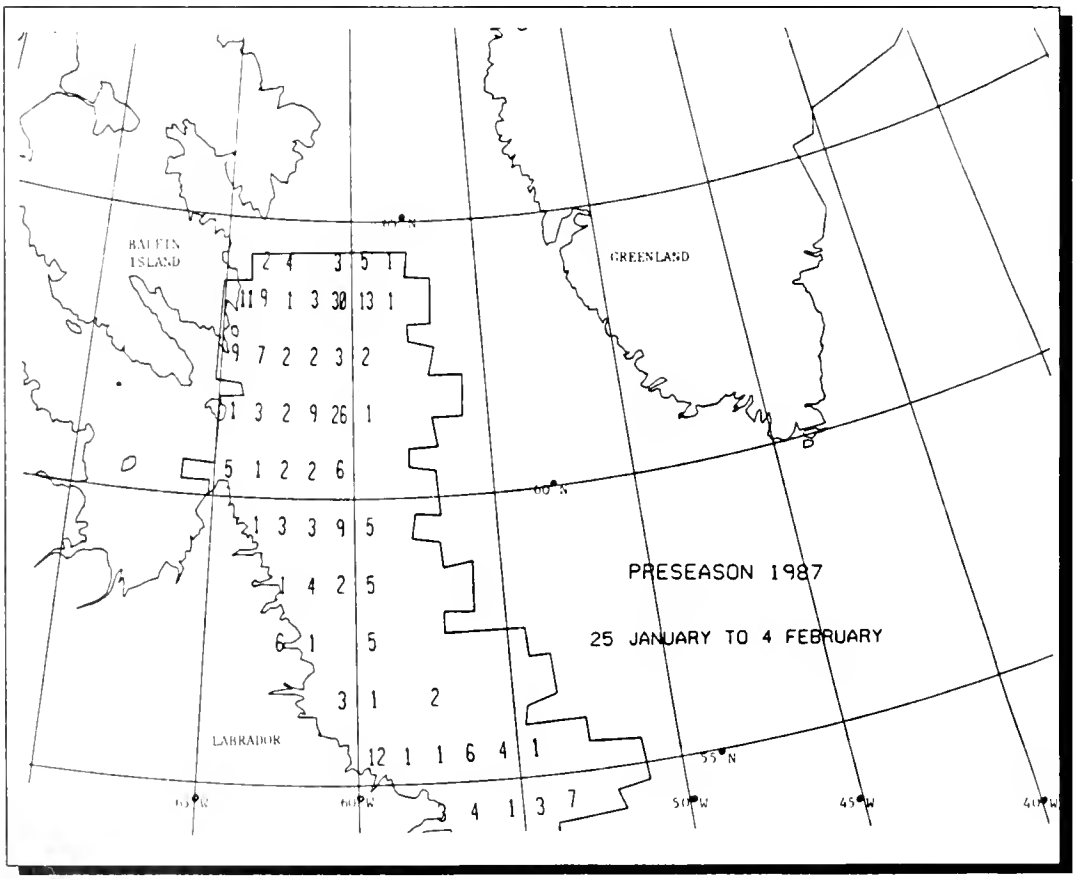

Figure 1. Area of iceberg census and iceberg count January 25 to February 4, 1987. Numbers shown are number of icebergs per 1° latitude by 1° longitude square.

previous years. These AES-IIP joint surveys will continue in the future whenever it is mutually beneficial.

Based on the second pre-season deployment, the 1987 season opened on March 12 and regular aircraft deployments started on March 18. From the later date until August 2, 1987, an aerial Iceberg Reconnaissance Detachment (ICERECDET) operated from Gander, Newfoundland, one week out of every two. The season officially closed on July 31, 1987.

Watchstanders at IIP's Operations Center in Groton, Connecticut, analyze the iceberg sighting information from the ICERECDET, along with sighting information from commercial shipping and AES sea ice/iceberg reconnaissance flights. Only those iceberg sightings within IIP's operations area (40°N - 52°N, 39°W - 57°W) are entered into the IIP iceberg drift prediction computer model (ICEPLOT). The watchstanders determine whether each sighting is a resight of an iceberg IIP already has on ICEPLOT, or whether the sighting is a sighting of a new iceberg which had not been previously reported. Iceberg sightings near the Newfoundland coast are not entered into the computer model due to lack of current information in the model in these areas to drift the icebergs. Each sighting is labelled in the computer model as either a resight or a new sighting. During the 1987 ice year, 755 icebergs were sighted in IIP's operations area (south of 52°N), compared to 415 icebergs in the 1986 ice year.

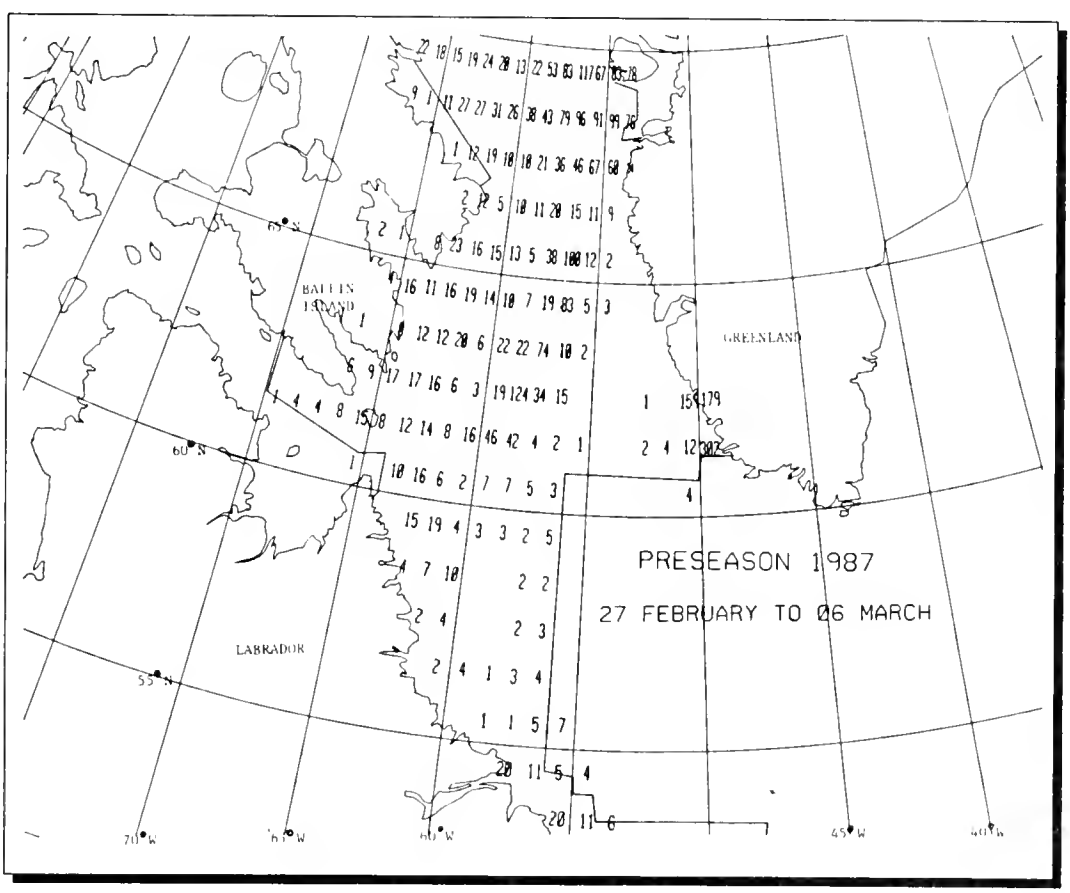

Figure 2. Area of iceberg census and iceberg count February 7 to March 6, 1987. Numbers shown are number of icebergs per 1° latitude by 1° longitude square.

Table 1. Source of International Ice Patrol Iceberg Reports by Size.

Sighting Source	Growler	Small	Medium	Large	Radar Target	Total	Percent of Total
Coast Guard SLAR	29	94	82	30	12	247	12.9
Coast Guard Visual	40	94	85	26	0	245	12.8
CanadianSLAR	2	34	23	12	245	316	16.6
Canadian Visual	11	253	124	49	0	437	22.9
Ship Radar	5	5	18	3	49	80	4.2
Ship Visual	43	95	195	61	0	394	20.6
Offshore Oil Industry	9	35	24	8	4	80	4.2
Lighthouse/Shore	0	0	1	0	0	1	0.1
DOD Sources	0	14	53	34	0	101	5.3
Other	0	4	1	0	3	8	0.4
Total	139	628	606	223	313	1909	100.0

IIP's computer model consists of a routine which predicts the drift of each iceberg, and a routine which predicts the deterioration of each iceberg. The drift prediction program uses a historical current data file to drift the icebergs. This historical data file is modified weekly using satellite-tracked ocean drifting buoy data to take into account local, short-term current fluctuations. Murphy and Anderson (1985) describe the IIP drift model in more detail, along with an evaluation of the model which was conducted in 1985.

The IIP iceberg deterioration program uses daily wind, sea surface temperature, and wave height information from the U.S. Navy Fleet Numerical Oceanography Center to melt the icebergs. Anderson (1983) describes the IIP deterioration model in detail. It is the ability of the SLAR to detect icebergs in all weather, and the IIP's computer models to estimate iceberg drift and deterioration, which has enabled IIP to reduce its ICERECDET operations from weekly deployments to every other week deployments.

Table 1 shows the total iceberg sightings reported to IIP in 1987 (including resights), broken down by the sighting source and iceberg size. The number of iceberg sightings shown in Table 1 are only those which were in IIP's operations area and away from the Newfoundland coast. For example, more than one iceberg sighting was received from the Canadian lighthouses, but since most were nearshore, only one was entered into IIP's computer model. Appendix A lists all iceberg sightings received from commercial shipping, regardless of the sighting location.

The SLAR continued to be an important instrument in iceberg detection in 1987. IIP and Canadian (AES) SLAR observations accounted for 29.5 percent of all 1987 iceberg reports (Table 1). Visual and SLAR observations from Canadian (AES) sea ice/iceberg reconnaissance flights accounted for 39.5 percent of all 1987 iceberg reports. This is a significant increase from the past, representing greater emphasis on iceberg reporting by AES, and again indicating the increased mutually-beneficial cooperation between IIP and AES.

Table 2 shows monthly estimates of the total number of icebergs that crossed 48°N for the pre-International Ice Patrol era, and for the ship, aircraft visual, and aircraft SLAR reconnaissance eras. Table 3 compares the estimated number of icebergs crossing 48°N for each month of 1987 with the monthly mean number of icebergs crossing 48°N for each of the four different eras.

During the 1987 ice year, an estimated 318 icebergs drifted south of 48°N latitude, compared to 204 icebergs drifting south of 48°N during 1986. The number of icebergs crossing 48°N during 1987 was less than the SLAR reconnaissance era average. It is important to note, however, that this average is based on only four years of data. The average number of icebergs drifting south of 48°N from 1913 to 1987 is 395 icebergs (Appendix B). With 318 icebergs drifting south of 48°N, 1987 was deemed an intermediate or average ice year (Appendix B).

April 15, 1987, marked the 75th anniversary of the sinking of the RMS TITANIC. A memorial wreath was placed near the site of the sinking during an ice reconnaissance patrol to commemorate the nearly 1500 lives lost.

Table 2. Total Icebergs South of 48° N - The four periods shown are pre-International Ice Patrol (1900-1912), ship reconnaissance (1913-1945), aircraft visual reconnaissance (1946-1982), and SLAR reconnaissance (1983-1986).

	Total 1900-12	Total 1913-45	Total 1946-82	Total 1983-86	1987
OCT	27	80	2	3	0
NOV	13	93	4	11	0
DEC	38	42	11	9	5
JAN	33	87	65	11	2
FEB	79	372	273	225	14
MAR	898	1204	1172	394	48
APR	1537	3308	3131	1560	76
MAY	1611	5472	2993	1213	29
JUN	1004	2514	1865	666	127
JUL	423	773	489	552	15
AUG	160	229	100	136	2
SEP	58	188	10	41	0
Total	5,881	14,362	10,115	4,821	318

Table 3. Average Number of Icebergs South of 48° N - The four periods shown are pre-International Ice Patrol (1900-1912), ship reconnaissance (1913-1945), aircraft visual reconnaissance (1946-1982), and SLAR reconnaissance (1983-1986).

	Avg 1900-12	Avg 1913-45	Avg 1946-82	Avg 1983-86	1987
OCT	2	2	0	1	0
NOV	1	3	0	3	0
DEC	3	1	0	2	5
JAN	2	3	2	3	2
FEB	6	11	7	56	14
MAR	69	36	32	98	48
APR	118	100	85	390	76
MAY	124	166	81	303	29
JUN	77	76	50	166	127
JUL	32	23	13	138	15
AUG	12	7	3	34	2
SEP	4	6	0	10	0
Era Average	452	435	273	1204	318

From March 23-25, IIP participated in the Labrador Ice Margin EXperiment (LIMEX) '87. This international experiment involved four remote sensing aircraft and a surface vessel. LIMEX '87 was a pilot study for the full experiment effort scheduled for 1989. The three objectives of LIMEX '87 were the verification of remote sensing algorithms for active and passive microwave sensors with the aim of applying these to future satellite-borne sensors, the investigation of oceanographic conditions in the marginal ice zone, and the determination of the characteristics of the Labrador ice pack in the region of maximum southerly advance. The IIP aircraft provided SLAR mosaics of the pack ice and the ice edge which were collected during the course of regular reconnaissance patrols.

Eleven satellite-tracked oceanographic drifters were deployed to provide operational data for IIP's iceberg drift model. Six of these drifters belonged to AES and were deployed by IIP. AES and IIP each had access to the data these eleven drifters provided. The drifters' data are discussed in Appendix C.

No U. S. Coast Guard cutters were deployed to act as surface patrol vessels this year. Two cruises were performed during the 1987 season to conduct oceanographic research for the Ice Patrol. The first was conducted from U.S. Coast Guard Cutter (USCGC) BITTERSWEET (WLB-389) during the period April 27 through May 26. The primary objective of this cruise was to study water mass and frontal boundary identification in conjunction with the SLAR. The second cruise was conducted from USCGC TAMAROA (WMEC-166) during the period June 8-27. The primary objectives of this cruise were to compare the environmental inputs to the IIP's iceberg drift and deterioration model with observed conditions, and evaluate any errors in the model. The results of these studies are presented in Appendices D, E, and F.

These cruises were the first deployments of IIP's transportable oceanographic equipment, including a Mobile Oceanographic Laboratory, portable hydrographic winch, and A-frame platform. This transportable equipment allows IIP to perform oceanographic research from many types of Coast Guard cutters. Alles and Alfultis (1988) discuss the assembly and operation of this system in detail.

Iceberg Reconnaissance and Communications

During the 1987 Ice Patrol year (from October 1, 1986, through September 30, 1987), 80 aircraft sorties were flown in support of the International Ice Patrol. These included pre-season flights, ice reconnaissance flights during the season, post-season flights, and logistics flights. Pre-season flights determined iceberg concentrations north of 48°N. These iceberg concentrations were needed to estimate when icebergs would threaten the North Atlantic shipping lanes in the vicinity of the Grand Banks of Newfoundland. During the active season, ice reconnaissance flights located the southwestern, southern, and southeastern limits of icebergs. Logistics flights were necessary to support patrol aircraft with aircraft maintenance problems. Post-season flights were made to check on the iceberg distribution, to retrieve parts and equipment from Gander, and to close out all business transactions from the season.

U.S. Coast Guard aircraft, deployed from Coast Guard Air Station Elizabeth City, North Carolina, conducted all the aircraft missions. Aerial ice reconnaissance was conducted solely with SLAR-equipped HC-130H aircraft. HC-130H and HU-25A aircraft were used on logistics flights. Table 4 shows aircraft use during the 1987 season.

Table 4. Aircraft use during the 1987 IIP Year (October 1, 1986 - September 30, 1987)

Aircraft Deployment	Sorties	Flight Hours
Pre-season	14	69.9
Regular Season	58	370.2
Post season	8	38.0
Total	80	478.1

Iceberg Reconnaissance Sorties by Month

Month	Sorties	Flight Hours
Jan	1	4.7
Feb	2	13.5
Mar	11	81.4
Apr	6	43.4
May	13	90.3
Jun	10	69.3
Jul	7	46.8
Aug	3	19.5
Total	53	368.9

Table 5. Iceberg and SST Reports.

Number of ships furnishing Sea Surface Temperature (SST) reports	91
Number of SST reports received	416
Number of ships furnishing ice reports	256
Number of ice reports received	505
First Ice Bulletin	120000Z MAR87
Last Ice Bulletin	311200Z JUL 87
Number of facsimile charts transmitted	141

The IIP prepares the ice bulletin warning mariners of the southwestern, southern, and southeastern limits of icebergs twice a day for broadcast at 0000Z and 1200Z. The IIP also prepares a facsimile chart graphically depicting these limits for broadcast at 1600Z. U.S. Coast Guard Communications Station Boston, Massachusetts, NMF/NIK, was the primary radio station used for the dissemination of the daily ice bulletins and facsimile charts . Other transmitting stations for the 0000Z and 1200Z ice bulletins included Canadian Coast Guard Radio Station St. John's, Newfoundland/VON; Canadian Forces Meteorological and Oceanographic Center (METOC) Halifax, Nova Scotia/CFH; and U.S. Navy LCMP Broadcast Stations Norfolk/NAM; Thurso, Scotland; and Keflavik, Iceland.

Canadian Forces METOC, Halifax/CFH, as well as AM Radio Station Bracknell, United Kingdom/GFE, are radiofacsimile broadcasting stations which used International Ice Patrol limits in their broadcasts. Canadian Coast Guard Radio Station St. John's/ VON and U.S. Coast Guard Communications Station Boston/NIK provided special broadcasts.

The International Ice Patrol transmissions requested that all ships transiting the area of the Grand Banks report ice sightings, weather, and sea surface temperatures via the above communications/radio stations. Response to this request is shown in Table 5, and Appendix A lists all contributors. Commander, International Ice Patrol extends a sincere thank you to all stations and ships which contributed.

Environmental Conditions 1987 Season

The wind direction along the Labrador and Newfoundland coasts can affect the iceberg severity of each year. The mean wind flow can influence iceberg drift. Dependent upon wind intensity and duration, icebergs can be accelerated along or driven out of the main flow of the Labrador Current. Departure from the Labrador Current normally slows their southerly drift, and in many cases speeds up their rate of deterioration.

The wind direction and air temperature affect the iceberg severity of each year in an indirect way by influencing the extent of sea ice. Sea ice protects the icebergs from wave action, the major agent of iceberg deterioration. If the air temperature and wind direction are favorable for the sea ice to extend to the south and over the Grand Banks of Newfoundland, the icebergs will be protected longer as they drift south. When the sea ice retreats in the spring, large numbers of icebergs will be left behind on the Grand Banks. Also, if the time of sea ice retreat is delayed by below normal air temperatures, the icebergs will be protected longer, and a longer than normal ice season can usually be expected. The opposite is true if the southerly sea ice extent is minimal, or if above normal temperatures cause an early retreat of sea ice from the Grand Banks.

The following discussion summarizes the environmental conditions along the Labrador and Newfoundland coasts for the 1987 ice year. The Gander Airport Weather Office provided the data for Table 6.

January: The mean pressure distribution in Figure 3 shows the Icelandic Low was southwest of its mean position, with stronger than normal pressure gradients surrounding it. The resulting stronger northerly flow brought more Polar Continental air to Labrador causing colder, drier than normal conditions, and more Polar Maritime air to Newfoundland causing colder, wetter conditions (Table 6). The Grand Banks conditions were probably similar to the Newfoundland conditions, colder, wetter than normal.

February: The Icelandic Low remained intense in February and shifted farther to the southwest, bringing a northeasterly flow to Labrador and Newfoundland (Figure 4). The conditions in Labrador were warmer and wetter than normal, while the temperatures on Newfoundland were about normal with above normal precipitation (Table 6). These conditions were caused by the northeasterly flow bringing in large amounts of Polar Maritime air to the region. This maritime air would have a warmer temperature and more moisture than the continental air usually influencing Labrador's weather.

March: The Icelandic Low returned to its usual position and nearly normal intensity for March (Figure 5). In addition to the Icelandic Low, a low pressure trough extended from the Grand Banks south. Conditions in Nain and Gander returned to nearly normal while Goose Bay was drier than normal and St. John's was colder and wetter than normal (Table 6). The northwesterly flow brought dry polar air to Goose Bay instead of the maritime air it is usually influenced by. The low pressure trough off the Grand Banks brought moisture to St. John's from the south. The conditions on the Grand Banks were probably similar to those at St. John's, colder and wetter than normal.

April: The Icelandic Low was more intense than normal for April, and the position of the Bermuda High was more to the northwest than normal (Figure 6). This pressure distribution brought a southwesterly flow to Newfoundland, and a westerly flow to Labrador. The conditions at Newfoundland were warmer and wetter than normal, while the conditions on Labrador were warmer and drier than normal (Table 6). These conditions were caused by the southwesterly flow bringing warmer, moister, maritime air to Newfoundland,

and the westerly flow bringing warmer, drier, continental air to Labrador, instead of the Polar Maritime air usually influencing Newfoundland and Labrador. The conditions over the Grand Banks were likely warmer, wetter, than normal due to the southwesterly flow again bringing warm, moist, air to the Grand Banks from the south.

May: A ridge of high pressure extended across the North Atlantic in May (Figure 7). The resulting southwesterly flow around this ridge brought air from farther south than normal to Newfoundland. This warm, moist air brought warmer than normal temperatures to Newfoundland and southern Labrador (Table 6). The conditions on the Grand Banks were likely to be warmer and moister than normal in May. The colder, wetter, than normal weather at Nain (Table 6) was caused by the low pressure system off of the Labrador coast bringing Polar Maritime air to northern Labrador rather than the warmer, drier, continental air usually influencing the region.

June: With the Bermuda High still farther west than normal in June, the flow of air to Newfoundland was more out the west than normal (Figure 8). This brought cooler, drier, continental air to Newfoundland rather than the warm, moist, maritime air usually coming to the region from south. This resulted in cooler, drier, than normal weather in St. John's and Gander (Table 6). Labrador was also under the influence of the continental air mass, as it usually is, and nearly normal conditions were reported in Nain and Goose Bay.

July: The pressure distribution in July was nearly normal (Figure 9). This distribution brought normal temperatures to Newfoundland (Table 6). The colder, wetter, than normal conditions in northern Labrador were caused by the area of low pressure off of Greenland bringing the cold, but wet, Polar Maritime air to the region rather than the warmer, drier, continental air which normally influences northern Labrador in July.

August: A low pressure trough formed north of Labrador in August (Figure 10). The resulting flow was northerly, rather than the the normal southwesterly flow. This caused conditions in Newfoundland and southern Labrador to be colder and drier than normal (Table 6).

September: September saw the return of the Icelandic Low, deeper than normal, and the diminishing of the Bermuda High (Figure 11). The westerly flow over Newfoundland and Labrador was nearly normal. Conditions on Newfoundland were colder than normal, while the conditions on Labrador were warmer than normal (Table 6).

NOTE: Temperature and precipitation data for Nain, Labrador, are compared to 1985 values in Table 6. The reporting station at Hopedale, Labrador, was closed in 1984 and the Nain station opened. A historical mean for Nain does not exist.

Table 6. Environmental Conditions for the 1987 IIP Year.

	Station	Temp °C Monthly Mean	Temp °C Diff. from Norm.	Total Precipitation (mm)	% of Normal Precipitation	% of Normal Snowfall
OCT 1986	Nain	-1.7	-4.1	42.3	67.4%	
	Goose	0.4	-2.3	88.9	116.1%	87.9%
	Gander	3.8	-2.2	113.4	108.3%	198.4%
	St. John's	5.4	-1.5	157.2	108.0%	50.0%
NOV	Nain	-11.0	-7.8	31.0	54.0%	
	Goose	-10.3	-6.5	71.7	95.3%	152.8%
	Gander	-1.4	-3.2	138.7	129.3%	351.6%
	St. John's	0.7	-2.7	203.1	125.0%	306.1%
DEC	Nain	-14.9	-4.2	29.3	51.7%	
	Goose	-14.4	-1.4	38.1	52.4%	64.1%
	Gander	-5.6	-1.8	68.0	62.8%	82.5%
	St. John's	-3.9	-2.4	80.8	50.1%	77.7%
JAN 1987	Nain	-16.5	-0.7	20.6	33.1%	
	Goose	-17.2	-0.8	14.6	19.6%	26.3%
	Gander	-8.2	-2.0	163.2	149.6%	201.8%
	St. John's	-5.5	-1.6	174.4	111.9%	158.7%
FEB	Nain	-12.9	2.2	178.0	355.3%	
	Goose	-11.6	2.9	131.5	217.0%	257.3%
	Gander	-6.3	0.5	129.1	129.5%	153.8%
	St. John's	-5.0	-0.5	175.1	125.0%	177.5%
MAR	Nain	-11.2	-0.7	60.5	109.2%	
	Goose	-8.1	0.5	35.3	48.9%	42.5%
	Gander	-3.9	-0.4	99.7	90.6%	27.1%
	St. John's	-3.4	-1.1	149.7	113.5%	78.2%
APR	Nain	-1.8	3.1	23.5	50.5%	
	Goose	2.3	4.0	28.5	46.6%	13.4%
	Gander	2.4	1.5	100.7	108.0%	27.6%
	St. John's	2.0	0.8	120.9	104.6%	3.8%
MAY	Nain	1.1	-0.3	58.0	114.4%	
	Goose	6.5	5.3	46.9	73.5%	39.7%
	Gander	7.7	1.5	90.6	129.4%	3.1%
	St. John's	7.4	2.0	79.8	78.4%	10.8%
JUN	Nain	6.4	0.0	44.4	69.5%	
	Goose	11.7	0.4	83.7	89.9%	0%
	Gander	11.1	-0.7	59.6	74.2%	0%
	St. John's	9.8	-1.1	37.9	44.3%	0%
JUL	Nain	8.8	-1.7	110.6	130.9%	
	Goose	15.7	-0.1	105.2	100.1%	*
	Gander	17.3	0.8	10.5	15.2%	*
	St. John's	15.5	0.0	50.8	61.1%	*
AUG	Nain	9.2	-0.5	83.6	121.7%	
	Goose	14.0	-5.3	76.8	74.4%	*
	Gander	15.5	-0.1	51.4	52.8%	*
	St. John's	14.5	-0.8	70.9	58.3%	*
SEP	Nain	7.3	1.4	76.4		
	Goose	10.9	1.8	92.3	109.2%	*
	Gander	10.4	-5.2	68.0	83.7%	*
	St. John's	11.2	-4.7	112.8	100.7%	*

* No snowfall recorded during this month.

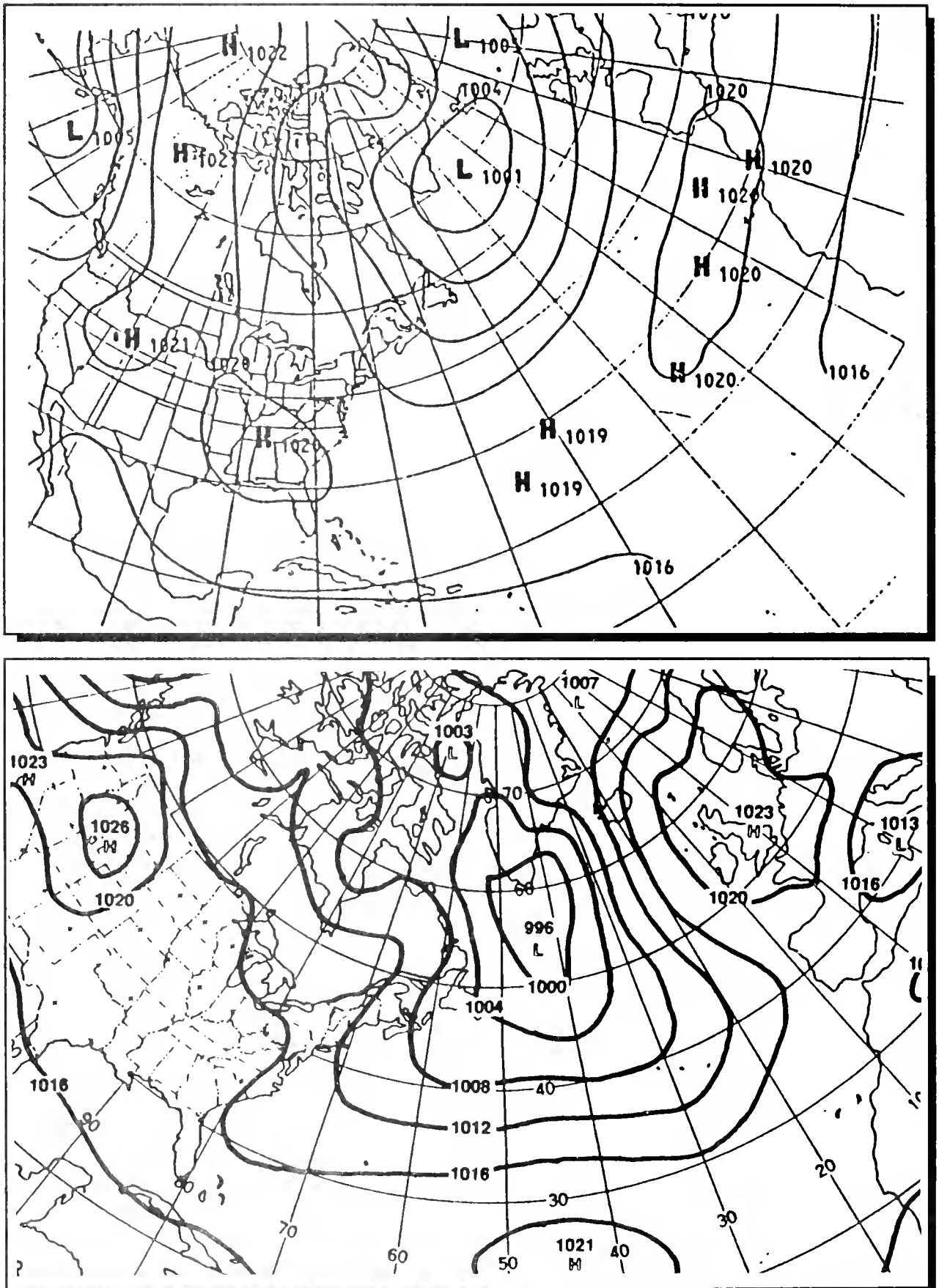

Figure 3. Comparison of January 1987 monthly mean surface pressure in mb (bottom, from Mariner's Weather Log, 1987b) with January historical average, 1948-1970 (top).

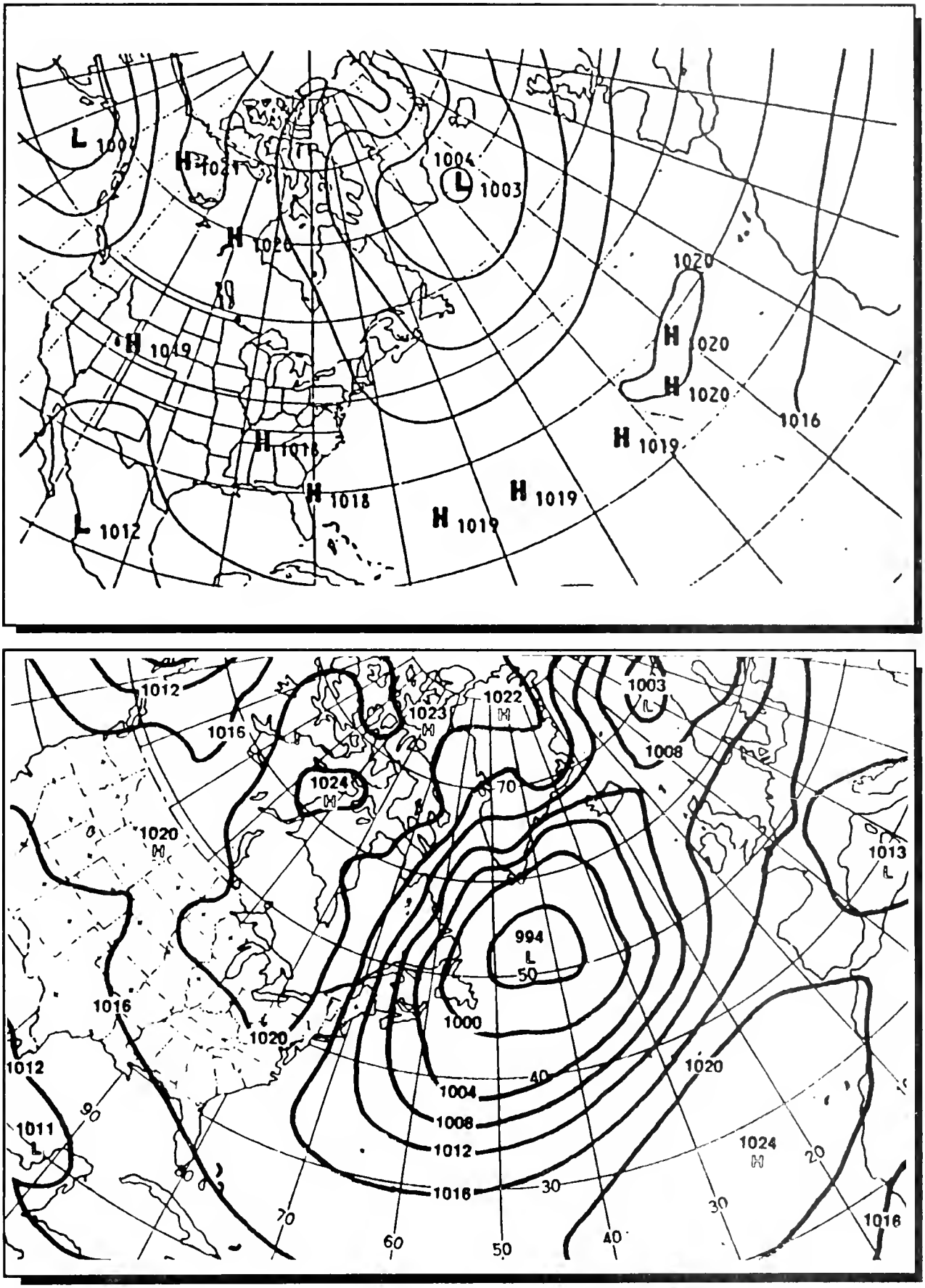

Figure 4. February 1987 (from Mariner's Weather Log, 1987b).

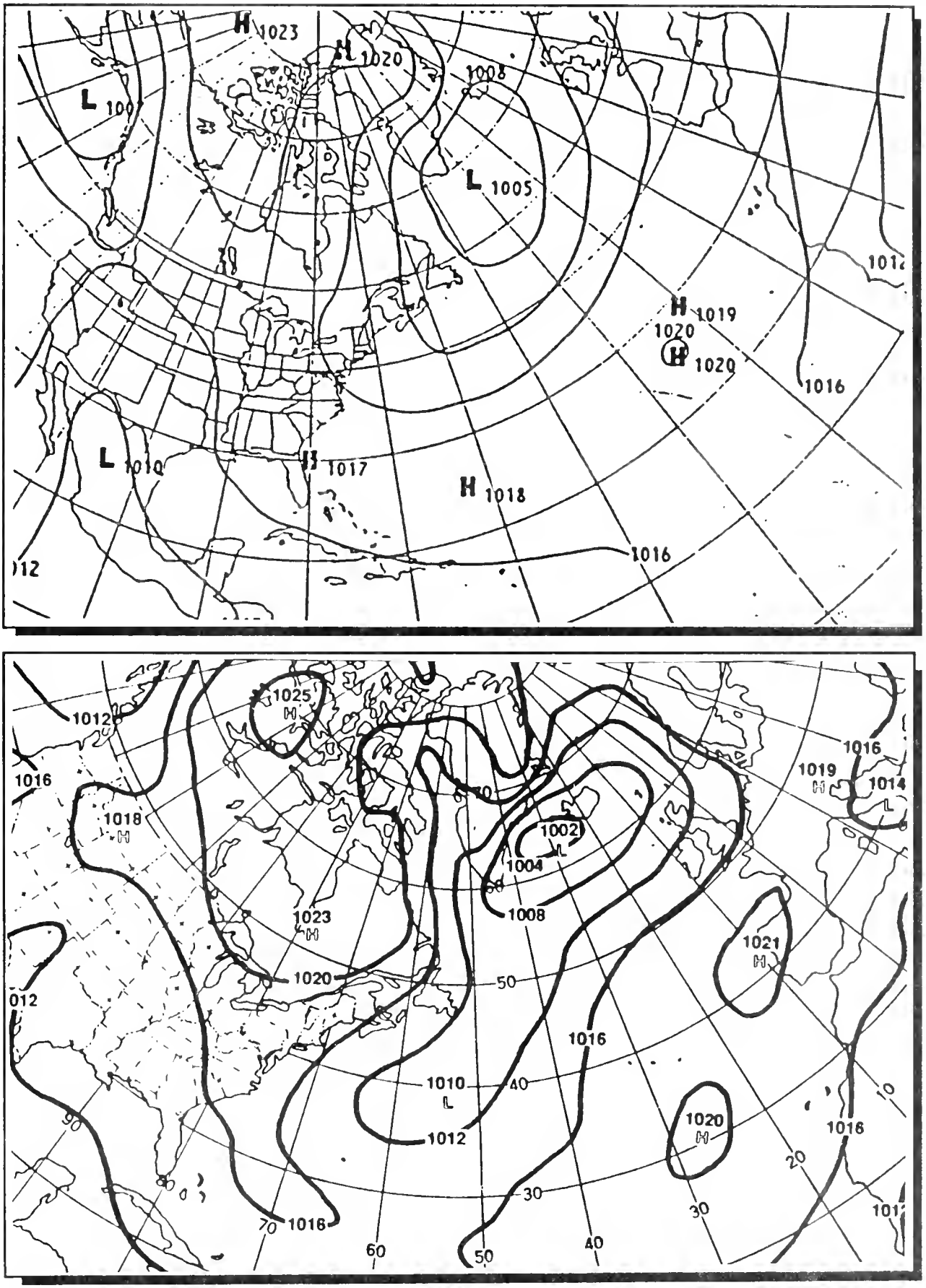

Figure 5. March 1987 (from Mariner's Weather Log, 1987b) .

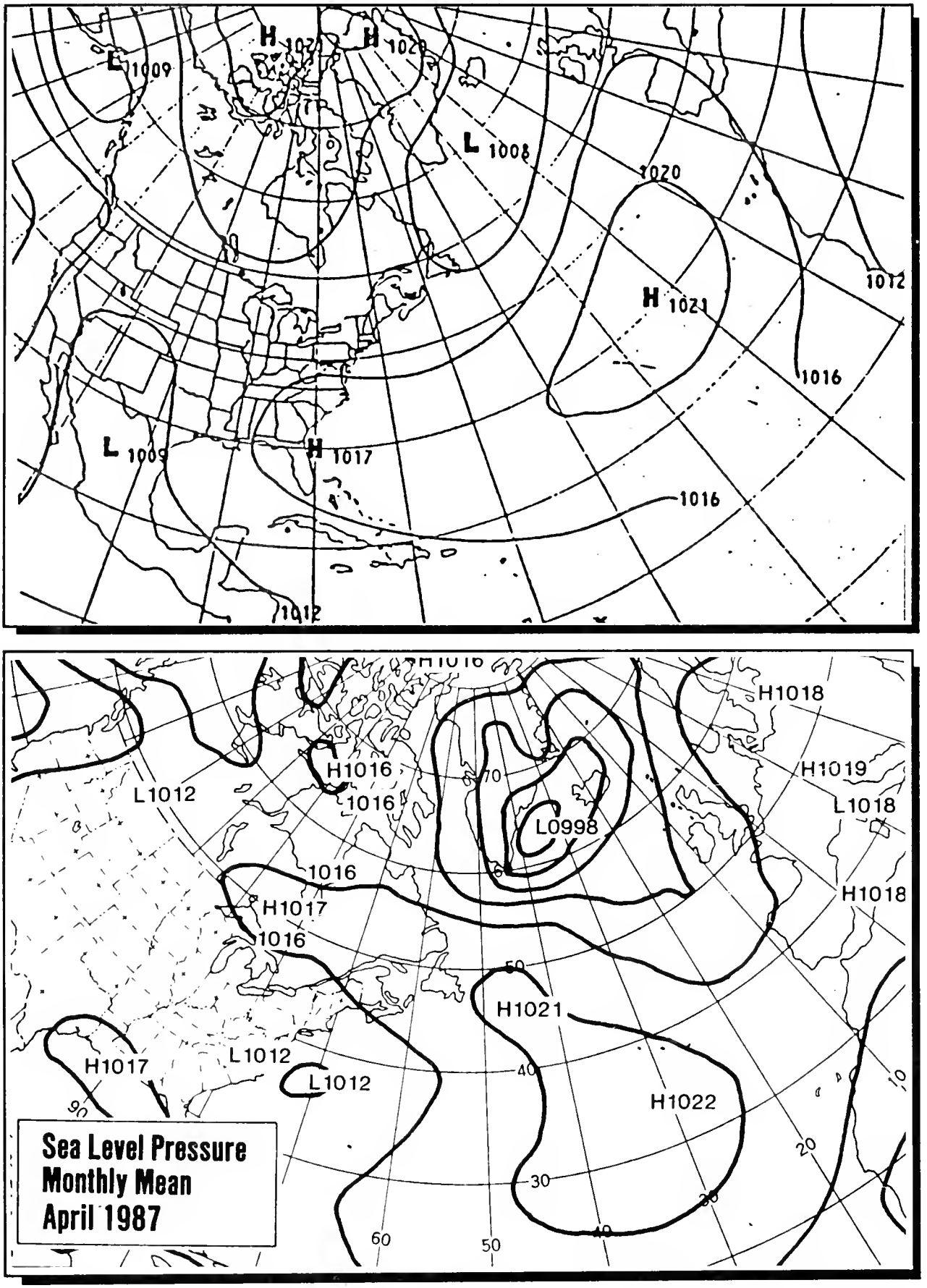

Figure 6. April 1987 (from Mariner's Weather Log, 1987c).

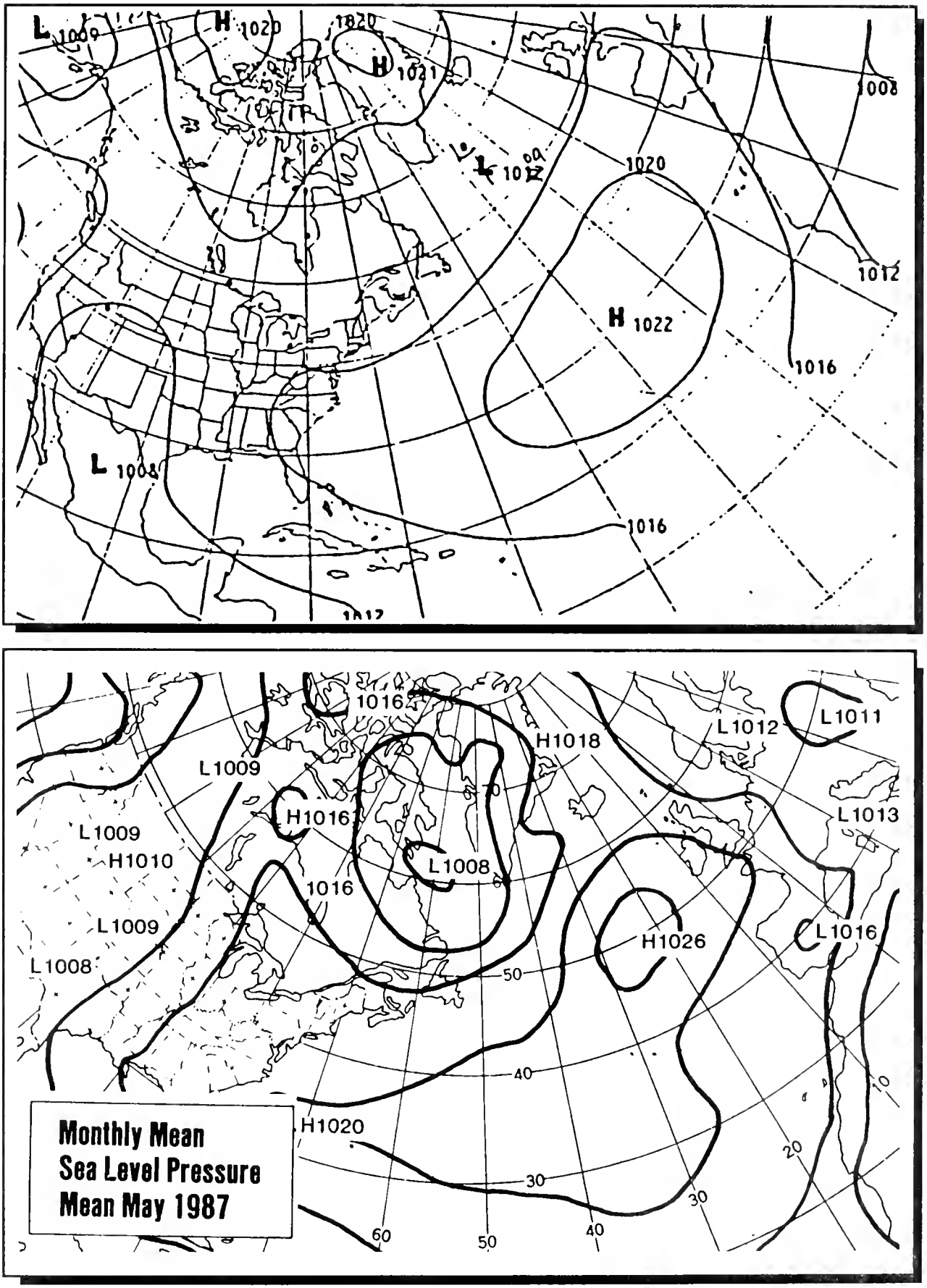

Figure 7. May 1987 (from Mariner's Weather Log, 1987c).

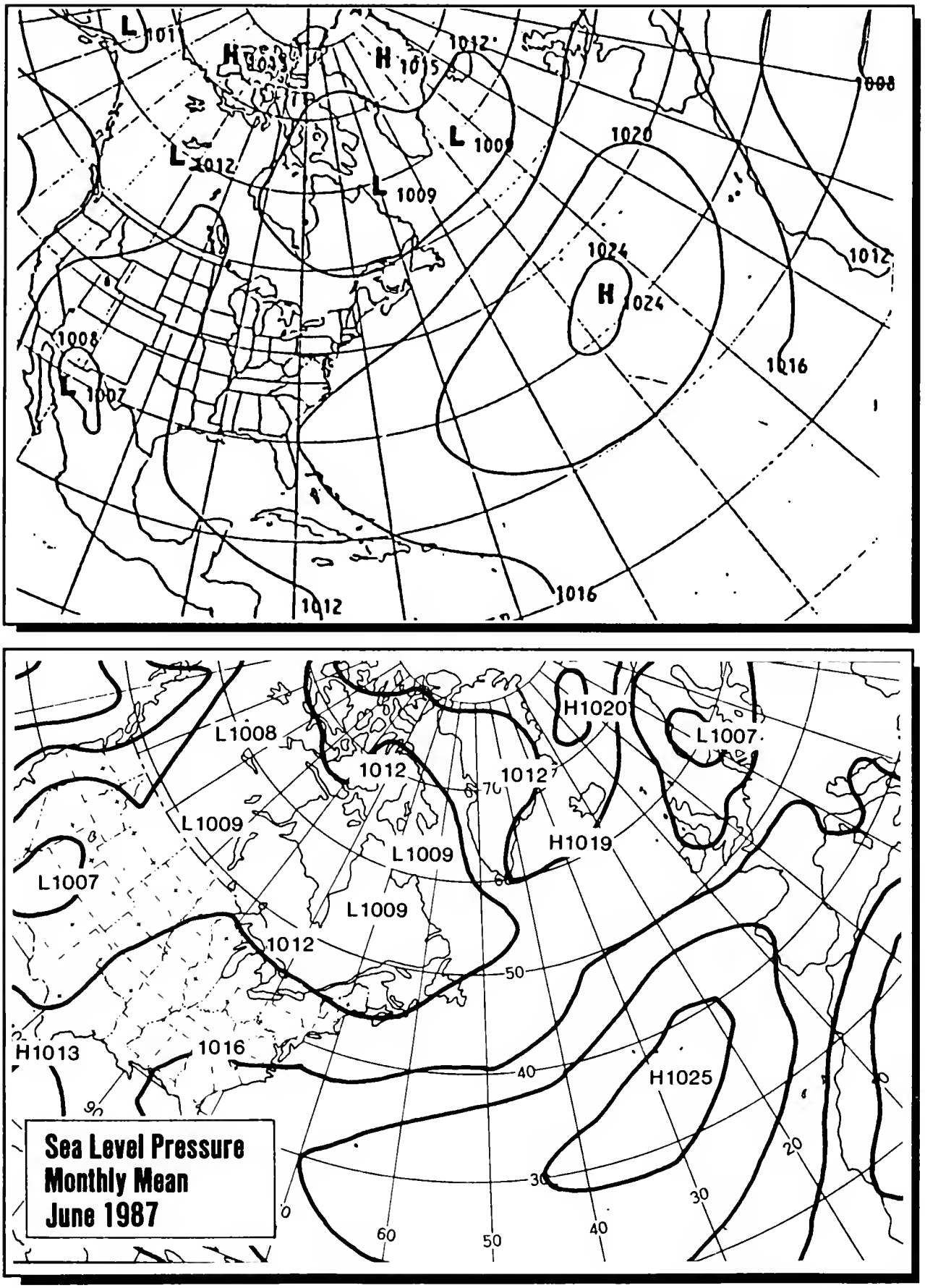

Figure 8. June 1987 (from Mariner's Weather Log, 1987c).

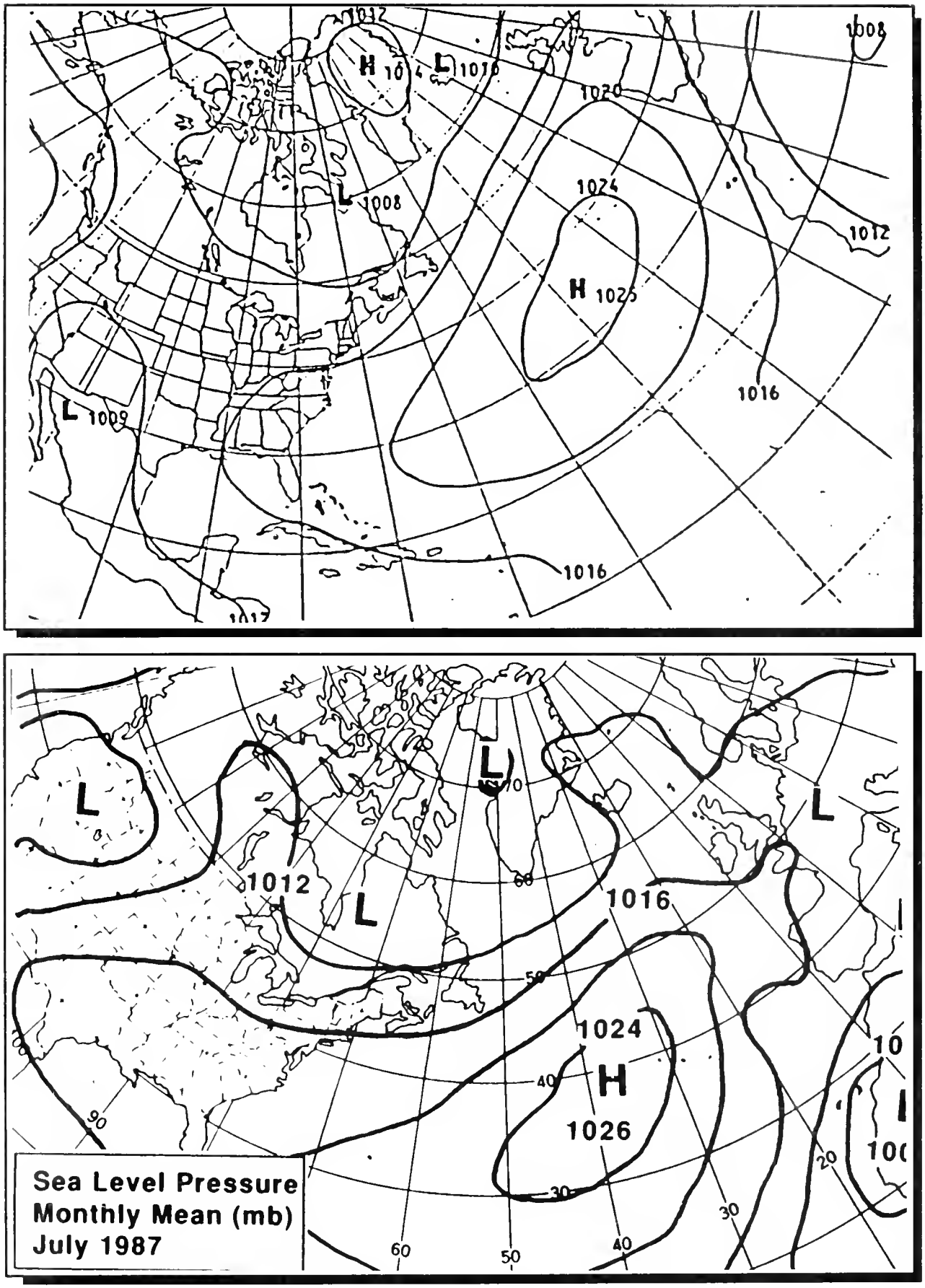

Figure 9. July 1987 (from Mariner's Weather Log, 1988) .

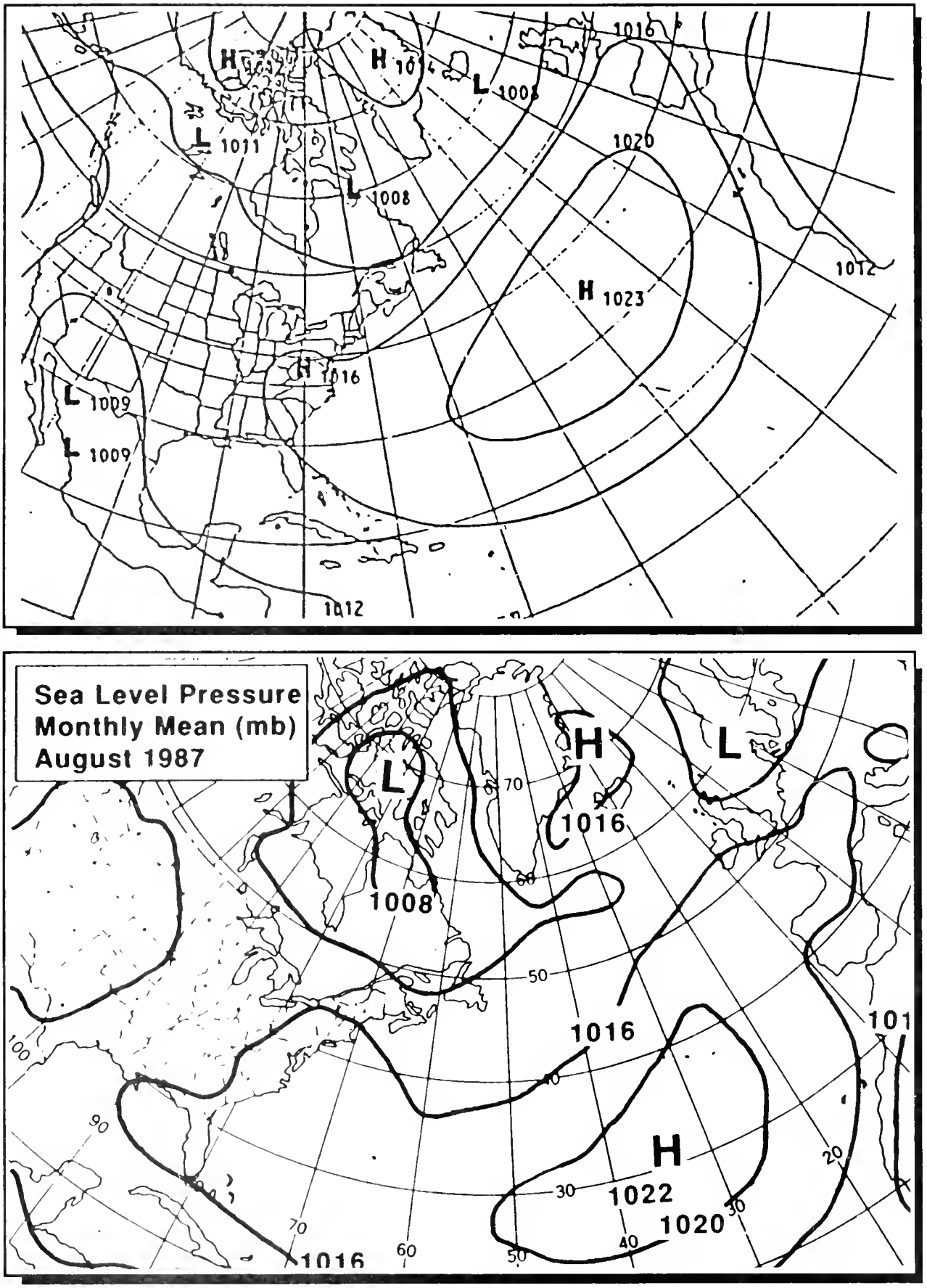

Figure 10. August 1987 (from Mariner's Weather Log, 1988).

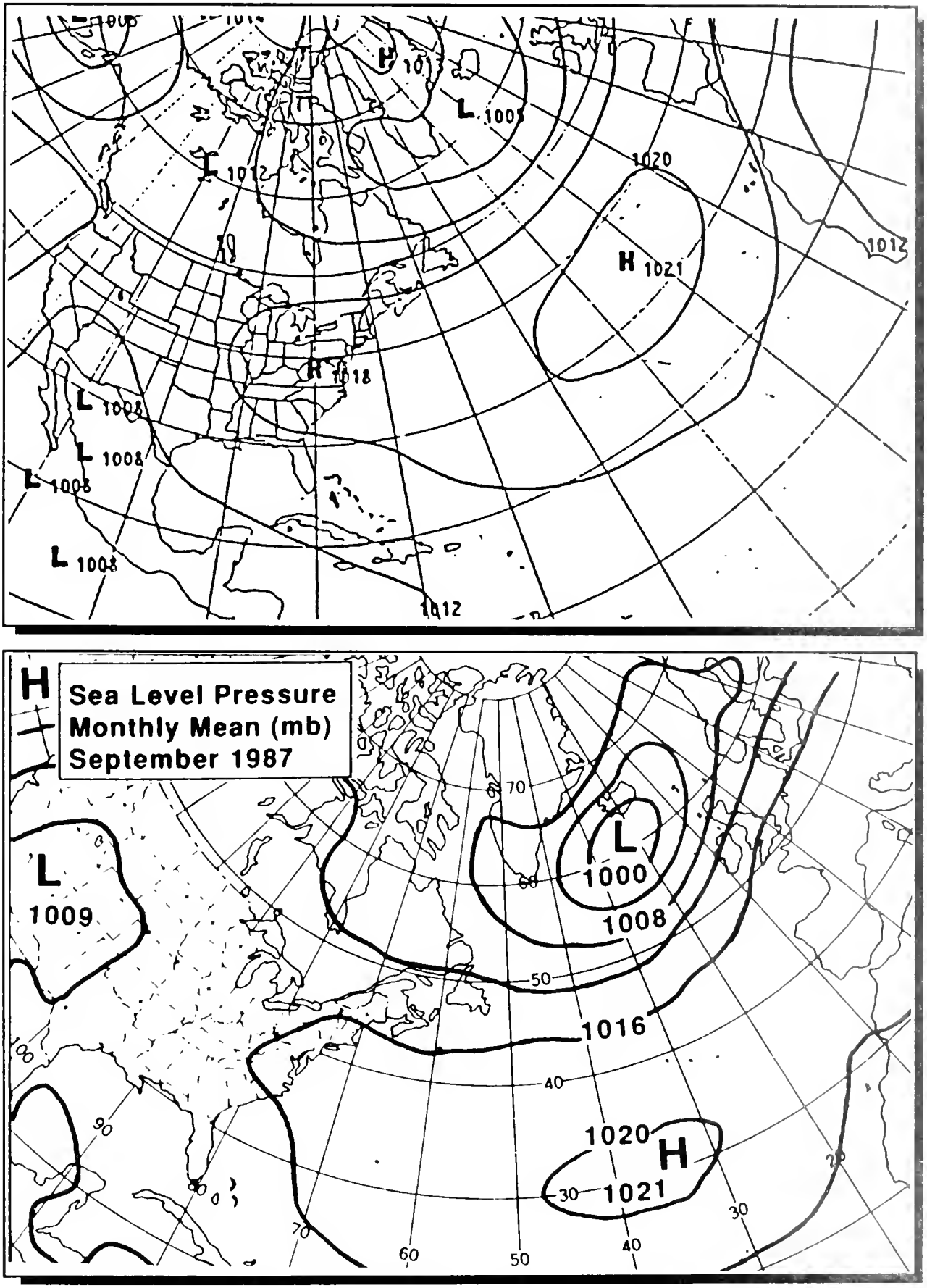

Figure 11. September 1987 (from Mariner's Weather Log, 1988).

Ice Conditions 1987 Season

The following discussion summarizes the sea ice and iceberg conditions along the Labrador and Newfoundland coasts and on the Grand Banks of Newfoundland for the 1987 ice year. The sea ice type and concentration information used in this discussion came from the Monthly Thirty Day Ice Forecast for Northern Canadian Waters published monthly by the Atmospheric Environment Service (AES) of Canada and the Southern Ice Limit published twice-monthly by the U.S. Navy-NOAA Joint Ice Center. Information on the maximum, mean, and minimum sea ice extent was obtained from Naval Oceanography Command, 1986.

October 1986: No sea ice was seen south of 65°N in October, which is normally the case (Figure 12). There were no icebergs reported south of 52°N in October.

November 1986: In mid-November, new, young, and thin first-year sea ice began to form in Ungava Bay, Hudson Strait, and Davis Strait (Figure 13). The mean extent of sea ice in November is confined to the southern tip of Baffin Island with the maximum sea ice extent covering Hudson Strait, and Ungava Bay. Ice conditions in November 1986 were close to the maximum conditions. An unusually deep Icelandic Low (Mariner's Weather Log, 1987a) brought below normal temperatures to Labrador (Table 6) which enhanced the sea ice growth. There were 8 icebergs reported south of 52°N in November.

December 1986: Aided by continued below normal temperatures (Table 6), the sea ice edge continued to be farther south than the mean and close to the maximum extent of sea ice. In mid-December, thin first-year, young and new sea ice were just north of the Strait of Belle Isle (Figure 14). Concentrations were generally 8-10 tenths. There were 9 icebergs reported south of 52°N in December; 5 of these icebergs were south of 48°N.

January 1987: In mid-January, new and young sea ice were north of the Avalon Peninsula and along the eastern coast of Newfoundland (Figure 15). The Strait of Belle Isle was now ice covered with new and young sea ice. The sea ice again extended beyond the mean limits of sea ice, but did not extend to the maximum limits of sea ice extent. By the end of January, the sea ice growth and spread was 2-3 weeks ahead of normal (AES, 1987). This above average sea ice growth can again be attributed to below normal temperatures in Labrador and Newfoundland (Table 6). There were 5 icebergs reported south of 52°N in January; 2 of these were south of 48°N.

February 1987: By mid-February, a tongue of 9-10 tenths first-year sea ice extended along the Labrador coast, into the Strait of Belle Isle, and along the eastern coast of Newfoundland down to the Avalon Peninsula (Figure 16). Young, thin first-year, and first-year sea ice were west of Newfoundland with concentrations of 9-10 tenths. The extent of sea ice in February was close to the mean extent. The increase in temperatures to warmer than normal in Labrador and near normal on Newfoundland (Table 6) returned the sea ice extent to near normal. There were 14 icebergs observed south of 52°N in February; all of these icebergs were south of 48°N.

March 1987: The 1987 International Ice Patrol season opened on March 12. Figure 24 shows the iceberg distribution at the beginning of the season. In mid-March, thin first-year sea ice advanced from the Avalon Peninsula south over the Grand Banks (Figure 17). The sea ice edge was again close to its mean extent. Towards the end of March, drastic changes in the sea ice extent occurred. Figure 26 shows the sea ice pushed off the Grand Banks with all the remaining sea ice confined to close to the east and south coast of Newfoundland. The iceberg distribution on March 30 showed a marked shift to the west compared to March 15 (Figure 25). Between March 15 and March 30, the prevailing winds were easterly (AES 1987), forcing the sea ice and icebergs westward. There were 57 new icebergs south of 52°N in March; 48 of these icebergs were south of 48°N. At the end of March, there were 25 icebergs on plot (Figure 26).

April 1987: The unusual sea ice distribution created by the easterly winds at the end of March continued into April. There was no sea ice on the Grand Banks or the west coast of Newfoundland (Figure 18). The southern coast of Newfoundland, usually ice free, had 9-10 tenths of sea ice. The extent of sea ice was still near average for April . The iceberg distribution on April 15 (Figure 27) only extended to 47°W. By April 30, the iceberg distribution extended to 43°W (Figure 28). There were 117 new icebergs south of 52°N; 76 of these were south of 48°N. There were 142 icebergs on plot at the end of April (Figure 28).

May 1987: In mid-May, the southern and eastern coasts of Newfoundland became ice-free as the sea ice retreated northward (Figure 19). A large polynya (an area of open water surrounded by ice) formed along the Newfoundland and Labrador coasts between 50 and 55°N. This polynya was formed from southwesterly winds pushing the ice off-shore (AES, 1987). Above average temperatures on Newfoundland and southern Labrador had accelerated the sea ice retreat in these regions. As the sea ice retreated northward, large numbers of icebergs were released to drift southward. With 236 new icebergs south of 52°N, May was the heaviest month for new icebergs. Only 29 of these icebergs were south of 48°N. Only a few of these icebergs drifted with the Labrador Current through Flemish Pass. There were 158 icebergs on plot the end of May (Figure 30).

June 1987: By mid-June, the ice edge had retreated to Goose Bay (Figure 20). This is the typical pattern of retreat in June (Naval Oceanographic Command, 1986). The number of new icebergs south of 52°N was again high in June. There were 215 new icebergs south of 52°N in June; 127 of these were south of 48°N. By mid-June, a large number of icebergs had drifted onto the Grand Banks (Figure 31). Most of these icebergs were gone by the end of June with most of the remaining icebergs north of 48°N (Figure 32). There were 64 icebergs on plot the end of June (Figure 32).

July 1987: The sea ice edge continued to retreat northward, but at a slower rate than normal. By mid-July, the sea ice edge has usually retreated to Baffin Island, with some sea ice also persisting in Ungava Bay. In mid-July 1987, however, the sea ice edge was still down along the Labrador Coast (Figure 21). The temperatures in July on Labrador were colder than normal (Table 6) and these cooler temperatures may have caused the sea ice edge to retreat slower than it would have normally. There were 25 new icebergs south of 52°N; 15 of these were south of 48°N. There were 10 icebergs on plot the end of July (Figure 34). The 1987 International Ice Patrol season was closed on July 31,1987.

August 1987: The retreat of the sea ice edge to just north of Frobisher Bay in August left Hudson Strait and most of Davis Strait ice free (Figure 22). There were 57 icebergs reported south of 52°N in August; 2 of these were south of 48°N.

September 1987: The only sea ice observed south of 65°N in September was near Frobisher Bay (Figure 23).

Figure 12.

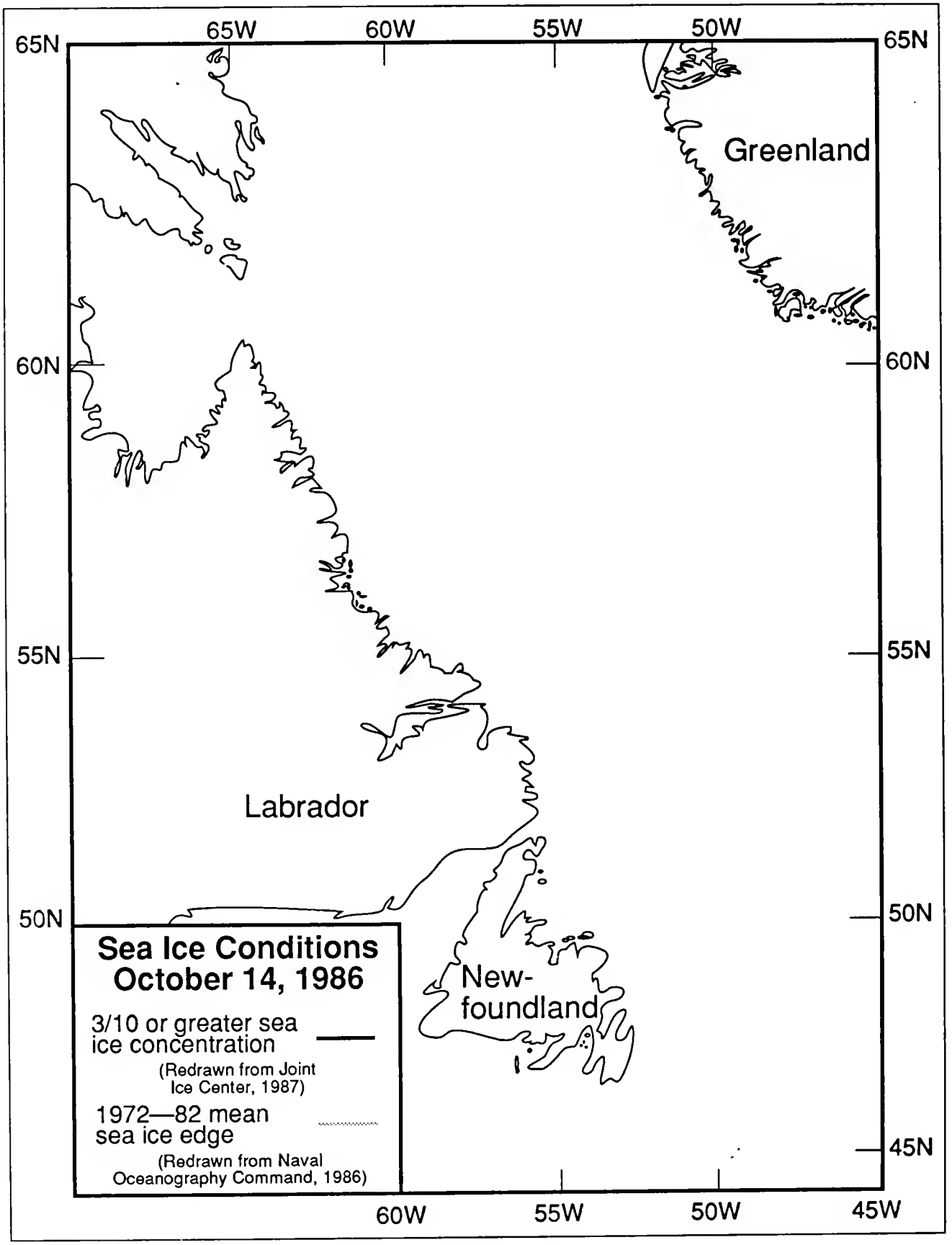
65W
60W
55W
50W
65N
60N
55N
50N
45N
Greenland
Labrador
New-
foundland
Sea Ice Conditions
October 14, 1986
3/10 or greater sea ice concentration
(Redrawn from Joint Ice Center, 1987)
1972—82 mean sea ice edge
(Redrawn from Naval Oceanography Command, 1986)

Figure 13.

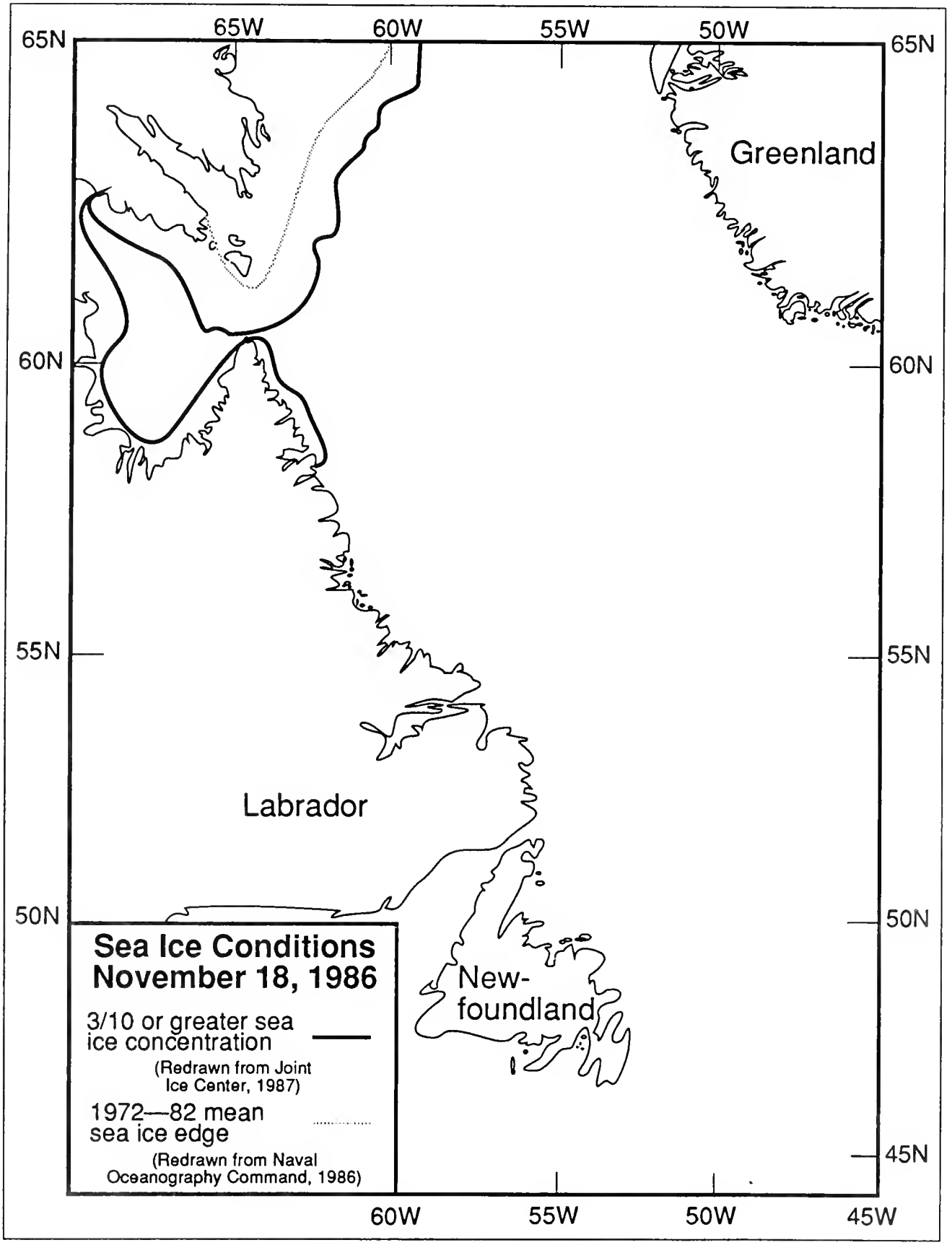
65N
65W
60W
55W
50W
Greenland
60N
55N
Labrador
50N
New-
foundland
45N
60W
55W
50W
45W
Sea Ice Conditions
November 18, 1986
3/10 or greater sea ice concentration
(Redrawn from Joint Ice Center, 1987)
1972—82 mean sea ice edge
(Redrawn from Naval Oceanography Command, 1986)

Figure 14.

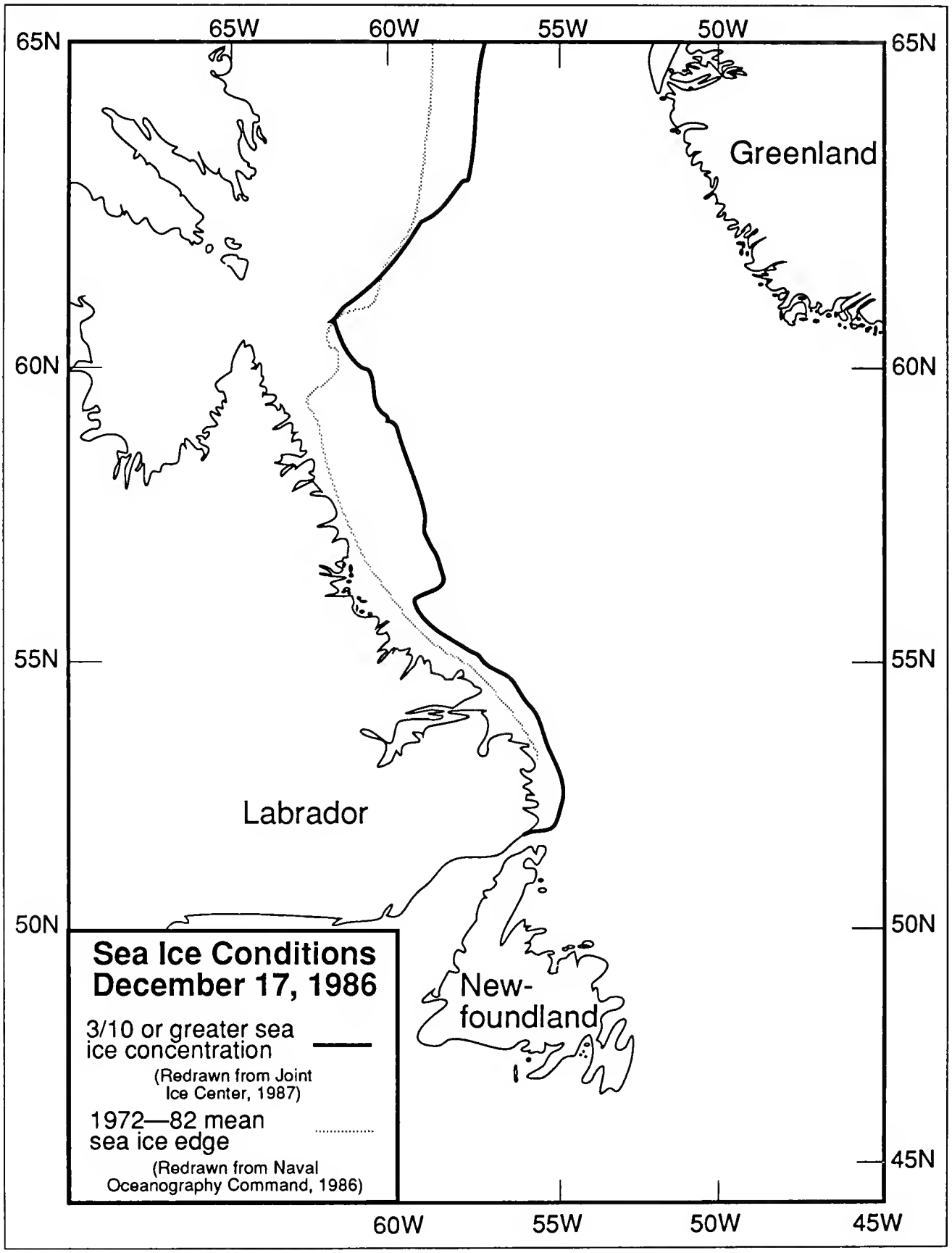
65W
60W
55W
50W
65N
60N
55N
50N
45N
Greenland
Labrador
New-
foundland
Sea Ice Conditions
December 17, 1986
3/10 or greater sea ice concentration
(Redrawn from Joint Ice Center, 1987)
1972—82 mean sea ice edge
(Redrawn from Naval Oceanography Command, 1986)

Figure 15.

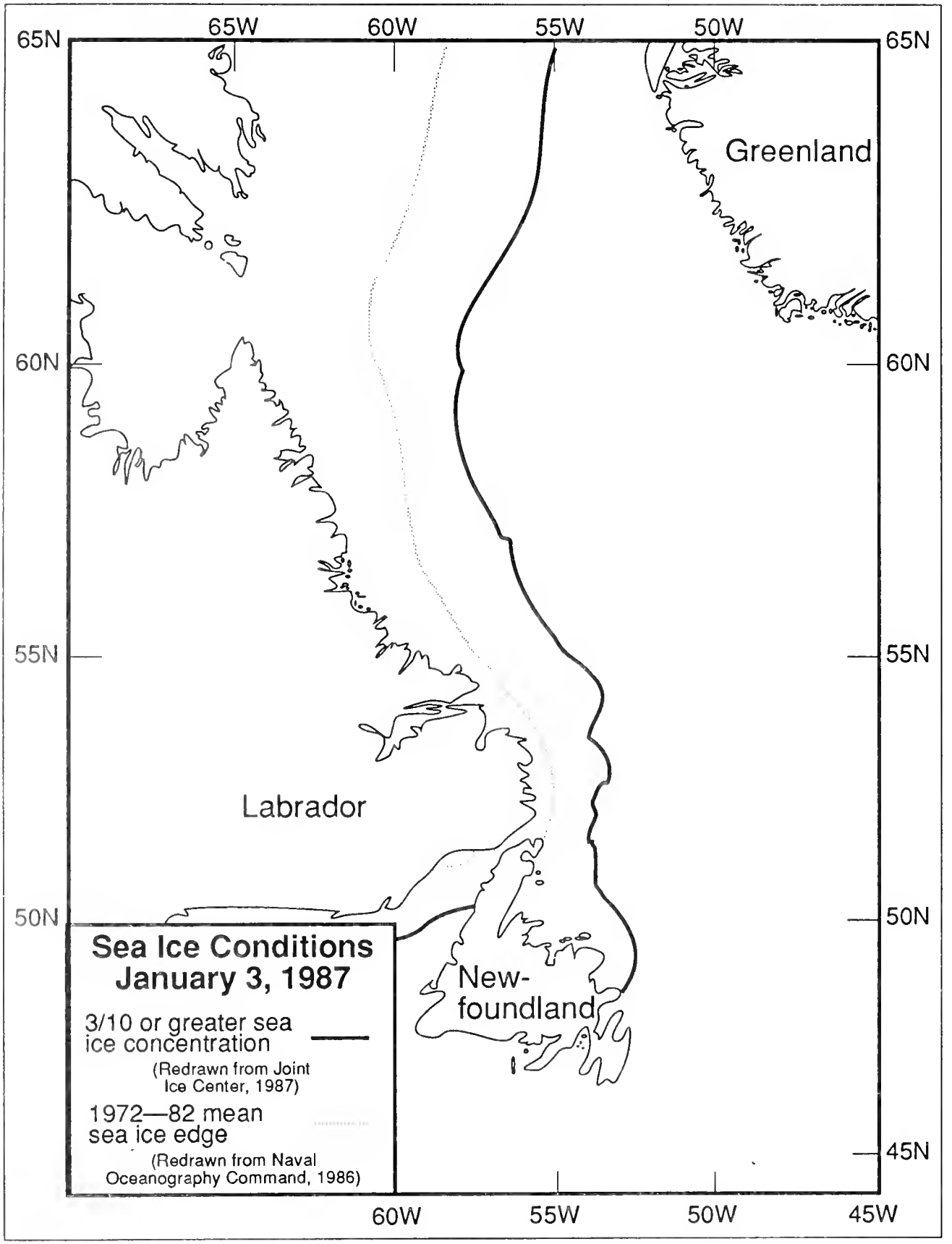
65N
65W
60W
55W
50W
65N
Greenland
60N
60N
55N
55N
Labrador
50N
50N
Sea Ice Conditions
January 3, 1987
3/10 or greater sea ice concentration
(Redrawn from Joint Ice Center, 1987)
1972—82 mean sea ice edge
(Redrawn from Naval Oceanography Command, 1986)
New-
foundland
45N
60W
55W
50W
45W

Figure 16.

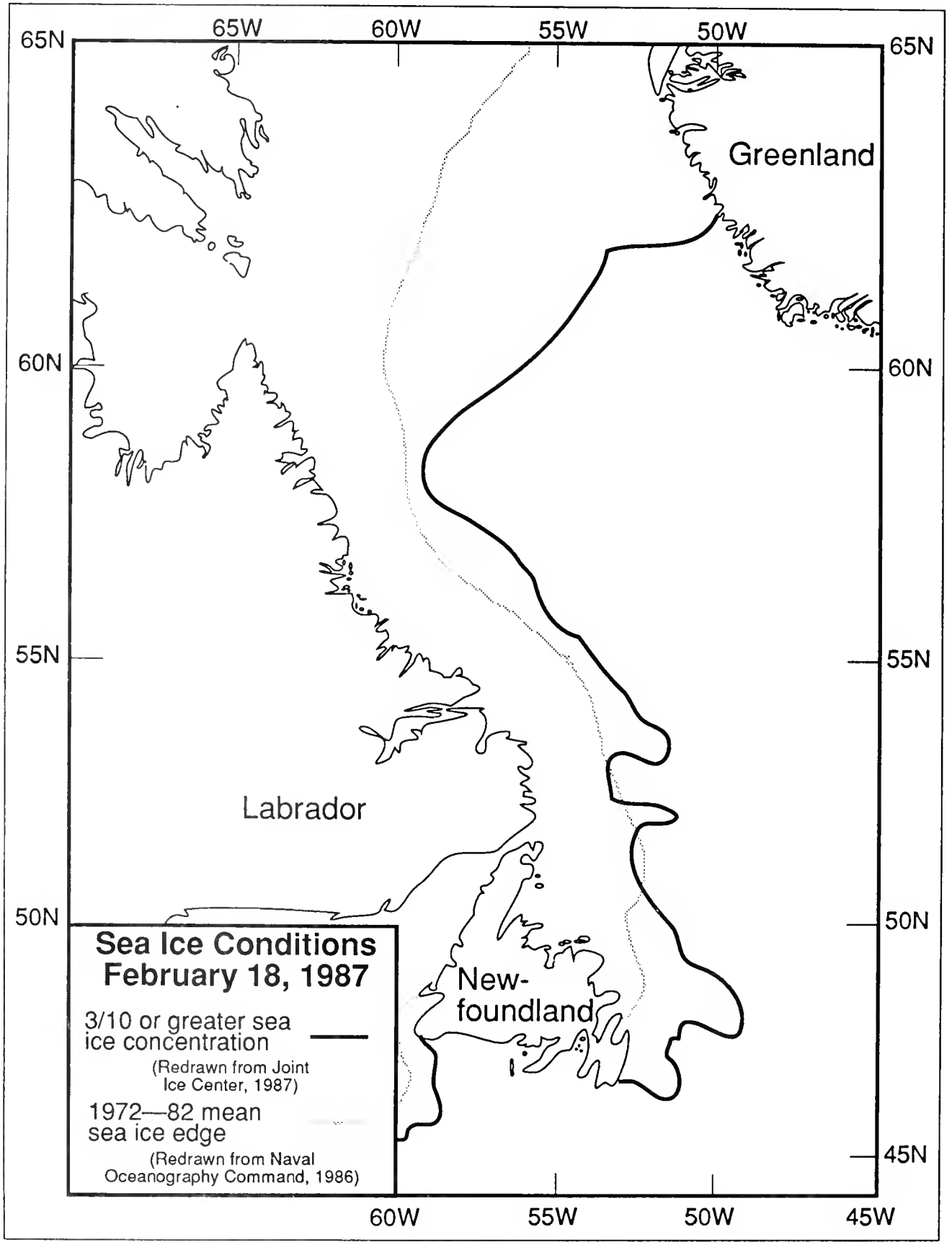
65N
65W
60W
55W
50W
Greenland
60N
55N
Labrador
50N
New-
foundland
45N
60W
55W
50W
45W
Sea Ice Conditions
February 18, 1987
3/10 or greater sea ice concentration
(Redrawn from Joint Ice Center, 1987)
1972—82 mean sea ice edge
(Redrawn from Naval Oceanography Command, 1986)

Figure 17.

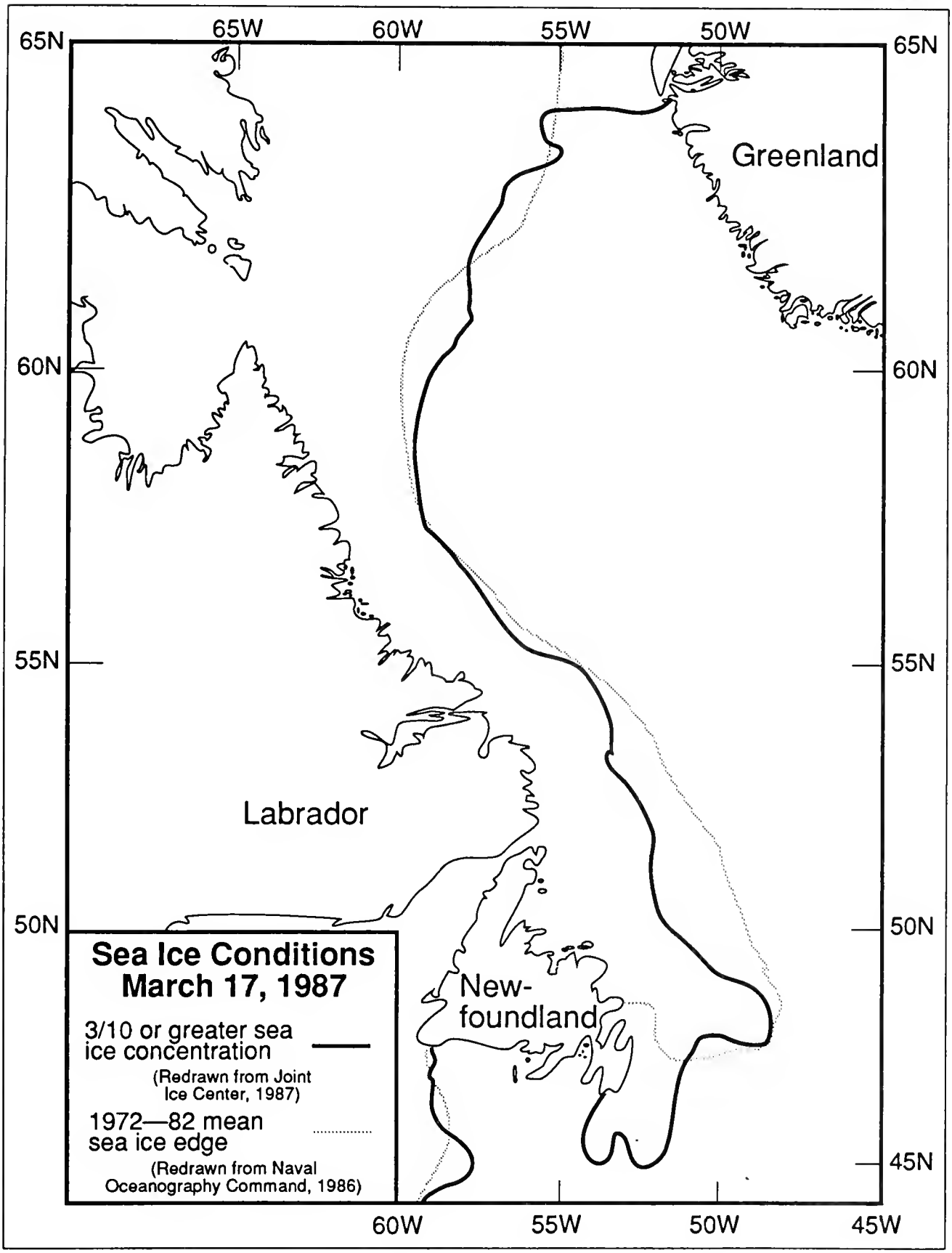
65N
65W
60W
55W
50W
65N
Greenland
60N
60N
55N
55N
Labrador
50N
50N
Sea Ice Conditions
March 17, 1987
3/10 or greater sea ice concentration
(Redrawn from Joint Ice Center, 1987)
1972—82 mean sea ice edge
(Redrawn from Naval Oceanography Command, 1986)
New-
foundland
45N
60W
55W
50W
45W

Figure 18.

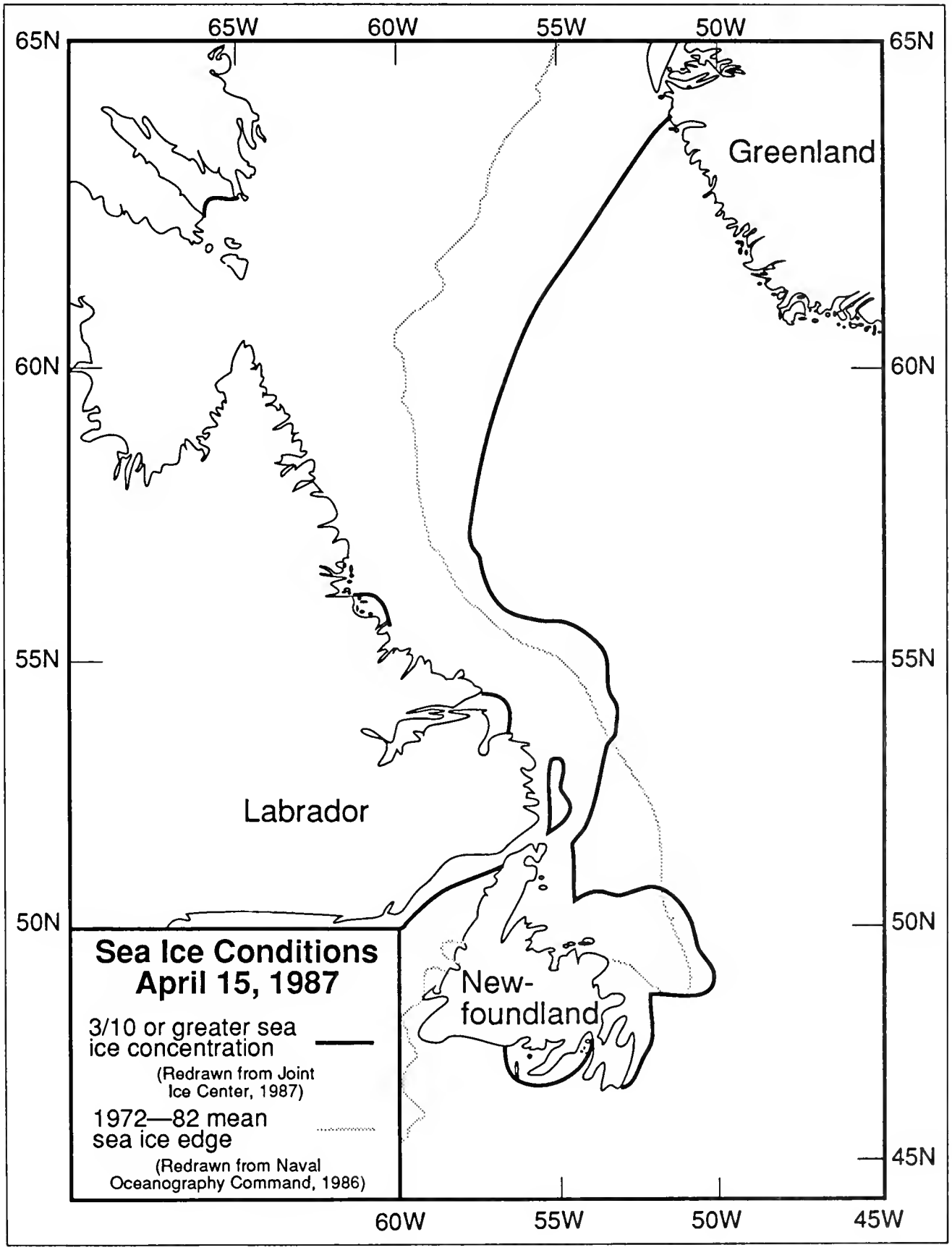
65N
65W
60W
55W
50W
Greenland
60N
55N
Labrador
50N
Sea Ice Conditions
April 15, 1987
3/10 or greater sea ice concentration
(Redrawn from Joint Ice Center, 1987)
1972—82 mean sea ice edge
(Redrawn from Naval Oceanography Command, 1986)
New-foundland
45N
45W

Figure 19.

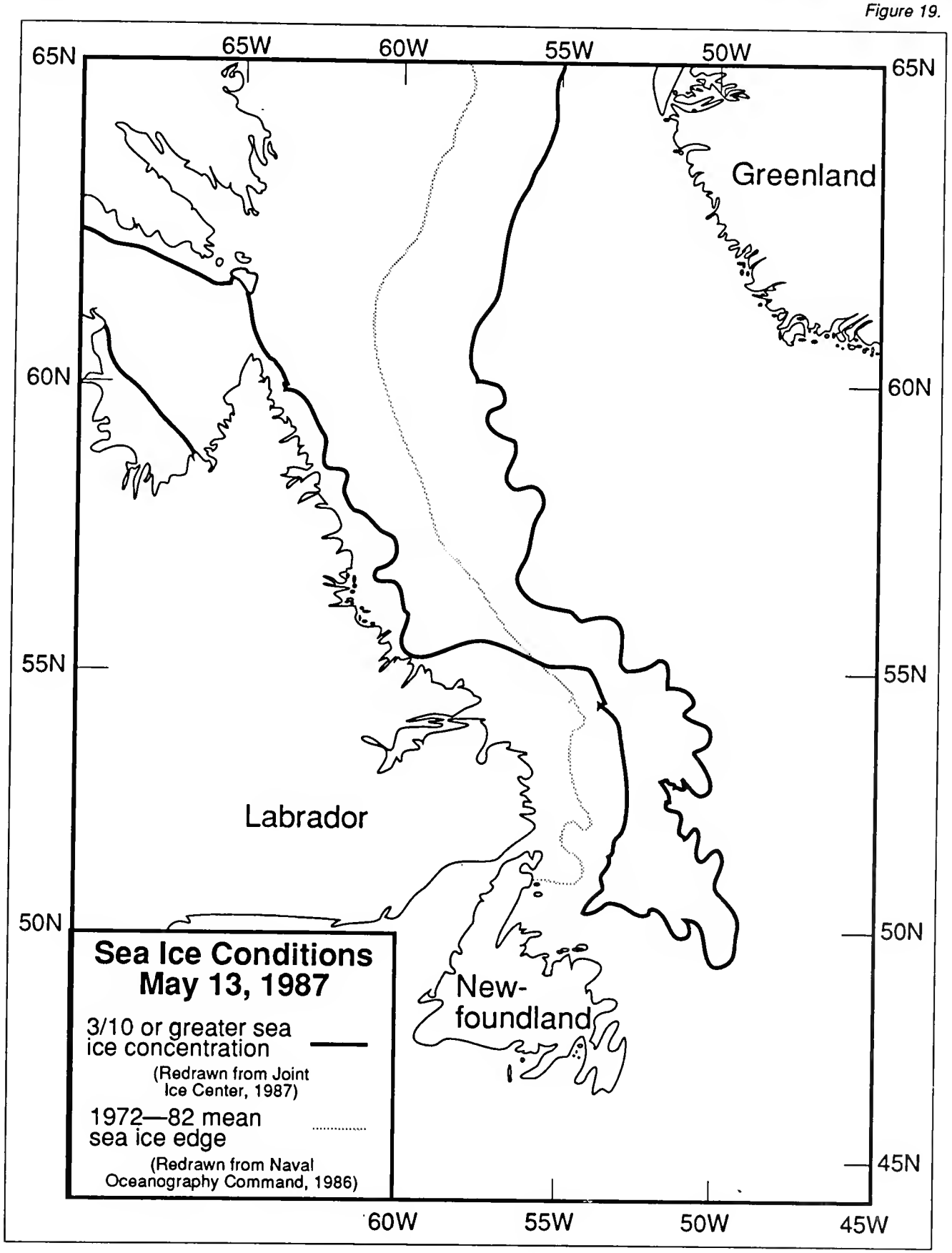
65N
65W
60W
55W
50W
65N
Greenland
60N
60N
55N
55N
Labrador
50N
50N
New-
foundland
45N
60W
55W
50W
45W
Sea Ice Conditions
May 13, 1987
3/10 or greater sea ice concentration
(Redrawn from Joint Ice Center, 1987)
1972—82 mean sea ice edge
(Redrawn from Naval Oceanography Command, 1986)

Figure 20.

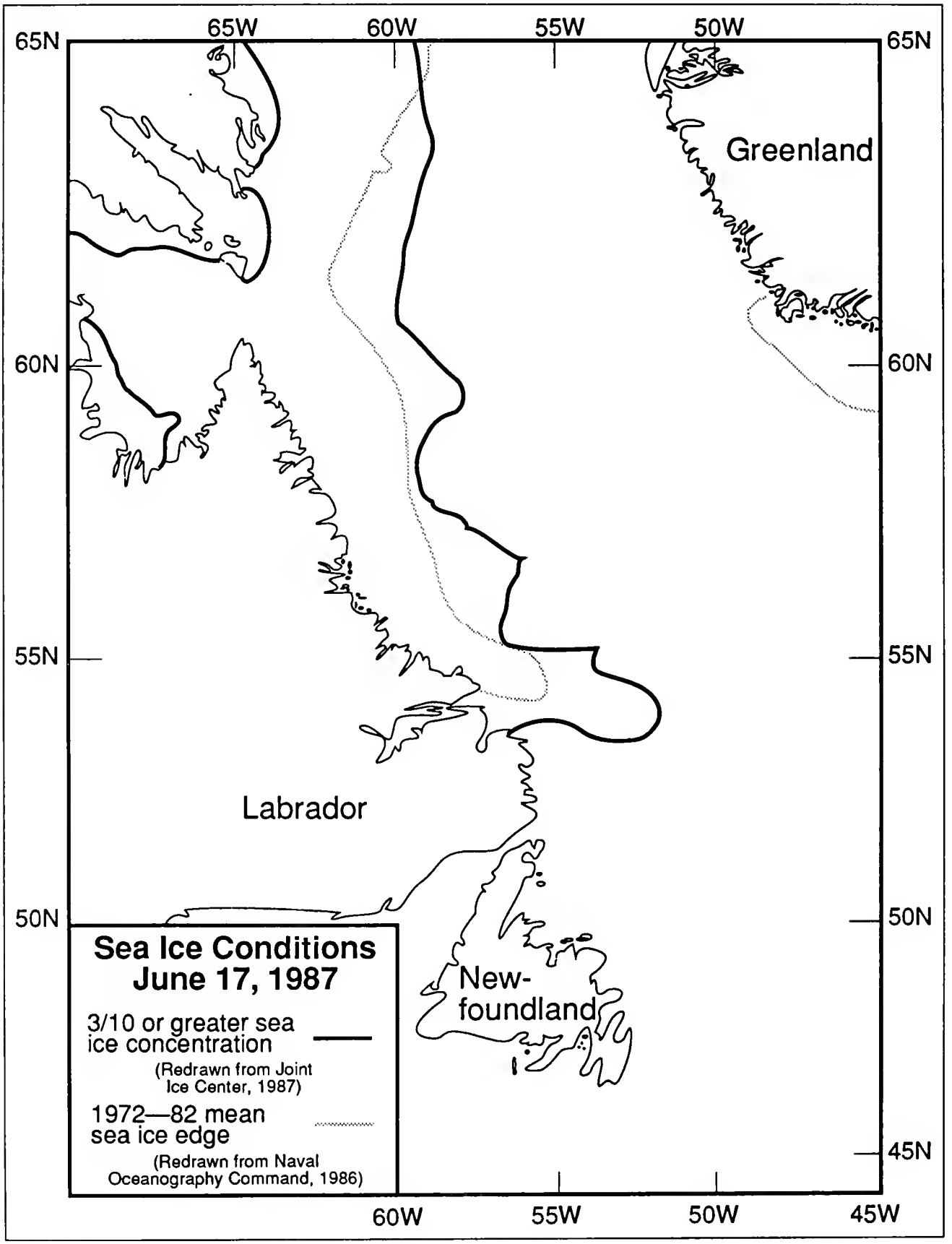
65W
60W
55W
50W
65N
60N
55N
50N
45N
Greenland
Labrador
New-
foundland
Sea Ice Conditions
June 17, 1987
3/10 or greater sea ice concentration
(Redrawn from Joint Ice Center, 1987)
1972—82 mean sea ice edge
(Redrawn from Naval Oceanography Command, 1986)

Figure 21.

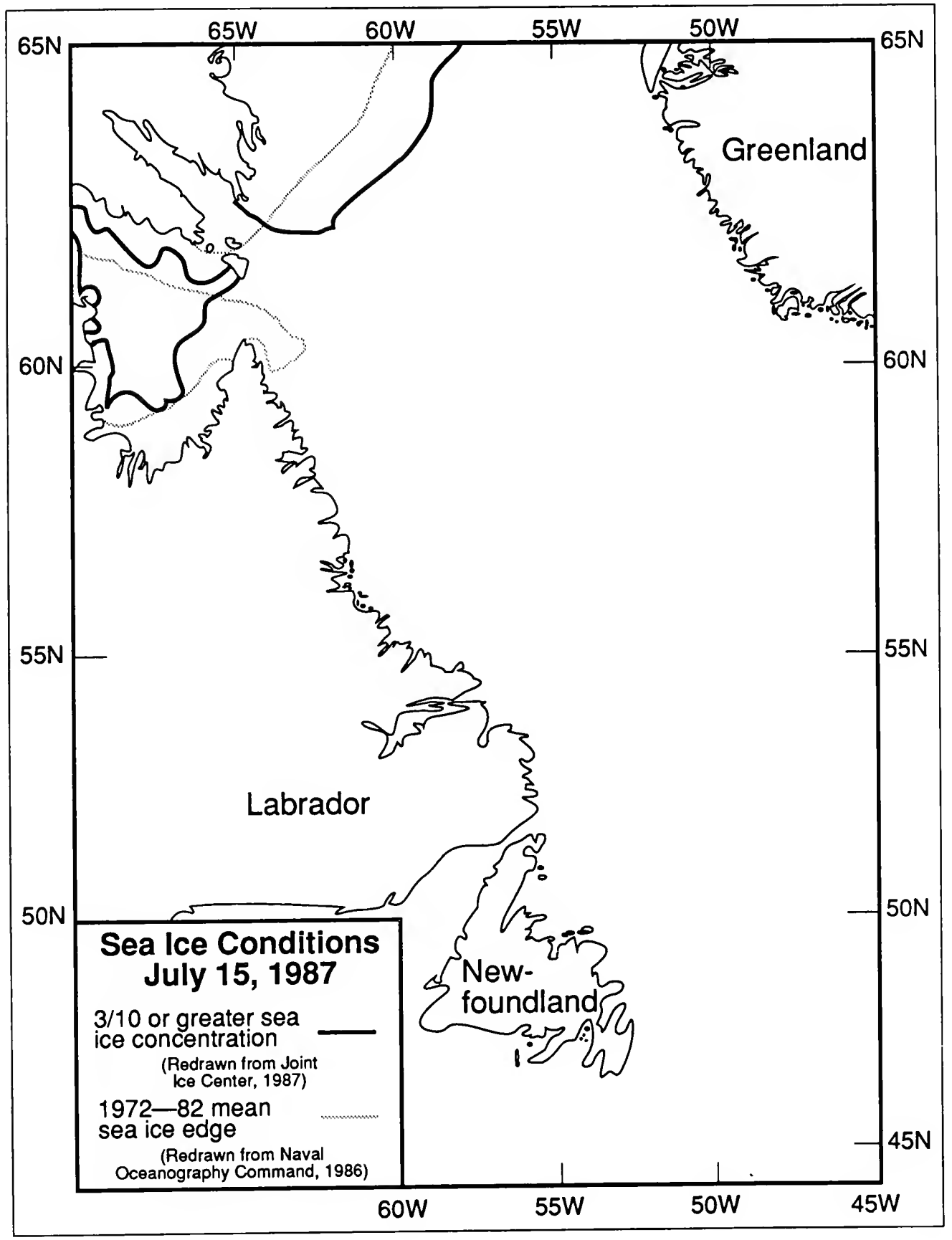
65W
60W
55W
50W
65N
60N
55N
50N
45N
Greenland
Labrador
New-
foundland
Sea Ice Conditions
July 15, 1987
3/10 or greater sea ice concentration
(Redrawn from Joint Ice Center, 1987)
1972—82 mean sea ice edge
(Redrawn from Naval Oceanography Command, 1986)

Figure 22.

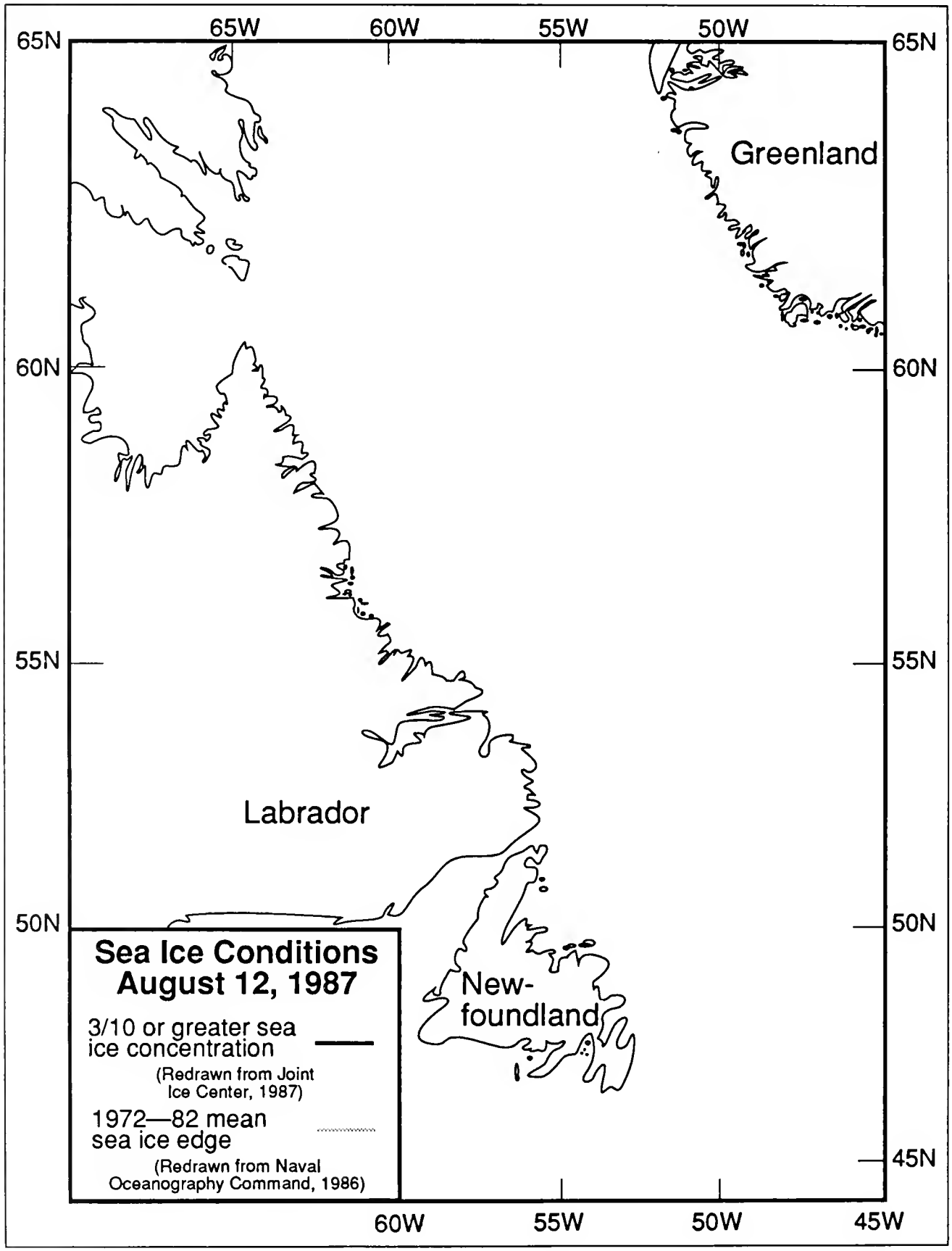
65W
60W
55W
50W
65N
60N
55N
50N
45N
Greenland
Labrador
New-
foundland
Sea Ice Conditions
August 12, 1987
3/10 or greater sea ice concentration
(Redrawn from Joint Ice Center, 1987)
1972—82 mean sea ice edge
(Redrawn from Naval Oceanography Command, 1986)

Figure 23.

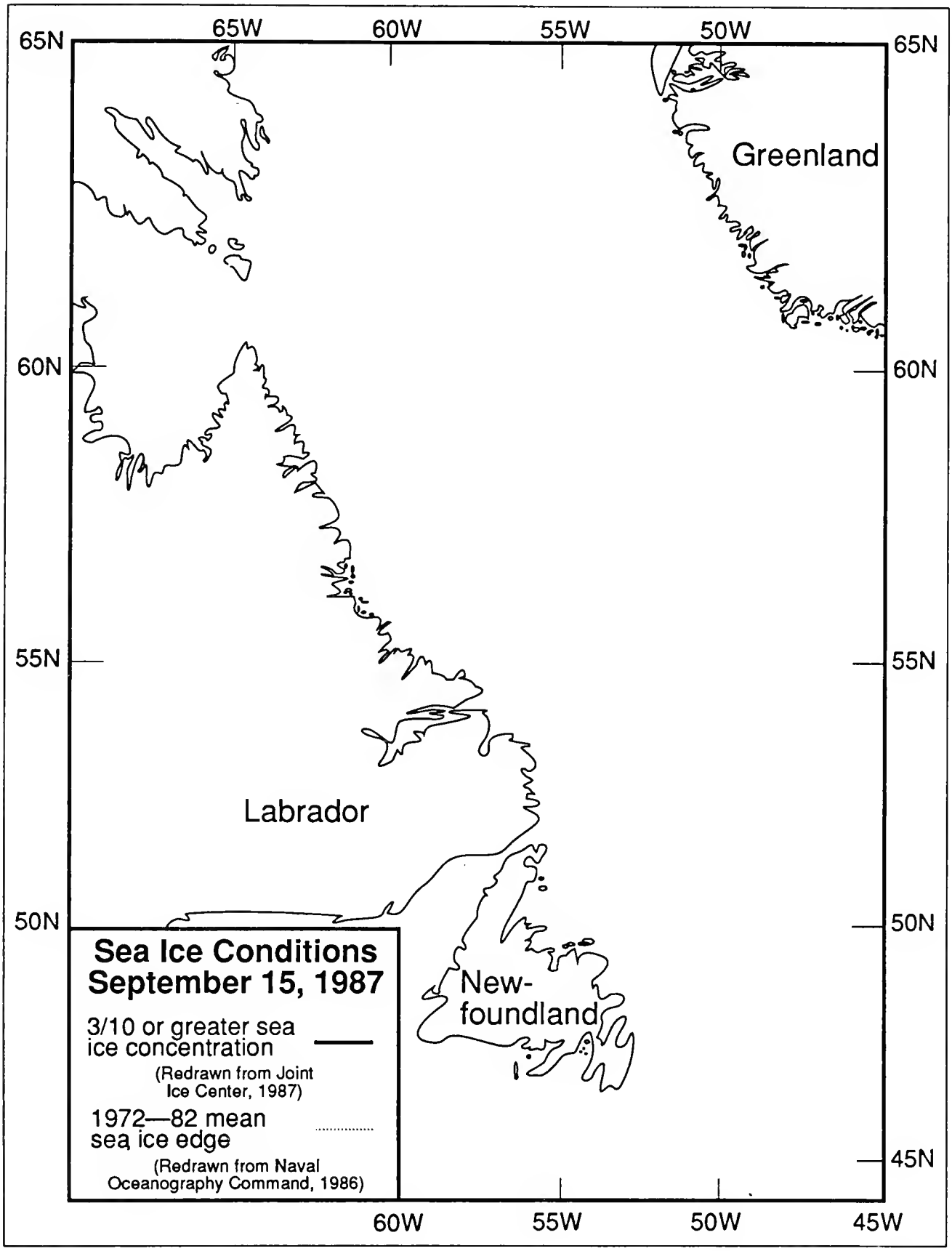
65N
65W
60W
55W
50W
65N
Greenland
60N
60N
55N
55N
Labrador
50N
50N
Sea Ice Conditions
September 15, 1987
3/10 or greater sea ice concentration
(Redrawn from Joint Ice Center, 1987)
1972—82 mean sea ice edge
(Redrawn from Naval Oceanography Command, 1986)
New-
foundland
45N
60W
55W
50W
45W

Figure 24. Graphic Depiction of International Ice Patrol Plot for 1200 GMT March 12, 1987, Based on Observed and Forecast Conditions.

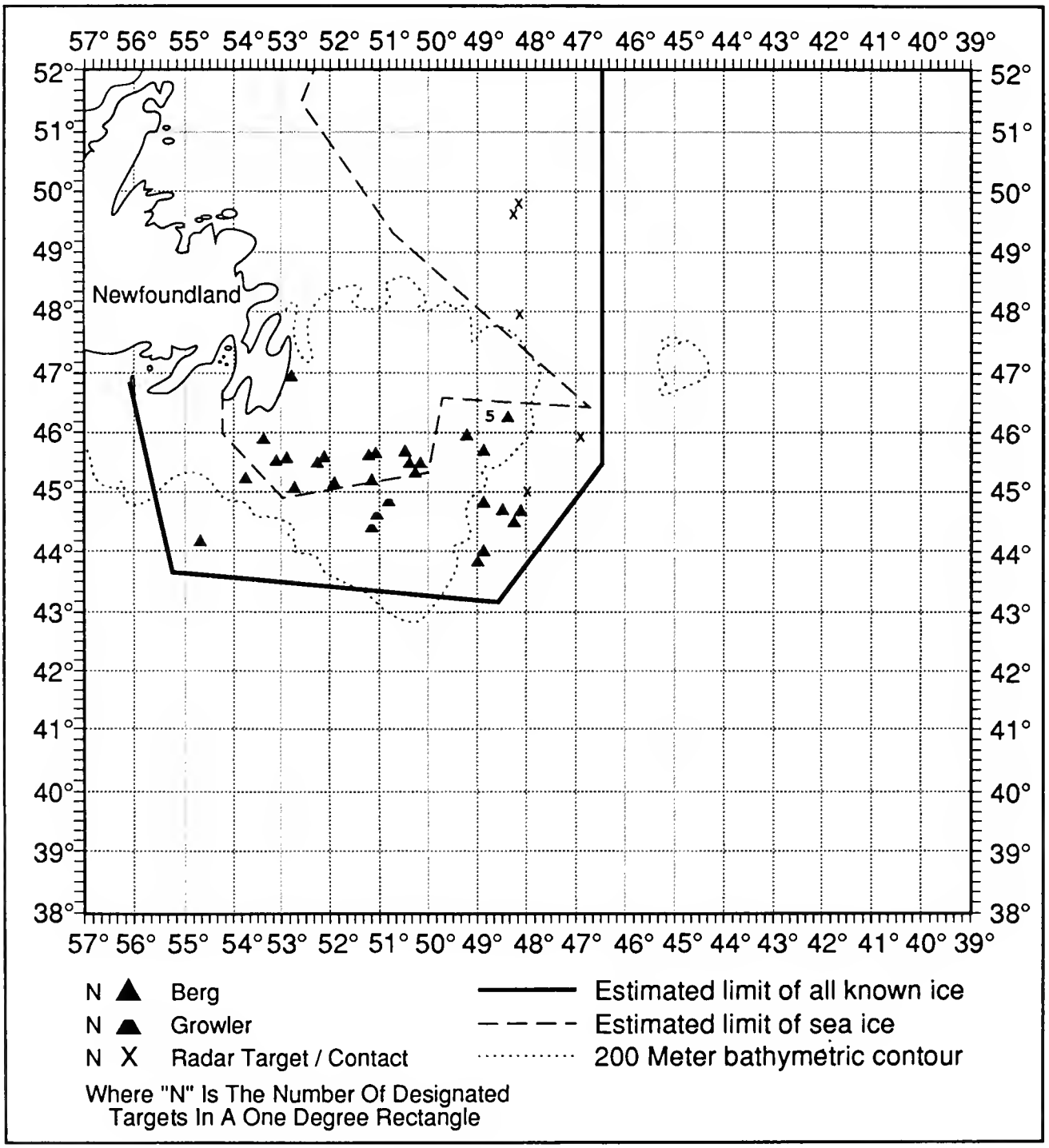

Figure 25. Graphic Depiction of International Ice Patrol Plot for 1200 GMT March 15, 1987, Based on Observed and Forecast Conditions.

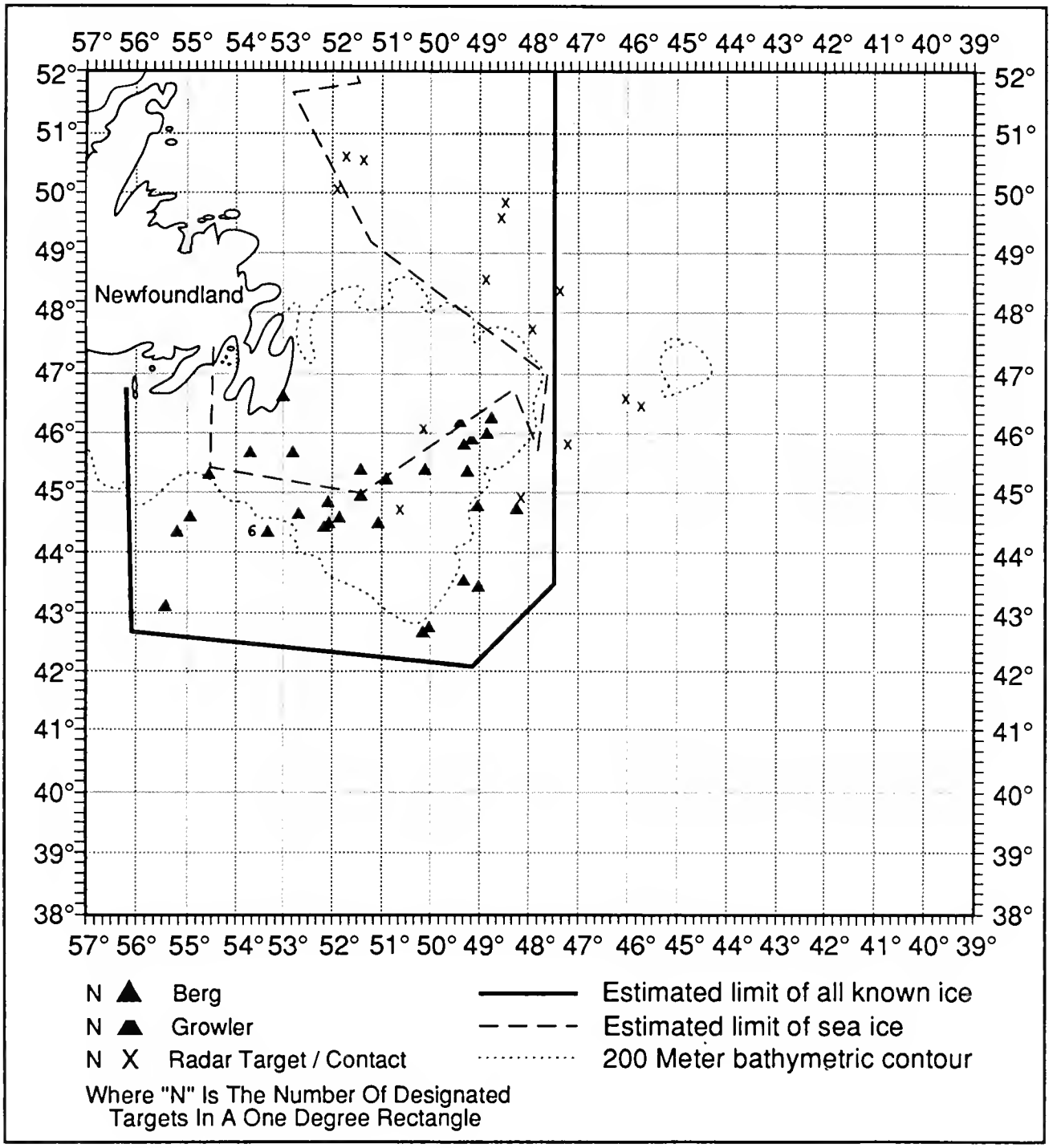

Figure 26. Graphic Depiction of International Ice Patrol Plot for 1200 GMT March 30, 1987, Based on Observed and Forecast Conditions.

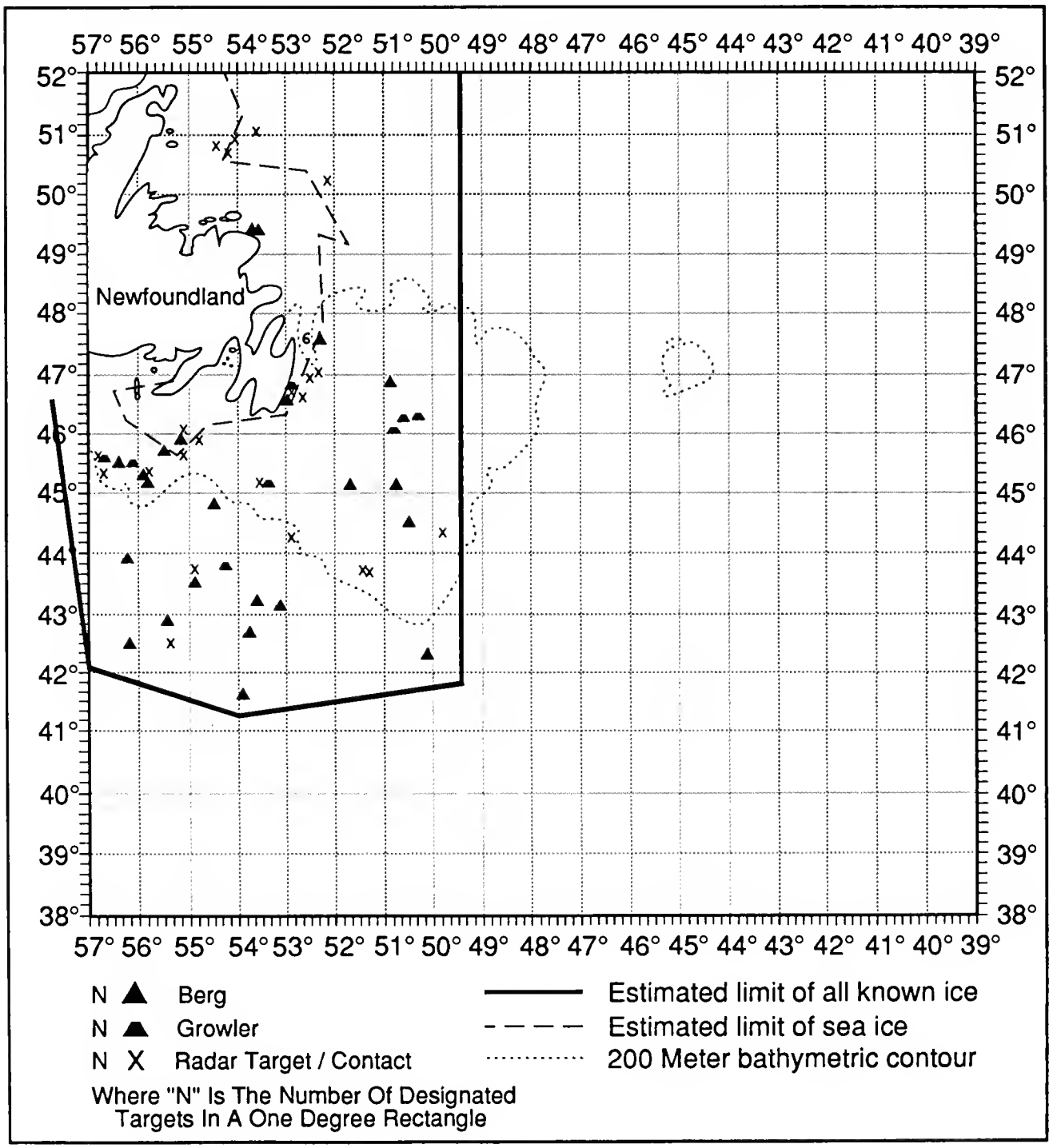

Figure 27. Graphic Depiction of International Ice Patrol Plot for 1200 GMT April 15, 1987, Based on Observed and Forecast Conditions.

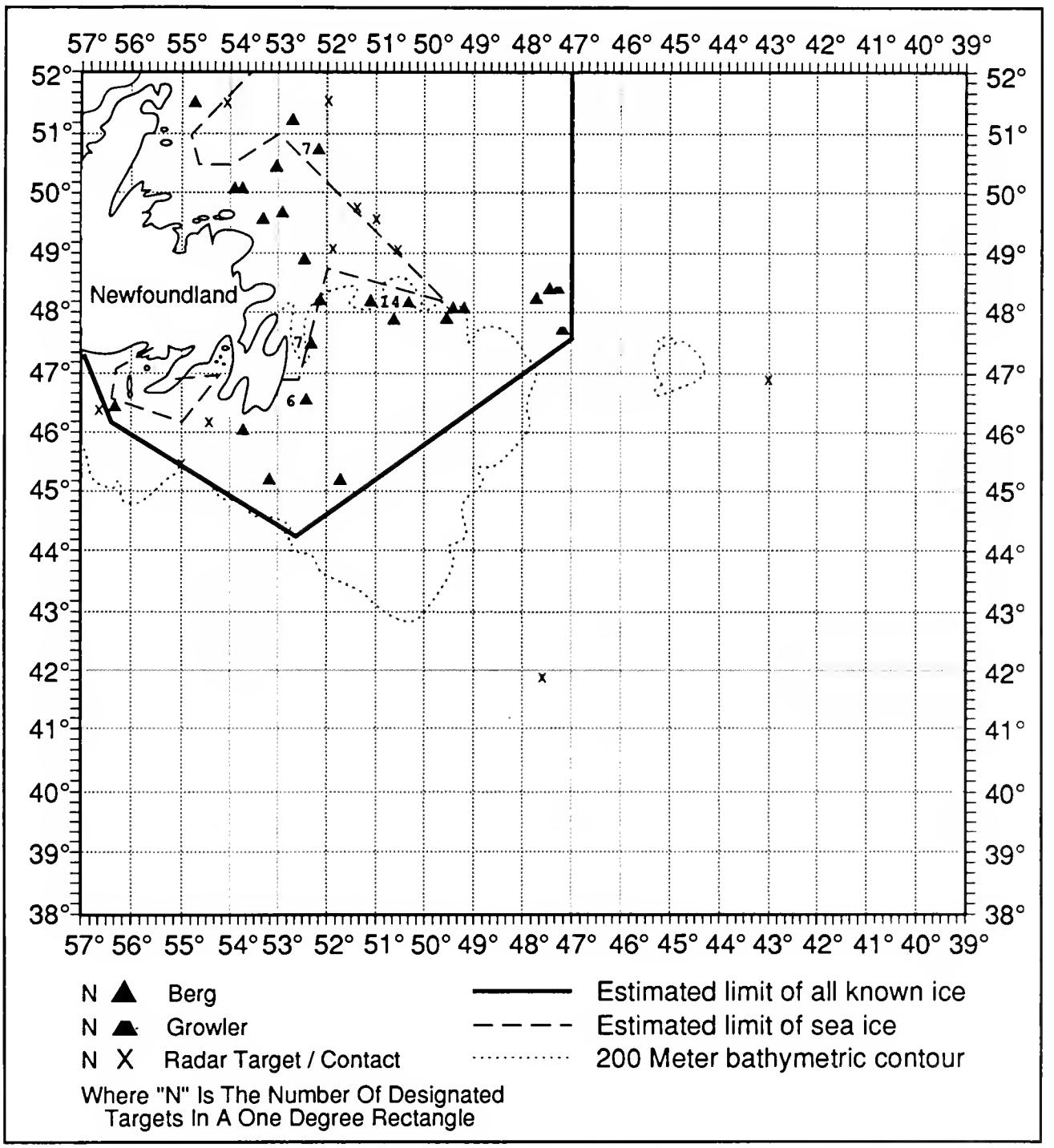

Figure 28. Graphic Depiction of International Ice Patrol Plot for 1200 GMT April 30, 1987, Based on Observed and Forecast Conditions.

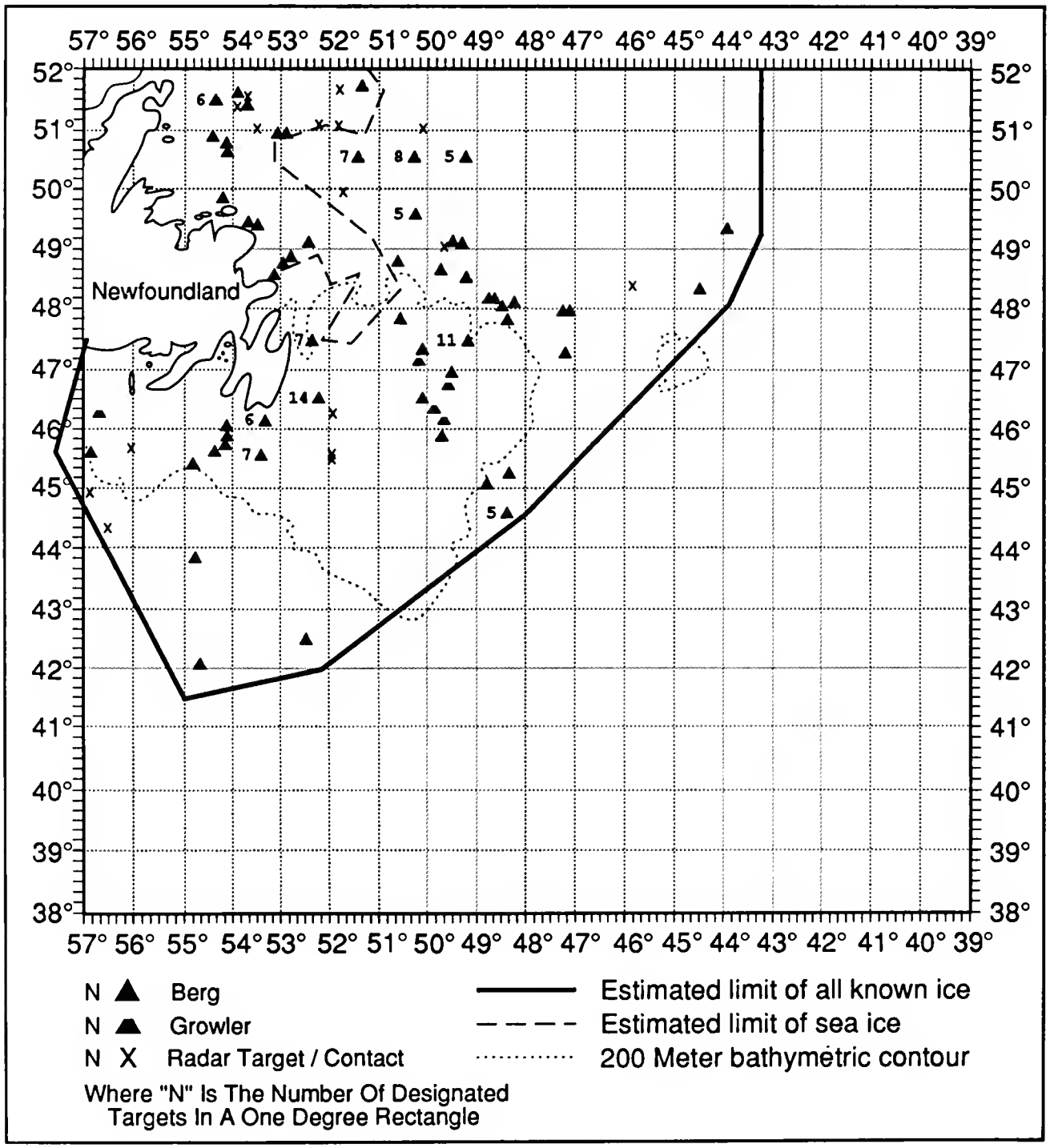

Figure 29. Graphic Depiction of International Ice Patrol Plot for 1200 GMT May 15, 1987, Based on Observed and Forecast Conditions.

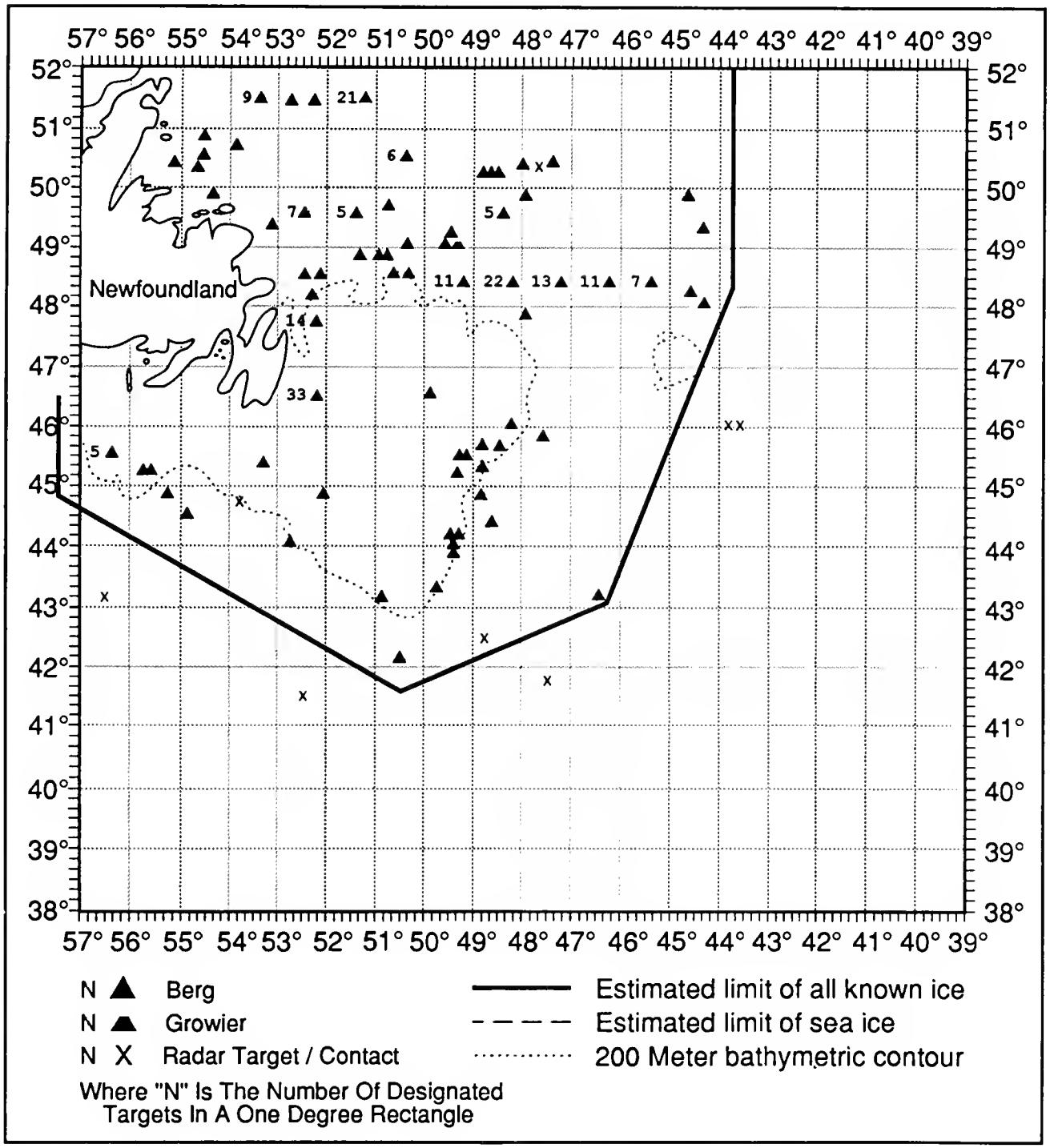

Figure 30. Graphic Depiction of International Ice Patrol Plot for 1200 GMT May 30, 1987, Based on Observed and Forecast Conditions.

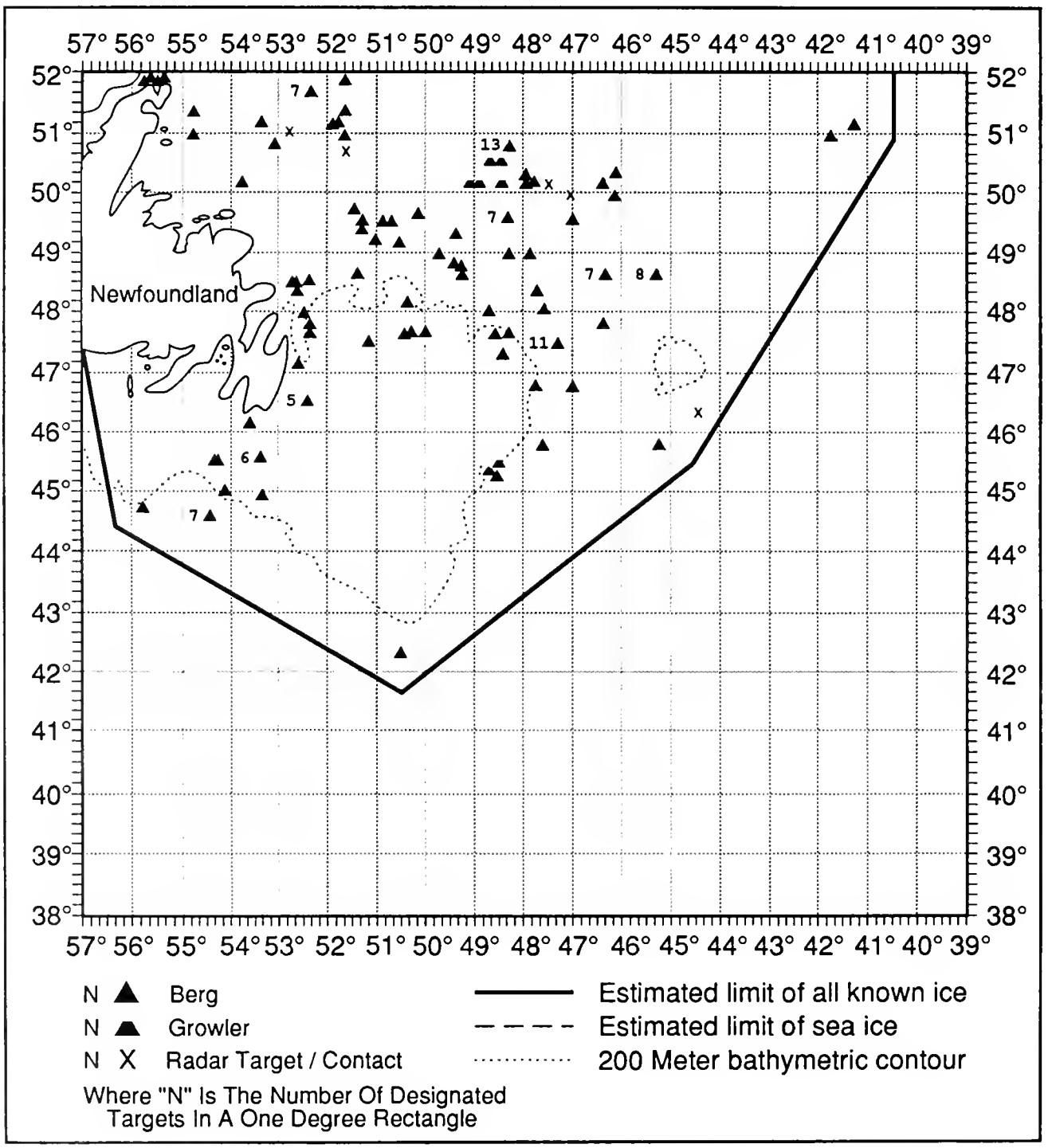

Figure 31. Graphic Depiction of International Ice Patrol Plot for 1200 GMT June 15, 1987, Based on Observed and Forecast Conditions.

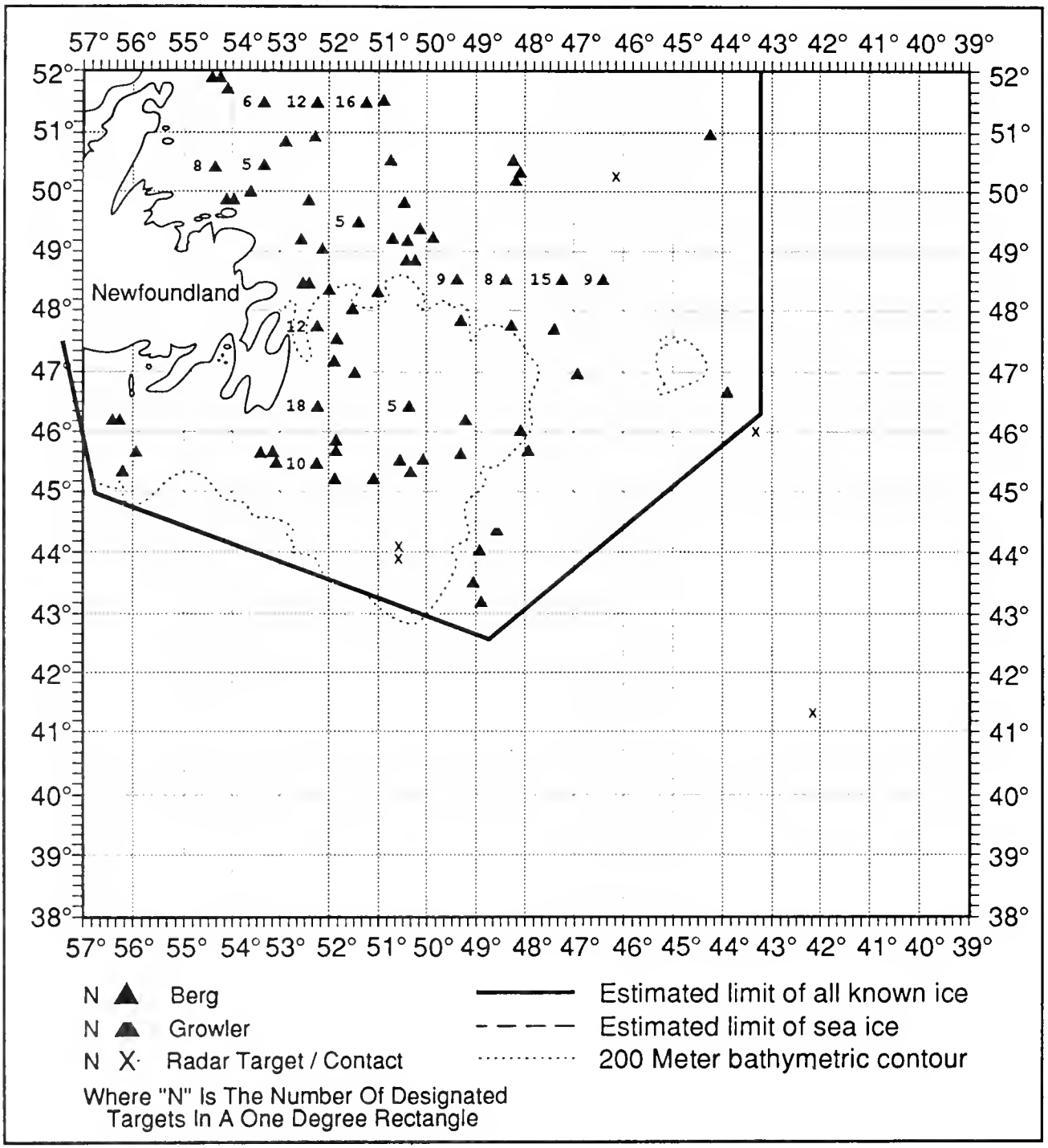

Figure 32. Graphic Depiction of International Ice Patrol Plot for 1200 GMT June 30, 1987, Based on Observed and Forecast Conditions.

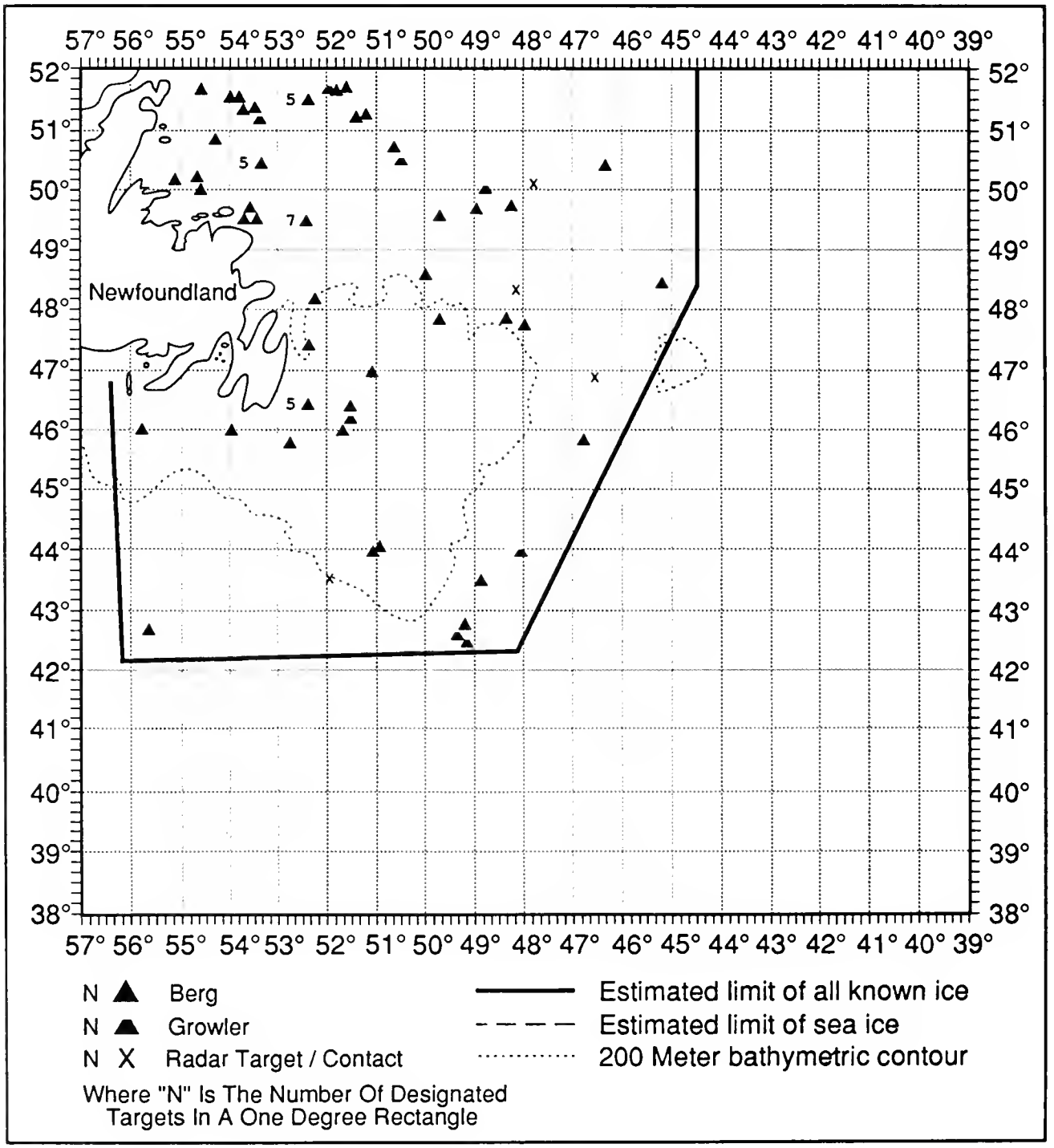

Figure 33. Graphic Depiction of International Ice Patrol Plot for 1200 GMT July 15, 1987, Based on Observed and Forecast Conditions.

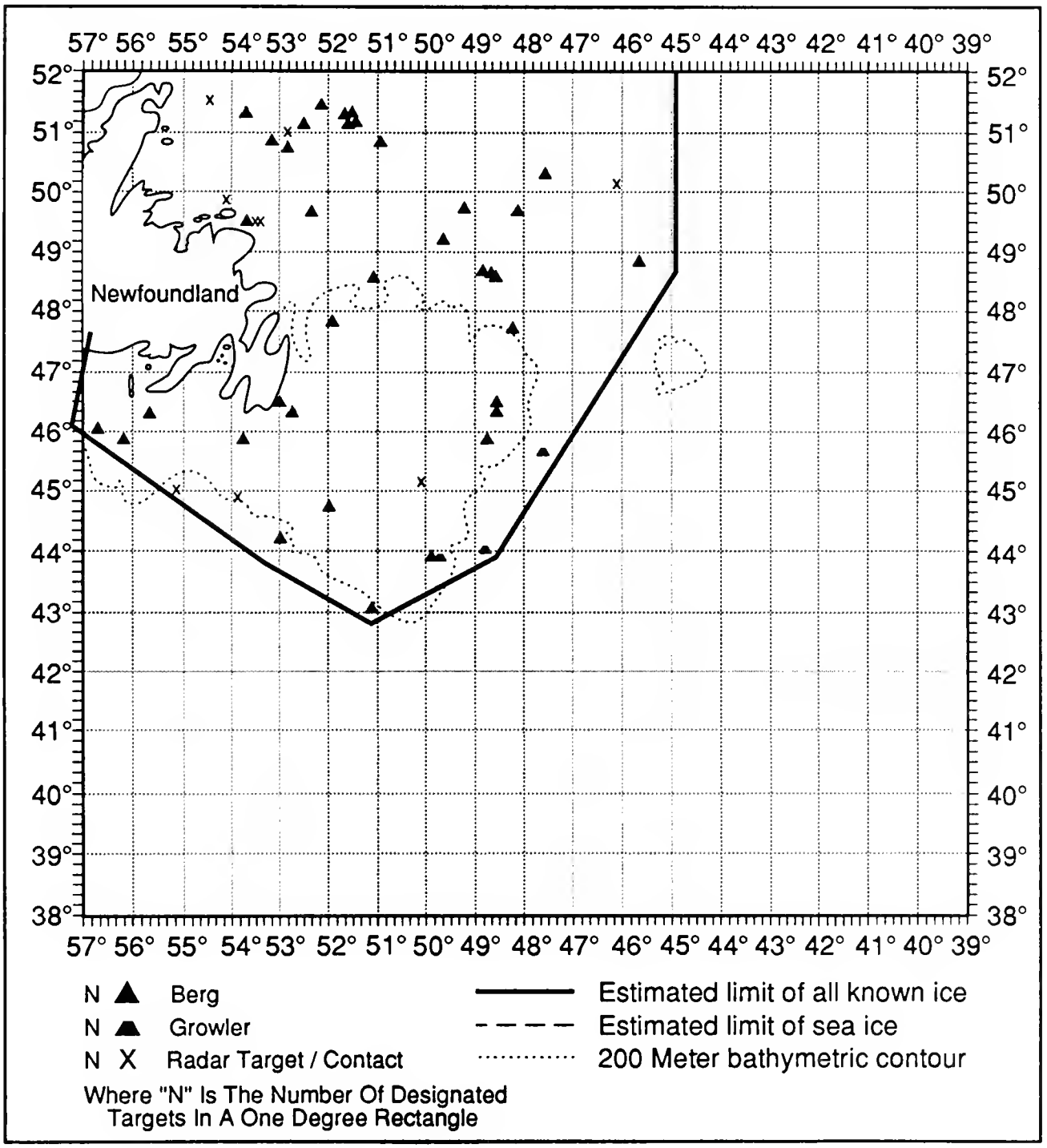

Figure 34. Graphic Depiction of International Ice Patrol Plot for 1200 GMT July 30, 1987, Based on Observed and Forecast Conditions.

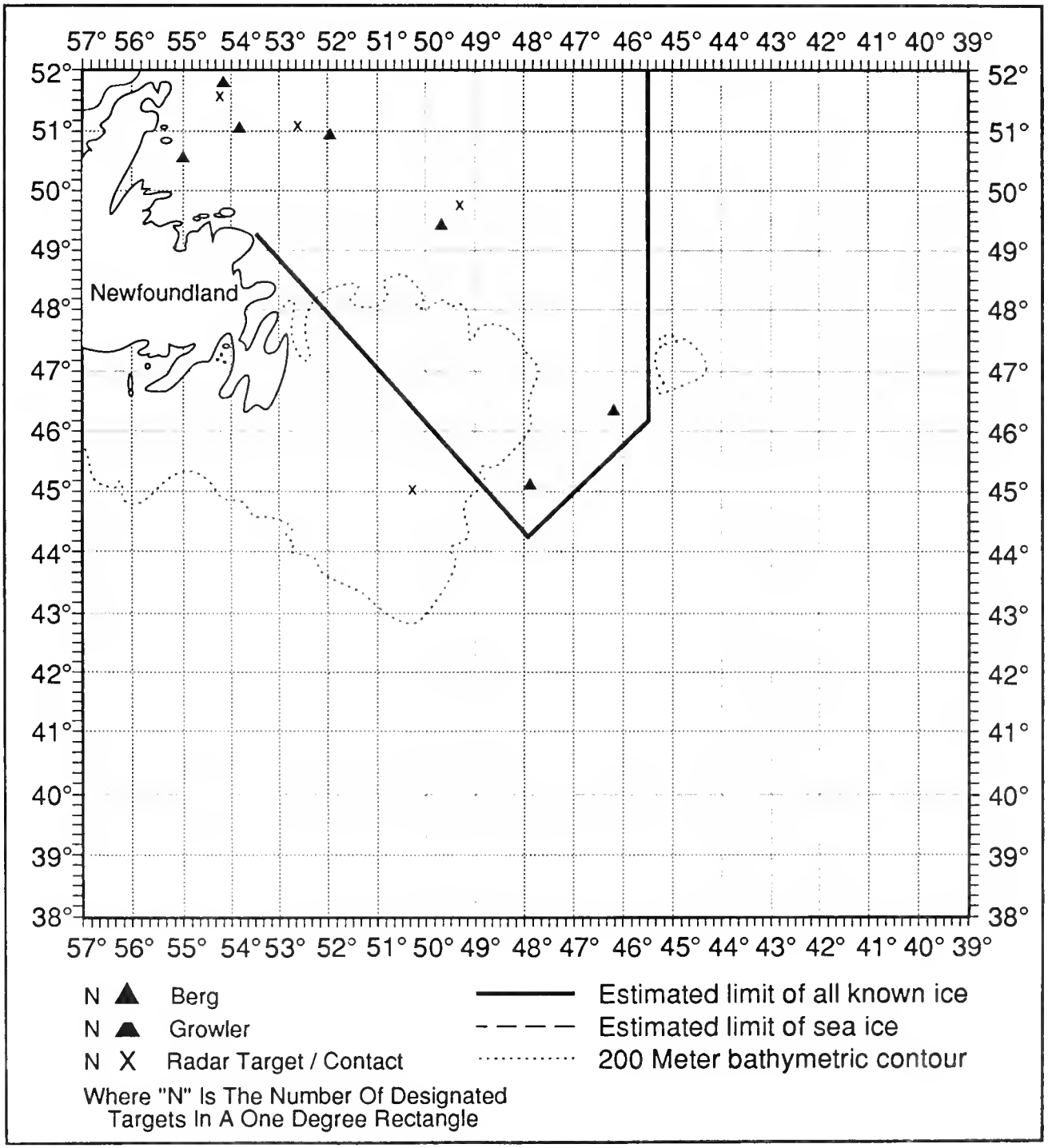

Discussion of Ice and Environmental Conditions

The number of icebergs that pass south of 48°N in the International Ice Patrol area is the measure by which the International Ice Patrol has judged the severity of each year since 1913 (Appendix B). With 318 icebergs south of 48°N, the severity of 1987 was below the 1913-1986 average (Appendix B).

Since the number of icebergs calved each year by Greenland's glaciers is in excess of 10,000 (Knutson and Neill, 1978), a sufficient number of icebergs exist in Baffin Bay during any year. Therefore, annual fluctuations in the generation of Arctic icebergs are not a significant factor in the number of icebergs passing south of 48°N annually. The number of icebergs passing south of 48°N each season is determined by the supply of icebergs available to drift south onto the Grand Banks, as well as factors affecting iceberg transport (currents, winds, and sea ice) and the rate of iceberg deterioration (wave action, sea surface temperature, and sea ice).

Sea ice impedes the transport of icebergs by winds and currents and protects icebergs from wave action, the major agent of iceberg deterioration. Although it slows current and wind transport of icebergs, sea ice is itself an active medium, for it is continually moving toward the ice edge where melt occurs. Therefore, icebergs in sea ice will eventually reach open water unless grounded. The melting of sea ice itself is affected by snow cover (which slows melting) and air and sea water temperatures. As sea ice melt accelerates in the spring and early summer, trapped icebergs are rapidly released and are then subject to normal transport and deterioration.

The Labrador Current, aided by northwesterly winds in winter, is the main mechanism transporting icebergs south to the Grand Banks. In addition to transporting icebergs south, the relatively cold waters of the Labrador current slow the deterioration of icebergs in transit.

Sea ice conditions were above normal for the first part of the 1987 season. The sea ice edge was farther south than normal in December and January, and at its mean location in February. This would have the affect of protecting the icebergs longer and releasing them farther south than normal. These ice conditions would normally lead to a season of average or above average iceberg severity.

The AES/IIP pre-season surveys in January and February indicated an adequate supply of icebergs available to drift south onto the Grand Banks (Osmer and McRuer, 1987).

Based on the sea ice conditions and availability of icebergs, International Ice Patrol was expecting an average to above average season. The question of how and why the iceberg season develops as it does is always of interest to International Ice Patrol. This is particularly true when the season does not develop as expected, as happened in 1987.

In February, the sea level pressure distribution indicated the mean flow pattern for the month was northeasterly rather than northwesterly. This would result in an unfavorable drift to the west, out of the Labrador Current and against the Labrador coast. The icebergs would get grounded or trapped in the many bays and inlets along the Labrador coast. The easterly winds in March pushed all the sea ice off the Grand Banks, and packed it against the Newfoundland coast. Again, the winds in March were unfavorable for iceberg drift. The icebergs were pushed out of the Labrador Current, and along the coasts of Labrador and Newfoundland.

In summary, it appears that in spite of adequate supply of icebergs and favorable sea ice conditions, an average or above average 1987 iceberg season failed to occur because wind conditions were not favorable in February and March for the transport of icebergs south of 48°N.

References

Alles, M.F., and M.A. Alfultis. A Mobile Oceanographic Data Collection System, International Ice Patrol Technical Report, In Press.

Anderson, I. Iceberg Deterioration Model, *Report of the International Ice Patrol in the North Atlantic, 1983 Season, CG-188-38*, U.S. Coast Guard, Washington D.C., 1983.

Atmospheric Environment Service (AES), Thirty Day Ice Forecast for Northern Canadian Waters, January 1987.

Atmospheric Environment Service (AES), Thirty Day Ice Forecast for Northern Canadian Waters, March 1987.

Atmospheric Environment Service (AES), Thirty Day Ice Forecast for Northern Canadian Waters, May 1987.

Knutson, K.N. and T.J. Neill, *Report of the International Ice Patrol Service in the North Atlantic Ocean for the 1977 Season, CG-188-32*, U.S. Coast Guard, Washington D.C., 1978.

Mariners Weather Log, Spring 1987, Vol. 31, Number 2, 1987a.

Mariners Weather Log, Summer 1987, Vol. 31, Number 3, 1987b.

Mariners Weather Log, Fall 1987, Vol 31, Number 4, 1987c.

Mariners Weather Log, Winter 1988, Vol. 32, Number 1, 1988.

Murphy, D.L. and I. Anderson. Evaluation of the International Ice Patrol Drift Model, *Report of the International Ice Patrol in the North Atlantic, 1985 Season, CG-188-40*, U.S. Coast Guard, Washington D.C., 1985.

Naval Oceanography Command, Sea Ice Climatic Atlas: Volume II Arctic East, 1986.

Navy-NOAA Joint Ice Center, Naval Polar Oceanography Center, Southern Ice Limit, Published Bi-monthly, 1987.

Osmer, S. R. and H. McRuer, 1987 Preseason Iceberg Survey and Season Prediction, Proc. Oceans '88, Oct. 1987, Halifax, N.S.

Acknowledgements

Commander, International Ice Patrol acknowledges the assistance and information provided by the Atmospheric Environment Service (AES) of Environment Canada, the U.S. Naval Fleet Numerical Oceanography Center, U.S. Naval Eastern Oceanography Center, and the U.S. Coast Guard Research and Development Center.

We extend our sincere appreciation to the staffs of the Canadian Coast Guard Radio Station St. John's, Newfoundland/ VON, Ice Operations St John's, Newfoundland, Air Traffic Control Gander, Newfoundland, Canadian Forces Gander and St. John's, Newfoundland, and the Gander Weather Office, and to the personnel of U.S. Coast Guard Air Station Elizabeth City, US Coast Guard Communications Station Boston, USCGC BITTERSWEET, and USCGC TAMAROA for their excellent support during the 1987 International Ice Patrol season.

It is also important to recognize the efforts of the personnel at the International Ice Patrol: LCDR S. R. Osmer, LCDR W. E. Hanson, Dr. D. L. Murphy, LT I. Anderson, LT N. B. Thayer, LT M. A. Alfultis, MSTCS G. F. Wright, MSTC M. F. Alles, YN1 S. A. Cooper, MST1 P. O. Pelletier, MST1 M. G. Barrett, MST2 D. A. Hutchinson, MST2 D. D. Beebe, MST2 W. A. Henry, MST2 K. A. Austin, MST3 P. B. Reilley, and MST3 C. F. Weiller.

Appendix A
List of Participating Vessels, 1987

VESSEL NAME	FLAG	SST	ICE REPORTS
ABITIBI MACADO	FED. REP. OF GERMANY		4
ABTARTICO	PORTUGAL		1
ACADIAN GAIL	CANADA		1
ACADIAN TEMPEST	CANADA		1
ADA GORTHON	SWEDEN		3
AFRICAN EVERGREEN	LIBERIA	1	
AFRICAN GARDENIA	LIBERIA	10	
AGIATHALASSINI	PANAMA	1	2
AIFANOURIOS	LIBERIA	17	
AKRANES	ICELAND		1
ALBERRY	SAUDI ARABIA	3	
ALBRIGHT EXPLORER	UNITED KINGDOM		1
ALBRIGHT PIONEER	UNITED KINGDOM		1
ALGERIAN	SWEDEN	5	
ALMARE SETTIMA	ITALY		1
ALMESSILAH	KUWAIT	16	2
AMERICANA	ITALY		1
APOLLO	UNITED KINGDOM	1	
ARABELLA	GREECE		1
ARCTIC	CANADA		2
ARGUS TRAUCHER	LIBERIA	9	
ARKA	UNKNOWN		3
ARMERIA	JAPAN	1	1
ASTOR	ST. VINCENT THE GRENADINES		3
ATLANTIC	NETHERLANDS		1
ATLANTIC AMITY	UNITED KINGDOM	1	1
ATLANTIC LINK	BAHAMAS		3
ATLSGA	SWEDEN		1
BAFFIN	CANADA	2	
BALAO	LIBERIA	7	1
BALTIC	CYPRUS		7
BALTIC SUN	NETHERLANDS	1	1
BARBER NARA	SWEDEN		1
BARON	PANAMA		1
BARTLETT	CANADA		5
BELLE ETOILE	MAURITUIS		1
BIENDIE	LIBERIA	1	
BIRDIE	AUSTRALIA	5	
BISHAH	SAUDIA ARABIA	5	

VESSEL NAME	FLAG	SST	ICE REPORTS
BITTERSWEET	USA	3	1
BLUE PINE	PANAMA		2
BOKA	JAPAN	4	
BOKHTARMA	PEOPLES REP. OF CHINA		1
BONNY	BAHAMAS	8	
BRIDGEWATER	FED. REP. OF GERMANY		2
BRITISH STEEL	UNITED KINGDOM		1
BROOMPARK	UNITED KINGDOM		1
CANMAR AMBASSADOR	CANADA		8
CANMAR (DART) EUROPE	BELGIUM		4
CANADIAN EXPLORER	UNITED KINGDOM		1
CAPETAN HALARIS	UNKNOWN		1
CAPE BYRON	FED. REP. OF GERMANY		1
CAPE ROGER	CANADA		1
CARMEN MARE	GREECE	39	
CAST CARIBOU	LIBERIA	1	2
CAST HUSKEY	UNITED KINGDOM		2
CAST MUSKOX	UNITED KINGDOM		1
CAST OTTER	UNITED KINGDOM		1
CAST POLAR BEAR	LIBERIA	10	4
CAVELIER DELASSALLE	FRANCE		1
CECELIA DESGAGNES	CANADA		1
CHARLOTTE BASTIAN	FED. REP. OF GERMANY		3
CHIPPEWA	LIBERIA	1	1
CHERRY VALLEY	USA		2
CIECERO	CANADA		4
COASTAL CANADA	CANADA		4
CZANTORIA	POLAND	1	4
DAMODAR DR. A. BLOCK	INDIA		1
DANAU MARU	JAPAN		1
DART AMERICA	PANAMA		2
DART ATLANTIC	UNITED KINGDOM		2
DART BRITAIN	UNITED KINGDOM		1
DONNY	SWEDEN		1
DORTHE OLDENDORFF	SINGAPORE		4
DUESSELDORF EXPRESS	FED. REP. OF GERMANY		2
DUKE OF TOPSAIL	UNITED KINGDOM		1
DOZE VALE	BRAZIL	8	
EASTERN UNICORN	PANAMA	7	7
ECAREG LIRIA	SPAIN		1

VESSEL NAME	FLAG	SST	ICE REPORTS
EDCO	EGYPT		1
EIRMNES	LIBERIA		1
ENERCHEM FUSION	CANADA		5
ENSORTFONAH	BELGIUM		1
ESSICAMILLA	SINGAPORE		1
ESSO PROVIDENCE	LIBERIA		2
EUROPEGASUS	LIBERIA		1
EUTERPE	CYPRUS		1
EVRYALOS	GREECE	1	2
FAIR SPIRIT	LIBERIA	3	
FALCON	LIBERIA	1	
FALKOFN	SWEDEN		1
FEDERAL CALUMET	SWEDEN		1
FEDERAL FUJI	JAPAN		2
FEDERAL POLARIS	JAPAN		1
FEDERAL ST. CLAIR	LIBERIA		1
FINNARCTIS	UNITED KINGDOM		1
FINN FALCON	UNITED KINGDOM		12
FINNFIGHTER	FINLAND	2	2
FINNPOLARIS	UNITED KINGDOM	7	5
FINNSNES	LIBERIA		1
FLAME	CYPRUS		1
FRED J. AGNICH	CANADA		1
FROST CASTOR	CYPRUS	1	
FURIA	LIBERIA	3	
GALASSIA	ITALY	15	
GAUDREAU	CANADA		1
GENERAL GARCIA	PHILIPPINES		1
GENERAL VARGAS	PHILIPPINES		1
GRAND COURT	USSR		2
GRAND KNIGHT	USSR		1
GRAND PRINCE	UNKNOWN		1
GRENFELL	CANADA		4
GROSEWATER	CANADA		2
GULF HARVEST	PANAMA		1
HANSEATIC	PANAMA		1
HARITAS	CYPRUS	5	
HELENA OLDENDORFF	PANAMA		2
HELLESPONT MARINER	GREECE		1
HELLESPONT VALOUR	GREECE	6	

VESSEL NAME	FLAG	SST	ICE REPORTS
HENRI TE' LLIER	CANADA		1
HEXMARRDO	UNITED KINGDOM	1	1
HIGH AEUT	SINGAPORE		4
HOFSJOKULL	ICELAND		4
HOLCAN MAAS	URUGUAY		1
HUAL TRAPPER	PANAMA	5	
HUBERT GAUCHER	CANADA		1
HUDSON	CANADA		5
ICE LACKENKY	UNITED KINGDOM		2
ICE TECHNO VENTURE	CANADA		2
IMPERIAL BEDFORD	CANADA		2
IMPERIAL QUEBEC	CANADA		2
INGRID GORTHON	BAHAMAS		1
IRONMASTER	PANAMA		3
IRVING OURS POLAIRE	CANADA		16
IRVING WOOD	UNITED KINGDOM		4
ISHIKARIMARU	JAPAN	10	1
JACKMAN	CANADA		6
JESSIE STOVE	SINGAPORE	11	
JOHANNA SCHULTE	CYPRUS	3	3
JOKULFELL	ICELAND		3
JUGOAGENT	UNKNOWN		1
KANGUK	CANADA		2
KATTEGAT	PHILIPPINES		1
KAZIMIERZ PULASKI	SUDAN		1
KHUDOYHNIK PAKHOMOV	USSR		1
KHUDOYHNIK ROMAS	USSR		4
KOELN EXPRESS	FED. REP. OF GERMANY	1	2
KOLL BJORG	NORWAY	2	
KRISTINA LOGOS	USSR		1
KRITI CORAL	GREECE		3
LABRADOC	CANADA		1
LA CHENE	CANADA		2
LADY HIND	BELGIUM	11	2
LAKENBY	UNITED KINGDOM		1
LAKESTAR	CYPRUS	2	
LAPPONIA	BAHAMAS	1	1
LAURENCE H. GIANELLA	UNKNOWN		1

VESSEL NAME	FLAG	SST	ICE REPORTS
LEBRAVE	UNKNOWN		2
LECEDREN	CANADA		3
LECH	AUSTRIA	2	2
LEERORT	FED. REP. OF GERMANY	3	
LEONARD J. COWLEY	UNKNOWN		5
LIBERTY BELL VENTURE	LIBERIA		1
LIPNO	CZECHOSLAVIA	8	
LONE VENTURE	CANADA		1
LONG CHALLENGER	LIBERIA	2	
LOTILA	BAHAMAS		1
L. ROCHETTE	CANADA		1
LUCIEN PAGUIN	CANADA		6
LUCKY MAN	CYPRUS	1	1
LUDOLF OLDENDORFF	SINGAPORE		1
MAERSK SEBAROK	SINGAPORE	1	1
MAHONE BAY	CANADA		2
MALOJA	CYPRUS		4
MANCHESTER CHALLENGE	UNITED KINGDOM		7
MANGA	UNITED KINGDOM		2
MARIA AUXILIDORA	BRAZIL		1
MARIA G L	GREECE		1
MARIN	LIBERIA		2
MARINE PACKER	CANADA		1
MASHUMARU	JAPAN	6	
MEDALLION	DENMARK		4
MELA	PANAMA		1
METRO STAR	CANADA		2
ML JET	YUGOSLAVIA		2
MOCHIZUKI	JAPAN		1
MOSIL ORE	LIBERIA		1
MT BONNY	BAHAMAS	3	
MUO	ST. VINCENT	1	1
MUSKOX	UNITED KINGDOM		1
MYRSINIDI	LIBERIA		1
NADEZHDA OBUKHOVA	USSR		1
NARWHAL	UNITED KINGDOM		6
NELVANA	LIBERIA	2	2
NEMEMCHA	ALGERIA		
NEPTUNE JADE	SINGAPORE		1
NORDHEIDI	SINGAPORE		5
NORDIC SUN	LIBERIA		1

VESSEL NAME	FLAG	SST	ICE REPORTS
NORDMARK	SINGAPORE		2
NORD PACIFIC	SINGAPORE	10	2
NORDSTAR	SINGAPORE		3
NORLANDIA	FED. REP. OF GERMANY		1
NORTHERN ENTERPRISE	BERMUDA		1
NORTHERN PRINCESS	CANADA		1
NORTHWIND	USA	11	2
NORWIND	NETHERLANDS	2	1
NOSAC LAKAYAMA	LIBERIA	1	
NURNBERG EXPRESS	FED. REP. OF GERMANY		9
OKANAGAN	CANADA	1	1
OLIVIA	BRAZIL		1
ORIENTAL RUBY	JAPAN	1	1
ORIENT PIONEER	LIBERIA		1
ORLANDO	LIBERIA		1
PENALARA	FRANCE	2	2
PENNY LUCK	UNKNOWN		1
PEONIA	LIBERIA		2
PLACENTIA BAY	CANADA		8
POLAR BEAR	LIBERIA	2	
PONIA	HONDURAS		1
PRIMOSTEN	YUGOSLAVIA	1	3
PRODUCT SPLENDOR	UNITED KINGDOM	4	1
PROTECTEUR	CANADA	6	
PUHOS	BAHAMAS		1
RAVIDAS	INDIA		1
REED VOYAGER	PANAMA		6
RIVER PRINCESS	LIBERIA	1	1
ROBERT MAERSK	DENMARK	3	1
RODRIGOTORREABLA	BRAZIL	7	
ROVER	USA	1	
SAINT DIMITIRIOS	LIBERIA	6	
SAINT LAWRENCE	PAKISTAN		1
SAINT VASSILLOS	CYPRUS	1	
SAMBURG	USSR		2
SAM JOHN PIONEER	PANAMA		1
SAMUEL L COBB	USA	10	8
SANDNESS	PANAMA		2
SANTA MALFALDO	PORTUGAL		1

VESSEL NAME	FLAG	SST	ICE REPORT
SEASTAR 2	CYPRUS		1
SELKIRK SETTLERR	CANADA		1
SENTIS	UNITED KINGDOM	3	
SIR H. GILBERT	CHILE		9
SIR ROBERT BOND	CANADA		4
SKIDEGATE	CANADA		10
SOREN TOUBRO	INDIA	6	3
SOVETSK	USSR		1
SPYROS A. LEMOS	GREECE		1
STALWART	USA	4	
STARWORLD	UNITED KINGDOM		1
STEFAN BATORY	POLAND		4
STEFAN STARZYNSKI	POLAND		2
STILLANOVA	NETHERLANDS		1
STOLT CASTLE	LIBERIA		2
STOLT CROWN	LIBERIA		2
STOLT SAPPHIRE	LIBERIA	4	2
STOLT SPAN	LIBERIA		1
STOLT SYDNESS	LIBERIA	3	
STUTTGART EXPRESS	FED. REP. OF GERMANY		1
SUMMIT	LIBERIA		3
TAMAROA	USA	5	1
TAVERNER	CANADA		1
TEAM FROSTA	SINGAPORE	5	
TEVERA	CYPRUS	1	
THAMES	LIBERIA		1
TILIA GORTHOU	SWEDEN		1
TOKI ARROW	NORWAY	1	1
TORONTO	BERMUDA	1	
TRINITY BAY	CANADA		4
UNDERWOOD	USA	6	
VADASTEINUR	DENMARK		1
VALOR	PHILIPPINES		1
VAYGACH	USSR		1
VESALIUS	BELGIUM		1
VICTORIUS	PANAMA		2
VIKING OSPREY	BAHAMAS		1
VIKTOR TKACHYOV	USSR		2
VISHVA PALLAV	INDIA		1
VOLOS	LIBERIA	3	

VESSEL NAME	FLAG	SST	ICE REPORT
WESER HARBOUR	FED. REP. OF GERMANY		1
WEST BRIDGE	LIBERIA		2
WILFRED TEMPLEMAN	CANADA		3
WINONA	LIBERIA		1
WOODLAND	CANADA		4
YAYAMARIA	CYPRUS		1
YOUNG SHINKO	JAPAN	3	
YUKOVA	LIBERIA		2
ZAGREB	YUGOSLAVIA		1
ZANDAM	INDIA		1
ZANDBERG	CANADA		1
ZAWRAT	POLAND		1
ZIEMIA LUBELSKA	POLAND		1
ZIEMIA OLSZTYNSKA	POLAND		3
ZIEMIA OPOLSKA	POLAND	3	
ZIEMIA TARNOWSKA	POLAND		1
ZIM KEELUNG	ISRAEL		1

Appendix B

Iceberg Populations South of 48° N Since 1900

LT Michael A. Alfultis, USCG

Since its beginning, the International Ice Patrol has maintained an annual count of the number of icebergs crossing latitude 48°N. Each year the number of icebergs south of 48°N is used by International Ice Patrol to gauge the potential threat to North Atlantic shipping, and, therefore, the opening and closing date of each Ice Patrol Season.

Table B-1 provides a monthly breakdown of the estimated number of icebergs crossing 48°N each year since 1900. This updates the historical iceberg statistics last published in the 1977 Ice Patrol Bulletin No. 63. Table B-1 is in a slightly different format from that published previously. Recently, International Ice Patrol began using as its ice year the period from October through September rather than the calendar year or the period September through August, as was done in the past. The data published in 1977 have been updated to reflect this, and the iceberg counts since 1977 added.

The monthly counts are broken into four eras, 1900-1912, 1913-1945, 1946-1982, and 1983-1987. The first era is the pre-International Ice Patrol period when icebergs sighted by commercial shipping were reported to the U. S. Hydrograhic Office. During the next era, the International Ice Patrol estimated the iceberg distribution from surface observations made from U. S. Coast Guard cutters and commercial vessels transiting the area. Visual reconnaissance from aircraft became International Ice Patrol's primary method for iceberg detection during the third era. During the final era, the Side-Looking Airborne Radar (SLAR) provided International Ice Patrol with an all-weather capability to detect icebergs. Iceberg sightings provided by commercial shipping have been, and continue to be, an important source of information to International Ice Patrol.

International Ice Patrol defines those ice years with less than 300 icebergs crossing 48°N as light or low ice years; those years with 300 to 600 icebergs crossing 48°N as average or intermediate ice years; those years with 600 to 900 icebergs crossing 48°N as heavy or severe ice years; and those ice years with more than 900 icebergs crossing 48°N as extreme ice years.

Figure B-1 is a bar graph of icebergs crossing 48 N since 1912. The variability in the record is readily seen. The factors that determine this variability are the supply of icebergs available to drift onto the Grand Banks, those affecting iceberg transport (currents, winds, and sea ice), and those affecting deterioration (wave action, sea surface temperature, and sea ice). These factors are often unpredictable. During the 1987 season, short term changes in the mean wind flow dramatically affected the iceberg distribution, and changed the character of an anticipated severe iceberg season to barely an average season (318 icebergs).

Table B-1. Iceberg Populations South of 48° N Since 1900.

ICE YEAR	OCT	NOV	DEC	JAN	FEB	MAR	APR	MAY	JUN	JUL	AUG	SEP	ANNUAL TOTAL
Pre-International Ice Patrol													
1900	0	0	0	10	0	0	5	32	33	6	1	1	88
1901	1	0	0	1	0	0	4	13	29	22	6	5	81
1902	1	2	5	3	0	1	1	13	5	16	1	0	48
1903	1	0	0	0	2	400	166	151	52	23	7	0	802
1904	0	0	1	0	0	12	63	82	89	14	3	2	266
1905	0	0	0	3	2	168	373	109	100	50	9	8	822
1906	8	0	15	14	11	77	49	133	87	18	16	0	428
1907	0	0	0	0	1	11	162	248	138	64	11	0	635
1908	0	0	3	1	0	7	39	82	51	2	2	20	207
1909	15	3	0	0	55	147	134	321	181	121	45	19	1,041
1910	1	0	0	0	0	0	34	10	3	3	0	0	51
1911	0	0	0	0	8	41	112	72	77	21	40	3	374
1912	0	8	14	1	0	34	395	345	159	63	19	0	1,038
TOTAL 1900-1912	27	13	38	33	79	898	1,537	1,611	1,004	423	160	58	5,881
AVERAGE 1900-1912	2	1	3	2	6	69	118	124	77	32	12	4	452
Surface Patrol Vessels													
1913	0	3	0	2	4	37	109	292	71	14	4	7	543
1914	0	6	4	1	41	32	27	419	71	22	46	52	721
1915	13	1	6	14	72	67	96	97	71	28	17	5	487
1916	0	1	0	0	0	0	0	25	29	0	0	0	55
1917	0	0	0	0	0	13	3	3	9	10	0	0	38
1918	0	0	0	0	0	12	23	26	37	27	34	22	181
1919	1	14	3	3	4	5	25	75	56	26	36	69	317
1920	2	12	4	6	43	20	5	211	86	18	5	18	430
1921	19	10	4	17	5	43	210	198	175	53	24	4	762
1922	10	1	6	0	3	35	71	245	83	21	11	6	492
1923	27	21	0	0	3	28	65	83	42	10	3	2	284
1924	0	0	0	3	0	6	2	0	0	0	0	0	11
1925	0	0	0	0	3	5	8	58	22	13	0	0	109
1926	0	0	0	0	3	15	58	168	85	4	6	2	341
1927	3	1	0	4	10	26	93	153	95	5	3	0	393
1928	0	0	0	0	0	14	156	190	87	55	5	0	507
1929	4	4	0	0	0	45	332	460	376	107	1	0	1,329
1930	0	18	12	14	116	87	89	101	62	3	1	1	504
1931	1	0	0	0	0	2	1	10	0	0	0	0	14
1932	0	0	0	0	1	43	321	90	58	1	0	0	514
1933	0	0	0	0	2	4	12	162	36	0	0	0	216
1934	0	0	0	1	0	0	245	228	87	14	1	0	576

Table B-1 (Continued).

ICE YEAR	OCT	NOV	DEC	JAN	FEB	MAR	APR	MAY	JUN	JUL	AUG	SEP	ANNUAL TOTAL
1935	0	0	0	0	0	46	177	501	134	11	3	0	872
1936	0	0	3	0	0	0	8	14	0	0	0	0	25
1937	0	0	0	20	53	121	124	137	14	1	0	0	470
1938	0	0	0	2	3	38	212	286	110	13	0	0	664
1939	0	0	0	0	0	22	173	471	150	28	6	0	850
1940	0	0	0	0	0	0	0	1	0	0	0	0	1
1941	0	1	0	0	0	0	1	1	0	0	0	0	3
1942	0	0	0	0	0	30	0	0	0	0	0	0	30
1943	0	0	0	0	0	25	90	298	270	150	7	0	840
1944	0	0	0	0	0	31	319	213	106	30	1	0	700
1945	0	0	0	0	6	352	253	256	92	109	15	0	1,083
TOTAL 1913-1945	80	93	42	87	372	1,204	3,308	5,472	2,514	773	229	188	14,362
AVERAGE 1913-1945	2	3	1	3	11	36	100	166	76	23	7	6	435
Visual Aircraft Reconnaissance													
1946	0	0	0	0	2	67	98	168	88	7	0	0	430
1947	0	0	0	3	1	2	5	11	26	15	0	0	63
1948	0	0	0	0	0	60	210	185	68	0	0	0	523
1949	0	0	0	0	0	1	23	20	3	0	0	0	47
1950	0	0	0	0	12	61	183	135	58	7	0	1	457
1951	1	2	0	0	3	2	0	0	0	0	0	0	8
1952	0	0	1	0	0	0	12	2	0	0	0	0	15
1953	0	0	0	0	0	21	11	18	6	0	0	0	56
1954	0	0	0	1	16	47	165	65	16	2	0	0	312
1955	0	0	0	0	0	10	32	14	5	0	0	0	61
1956	0	0	0	0	0	9	13	34	21	3	0	0	80
1957	0	0	0	3	43	41	172	265	288	113	6	0	931
1958	0	0	0	0	0	0	0	0	0	1	0	0	1
1959	0	0	0	0	0	14	266	180	186	43	0	0	689
1960	0	2	3	3	0	0	41	161	44	4	0	0	258
1961	0	0	0	0	6	60	30	16	1	0	1	0	114
1962	1	0	1	0	0	14	72	21	10	3	0	0	122
1963	0	0	0	0	0	4	20	0	1	0	0	0	25
1964	0	0	0	0	3	88	225	19	28	5	1	0	369
1965	0	0	0	0	1	19	33	22	1	0	0	0	76
1966	0	0	0	0	0	0	0	0	0	0	0	0	0
1967	0	0	0	0	0	25	134	209	65	8	0	0	441
1968	0	0	0	0	0	0	104	44	60	14	4	4	230
1969	0	0	0	0	0	0	0	35	17	1	0	0	53
1970	0	0	0	0	0	0	5	2	70	8	0	0	85

Table B-1 (Continued).

ICE YEAR	OCT	NOV	DEC	JAN	FEB	MAR	APR	MAY	JUN	JUL	AUG	SEP	ANNUAL TOTAL
1971	0	0	0	0	0	31	4	20	7	11	0	0	73
1972	0	0	0	0	40	185	501	559	225	48	26	4	1,588
1973	0	0	6	54	110	134	212	159	151	19	1	0	846
1974	0	0	0	0	1	99	345	446	266	168	61	1	1,387
1975	0	0	0	0	24	41	10	20	5	0	0	0	100
1976	0	0	0	0	0	33	13	67	35	3	0	0	151
1977	0	0	0	0	3	7	12	0	0	0	0	0	22
1978	0	0	0	0	0	5	28	35	7	0	0	0	75
1979	0	0	0	0	5	20	81	34	9	3	0	0	152
1980	0	0	0	1	3	7	0	9	4	0	0	0	24
1981	0	0	0	0	0	48	10	5	0	0	0	0	63
1982	0	0	0	0	0	17	61	13	94	3	0	0	188
TOTAL 1946-1982	2	4	11	65	273	1,172	3,131	2,993	1,865	489	100	10	10,115
AVERAGE 1946-1982	0	0	0	2	7	32	85	81	50	13	3	0	273
Aircraft SLAR Reconnaissance													
1983	0	0	2	9	165	124	339	465	168	76	4	0	1,352
1984	0	0	0	0	0	101	953	484	227	335	93	9	2,202
1985	3	11	7	2	57	129	208	205	247	123	39	32	1,063
1986	0	0	0	0	3	40	60	59	24	18	0	0	204
1987	0	0	5	2	14	48	76	29	127	15	2	0	318
TOTAL 1983-1987	3	11	14	13	239	442	1,636	1,242	793	567	138	41	5,139
AVERAGE 1983-1987	0	2	3	3	48	88	327	248	159	113	28	8	1,027
TOTAL 1900-1987	112	121	105	198	963	3,716	9,612	11,318	6,176	2,252	627	297	35,497
AVERAGE 1900-1987	1	1	1	2	11	42	109	129	70	26	7	3	403
TOTAL 1913-1987	85	108	67	165	884	2,818	8,075	9,707	5,712	1,829	467	239	29,616
AVERAGE 1913-1987	1	1	1	2	12	38	108	129	69	24	6	3	395

Number of Icebergs South of 48°N (1912-87)
Number of Icebergs
Ice Patrol Season
2500
2000
1500
1000
500
0
1912
1915
1920
1925
1930
1935
1940
1945
1950
1955
1960
1965
1970
1975
1980
1985
January 20, 1914
IIP established
1917-1918,
No patrols due to WWI
Southernmost berg to date
30°20'N 62°32'W
1942-1945
No patrols due to WW2
1945 First use of aircraft for
iceberg reconnaissance
1983-IIP first uses SLAR

Appendix C

1987 International Ice Patrol Drifting Buoy Program

Donald L. Murphy
LT Neal B. Thayer, USCG

INTRODUCTION

This report documents the operational portion of the 1987 drifting buoy program of the International Ice Patrol. The program, which began in 1976, supports Ice Patrol operations and research.

Eighteen separate buoy deployments were made in 1987. Of these, nine were launched from Ice Patrol reconnaissance aircraft and the data used primarily for operational purposes (Summy and Anderson, 1983 and Summy, 1982). The remainder were deployments from U.S. Coast Guard vessels conducting Ice Patrol research cruises. Most of the latter were drift tracks of short duration, with the buoy being recovered at the end of each experiment. Two of the aircraft-deployed buoys were launched by Ice Patrol off northern Labrador as part of a Canadian Atmospheric Environment Service (AES) test of their iceBerg Analysis and Prediction System (BAPS).

Ice Patrol sponsored two oceanographic research cruises in 1987. The first, (IIP 87-1) from 27 April to 20 May, was conducted aboard USCGC BITTERSWEET (WLB 389). The objective of IIP 87-1 was to investigate the ability of IIP's side-looking airborne radar (SLAR) to detect warm-core eddies. Six separate buoy deployments were made during this research. Of these, two buoys were not recovered at the end of the experiment, and their data were used for operational purposes. The buoy tracks during the cruise period are discussed in Appendix D of this Bulletin.

The second 1987 Ice Patrol research cruise (IIP 87-2) was an iceberg drift and deterioration study conducted aboard USCGC TAMAROA (WMEC 166), from 8 June to 27 June. TAMAROA deployed three buoys, all of which were recovered at the end of the experiment. The results of this cruise are discussed in Appendix E.

With the exception of the buoys deployed solely for research, Ice Patrol enters all of its buoy data onto the Global Telecommunications System (GTS). Although Ice Patrol is directly interested in sea surface temperature and position data only when the buoys are within its operations area, the buoys frequently leave the area and move eastward across the North Atlantic. Tracking the buoys eastward serves the dual purpose of providing useful oceanographic data to the world oceanographic community and providing the opportunity to recover a buoy when it beaches or crosses the path of a ship willing to recover it. Approximately one buoy per year is recovered and returned to Ice Patrol for reuse.

All of the buoys used in 1987 had a 3 meter long spar hull with a 1 meter diameter flotation collar. Each buoy was equipped with a 2 by 10 meter window-shade drogue attached to the buoy with a 50 meter tether of 1/2" (1.3 cm) nylon. The center of the drogue was at 58 m. In addition, each buoy had a temperature sensor mounted approximately 1 m below the waterline, a drogue tension monitor, and a battery voltage monitor. The sea surface temperature is accurate to approximately 1°C.

The drogue sensor data should be viewed with some caution. Although recent experience (Anderson, 1986) suggests that the sensor reliably reports drogue status, it sometimes fails. In some cases the buoy's drift track can provide evidence of drogue separation. For example, an abrupt increase in variability with a period of several days might suggest that the drogue has detached and the buoy drift is being affected by the wind and wind-driven currents. However, short of relocating and recovering the buoy, there is no way to know with certainty that the drogue remained attached for the period of interest.

The data from the buoys are acquired and processed by Service ARGOS. Ice Patrol queries and stores the data files once daily.

Table C-1 summarizes the 18 buoy deployments in 1987. This table reflects the status of all the buoys as of 31 December 1987.

Table C-1. Summary of the 18 buoy deployments in 1987. This Table reflects the status of all buoys as of 31 December 1987.

Buoy ID	Date Deployed	Deployment Platform	Deployment Position	Recovered/Stopped Transmitting
4511a	07 MAY	BITTERSWEET	43°59'N 48°09'W	11 MAY (1)
4511b	17 MAY	BITTERSWEET	43°13'N 47°43'W	ACTIVE
4528	15 AUG	HC-130	60°00'N 61°43'W	ACTIVE
4536	07 MAY	BITTERSWEET	43°39'N 48°12'W	09 DEC
4545a	04 MAR	HC-130	47°48'N 48°45'W	05 MAY (2)
4545b	05 MAY	BITTERSWEET	45°14'N 48°46'W	11 MAY
4545c	17 MAY	BITTERSWEET	44°40'N 49°00'W	20 MAY
4545d	15 JUN	TAMAROA	51°06'N 53°28'W	19 JUN
4547a	07 MAY	BITTERSWEET	44°10'N 48°10'W	11 MAY
4547b	15 JUN	TAMAROA	51°06'N 53°28'W	20 JUN
4553	25 JUN	HC-130	52°44'N 51°55'W	ACTIVE
4554	25 MAR	HC-130	50°00'N 50°40'W	28 MAY
4555	25 MAR	HC-130	48°20'N 48°26'W	03 JUL
4556	14 APR	HC-130	48°20'N 49°19'W	19 JUN
4558	14 JUN	TAMAROA	51°14'N 53°20'W	20 JUN
4559	06 JUN	HC-130	49°40'N 50°52'W	06 AUG (3)
4560	06 MAY	HC-130	49°00'N 50°36'W	ACTIVE
4562	15 AUG	HC-130	59°13'N 60°18'W	ACTIVE

Notes:
(1) A letter behind a buoy number indicates that the buoy was deployed more than once during the year.

(2) Buoy 4545 was recovered by USCGC BITTERSWEET on 5 May at position 45°42' N, 49°21'W. The missing drogue was replaced and the buoy redeployed on 5 May.

(3) Buoy 4559 was picked up by an unknown vessel on 6 August. The buoy track from that point headed toward Europe at approximately 12 knots.

BUOY DEPLOYMENT FROM AIRCRAFT

Ice Patrol has deployed satellite-tracked buoys from HC-130's since 1979. The buoy is strapped into an air-deployment package and launched out the rear door of an HC-130 flying at an altitude of 500 feet (150 m) at 150 knots (77 m/s). The air-deployment package consists of a wooden pallet and a parachute, both of which separate from the buoy after it enters the water. The parachute riser is cut by a cable-cutter that is activated by a battery that energizes when immersed in salt water. The pallet separates when salt tablets dissolve and release straps holding the buoy to the pallet. The buoy then floats free and the drogue falls free and unfurls.

Nine buoys were air-deployed in 1987. Of these, three pallets (4528, 4553, and 4559) failed upon entry into the HC-130's airstream. When this occurs, the buoy and drogue usually survive intact, but frequently the wires to the parachute cutter break. This means that the parachute remains attached to the buoy hull and can act as a near-surface drogue. Aerial inspections and shipboard recoveries of buoys have shown that the parachutes collapse and become entangled with the buoy hull or the upper part of the drogue tether. It is not likely that these failures contaminated the drift data significantly.

BUOY DEPLOYMENT STRATEGY

It is not possible to obtain adequate temporal and spatial coverage of the Ice Patrol operations area (40-52N, 39-57W) over a 5 or 6-month period with a few (< 12) buoys. As a result, the buoy deployment strategy focuses on the current that is the major conduit of icebergs into the North Atlantic shipping lanes, the southward-flowing off-shore branch of the Labrador Current. The goal is to monitor this current for the entire ice season by keeping one or two buoys in it at all times. With two exceptions (4511 and 4536), all of the 1987 buoys were deployed in the Labrador Current. The two exceptions were deployed in and near a warm-core eddy that was affecting the flow of the Labrador Current near 44°N. No buoys entered, nor were any deployed, in the inshore branch of the Labrador Current. Previous attempts at deployments in this near-shore region resulted in short drift tracks because the buoys became entangled in fishing gear and were recovered by fishermen.

DATA PROCESSING

Most of Ice Patrol's buoy position data fall within the standard location accuracy (LeTran and Liabet, 1987) provided by Service ARGOS. The data are reported to 0.001° of latitude and longitude, which far exceeds this standard location accuracy. For 46°N, the center latitude of the Ice Patrol operations area, the positions are accurate to 0.003° of latitude and 0.005° of longitude. The raw position data are unevenly-spaced in time, with virtually no data from the period from 00Z to 004Z each day. This null period is due to the orbits of the NOAA satellites. Approximately 10 fixes are determined each day for each of the buoys.

Although the data are relatively noise free, all records are scanned before processing to ensure quality control. First, duplicate positions and positions with time separations of 30 minutes or less are deleted. Then, positions < 700 m from adjacent positions are deleted, unless the deletion results in a time separation of 4 or more hours.

The error-free position data are then fitted to a cubic spline curve to arrive at an evenly-spaced record with an interval of 3 hours. This process results in a slight reduction in the number of fixes per day (from 10 to 8). Next, the position records are filtered using a low-pass cosine filter with a cut-off of 1.16 X 10-5 Hz (one cycle per day). This filter removes most tidal and inertial effects. Finally, the buoy drift speeds are calculated at three-hour intervals using a two-point backward differencing scheme.

Most of the trajectory plots presented in this report are from the filtered records. Also presented for each buoy is a plot of

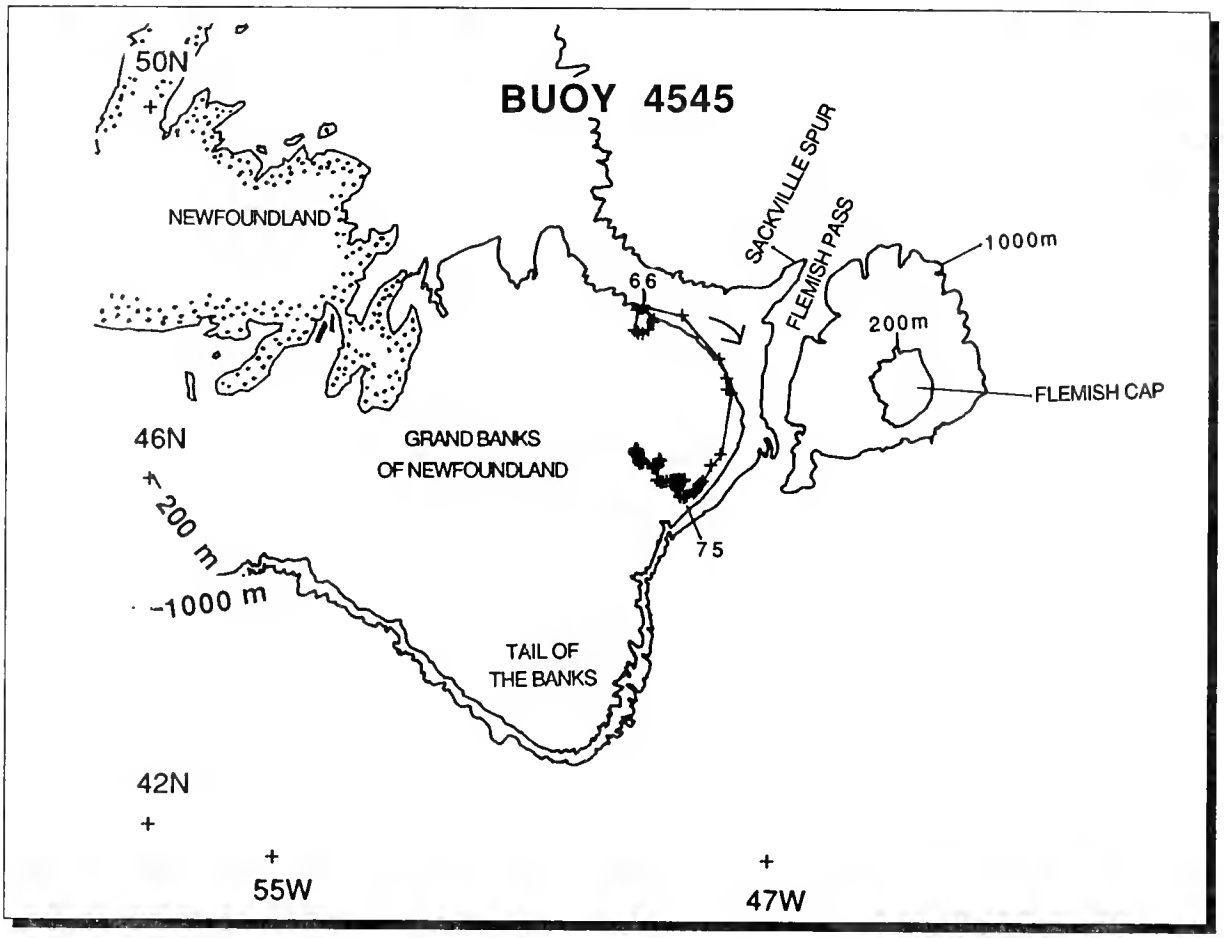

Figure C-1. Trajectory of Buoy 4545.

the time history of the U (east is positive) and V (north is positive) components of velocity from the filtered records. Finally, a time history of the raw sea surface temperature data is plotted for each buoy. The dates used in all of the plots are year-dates, which are numbered sequentially from January 1. In the text, the year-dates are included parenthetically.

BUOY TRAJECTORIES

In the following sections each buoy trajectory is discussed separately, presented in chronological order by deployment date. Only the operational buoys are discussed. This includes two buoys that were deployed from BITTERSWEET and allowed to drift free at the end of the experiment and two buoys purchased by, and deployed for, AES. Buoys 4547 and 4558 were used only during the research cruises. Their data are reported in Appendices D and E.

The intent of the following discussions is to summarize each buoy's performance and the data that it contributed to Ice Patrol operations. It is not intended to be an exhaustive data analysis. The buoy data from the area east of 39°W, the eastern boundary of the Ice Patrol operations area, are not presented. All of the data from the IIP drifting buoy program are archived at the IIP office in Groton, Connecticut.

BUOY 4545

Buoy 4545 (Figure C-1, C-2) was deployed and recovered four times in 1987 (Table C-1), but only one deployment was for operational use. On 4 March (63) it was air-deployed at 47-45N, 48-45W. It provided position and temperature data for 63 days until it was recovered on 5 May (125) at 46-42N, 49-21W by USCGC BITTERSWEET during IIP 87-1. During the entire period, the drogue sensor showed that the drogue remained attached; however, when the buoy was recovered only the 50 m nylon drogue tether and the chain bridle that supports the drogue were attached to the buoy. The chain was badly abraided, suggesting that it had dragged

across the bottom. The position data presented and discussed in this section are the raw data, not filtered. The record was short and the data return from the buoy immediately after its deployment was poor (2-3 fixes per day) so much of the interesting data would be lost filling the filter.

Buoy 4545 was deployed near the 200 m isobath. During the first 48 hours after deployment, it moved onto the Grand Banks and made an anticyclonic loop with a diameter of about 35 km. Typical buoy speeds during this period were 30-40 cm/s. For the next 10 days (7 - 16 March, 66-75) it moved southward through Flemish Pass, near and parallel to the 200 m isobath. Buoy speeds during this period were 40-50 cm/s and the temperature changed little (-0.8 to -1.4°C).

On 16 March (75), 4545 started to move northwestward onto the continental shelf. By 8 April (98) the buoy had moved into a region where it is likely that the drogue was dragging on the bottom, so the drift data after this date are of little use. The surface temperature continued to increase slowly but persistently. The surface temperature when the buoy was recovered was 3.3°C.

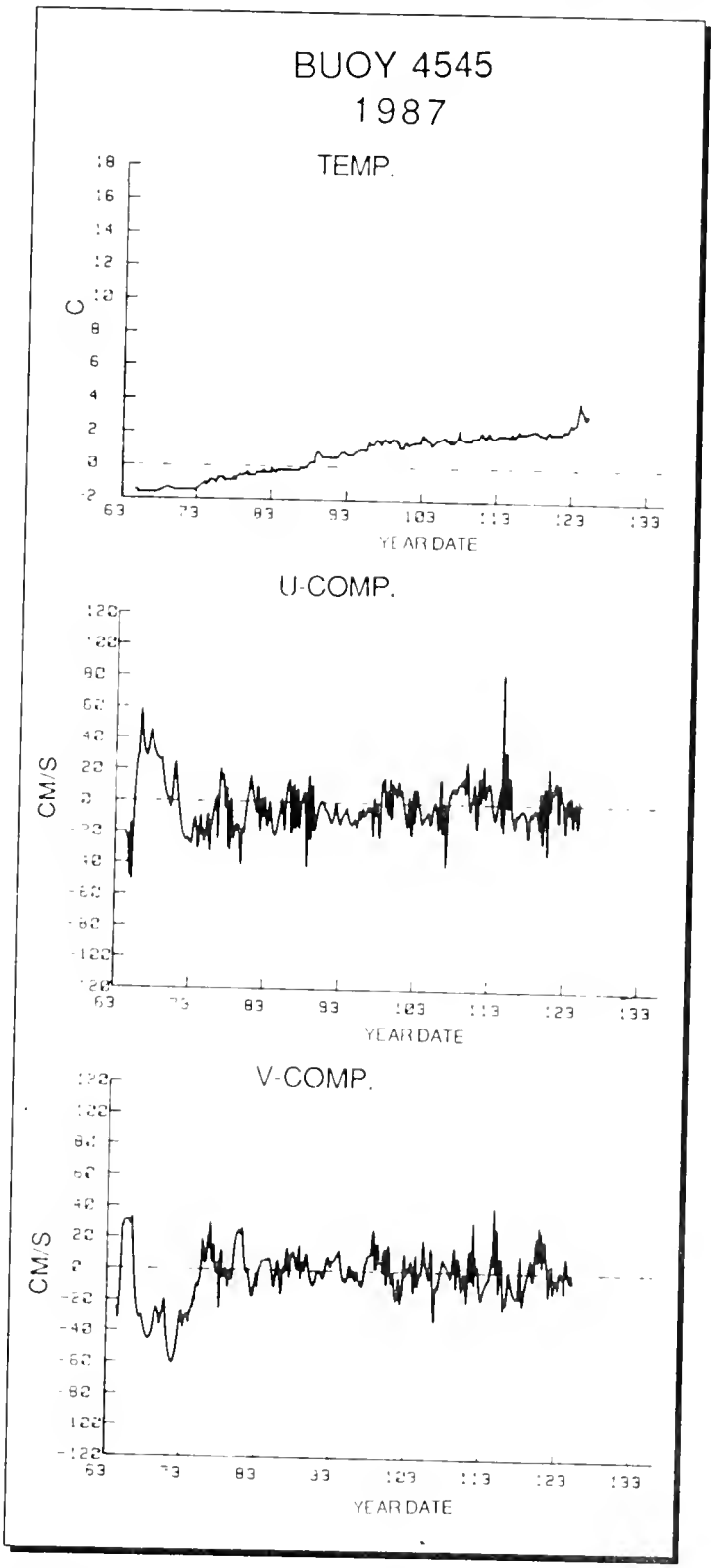

Figure C-2. Temperature, U and V velocity components for buoy 4545.

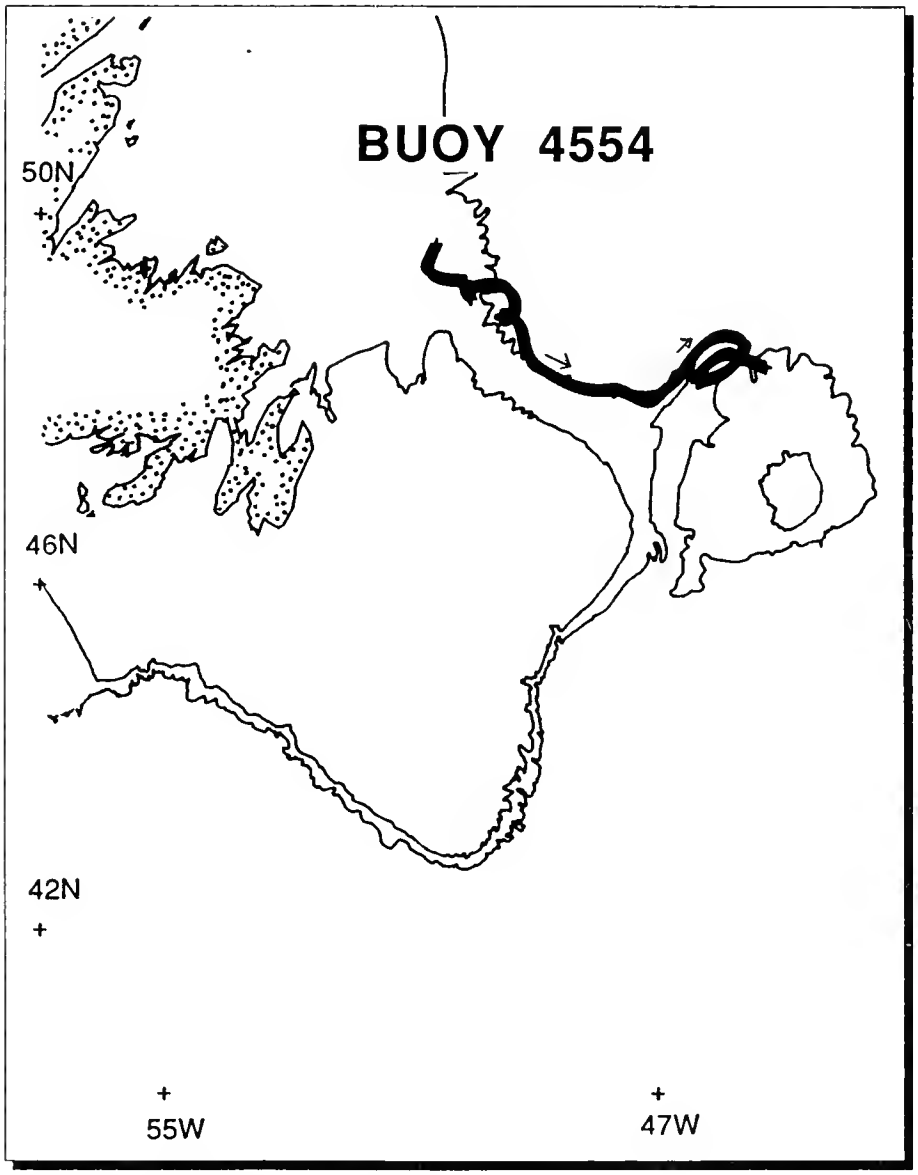

Figure C-3. Trajectory of Buoy 4554.

BUOY 4554

Buoy 4554 (Figure C-3, C-4) was air-deployed at 50-00N, 50-40W on 25 March (84). It transmitted position and temperature data for 65 days, failing on 28 May (148). The buoy's battery voltage and the number of fixes per day were normal until failure. The drogue remained attached during the entire drift period.

After its deployment, 4554 moved southeastward, approximately following the 1000 m isobath. Over this period, the filtered buoy speeds varied over the range of 5 to 30 cm/s. The temperature record is unremarkable, with a slow increase in temperature of from 0 to 6°C over the 65 days (0.1°C/day) of the buoy's life.

At Sackville Spur, 4554 turned to the northeast, after which it made an anticyclonic loop (~50 km diameter). It failed shortly thereafter.

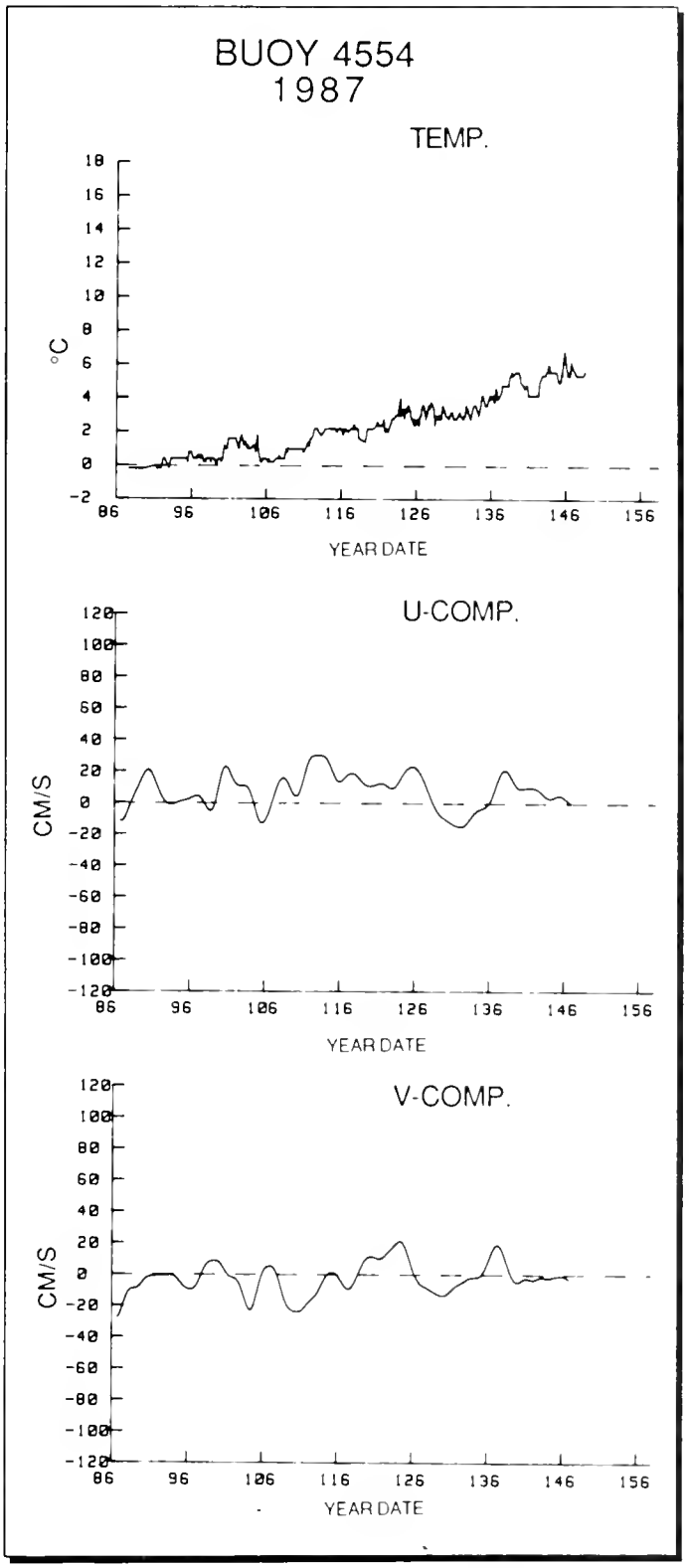

Figure C-4. Temperature, U and V velocity components for buoy 4554.

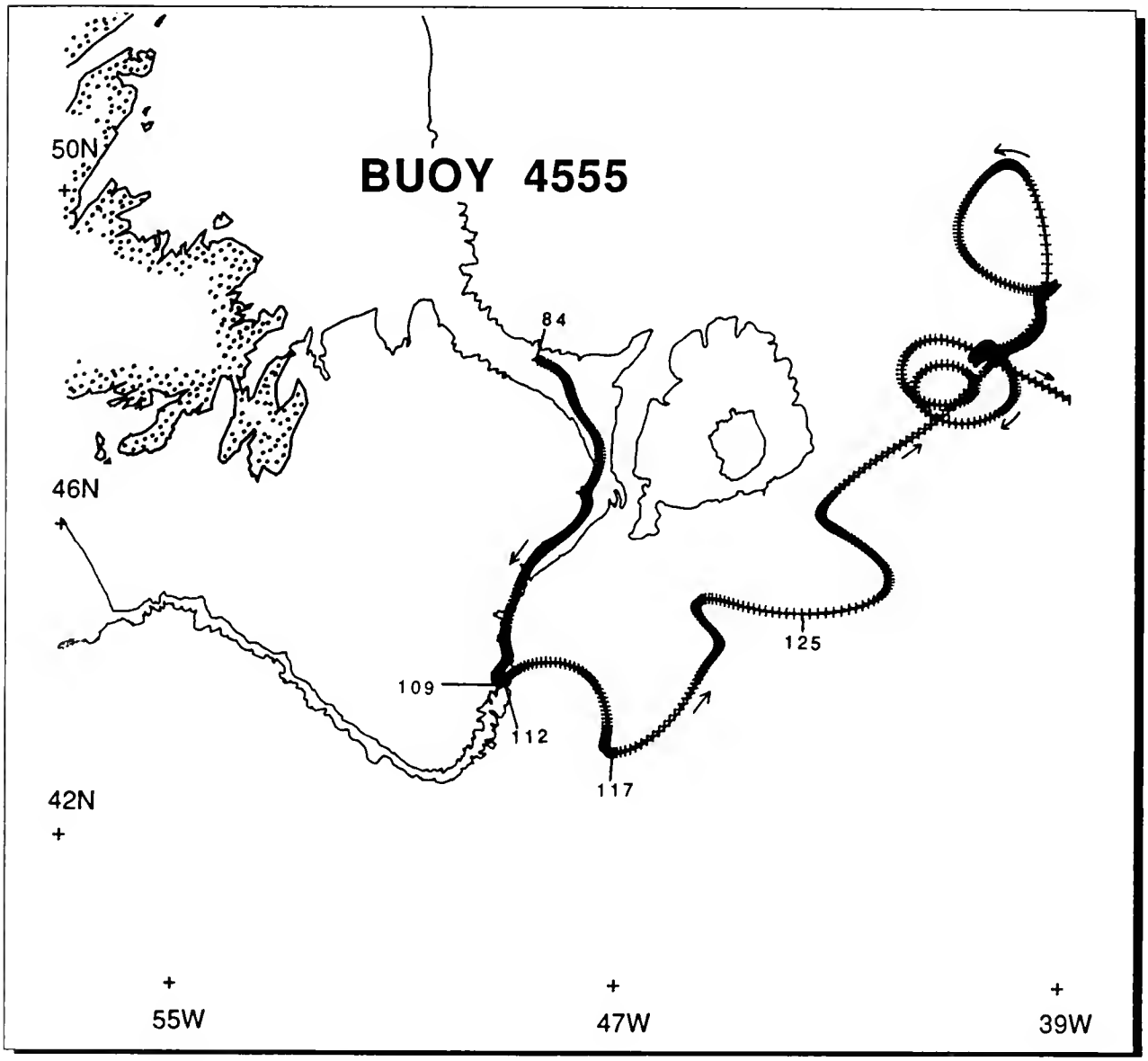

Figure C-5. Trajectory of Buoy 4555.

BUOY 4555

Buoy 4555 (Figure C-5, C-6) was air-deployed at 48-20N, 48-26W on 25 March (84). It remained in the Ice Patrol operations area for 91 days, passing east of 39°W on 23 June (174). The drogue remained attached to the buoy for the entire 91-day drift period, detaching on 29 June (180). Shortly thereafter (3 July, 184), 4555 was recovered by an unknown vessel at 46-28°N, 37-06°W and taken in the direction of Europe.

After deployment, 4555 moved southeastward and then southward through Flemish Pass, approximately following the 200 m isobath. During this 25-day period, from 25 March to 19 April (84-109), the temperature increased slowly from -1.4 to 1.4°C and the speed varied widely (10-50 cm/s).

At approximately 44°N, the trajectory of 4555 changed abruptly under the influence of a warm-core eddy centered at 43-30N, 48-10W. The buoy slowed, reversed direction, and then moved eastward and southward, tracing an anticyclonic path approximately one-half the way around the boundary of the eddy. This occurred over a 6-day period, during which the buoy moved at speeds of 50-70 cm/s. During the period that 4555 was moving around the outside of the eddy, the temperature record shows a considerable variability over the range from 0.8 to 13°C, suggesting that the buoy was

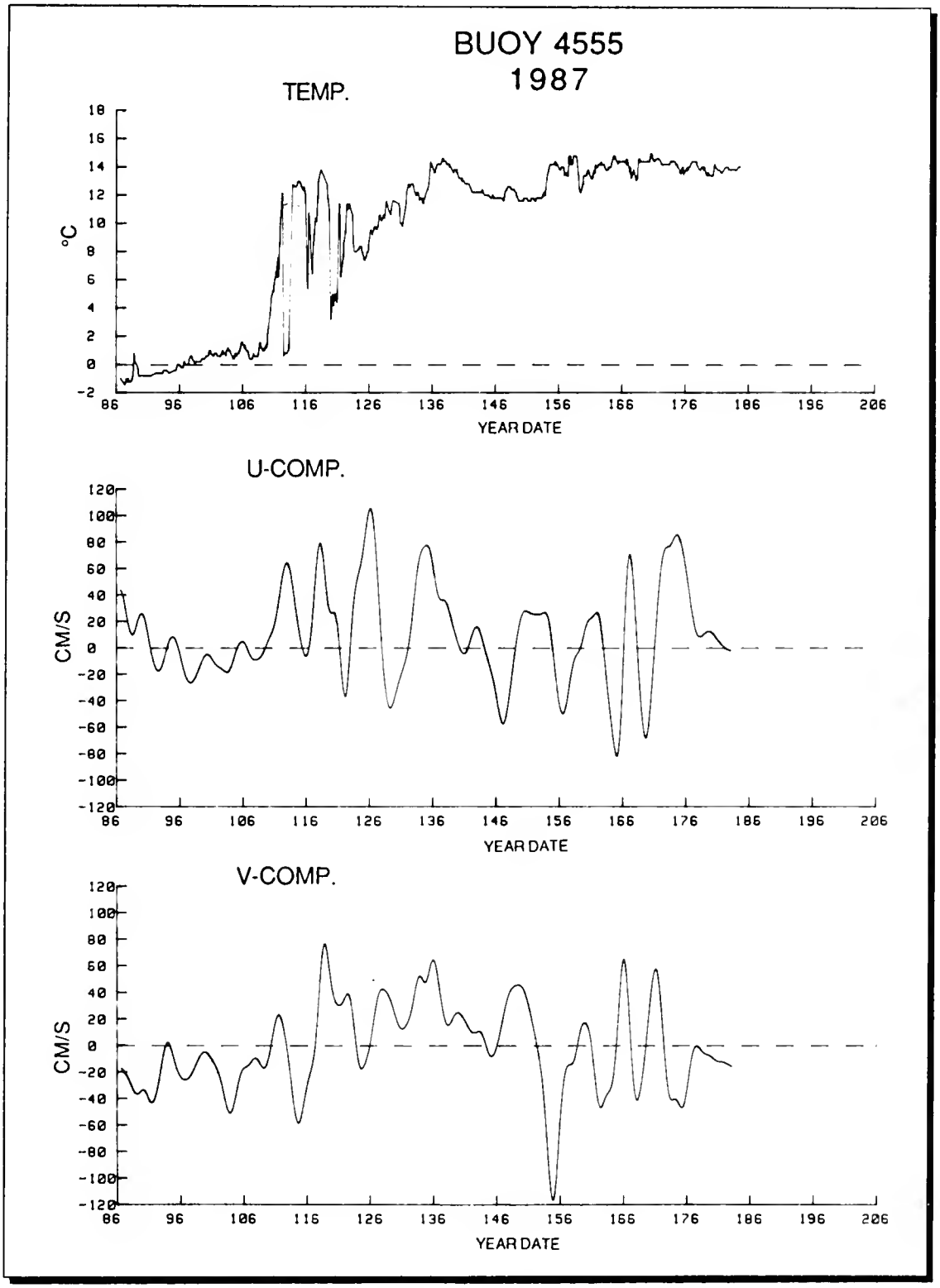

Figure C-6. Temperature, U and V velocity components for buoy 4555.

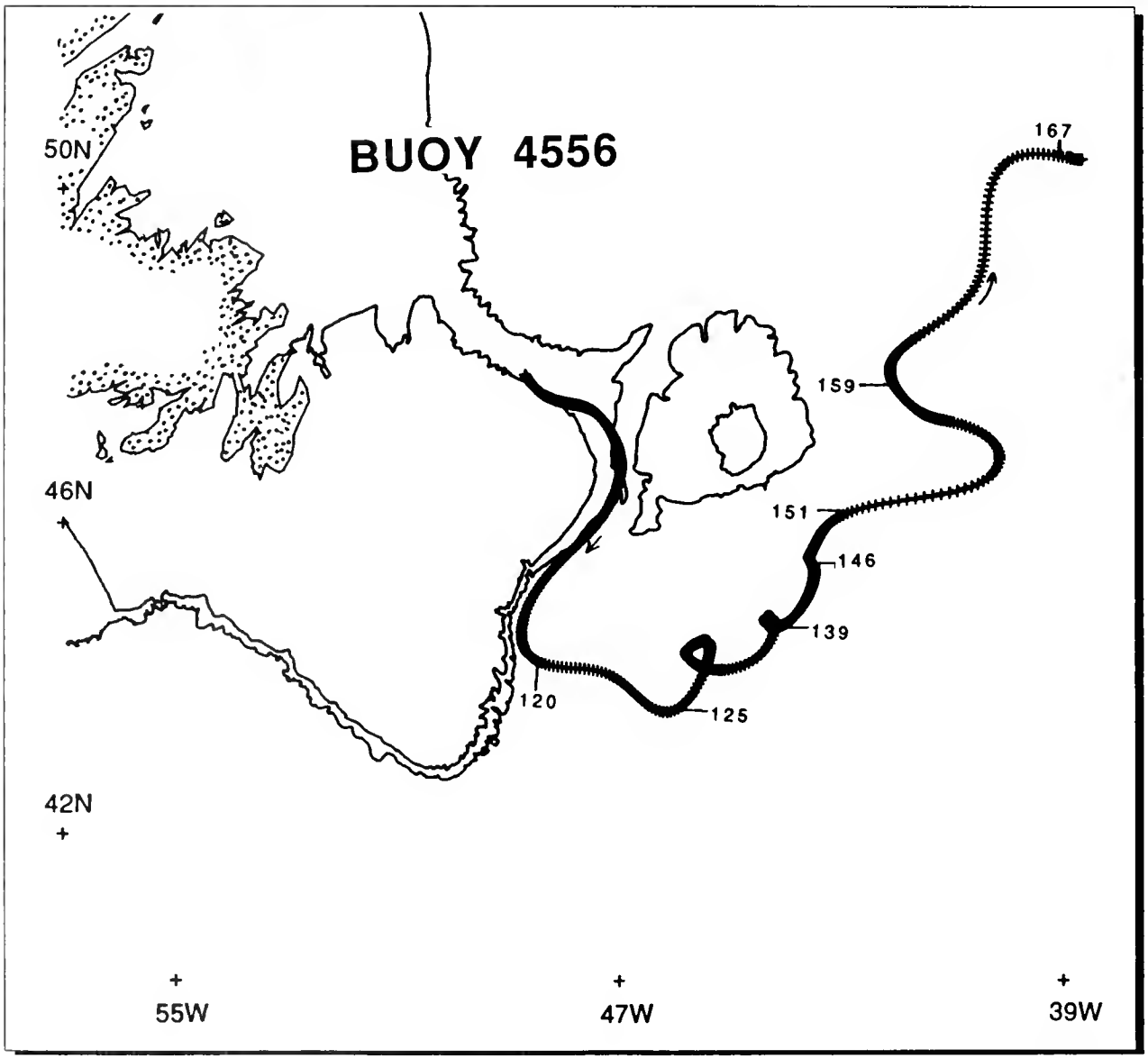

Figure C-7. Trajectory of Buoy 4556.

close to the eddy's boundary. It is likely that the drogue (~58 m) remained in the cold, subsurface core of the Labrador Current while the temperature sensor at the surface was moving through surface waters of various temperatures near the eddy's boundary.

The track of 4555 after it left the vicinity of the eddy was generally northeastward, with wide fluctuations in the filtered speeds. The temperature record shows that the buoy remained in waters greater than 8°C, with most of the readings in the range of 12-14°C. The buoy's subsequent movement is complex, with evidence of eddies and meanders associated with the North Atlantic Current, particularly in the area east of Flemish Cap.

BUOY 4556

Buoy 4556 (Figure C-7, C-8) was deployed from an aircraft on 14 April (104) at 48-20.1N, 49-19.8W. It remained in the Ice Patrol operation area for 63 days, passing east of 39°W on 16 June (167). Three days later (170), the buoy stopped transmitting, although there was no prior indication of a reduction in the buoy's battery voltage or the number of fixes per day. The drogue indicator showed that the drogue detached on 31 May (151), thus it remained attached to the buoy for 48 days.

After its deployment, the buoy moved southward through the Flemish Pass and along the eastern edge of the Grand Banks, approximately following the 1000 m isobath. During this period (14-20 April, 104-120), the average speed was 30-45 cm/s and the sea surface temperature increased slightly from -1.4°C to 0.6°C.

On 30 April (120), 4556 began to move rapidly (50-70 cm/s) to the east, north of the warm core eddy that was surveyed during IIP 87-1. This eastward motion of a buoy deployed in the Labrador Current and encountering a warm core eddy near the eastern edge of the Grand Banks is similar to that observed in 1986 (Murphy et al, 1986). The buoy's motion around the eddy suggests that a portion of the Labrador Current left the eastern edge of the Grand Banks at approximately 44-10N and traced a path partially around the eddy. Buoy 4556's temperature record, which showed a slow increase in temperature (0.6 to 2.0°C), suggests that it did not enter the eddy, instead remaining in the Labrador Current.

On 4 May (124), 4556 started a general northeastward drift, which is typical of many IIP buoys that become entrained in the North Atlantic Current. Over the next twelve days the temperature increased 8°C (2-10°C). This period is also remarkable in that the buoy's trajectory shows that it became entrained in a small (< 40 km in diameter) cyclonic eddy that was propagating northeastward and apparently decreasing in size. The trajectory shows that the buoy made three circuits of the eddy while the eddy moved northeastward at about 5 km/day.

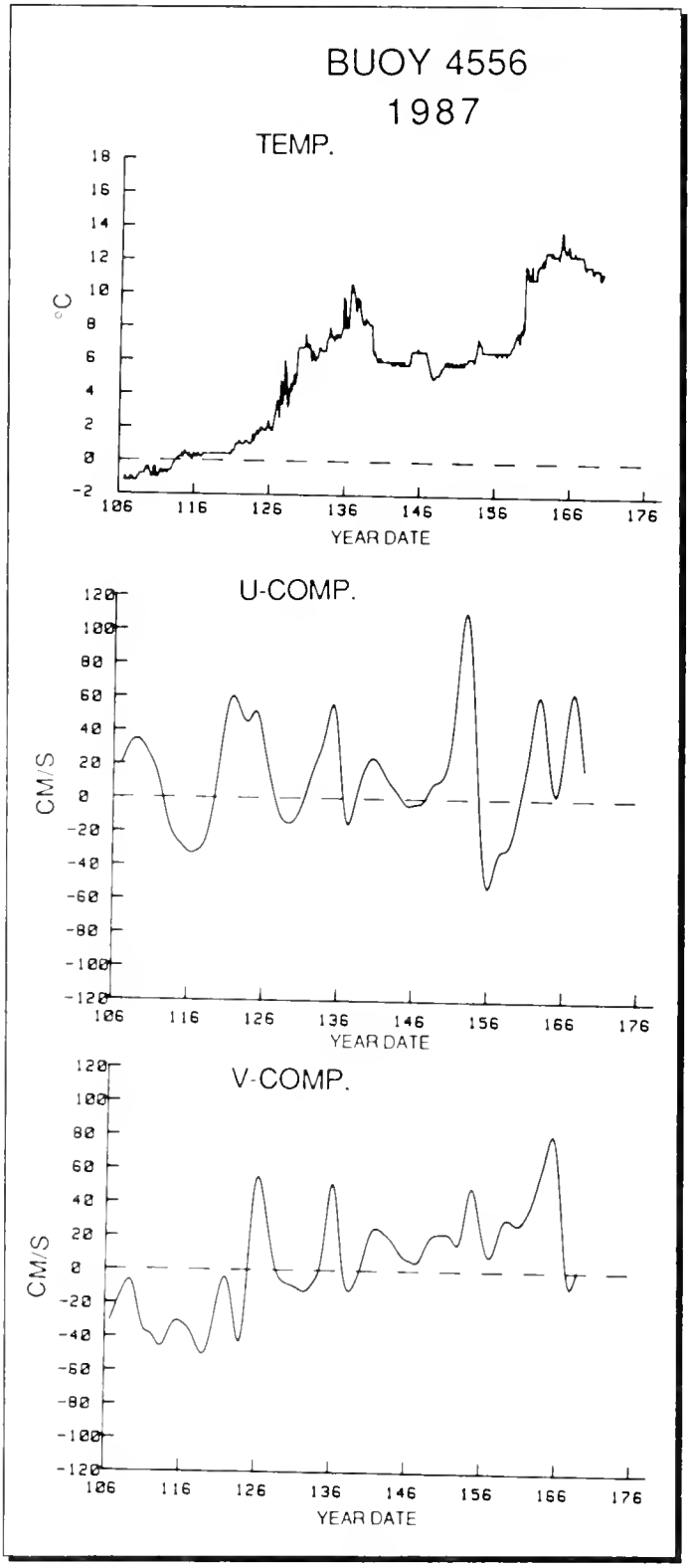

Figure C-8. Temperature, U and V velocity components for buoy 4556.

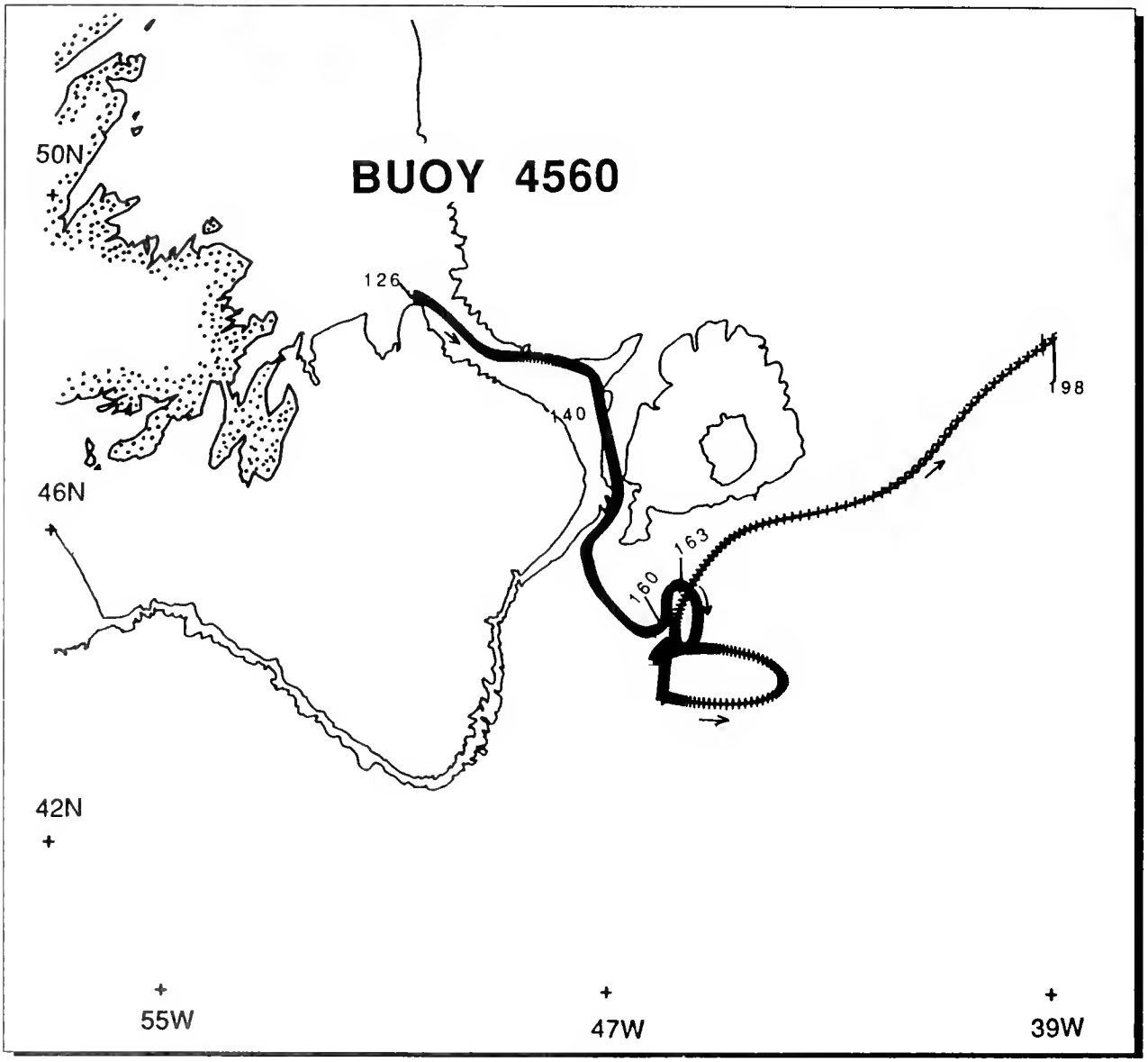

Figure C-9. Trajectory of Buoy 4560.

The temperature record during the period that 4556 was moving in the anticyclonic eddy (125-146) cannot be easily explained. First, the temperature increased from 2-10°C, then it decreased rapidly to 5-6°C. It is possible that the low temperature recordings from 19 May to 8 June (139-159) are the result of a sensor malfunction. However, other than the loss of the drogue on 30 May (150), there is no evidence of a buoy malfunction.

On 8 June (159) the temperature record shows an increase from 8.2 to 11.8°C on successive satellite passes (about three hours apart). Eight days later (167), 4556 crossed east of 39°W. On 19 June (170), 66 days after its deployment, 4556 stopped transmitting.

Buoy 4556 was recovered by the Irish Navy and returned to Ice Patrol in August 1988. It was severely damaged and could not be returned to service.

BUOY 4560

Buoy 4560 (Figure C-9, C-10) was air-deployed on 6 May (126) at 49-00N, 50-36W. It provided data in the Ice Patrol operations area for 73 days, passing east of 39°W on 17 July (198). The drogue remained attached for the entire period, detaching on 17 October (290) 175 days after deployment. The buoy continued to transmit data for the remainder of the calendar year.

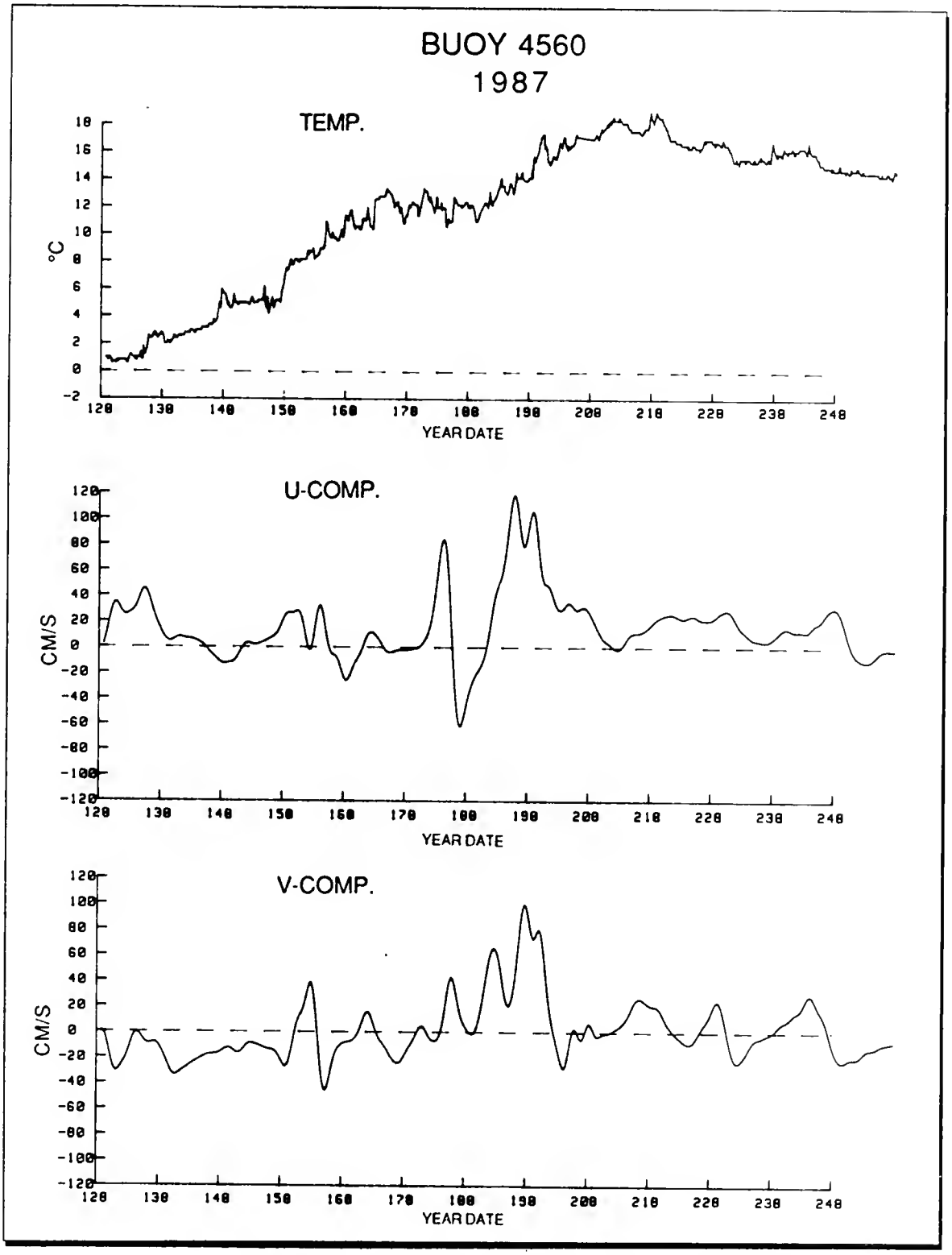

Figure C-10. Temperature, U and V velocity components for buoy 4560.

During the first 14 days following its deployment (6-20 May,126-140), 4560 moved southeastward to the northern part of Flemish Pass. During this period the buoy's speed varied over the range 25-40 cm/s while the temperature increased slightly (1-3°C). The southward motion through Flemish Pass approximately followed the 1000 m isobath. The buoy speed through Flemish Pass varied from 20-35 cm/s, while the temperature remained about 2-3°C.

After departing Flemish Pass, 4560 left the slope and moved slowly (< 20 cm/s) southeastward. During this period the temperature changed little. The buoy trajectory in the region south of Flemish Cap is complex. Buoy 4560 remained in this region for 31 days (9 June-10 July,160-191), during which the surface temperature increased from 8 to 12°C.

On 10 July (191), 4560 began a rapid and persistent movement northeastward with speeds varying over the range of 65-135 cm/s. During this period the surface temperature increased rapidly, from 12 to 16°C.

BUOY 4536

Buoy 4536 (Figure C-11, C-12) was deployed from BITTERSWEET at 43-39N, 48-12W on 7 May (127) in a warm-core eddy. It provided data in the Ice Patrol operations area for 152 days, passing east of 39°W on 5 October (278). The drogue sensor indicated an early drogue failure, with detachment occurring on 20 May (140), 14 days after deployment. The buoy ceased transmitting on 9 December (343).

Buoy 4536 remained in the eddy for only 3 days. The data from that period are presented in Appendix D. The departure of 4536 from the eddy was marked by an abrupt decrease in surface temperature (10.2 to 7.8°C in about 5 hours) and a persistent movement to the east. Over this 5-day period, 11-15 May (131-135), the buoy accelerated form 40 to 110 cm/s and the surface temperature increased from 6 to over 13°C. This motion and temperature increase suggest 4536 entered the North Atlantic Current.

During the next 34 days (17 May - 20 June, 137-171) 4536 remained in the region directly south of Flemish Cap. The buoy's trajectory in this area is complex, with three anticyclonic and one cyclonic loop. At times 4536 moved at over 60 cm/s. The surface temperature varied form 8-12°C. These data suggest an area characterized by North Atlantic Current meanders and eddies.

Over the next 6 days (20-25 June, 171-176), 4536 moved rapidly (70-125 cm/s) eastward and then northward. The temperature over the period remained within 10-13°C. For the remainder of its period in the Ice Patrol operations area (26 June - 5 October, 177-278) 4536 remained north of Flemish Cap. The trajectory is complex but it suggests that the flow in the region was dominated by North Atlantic Current meanders. The temperature varied over the range of 13-18°C.

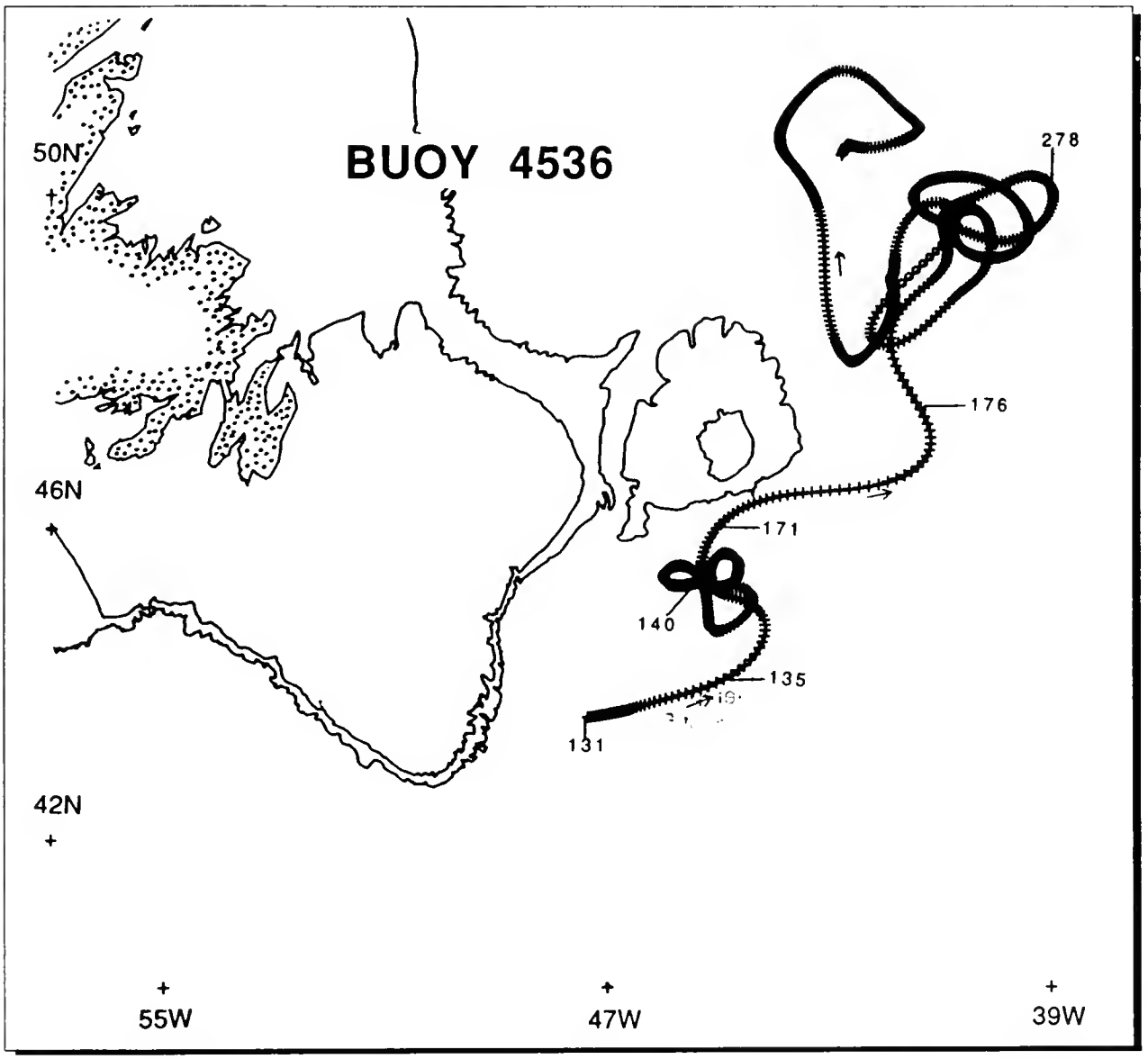

Figure C-11. Trajectory of Buoy 4536.

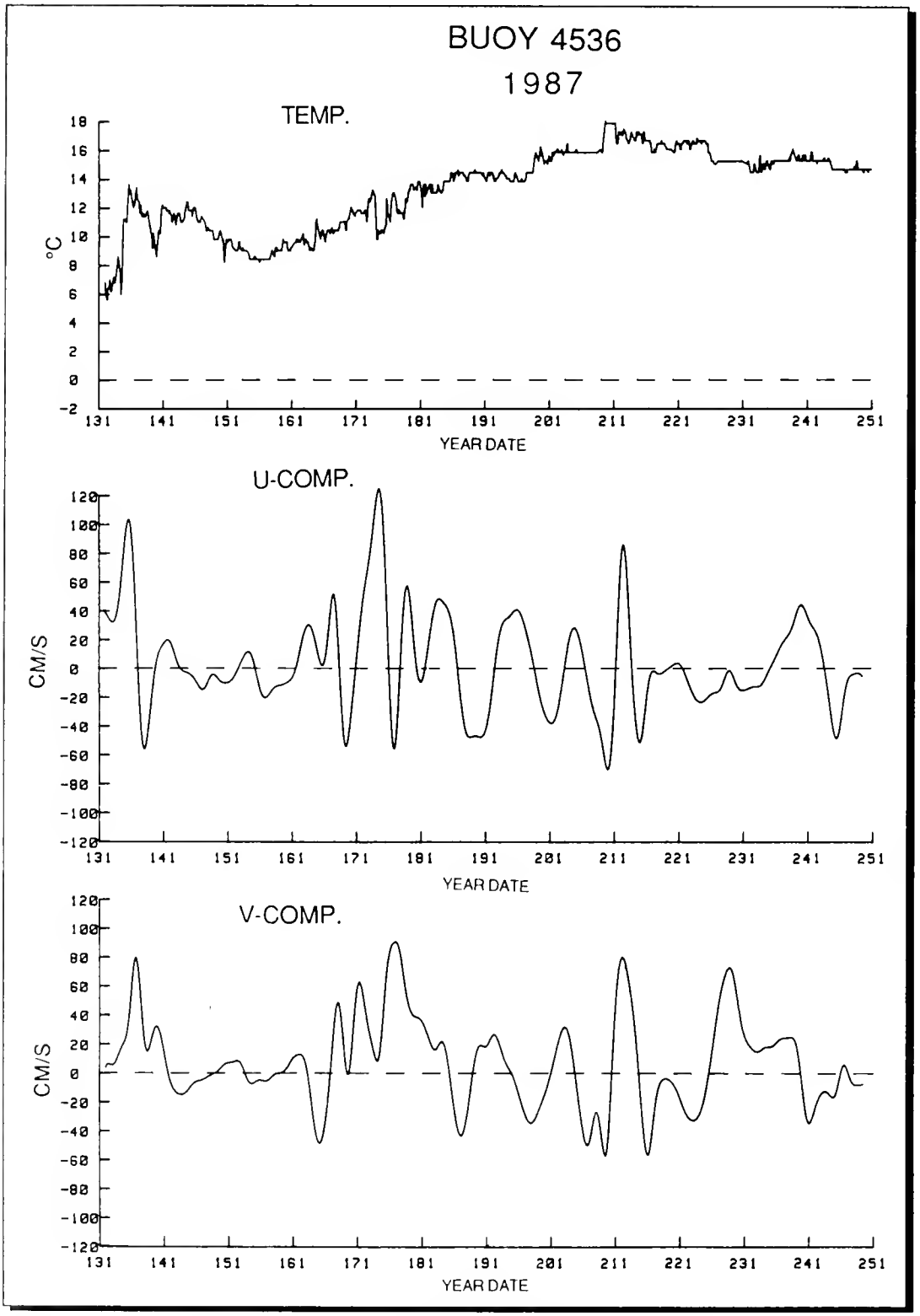

Figure C-12. Temperature, U and V velocity components for buoy 4536.

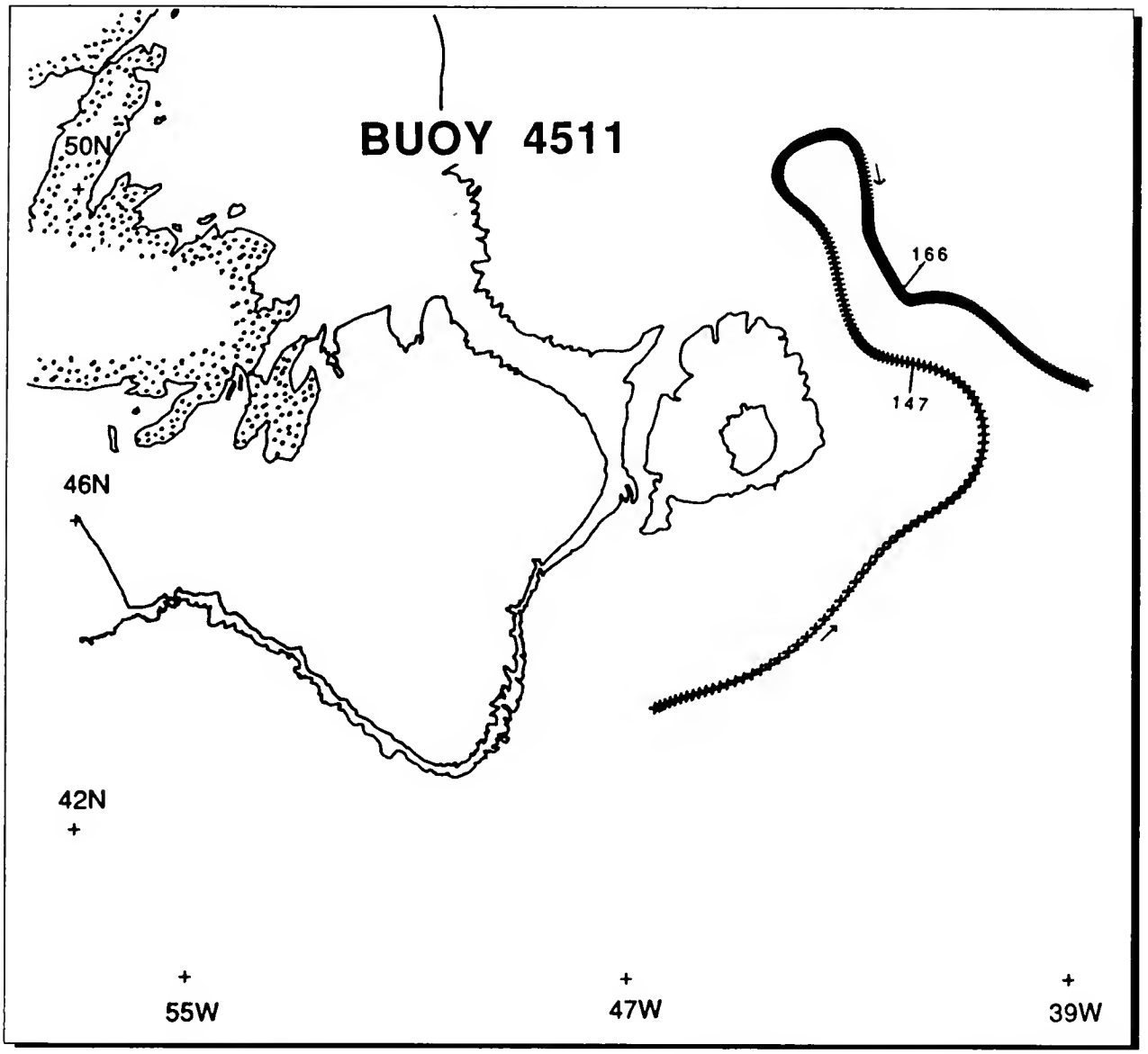

Figure C-13. Trajectory of Buoy 4511.

BUOY 4511

Buoy 4511 (Figure C-13, C-14) was deployed twice in 1987, the second time to collect operational data. On 17 May (137) it was deployed at 43-13N, 47-43W by USCGC BITTERSWEET (WLB 389). It provided 37 days of operational data in the Ice Patrol operations area, before passing east of 39°W on 22 June (173). Due to a data formatting error, no data regarding drogue status was received from the ARGOS processing center after 15 June (166). The earlier data indicate that the drogue was attached until that time. Buoy 4511 continued to transmit data throughout the remainder of 1987 as it moved eastward across the Atlantic Ocean.

Buoy 4511 was deployed south of the eddy surveyed by BITTERSWEET. This shipboard deployment provided an opportunity to compare the sea surface temperature as determined by the buoy and a CTD (conductivity, temperature, and depth) measurement made at the depth of the buoy's temperature sensor. The agreement was excellent. The buoy measured 16.3-16.4°C while the CTD measurement was 16.4°C. The two measurements were taken approximately 15 minutes apart.

After its deployment, 4511 moved persistently and rapidly to the northeast, with speeds, at times, exceeding 150 cm/s. During the

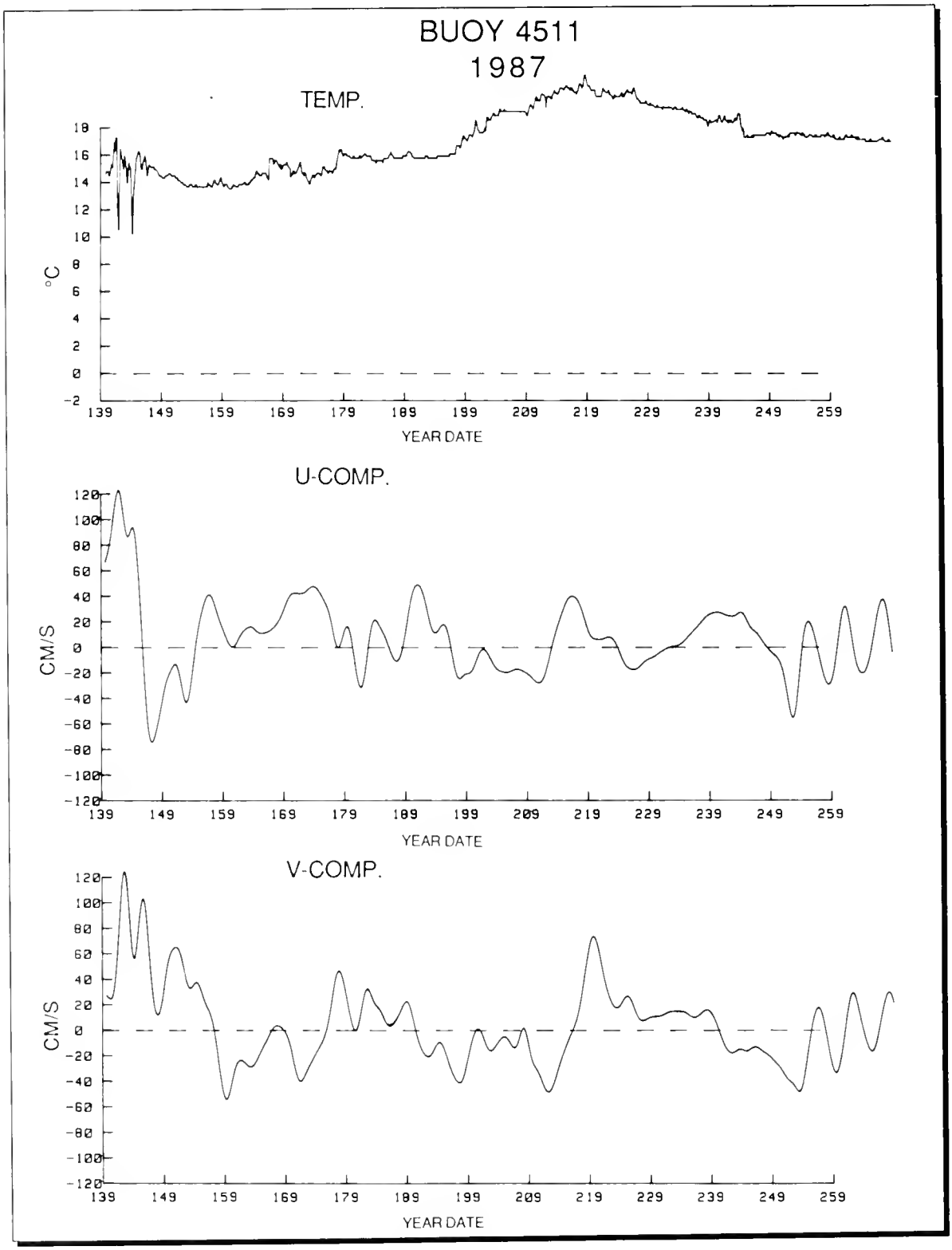

Figure C-14. Temperature, U and V velocity components for buoy 4511.

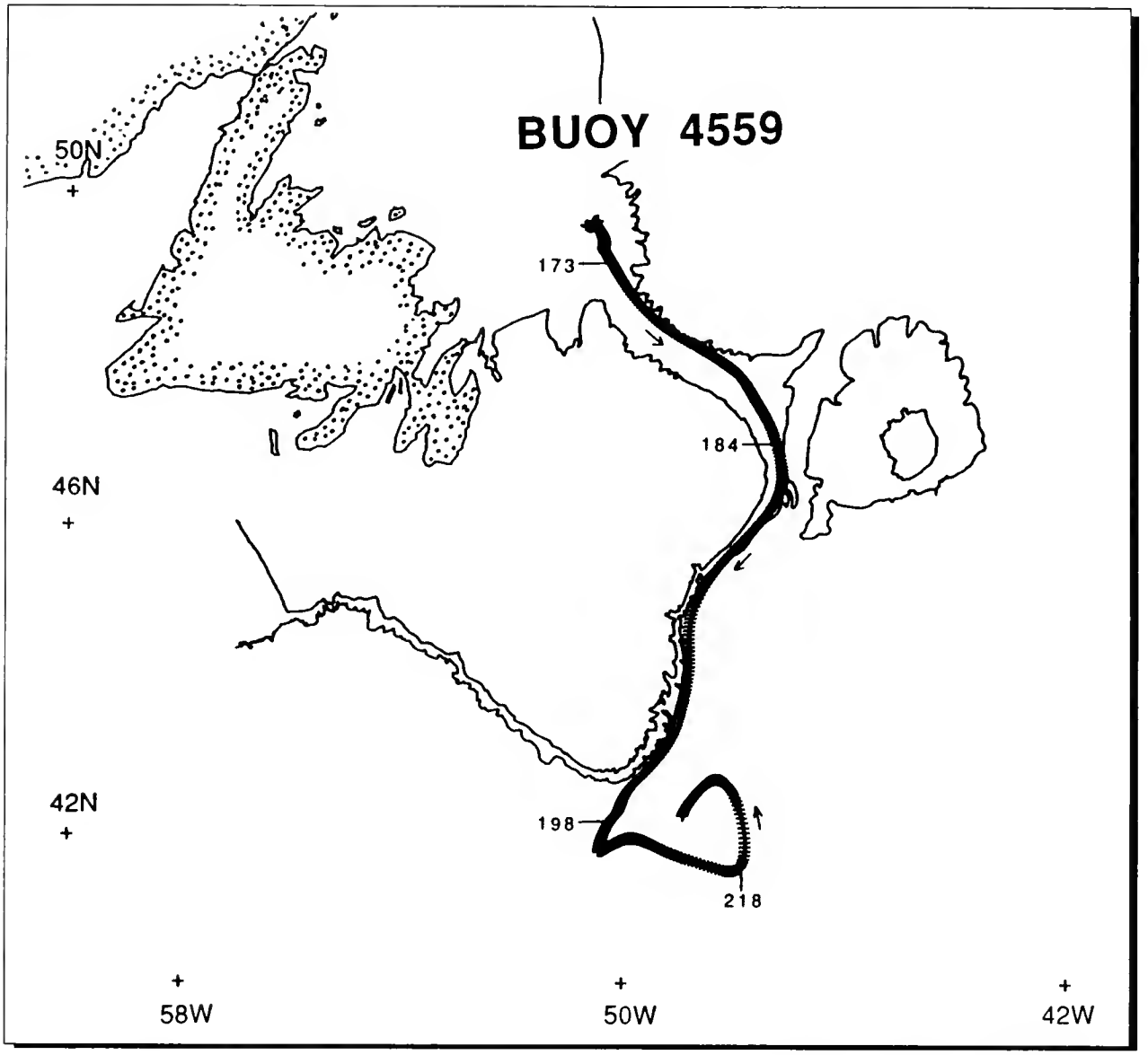

Figure C-15. Trajectory of Buoy 4559.

same period (17-27 May, 137-147), the temperature record shows considerable variability over the range 10-17°C. At the end of this period, 4511 turned abruptly to the northwest and slowed substantially with the typical speeds varying over the range of 20-70 cm/s. It is likely that this motion was due to a northwestward-projecting meander of the North Atlantic Current near Flemish Cap. During this entire period, the temperature remained stable near 14°C.

BUOY 4559

Buoy 4559 (Figure C-15, C-16) was air-deployed at 49-40N, 50-52W on 6 June (157). It provided data in the Ice Patrol operations area for 62 days, during which the drogue remained attached. On 6 August (218) it appears that the buoy was recovered by a vessel. The temperature showed an abrupt 6°C increase to 23.8°C, accompanied by an indication of drogue detachment. Shortly thereafter, the buoy ceased transmitting.

The first 16 days after deployment were characterized by a sluggish (< 20 cm/s) movement to the southeast, with the sea surface temperature remaining in the 2-5°C range. On 12 June (163), six days after its deployment, 4559 was inspected by the Ice Patrol field party aboard TAMAROA at 49-39.9N, 50-32.8W. The drogue was properly deployed, but the parachute had not cut and was fouled around the wooden pallet. The parachute was cut free. On 22 June (173),

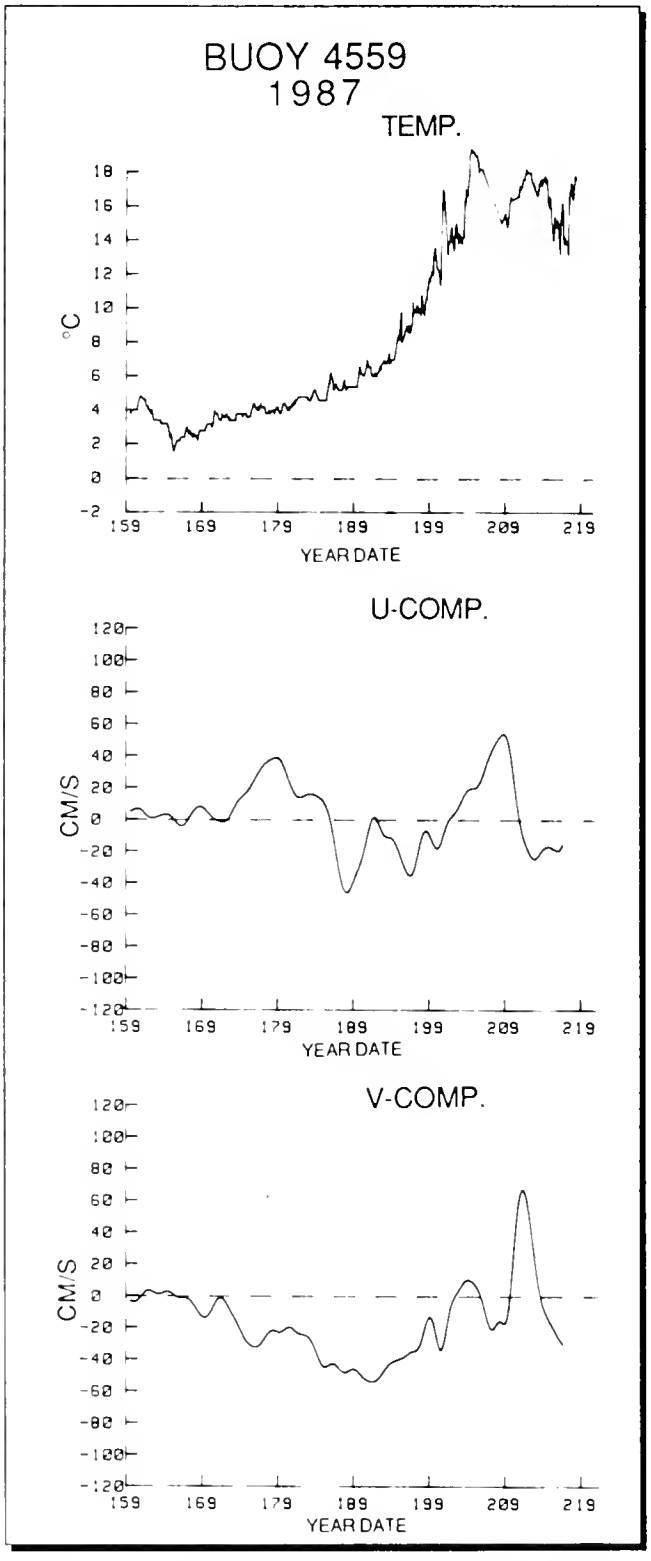

Figure C-16. Temperature, U and V velocity components for buoy 4559.

when the buoy reached the vicinity of the 1000m isobath, 4559 began a more vigorous (30-40 cm/s) southeastward movement along that isobath. During this 11-day period (22 June - 3 July, 173-184) the sea surface temperature changed little.

On 3 July (184), 4559 started to move southward through Flemish Pass. It then moved southward in the Labrador Current along the eastern edge of the Grand Banks, approximately following the 1000 m isobath to the Tail of the Bank with speeds mostly in the 40-60 cm/s range and some peak readings approaching 70 cm/s. During this two-week period (3-17 July, 184-198) the surface temperature increased about 5°C (5 to 10°C).

After leaving the 1000 m isobath at the Tail of the Bank, 4559 moved southward and then eastward. During this period there is a data gap of three days duration due to communications problems within the ARGOS system. Finally, the track of 4559 traced a cyclonic loop with a diameter of approximately 110 km. The surface temperature during this period varied considerably over the range of 14 to 18°C.

BUOY 4553

Buoy 4553 (Figure C-17, C-18) was air-deployed on 25 June (176) at 52-44N, 51-55W. It was the last operational buoy deployed during the 1987 iceberg season. It provided position and sea surface temperature data for 100 days in the Ice Patrol operations area, passing east of 39°W on 22 September (265). It was still transmitting as of 31 December 1987. The drogue sensor showed that the drogue remained attached for

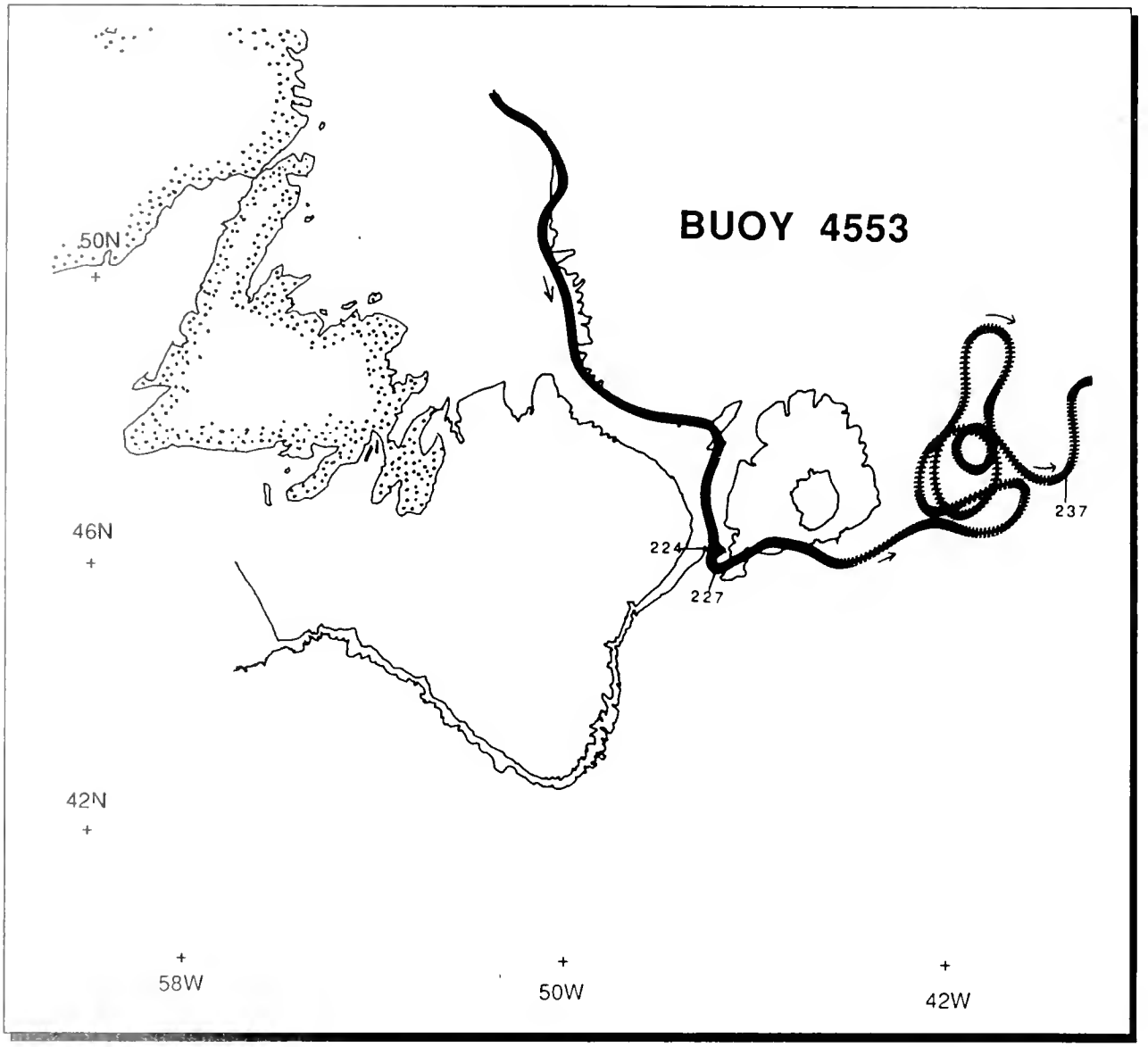

Figure C-17. Trajectory of Buoy 4553

approximately one-half of the 100-day period, detaching on 12 August (224).

Buoy 4553's southeastward motion after deployment almost exactly traces the 1000 m isobath down to 46°N, including the movement southward through Flemish Pass. While moving southward through Flemish Pass, 4553 recorded a 5.2°C increase in temperature over a 21-day period (~.25 deg/day). During this period the buoy's speed varied from near zero to 30 cm/s. It is also during this period that the drogue sensor showed drogue detachment. The detachment of the drogue added no noise to the position record, as might be expected due to wind effects on the above-water portion of the buoy hull.

On 15 August (227) at approximately 46°N, 4553 began an eastward motion south of Flemish Cap. During the next 10 days the temperature continued to increase until it reached about 15°C on 25 August (237), while the buoy moved persistently eastward at 15-35 cm/s. At this point the temperature leveled off and remained within 2°C of 15°C for the remainder of the drift period in the Ice Patrol operations area. At the same time, 25 August (237), the buoy's movement changed substantially. Figure C-18 shows that on this date 4553 entered a region east of Flemish Cap where the flow was vigorous, apparently dominated by eddies and meanders of the North Atlantic Current.

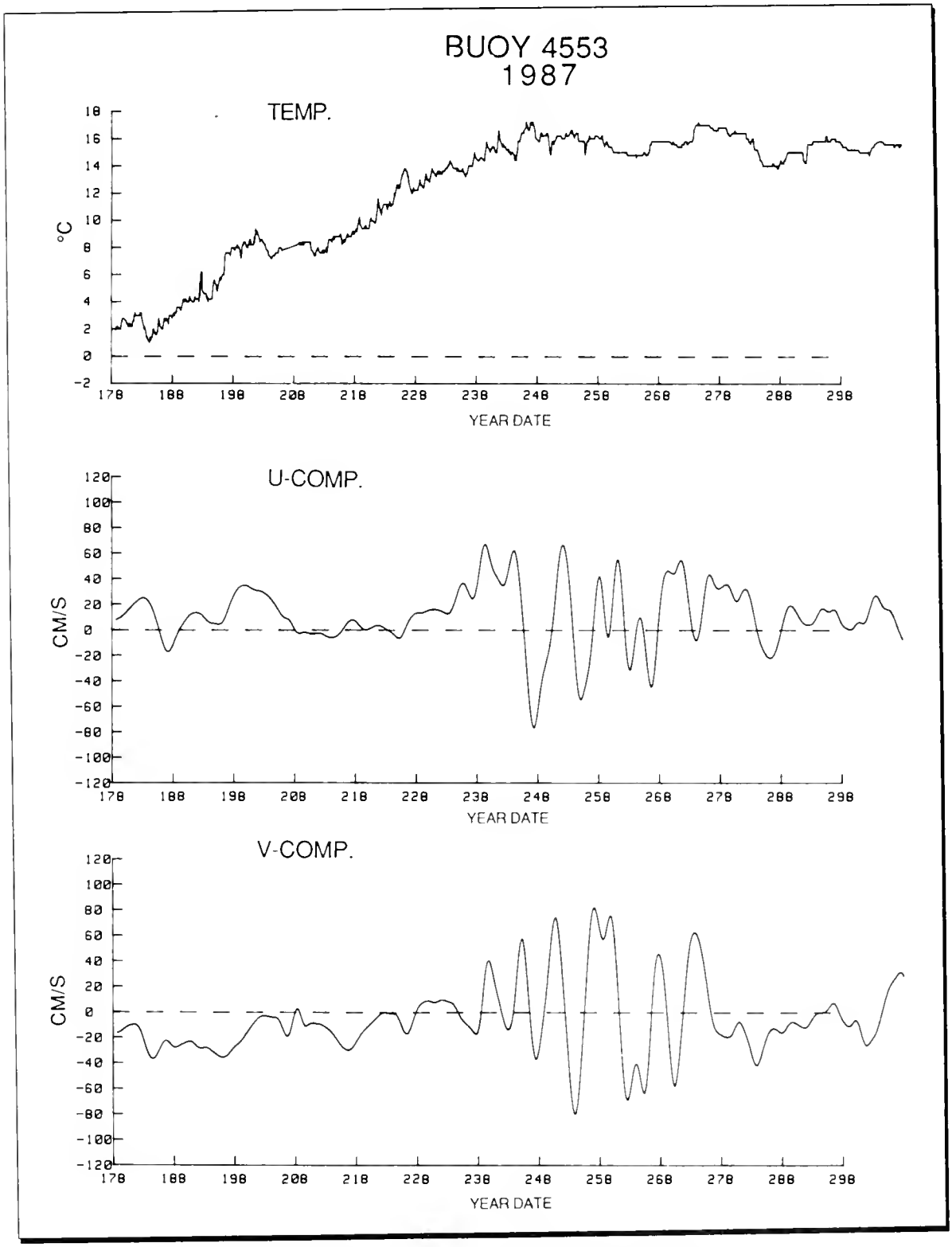

Figure C-18. Temperature, U and V velocity components for buoy 4553.

BUOY 4562

Buoy 4562 (Figure C-19, C-20) was launched from an aircraft on 15 August (227) at 59-13N, 60-18W. It entered the Ice Patrol operations area on 26 November (330) when it passed south of 52°N and transmitted data throughout the remainder of 1987. The drogue sensor indicated drogue detachment on 24 October (297), 70 days after the buoy's deployment.

For the first 28 days (15 August-11 September (227-254)) after its deployment, 4562 moved to the southeast, mostly between the 200 m and 1000 m isobaths. The speeds were in the range of 20 to 55 cm/s, while the temperature remained nearly constant (4-5°C). On 13 September (256), 4562 moved onto Hamilton Bank into water that was too shallow for the buoy's drogue. It remained in that vicinity for about 57 days, during which it moved slowly, with frequent direction changes. About halfway through this period (3 October (276)) the temperature record shows an abrupt decrease in temperature (3°C over 18 hours).

The remainder of 4562's southward movement occurred well inside the 1000 m isobath (3 days). The buoy speeds varied widely (0 to 35 cm/s), while the temperature decreases slowly but persistently from 3°C to 0°C.

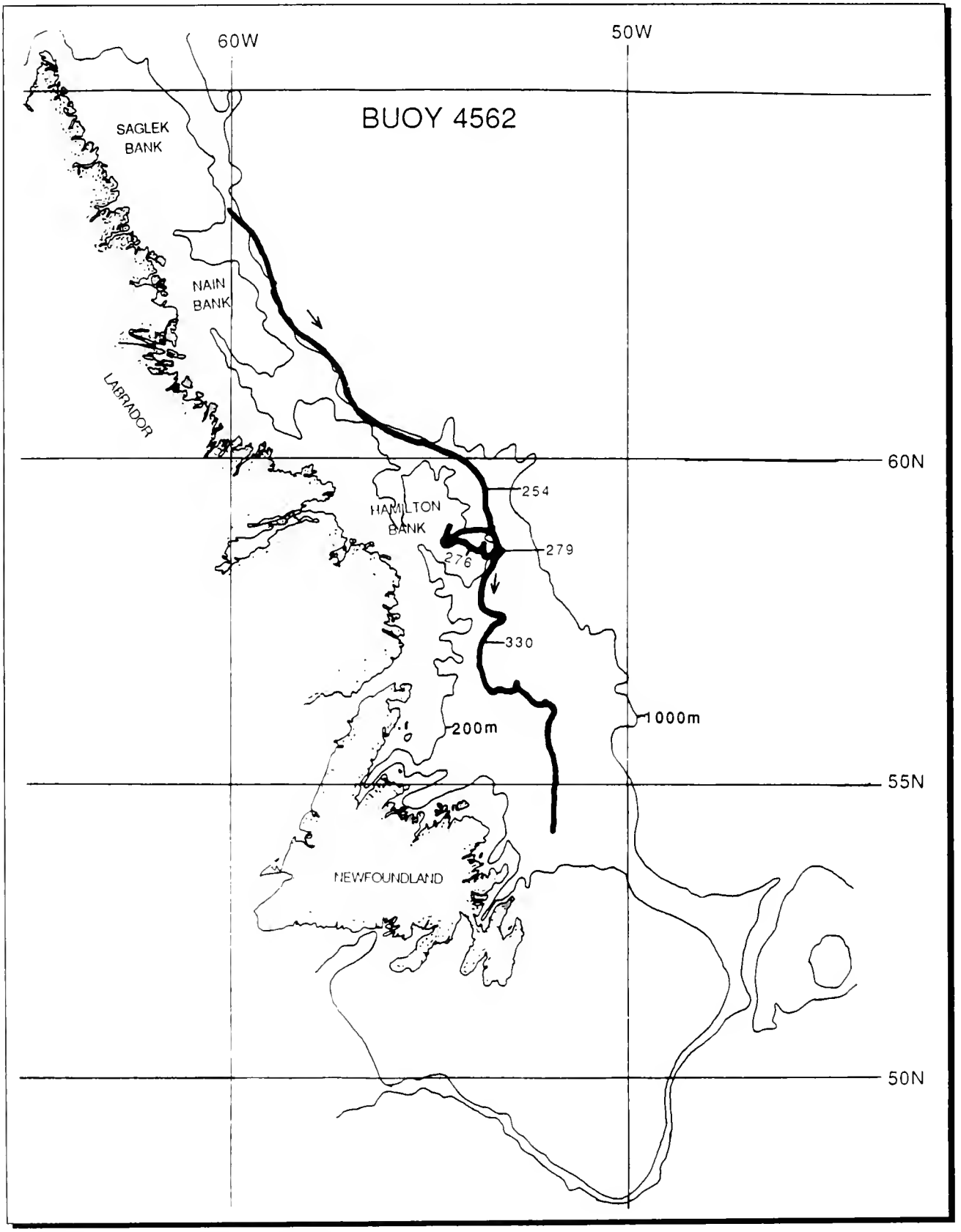

Figure C-19. Trajectory of Buoy 4562.

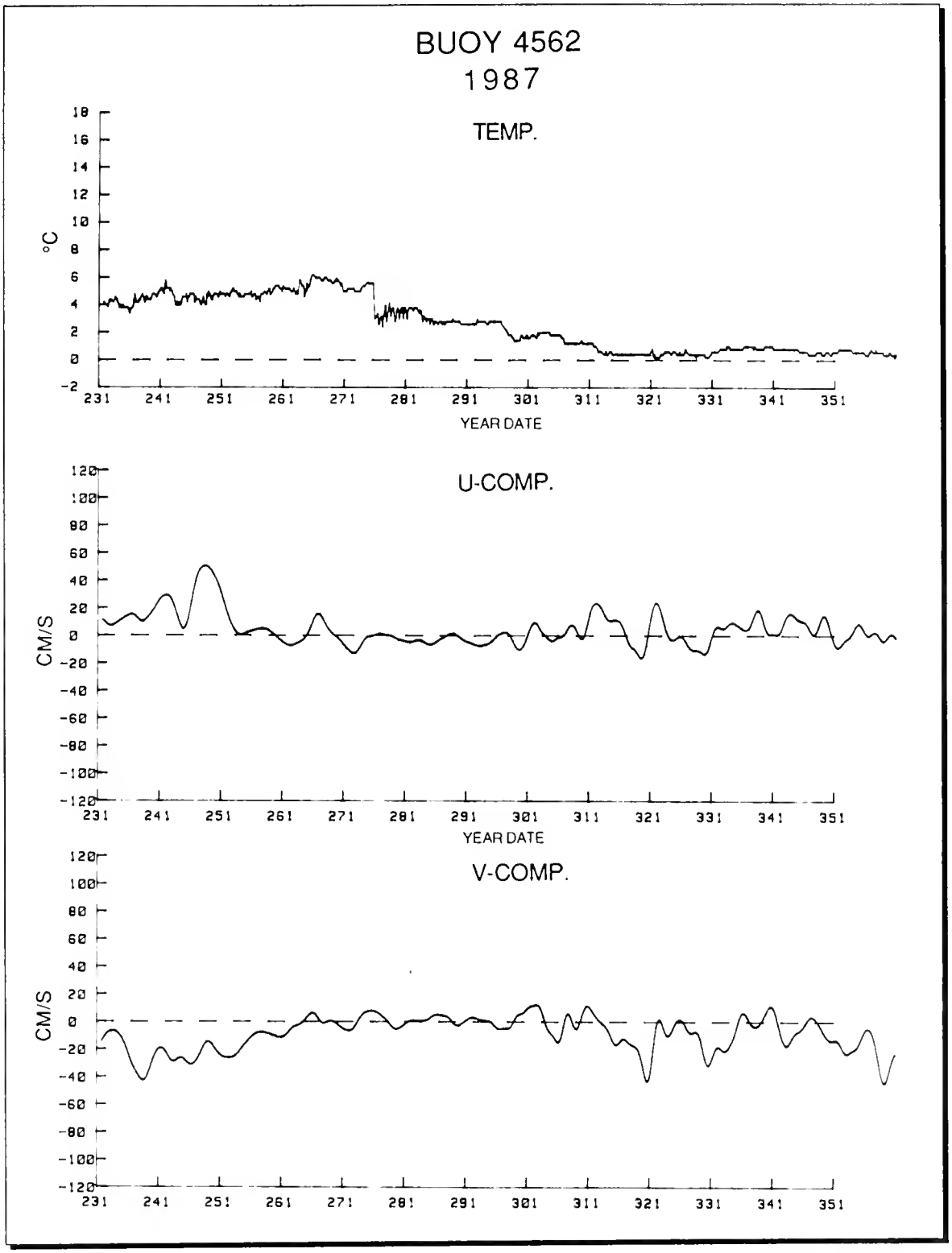

Figure C-20. Temperature, U and V velocity components for buoy 4562.

BUOY 4528

Buoy 4528 (Figure C-21, C-22) was deployed from an aircraft at 60-00N, 61-43W on 15 August (227), after the close of the 1987 iceberg season. Due to a data formatting error, no data regarding the status of the drogue were received from the ARGOS processing center. Buoy 4528 transmitted data throughout the remainder of 1987. It entered the Ice Patrol operations area on 13 October (286) when it crossed south of 52°N.

Buoy 4528 was deployed near the 200m isobath, which it then followed southward to approximately 55°N. Along this track, the buoy's speed varied over the range of 20-30 cm/s. However, there was one 5-day period (1-5 September, 244-248) during which it slowed to about 10 cm/s. This occurred between Saglek and Nain Banks, where the buoy made a small westward excursion. The temperature record during the period, between launch and 55°N, is unremarkable, with a slow increase from 1 to 6°C.

After passing south of 55°N (25 September, 268), 4528 followed the 1000 m isobath for the next 50 days, during which period it moved southward then eastward to a region directly north of Flemish Pass. During this period, the buoy's speed varied mostly over the range of 20-45 cm/s, with two brief periods of slower motion. The temperature record is remarkably constant during the southward motion, but when 4528 began its eastward motion (6 November, 310) the temperature increased rapidly from 3.5 to 6°C.

Buoy 4528 continued its eastward motion, moving to the north of Flemish Cap. Its subsequent motion is complex. First it moved around Flemish Cap, approximately following the 1000 m isobath. Then it apparently became entrained in the North Atlantic Current, as indicated by an abrupt eastward (2 December, 336) then northward motion. During the first part of the period the temperature increased slowly from 6 to 8.5°C, then during a 28-hour period (8-9 December, 342-343) the temperature increased by nearly 8°C. Over the same period the buoy's speed increased from 50 to 85 cm/s. This indicates that the buoy had entered a portion of the North Atlantic Current dominated by meanders and eddies.

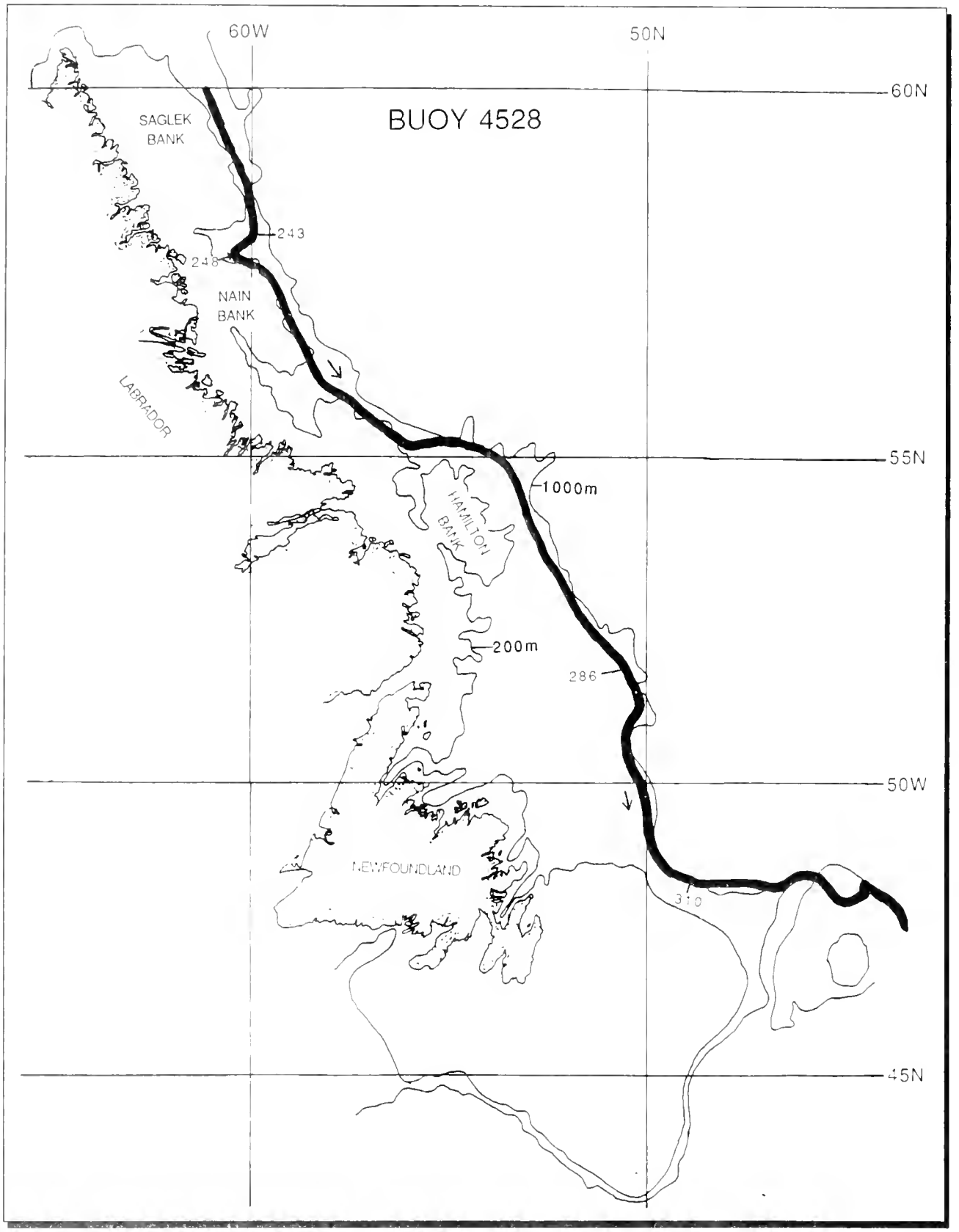

Figure C-21. Trajectory of Buoy 4528.

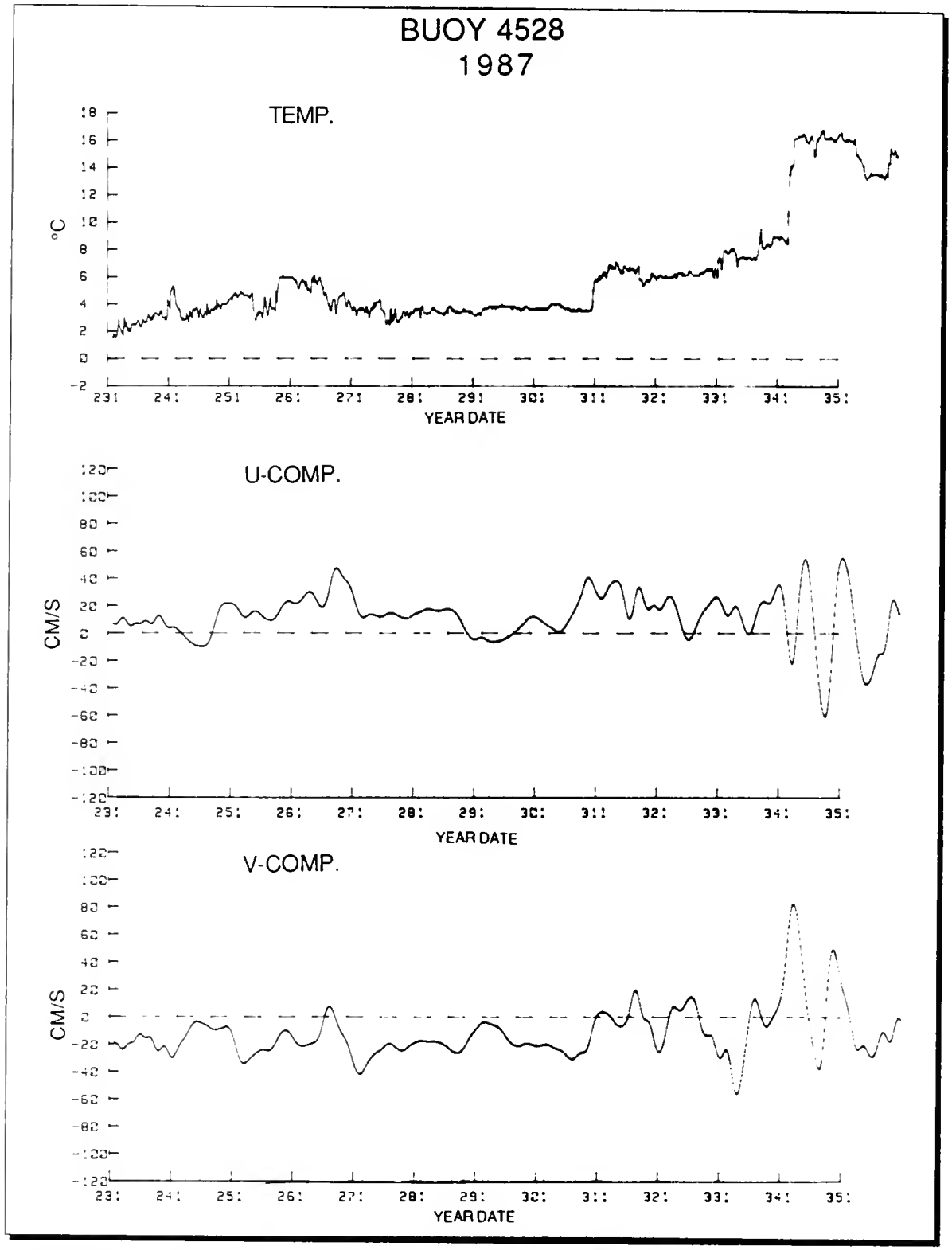

Figure C-22. Temperature, U and V velocity components for buoy 4528.

SUMMARY AND CONCLUSIONS

In 1987 the data return from the buoys was good. The average length of time that a buoy transmitted data from the Ice Patrol operations area was 78 days. According to the drogue sensor data, the average drogue life span was somewhat shorter (70 days), but its survival is well-matched to the requirement that it remain attached during the period the buoy drift is used for operations.

Most buoys transmit data far longer than the 78 days they spend in the Ice Patrol operations area. Five continued to transmit for the remainder of the calendar year. Three buoys were recovered before leaving the area, one by an Ice Patrol research vessel (for redeployment), and two by unknown vessels. Two buoys suffered premature failures, after 65 days and 67 days. It is possible that they were recovered by unknown vessels, but their fate remains uncertain.

The 1987 buoy program did an excellent job of monitoring the Labrador Current, particularly from Flemish Pass southward. The trajectories showed strong bathymetric steering of the current, with most buoys following the continental slope (200-1000 m) southward through Flemish Pass.

Substantial temporal variability in the Labrador Current is also evident in the data. Early in the iceberg season (April - May), two buoys (4555 and 4556) left the slope at 44° and moved rapidly to the east, north of a warm-core eddy at the shelf edge. A similar event occurred in 1986 (Anderson, 1986). Later in the season (July), the track of 4559 suggests that neither the eddy nor any North Atlantic Current meanders were significant factors in the southward movement of the Labrador Current along the slope. After departing Flemish Pass, buoy 4559 moved to the region south of Tail of the Bank (41-50N) in 14 days. This is the most dangerous flow pattern in terms of icebergs moving into the North Atlantic shipping lanes. However, it occurred in July when no icebergs were moving southward through Flemish Pass. Had Ice Patrol relied solely on its historical current data base, which is based on many years of hydrographic data and is time-invarient (Murray, 1979), there would have been no recognition of this observed temporal variability of the Labrador Current.

The 1987 drifting buoy data suggest that the Labrador Current speeds in Ice Patrol historical current data base for the region south of Flemish Pass are too high. [During the iceberg season IIP operations center personnel had to reposition many resighted icebergs upstream from where the drift model had predicted.]

Six buoys passed southward through Flemish Pass, three of which continued their southward movement along the continental slope well south of the pass. In the data base, typical Labrador Current speeds in the area along the slope from 44-46°N are 90-110 cm/s. None of the 1987 buoys recorded speeds as high as this, even for short periods (3 hr). Buoy 4559, which moved from the pass the the Tail of the Bank, recorded the highest speeds, but most were in the 40-60 cm/s range. Ice Patrol has undertaken a program that will make use of all available drifter data to investigate the accuracy of its historical data base. In the regions where sufficient data exist, the data base will be modified to reflect these observations.

No current data were collected on the Grand Bank or in the inshore branch of the Labrador Current in 1987. The distribution of icebergs for this year shows that this is a problem that needs to be addressed. Many icebergs were sighted along the Newfoundland Coast and directly south of the island, a region where the Ice Patrol data base is particularly poor. Little attention has been given to this region. A new generation of smaller, less expensive satellite-tracked buoys is now available. Ice Patrol has been evaluating these buoys and expects to integrate them into the buoy program within the next few years. They will be particularly

useful on the continental shelf and in the near-shore areas where there is a greater risk of unauthorized recovery. They are smaller, more difficult to see, and less of a financial loss when they are recovered by unknown vessels.

REFERENCES

Anderson, I, 1986. TIROS Oceanographic Drifter Tracks on the Grand Banks During the 1986 International Ice Patrol Season. Appendix B, *Report of the International Ice Patrol in the North Atlantic Ocean , Season of 1986, (CG-188-41), Bulletin No. 72.* International Ice Patrol, Avery Point, Groton, CT 06340-6096, U.S.A.

Le Tran, P.Y. and R. Liaubet, 1987. Location: Matching Service To User Needs ARGOS Newsletter No. 30, July 1987. Service ARGOS Inc., 1801 McCormick Drive, Suite 10, Landover, MD 20785 (USA).

Murray, J.J., 1979. Oceanographic Conditions. Appendix B, *Report of the International Ice Patrol Service in the North Atlantic Ocean, Season of 1979 (CG-188-34), Bulletin No. 65.* International Ice Patrol, Avery Point, Groton, CT 06340-6096, U.S.A.

Murphy, D.L., I. Anderson, and N.B. Thayer, 1986. Observations of an Oceanic Front South of Flemish Pass. Appendix C, *Report of the International Ice Patrol in the North Atlantic Ocean, Season of 1986 (CG-188-41), Bulletin No. 72* . International Ice Patrol, Avery Point, Groton, CT 06340-6096, U.S.A.

Summy, A.D.; "Oceanographic Conditions on the Grand Banks During the 1982 Ice Patrol Season"; Appendix B, *Report of the International Ice Patrol Service in the North Atlantic, Season of 1982 (CG-188-37) Bulletin No. 68.* International Ice Patrol, Avery Point, Groton, CT 06340-6096, U.S.A.

Summy, A.D. and I. Anderson; "Operational Uses of TIROS Oceanographic Drifters by International Ice Patrol (1978 - 1982)", *Proceedings 1983 Symposium on Buoy Technology*, Marine Technology Society, Gulf Coast Section, pp. 246-250.

Appendix D

Observations of a Warm-Core Eddy Near the Grand Banks of Newfoundland

Donald L. Murphy

INTRODUCTION

In April - May 1987, the International Ice Patrol conducted a surface hydrographic and remote sensing study of a warm core eddy near the eastern edge of the Grand Banks of Newfoundland (Figure D-1). The surface vessel was USCGC BITTERSWEET (WLB 389). The primary objective of the study was to improve Ice Patrol's ability to interpret images of the ocean's surface made with its side-looking airborne radar (SLAR).

Imaging radars map the sea surface roughness primarily through Bragg scattering (Robinson, 1985), which for the 3 cm wavelength and incidence angles (45° to 87°) of the Ice Patrol SLAR, results in a sensitivity to wavelengths of 2 cm. These waves are in the capillary-gravity part of the spectrum, thus they are influenced by molecular viscosity, which is a function of sea surface temperature and salinity. The physics of radar returns from the sea surface is receiving increased research attention (see for example, Phillips, 1988 and Donelan and Pierson, 1987) mostly because radar is used to measure oceanic wind distributions. Ice Patrol is interested in using radar images of the sea surface to map the major water-mass boundaries within its operations area.

A previous study (Murphy et al, 1986 and Thayer and Murphy, 1987) showed that the SLAR mapped the location of sharp surface thermal gradients that marked the boundary between a warm-core eddy and the Labrador Current. They found that the warm surface-water within the eddy was always marked by a stronger radar return than the surrounding cooler water. However, they were unable to map the entire boundary around the eddy. A likely explanation of this observation is that their flight patterns permitted only two look angles (with respect to the wind) at the eddy boundary and these were reciprocals of each other. This means that along some portions of the eddy's boundary, the radar was looking along the Bragg wave field rather than into it. This reduces the intensity of the radar return from within the eddy and makes the location of the thermal front difficult to determine.

One of the goals of the 1987 experiment was to improve on the previous experimental design by including four look angles at the eddy in hopes of defining the entire boundary of the feature. In addition, the 1987 experiment provided an opportunity to conduct the surveys under different environmental conditions than those encountered in 1986.

The intent of this report is to describe the experiment that was conducted in 1987 and to present some of the preliminary results. None of the SLAR data are available for presentation at this time, but a portion of the surface-truth data is. This presentation, made before a thorough analysis is completed, is nonetheless worthwhile because it helps understand the oceanographic conditions in the Ice Patrol operations area during 1987. The eddy studied during IIP-87-1 dominated the circulation near the southeastern edge of the Grand Banks early in the season

OBSERVATIONAL PROGRAM

The study site was chosen prior to BITTERSWEET's departure from port based on a satellite infrared image obtained from the National Marine Fisheries Service (NMFS) laboratory at Narragansett, Rhode Island. It showed a warm-core eddy near the eastern slope of the Grand Bank at about 44°N. In addition, data from Ice Patrol operational drifting buoys showed apparent eastward movement in the Labrador Current north of the eddy. Hence, the region had waters of the cold and relatively fresh (< 2°C and < 34.3 ppt) Labrador Current and the warm and more saline (> 12°C and > 35.5 ppt) North Atlantic Current in close proximity. The substantial surface temperature gradients presented a good location to test the SLAR.

Hydrographic Survey

The hydrographic survey was divided into two phases, the first during 5-10 May and the second from 16-20 May. The objective was to survey the eddy and its surroundings twice, in an attempt to describe the evolution of the feature over the entire three-week

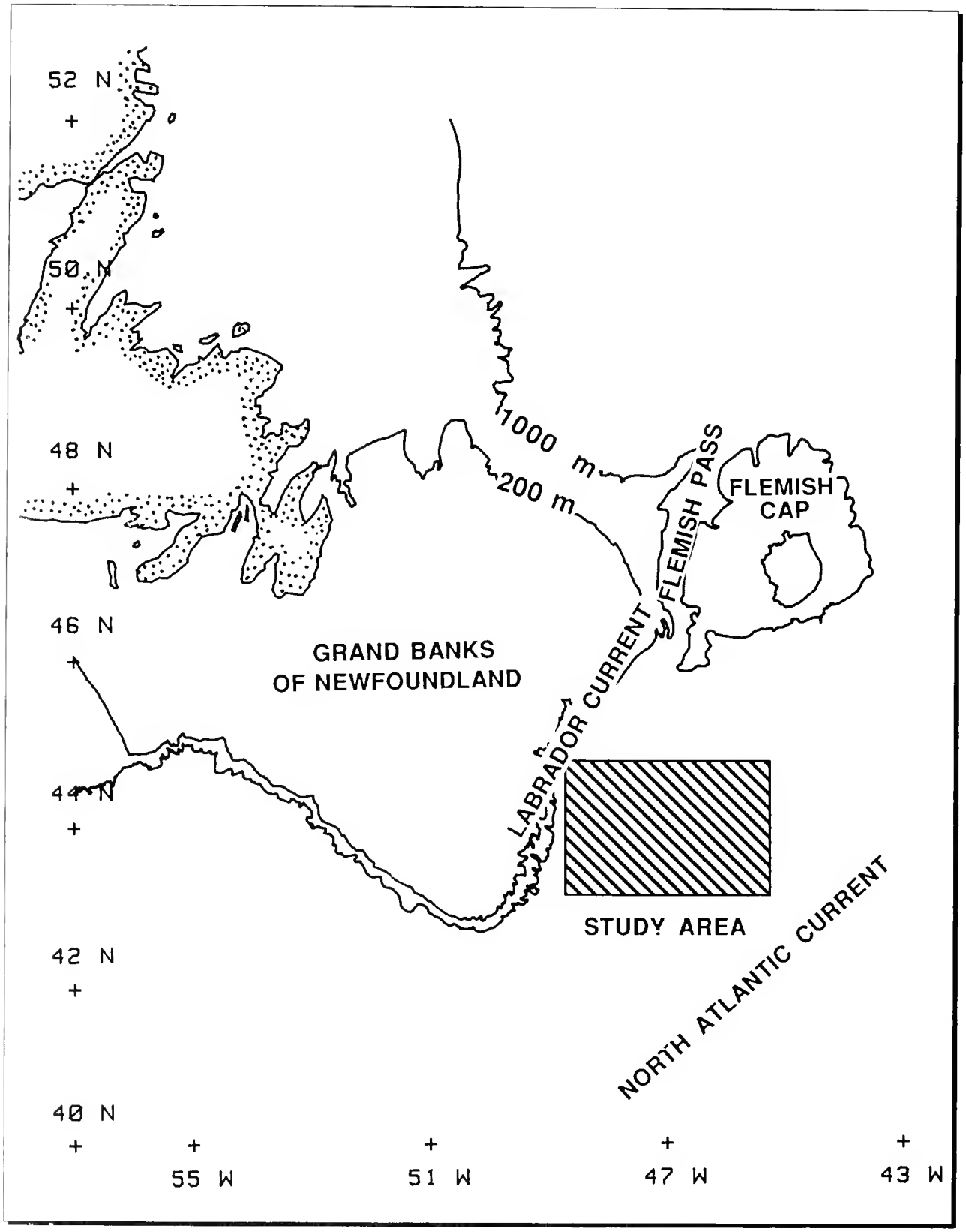

Figure D-1. Schematic of the major current systems near the Grand Banks of Newfoundland. The study area is shown by the shaded rectangle.

study period. In particular, a knowledge of the movement of the thermal fronts over the period of the SLAR surveys is essential when the images are compared to the surface data. The length of each hydrographic phase was limited to no more than 6 days due to the short endurance of the survey vessel.

Phase one consisted of 50 CTD (conductivity, temperature, and depth) stations and 70 XBT stations. This phase consisted of six hydrographic lines, four oriented north-south and two east-west, and one XBT line, a diagonal. The CTD station spacing along the hydrographic lines was 18 km (10 nm), with an XBT cast taken half way between the CTD stations. The station spacing along the XBT line was 9 km (5 nm).

The CTD casts were taken to about 1000 m or to within 50 m of the bottom at stations shallower than 1000 m. To verify CTD results, deep quality control samples were taken at most stations using a Nansen bottle with reversing thermometers. XBT stations were made with T-4 XBT's, which provide a temperature profile to 450 m.

High winds and seas further constricted the time available for sampling during phase two. BITTERSWEET was unable to complete the originally-planned 45 station star pattern, and completed 38 CTD stations and 48 XBT deployments. As in phase one, CTD station spacing was 18 km (10 nm) and XBT casts were conducted about halfway between the CTD stations.

This research cruise marked the first operational use of Ice Patrol's Mobile Oceanography Laboratory (MOL). BITTERSWEET is a buoy tender with no special equipment for oceanographic sampling, thus all sampling and analysis equipment had to be brought aboard for the cruise and removed after its completion.

The MOL consists of a 4.2 X 2.4 X 2.4 m (14 X 8 X 8 ft) steel shipping container, which was attached to brackets welded to BITTERSWEET's buoy deck. The interior of the MOL is fitted with desks and equipment racks containing the computers that retrieve and store data from the CTD and XBT systems, as well as a global positioning system (GPS) receiver.

An electrically-powered, portable oceanographic winch with about 2000 m of 1/4" (0.6 cm) armored hydrographic cable was chained to the buoy deck. The final component of the sampling system was a portable hydrographic platform with a hydraulically operated A-frame, which was placed in the buoy port. All of this equipment can be installed in one day and removed in about four hours.

Drifting Buoys

The drifts of satellite-tracked buoys were used to determine the current speed and direction in the study area. The buoys were 3 meter long spars with a 2 X 10 meter window-shade drogue attached at the end of a 50 meter tether. The accuracy of the position data is about 350 m. The buoys were fitted with temperature sensors (accuracy ~ 1°C) mounted approximately 1 m below the buoy's waterline. Each buoy received about 8 fixes per day.

Eight drift tracks are used for this study. Of these, two are from operational buoys deployed in the Labrador Current well north of the study area by Ice Patrol's reconnaissance aircraft (HC-130). They moved southward along the eastern edge of the Grand Banks (Murphy and Thayer, 1987) and passed through the study area shortly before BITTERSWEET arrived on scene. The remaining drift tracks are from buoys deployed from BITTERSWEET, most of which were recovered after the experiment concluded.

SLAR Surveys

Four SLAR surveys, on 2, 6, 14 and 20 May, mapped the features in the study area. On two dates (15, 18 May) portions of the study area were mapped during routine iceberg patrols. The Ice Patrol SLAR is an X-band (3 cm wavelength), real-aperture radar that produces a continuous 9" (23 cm) analog image on film. When the

aircraft is flown at 8000 ft (2440 m), the radar maps a 50 km wide swath on each side of the aircraft with a blind spot 5 km wide directly under the aircraft. Both antennas are vertically polarized.

Several different flight patterns were used during the survey. The intent of the various patterns was to obtain several different directions of look relative to the wind, in addition to looking at the thermal fronts from various ranges.

RESULTS

The following sections describe some of the data that constitute the surface-truth for the SLAR interpretation experiment. The radar data are currently being analyzed. The surface-truth data presented here are limited to the first phase because it is the more complete of the two data sets and the first to be analyzed.

Hydrography

Figure D-2 shows the surface temperature on the first phase hydrography. A small, warm-core eddy, centered at 43-50N, 48-20W and with a diameter of about 65 km dominates the temperature field in survey area. North of the eddy is cold water (< 3°C) of Labrador Current origin, while warm water (> 12°C) from the North Atlantic Current is evident in the southeastern part of the study area. Although it appears from the surface temperature distribution that the eddy was separate from the North Atlantic Current, their proximity makes it likely that they were interacting.

The greatest surface temperature gradient, about 8°C, is located at the northern boundary between the eddy and the Labrador Current. Over an 18 km distance, the surface temperature changes from less than 3°C to greater than 10°C. It is in this region that the SLAR is most likely to detect a difference in radar return.

A vertical temperature section (Figure D-3) along the center of the 5 north-south transects (A-B on Figure D-2) shows that the 10°C isotherm extends to about 160 m. It also shows the locations where three of the drifting buoys were deployed. Buoy 4536 was deployed in 13°C water near the center of the eddy. Buoy 4547 was deployed in 3-4°C water north of the eddy. Finally, buoy 4511 was deployed near the eddy's northern edge. The center of the drogues for all of the buoys is at ~ 58 m.

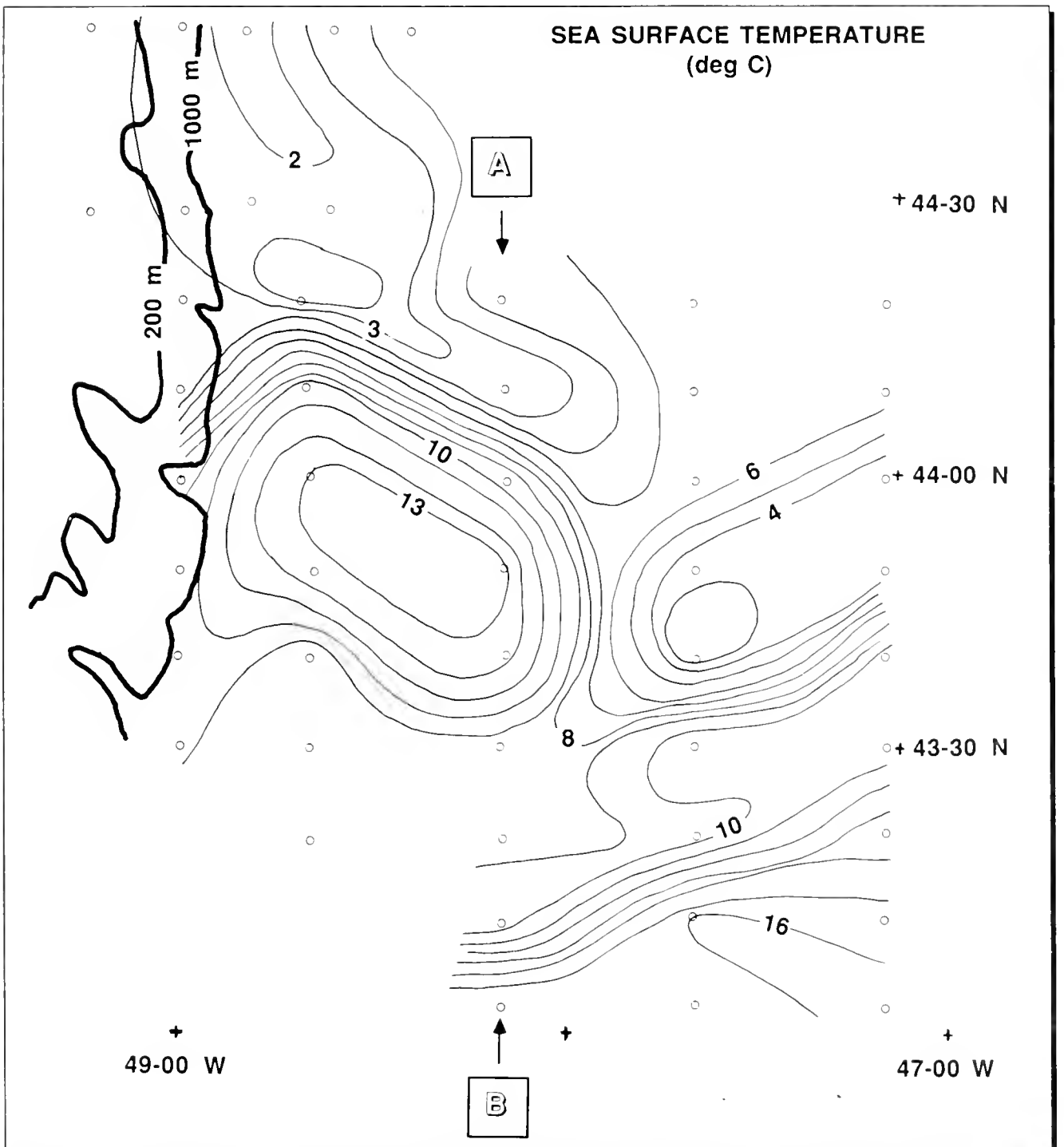

Figure D-2. Distribution of sea surface temperature based on the first phase (5-10 May) hydrographic survey.

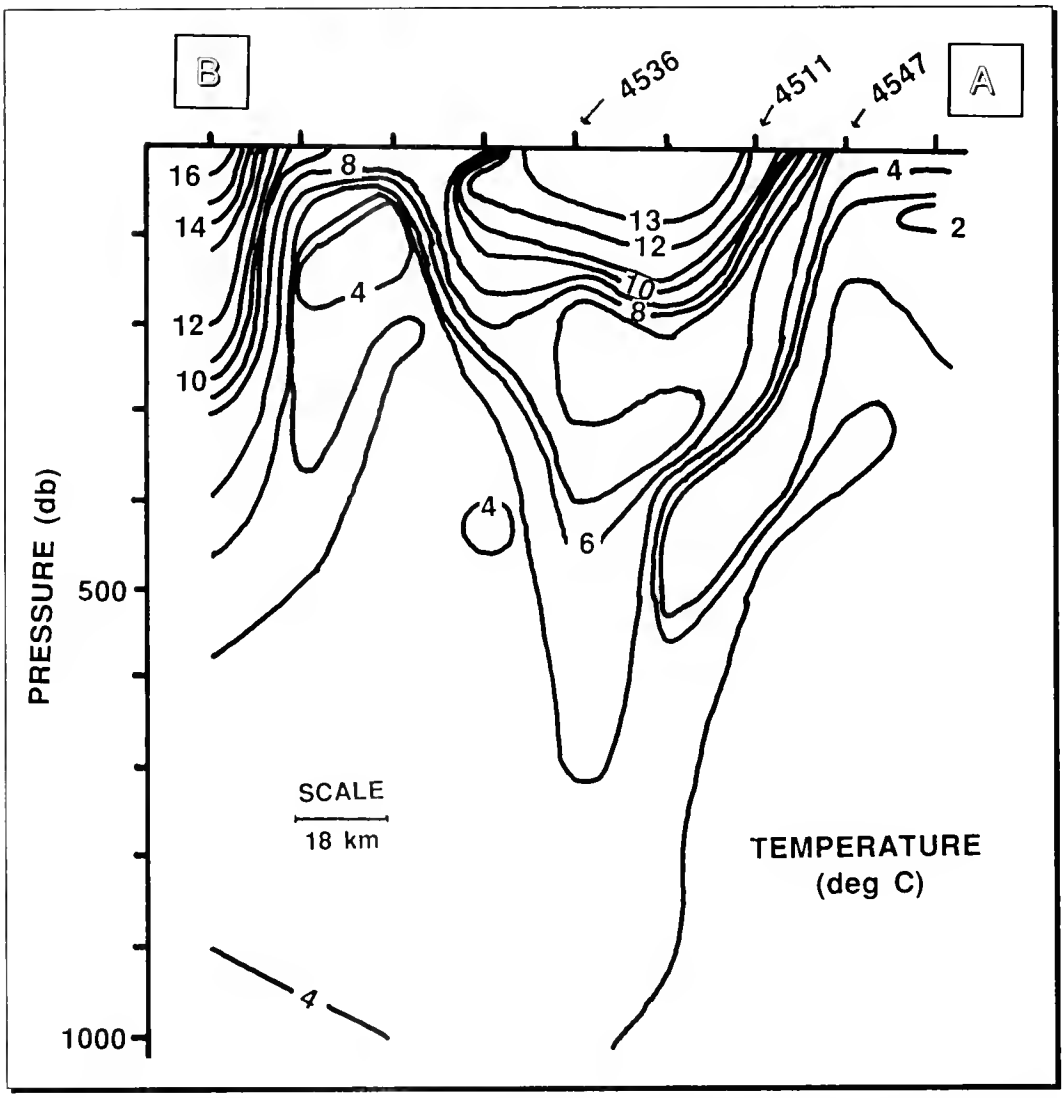

Figure D-3. Vertical distribution of temperature along transect marked A-B in Figure D-2.

Drifters

The drifter data are presented in two plots. The first (Figure D-4) presents trajectories of 4555 and 4556, both of which were Ice Patrol operational drifters deployed in the Labrador Current north of Flemish Pass.

Buoy 4555 arrived in the study area on 20 April, approximately two weeks before the start of the hydrographic survey. Over the next 6 days it traced an anticyclonic path approximately one-half the way around the eddy's boundary. The buoy speeds over this period varied over the range of 50-70 cm/s, while the temperature varied over the range from 0.8 to 13°C, suggesting that the buoy was close to the eddy's boundary.

On 30 April, 4556 entered the study area. Like 4555, buoy 4556 moved rapidly (50-70 cm/s) to the east, north of the eddy. However, buoy 4556's temperature record was quite different, with a slow increase from 0.6 to 2.0°C over the period during which it remained in the area.

Figure D-5 presents the drifter data from the four buoys deployed by BITTERSWEET. They are plotted on a map of the surface dynamic topography (relative to 1000 db) calculated from the first phase (5-10 May) hydrographic survey. The buoy tracks are for the same period as the survey.

Both the dynamic topography and 4536's drift track suggest that the eddy was interacting with the North Atlantic Current. Buoy 4556 did not complete one entire circuit around the eddy before it departed to the east and left the study area.

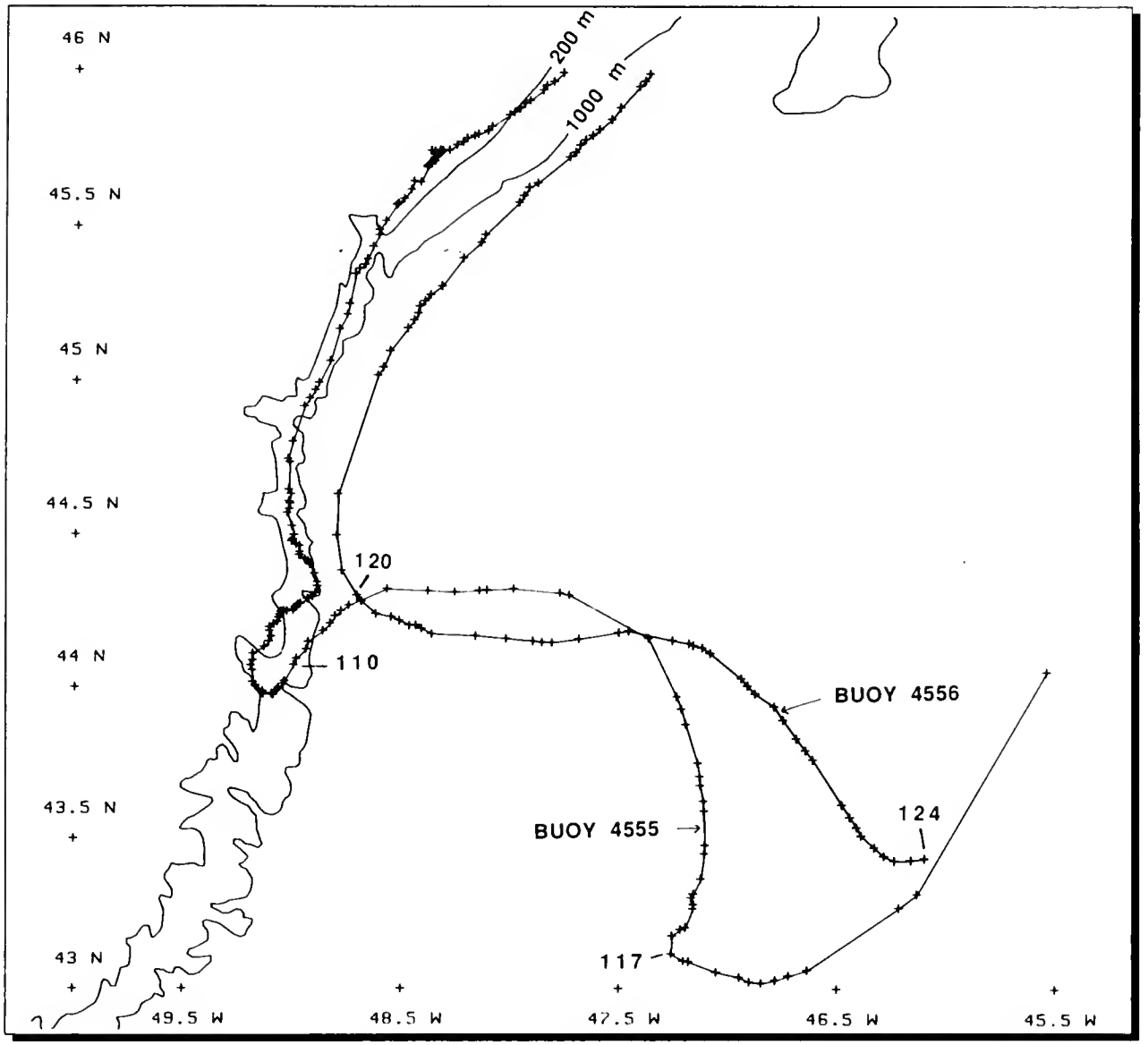

Figure D-4 Trajectories of 4555 and 4556, both of which were deployed north of Flemish Pass.

The track of 4547 is remarkable in that shortly after deployment it moved southward and eventually intersected the path of 4511. The drifter tracks are in general agreement with the surface dynamic topography.

CONCLUSIONS

The data presented here show a small, warm-core eddy centered at 43-50N, 48-20W and interacting with the North Atlantic Current. Although the detailed dynamics of the eddy cannot be resolved by the coarse sampling scheme, its effect on the Labrador Current is clear. During the period that the eddy was close to the continental slope (April-May), a portion of the Labrador Current departed the slope and moved to the east at about 44°N.

The tracks of 4555 and 4556, which were deployed in the Labrador Current but moved eastward off the slope at 44°N, are consistent with the existence of an eddy at this location. The eddy had a major influence on the Labrador Current as early as 20 April, and perhaps before.

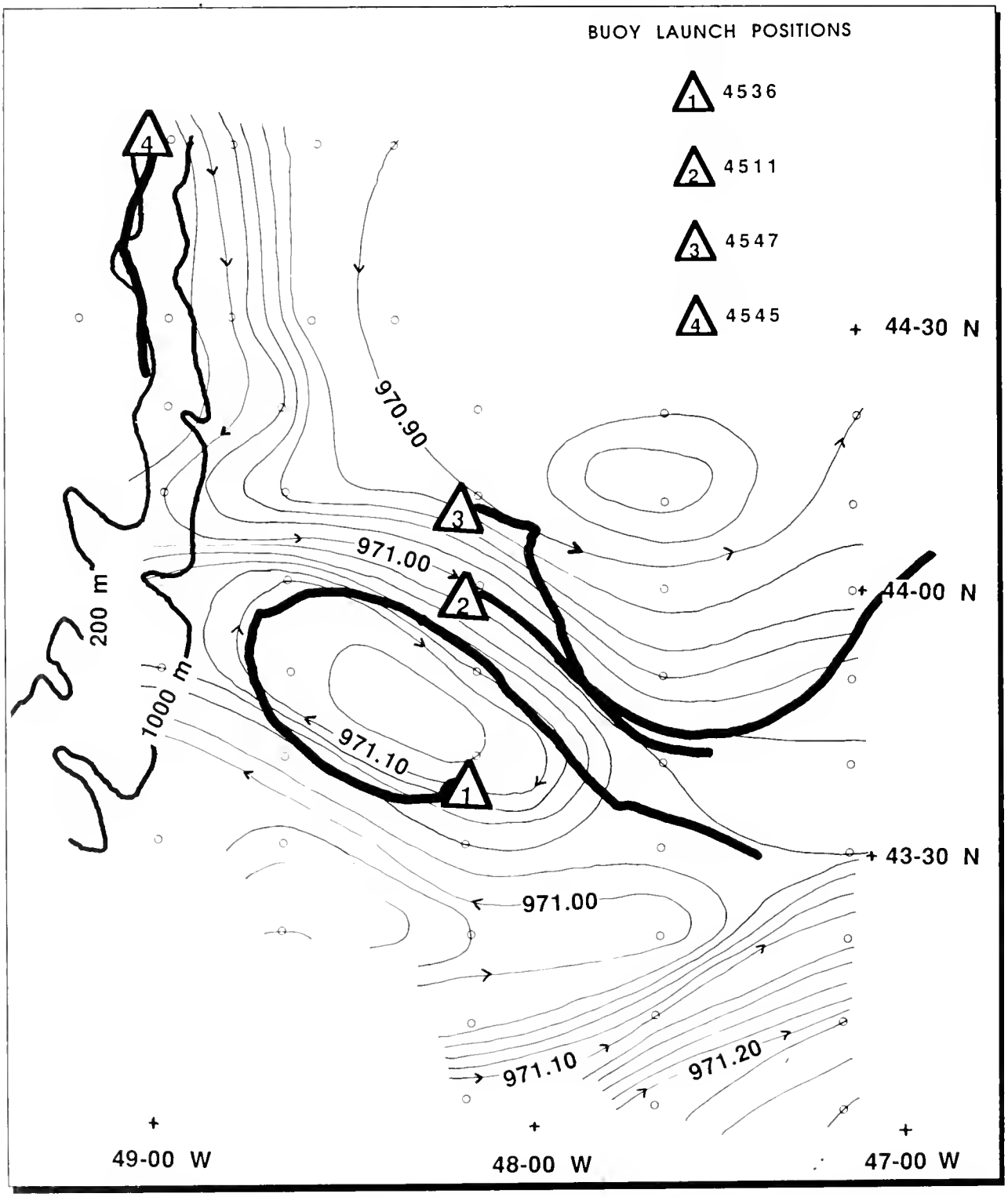

Figure D-5. Trajectories of four buoys (4511, 4536, 4545, and 4547) plotted on a map of the surface dynamic topography (with respect to 1000db) based on the first phase hydrographic survey.

ACKNOWLEDGEMENTS

Sincere appreciation is extended to the Marine Science Technicians of International Ice Patrol who collected and are currently analyzing the data from the experiment described herein. Without their efforts this work could not have been accomplished.

The officers and crews of USCGC BITTERSWEET (WLB 389) and CG 1503 and CG 1504, both of Coast Guard Air Station Elizabeth City, North Carolina enthusiastically supported Ice Patrol's research. Their efforts are greatly appreciated.

REFERENCES

Donelan, M. A. and W. J. Pierson, Jr., 1987. Radar Scattering and Equilibrium Ranges on Wind-Generated Waves With Application To Scatterometry. *Journal of Geophysical Research*, Vol 92 (C5): 4971-5029.

Murphy, D. L., I. Anderson, and N. B. Thayer, 1986. Observations of an Oceanic Front South of Flemish Pass. Appendix C, *Report of the International Ice Patrol in the North Atlantic Ocean, Season of 1986 (CG-188-41), Bulletin No. 72.* International Ice Patrol, Avery Point, Groton, Connecticut 06340 U.S.A.

Murphy, D. L. and N. B. Thayer, 1987. 1987 International Ice Patrol Drifting Buoy Program. Appendix C, *Report of the International Ice Patrol in the North Atlantic Ocean, Season of 1987 (CG-188-42), Bulletin No. 73.* International Ice Patrol, Avery Point, Groton, Connecticut 06340 U. S. A.

Phillips, O. M., 1988. Radar Returns From The Sea Surface - Bragg Scattering And Breaking Waves. *Journal of Physical Oceanography*, Vol 18: 1065-1074.

Thayer, N. B. and D. L. Murphy, 1988. SLAR Observations of Ocean Fronts East of the Grand Banks of Newfoundland. Proceedings of the 11th Canadian Symposium on Remote Sensing, University of Waterloo, Waterloo, Ontario, Canada N2L 3G1. (In press).

Robinson, I. S., 1985. *Satellite Oceanography: An Introduction for Oceanographers and Remote Sensing Scientists.* West Sussex, England: Horwood Limited. 455 pp.

Appendix E

Operational Forecasting Concerns Regarding Iceberg Deterioration

LCDR Walter E. Hanson Jr., USCG

INTRODUCTION

Since 1971, the International Ice Patrol (IIP) has used computer-based drift prediction models to help evaluate the extent of the iceberg danger to North Atlantic shipping in the vicinity of the Grand Banks of Newfoundland. A dynamic model began operational use in 1979 (Mountain, 1980). This model, along with a parametric iceberg deterioration model which began operational use in 1983 (Anderson, 1983), has grown in importance as iceberg reconnaissance has gone to an every other week schedule. During the peak of the iceberg season, April through June, the iceberg danger covers a large area, requiring reconnaissance missions to concentrate on patrolling the limits. Often icebergs go several weeks before being resighted. Resighting icebergs depends heavily on these models effectively predicting drift and deterioration rates. These predictions are also routinely used to set the limit of all known ice, as reported in the IIP bulletins.

As evidenced by the many years of safe passage by trans-Atlantic shipping, the IIP seems to have some skill in determining the extent of the ice danger. (To assess the model's predictions there is a need for accurate data to represent the initial iceberg, interim iceberg, and environmental conditions.) Iceberg drift prediction is highly dependent upon iceberg mass (size and shape). Consequently, the ability to accurately predict changes in iceberg size for the majority of icebergs, which are infrequently resighted, becomes very important.

Between 1983 and 1985, the IIP studied the drift and deterioration of four icebergs. Although no firm conclusions could be drawn from such a small data set, which represented an average drift of 4.5 days, the prediction models did fairly well hindcasting the drift and deterioration when observations were used as inputs (Anderson, 1985). A similar study was performed, using U. S. Coast Guard iceberg data, for the Atmospheric Environment Service of Canada (El-Tahan et al, 1987). The results were mixed. Thus in June 1987, the IIP conducted another cruise to collect similar data for a cluster of icebergs.

The objectives of this study were to compare iceberg deterioration predictions derived from environmental data collected in situ to inputs available from operational data centers. These latter inputs were divided between global and regional scale products.

BACKGROUND

The iceberg deterioration model used by the IIP provides its watch officers with a daily estimate of the "melt" status of each iceberg entered in the drift model. The computer-based application (Anderson, 1983), which computes the melt rate, is derived from White, et al 1980. The model sums the effects of the following processes which are depicted in order of importance in Figure E-1:

- solar radiation;
- buoyant heat convection;
- heat convection caused by iceberg movement relative to the water mass (forced heat convection); and
- waterline wave erosion, followed by calving of the resultant ice overhang.

Based on the 1980 report, warm air heat convection is considered insignificant and not calculated. The report also identified other iceberg deterioration processes; however, they were only partially addressed and difficult to quantify. Consequently those processes are not modelled.

The model calculates melt in terms of length instead of mass. This measure of melt accommodates IIP's operational procedures, in which nearly all iceberg dimensions are reported by size categories. These categories are based primarily on the maximum observed length of the iceberg.

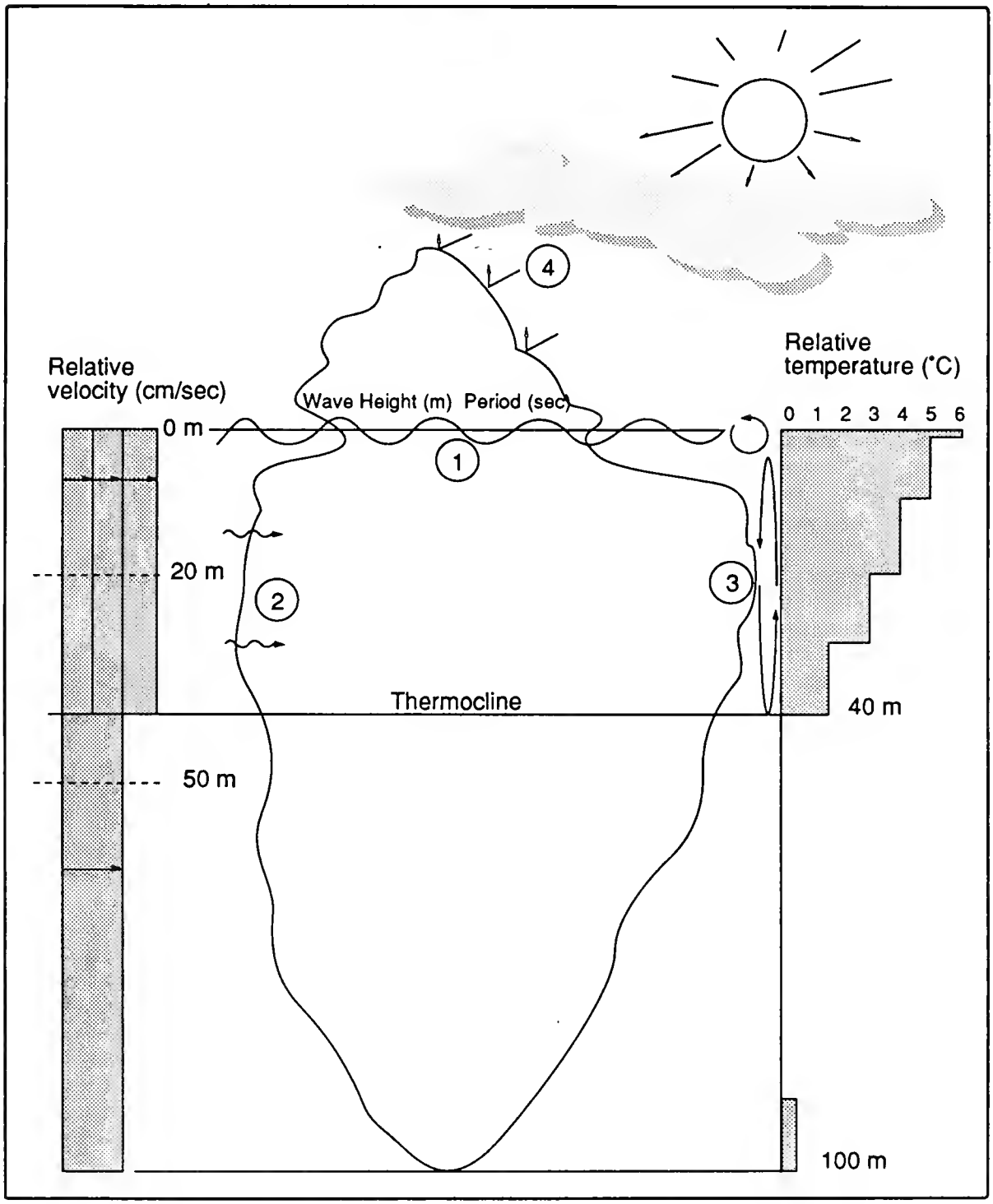

Figure E-1. Modelled Iceberg Deterioration Processes. This figure depicts four processes used by the IIP deterioration model to "melt" icebergs. The four processes, which are labelled in order of importance are: (1) wave erosion; (2) forced heat convection; (3) buoyant heat convection; and (4) solar radiation. The figure also identifies the variable environmental terms used to model each process and their influence on "melt" for the icebergs studied by IIP. These terms are: relative velocity; wave height; wave period; and relative temperature. Other terms used to model iceberg "melt" are: cloud cover, which is constant; and maximum waterline length of the iceberg.

1987 DATA COLLECTION EFFORT

This study collected data on six medium to small icebergs for a period ranging from 2.1 to 6.3 days. The icebergs were studied as they drifted south with the Labrador Current on the northeast Newfoundland Shelf (centered around position 50-45°N, 53-30°W); see Figure E-2. The study was conducted between 15 and 21 June 1987 using the USCGC TAMAROA, a 68m (205 ft) U. S. Coast Guard cutter.

Iceberg above water dimensions were taken during daylight using a camera and reticulated laser rangefinder. Iceberg shape and size were calculated from photographic images scaled according to rangefinder measurements. This required a 360 degree look at each iceberg; measuring and photographing all prominent faces. Measurements were accurate to +/- 8% of the observed dimensions. No underwater iceberg dimensions were measured.

The rangefinder-derived distances were used with visual bearings to fix the icebergs' positions during daylight. At night, radar bearings and ranges were used. The cutter used LORAN-C and SATNAV to fix its position. Positional accuracy for iceberg positions was estimated (by summing system errors) to be +/- 750m. Table E-1 summarizes the observed dimensions and estimated drift of the icebergs.

Hourly environmental observations included: air and sea surface temperature, cloud cover, and wind (at 22.3m). Sea surface temperature was taken by bucket thermometer (error was +/- 0.1°C); wind was measured by the ship's anemometer. Wave height, period and direction were visually estimated every six hours. Visual wave observations were estimated to have an error of +/- 0.5m for wave height; and +/- 2sec for period. Surface currents were inferred from the drift of two satellite-tracked drifters (FGGE-hulled), which had window-shade (2m X 10m) drogues. Both drifters were deployed at the same time near the center of the cluster. One was drogued near the surface (center of the drogue: 8m deep), while the other was drogued at 58m, at the core of the Labrador Current. Temperature vs. depth profiles were taken in the vicinity of each iceberg and transects were made at the beginning and end of the study to determine iceberg drift in relation to the

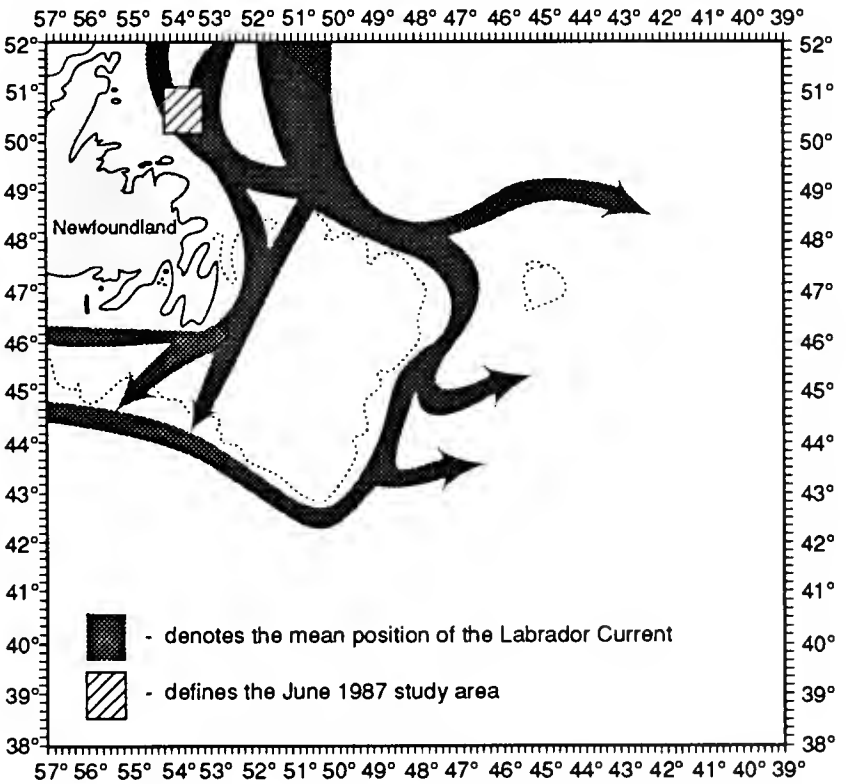

Figure E-2. International Ice Patrol Study Area. This figure depicts the area in which iceberg drift and deterioration is operationally modelled by IIP. The 200m bathymetric contour is shown to describe the Grand Banks of Newfoundland and Flemish Cap.

Table E-1: Observed Size, Shape, and Estimated Drift of Icebergs.

Elapsed Days	Maximum Dimensions (in meters) Length	Height	Shape	Interpolated 12-hourly Speed (cm/sec)	Direction (T)
Berg #620					
0.0	43	11	Wedged		
0.6				19	231
0.9	41	10	Pinnacled		
1.1				18	201
1.6				22	209
1.7	36	11	Domed		
2.1				35	186
2.6				45	171
2.9	41	12	Pinnacled		
3.1				32	165
3.6				46	193
4.0	52	27	Pinnacled		
4.1				38	192
4.6				24	127
4.8	58	7	Pinnacled		
Berg #744					
0.0	32	7	Domed		
0.1				6	295
0.6				20	295
0.8	77	18	Pinnacled		
1.1				8	229
1.6				37	140
2.0	55	16	Pinnacled		
2.1				45	138

Table E-1 (Continued).

Elapsed Days	Maximum Dimensions (in meters) Length	Height	Shape	Interpolated 12-hourly Speed (cm/sec)	Direction (T)
Berg #747					
0.0	114	24	Wedged		
0.9	70	24	Wedged		
1.0				16	234
1.5				13	183
1.7	96	25	Wedged		
2.0				18	163
2.5				33	150
2.9	86	28	Pinnacled		
3.0				41	146
3.5				32	154
4.0				25	173
4.5				23	142
4.7	115	22	Pinnacled		
5.0				21	107
5.5				6	065
6.0	96	23	Pinnacled	14	118
6.3	86	27	Pinnacled		
6.5				33	131
Berg #784					
0.0	89	31	Pinnacled		
0.8				23	121
1.0	110	49	Pinnacled		
1.3				28	153
1.8				36	166
2.0	107	43	Pinnacled		
2.3				44	168
2.8				38	178
3.0	112	24	Pinnacled		
3.3				35	182
3.8	117	43	Pinnacled	21	185
4.3				4	147
4.8				9	274
4.9	113	33	Pinnacled		
5.3				3	275

Table E-1 (Continued).

Elapsed Days	Maximum Dimensions (in meters) Length	Height	Shape	Interpolated 12-hourly Speed (cm/sec)	Direction (T)
0.0	97	37	Pinnacled		
0.4				26	355
0.8	94	32	Drydock		
0.9				12	293
1.4				21	191
1.9	92	30	Drydock	35	169
2.4				37	143
2.8	84	25	Drydock		
2.9				43	136
3.4				31	145
3.9				15	164
4.4				11	182
4.8	71	7	Domed		
4.9				15	164
Berg #787					
0.0	81	34	Pinnacled		
0.3				49	169
0.8				52	194
1.1	75	23	Pinnacled		
1.3				34	192
1.6	57	25	Pinnacled		
1.8				22	208
2.3				10	250
2.8				8	152
3.1	59	23	Pinnacled		
3.3				21	308

Labrador Current. The measurements were made to a depth of about 300m using T-4 eXpendable BathyThermographs (XBT).

Having only one observation platform to monitor the drift and deterioration of six icebergs, which were within a circle of approximately 55km radius, made both compiling environmental factors affecting each iceberg and verifying iceberg identity difficult. The distance between the cutter and each iceberg determined the applicability of environmental observations. Table E-2 summarizes the distances between observations and icebergs. The average distance wave data were collected from each iceberg was 48km; wind and weather data, 61km; and sea temperature data, 7km. These distances were computed from the interpolated positions of each iceberg for 0000Z and 1200Z as derived from a cubic spline.

The spatial separation of the wind and wave observations is much smaller than the 250km data grid-spacing on which global environmental products are prepared by FLENUMOCEANCEN for IIP use (COMNAVOCEANCOM, 1986). Because the study area was at least 105km offshore, the wind and wave fields were assumed to be spatially uniform.

In mapping the sea surface temperature, the icebergs were in a tongue-like feature of cold water which protruded southeastward. The feature, which measured about 18km across, complicated the data analysis, since the temperature field could not be assumed uniform. As a compromise, only observations within 9km of an iceberg's position were accepted. Because of this restriction and having only one observation platform, the data sets for some icebergs were incomplete. The temperature values necessary to model deterioration were linearly interpolated from these data sets.

Table E-2: Distance of Observations from Individual Icebergs.

Type of Data Collected		Distance (in km) From Iceberg		
	Wind	Min	Max	Avg
Berg#	620	3	104	49
	744	9	71	45
	747	9	121	69
	784	1	136	60
	785	1	111	52
	787	13	103	49
	Sea Surface Temperature	Min	Max	Avg
Berg#	620	3	15	7
	744	3	14	9
	747	1	11	7
	784	0	16	9
	785	1	7	4
	787	4	9	6
	Wave	Min	Max	Avg
Berg#	620	14	53	31
	744	1	76	52
	747	73	127	106
	784	1	31	16
	785	0	61	17
	787	11	107	65

THE ICEBERGS STUDIED

Six non-tabular icebergs were studied. Five were classified medium in size; one was small (#620). Most icebergs did not deteriorate enough to change size. The numbers (e.g. #620) refer to the sequential numbering system that IIP uses to identify individual icebergs during the course of the ice season. These are the same numbers used in archived IIP iceberg data at the World Data Center for Glaciology, Boulder, Colorado.

Although the icebergs did not change size category during the course of the study, all were deteriorating rapidly. Because of the recurring presence of growlers and bergy bits in the vicinity of all icebergs except #620 and #744, calving was assumed to be a major factor in the cluster's deterioration. Table E-3 describes the amount of calved ice in the vicinity of each iceberg during daily sizing measurements. The study could not document all calving for any one iceberg since no iceberg was observed around-the-clock. However, two events were documented: iceberg #784 on 19 June; and #747 on 21 June. Because of the warm water (greater than 3°C), the brash melted between daily observations. Bergy bits and growlers which did not fully melt between observations were tracked (in one case up to 18 hours), to keep calving statistics for the cluster from being inflated.

Only icebergs #785 and #787 appeared stable throughout the study period. Stability in this context meant that the iceberg length and height constantly decreased. Figure E-3 describes the areal dimensions for these icebergs at the beginning and end of the study period. Most of the icebergs changed shape during the study, probably from rolling. Iceberg #784 rolled while the cutter was nearby on 19 June. In this case, the rolling caused height to double although length increased insignificantly (5%).

Table E-3. Total Amount of Calved Ice Observed Daily in the Vicinity of Icebergs.

	Iceberg #					
Date (June)	620	744	747	784	785	787
14	fog	-	-	-	-	-
15	0	fog	fog	fog	brash	
16	4G	0	brash	0	brash	
17	0	brash	4G+1B	0	4G	3G+1B
18	0	-	-	8G+1B	3G	5G+2B
19	0	-	1G+1B	5G	-	1G
20	-	-	-	0	2B	fog
21	-	-	5G	-	-	-

fog - observations obscured by dense fog

(-) - no observation made during 24-hour period

G - growler, which is less than 1m high and/or 5m long

B - bergy bit, which is larger than a growler, but less than 5m high and/or 15m long

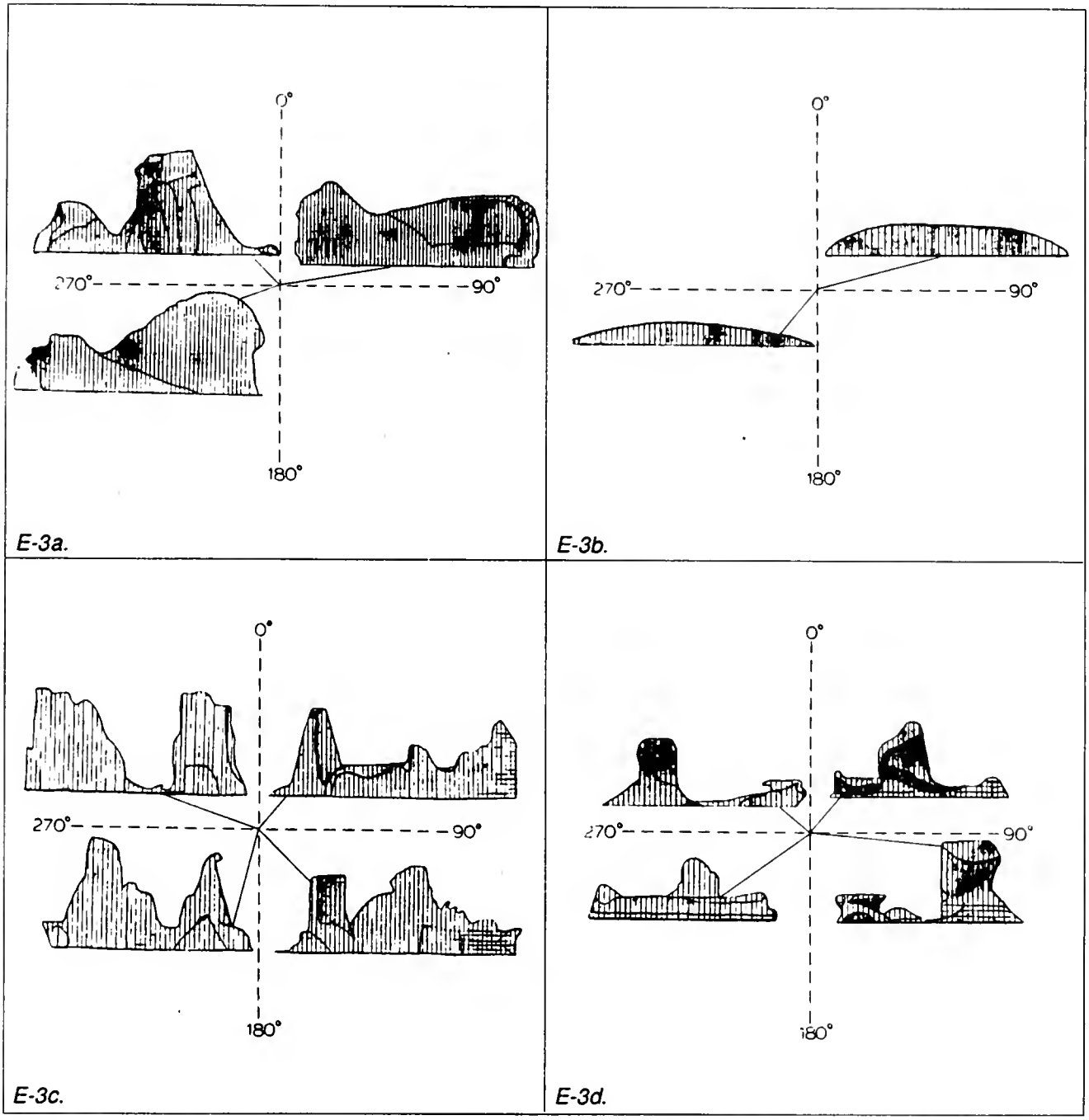

Figure E-3. Areal Dimensions of Icebergs.
These figures describe the major faces of two medium-sized, non-tabular icebergs studied during June 1987. The initial and final dimensions of each iceberg are presented. The scale is the same for all figures (1 unit = 3.1m (10 ft)). The orientation of each face to true North is also shown. The faces depicted in the initial and final sizing are dissimilar.

Figure E-3a. depicts the inital dimensions of iceberg #785 (maximum height = 37m, maximum length = 97m); Figure E-3b shows the same iceberg 4.8 days later (maximum height = 7m, maximum length = 71m).

Figure E-3c depicts the initial dimensions of iceberg #787 (maximum height = 34m, maximum length = 81m); Figure E-3d shows the same iceberg 3.1 days later (maximum height = 23m maximum length = 59m).

THE WATER COLUMN

The cluster of icebergs was in a tongue of the Labrador Current as evidenced from both sea surface temperatures and the XBT profiles (see Figure E-4). The tongue of Labrador water had a cold (-1°C) core at 60m, below a shallow thermocline at 40m. Surface temperatures ranged between 3.4 and 7.6°C. Temperatures of -1°C or colder, that would preclude melt (White et al, 1980), existed from 40m to 90m in the eastern portion of the study area, and from 40m to 160m in the western portion. XBT casts taken in the vicinity (within 28km) and within 6 hours of the 0000Z interpolated iceberg's positions were used to estimate the average heat available in the water column to melt the iceberg. When there was no XBT cast near a particular iceberg within six hours of 0000Z, the temperature information was calculated by linearly interpolating in time. The water temperature, relative to -1°C, was averaged over 10m intervals over the estimated draft of the iceberg. Iceberg draft was estimated as 3.95 times the average sail height observed during the study (Robe, 1975).

From analyzing temperature profiles taken about four days apart, this tongue of the Labrador Current had advected south 74km. The advection of the cold core at 60m agrees well with the deep-drogued drifter. Its drift indicated a predominantly southerly flow (186°T at 21cm/sec) for 4 days (from 15 June/0000Z through 19 June/0000Z), then an easterly flow (112°T at 12cm/sec) for the last 1.5 days of drift. The westward displacement of the thermal field above the thermocline agreed well with the shallow-drogued drifter. From 15 June/0000Z to 17 June/1600Z the drift was 193°T at 27cm/sec. From 17 June/1600Z until recovered on 20 June/1243Z, the drifter showed a steady deceleration, averaging 206°T at 9cm/sec. Figure E-5 summarizes the drifts of all icebergs and drifters and shows the XBT transects used to describe the thermal characteristics of the water column. All of the drifters recorded sea temperature at 1m depth between 3 and 5°C, which agreed well with the bucket thermometer measurements.

DETERIORATION MODEL EVALUATION CRITERIA

The deterioration processes were evaluated based on observations compiled for the four medium, non-tabular icebergs #747, #784, #785, and #787 which had estimated drafts from 98 to 146m. This cluster was studied for 5 days.

Based on in situ temperature, icebergs #747 and #787 had insignificant melt from convective processes below 40m depth. Therefore the buoyant and forced heat convection contributions below 40m depth were calculated and evaluated for only icebergs #784 and #785.

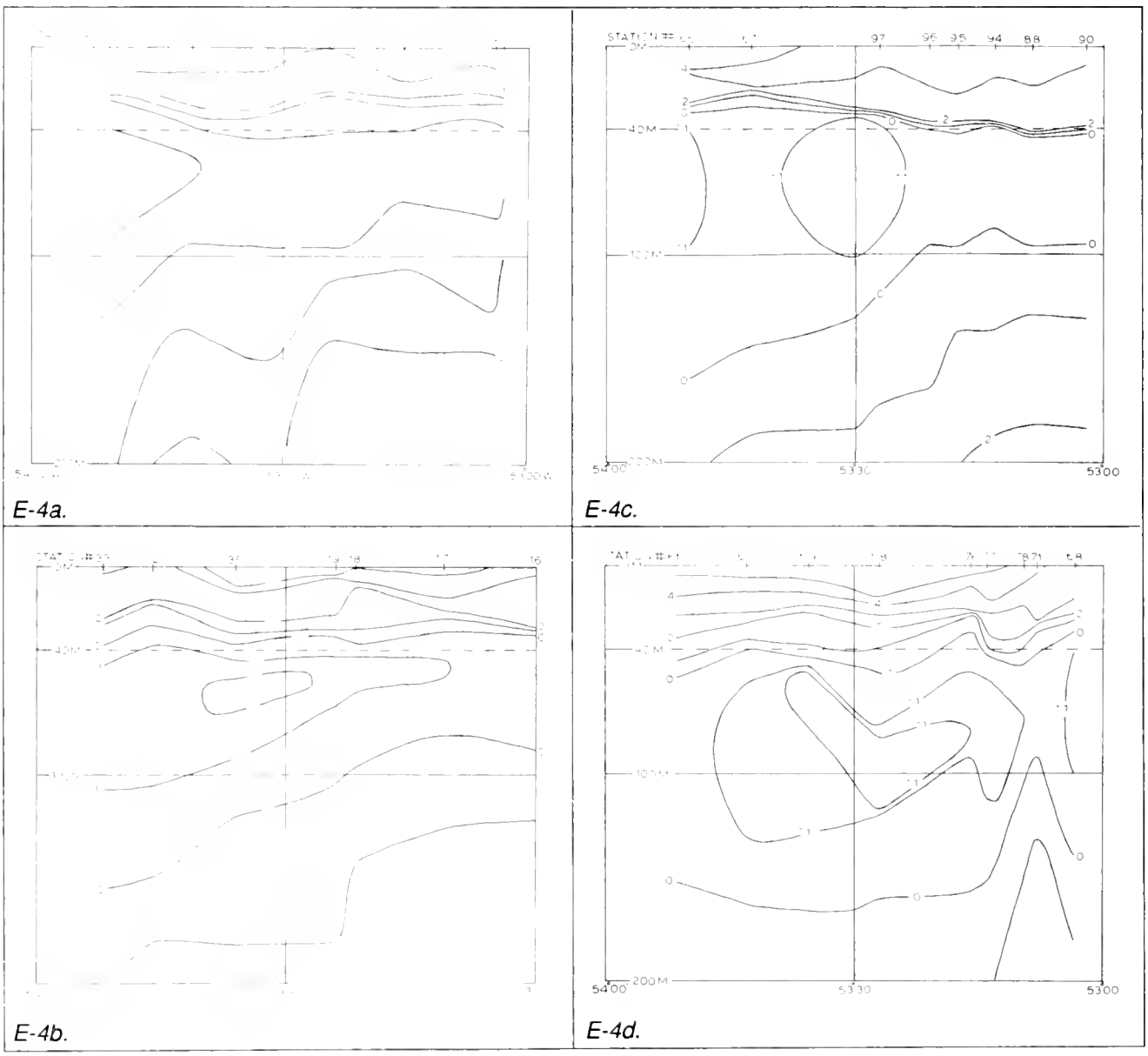

Figure E-4. Thermal Structure of the Water Column.
These figures depict the thermal structure along four eXpendable BathyThermograph transects taken during the IIP June 1987 study. These transects were nearly orthogonal to the flow of the Labrador Current. The XBT positions are noted by cast numbers along the top of each figure. The geographic positions of the transects are shown in Figure E-5. Figure E-4a depicts transect A1, which was measured between 0645Z June 15 and 0631Z June 16. Figure E-4b depicts transect B1, which was measured between 1949Z June 14 and 0151Z June 16. Figures E-4c and E-4d represent transects taken about 4 days later approximately 74km downstream from the A1 and B1 transects. Figure E-4c depicts transect A2, which was measured between 0819Z June 19 and 1234Z June 20. Figure E-4d depicts transect B2, which was measured between 0429Z and 2008Z June 19.

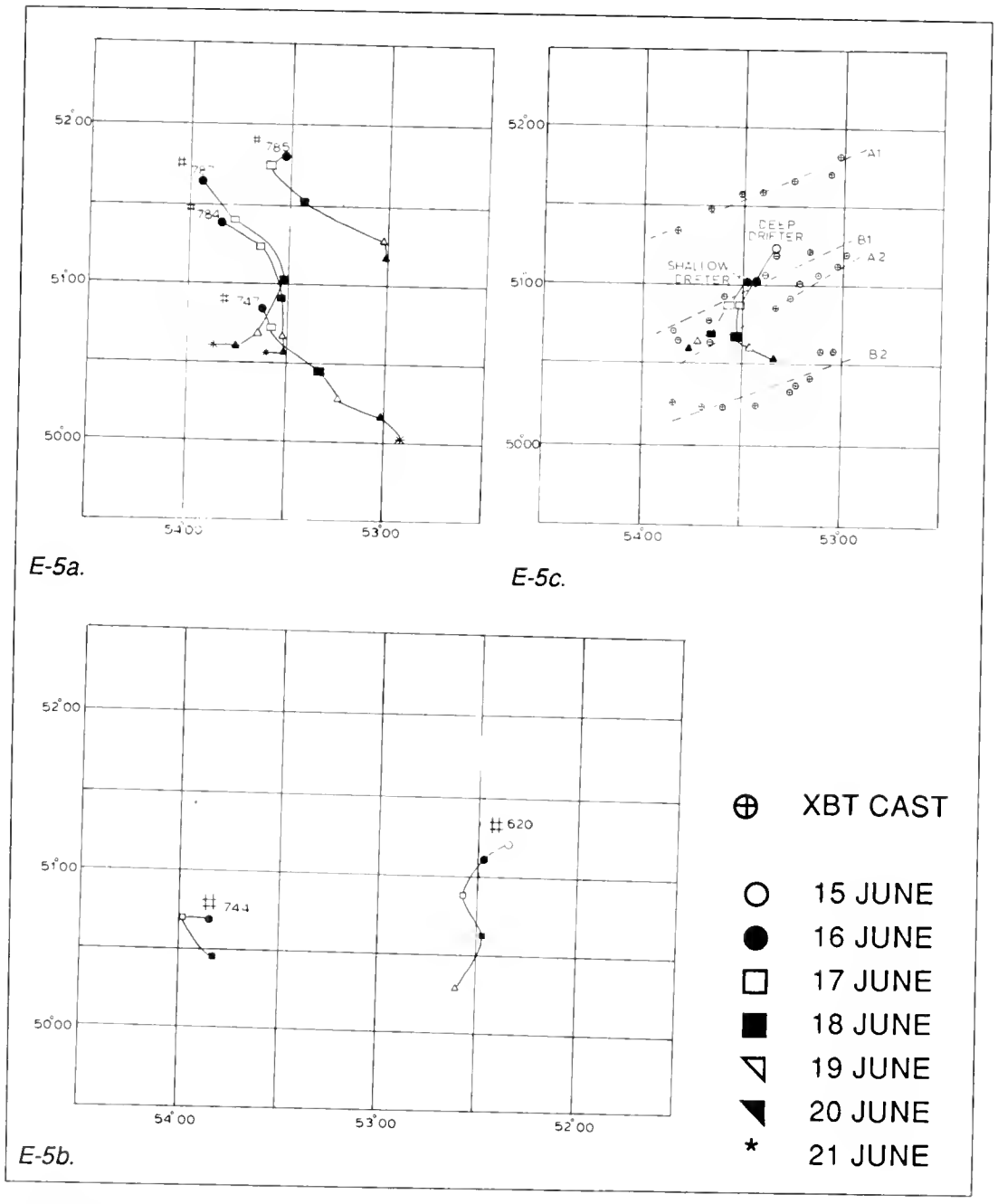

Figure E-5. Iceberg and Bathythermograph (XBT) Position Data.
Figures E-5a and E-5b show the interpolated 0000Z positions for the six icebergs studied during June 1987. The icebergs in Figure E-5a were used to evaluate the deterioration model; the icebergs in Figure E-5b were not. Figure E-5c shows the interpolated 0000Z positions for the shallow and deep-drogued drifters and the positions of the four XBT transects described in Figure E-4.

The rest of this paper evaluates modelled iceberg deterioration by examining environmental terms used in the formulae. The environmental assumptions regarding each melt process are also reviewed. Building on White's research (White et al, 1980), various observed thermal and velocity parameters are independently compared to determine which of each best represent the terms in the formulae. Using Anderson's operational computer model (Anderson, 1983), melt estimates are calculated from operational data center inputs. Figure E-6 depicts the contribution of each deterioration process to illustrate its relative importance and the changes in contribution caused by using different parameters to represent terms in formulae. The implications of error estimates for various model inputs on IIP operations are then discussed.

WARM AIR CONVECTION

Melt from warm air convection is ignored in the model. For March through mid-May, no melt is estimated for air convection. For July through September, the average melt is estimated at 8cm/day, assuming an average daily air temperature of 10°C and average wind of 37km/hr.

The daily average air temperature warmed during the study period from 6°C on 15 June to 8°C on 21 June. The average wind speed for the study period was 33km/hr. Warm air heat convection was estimated at 4cm/day.

Climatological average air temperatures for the IIP region could be used to make monthly melt estimates. Likewise, daily global-scale air temperature values could be requested from an operational data center; however, this level of effort for a relatively insignificant deterioration process seems impractical for operational forecasting purposes.

SOLAR RADIATION

The modelled melt due to solar radiation is fixed at 2cm/day, which represents the minimum melt rate for the period March through August (Anderson, 1983). The model assumes cloudy conditions.

The daylight (0800Z to 2400Z) was obscured (100%) by cloud cover or fog every day of the study except for the afternoon of 17 June and morning of 19 June. For those half day periods the skies were partly (averaged 50%) cloudy. Assuming a 35% albedo for an iceberg, the average melt rate for the June study period was 4cm/ day (White et al, 1980).

The model could be adapted to the monthly melt estimates derived by White, although the benefit would be minimal. Likewise, global-scale radiation estimates could be requested from operational data centers (COMNAVOCEANCOM, 1986); however, the level of effort to identify those periods of clear skies would only provide an additional melt of 2cm/day.

Again this level of effort for a relatively insignificant deterioration process seems impractical for operational forecasting purposes.

WATER TEMPERATURE

The model uses sea surface temperature to estimate both buoyant and forced convection contributions to iceberg melt. The melts due to buoyant and forced convection were computed as a function of observed sea surface temperature (T_o) and as a function of the in-situ temperature of the water column integrated over the estimated draft of the iceberg ($\int T_o$).

Buoyant Vertical Convection

Buoyant convection is considered solely dependent upon the "relative" temperature between a near vertical wall of ice and the water column. The cluster's average daily melt due to buoyant convection using $\int T_o$ was estimated at 2cm/day with average values for individual icebergs ranging from 1cm/day (#787) to 3cm/day (#785). The melt rate as a function of T_o averaged 7cm/day greater; with daily differences ranging from +3cm/day (#787/21 June) to +11cm/day (#747/20 June). These differences were associated with surface temperatures which were approximately 1.5°C warmer than the averaged temperature for the first ten meters of the water column.

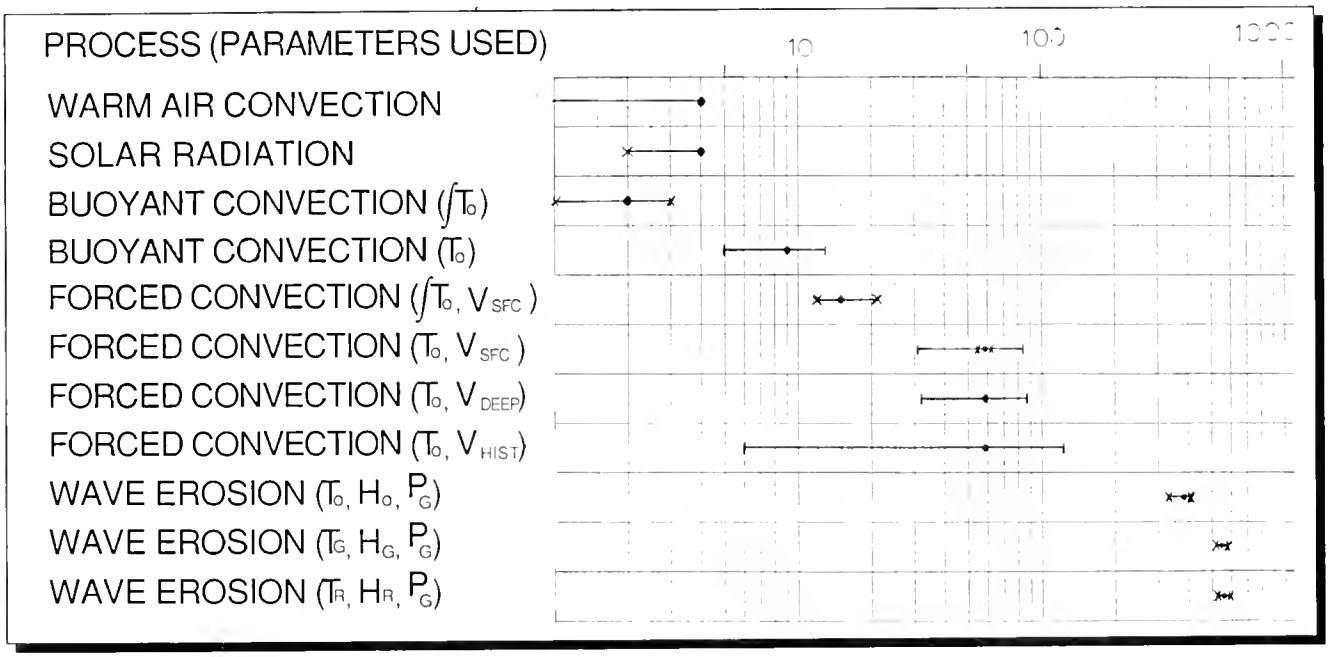

Figure E-6. COMPARISON OF ICEBERG DETERIORATION PROCESSES. This figure graphically describes both the significance of each process and the affects that different parameters have on the "melt" contribution for these processes. The "melt" contributions, which are denoted by a (•), are the five-day average for a cluster of four medium-sized, non-tabular icebergs. An (X) denotes the minimum and maximum five-day average for an individual iceberg. A (I) denotes the minimum and maximum daily "melt" for an individual iceberg.

T_o = *Observed sea surface temperature*
$\int T_o$ = *In situ temperature as a function of depth*
T_G = *Global-scale sea surface temperature product*
T_R = *Regional-scale sea surface temperature product*
H_o = *Observed significant wave height*
H_G = *Global-scale significant wave height*
H_R = *Regional-scale significant wave height*
P_G = *Global scale primary wave period product*
V(sfc) = *Differential velocity between iceberg and surface-drogued drifter*
V(deep) = *Differential velocity between iceberg and deep-drogued drifter*
V(hist) = *Differential velocity between iceberg and historical current field*

Forced Heat Convection

Forced convection is primarily dependent upon the relative temperature between iceberg and the water flowing past the iceberg. The cluster's average daily melt due to forced convection using $\int T_o$ was approximately 15cm/day with average values for individual icebergs ranging from 12cm/day (#787) to 21cm/day (#785). The melt rate as a function of T_o averaged 47cm/day greater; with daily differences ranging from +17cm/day (#784/20 June) to +69cm/day (both #747 and #784 on 18 June). These differences were associated with surface temperatures which were about 0.9°C warmer than the averaged temperature for the first ten meters of the water column.

Combined Effect in Using Sea Surface Temperature

By using sea surface temperature to derive the relative temperature term, the waterline loss could be overestimated by 20 to 80cm/day. This error represents summer conditions (surface warming). Errors for the period March through mid-May should be significantly smaller. Although the error associated with summer sea surface temperatures appears significant, it is an order of magnitude less than the sum of all modelled deterioration processes.

Subsurface temperature values can be requested from operational data centers; however, the quality of the analyses are highly dependent upon the availability of bathythermograph data. More daily observations occur in the IIP region for surface than for subsurface temperature. Additionally, the thermal structure of the water column depicted by data center products often have an accuracy no better than the temperature differences between surface and near surface values (Clancy et al, 1987). Using a subsurface temperature profile would mean substituting a known small bias in melt rate for errors which could vary as described. It would also mean a two- to four-fold increase in data input. For these reasons, IIP could not justify requesting and using subsurface temperature fields from operational data centers.

RELATIVE VELOCITY

Forced convection is also a function of relative velocity between the iceberg and the surrounding water column. The model equates relative velocity to the difference between iceberg drift and the IIP historical current in the iceberg's vicinity. The wind-induced component of the current is ignored.

Melt rates for forced convection using relative velocities derived from different current inputs were compared. The shallow-drogued drifter was assumed to represent the velocity of the water mass between the surface and the 40m thermocline, that portion of the water column which contributed most to iceberg deterioration. The relative velocity between each iceberg and the following were calculated as inputs to the model: shallow- and deep- drogued drifters, and the IIP's "master" historical current field velocity, which for the entire study area was 160°T at 23cm/sec. The deep-drogued drifter represents real-time current data which, when available, is used to "modify" the historical current. (Summy et al, 1983) Sea surface temperature was used to compute the relative temperature term. The melt rates derived using the deep-drogued drifter and "master" current as inputs were compared to the melt rate derived from the shallow-drogued drifter input.

The average daily melt due to forced convection, using iceberg drift relative to the shallow-drogued drifter, was estimated at 59cm/day with average values for individual icebergs ranging from 55cm/day (#785) to 62cm/day (#747). The melt rate as a function of iceberg drift relative to the deep-drogued drifter ranged from 25cm/day slower (#747/19 June) to 38cm/day faster (#784/20 June). Using the "master" historical current, the melt rate ranged from 53cm/day slower (#747/19 June) to 63cm/day faster (#784/20 June).

These differences in melt equated to velocity differences between the shallow-drogued drifter and the deep-drogued drifter (i.e. the "modified" current) and between the shallow-drogued drifter and the "master" current of +/- 9cm/sec

and +/- 16cm/sec respectively. In comparing the melts due to forced convection between the "master" and "modified" currents, the real-time input serves to reduce the daily differences for each iceberg by nearly half. The meteorological conditions during the study also helped to reduce the daily differences in melt between using the shallow- and deep-drogued drifter velocities. Rapid changes in the weather prevented wind direction from remaining constant (within a 60° arc of the compass) for periods longer than 27 hours; wind shifts averaged every 12 hours. Consequently, the sum of the differences for each iceberg never exceeded +/- 70cm for the study period, or an averaged error of +/- 21cm/day.

These statistics probably represent the minimum errors. In the IIP region 5- to 7-day wind events occur. An effort to control the growth of these errors may be appropriate. Wind-induced components of the current could be extracted from the dynamic iceberg drift model and substituted for the existing input. This is perceived to be a moderate level of effort for the IIP.

WAVE EROSION: GLOBAL VS REGIONAL SCALE PRODUCTS

Wave erosion, which is induced by heat convection from the turbulent maximum orbital velocity caused by the wave field surrounding the iceberg, is computed by the model. This convection is proportional to wave height (H) times relative temperature (T), and inversely proportional to wave period (P). The model assumes the effects of the wave field are non-directional, implying that the iceberg is melted uniformly from all directions (White et al, 1980). This assumption probably overestimates melt due to wave erosion. Regardless, its melt contribution is up to ten times greater than melt by forced convection, and around 100 times greater than buoyant convection. The applicability and accuracy of the environmental parameters used to model wave erosion thus greatly affect the daily melt rate estimated by the model.

The model computes T from sea surface temperature. Significant wave height and a primary wave period, which is that period associated with peak energy observed in the full wave spectrum, are currently used by the model for H and P respectively. Sea surface temperature is assumed to be the best parameter from which the relative temperature term for wave erosion is calculated, and it is readily available from data centers. Data center products representing H are significant wave height, sea height, or swell height, and products representing P are peak periods for the full, sea, or swell energy spectra (Clancy, 1987). When the model was implemented in 1983, the wave parameters currently used were the only ones available.

Table E-4 shows the differences between our observations and those analysis values produced by operational data centers: U. S. Navy Fleet Numerical Oceanography Center, Monterey, CA (FLENUMOCEANCEN); and Canadian Forces Meteorological and Oceanographic Center, Halifax, Nova Scotia (METOC). The global-scale (250km grid-spacing) analyses were produced by FLENUMOCEANCEN using its computerized Expanded Ocean Thermal Structure (EOTS) analysis and Global Spectral Ocean Wave Model (GSOWM) (COMNAVOCEANCOM, 1986). The regional-scale (estimated from 50 to 100km grid-spacing) analyses were produced by METOC Halifax. METOC depends on human interpretation of surface thermal observations and uses a parametric ocean-wave model (MacDonald et al, 1987) which is qualitatively blended with ship observations. All data center values were interpolated to each iceberg's 0000Z position. All values are for 0000Z, except for the METOC sea state analyses, which were analyzed at 1800Z. The METOC 1800Z sea state analysis normally contains more ship observations than the METOC 0000Z analysis, thereby improving the quality of the 1800Z analysis.

FLENUMOCEANCEN and METOC sea surface temperature products differed. The FLENUMOCEANCEN-produced temperatures averaged 1.3°C colder than the observed values for the cluster; the METOC-produced

temperatures were 0.6°C colder. Averaged differences between observations and FLENUMOCEANCEN products for individual icebergs ranged from 1.9°C (#784) to 0.6°C (#785) colder. The differences listed in Table E-4 which are greater than the reported system error are due to the presence of sub-scalar thermal features. In this case, iceberg #747 and #784 had crossed the surface thermal front between the colder Labrador water and the warmer Newfoundland Shelf water.

Little difference existed between the wave height products by FLENUMOCEANCEN and METOC. The FLENUMOCEANCEN-produced wave heights averaged 0.9m higher than the observed height for the cluster; the METOC-produced height was 0.8m higher. Daily differences between observed and predicted wave heights for individual icebergs ranged: from 0.3m (all/17 June) to 1.5m (#785/20 JUNE) for FLENUMOCEANCEN products; and from 0.2m (all 19 June) to 1.2m (all/18 June) for METOC products. The wave period differences in Table E-4 which exceeded system error may be based partly on the limitations of visual observations and the expertise of each observer.

The cluster's average daily melt due to wave erosion using observed values was estimated at 379cm/day with average values for individual icebergs ranging from 330cm/day (#785) to 408 cm/day (#747). The cluster's average daily melt rate using FLENUMOCEANCEN (global-scale) products averaged 152cm/day faster. Individual icebergs' average melt ranged from 144cm/day (#784) to 200cm/day (#785) faster. The cluster's average daily melt using METOC (regional-scale) products averaged 195cm/day faster. Individual iceberg's average melt ranged from 149cm/day (#785) to 218cm/day (#787) faster.

Table E-4. Average Difference Between Data Center Products and Observations.

		OBSERVED - FLENUMOCEANCEN			OBSERVED - METOC	
Date 0000Z	# of Icebergs	SST (°C)	Wave HT (m)	Wave PD (sec)	SST (°C)	Wave HT (m)
15 JUN	2	+1.1	-1.2	-8 (2)	+0.5	-0.9
16JUN	5	+0.7	-0.9	-5 (5)	+1.0	-0.6
17 JUN	5	+0.3	-0.3	-5 (5)	+0.5	-0.6
18 JUN	6	+1.0	-0.9	-4	+0.2	-1.2
19 JUN	5	+1.5 (2) *	-0.9	-2	-0.1	-0.3
20 JUN	4	+1.8 (2)	-1.2	-4 (1)	+0.2	-0.9
21 JUN	3	+2.5 (2)	-0.6	-2	+0.7	-1.2

**Note: Numbers in parentheses indicate number of times a value was outside the following error bounds:*

SST +/- 1.6°C *Wave Height +/- 1.8 m* *Wave Period +/- 4 sec*

The higher melt estimate derived from using either FLENUMOCEANCEN or METOC products was a function of their higher wave height analyses. The melt estimate using FLENUMOCEANCEN products appeared better than METOC because the underestimation of the temperature analyses offset the overestimation in the wave height analyses. The model's sensitivity to wave height makes that term just as important as the temperature term.

The significant overestimation of wave erosion justifies IIP seeking better temperature and wave data from operational data centers. Regional-scale temperature analyses are available and could reduce the variable error associated with features (i.e. the Labrador Current) which are sub-scaler to the analysis grid. Unfortunately, no digital product is presently available for regional-scale wave analyses. However, the global-scale sea height and associated peak period may reduce the bias evident in the global-scale significant wave height data. Any shift to new inputs should be evaluated by IIP to determine the combined effect of input errors before their final acceptance for operational use.

SUMMARY

Table E-5 summarizes the deterioration processes examined by this paper. For this ensemble of medium-sized, non-tabular-shaped icebergs, a daily melt rate was estimated by the model to be 4.0 m/day. Using FLENUMOCEANCEN products, the melt rate was overestimated by 1.7 m/day. METOC products overestimated the melt by 2.2 m/day. These melt estimates are of the same magnitude as the iceberg sizing error. Because of the short duration of the study, no firm conclusions could be drawn from the observed iceberg measurements. Icebergs #785 and #787, which were the only icebergs to constantly decrease in length and height throughout the study period, appeared to have melted faster than the predictions based on the optimum, observed environmental parameters. Melt predictions based on data center products were within measurement error bounds.

Sea surface temperature appears to be a suitable input for calculating the relative temperature term. In this study the use of sea surface temperature to solely represent the relative temperature term vice using temperature versus depth to represent the term for buoyant and forced convection, caused the melt rate to be overestimated by 12%. Global-scale thermal products cannot adequately represent the Labrador Current. Regional-scale temperature products currently available can improve the resolution of the temperature data.

Oversimplification by IIP of methods used to derive the relative velocity between icebergs and the surrounding water contributed to an error of up to 16% of total melt. Because the wind-induced component of the ocean surface layer (between the surface and 50m depth) is computed in the IIP iceberg drift model, this velocity component could be added to the "modified" or historical surface current. The resultant current value could then be used to compute relative velocity to reduce the magnitude of this error.

Wave height overestimation causes daily melt to be overestimated. This significant (about 38% of total melt) error in determining the wave erosion contribution probably compensates for the model's inability to represent all deterioration processes. New wave products that have recently become available should improve the melt estimate due to wave erosion.

The iceberg sizing method and study time constraints made comparisons of model estimations to observed lengths inconclusive. Either a better method must be used in future studies or studies must be extended over much longer periods (14-21 days). Given the potential for errors associated with operational reconnaissance, which depends heavily on arbitrary size classifications, and the inability to model all deterioration processes, the IIP policy to require icebergs to deteriorate 175% of their original length is prudent.

Table E-5: Average Melt Rate for Various Inputs.

MODEL TERMS	PARAMETERS USED				
Relative Temperature	$\int T_O$	T_O	T_O	T_G	T_R
Relative Velocity	V(sfc)	V(sfc)	V(deep)	V(sfc)	V(sfc)
Wave Height	H_O	H_O	H_O	H_G	H_R
Wave Period	P_O	P_O	P_O	P_G	P_R
DETERIORATION PROCESSES	**MELT RATE (cm/day) USING ABOVE PARAMETERS**				
Warm Air Convection	4	4	4	2	2
Solar Radiation	4	4	4	0	0
Buoyant Radiation	2	9	9	6	8
Forced Convection	15	62	6-122	33	41
Wave Erosion	379	379	379	531	574
Total Average Melt	404	458	402-520	572	625

T_O = Observed sea surface temperature
$\int T_O$ = In situ temperature as a function of depth
T_G = Global-scale sea surface temperature product
T_R = Regional-scale sea surface temperature product
H_O = Observed significant wave height
H_G = Global-scale significant wave height
H_R = Regional-scale significant wave height
P_G = Global-scale primary wave period product
V(sfc) = Differential velocity between iceberg and surface-drogued drifter
V(deep) = Differential velocity between iceberg and deep-drogued drifter

ANDERSON, I., 1983. Iceberg Deterioration Model. *Report of the International Ice Patrol in the North Atlantic Ocean, Season of 1983, (CG-188-38)*, p 67-73.

ANDERSON, I., 1985. Oceanographic Conditions On The Grand Banks During The 1985 IIP Season. *Report of the International Ice Patrol in the North Atlantic Ocean, Season of 1985, (CG-188-40)*, p 56-67.

CLANCY, R. M., B. L. SAMUELS, and K. D. POLLACK, 1987. Technical Description Of The Optimum Thermal Interpolation System (OTIS): A Model For Oceanographic Data Assimilation. Fleet Numerical Oceanography Center Tech Note 422-86-02, 22 May 1987. pp 110.

CLANCY, R. M., 1987. Real-Time Applied Oceanography At The Navy's Global Center. *Marine Technology Society Journal*, Vol 21, No 4, December 1987, p 33-46.

EL-TAHAN, M., S. VENKATESH, and H. EL-TAHAN, 1987. Validation and Quantitative Assesment Of The Deterioration Mechanisms Of Arctic Icebergs. *Journal of Offshore Mechanics and Arctic Engineering*, February 1987, Vol 109, p 102-108.

MACDONALD, K. A., and S. CLODMAN, 1987. The AES Parametric Ocean-Wave Forecast System. *Proceedings of the International Workshop on Wave Hindcasting Forecasting. Report 065.* Environmental Studies Revolving Funds, Ottawa, pp 119-132.

MOUNTAIN, D. G., 1980. On Predicting Iceberg Drift. *Cold Region Science and Technology*, Vol I (3/4), p 273-282.

ROBE, R. Q., 1975. Height To Drift Ratios Of Icebergs. *Proceedings of the Third International Conference on Port and Ocean Engineering Under Arctic Conditions*, 11-15 August 1975, Vol I, p 407-415.

SUMMY, A. D. and I. ANDERSON, 1983. Operational Uses Of TIROS Oceanographic Drifters By the International Ice Patrol (1978-1982). *Proceedings 1983 Symposium On Buoy Technology*, 27-29 April 1983, p 246-250.

WHITE, F. M., M. L. SPAULDING, and L. GOMINHO, 1980. Theoreti cal Estimates Of The Various Mechanisms Involved In Iceberg Deterioration In The Open Ocean Environment. Report CG-D-62-80, U. S. Coast Guard Research and Development Center, Groton, Connecticut 06340-6096, pp126.

Numerical Environmental Products Manual, Vol II, August 1986 Prepared under authority of Commander, Naval Oceanography Command, Stennis Space Center, Mississippi 39525, pp 200.

Appendix F

Evaluation of Shipboard Visual Estimation of Iceberg Size

LCDR Walter E. Hanson, USCG

INTRODUCTION

During 1987, approximately 21 per cent of all sightings entered into the International Ice Patrol (IIP) computer were from visual ship observations. Shipping has each year contributed a significant number of visual sightings. Many studies have assessed the ability of ships to detect icebergs, primarily by radar (Budinger, 1960; Ryan et al, 1985; and Harvey et al, 1986). However, little information is known about the sizing accuracy of visual sightings. Consequently, the 1987 iceberg IIP iceberg deterioration study, described in Appendix E, presented an opportunity to evaluate the ability of shipboard observers to visually estimate iceberg size.

This study evaluates visual sizing efforts which had neither the aid of visual cues (i.e. an object in close proximity for size comparison) nor the aid of stadimeter or sextant. This sizing technique may mirror that of the shipping community. The icebergs studied by IIP were primarily medium-sized, non-tabular shaped. This category of iceberg seems to be the most often sighted by shipping.

BACKGROUND

The IIP uses iceberg size and shape in sighting reports to predict their drift and deterioration. For operational purposes, only seven different categories of icebergs are modelled (Mountain, 1980). They are:

- Growler
- Small, Non-Tabular
- Small, Tabular
- Medium, Non-Tabular
- Medium, Tabular
- Large, Non-Tabular
- Large, Tabular

Drift and deterioration predictions are computed twice daily using computerized models. Iceberg size is used differently by the two models.

In the drift model, the size and shape parameters together select one of seven profiles. Each profile is a different cross-sectional representation of above-surface and sub-surface area. The profile represents the average dimensions for icebergs in that size and shape category. The iceberg is drifted based on the forces acting upon the profile. The profile is not changed until a new size and/or shape is specified.

In the deterioration model, the size and shape parameters together select one of seven waterline lengths. The model calculates "melt" in terms of length instead of mass. Each of the seven lengths is assumed to be the maximum value for the particular size and shape category. Environmental conditions and waterline length are then used as inputs for the daily "melt" of the iceberg.

DATA COLLECTION

The USCGC TAMAROA, a 68 m (205 ft) U. S. Coast Guard cutter, was used for the 6.3 day study. Visual observations were made from the bridge wing; height of eye was 10.8 m. Two IIP ice observers, who each had at least two years of aerial iceberg reconnaissance experience, made the observations.

Iceberg above the waterline dimensions were measured during daylight (from 0800Z to 2400Z) in all weather and light conditions. Table F-1 shows the hours when iceberg sizing occurred. Iceberg shape and size were both estimated by the ice observers and calculated from photographic images scaled according to rangefinder measurements. This required a 360 degree look at each iceberg; measuring and photographing all prominent faces. Measurements were accurate to +/- 8% of the observed dimensions; see Table F-1.

The cutter circled each iceberg twice; once to identify the prominent faces; and during the second pass, to make measurements. When perpendicular to each face the true bearing and laser-derived distance to it were recorded, a

Table F-1. TIMES OF ICEBERG SIZING MEASURMENTS. Dates and times to the nearest hour when icebergs were sized are listed. Iceberg numbers refer to the sequential numbering system that IIP uses to track individual icebergs during the course of the ice season.

ICEBERG # DATE/TIME	620	747	744	784	785	787
14 June	22Z	-	-	-	-	-
15	19Z	00Z/21Z	23Z	16Z	08Z	-
16	15Z	17Z	19Z	13Z	09Z	-
17	20Z	21Z	23Z	17Z	12Z	16Z
18	22Z	-	-	16Z	11Z	18Z
19	18Z	16Z	-	10Z	-	08Z
20	-	-	-	13Z	09Z	18Z
21	-	00Z/08Z	-	-	-	-

photograph taken, and the scalar dimensions recorded. (Scalar dimensions were converted to length and height after all the field work was completed.) At the end of the second pass, the ice observers collectively estimated the iceberg's maximum height and length. No visual cue, like a ship's boat or another vessel, was available to help size the iceberg; only the horizon, when weather permitted. Neither stadimeters nor sextants were used.

Iceberg size measurements were conducted within 1900 m of each iceberg; distances for each observation are listed in Table F-2. These distances were dependent upon weather and the ability to view/measure the entire face of the iceberg through the reticulated binoculars.

STUDY FINDINGS

Thirty-one visual estimations of both height and length were compared to measured dimensions. The results indicated that the trained observer tended to underestimate both length and height.

All but one of the visually-estimated lengths were less than the measured length; see Figure F-1a. For this set, a linear regression indicated the estimated length was about 56 per cent of the measured length. The data set's linear correlation was 0.72.

The observers better estimated height. All but seven of the visually-estimated heights were less than the measured height; see Figure F-1b. For this set, the regression indicated the estimated height was about 66 per cent of the measured height. The correlation was 0.81.

CONCLUSIONS

Visual observations made close to medium-sized, non-tabular icebergs without the aid of measurement devices (i.e. stadimeters, sextants, or reference objects) may underestimate their size. Therefore, if an iceberg appears on the border between two size categories, the IIP recommends assigning the iceberg to the larger of the two size categories. Given the difficulty in properly estimating size, IIP encourages the use of all measurement devices at one's disposal.

Table F-2. DISTANCE AT WHICH ICEBERG SIZING MEASUREMENT MADE. The beginning and ending distance in meters from the iceberg are listed.

ICEBERG # DATE/TIME	620	747	744	784	785	787
14 June	890-620	-	-	-	-	-
15	490-310	1880-1160	300-260	517-390	960-710	-
		580-380				
16	1060-870	1190-940	1280-930	1130-710	780-550	-
17	720-550	1070-700	1350-690	1210-990	1270-990	1350-980
18	1040-750	-	-	1340-1050	1020-860	1230-710
19	1370-580	1140-850	-	1450-810	-	700-540
20	-	-	-	1430-870	790-570	560-420
21	-	1360-860	-	-	-	-
		1780-570				

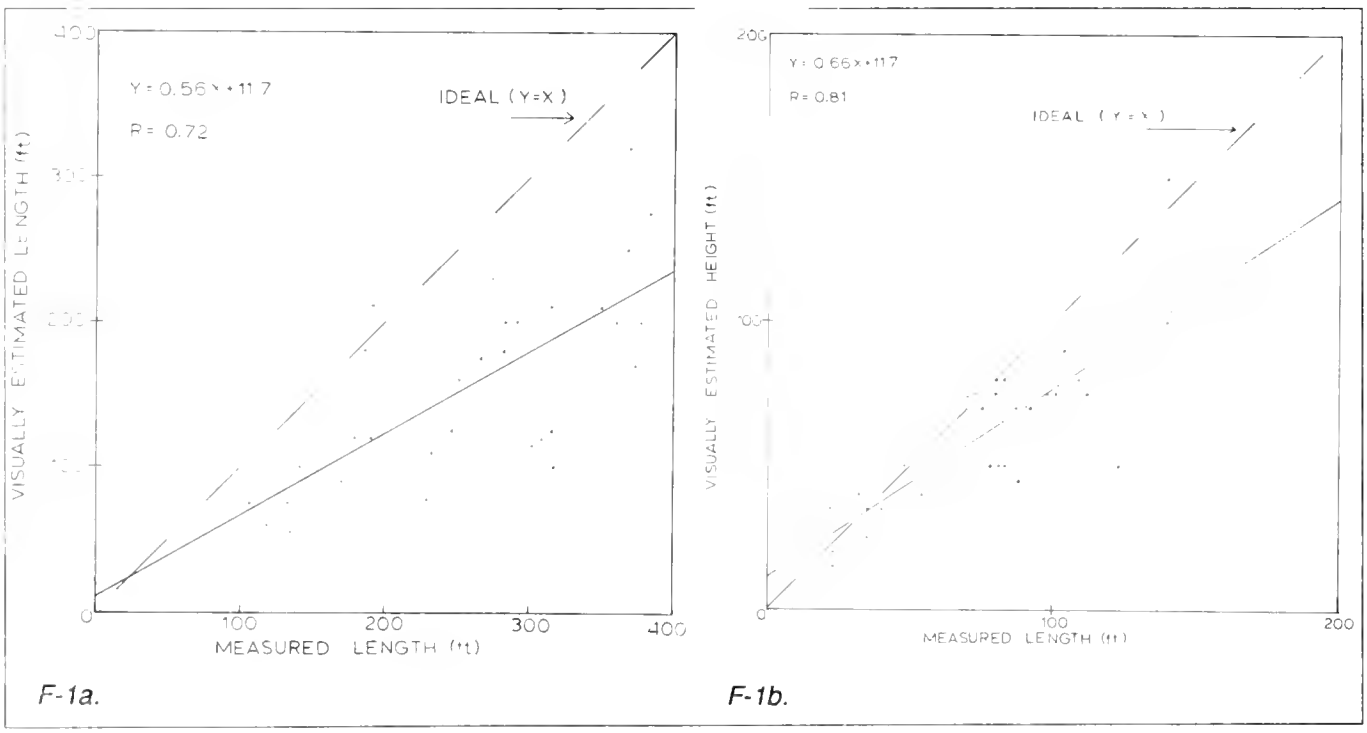

F-1a. *F-1b.*

Figure F-1. VISUAL ESTIMATION VS. ACTUAL MEASUREMENTS. These scatter diagrams show the estimated and the measured dimensions of icebergs sized during the IIP June 1987 iceberg deterioration study. The linear regression is the solid line; its equation (in which Y = estimated feet and X = measured feet) and its correlation coefficient are in the upper lefthand corner. The ideal condition (estimated = measured) is shown by the dashed line.

Figure F-1a compares estimated vs measured lengths; Figure F-1b compares heights.

REFERENCES

Budinger, T. F., 1960. Iceberg Detection by Radar. *International Ice Observation And Ice Patrol Service In The North Atlantic Ocean, Season of 1959*, Bulletin No. 45, p 49-97.

Ryan, J. P., M. J. Harvey, and A. Kent, 1985. Assessment Of Marine Radars For The Detection Of Ice And Icebergs. Environmental Studies Revolving Funds Report 008, Ottawa pp 127.

Harvey, M. J. and J. P. Ryan, 1986. Further Studies On The Assessment Of Marine Radars For The Detection Of Icebergs. Environmental Studies Revolving Funds Report 035, Ottawa pp 82.

Mountain, D. G., 1980. On Predicting Iceberg Drift. *Cold Region Science And Technology*, Vol I (3/4) p 273-282.

U. S. GOVERNMENT PRINTING OFFICE 1989/601-414/00022